

ISSN - 2278-5655
VOL -VII , SPECIAL ISSUES -IX

Impact Factor
5.18

AMIERJ

*Aarhat Multidisciplinary
International Education
Research Journal*

A Peer Reviewed Multidisciplinary Journal
UGC Approved Journal No 48178, 48818

Edited by-
Dr. N. K. Shinde
Dr. Mrs. S.K. Mengane
Dr. R. P. Patil
Dr. S. R. Londhe



M.H. Shinde, Mahavidyalya, Tisangi
Tal- Gaganbavada, Dist- Kolhapur
Maharashtra, India



Aarhat Publication & Aarhat Journal's

108, Gokuldham Park, Dr. Ambedkar Chowk, Near TV Tower, Badlapur(E), 421503
Email ID: aarhatpublication@gmail.com • Ph.: 9822307164
Website : www.aarhat.com

*"National conference
on
"Innovative Research in Physical, Chemical and Life Sciences"*

NCIRS—2018

*Aarhat Multidisciplinary International Education
Research Journal (AMIERJ)*

VOL VII SPECIAL ISSUES IX

TABLE OF CONTENTS

Research Article

1.	<i>The Effect of Boron on Yield and Yield Parameters of Sweet Sorghum var. Madhura(S. S.Jadhav and S.B.Bhamburdekar).....</i>	<i>1-4</i>
2.	<i>Ethnomedicinal and pharmacognostical studies on the leaves of Caseariachampioniithw.,enum(ArunPatil and VarshaJadhav(Rathod).....</i>	<i>5-10</i>
3.	<i>Effect of different carbon and nitrogen sources on growth of Fusariumoxysporumf.sp. Crysanthemi causing wilt of Chrysanthemum(S.S.Patil and M.B. Waghmare).....</i>	<i>11-14</i>
4.	<i>Checklist of the freshwater molluscs from Panchganga River, Kolhapur, (MS) India (Sanindhargaikwad, Priyanka Prakash Chavan and NitinAnandraoKamble).....</i>	<i>15-20</i>
5.	<i>Haematological alterations against chronic exposure of Monosodium glutamate (MSG) on male mice Musmusculus. (Sunny Bhivate and NitinKamble).....</i>	<i>21-24</i>
6.	<i>Effect of heavy metal on the behavior of some selected aquatic Molluscan species: a comparative study (Sunil Londhe and NitinKamble).....</i>	<i>25-32</i>

-
- 7 *Effect of phosphate and salt sources on growth of Alternaria zinniae caused by flower blight of marigold (Tagetes erecta) (A.B. Nangare, M.B. Waghmare and M.M. Patil).....* 33-36
 - 8 *Effect of Carbon and Nitrogen Sources on the Growth of Fusarium oxysporum f.sp. cubense causing Panama wilt of banana. (M. S. Desai, A. A. Jagtap and S. S. Kamble).....* 37-42
 - 9 *Biocontrol capability of Trichoderma virens lcf on the Fusarium equiseti causing blossom blight of Polianthes tuberosa l. (S.A. Shinde, M. B. Waghmare and M. M. Patil).....* 43-46
 - 10 *Intellectual medicinal properties of Withania somnifera (L.) Dunal: a review (Nilofar Shaikh and Madhuri Walvekar).....* 47-54
 - 11 *MSG (Monosodium Glutamate) induced male gonadal lesions and reproductive disabilities in vertebrate model Mus musculus. (Gondil K. A., Kusarkar S. P., Babar K. K., Kasar P. M., Bhivate S. B. and Kamble N. A.).....* 55-58
 12. *Histopathological study of Etova P-400 on liver and kidney of Mus musculus (Tushar Kakade, Sanindhar Gaikwad and Rajan More).....* 59-62
 13. *Use of Agrochemicals in the Management of Sesamum Blight Caused by Bavistin Resistant Alternaria sesame (A. B. Patil and S. S. Kamble.).....* 63-66
-

-
14. Effect different pH levels on the growth of *Colletotrichum capsici* (Syd E J Butler & Bisby) causing anthracnose disease. (M.S.Sutare)..... 67- 68
15. Sustainable capability of carbendazim resistance *Alternaria alternata* causing leaf spot *Aloe vera* in the mixed population. (M.B. Waghmare)..... 69-70
16. Seasonal Abundance of Mayflies (Ephemeroptera) In Kolhapur District (Rohini Kamble and T.V.Sathe)..... 71-76
17. A study of fitness performance and maximum oxygen consumption ($VO_{2\max}$) in the residential and non-residential school children's of Kolhapur District, MS, India (Manjare K.G. Sanadi R.A. and Jadhav A.D.)..... 77-84
18. Seasonal abundance of Ichneumonids from Western Maharashtra (Sutar Mahesh and T.V.Sathe)..... 85- 92
19. Application of Morphometrics to Reveal the Similarity Matrix and Distance Matrix among Closely Related *Cleome L.* Species from Kolhapur District (S. A. Deshmukh and D. K. Gaikwad)... 93-96
20. Bio-control of *Fusarium udum*, the causal organism of pigeonpea wilt utilising *Trichoderma* spp. (U.A. Desai and S. S. Kamble)... 97-102
-

21	<i>Evaluation of Antimicrobial Properties and Phytochemical Content of Leaf and Fruit Peel Extract of Capparis divaricate (ManjunathGopika, Vhanmane R. S, Vhankade A. M, Swami V. R.).....</i>	<i>103-108</i>
22	<i>Histology of male reproductive system in longhorn beetle AeolesthesholosericeaFabricius (Coleoptera: Cerambycidae). (Patil N. K. and S. M. Gaikwad.).....</i>	<i>109-114</i>
23	<i>Diversity of Bivalve Molluscs from Karanja Estuary, UranDist-Raigad (ms) - a systematic survey (Kamble S. P.).....</i>	<i>115-118</i>
24	<i>Acute toxic effect of sugar factory effluent on behavior and mortality in fresh water fish, Labeocalbasu(VinodKakade)...</i>	<i>119-124</i>
25	<i>Water quality assessment of takve lake of shiralataluka, Sangli district(Shakila P. Maldar, Niranjana S. Chavan.).....</i>	<i>125-130</i>
26	<i>Detection of seed mycoflora of some important oil seeds from Kolhapur (S.C.Vhandrao, J.D.Babar, G.B.Gosavi, R.K.Kamble, S.A.Magdum, S.L.Soudagar and S. S. Kamble.).....</i>	<i>131-132</i>
27	<i>Zinc ferrite as efficient H₂S gas sensor(S. D. Jadhav, A.D.Pinjarkar, S.L.Pawar, R. P. Patil).....</i>	<i>133-138</i>
28	<i>Effect of Sn doping on Structural Properties of Cobalt Ferrites Synthesized by Sol Gel Method(P. V. Gaikwad and P.D. Kamble)</i>	<i>139-144</i>
29	<i>Synthetic studies on 1, 2, 4-triazoles derivatives and biological evaluation as antifungal and antibacterial agents (Sujatha.k, A.M.A.KhaderBalakrishnaKalluraya).....</i>	<i>145-152</i>

30	<i>Synthesis of Nanoropes, Nanorods, Nanodiscs and Nanoflowers of ZrO₂ Thick Films for various Applications and Their Characterizations (G. B. Shelke and D. R. Patil).....</i>	<i>153-158</i>
31	<i>Photoelectrochemical applications of NiSe thin films prepared by Chemical bath deposition method (B. V. Jadhav).....</i>	<i>159-164</i>
32	<i>Simple Method for Synthesis of Pd Supported Nanoparticals and Its Applications in Organic Transformation (A. V. Mali A. V. Tapase and P.P. Hankare).....</i>	<i>165-168</i>
33	<i>Comparative Study of Germination of Seed of Vignaradiata and Vigna conitifolia by Treatment of Ultrasonic Wave using Sonicator (Avinash A Ramteke and Shivaji R Kulal).....</i>	<i>169-172</i>
34	<i>Comprehensive Structural Investigations of Nanocrystalline MoO₃ thin films (S.V.Kitea, P.A.Chate, K.M.Garadkar, U.B.Sankpal, Z.D. Sande, D.J.Sathe).....</i>	<i>173- 178</i>
35	<i>Effect Of Tin (Sn) Substitution On The Structural Properties Of Co Ferrite Nano Particle Synthesized Via Sol-gel Route. (S.D. Zimur, P.D. Kamble ,M.R. Kadam , P.V. Gaikwad.).....</i>	<i>179-184</i>
36	<i>Synthesis and Electrical, Magnetic studies of Cu_{1-x}Co_xFe₂O₄ Ferrite (SM R. Kadam, P.D.Kamble, S. A. Shivade).....</i>	<i>185-192</i>
37	<i>Application of Pomegranate Albedo for Biosorption of Methylene Blue Dye (Prakash Patil_{1,2}, Bharat Pawar₁ and Sunil Mirgane₂)..</i>	<i>193-194</i>
38	<i>Development of growth charts for 5-10 year aged children (S.S.Shinde, S. V. Kakade).....</i>	<i>195-204</i>
39	<i>Degradation of methyl orange by using ternary TiO₂/SnO₂/WO₃ nanocomposite as an efficient visible light active photocatalyst (Satish M. Patil, Shamkumar P. Deshmukh, and Sagar D. Delekar).....</i>	<i>205-210</i>

-
- 40 Use of some agrochemicals in the management of leaf spot of ginger caused by *Phyllosticta zingiberi* resistant to carbendazim (J. M. Gorule and S. S. Kamble)..... 211-216
- 41 Effect of interactions between symbiotic VAM fungus and diazotrophic bacteria, *Rahnella* on carbohydrate and mineral contents of non-leguminous plant, *Abelmoschus esculents* (L.) Moench. (D. D. Gharge and B. A. Karadge)..... 217-226
- 42 Effect of NaCl on growth and development, polyphenol content and proline accumulation in the leaves of *Trianthem portulacastrum* L. grown in sand and soil culture. (J.M. Patil and B. A. Karagade)..... 227-232
- 43 Floristic Diversity of Wild Relatives of Grain Legumes from Nashik District. (Mayur S Patil and Sanjay G Auti)..... 233-236
- 44 Effect of Foliar Acetyl Salicylic Acid Application on Total Nitrogen and Soluble Nitrogen Fractions of Groundnut (S H Jadhav)..... 237-240
- 45 Biopotential of *Trichoderma sp.* against *Fusarium oxysporum f. sp. dianthi* causing wilt of carnation in the presence of micronutrients (R. M. Waghmare, M. B. Waghmare, S.K Mengane, D.S Pawar, S.S. Kamble)..... 241-244
-

46	<i>Qualitative analysis of secondary metabolites from some phytofungicidal plants (Dhanajipawar, Mengane S.K Waghmare R.M and B. J. Patil).....</i>	245-248
47	<i>Effect of interactions between symbiotic VAM fungus and nitrogen fixing bacteria, Rhizobium on growth and chlorophyll content of non-leguminous plant, spinach (Spinaciaoleracea L.) (Gharge D. D. and Karadge B. A.).....</i>	249- 256
48	<i>Bioefficacy of plant extracts on Macrophominaphaseolina (tassi)goid causing charcoal rot of maize (S.G.Jagtap, .R.Kavale and S.S. Kamble).....</i>	257-260
49	<i>Synergistic effect of herbicides on the development of carbendazim resistance in Alternariadauci causing leaf blight of carrot (M. S. Mishrakoti and S. S. Kamble).....</i>	261-264
50	<i>Effect of biofertilizers on growth of paddy (Oryza sativa L.) CV. JAYA. (N.B. Pawar, N.S. Suryawanshi and A.G. Rokade).....</i>	265-270
51	<i>Effect of Trichodermaoningii culture filtrate on seed germination and growth of some vegetables (in vitro) (PrajaktaPatil , SnehaDevardekar, RaginiPatil, ManaliJadhav, SupriyaPatil, SnehalPatil, TruptiGhadge , Swapnali Shinde*, M. B. Waghmare).....</i>	271-278
52	<i>Influence of plant growth regulators on total alkaloids content of Amaranthusgangeticus l. under salt stress. (Priyanka P. Jadhav and D. K. Gaikwad).....</i>	279-284
53	<i>Water quality assessment of takve lake of shiralataluka, Sangli district. (1Shakila P. Maldar*, 2Niranjana S. Chavan.).....</i>	285-290

54	<i>Kinetics and Mechanism of Oxidation of Maltose by keggin type 12-tungstocobaltate (III) in hydrochloric acid Medium(Sunil N. Zende).....</i>	291- 296
55	<i>Ecofriendly Solvent Free Synthesis of Dihydropyrimidine Derivatives by Biginelli Reaction (A.C.Bhosale, S. A. Kenawade).....</i>	297-300
56	<i>Manganese doped Co-Zn Ferrite Nanoparticle Synthesis and Characterization; Effects of Annealing Temperature on the Size of nanoparticles.(Bhagvan V. Jadhav¹, Sajid F. Shaikh², Rajendra P. Patil³).....</i>	301- 306
57	<i>Green synthesis and characterisation of silver nano-particles (Apoorva U. Sammitha D.Hebbar LeenaHublikar).....</i>	307- 308
58	<i>Synthesis, Characterization and gas sensing study of Cd-Mn Ferrite (N. M. Patil*, R. P. Patilb*).....</i>	309-314
59	<i>Analysis of habitable site of M. cymbalaria. Hook. f. (S.V.Madhale).....</i>	315-318
60	<i>A comparative study of different compatibilisers on thermoplastic polyurethane/polyolefin blends. (Atul DinkarKamble@1, Merlin Thomas2, Neetha John3.).....</i>	319-330
61	<i>Investigation of structural and magnetic properties of TiO₂ supported Zinc ferrite (R.P.Patila*, B. L. Shindeb, M. N. Gadsingc, R. K. Dhokaled).....</i>	331-334

62	<i>Synthesis and characterization of Zn-Cr ferrite (S. B.Patila, N.M.Patil, A.J.Davaric, M.N.Patil, R. P. Patil*)</i>	335- 338
63	<i>Synthesis, characterization and catalytic application of Cr substituted Zinc Manganese Ferrite (A.S.Chavan, C. F. Rajmahadik, R.S.Pandav, R. P. Patila*)</i>	339-346
64	<i>Electrochemical synthesis of Mn(OH)₂ and Co(OH)₂ thin films for supercapacitor electrode application (N. C. Maile, S. D. Ghongade, S. K. Khare, H. B. Kamble and V. J. Fulari)</i>	347- 356
65	<i>Sol-Gel Deposition of Nanocrystalline TiO₂ Films and Natural dye for Dye Sensitized Solar Cell Application (M. T. Sarode)</i>	357- 362
66	<i>Phytochemical constitute and antioxidant potential of Lantana camera (S.B.Patil and S.K.Mengane)</i>	363- 366
67	<i>Green synthesis of silver nanoparticles from Lantana camera (S.K.Mengane and S.S.Patil)</i>	367-370
68	<i>STUDIES ON LPG SENSING BEHAVIOUR OF Cs DOPED PHOSPHOMOLYBDIC ACID BY HYDROTHERMAL ROUTE (S. N. NADAP, V. A. KALANTRE, B. M. SARGAR, K. S. PAKHARE AND S. R. MANE)</i> -----	371-374
69	<i>The effect of Copper doping on the structural and Optical properties of ZnFe₂O₄ (Deepa M Audi)</i>	375-379



The Effect of Boron on Yield and Yield Parameters of Sweet Sorghum var. Madhura

¹S. S.Jadhav*, ²S.B.Bhamburdekar

¹*Department of Botany, Shrimant Bhaiyyasaheb Rajemane College Mhaswad, Tal. Man, Dist. Satara (MS).

² Department of Botany, Krishna Mahavidyalaya, Rethare (BK), Karad, Dist. Satara (MS).

KEYWORDS

Yield, sweet Sorghum,
Boron, Concentration,
Micronutrient

ABSTRACT

Yield is the ultimate reflection of the various yield components as it is important and combined effect of various morphological, environmental, physiological and growth characters, which are showing differences in cultivars. Yield contributing characters are directly related with economic yield of the plant. Sweet Sorghum is a very important crop as a food, fodder, fuel and fertilizer. Boron is important micronutrient which plays role in pollen germination and pollen tube formation which leads to improve yield. In the present investigation the effect of different boron concentrations like 0 ppm (Control), 10 ppm, 50 ppm and 100 ppm on sweet Sorghum var. Madhura has been studied. The pot culture technique was used for this investigation. The objective was to identify the correct dose of boron to improve yield in sweet Sorghum which is a semi-arid crop. The data was collected after the full growth of plant. The results are showing that the lower doses of boron like 10 ppm and 50 ppm have positively influenced the yield parameters and yield components. The sweet Sorghum var. Madhura shows increased grains per panicle, grain yield, biological yield and harvest index due to 50 ppm boron concentration.

Corresponding Author
Email

sujit_jadhav275@rediffmail.com

Introduction

Generally, plant comprises yield in two ways, forage/ straw yield and grain yield. There are various factors in the nature that have direct or indirect influence on the crop yield. These factors include water deficit, mineral imbalance, and non-availability of macro or micro nutrients in soil, environmental factors along with this excess availability or use of a particular or more macro/ micro fertilizers and or water in the crop field. The amount of soil moisture available to plants in arid and semiarid regions is also one of the major limiting factors for crop yield.

Boron is one of the microelements required for healthy crop growth and development of reproductive tissues. It is required in very small amount. However, the deficiency and excess use of boron may affect crop growth. Boron is important micronutrient which plays role in pollen germination and pollen tube formation which leads to improve yield (Wojcik and Klamkowski, 2008). As boron is important micronutrient required for plant growth and yield (Soomro *et al.*, 2011) which play vital function in cell wall formation, nitrogen fixation, nucleic acid, membrane stability, sugar transport, carbohydrate and Indol Acetic Acid metabolism. Due to all these roles, boron leads to an

Acid metabolism. Due to all these roles, boron leads to an increase in plant height and production (Ali, 2012; Masoud *et al.*, 2012).

Sorghum bicolor is an important dry land annual cereal crop grown in India. In semiarid tropics when other plants fail to survive, sweet Sorghum can grow successfully. Sweet Sorghum is said to be valued for 4-F's. These 4-F's are Food, Feed, Fuel and Fertilizer. It can produce along with grains, a sugary juice that is useful to produce ethanol, jaggery, syrup and flour. As sweet Sorghum produces food as well as fuel so it can help to meet the countries fuel needs without compromising our food supply.

Material and Methods:

The sweet Sorghum variety Madhura is grown in individual pots which were treated with 10 ppm, 50 ppm and 100 ppm boron along with one pot untreated i.e. 0 ppm named as control. These treatments were given at 15 days old seedlings and the treatment was repeated at 40 days and 70 days old plant after sowing. At maturity plants from each treatment and control were harvested and various components namely length of earhead, weight of 100 grains, biological yield, harvest index, total yield were calculated.

The plant height was measured simply by adding root length and shoot length together. Plant height along with root and shoot, length was expressed in cm. Average number of leaves per plant was determined by counting total number of leaves developed on selected plants from the pots. Length of panicle and number of grains were measured from selected earheads.

Result and Discussion:

The effect of soil application of different boron concentrations on yield and different yield parameters is shown in table 1 and 2. The variety studied under this investigation shows remarkable increase in yield and yield parameters. The lower doses of boron like 10 and 50 ppm positively influenced the yield parameters like total height,

diameter of stem, number of nodes per plant, number of leaves per plant, number of grains, weight of 100 seeds, grain yield, biological yield and harvest index with 50 ppm boron treatment. The higher dose of 100 ppm boron reported to decrease in biological yield.

There are various reports of effect of boron on yield and yield components. A study of boron requirement on sugar-beet plant by Hellalet *et al.* (2009) shows increased root and shoot length due to boron at 50 ppm concentration when compared with other non-boron treatments which ultimately increases total height of the plant. Similar results were obtained in the present investigation where total height was increased due to 50 ppm boron treatment. According to Moniruzzaman *et al.* (2007) significant increase in number of leaves per plant, length and width of highest leaf in broccoli plant treated with 1.5 kg boron ha⁻¹. Number of leaves is increased in onion when plant treated with 0.1 % to 0.5 % of boron (Dakeet *et al.*, 2011; Manna, 2013). Our results are showing increased leaf number due to all the boron treatments. Mehdi *et al.* (2006) in an experiment on rice under saline sodic soil found that residual boron increased plant height, straw yield, number of tillers and panicles per plant.

Howard *et al.* (2000) worked on different plant and find combined effect of boron and zinc correlated with increased yield. The highest grain yield was observed due to 50 ppm boron treatment in the present investigation which shows similarity with the reports of Rakshit *et al.* (2002) and Rashid *et al.* (2004) who worked on rice plant and suggested that boron with optimum dose can improve yield. Uddin *et al.* (2002) stated that significantly higher yield was recorded with boron treatment along with Zn and sulphur. The maximum panicle length of rice was recorded by Ahmad *et al.* (2012) under the treatment of boron application finally which increases yield. The increased biological yield and harvest index due to boron application was confirmed by Alam *et al.* (2000), Shah (2008), Tomboet *et al.* (2008). Recently Muthanna *et al.* (2017) reported that application of boron along with sulphur increases yield of potato plant. Our



findings in the present investigation were in correlation with the previous reports of various workers.

Table 1. Effect of boron on yield and yield parameters of sweet Sorghum cultivar Madhura.

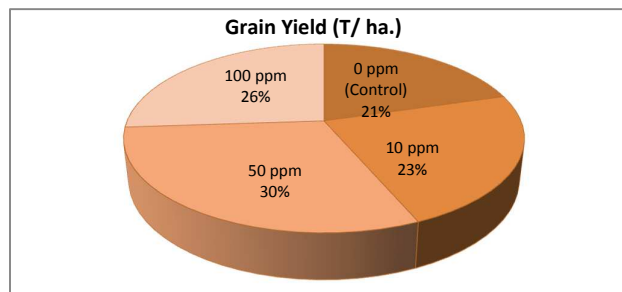
Boron Treatments ↓	Total Height Pl ⁻¹ (cm)	Diameter of the stem(cm)	No. Of Nodes/Plant	No. of Leaves/Plant
0 ppm (Control)	172.3 ± 0.60	1.85 ± 0.028	8 ± 0.57	9 ± 0.57
10 ppm	219 ± 2.54	2.09 ± 0.064	13 ± 1.52	19 ± 1.0
50 ppm	289.4 ± 1.85	2.69 ± 0.092	14 ± 1.52	26 ± 0.57
100 ppm	173.5 ± 0.86	1.47 ± 0.017	10 ± 1.52	12 ± 1.0

± SEM

Table 2. Effect of boron on yield and yield parameters of sweet Sorghum cultivar Madhura.

Boron Treatments ↓	Length of ear head (cm)	No. of grains panicle ⁻¹	Weight of 100 seeds (gms)	Grain Yield (T/ha.)	Biological yield (T/ha.)	Harvest Index (%)
0 ppm (Control)	16.9	240	3.26	1.403	9.283	17.8
10 ppm	21.6	268	3.28	1.576	8.826	21.73
50 ppm	18.6	318	3.64	2.084	10.244	25.53
100 ppm	10.6	298	3.34	1.785	9.045	24.58

Chart 1: Effect of boron on grain yield of sweet Sorghum var. Madhura.



Conclusion:

The enhancement in total height, diameter of stem, number of nodes and leaves per plant and number of grains per plant ultimately increases biological yield and harvest index of the sweet Sorghum var. Madhura showing that boron application is required for improving yield and yield parameters.

References:

Ahmad A, Tahir M, Ullah E, Naeem M, Ayub M, Haseeb– Ur- Rehman and Talha M (2012). Effect of silicon and boron foliar application on yield and quality of rice. *Pak. J. Life Soc. Sci.*, **10**(2): 161-165.

Alam S M, Iqbal Z and Latif A (2000). Effect of boron application with or without zinc on yield of wheat. *Pak. J. Soli. Sci.*, **18**: 95-98.

Ali E A (2012). Effect of iron nutrient care sprayed on foliage at different physiological stages on yield and quality of some durum wheat (*Triticum durum* L.) varieties in sandy soil. *Asian journal of Crop Science*, **4**(4): 139-149.

Dake S D, Hiwale B G, Patil V Kand Naik P G (2011). Effect of micronutrients on growth, yield and quality of onion (*Allium cepa* L.) c.v. Baswant 780. National symposium on Alliums: current Scenario and Emerging Trends, 12-14 March, 2011, Pune. pp. 205.

Hellal F A, Taalab A S and Safaa A M (2009). Influence of nitrogen and boron nutrition on nutrient balance and sugar beet yield grown in calcareous soil. *Ozean Journal of Applied sciences* **2**(1):1-10.

Howard D D, Essington M E, Gwathmey C O and Percell W M (2000). Buffering of foliar potassium and boron solutions for no-tillage cotton production. *J. Cotton Sci.*, **4**: 237-244.

- Manna D. (2013).** Growth, yield and bulb quality of onion (*Allium cepa* L.) in response to foliar application of boron and zinc. *Saarc J. Agri.*, **11**(1): 149-153.
- MasoudBameri, Abdolshahi R, Mohammadi-Nejad G, Yousefi K and Sayed M. Tabatabaie (2012).** Effect of different microelement treatment on wheat (*Triticumaestivum*L.) growth and yield. *Int. Res. J. Appl. Basic. Sci.*, **3** (1): 219-223.
- Mehdi S M, Sarfraz M, Hassan N M and Sadiq M (2006).** Rice and wheat yield improvement by the application of boron in salt affected soils. *Sci. Inter.*, **4**: 112-115.
- Moniruzzaman M, Rahman S M L, Kibria M G, Rahman M A and Hossain M M (2007).** Effect of boron and nitrogen on yield and hollowstem of broccoli. *J. Soil Nature*, **1**(3): 24-29.
- Muthanna M A, Singh A K, Tiwari A, Jain V K and Padhi M (2017).** Effect of boron and sulphur application on plant growth and yield attributes of potato (*Solanum tuberosum* L.) *Int. J. Curr. Microbiol. App. Sci.* **6** (10): 399-404.
- Rakshit A, Bhadoria P B S and Ghosh D (2002).** Influence of boron on NPK uptake of rice (*Oryza sativa* L.) in acid alluvial soils of Coochbehar, West Bengal. *and Ecol.*, **20** (1): 188-190.
- Rashid, A., M. Yaseen, M. Ashraf and R. A. Mann (2004).** Boron deficiency in calcareous soils reduces rice yield and impairs grain quality. *Inter. Rice Res. Notes*, **29**: 58-60.
- Shah T J (2008).** Yield response of wheat (*Triticumaestivum*L.) to boron application at various growth stages. M.Sc. (Hons). Thesis, Dept. Of Agron. Univ. of Agric. Faisalabad, Pakistan.
- Soomro Z H, Baloch P A and Gandhai A W (2011).** Comparative effects of foliar and soil applied boron on growth and fodder yield of maize, *Pak. J. Agri., Engg. Vet. Sci.*, **27**(1): 18-26.
- Tombo Y N, Tombo F C, Erman M and Celen A E (2008).** The effect of boron application on nutrient composition, yield and some yield components of barley (*Hordeum vulgare* L.) *Afric. J. Biotech.*, **7** (18): 3255-3260.
- Uddin M K, Islam M R, Rahman M M and Alam S M K (2002).** Effect of Sulphur, Zinc and Boron supplied from chemical Fertilizer and poultry manure to wetland rice (Cv. BRRI Dhan -30). *J. Biol. Sci.*, **2**: 165-167.
- Wojcik M and Klamkowski K (2008).** Response of apple trees to boron fertilization under conditions of low soil boron availability. *Sci. Hort.*, **116**: 58-64.



Ethnomedicinal and pharmacognostical studies on the leaves of *Casearia championii* thw., enum.

Arun Patil* and ¹Varsha Jadhav(Rathod)

*Department of Botany, Yashawantrao Chavan College, Halkarni, Kolhapur(M.S.), India

¹Department of Botany, Shivaji University, Kolhapur (M.S.), India

KEYWORDS

Casearia championii,
Flacourtiaceae, Leaf,
Pharmacognostical,
Phytochemical.

ABSTRACT

The present paper deals with ethnomedicinal and pharmacognostical studies on leaves of *Casearia championii* Thw.,Enum. It is a known fact that over 80% of the world population depends on herbal medicines and product for healthy living. *Casearia championii* Thw.,Enum. belonging to family Flacourtiaceae and commonly called as modi or Hadmodi or Kirmira. It is a small evergreen tree with yellowish white smooth bark. Leaves of this plant have been employed as herbal medicine in the treatment of bone fracture. The present paper deals with pharmacognostical and phytochemical studies on leaves of *Casearia championii* Thw., Enum. It includes macro and microscopic characters, analysis of ash, dry matter, moisture content, fluorescence analysis and analysis of powdered drug reactions with different chemical reagents. Transverse section of the leaf lamina showed the presence of two layered upper epidermis and single layered lower epidermis with thin cuticle and spongy parenchyma with intercellular spaces. Powder microscopy shows epidermal cells, trichomes, starch grains and fragments of xylem vessels with spiral thickenings. The powdered crude drug was extracted with different solvents and screened for their phytochemical constituents. Qualitative phytochemical analysis of these extracts revealed the presence of phenols, alkaloids, flavones, tannins, coumarins, saponins, reducing sugars, xanthoproteins and glycosides. The morphological, microscopic, physicochemical and chromatographic studies would serve as standard reference for identification, authentication and distinguishing the plants from its adulterants. This is the first such study on standardization of *Casearia championii* leaf.

Corresponding Author
Email
arunpatil545@gmail.com

Introduction

India is considered to be a store house of medicinal plants. It harbors over 2000 medicinal plant species of which 443 have been recorded for the state of Maharashtra (Yadav and Sardesai 2002). Ayurveda is gaining popularity not only in India but also abroad. The ancient knowledge of herbal medicine is a great source of information for scientific community, researchers and medical practitioners. In last couple of decades a new trend in the preparation and marketing of drugs based on medicinal plants has become increasingly apparent (Bisset 1994). The curative properties of medicinal plants are mainly due to presence of various complex chemical substances of different composition which occur as secondary metabolites (Karthikeyan 2013). Pharmacognosy is the study of medicines derived from natural sources. It is the study of physical, chemical, biochemical and biological properties of drug substance. Pharmacognostical study is the preliminary step in the standardization of crude drugs. Standardization of drug means confirmation of its identity and determination of its quality and purity. The standardization of crude drug material includes many steps such as authentication, macro and microscopic examination, removal of foreign organic matter, organoleptic evaluation, analysis of ash values and dry matter, moisture content determination, extractive values, qualitative chemical evaluation and chromatographic examinations.

Kolhapur district has a valuable heritage of herbal remedies. The climate of the district is healthy and favorable for growth and development of plants. So district shows rich biodiversity. Its rural people living in remote forest area are till depending on the local plant resources for medical treatment. *Casearia championii* Thw., Enum. belonging to family Flacourtiaceae and commonly called as modi or Hadmodi or Kirmira. It is a small evergreen tree with yellowish white smooth bark. Leaves of this plant have been employed as herbal medicine in the treatment of bone fracture.

Material and Methods

Ethnomedicinal information was collected through interview with traditional rural practitioners (Vaidus) as suggested by Jain (Jain 1987). Fresh plant material was collected from Kolhapur district of Maharashtra (India). Plant was identified with the help of Flora of Kolhapur District (Yadav and Sardesai 2002). For microscopic studies uniform, thin, free hand sections of stem bark were taken and stained as per the procedure of Johansen (Johansen 1940). Macro and microscopic character were studied as described by Trease and Evans (Trease and Evans 2002). Ash value, dry matter and moisture content of the material were determined by following the method of AOAC 1990. Bark material was dried in shade so as to prevent decomposition of active principles and made into fine powder for the studies of power behavior, fluorescence study and phytochemical tests as per given in Indian Pharmacopeia. Fluorescence analysis of the powdered was examined under U.V light according to the method suggested by Chase and Pratt 1949 and Kokoski et al. 1958.

Results and Discussion

Macroscopic Characters

Casearia championii belonging to family Flacourtiaceae is a small evergreen tree reaching 20 - 30 ft. in height (Fig.1). Young branches slender, pale, and glabrous. Leaves closely arranged, thinly coriaceous, elliptic, ablong to elliptic - lanceolate, subacute, main nerves 6 -10 pairs, stipules minute scale like. Flowers in clusters in the axils of fallen and present leaves. Pedicels longer than the calyx and articulated above the base. Sepals pellucid - punctate and lineolate, hairy both inside and outside. Ovary densely hirsute at apex. Capsule ellipsoid, orange yellow, glabrous, seeds many covered by a large fleshy lacerate scarlet aril.



Microscopic Characters

T. S. of leaf showed upper and lower epidermis formed of barrel shaped elongated cells. Upper epidermis was two layered. Externally epidermis was covered with thin cuticle. Epidermis shows presence of crystal idioblast. Mesophyll differentiated into upper palisade tissue and lower spongy parenchyma. Upper palisade consists of two layers of columnar elongated palisade cells which were compactly arranged with chloroplasts. Spongy parenchyma composed of loosely arranged cells with small intercellular spaces (Fig.2). Mesophyll cells at some places shows presence of secretory cavities. Simple unicellular trichomes appear on both the surfaces. Anomocytic stomata observed only on lower surface (Fig.3). Upper epidermis shows many rosette crystals (Fig.4). The stomatal index was 24.32.

Ash value: 4.3%,

Dry matter: 30.50%,

Moisture content: 69.50%.

Powder study: Leaf powder of *Casearia championii* was olive green in color and coarse in texture. Powder microscopy shows epidermal cells, trichomes, starch grains and fragments of xylem vessels with spiral thickenings.

Behavior of bark powder with different chemical reagents

Leaf powder indicates presence of alkaloids, flavonoids, cystein, steroids, tannins, glycosides, proteins and oils. Powder treated with ferric chloride has produced dark green ppt indicating high concentration of tannins. Tests for starch, xanthoproteins and oils were negative (Table - 1).

Fluorescence character of bark powder under visible and UV light

Leaf powder of *Casearia championii* treated with NaOH in

alcohol produces brown fluorescence under visible light, 254nm and 366nm UV light. Powder treated with conc. HNO₃ produces brown fluorescence under visible and 366nm UV light and green fluorescence under 254nm UV light. Leaf powder treated with iodine produces green fluorescence under visible and 254 nm light while produces black fluorescence under 366nm UV light (Table - 2).

Phytochemical screening

Leaf extract shows high concentration (+++) of phenols, flavones, tannins, xanthoproteins and saponins and moderate concentration (++) of coumarins, alkaloids, glycosides and reducing sugars. Test was negative for anthraquinones (Table - 3).

Studies on morpho-microanatomical evaluation of the leaves of *Tridax procumbence* Linn. have been done by Salahuddin *et al.* (2010). The plant material was collected from Herbal Garden, Noida Institute of Engineering and technology, Greater Noida U.P. India. The leaves were opposite, lanceolate to ovate with acute apex and short petiole. Leaf lamina shows double layered elongated palisade layer and mid rib shows central, concentric, conjoint, collateral vascular bundle surrounded by parenchymatous cells. In present work pharmacognostical studies of leaves of *Caesaria championii* was done. The present pharmacognostical results were compared with the above results. Point of similarities in morphological characters and some differences were noticed. Opposite lanceolate to ovate leaves with short petiole, presence of double layered elongated palisade and concentric conjoint collateral vascular bundle were present in both the plants. However unicellular trichomes occurs in *C. championii* and multicellular trichomes were recorded in *T. procumbence*. Presence of two layered upper epidermis, secretory cavities in the mesophyll, sclerenchymatous layer surrounding the vascular bundle was observed in *C. championii*.

Devi et al. (2003) carried out studies of pharmacognostical profile of *Cleome viscosa* belonging to family Capparidaceae. The plant material was collected from the Jhilimili, Bankura, West Bengal, India. As evident from the result, the methanol leaf extract of above plant contains sterols, saponins, alkaloids, tannins and reducing sugars. In present work preliminary phytochemical analysis of leaf extract of *Caesaria championii* belonging to family Flacourtiaceae was done. The results of present work reveals that methanol leaf extract shows positive tests for phenols, flavones, tannins, saponins, alkaloids and xanthoproteins. Leaf extract of *C. championii* shows high concentration of phenols, flavones, tannins and saponins and moderate concentration of coumarins, alkaloids and reducing sugars.

Conclusion

The present study on pharmacognostical and phytochemical evaluation of stem bark of *Casearia championii* provide useful information for its identification. Macroscopic and microscopic characters, behavior of bark powder analysis, fluorescence characters of bark powder and phytochemical tests can be used as a diagnostic tool in the correct identification of plant. Phytochemical tests revealed the presence of tannins, phenols, flavones, reducing sugars, coumarins, saponins, xanthoproteins, alkaloids and glycosides. These phytochemicals are responsible for various pharmacological actions. The adulterants if any in the plant material can also easily identified by these studies. The study scientifically validates the use of plant in traditional medicine.



Fig. 1: Flowering twig

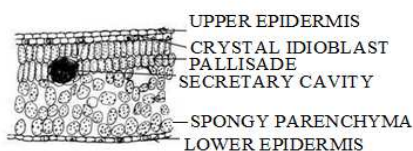


Fig. 2: T. S. of leaf

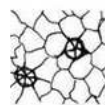


Fig. 4: Rosette crystals



Fig. 3: Anomocytic stomata

Table 1: Behavior of powdered drug with different chemical reagents

SN	Treatment / Reagent	Behaviour	Inference
1	Powder as such	Olive green	--
2	Powder + 1 N NaOH	Brown	Flavonoid
3	Powder + 5% Iodine	Olive green	--
4	Powder + 40% NaOH + Lead acetate	Yellowish green	Cystein
5	Powder + Conc. H ₂ SO ₄	Brown	Steroid
6	Powder + Conc. HNO ₃ + Ammonia	Olive green	--
7	Powder + 5% FeCl ₃	Dark green	Tannin
8	Powder + 5% KOH	Brown	Glycoside
9	Powder + 1% AgNO ₃	Grey	Protein
10	Powder + Sudan III	Brown	Oil
11	Powder + Glacial acetic acid	Dark olive green	--
12	Powder + Picric acid	Yellowish green	Alkaloid



Table 2: Fluorescence characters of powdered drug under Visible and U.V. light

SN	Treatment / Reagent	Visible	254nm	366nm
1	Powder as such	Dark olive green	India green	Brown
2	Powder + NaOH in water	Brown	Reddish brown	Black
3	Powder + NaOH in Alcohol	Seal brown	Dark brown	Dark brown
4	Powder + Conc. HCl	Office green	Pakistan green	Black
5	Powder + Conc. H ₂ SO ₄	Black	Black	Black
6	Powder + Conc. HNO ₃	Yellowish brown	Yellowish green	Dark brown
7	Powder + 10% HCl	Office green	Pthalo green	Black
8	Powder + Acetone	Asparagus green	Green	Black
9	Powder + 5% KOH	Reddish brown	Black brown	Black
10	Powder + Iodine	Dark olive green	Office green	Black
11	Powder + FeCl ₃	Dark olive green	Office green	Black
12	Powder + D.W.	Dark olive green	Hunter green	Brown

Table 3: Phytochemical tests

Chem. constituents	Solvents					
	Methanol	P. ether	Acetone	Chloroform	Ethanol	Aqueous
Phenols	+++	-	+++	-	+++	+++
Antraquinones	-	-	-	-	-	-
Flavones	+++	-	++	-	+++	-
Tannins	+++	-	+	-	+++	++
Coumarins	-	++	++	-	-	-
Saponins	+++	-	-	-	++	+++
Alkaloids	++	+	+	+	-	-
Reducing sugars	-	-	-	-	-	++
Xanthoprotein	+++	-	-	-	++	-
Glycosides	-	-	-	-	-	++

(+ = Low, ++ = Medium, +++ = High, -- = Absent)

References

- AOAC (1990)** Official Methods of Analysis. Association of official Analytical Chemists, Washington. DC.
- B.P.Devi, R.S. Boominathan, C. Mandal, (2003).** Studies of pharmacognostical profile of *Cleome viscosa* L. Ancient sci. of life. XXII (4): 30 - 35
- C.R. Chase, R Pratt, (1949).** Fluorescence of powdered vegetable drugs with particular reference to development of a system of identification. *J. Amer. Pharm. Assoc.* 38 (6): 324 - 331
- D.A.Johansen, (1940).** Plant micro technique. McGraw Hill Publication, New York
- F.S. Salahuddin, S. Pahula, S.Kumari, S.K. Gupta (2010).** Studies on morpho- microanatomical evaluation of leaves of *Tridax procumbens* Linn. *J. Sci. Res.* 2 (3): 613 - 619
- G.E. Trease and W.C. Evans. (2002).** Pharmacognosy. 15th Edition London: Saunders Publishers.
- J.C. Kokoski, R.J. Kokoshi and F.J. Slama, (1958).** Fluorescence of powder vegetable drugs under ultra violet radiations. *J. American Association.* 47: 715

NG Bisset, (1994). Herbal drugs and Pharmaceuticals. CRC Press, Boca Raton.

S. Karthikeyan, A. Sivakumar , M. Anbalagan,E. Nalini, K.M.Gothandam, (2013). Fingerprinting of alkaloids, steroids and flavonoids using HPTLC of *Leuca saspara L.* whole plant methanolic extract. *J. Pharmaceutical Sci. and Res.* 5(3): 67-71.

S.K. Jain, (1987). A manual of Ethnobotany. Scientific Publishers, Jodhapur, India

S.R. Yadav M.M. Sardesai. (2002).Flora of Kolhapur District. Shivaji University, Kolhapur



Effect of different carbon and nitrogen sources on growth of *Fusarium oxysporum f.sp. Chrysanthemi* causing wilt of *Chrysanthemum*

S.S.Patil and M.B.Waghmare

Department of Botany, The New College, Kolhapur.

KEYWORDS

Carbon source, Nitrogen source, *Chrysanthemum*, *Fusarium oxysporum*

Corresponding Author

Email
shitalpatil1405@gmail.com

ABSTRACT

In the present study investigation has made on the effect of different carbon sources (Sucrose, Glucose, Fructose, Dextrose, Maltose and Lactose) and nitrogen sources (Sodium nitrate, Potassium nitrate, Ammonium nitrate, Bismuth nitrate and Barium nitrate) on the mycelial growth of *Fusarium oxysporum f. sp. chrysanthemi* causing wilt of *Chrysanthemum indicum* L. Sucrose was found to be the best source of carbon whereas, Sodium nitrate was the best source of nitrogen.

Introduction

In the present study investigation has made on the effect of different carbon sources (Sucrose, Glucose, Fructose, Dextrose, Maltose and Lactose) and nitrogen sources (Sodium nitrate, Potassium nitrate, Ammonium nitrate, Bismuth nitrate and Barium nitrate) on the mycelial growth of *Fusarium oxysporum f. sp. chrysanthemi* causing wilt of *Chrysanthemum indicum* L. Sucrose was found to be the best source of carbon whereas, Sodium nitrate was the best source of nitrogen.

Chrysanthemum indicum L. is small herbaceous annual plant belongs to family Asteraceae. *Chrysanthemum* is commonly known as "Queen of East." In the International florist trade it is an important commercial flower at 2nd position in the rank after Rose. In India *Chrysanthemum* is traditional and religious flower (Kher, 1990). In India, a flower of *Chrysanthemum* has been constant demand. However, it is very difficult to produce good quality of flowers because it suffered from wilt caused by *Fusarium oxysporum f. sp. chrysanthemi*.

For the proper growth, pathogen requires various nutritional sources. Carbon is one of the most important and essential nutrition required for their proper growth and development while nitrogen is also an important component required for protein synthesis and other vital functions. Therefore in the present study investigation is made on the effect of various carbon and nitrogen sources on the mycelial growth of *Fusarium oxysporum f. sp. chrysanthemi*. This work helps to manage the growth of pathogen.

Material and method

Isolation of fungi

Naturally infected samples of *Chrysanthemum* were collected from different districts of Maharashtra and brought to the laboratory in the sterile polythene bags. Surface sterilization of wilted roots were made with 0.1% mercury chloride, then washed with sterile distilled water and removed the traces of mercury chloride. Sterilized wilted roots were cut longitudinally into small pieces by the sterilized blade and cultured on the Czapek Dox Agar (CDA) medium. After 4-5 days different fungal

colonies observed in the petriplates. Identification of the pathogen was made with the help of available mycological literature (Subramanian 1971) as *Fusarium oxysporum f. sp.chrysanthemi*. Then pathogen was sub-cultured on same media to obtain pure culture and maintained in the BOD incubator.

Effect of carbon sources

Five different carbon sources viz., sucrose, glucose, fructose, dextrose, maltose and lactose were added to 1000 ml of CDA medium at the concentration of 3 % percent prior to autoclaving. After autoclaving, 15ml of medium from source were poured into petriplates. The plates were inoculated with 8mm discs of actively growing eight days old culture of *Fusarium oxysporum f. sp.chrysanthemi* and incubated at 25±5°C. The linear growth of mycelium was measured at 2 days intervals. The medium without any carbon source served as control.

Effect of nitrogen sources

In the studies of the effect of five different nitrogen sources (Sodium nitrate, Potassium nitrate, Ammonium nitrate, Bismuth nitrate and Barium nitrate) on the growth of *Fusarium oxysporum f. sp.chrysanthemi*, the sources were added to 1000 ml of CDA medium at the concentration of 0.2 % prior to autoclaving. After autoclaving, 15 ml of medium from source were poured into petriplates. The plates were inoculated with 8mm discs of actively growing eight days old culture of *Fusarium oxysporum f. sp.chrysanthemi* and incubated at 25±5°C. The linear growth of mycelium was measured at 2 days intervals. The medium without any nitrogen source served as control.

RESULT AND DISCUSSION

Effect of carbon sources

The results are shown in Table no.1 which indicated that all the carbon sources were suitable for the growth of

Table 1: Effect of different carbon sources on the radial growth (mm) of benomyl sensitive and resistant isolates of *Fusarium oxysporum f. sp. chrysanthemi* on Czapek Dox agar medium

Carbon sources (3%)	Sensitive isolate				Resistant isolate			
	Days				Days			
	2	4	6	8	2	4	6	8
Sucrose	19.66	39.00	58.66	82.66	22.66	46.00	67.00	90.00
Glucose	18.33	37.66	53.66	70.33	19.00	38.33	56.66	72.00
Dextrose	17.33	36.33	58.00	72.00	18.00	37.33	56.00	76.66
Fructose	13.00	28.00	42.00	55.66	14.66	30.00	44.66	58.00
Maltose	15.66	33.33	42.33	59.33	17.00	35.33	45.00	61.00
Lactose	11.33	23.66	35.33	39.00	14.66	27.33	37.33	41.00
Control	10.33	17.00	25.33	35.00	12.00	19.33	27.00	37.33



Table 2: Effect of different nitrogen sources on the radial growth (mm) of benomyl sensitive and resistant isolates of *Fusarium oxysporum f. sp. chrysanthemi* on Czapek Dox agar medium

Nitrogen sources (0.2%)	Sensitive isolate				Resistant isolate			
	Days				Days			
	2	4	6	8	2	4	6	8
Sodium nitrate	21.00	39.33	59.66	88.33	22.33	45.00	64.00	90.33
Peptone	19.00	37.33	59.66	82.00	20.00	38.66	61.66	83.00
Potassium nitrate	10.33	21.00	32.33	44.00	11.33	22.00	34.00	46.33
Ammonium nitrate	15.00	33.66	47.00	70.00	17.33	35.00	53.66	73.00
Bismuth nitrate	09.00	12.00	16.00	21.33	11.00	13.66	17.00	23.66
Barium nitrate	00.00	00.00	10.33	13.00	00.00	00.00	11.00	14.33
Control	00.00	00.00	09.00	09.66	00.00	00.00	10.00	11.66

Result and Discussion

Effect of carbon sources

The results are shown in Table no.1 which indicated that all the carbon sources were suitable for the growth of *Fusarium oxysporum f. sp. chrysanthemi* as compared to control. However, sucrose was found to be the best carbon source for the growth of sensitive (82.66 mm) and resistant (90.00 mm) isolates of *Fusarium oxysporum f. sp. chrysanthemi*. It was followed by dextrose, glucose, maltose, fructose and lactose. Similar observations were made by Ramteke and Kamble (2011) among different five carbon sources (sucrose, dextrose, fructose, maltose and lactose), sucrose was found to be the best carbon source for the growth of *Fusarium solani*. It was followed by lactose, maltose, dextrose and fructose. U.N. Bhale (2010) reported that growth rate of sucrose is higher in fungicide resistant and sensitive *Fusarium oxysporum f. sp. spinaciae* which were isolated from the wilt of Spinach. Gangadhara *et.al.* (2010) observed that all the carbon sources were suitable for the growth of isolates of *F. oxysporum f. sp. vanillae*. However, maximum growth of

isolates was best on sucrose followed by fructose and maltose.

Effect of nitrogen sources

The results are shown in Table no.2. The maximum growth of the sensitive (85.33mm) and resistant 88.33mm isolates of *Fusarium oxysporum f. sp. chrysanthemi* was observed in sodium nitrate followed by peptone, ammonium nitrate, potassium nitrate, bismuth nitrate and barium nitrate. U.N. Bhale (2010) have also reported similar findings in case of *Fusarium oxysporum f. sp. spinaciae*. Sodium nitrate supported maximum growth of the pathogen followed by ammonium nitrate and magnesium nitrate.

ACKNOWLEDGEMENT

Authors are very much thankful to Dr. N.V. Nalawade principal, The New College, Kolhapur and T.G. Nagaraja Head of the Department, The New College, Kolhapur for providing the laboratory facilities.

Reference

- Bhale UN (2012)** Physiological studies of fungicide resistant and sensitive *Fusarium oxysporum f. sp. Spinaciae*. International Journal Of Ayurvedic And Herbal Medicine 2:1 171:175.
- Gangadhara NB, Nagaraja R, Basavaraja MK, Krishna NR (2011)** Variability studies of *Fusarium oxysporum f. sp. vanillae* isolates. *International Journal of Science and Nature*. Vol.1(1):12-16.
- Kher MA(1990)** *Chrysanthemum* “Queen of the East’. *Indian Hort.*,35(1): 10-13.
- Ramteke PK, Kamble SS (2011)** Physiological studies in *Fusarium solani* causing rhizome rot of Ginger (*Zingiber officinale* Rosc.) An International Quarterly Journal of Life Science. 6(2):195-197.
- Subramanian C V (1971)** Hyphomycetes. An account of Indian species except *Cercospora*. Indian Council of Agric. Research, New Delhi, pp. 930.



Checklist of the freshwater molluscs from Panchganga River, Kolhapur, (MS) India

¹Sanindhar Shreedhar Gaikwad ²Priyanka Prakash Chavan ³Nitin Anandrao Kamble

¹ Assistant Professor, Department of Zoology, Eknath Sitaram Divekar College, Varvand - 412 215, (MS) India.

² Assistant Professor, Department of Zoology, Yashavantrao Chavan Institute of Science, Satara - 415 001, (MS) India.

³Assistant Professor, Department of Zoology, Shivaji University, Kolhapur- 416 004, (MS) India.

KEYWORDS

Freshwater molluscs, Panchganga river, Gastropods, Bivalves.

Corresponding Author
Email

sanindhargaikwad@rediffmail.com

ABSTRACT

A total of 13 freshwater species belonging to the 10 genera 04 orders and seven families were noticed during the investigation. A new record of the molluscan species *Physa acuta* was also assessed from the study region. Assessed checklist describes the abundance of the freshwater molluscan species at the Panchganga River. However, regional population of malacofauna may be due to the abundance of planktonic mass at the respective sites of the river that reflects the variations of molluscan species. metal.

Introduction

Invertebrates are a ubiquitous and diverse group of long-lived species, which react strongly and often predictable to human influences in natural ecosystem (George et al., 2010). Most of them are sedentary; therefore, their body burden reflects local conditions, allowing for detection of a variety of perturbations in a range of aquatic habitats (Rosenberg and Resh, 1993 and Darwall et al., 2011). Benthic invertebrates are important and integral part of any aquatic ecosystem, as they form the basis of the trophic level (Butchart et al., 2010).

Freshwater molluscs are common, conspicuous and commercially important group of animals. These animals are highly adaptive and found in every possible habitats of the mother earth except aerial one (Wilbur and Yong, 1964 and Jorden and Verma, 2010). Each organism of the phyla has

peculiar body shell which can be useful to differentiate the species from the other genera (Heller, 2011). The world's molluscan fauna comprises 1, 00, 000 valid and well described species that belong to the different taxa, families, orders and genera's (Bouchet et al., 2005). Diversified molluscan species showed varied morphological, physiological and reproductive characters along with high degree of adaptation. Since ancient time lakes and rivers were considered as key hotspots for molluscan diversity (Ponder and Lindberg, 1997). However many small streams, springs and groundwater systems had also significantly contributes in the molluscan population. Molluscs have variety of the economical and biological importance. Molluscs maintain the food chains and acts as members of ecosystems. Since long time they are source of important pearls, tyrian purple dye, sea silk etc (Ruppert, 2004).

Despite of mollusc's ecological importance, their systemic study is less attended and discussed (Strong et al., 2008). Hence, in order to build up the reliable understanding regarding the biodiversity of molluscs from the region, present investigation was carried out.

Material and Methods

Description of the study area:

River Panchganga is considered as one of the important and sacred river from Kolhapur district of eastern Maharashtra. River starts its journey at Prayag-Chikhali and continues its flows up to the Narsobawadi near Sangli. During this prolonged journey it receives the waters from the tributaries that continued it as big rivers from the region. After completing its flow finally river drains down in to the Krishna river at Narsobawadi. During its 81 Km stretch, it provides fruitful basin for the florishment of the aquatic flora and fauna.

From entire flow of the river Panchganga, five monitoring stations viz; Prayag- Chikhali (S₁), Shivaji Bridge (S₂), Rukdi bridge (S₃), Ichalkaranji (S₄) and Narsobawadi (S₅) were selected for regular collection of the malacofauna. Amongst the selected stations S₁ and S₂ were from upstream and S₃, S₄ and S₅ were located to the downstream of the river. Latitude and longitudinal co-ordinates of these monitoring stations were expressed in the Table No. 01.

Method of Collection:

Molluscan species were collected by simple hand picking method by applying Stratified Random Quadrant Sampling Method (Christian and Harris, 2005), from all along the marginal area sandy and muddy substratum of the Panchganga river. Samplings were carried out up to depth of 1 to 2 meters from water level. Identification was done by using standard keys provided by Zoological Survey of India (Ramakrishna and Dey, 2007).

Result and Discussion

Assessed literature listed 13 species of the freshwater molluscs with all forms and varieties belonging to the 10 genera under seven families. Present checklist describes the analysis of shell fishes from the region. There binary orders wise distributions from the different sampling areas were mentioned in the Table No. 02 to 05. The observed values confirmed the rich diversity of the molluscan fauna from the study region.

1. *Bellamyia bengalensis* (Lamarck, 1822)
2. *Melanoides tuberculata* (Mueller, 1774)
3. *Tarebia lineata* (Gray, 1828)
4. *Lymnaea acuminata typica* (Lamarck, 1822)
5. *Lymnaea luteola typica* (Lamarck, 1822)
6. *Physa acuta* (Draparnaud, 1805)
7. *Indoplanorbis exustus* (Deshayes, 1834)
8. *Parreysia favidens* (Benson, 1862)
9. *Parreysia corrugata* (Mueller, 1774)
10. *Pyressia corrugata nagpoorensis* (Lea, 1859)
11. *Lamellidens marginalis* (Lamarck, 1819)
12. *Lamellidens corrianus* (Lea, 1834)
13. *Corbicula striatella* (Deshayes 1854)

Abundance of the species along with level of dominance at respective sampling regions reveals suitability of the habitat along with balanced aquatic ecosystem. Although, at some places the absence of the species denotes the progressive contamination of the study region. However, cumulative analysis of the study region insures the favorability of the sites for molluscan availability Amongst collected molluscan species *B. bengalensis*, *L. marginalis* and *L. corrianus* were considered as good biomonitoring agents (Johnpaul et al., 2010 and Rao and Day, 1986). However, dominance of *M. tuberculata* in the region describes the increasing level of deposition in to the study region as previously mentioned by Gutierrez and Vogler, (2010).



Monitoring sites				
Code	Name	Longitude	Latitude	Elevation from Sea level
S ₁	Prayag-Chikhli	16° 44' N	74 ° 10' E	1780 ft.
S ₂	Shivaji Bridge	16° 42' N	74 ° 13' E	1786 ft.
S ₃	Rukdi	16° 42' N	74 ° 20' E	1770 ft.
S ₄	Narsobawadi	16° 41' N	74 ° 36' E	1754 ft.
S ₅	Ichalkaranji	16° 41' N	74 ° 35' E	1763 ft.

Table No. 01: Geographical distribution of the selected monitoring stations.

Family	Species	Monitoring Stations				
		S ₁	S ₂	S ₃	S ₄	S ₅
Viviparidae	<i>Bellamya bengalensis</i>	+	-	+	-	+
Thiaridae	<i>Melanoides tuberculata</i>	+	+	+	+	+
	<i>Tarebia lineata</i>	+	-	+	+	+

Table No. 02 - Binary (presence or absence) data of the order- Mesogastropoda.

Family	Species	Monitoring Stations				
		S ₁	S ₂	S ₃	S ₄	S ₅
Lymnaeidae	<i>Lymnaea acuminata typica</i>	+	-	+	-	+
	<i>Lymnaea luteola typica</i>	+	+	+	+	+
Physidae	<i>Physa acuta</i>	+	-	+	-	-
Bullinidae	<i>Planorbella scalaris</i>	+	-	-	-	-
	<i>Indoplanorbis exustus</i>	+	+	+	+	+

Table No. 03 - Binary (presence or absence) data of the order- Basommatophora

Family	Species	Monitoring Stations				
		S ₁	S ₂	S ₃	S ₄	S ₅
Unionidae	<i>Parreysia favidens</i>	+	-	+	-	+
	<i>Parreysia corrugata</i>	+	-	+	-	+
	<i>Pyressia corrugata nagpoorensis</i>	+	-	+	-	+
	<i>Lamellidens marginalis</i>	+	-	+	-	+
	<i>Lamellidens corrianus</i>	+	-	+	-	+

Table. No. 04 - Binary (presence or absence) data of the order- Unionoida

Family	Species	Monitoring Stations				
		S ₁	S ₂	S ₃	S ₄	S ₅
Corbiculidae	<i>Corbicula striatella</i>	+	-	+	-	+

Table. No. 05- Binary (presence or absence) data of the order- Veneroida.

Sr. No.	Scientific Name	Status
1	<i>Bellamya bengalensis</i> (Lamarck, 1822)	**
2	<i>Melanoides tuberculata</i> (Mueller, 1774)	***
3	<i>Tarebia lineata</i> (Gray, 1828)	**
4	<i>Lymnaea acuminata typica</i> (Lamarck, 1822)	***
5	<i>Lymnaea luteola typica</i> (Lamarck, 1822)	***
6	<i>Physa acuta</i> (Draparnaud, 1805)	**
7	<i>Indoplanorbis exustus</i> (Deshayes, 1834)	**
8	<i>Parreysia favidens</i> (Benson, 1862)	**
9	<i>Parreysia corrugata</i> (Mueller, 1774)	***
10	<i>Pyressia corrugata nagpoorensis</i> (Lea, 1859)	**
11	<i>Lamellidens marginalis</i> (Lamarck, 1819)	*
12	<i>Lamellidens corrianus</i> (Lea 1834)	**
13	<i>Corbicula striatella</i> (Deshayes 1854)	*

Table No. 06- Checklist of the freshwater molluscs from Panchganga river.

***- Most Abundant, **- Abundant, *- Less abundant



Similar lines of results were also mentioned by the Dhanalakshmi et al., (2013) for Anicut reservoir of Tamilnadu. Subba, (2003) also mentioned the resembling regional population of molluscs in Ghodaghodi Taluka of Kailali district. Species distribution in accordance of the abundance was mentioned in to the Table No. 06.

Assessed molluscan population also noticed exotic species recorded firstly from the study region i.e. *P. acuta* which should be the cause of accidental release from aquarium or unsafe culture practices as mentioned by Matwal and Joshi, (2011); Bhave and Apte, (2012); Kumar et al., (2013) and Apte and Bhave, (2014) for some other molluscan species . Molluscan species *L. acuminata*, *L. luteola* and *I. exustus* also provides the valuable remarks on the water contamination and so can be effectively used for the biomonitoring. However, there is still need of the periodical and detailed biodiversity assessment from the study region that helps us to understand the biogeography of the region along with indication of the aquatic contaminants.

Acknowledgement

The Authors are thankful to the Head Department of Zoology, Shivaji University, Kolhapur for providing infrastructural facilities during the completion of work and Principal, Eknath Sitaram Divekar College, Varvand for their support and motivation. Authors are also thankful to the SERB, New Delhi, for providing the financial assistance for the implementation of the research work.

References

- Apte D. and Bhave V., (2014):** New records of opisthobranchs from Lakshadweep, India (Mollusca: Heterobranchia), *J. Threat. Tax.*, **6**(3): 5562–5568. Bakir and Katagan, (2013).
- Bhave V. and Apte D., (2012):** First record of *Okenia pellucida* Burn, 1967 (Mollusca: Nudibranchia) from India, *J. Threat. Tax.*, **4**(14): 3362–3365.
- Bouchet P., Rocroi J. P., Fryda J., Hausdorf B., Ponder W., Valdés A. and Waren A. (2005):** Classification and Nomenclature of gastropod families. *Malacologia: International Journal of Malacology*. Hackenheim, Germany: ConchBooks. **47** (1-2):1–397.
- Butchart S. H. M., Walpole M., Collen B., van Strien A., Scharlemann J. P. W., Almond R. A. E., Baillie J. E. M., Bomhard B., Brown B. and Bruno J., (2010):** Global biodiversity: indicators of recent declines, *Sci.*, **328**: 1164–1168.
- Christian A. D. and Harris J. L., (2005):** Development and assessment of a sampling design for mussel assemblages in large streams, *Amer. Mid. Natur.*, **153**: 284-92.
- Darwall W. R. T., Smith K. G., Allen D. J., Holland R. A., Harrison I. J., and Brooks E. G. E., (2011):** The Diversity of Life in African Freshwaters: Under Water, Under Threat. An analysis of the status and distribution of freshwater species throughout mainland Africa, Cambridge, United Kingdom and Gland, Switzerland: IUCN, pp: 347.
- Dhanalakshmi M., Sanjeevi S. B., Gayathri M. and Santhiya N., (2013):** A checklist of molluscs in lower Anicut reservoir in Tamil Nadu, *Res. Environ. Life Sci.*, **6**(4): 133-136.
- George A. D. I., Abowei J. F. N. and Alfred-Ockiya J. F. (2010):** “The distribution, abundance and seasonality of benthic macro invertebrate in Okpoka creek sediments, Niger Delta, Nigeria,” *Research Journal of Applied Sciences, Engineering and Technology*, **2**(1): 11–18.

- Gutierrez-Gregoric D. E. and Vogler R. E., (2010):** Riesgo de establecimiento del gasteropodo dulceacuicola invasor *Melanoides tuberculatus* (Thiaridae) en el Rio de la Plata (Argentina-Uruguay): Revi. Mexi. Biodiv., **81**:573–577.
- Heller J., (2011):** Marine Molluscs of the Land of Israel. Israel Heb.: Alon Sefer, pp: 323. ISBN 978-965-90976-9-2.
- Johnpaul A., Ragnathan M. B. and Selvanayagam M., (2010):** Population dynamics of freshwater molluscs in lentic ecosystems in and around Chennai., Rec. Res. Sci. Tech. **2**: 80-86.
- Jordan E. L. and Verma P. S., (2010):** Reprint, Invertebrate Zoology, S. Chand and Co Ltd., Ram Nagar, New Delhi.
- Kumar D. S. V., Anbalagan T., Nithyanandan M. and Namboothri N., (2013):** Watering Pot Shell, *Brechites penis* (Linnaeus, 1758), a new record to India (Mollusca: Bivalvia: Anomalodesmata): J. Threat. Tax., **5**(12): 4679–4681.
- Matwal M. and Joshi D., (2011):** Record of *Phyllidiella zeylanica* (Mollusca: Gastropoda: Opisthobranchia) after 42 years from Gujarat, India, J. Threate. Tax.,**3**(7): 1951–1954.
- Ponder W. F. and Lindberg D. R., (1997):** Towards a phylogeny of gastropod molluscs: an analysis using morphological characters, Zool. Jol. Linn. Soci., **119**: 83– 265. doi: 10.1111/j.1096-3642.1997.tb00137.x .
- Rao S. and Dey A., (1986):** Freshwater molluscs of Misoram, J. Hydrobiol. **2**: 25-32.
- Rosenberg D. and Resh V., (1993):** Freshwater Biomonitoring and Benthic macro invertebrates, Chapman hall publication.
- Ruppert E. E., Fox R. S., and Barnes R. D., (2004a):** Invertebrate Zoology (7 ed.): Brooks / Cole. pp. Front endpaper.
- Strong E. E., Gargominy O., Ponder W. F. and Bouchet P., (2008):** Global diversity of gastropods (Gastropoda; Mollusca) in freshwater, Hydrobiol., 595:149- 166.
- Subba B. R., (2003):** Molluscan checklist of Ghodaghodi Tal Area, Kailali District., Our Nat. 1: 1-2.
- Wilbur K. M. and Yonge C. M., (1964):** Physiology of Mollusca, Academic Press, New York, pp: 473.
- Ramakrishna and Dey A., (2007):** Handbook on Indian freshwater molluscs, Published by the Director of Zool. Surv. India., pp: 1-399.



Haematological alterations against chronic exposure of Monosodium glutamate (MSG) on male mice *Mus musculus*.

¹ Sunny Bhivate and ²Nitin Kamble

¹Assistant Professor, Department of Zoology, Mahaveer College, Kolhapur.

²Associate Professor, Department of Zoology, Shivaji University, Kolhapur

KEYWORDS

Monosodium glutamate, haematological parameters, serum triglyceride, PCV, MCV, MCH, MCHC.

Corresponding Author
Email

bhivatesunny@gmail.com
drknitinkumar@yahoo.in

ABSTRACT

Monosodium glutamate (MSG) is known to be flavour enhancer in fast food especially in Chinese meals. Investigation aimed to detect haematological changes in experimental animal. For present investigation animals were divided into 3 groups, each group contains 4 male mice. Control group were feed with normal diet and water, while remaining two groups were feed with diet including predetermined dose of MSG which were orally provided up to 3 weeks and 6 weeks respectively. Treated groups showed significant alterations in blood parameters in which RBC and haemoglobin content found altered. It was found that, WBCs count was elevated, while level of serum triglycerides and cholesterols were also found significantly increased. Packed cell volume (PCV), mean cell volume (MCV), mean corpuscular haemoglobin (MCH) and mean corpuscular haemoglobin concentration (MCHC) were markedly changed. The alterations in the corpuscular content and physiology of circulation were interpreted with metabolic changes and animal behaviour.

Introduction

Now a day's Monosodium glutamate (MSG) is familiar as Ajjinomoto which used as flavour enhancer. It is sodium salt of non essential amino acid- glutamic acid. Chemically MSG contains 78 % of glutamic acid, 22% of sodium and water (Samuels, 1999). MSG acts as taste stimulator and improves appetite; reports indicated that it has toxic impact on animal metabolism and behaviour also (Andrew, 2007). MSG content diet can cause histological changes in both hepatic and adipose tissues in both male and female mice (Ramos et al; 2011). Bhivate et. al., (2018) documented histopathology in cellular architecture of liver tissues leading to specific hypertopic and necrotic symptoms in liver cells. MSG disturbs the cyto-architecture of renal cortical structure and also causes cellular degeneration in neprotic cells of kidney (Eweka, 2007).

Literature has shown that ingestion of drugs can alter normal range of haematological parameters (Ajagbonna et. al., 1999). Taking account of increased used of MSG as flavour enhancer in the food which became one of the contaminant of diet has direct or indirect impact on the metabolism and system disfunctioning. So we have decided to carry out the work by chronic exposure of MSG against haematological parameters in male mice *Mus musculus*.

Material and Methods

For the chronic toxicity assessment of Monosodium glutamate (MSG), experimental animal *Mus musculus* was used as model. As per the standard protocol animals were reared and breed in animal house of Department of Zoology, Shivaji University, Kolhapur. The investigation was carried out with permission of authorized CPCSEA approval for animal experiment.

During the experimental procedure mice were kept in the departmental animal house for a week in maintained environmental conditions (24-28°C) provided normal diet and water. Healthy animals were selected for chronic exposure of MSG toxicity study. Dose dependent exposure period carried out is as follows-

Groups	A	B	C
Animals	4	4	4
Days	-	3 weeks	6 weeks
Dose	Control	80mg/100gm/day	80mg/100gm/day

After the completion of exposure period with respective dose, animals were sacrificed by cervical dislocation; thoracic cage was cut open to access heart. Blood samples were collected through cardiac puncture and the content of blood samples were subjected for assessment of qualitative and quantitative haematological parameters.

Result and Discussion

Blood as a fluid connective tissue plays vital role in physiology, metabolism and immunological functions also. From last decade the use of MSG, as flavour enhancer is highly increased. For present investigation when animals were exposed to doses of MSG we found some major alterations in quantities of blood related parameters. The data showed alterations in corpuscular content especially in RBC, WBC and haematocrite value which are significantly altered. Results showed that serum triglycerides and cholesterol level was also elevated. Similar results were recorded by Ashaolu et. al., (2011). So MSG found detrimental to chronic exposure as it showed alterations in various blood parameters in *Mus musculus*.

Statistical analysis- The results were expressed as the mean \pm SD of each group. The differences between different groups were analysed with respect to different haematological parameters.

Parameters	Control	3 weeks	6 weeks
RBCs $10^6/\text{mm}^3$	5.2 \pm 0.4	5.0 \pm 0.3	4.2 \pm 0.6
Hb gm/dl	15.2 \pm 0.3	13.2 \pm 1.0	11.6 \pm 0.6
WBCs	5500 \pm 100	6250 \pm 250	6600 \pm 400

Table No. 1- Showed effect of MSG on RBC, WBCs and Hb count with comparison with control group.

In comparison with controlled animals we found that the treated animals were showed depleted erythrocytic content were as leucocytes are qualitatively increased. This may be because of some toxic impact of induced MSG as per the exposure period (Table No. 1).

The haematocrit value including haemoglobin (Hb) was found depleted in direct correlation with erythrocytes. Our findings were coincides with the results documented by Hall, 2011, where they mentioned aplasia of progenitor cells in the mechanism of haemopoiesis.

Parameters	control	3 weeks	6 weeks
PCV (%)	40.5 \pm 4.5	40.4 \pm 1.2	27.3 \pm 1.3
MCV	51.12 \pm 1.2	52.5 \pm 1.5	52.5 \pm 1.3
MCH (pg)	16.2 \pm 0.24	16.6 \pm 0.8	19.4 \pm 0.24
MCHC (gm/dl)	33.6 \pm 1.04	32.7 \pm 1.20	31.07 \pm 1.6

Table No. 2 – Showed effect of MSG on different haematological parameters with respect to control mice group.

After laboratorial investigation we found that relative parameters of haematological content such as PCV, MCV, MCH and MCHC were showed alterations as per table No.2 in respect to dose and exposure period. These alterations may be because of MSG interference haemopoetic mechanism. Similar kind of results were documented by Meraiyebu . et. al., (2012), where they observed drastic effect of MSG against thrombocytes and coagulatory corpuscular cells of blood. Above table no- 2 described in graphically bellowed-

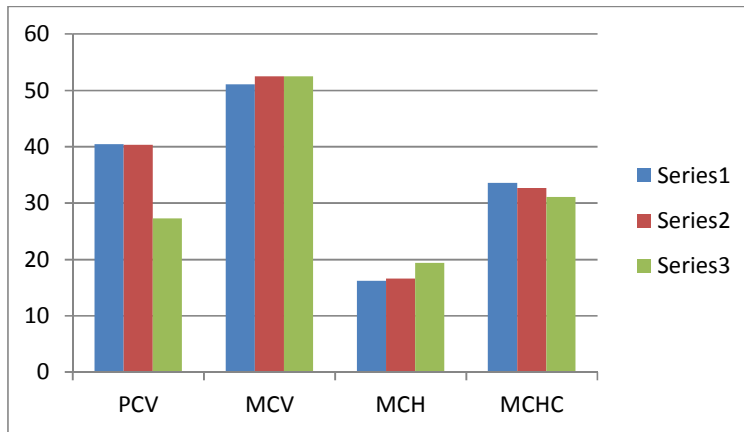


Fig-1 Showed effect of MSG on different haematological parameters with respect to control mice group.

Metabolic content	Control	3 Weeks	6 Weeks
Total cholesterol (mg/dL)	93	103	116
Serum triglycerides (mg/dL)	88.1	97.7	180.8

Table No. 3 – Showed effect of MSG Total Cholesterols and Serum triglycerides with respect to control mice group.

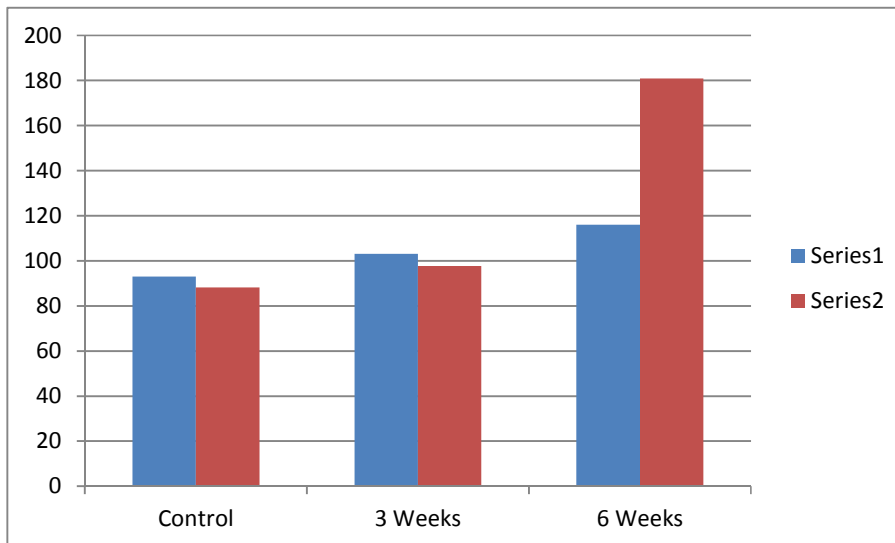


Fig-2 Showed effect of MSG Total Cholesterols and Serum triglycerides with respect to control mice group.

In addition we were interested in finding out the metabolic content against MSG doses where biochemical content such as cholesterol and serum triglycerides found highly elevated (Table No. 3). As a result externally we found bulginess in experimental animal with proportional weight gain. Similar kinds of obesity were observed against MSG content diet in the rat as documented by Dolnikoff et. al. (2001). Bopama et al. (1997) showed similar kinds of results were they mentioned breakdown of metabolism of triglycerides and mobilization of free fatty acids from peripheral fat depots..

Conclusion

MSG induction leads cause the abnormal haematological and biochemical activities. Depleted values of RBCs and Hb, increased values of WBCs and significantly altered values of cholesterol and serum triglycerides indicates that MSG has caused deleterious effect of physiology and metabolism of experimental animals. Excess consumption of MSG can cause behaviour changes in animals and also lethal if get bio accumulated at higher level.

Acknowledgements

The authors thankful to the Head of department of Zoology, Shivaji University, Kolhapur and The Principal of Mahaveer collage, Kolhapur for providing facilities to carry out work.

References

- Ajagbonna OP, Onifade KI, Suleiman U. (1999).** Haematological and biochemical changes in rats given extract of *Calotropis procera*. Sokoto J Vet Sciences. 1:36-42.
- Andrew O. E. Abieyuwa E, and Ferdinard A.E. Om'Iniabohs. (2010).** Histological studies of the effects of monosodium glutamate of the fallopian tubes of adult female Wistar rats. [N Am J Med Sci](#). Mar; 2(3): 146-149.
- Ashaolu J. O., Ukwenya V. O., Okonoboh A. B., Ghazal O. K., Jimoh A. A. G. (2011).** Effect of monosodium glutamate on hematological parameters in rats.
- Bhivate S. B. and Kamble N. A. (2018).** Cytotoxic effect of monosodium glutamate (MSG) on hepatocytes of *Mus musculus*. Int. J life sci.
- Bopama KN, Kanna J, Sushma G, Balaraman R, Rathod SP. (1997).** Ind J Pharmacol; 29: 162-167.
- Dolnikoff, M., Martin-Hidalgo, A., Machado, U. F., Lima, F. B. & Herrera, E. (2001).** "Decreased Lipolysis and Enhanced Glycerol and Glucose Utilization by Adipose Tissue Prior to Development of Obesity in Monosodium Glutamate (MSG) Treated Rats," International Journal of Obesity, 25(3), 426-33.
- Eweka, A. O., Ighighi, P. S. & Ucheya, R. E. (2011).** "Histochemical Studies of the Effects of Monosodium Glutamate on the Liver of Adult Wistar Rats," Annal of Medical & Health Sciences Research, 1(1), 21-9.
- Hall J. E. (2011).** Guyton and Hall textbook of Medical Physiology. 12th edition, Philadelphia, pp. 423-431.
- Meraiyebu, A., Akintayo, C.O., Uzoechi, A.C. and Okere, S. (2012).** The effects of orally administered monosodium glutamate MSG on blood thrombocyte, blood coagulation and bleeding in rats. IOSR Journal of Pharmacy and Biological Sciences, 4 1 : 4-8.
- Roman-Ramos, R., Almanza-Perez, J. C., Garcia-Macedo, R., Blancas-Flores, G., FortisBarrera, A., Jasso, E. I., Garcia-Lorenzana, M., Campos-Sepulveda, A. E., Cruz, M. & AlarconAguilar, F. J. (2011).** "Monosodium Glutamate Neonatal Intoxication Associated with Obesity in Adult Stage is Characterized by Chronic Inflammation and Increased mRNA Expression of Peroxisome ProliferatorActivated Receptors in Mice," Basic & Clinical Pharmacology & Toxicology, 108(6), 406-13.
- Samuels A. (1999).** The Toxicity/Safety of Processed Free Glutamic Acid (MSG): A Study in Suppression of Information. Accountability in Research, Vol. 6, pp. 259-310 ©, OPA (Overseas Publishers Association).



Effect of heavy metal on the behavior of some selected aquatic Molluscan species: a comparative study

¹Sunil Londhe and ²Nitin Kamble

¹Assistant Professor, Department of Zoology, M. H. Shinde Mahavidyalya, Tisangi.

²Assistant Professor, Department of Zoology, Shivaji University, Kolhapur

KEYWORDS

Molluscan Species,
Behavior,
Heavy metal

Corresponding Author
Email
drsunillondhe@gmail.com

ABSTRACT

Behavior of animal is quite disciplinary in normal mode of life but has quick responses to environmental disturbances in the form of pollution by contamination of toxic chemicals, pesticides, etc. In the study present study, control group of molluscan snail and bivalve were moving normally in the bioassay trough. Animals were showing quick response to any external stimuli. Bivalve *L. corrianus* showed normal behavior including opening and closing of shell valves with protruded foot, after immersion in water, animals showed rhythmic and controlled movement. Siphon was protruded outside of shell. In the present investigation, behavior of all experimental animals was altered behavior against lethal concentration of Hg and Zn. In conclusion, the behavior of animal was altered after toxicities of the heavy metal.

Introduction

Now a day, pollution problem is attracting the attention of people throughout world. Increase in agricultural development, urbanization with industrial development, has intensified the environmental pollution. Disposal of industrial effluents and municipal waste become major problem in developing cities. The major sources of terrestrial and aquatic contamination are due to industrial discharges, domestic waste disposal of the agrochemicals in the farmland. Thus at the end of 19th century and in the beginning of 20th century pollution has remarkably increased which has challenged new demands before society. Ghosh and Singh (2005), reported uncontrolled disposal of agricultural waste, drainage, spillage, mining and smelting of metalliferous contaminants into non-contaminated sites to disturb the ecosystem. Many of small scale, backyard industries have developed in the last ten years.

Agricultural activities, aquaculture, orchards, oil palm and rubber exacts, poultry, cattle and pig farm has increased problems of transportation, medication and housing. Deterioration of environment has contributed the accumulation of hazardous chemical including heavy metals, organotin compounds and organochlorine compound in environment especially in the aquatic ecosystem (Ahmed Ismail, 2006). Wills (2000), reported advancement in technology with increase in population resulting to dumping of refused industrial effluents, petroleum waste and crude oil spills with most commonly heavy metals in the environment.

In the last few decades, much attention has been paid to study the relationship between the contamination of heavy metals and their impact on environment. It is world widely accepted that, anthropogenic activity has made

significant contribution to the aquatic burden by inducing contaminant as source of aquatic contamination. Non point source contamination usually arises from agricultural, industrial and urban effluents, which reach by way of surface water runoffs and precipitations (Gupta and Singh, 2011).

Walker et al. (2003) reported behavioral changes representing organizational level of biomarker and documented behavioral differentiation related to biochemical and physiological processes. Thus, alteration in behavioral pattern found more comprehensive than physiological or biochemical alteration in body. According to Deshai et al. (2012), behavior can be defined as sum responses of an animal to internal and external stimuli. Qunfang et al. (2008), reported morphological and behavioral changes, which can provide direct effects of toxicant on the organism. Shaikh (2012) concluded, behavior changes, which affected on survivability of aquatic invertebrate and can provide reflection of integrated biochemical and physiological processes. Biomonitoring of environmental program related to metal pollution in terrestrial and aquatic media are based on the natural behavioral aspects. Therefore in the present study, behavior of organism considered for examination by intoxication to heavy metals.

Material and Methods

Animals for investigation

In the present investigation, two Freshwater gastropods were selected snail *Bellamyia bengalensis* and *Lamellidens corrianus*. Animals were collected from two different sites of Rajaram tank, near Shivaji University, District Kolhapur, Maharashtra.

Heavy metals under investigation

Two heavy metals viz; Mercury chloride ($HgCl_2$) and Zinc chloride ($ZnCl_2$) were selected for toxicological study against selected experimental animals.

b) Freshwater snail, *B. bengalensis* and bivalve *L. corrianus*

Laboratory acclimatized snails and bivalves were used for behavioral study. 50 animals were divided in to five sets (10 animals per set) as control, set-I (intoxicated up to 24 hr), set-II (intoxicated up to 48 hr), set-III (intoxicated up to 72 hr) and set-IV (intoxicated up to 96 hr). The experiments were carried out in 4 and 10 lit capacity plastic trough respectively. Mean LC_{50} concentration of $HgCl_2$, $ZnCl_2$ and $Co(NO_3)_2$ was intoxicated to each experimental set. Behavior of control and experimental animal was observed at each exposure period (24 hr, 48hr, 72 hr and 96 hr).

After completion of each exposure period following type of behavior of control and intoxicated animals were recorded.

For snail *B. bengalensis*:

1) Protective behavior, 2) Response to external stimuli, 3) Tentacular movement, 4) Foot movement, 5) Mucus secretion, 6) Courtship behavior.

For bivalve *L. corrianus*:

1) Protective behavior, 2) Response to external stimuli, 3) Opening and closing of shell valves, 4) Foot movement, 5) Siphonal activity, 6) Mucus secretion.

Result and Discussion

Experimental animal were intoxicated by Hg, Zn and Co. The detailed observations regarding behavioural changes in terrestrial slug *S. maculata*, freshwater snail *B. bengalensis* and bivalve *L. corrianus* from control and experimental group are as follows-

Freshwater Snail *B. bengalensis*

a. Control group

Control, snails were exhibited well courtship behaviour attached to the group with each other (Fig-1 A). Snail *B. bengalensis* creeping movement at bottom to surface with the help of foot. Snails were found tightly attached to the wall of trough and remain as it is (Fig-1 B).



The forward and backward movement of radula was observed for rasped food material. Tentacular movement was like whip, side to side (Fig-1 C). Foot movement was active. Protective responses were quick to external stimuli or to any disturbances so as to drag body inside shell. Mucus secretion by gills was not observed in control animal.

b. Behaviour of *B. bengalensis* against $HgCl_2$, and $ZnCl_2$ after 24, 48, 72 and 96 hrs exposures

Freshwater snail *B. bengalensis* were exposed the mean LC_{50} concentration of $HgCl_2$, and $ZnCl_2$ behavioural responses of *B. bengalensis* found altered. The detailed behaviour changes in experimental snail *B. bengalensis* after exposure to Hg and Zn at different exposure period were as follows-

After 24 hr, snails were tried to avoid the stress and dragged their body inside shell. Creeping movement was slowed down. Movement of foot and tentacles were slow as compared with control. Protective behaviour was strong when exposed to Hg and Zn. Slightly increased mucus secretion was found in foot region. After 48 hr of intoxication, snails were found reduced creeping and tentacular movement. Mucus secretion of foot was more as compared with 24 hr. Responses of snail to external stimuli was poor. Discharges of undeveloped and underdeveloped snails were found in trough.

Maximum excreta were seen in trough. Developing embryo was released in to trough against Hg, Zn and Co toxicity. Snails were less responsive to the mechanical stimuli. Mucus secretion was more by body and foot. Snails were detached in trough and not showing courtship behaviour. After 96 hr, snails were found totally disturbed and lost contact among themselves (Fig-1 D). Underdeveloped embryos were more in trough (Fig-1 E). Snails showed very poor responses to external stimuli, some were not responding to external stimuli (Fig-1 F). Foot movement was lost with increased mucus secretion (Fig-1 G). Operculum has lost its grip to the shell.

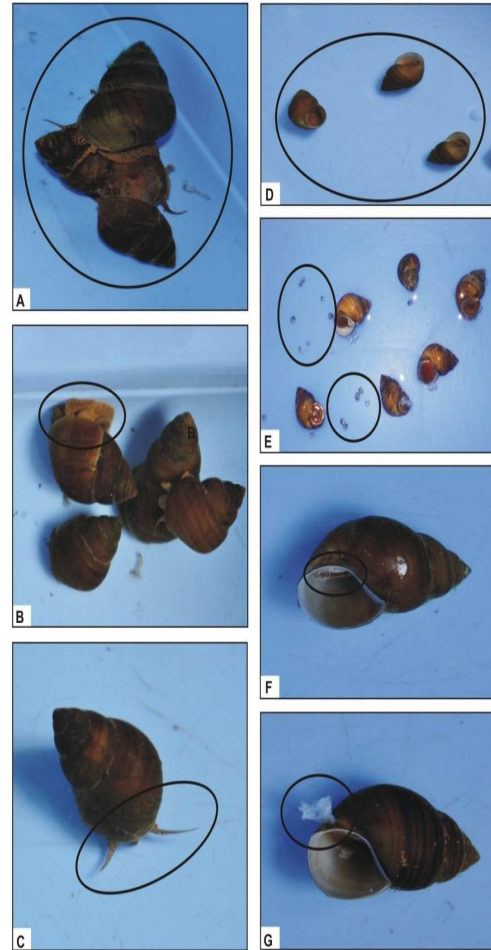


Fig-1. Behaviors of control and metal exposed freshwater snail *B. bengalensis*

A – Normal courtship behavior of snail *B. bengalensis*, B - Normal foot attachment with group, C – Normal tentacular movement, D – Scattered snail indicate disturbed courtship behavior, E- Discharge of undeveloped and underdeveloped embryos. F- Abnormal foot and tentacular movement, G – Increased mucus secretion.

Freshwater bivalve *L. corrianus*

a. Control group

In freshwater bivalve *L. corrianus*, shell valves were highly responding to stimuli, it was tightly closed shell valves (Fig-2 A). Siphons found outside the shell valves with normal activity (Fig-2 A). Valves were well extended foot movement in control group of animal (Fig-2 A). Normally mucus secretion of bivalve was not observed.

b. Behaviour of *L. corrianus* against HgCl₂ and ZnCl₂ after 24, 48, 72 and 96 hr exposure

Behavioural changes in freshwater bivalve *L. corrianus* were recorded after exposure to mean LC₅₀ concentration of HgCl₂, ZnCl₂ and Co (NO₃)₂. After 24 hr, shell valves of bivalve found closed. Protective responses to external mechanical stimuli were found strong. Slight mucus secretions was observed after intoxication by metals. Moderately altered protective behaviour was observed after 48 hr to the external stimuli. Foot movement was slowed down. Mucus secretion was increased in foot region. Responses to external stimuli were moderate. Siphonal activity was changed. Opening and closing of valves were changed. After 72 and 96 hr, foot muscles were dragged inside the shell valves. Whereas animals were responded to mechanical stimuli. Increased mucus secretion was observed over shell and foot region (Fig-2 D, E, G).

Comparative account of behavioural changes in *B. bengalensis* after Hg and Zn intoxication

Snail *B. bengalensis* recorded quick response to exposure of HgCl₂ than that of ZnCl₂ and Co (NO₃)₂ toxicity. Protective behaviour was fast to intoxication of Hg, Zn and Co at 24 and 48 hr. It was poor at 72 and 96 hr of exposure.

The movement of foot and tentacles were almost changed to exposure of Hg, Zn and Co. Mucus secretion of foot and body was increased to exposure of Hg and Zn as compared to Co. The behavioural alterations were directly proportional to the time of exposure. Comparative Hg toxicity found more affecting than Zn and Co. The increasing order for toxicity found as Hg > Zn. Comparative behaviour of *B. bengalensis* were recorded in the form of score in Table – 1.

Comparative account of behavioural changes in *L. corrianus* after Hg, Zn and Co induction

In freshwater bivalve *L. corrianus* after intoxication of Hg and Zn there protective behaviour was changed after 24, 48, 72 and 96 hr of exposure. Protective behaviour was more

responsive to intoxication of Hg at 24 and 48 hr, after which it was lost. The behavioural alteration was found directly proportional to the time of exposure. The increasing rank of metals intoxication to *L. corrianus* in relation with behaviour was, Hg > Zn . Behavioural changes in *L. corrianus* were recorded in the form of score in Table –2.

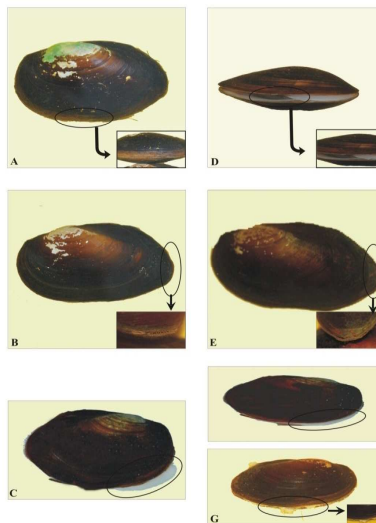


Fig- 2. Behaviors of control and metal exposed freshwater bivalve *L. corrianus*

A – Normal protective behavior of *L. corrianus*, B – Siphon outside the shell valves with normal activity, C – Normal foot movement, D – Weak protective behavior of shell, E- Siphon inside the shell valve with weak activity, F – Abnormal foot movement, G – Increased mucus secretion.

Discussion

In the study control molluscan animals as, slug, snail and bivalve were moving normally in the bioassay trough. Animals were showing quick response. Similarly, in 2004 Awati and Nanaware reported normal creeping movement of snail *Viviparous bengalensis* at bottom of trough with well protective behaviour from control group. Bivalve *L. corrianus* showed normal behaviour including opening and closing of shell valves with protruded foot, after immersion in water. Animals showed rhythmic and controlled movement. Siphon was protruded outside of shell.



Type of responses	Behavioral responses of <i>S. maculata</i> against intoxication of HgCl ₂ , ZnCl ₂ and Co (NO ₃) ₂ at different exposure period									
	HgCl ₂					ZnCl ₂				
	Control	24 hr	48 hr	72 hr	96 hr	Control	24 hr	48 hr	72 hr	96 hr
Protective behavior	+++	++	++	+	+	+++	+++	++	+	+
Response to external stimuli	+++	++	++	+	-	+++	+++	++	+	-
Tentacular movement	+++	++	+	+	+	+++	++	+	+	+
Foot movement	+++	++	+	+	+	+++	++	+	+	+
Mucus secretion	+	++	+++	+++	+++	+	++	+++	+++	+++
Courtship behavior	+++	++	++	+	-	+++	++	++	+	-

Table – 1 Comparative quantitative behavioral responses of control and experimental slug *S. maculata* against intoxication of HgCl₂ and ZnCl₂ at different exposure period. +++ - Strong response, ++ - Moderate response, + - Weak response, - - Not responding.

Type of responses	Behavioral responses of <i>B. bengalensis</i> against intoxication of HgCl ₂ , ZnCl ₂ and Co (NO ₃) ₂ at different exposure period									
	HgCl ₂					ZnCl ₂				
	Control	24 hr	48 hr	72 hr	96 hr	Control	24 hr	48 hr	72 hr	96 hr
Protective behavior	+++	+++	+	-	-	+++	+++	++	-	-
Response to external stimuli	+++	++	+	+	-	+++	+++	++	+	-
Tentacular movement	+++	+++	++	+	-	+++	+++	++	+	-
Foot movement	+++	+++	++	-	-	+++	+++	++	-	-
Mucus secretion	+	++	+++	+++	+++	+	++	+++	+++	+++
Courtship behavior	+++	++	+	-	-	+++	++	++	-	-

Table – 2 Comparative quantitative behavioral responses of control and experimental slug *B. bengalensis* against intoxication of HgCl₂, ZnCl₂ and Co (NO₃)₂ at different exposure period. +++ - Strong response, ++ - Moderate response, + - Weak response, - - Not responding.

Similarly, Shaikh (2012) documented normal opening and closing of shell valves, protruded foot with pallial edges and siphon outside the shell valves in *Lamellidens marginalis*. Salanki and Lukacsovics (1967), documented partially and rhythmic movement of valves including the sudden opening and closing.

In the present investigation, behaviour of all experimental animals were altered behaviour against lethal concentration of Hg, Zn and Co. Deshai et al (2012) observed , behavioural and morphological changes in organism when exposed to toxicity. They have co-related with nervous system in an animal. Rice and Armitage (1974) documented strong correlation between physiological activities, metabolic changes with behavioural alterations of in experimental animal. Kamble and Nanaware (2007), documented behavioural differentiation in freshwater snail *B. bengalensis* when exposed to cadmium sulphate, zinc sulphate and lead acetate. The content of aluminium and salicylic acid in the environment changed the behaviour of *Lymnaea stagnalis* (Comnbell et al. 2000). Nagarajh et al. (1985) noticed behavioural alterations in intertidal molluscs after exposure to water-soluble fraction of diesel. Behavioural changes in land snail *Helix aspersa* changed due to applications of organophosphorus compound (Rorke et al.1979). The doses of pesticide methyl parathion and thimet changed the normal behaviour in *Lymnaea stagnalis* (Bhide 1998).

Newman (1996) reported, acute toxicity of a chemical to more ecologically relevant processes, including animal behaviours providing valuable insight related to potential impacts of a chemical on real ecological system. Water contaminants has altered behavioural mechanism in animals (Crews et al. 2000; Lefcort et al. 2000) there life span (Jensen et al. 2001) and morphology (Fisher et al. 2003).

After intoxication of Hg, Zn and Co to freshwater, snails *B. bengalensis* immediately body dragged and operculum tightly closed, showing quick protective responses. Muley and Mane (1987), reported similar behaviour in freshwater snail *V. bengalensis* after toxicity of Folithion and

Lebaycide. Secretary functions were increased in the experimental animals. Ruangareerat (2004) showed increased mucus secretion around the head region of the golden apple snail *Pomacea* sp. against toxicity of Mercuric chloride, Cadmium nitrate and Copper nitrate. Mucus has showed avidly binding of polyhydroxy colloids of Aluminium (Desouky 2001). Under normal filtration, the slight mucus layer is continuously renewed, providing new binding site for the metal and thus restricting uptake of metal from the water column by binding to its negatively charged glycoproteins (Conrad et al. 1991). Increased mucus indicated the elimination mechanism of metal in bivalve *B. azoricus*, mucus prevent inhibitory effect of metal (Kadar 2005). Biogenic production of mucus by invertebrates was previously reported as to bind with trace elements as a dual internal and external detoxification mechanism in the alvinnelid polychaete worm (Juniper et al. 1986).

Intoxication of Hg, Zn and Co, to snail *B. Bengalensis* was found releasing embryos as a toxicity responses. Muley and Mane (1987) similar noted phenomenon in *V. bengalensis* when exposed to folithion and lebacida. Muley and Yelpale (1993), similarly reported release of egg capsule in bivalves *Indonaia caeruleus* when tested for textile mill effluent.

Freshwater bivalve *L. corrianus* showed closed shell valves after 24 hr of exposure to Hg, Zn and Co. Gokahe and Mane (1990) similarly observed in *L. marginalis* due to fluoride toxicity. Shaikh (2012) reported *L. marginalis* was documented closed shell valves after 12 hr to exposure of cadmium, but later on clams opened the shell valves for respiration and food intake. Closing of shell valves in *B. azoricus* indicated its respond to Hg toxicity and thus reduced uptake (Kadar et al. 2004). The mechanism of avoidance explained the ability of bivalves to respire anaerobically for longer periods, keeping their shells closed under stress, after Hg intoxication (Devi 1997).

After the 72 and 96 hr of exposure, shell valves and operculum found opened. *L. marginalis*, when cadmium



content penetrated inside the body, where clams widely opened the shell valves and unable to close again till the end. Siphonal activity from out side the shell valve was not found. Foot was swollen and found outside the shell valves. Similarly Shaikh (2012) documented swollen foot outside the valves and the bivalve *L. marginalis* dose not responded to any mechanical stimulus. The possible cause of the permanent opening of the shell valves may be because of loss of response ability of the adductor muscles due to prolonged cadmium exposure in the experimentation. Collectively we found, Hg has higher toxic effect than the Zn. The alteration in the behaviour of snail and bivalve were maximum due to Hg.

References

- Ahmad Ismail (2006)** The use of intertidal molluscs in the monitoring of heavy metals and organotin compounds in the west coast of Peninsular Malaysia. *Costal Marine Science* 30 (1): 401-406.
- Awati and Nanaware (2004)** Comparative study on toxic effects of synthetic and natural molluscicides on respiratory and reproductive physiology of aquatic snail *Viviparous bengalensis* (Lamarck). Ph. D thesis, Shivaji University, Kolhapur (India).
- Bhide M (1998)** Effect of nuvan, methyl parathion and thimet on the mortality, behavior and reproductive performance of freshwater molluscs, *Lymnaea stagnalis*. *J Environ Biol.* 19 (4), 325-332.
- Compbell MM, White KK, Jugdaohsingh R, Powell-jonathan J, Mc Crohan Catherine R (2000)**. Effect of aluminum and Silicic acid on the behavior of the freshwater sanil, *L. stagnalis* . *Canadian J. of Fisheries and Aquatic Sciences (Print)* 57 (6): 1151-1159.
- Crews D, Willingham E, Skipper JK (2000)** Endocrine disruptors:Present issues, Future directions. *Q Rev Biol*, 75: 243-260.
- Desouky MM (2001)** Amerlioration of behavioural toxicity of aluminium by oligomeric silicic and humic acid. *Journal of Biology* 3: 56-62.
- Deshai RB, Katore BP, Shinde VD, Ambore NE (2012)** Behavioral study of female crab *Brytelphusa guerini* under acute stress of dimethoate. *International Multidisciplinary Research Journal* 2(5): 1-4.
- Devi UV (1997)** Heavy metal toxicity to an intertidal gastropod *Morula granalata* (ducos) tolerance to copper, mercury, cadmium and zinc. *J Environ Biol* 18 (3): 291-305.
- Fisher MA, Jelaso AM, Predenkiewicz A, Schuster L, Means J, Ide CF (2003)** Exposure to the polychlorinated biphenyl mixture Arochlor 1254 alters melanocyte and tail muscle morphology in developing *Xenopus laevis* tadpoles. *Environ. Toxicol. Chem* 22: 321-328.
- Ghosh M, Singh SP (2005)** Review on phytoremedikation of heavy metal and utilization of its byproducts: *Applied Ecology Research* 3(1): 1-18.
- Gokhale SR, Mane UH (1990)** Acute fluoride toxicity to the freshwater bivalve molluscs, *Lamellidens marginalis* (Lamarck). *Ind J Inv Zool and Aqua Biol* 2(1): 11-14.
- Gupta SK, Singh J (2011)** Evaluation of mollusc as sensitive indicator of heavy metal pollution in aquatic system: A review. *The IIOAB Journal*, 2(1): 49-57.
- Jensen A, Forbes VE, Parker ED Jr. (2001)**. Variation in cadmium uptake, Feeding rate and life history effects in the gastropod *Potamopyrgus antipodarum*: Linking toxicant effects on individuals to the population level. *Environ Toxicol Chem* 20: 2503-2513
- Juniper SK, Thompson JAJ, Calvert SE (1986)** Accumulation of minerals and trace elements in biogenic mucus at hydrothermal vents. *Deep sea Res.* 33: 339-347.
- Kamble NA, Nanaware SG (2007)** Comparative studies on induced biotoxicity of three heavy metals (Cd, Pb and Zn) to freshwater snail *Bellamya bengalensis* (Lamarck). Ph. D. thesis Department of Zoology, submitted to Shivaji University, Kolhapur.

- Lefcort H, Amman E, Eiger SM (2000).** Antipredatory behavior as an index of heavy-metal pollution? A test using snails and caddisflies. Arch Environ Contam Toxicol 38: 311-316.
- Muley DV, Mane UH (1987).** Endosulfan induced changes in oxygen consumption in two species of freshwater lamellibranch molluscs. J. Environ. Biol 5(1): 28-33.
- Muley DV, Yelpale PY (1993)** Toxicity of textile mill effluent on the bivalve mollusc, *Indonaiia caeruleus*. Proc Acad Evt Biol. 2(1): 119-124.
- Nagarajah NN, Antonette Sophia AJ, Bakasubramaian T (1985)** Behavior of some intertidal mollusks exposed to water soluble fractions of diesel. Mar. Pollu. Bull. 16(7): 167-271.
- Qunfang Z, Jianbin Z, Jianie F, Jianbo S, Guibin J (2008)** Biomonitoring: An appealing tool for assessment of metal pollution in the aquatic ecosystem. Analytica Chimica Acta 606: 135-150.
- Rice PR, Armitage KB (1974)** The effect of photoperiod on oxygen consumption of the crayfish, *Orconectesnaiss*. Comp Biochem Physiol. 47(A): 261-270
- Rorke MA, Gardner DR and Greenhalgh R (1974).** Lethality and behavioral symptoms produced by some organophosphorus compounds in the *Helix aspersa*. Bull. Environ. Contam. Toxicol. 11: 417-424.
- Salanki J, Lukacsovics F (1967).** Filtration and oxygen consumption related to the periodic activity of freshwater mussel, *anodonta cygnea*. Annal. Biol. Tihany. 34: 85-98.
- Shaik Y, Suryawanshi GD, Dama LB, Mane UH (2012)** Behavioural changes of fresh water bivalve molluscs *Lamellidens marginalis* due to acute toxicity of cadmium. DAV International J of science 1: 103-106.
- Walker CH, Hopkin SP, Sibly RM, Peakall DB (2003)** Principles of Ecotoxicology, 2nd Edn. Taylor and Francis Group, Fetter Lane, London
- Wills J (2000)** A survey of offshore oil field drilling wastes and disposal techniques to reduce the ecological impact of sea dumping. Sakhalin Environ Watch 13: 23-29.



Effect of phosphate and salt sources on growth of *Alternaria zinniae* caused by flower blight of marigold (*Tagetes erecta*)

¹A.B. Nangare*, ²M.B. Waghmare, ³M.M. Patil

^{*1,2}Department of Botany, The New College, Kolhapur -416012, MH, India

³Department of Botany and Plant Protection, S. G. M College, Karad-415124, MH, India

KEYWORDS

Alternaria zinniae , Growth ,
Marigold , phosphate Source
, Salt source

ABSTRACT

In the present study investigation was made on effect of different phosphate and salt sources on growth of the *Alternaria zinniae* caused by flower blight of marigold. Total four phosphate sources (potassium dihydrogen phosphate, sodium dihydrogen phosphate, sodium dihydrogen orthophosphate and di-potassium hydrogen orthophosphate) and four salt sources (magnesium chloride, potassium chloride, sodium chloride and cobalt chloride) tested against the pathogen. In phosphate source, 80 mm mycelial growth was found in di-potassium hydrogen orthophosphate while in the sodium dihydrogen orthophosphate the growth was 66.66 mm. Similarly in salt source, 80 mm mycelial growth was found in potassium chloride while in the cobalt chloride the growth was 50.00 mm as compared to the control.

Corresponding Author

Email

asmitanangare90@gmail.com

Introduction

Marigold (*Tagetes erecta* L.) is annual, herbaceous plant belonging to family Asteraceae. It is a prominent plant in Indian culture and Mythology. It is originally a native plant of ancient Egypt and First introduced into Britain by Romans.

Tagetes erecta is rich in many compounds such as phenolic derivatives, thiophenes derivatives, steroids, alkaloids, flavanoids and carotenoids (Li wei xu *et al.* 2012). The essential oil of the flower contains antioxidants (Perez Gutierrez R.M. *et al.* 2006). It is popular source of natural dye. Medicinally this plant is very effective in headache, toothache, scars, rashes and eye diseases. Oil acts as a

repellent against ants and mosquitoes, apart from this the flowers of marigold used for folk medicine to treat fever, carminative, stomachic, scabies, liver complaints, skin and eye diseases. (Kadam Prasad Vijay *et al.* 2013). Such medicinally important plant suffering from flower blight disease caused by *Alternaria zinniae*. For getting high yield of the flower disease management is necessary. Proper nutritional source required for the growth and development of the pathogen. The present investigation was conducted to study the effect of phosphate and salt source on growth of *Alternaria zinniae* because if we know nutrition requirement that will help to control the pathogen.

potassium hydrogen orthophosphate were added to 100ml of CDA medium. The medium without any phosphate source served as control.

Material and Methods

Effect of phosphate and salt sources

Phosphate sources: Four phosphate sources (0.1%) viz potassium dihydrogen phosphate, sodium dihydrogen phosphate, sodium dihydrogen orthophosphate and di-potassium hydrogen orthophosphate were added to 100ml of CDA medium. The medium without any phosphate source served as control . After autoclaving, 15ml of medium from source were poured into plates. The plates were inoculated with 8mm discs of six days old culture of isolate and incubated at 28+2 C . The linear growth of test fungus was measured at different intervals.

Salt sources: Four sulphate sources (0.05%) viz magnesium chloride, potassium chloride, sodium chloride and cobalt chloride were added to 100ml of CDA medium. The medium without any salt source served as control . After autoclaving, 15ml of medium from source were poured into plates. The plates were inoculated with 8mm discs of six days old culture of isolate and incubated at 28+2 C . The linear growth of test fungus was measured at different intervals.

Result and Discussion

Among the four tested phosphate sources di-potassium hydrogen orthophosphate was found to be best phosphate source for the growth of *Alternaria zinniae* . In di- potassium hydrogen orthophosphate maximum growth was observed while in sodium di-hydrogen orthophosphate minimum growth was noticed. (Table -1). Similarly among the four tested salt sources potassium chloride was found to be best salt source for the growth of *Alternaria zinniae* . In potassium chloride maximum growth was observed while in cobalt chloride minimum growth was noticed.(Table - 2).

Phosphate and salts were the most important and essential component required for their growth and development. The present study was helps to investigate the phosphate and salt requirement for development of *Alternaria zinniae*. Similar studies were carried out by Khilare and Rafi, 2011 studied the effect of nutritional sources on *Fusarium oxysporum* f. Sp. Ciceri causing chickpea wilt. Khandare and Kamble, 2013 studied the effect of sulphate and salt sources on development of *Alternaria alternata* causing root rot of fenugreek. Similarly other workers studied the effect of nutritional sources on growth of other pathogen .

Phosphate sources in 0.1%	Readings in days (Resistant isolate)				Reading in days (Sensitive isolate)			
	2	4	6	8	2	4	6	8
Di-potassium hydrogen orthophosphate	21.00	41.33	60.33	80.00	19.33	38.66	57.00	78.33
Potassium dihydrngen phosphate	18.33	35.66	57.33	73.00	15.66	34.66	55.00	71.00
Sodium dihydrogen orthophosphate	12.00	19.66	36.33	66.66	10.33	17.66	33.66	65.00
Sodium dihydrogen phosphate	13.66	22.00	38.33	68.33	11.66	19.00	35.33	66.66
Control	11.00	16.33	31.00	62.66	10.00	14.66	29.00	60.66

Table 1: Effect of different Phosphate sources on the linear growth (mm) of *Alternaria zinniae* isolates of resistant and sensitive to carbendazim on marigold leaf extract Agar medium.



Table 2: Effect of different salt sources on the linear growth (mm) of *Alternaria zinniae* isolates of resistant and sensitive to carbendazim on marigold leaf extract agar medium.

Salt sources in 0.05%	Readings in days (Resistant isolate)				Reading in days (Sensitive isolate)			
	2	4	6	8	2	4	6	8
Cobalt chloride	12.66	17.00	28.33	50.00	11.00	15.33	25.66	48.66
Potassium chloride	19.33	38.66	56.33	80.00	17.66	35.66	54.00	77.66
Magnesium chloride	13.66	19.33	33.66	56.33	12.33	17.33	31.66	55.33
Sodium chloride	14.00	22.66	35.33	59.66	12.33	18.66	33.33	56.66
Control	11.00	18.33	31.66	52.00	11.00	16.66	28.33	51.33

Acknowledgement

Authors are very much thankful to Dr. N.V. Nalawade principal, The New College, Kolhapur for providing the laboratory facilities.

References

- Kadam P.V, Bhingare C.L, Sumbe R.B, Nikam R.Y, Patil M.J (2013)** Pharmacognostic, Phytochemical and physicochemical investigation of *Tagetes erecta* Linn flowers (Asteraceae). *Journal of Biological and Scientific opinion*, volume 1(1).
- Khilare VC, Rafi A (2011)** Effect of nutritional sources on the growth of *Fusarium oxysporum* f. Ciceri causing chickpea wilt . *International Journal of Sciences And Nature*. Vol. 2(3): 524-528.
- Khandare NK, Kamble SS (2013)** Effect of sulphate and salts salts sources on the development of *Alternaria alternata* causing root rot disease of fenugreek. *International Journal of Science and Research*. Vol. (4) Issue 6 .
- Li WX, Guo YW, Yan PS (2011)** Chemical constituents from *Tagetes erecta* flowers. *Chemistry of Natural Compounds*, Vol 47, Issue 2, PP 281-283.
- Patil JS, Suryawanshi NS (2015)** Effect of nutritional and physiological characters of *Alternaria alternata* causing fruit rot of strawberry. *Bionano Frontier*. Vol. 8 (1).
- Rosa MP, Heliodoro HL, Sergio H G (2006)** Antioxidant activity of *Tagetes erecta* L essential oil. *Journal of the Chilean chemical society* 51(2): 883-886.



Effect of Carbon and Nitrogen Sources on the Growth of *Fusarium oxysporum* f.sp. *cubense* causing Panama wilt of banana.

¹M. S. Desai*, ²A. A. Jagtap, ³S. S. Kamble

¹Department of Botany, Karmaveer Hire College, Gargoti. Dist. Kolhapur.

²D. P. Bhosale College, Koregaon Dist. Satara

³Dept. of Botany, Shivaji University, Kolhapur, Maharashtra

KEYWORDS

Fusarium oxysporum f.sp. *cubense*, carbon, nitrogen.

Corresponding Author

Email
desai.ms@rediffmail.com

ABSTRACT

Effect of different sources of carbon and nitrogen on the growth of *Fusarium oxysporum* f.sp. *cubense* was studied by amending them in the Czapek Dox Agar medium. There was highly significant increase in the growth of both the benomyl resistant and sensitive isolates on the carbohydrate sources except lactose. Growth of the resistant isolate was higher than the sensitive isolate. Maximum growth of pathogen was observed on potassium nitrate and calcium nitrate in case of sensitive and resistant isolates respectively. As well as minimum growth of pathogen was observed in ammonium nitrate and sodium nitrate in case of both sensitive and resistant isolates.

Introduction

Banana (*Musa* spp.) is forth most important staple food crop in the world. India ranks first by producing the largest number of banana followed by China, Philippines, Brazil, Ecuador. *Fusarium oxysporum* causes vascular wilt diseases in a wide variety of economically important crops (Beckman 1987). Panama wilt of banana caused by *Fusarium oxysporum* f. sp. *cubense* (Smith, 1910; Snyder and Hansen, 1940). It is also known as Banana wilt. The disease occurs in its severe form where the banana cultivation is there i.e. Asian countries, Australia, Pacific islands, African countries, North and South American countries. It was first reported in Panama and Costa Rica in 1890 (Rangaswami, 2002). The physiological studies of *Fusarium oxysporum* f. sp. *cubense* and how fungi cause disease will increase importance in

management of disease. Therefore the aim present work is to study effect of carbon and nitrogen sources on the fungi.

Materials and Methods

Effect of different carbon sources like sucrose, glucose, dextrose, fructose, lactose and maltose were amended in Czapek Dox Agar medium at 3 %. Different nitrogen sources like potassium nitrate, calcium nitrate, magnesium nitrate, sodium nitrate, ammonium nitrate and peptone were used for this study at 0.2 % in Czapek Dox Agar medium. The plates were inoculated with sensitive and resistant isolates and incubated at $28 \pm 2^\circ\text{C}$. Plates without carbon and nitrogen source served as control. The linear growth was measured at different intervals.

Result and Discussion

Various carbohydrate sources sucrose, glucose, fructose, maltose, lactose, dextrose (3%) were incorporated in the Czapek Dox Agar medium and linear growth of sensitive FOC - 4 and resistant EMS- FOC - 9 isolates was recorded at various intervals. It appeared that sugars are essential for the growth of both the sensitive FOC - 4 and resistant EMS- FOC - 9 isolates. There was highly significant increase in the growth of the both the isolates when compared with control. The growth rate of the resistant EMS- FOC - 9 was higher than the sensitive FOC - 4 isolate on all the sugars. In case of the sensitive and resistant isolates higher inhibition was seen on lactose. In case of sensitive and resistant isolates growth was higher on sucrose followed by glucose, dextrose, maltose and fructose. (Tables 1 and 2, Figs. 1 and 2). Sucrose was also found to favour growth of carbendazium sensitive and resistant isolates of *Macrophomia phaseolina* (Kamble,1991).

Different nitrogen sources like sodium nitrate, ammonium nitrate, magnesium nitrate, potassium nitrate, peptone and calcium nitrate were used (0.2%) for this study. Maximum growth of pathogen was observed on potassium nitrate and calcium nitrate in case of sensitive (FOC - 4) and resistant (EMS- FOC -9) isolates respectively. As well as minimum growth of pathogen was observed in ammonium nitrate and sodium nitrate , in case of both sensitive (FOC -4) and resistant (EMS -FOC -9) isolates respectively. (Tables 3 and 4, Figs. 3 and 4). There are various reports on the effect of different nutritional sources on growth and sporulation of resistant mutants of various pathogens. *Aspergillus flavus* resistant to eleven fungicides was different in several physiological aspects noted by Gangawane and Saler (1981).

Table 1. Effect of different carbon sources on the linear growth (mm) of *Fusarium oxysporum* f.sp. *cubeense* isolate sensitive to benomyl on Czapek Dox Agar medium.

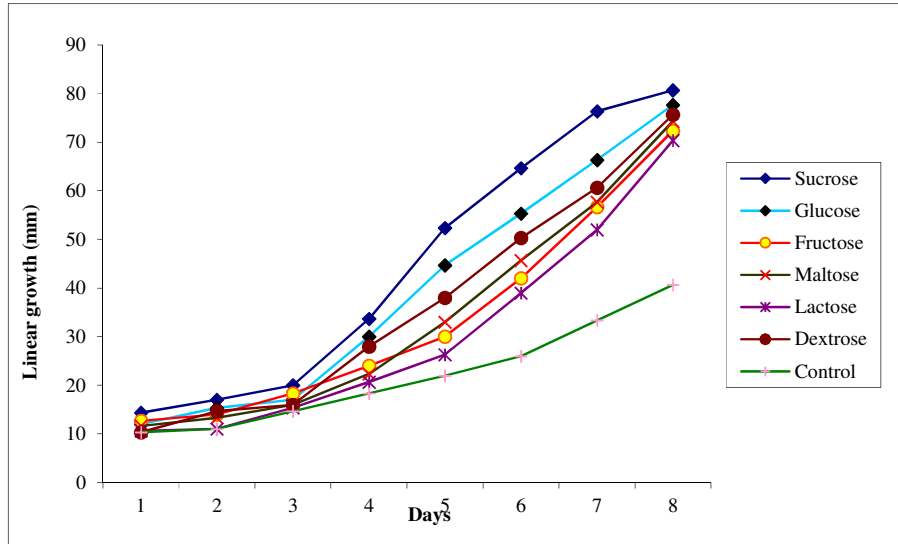
Sugars (3%)	Sensitive							
	Days							
	1	2	3	4	5	6	7	8
Sucrose	12.33	15.66	18.00	31.00	50.33	62.33	74.00	78.66
Glucose	10.00	13.00	15.66	28.66	42.66	50.33	61.33	75.66
Fructose	10.33	12.66	16.33	22.66	25.33	40.33	54.66	70.33
Maltose	11.66	12.00	17.66	22.33	29.00	43.66	55.33	72.33
Lactose	10.33	11.33	15.33	21.66	24.66	38.66	52.33	68.33
Dextrose	10.33	15.33	19.00	25.66	37.00	47.33	58.66	73.66
Control	10.00	11.00	14.00	18.00	22.00	26.66	33.00	40.00

P at 0.05 DF= 7 T value= 2.365
 Standard Error Mean = 7.542
 Critical Difference Mean = 17.84
 F (between carbon sources)= 91.250754 P < 0.0001
 F (between days) = 9.896221 P < 0.0001



Fig. 1.

carbon
linear
(FOC -



Effect of
different
sources on the
growth (mm) of
Fusarium
oxysporum f.sp.
cubense
sensitive isolate
4)

Table 2. Effect of different carbon sources on the linear growth (mm) of *Fusarium oxysporum* f.sp. *cubense* isolate resistant to benomyl on Czapek Dox Agar medium

Sugars (3%)	Resistant							
	Days							
	1	2	3	4	5	6	7	8
Sucrose	14.33	17.00	20.00	33.66	52.33	64.66	76.33	80.66
Glucose	12.00	15.33	17.00	30.00	44.66	55.33	66.33	77.66
Fructose	12.66	14.00	18.33	24.00	30.00	42.00	56.66	72.33
Maltose	11.66	13.33	16.00	22.33	33.00	45.66	57.66	74.33
Lactose	10.66	11.00	15.33	20.66	26.33	39.00	52.00	70.33
Dextrose	10.33	14.66	16.00	28.00	38.00	50.33	60.66	75.66
Control	10.33	11.00	14.66	18.33	22.00	26.00	33.33	40.66

P at 0.05 DF= 7 T value= 2.365
 Standard Error Mean =7.725
 Critical Difference Mean =18.27
 F (between carbon sources) = 92.481244 P < 0.0001
 F (between days) = 11.641197 P < 0.0001

Fig. 2. Effect of different carbon sources on the linear growth (mm) of *Fusarium oxysporum* f.sp. *cupense* resistant isolate (EMS- FOC -9)

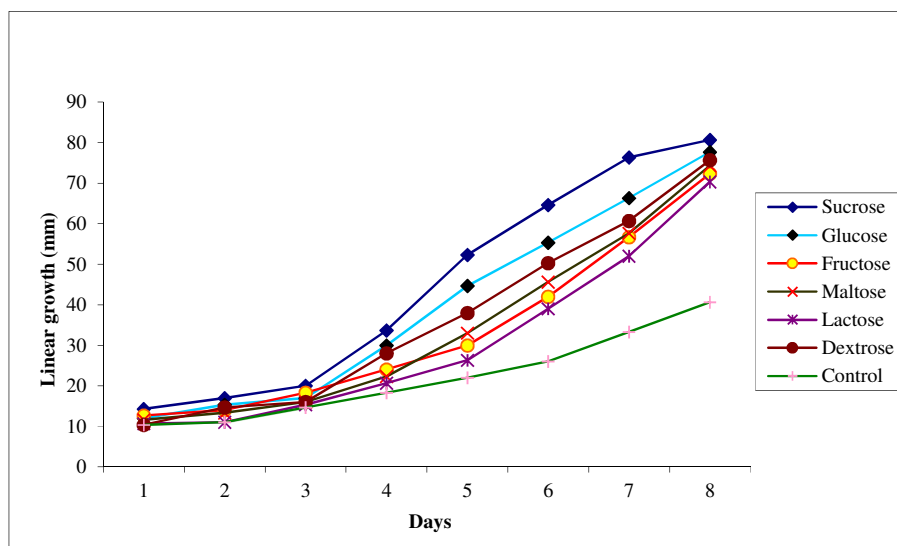


Table 3. Effect of different nitrogen sources on the linear growth (mm) of *Fusarium oxysporum* f.sp. *cupense* isolate sensitive to benomyl on Czapek Dox Agar medium

Nitrogen (0.2%)	Sensitive							
	Days							
	1	2	3	4	5	6	7	8
Sodium nitrate	10.33	11.66	16.33	22.66	24.33	42.66	50.33	60.66
Ammonium nitrate	11.66	14.66	17.66	21.00	24.33	30.66	41.33	50.33
Magnesium nitrate	10.33	11.00	16.33	22.00	26.66	40.33	52.66	65.66
Potassium nitrate	11.33	14.33	19.66	23.33	25.66	44.66	50.66	74.00
Peptone	11.00	15.66	23.00	29.00	33.66	43.33	55.33	66.00
Calcium nitrate	10.66	12.33	14.00	21.66	24.33	29.33	44.00	72.00
Control	10.33	11.66	12.00	20.66	24.00	28.00	43.33	53.00

P = 0.05 DF= 7 T value= 2.365
 Standard Error Mean = 6.560
 Critical Difference Mean = 15.51
 F (between nitrogen sources) = 149.398282 P < 0.0001
 F (between days) = 5.578103 P = 0.0003



Fig. 3. Effect of different nitrogen sources on the linear growth (mm) of *Fusarium oxysporum* f.sp. *cabense* sensitive isolate (FOC -4)

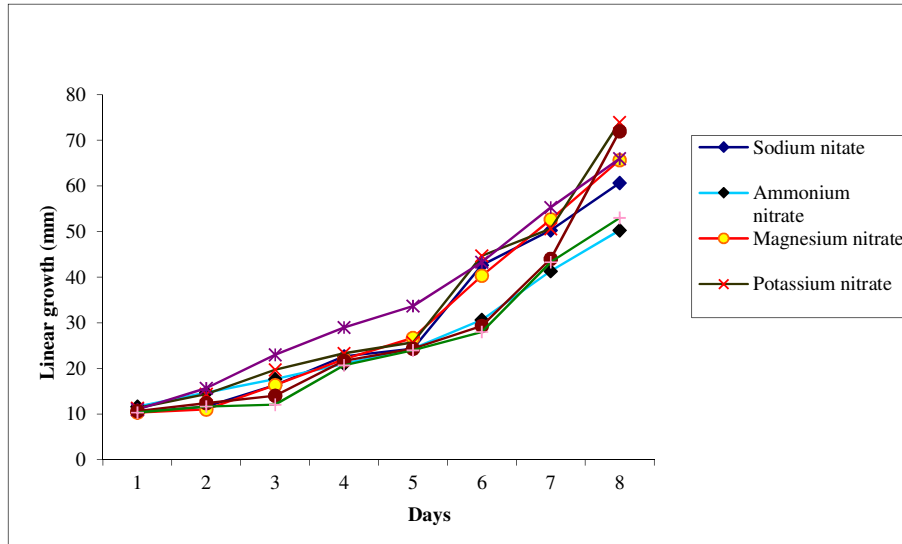
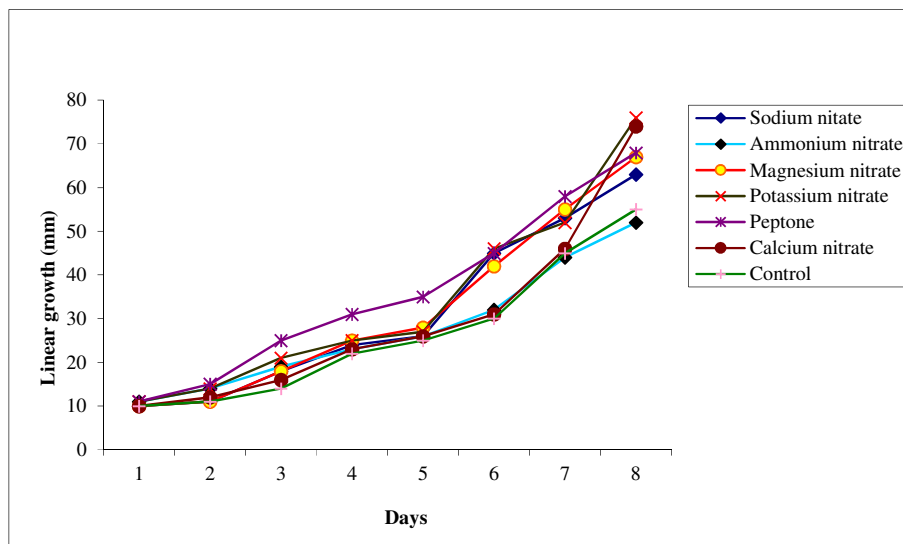


Table 4. Effect of different nitrogen sources on the linear growth (mm) of *Fusarium oxysporum* f.sp. *cabense* isolate resistant to benomyl on Czapek Dox Agar medium.

Nitrogen (0.2%)	Resistant							
	Days							
	1	2	3	4	5	6	7	8
Sodium nitrate	10.33	11.33	18.00	24.66	26.66	45.33	53.00	63.66
Ammonium nitrate	11.00	14.00	19.66	23.33	26.00	32.00	44.33	52.00
Magnesium nitrate	10.66	11.66	18.33	25.00	28.33	42.66	55.00	67.66
Potassium nitrate	11.66	14.00	21.33	25.66	27.00	46.33	52.66	76.33
Peptone	11.33	15.33	25.66	31.33	35.66	45.66	58.00	68.33
Calcium nitrate	10.00	12.00	16.66	23.00	26.33	31.00	46.66	74.33
Control	10.33	11.33	14.00	22.66	25.66	30.66	45.66	55.66

P at 0.05 DF= 7 T value= 2.365
 Standard Error Mean = 6.560
 Critical Difference Mean = 15.51
 F (between nitrogen sources) = 149.398282 P < 0.0001
 F (between days) = 5.578103 P = 0.0003

Fig. 4. Effect of different nitrogen sources on the linear growth (mm) of *Fusarium oxysporum* f.sp. *ubense* resistant isolate (EMS- FOC -9)



Conclusion

There was highly significant increase in the growth of both the benomyl resistant and sensitive isolates on the carbohydrate sources except lactose.

Nitrogen sources such as sodium nitrate, ammonium nitrate, magnesium nitrate, potassium nitrate, peptone and calcium nitrate were used. Growth of the resistant isolate was higher than the sensitive isolate. Maximum growth of pathogen was observed on potassium nitrate and calcium nitrate in case of sensitive and resistant isolates respectively. As well as minimum growth of pathogen was observed in ammonium nitrate and sodium nitrate, in case of both sensitive and resistant isolates.

References

Beckman, C.H.(1987) The nature of wilt diseases of plants. American Phytopathological Society, St. Paul .M. N., USA.175pp.

Gangawane, L. V. and Saler, R. S. (1981). Resistance to fungicides in *Aspergillus flavus*. Neth. J. Path.

Kamble, S. S. (1991). Studies on fungicide resistance in late blight and Charcoal rot of potato. Ph.D. Thesis, Marathawada University, Aurangabad.

Rangaswami, G. and Mahadevan, A. (2002). "Diseases of Crop Plants in India" Forth edition. Prentic-Hall of India Private Limited, New Delhi, 300-301.

Smith, E. F. (1910). A Cuban banana disease. (Abstract.) Science. 31: 754-755.

Snyder, W. C. and Hansen, H. N. (1940). The species concept in *Fusarium*. *American J. Bot.* 27: 64-67.



Biocontrol capability of *Trichoderma virens* lcf on the *Fusarium equiseti* causing blossom blight of *Polianthes tuberosa* l.

¹S.A. Shinde*, ¹M. B. Waghmare, ²M. M. Patil

¹The New College, Kolhapur

²S. G. M.College, Karad.

KEYWORDS

Fusarium equiseti,
Trichoderma virens, Liquid
culture filtrate ,
Antagonistic potential, Food
poisoning technique,
Biological control

ABSTRACT

Polianthes tuberosa L. is an ornamental and medicinal plant cultivated in field , gardens. It belongs to family Amaryllidaceae. It is night blooming herb, commonly known as Nishigandha. For cut flower trade and beautiful fragrance it is widely cultivated in our area. It is diuretic and gonorrhoea. Flower extract of *Polianthes tuberosa* used to produce high grade perfume. Flowers remains fresh for long time hence stands for long distance transportation. Such commercially important plant suffering from many fungal diseases, among all blossom blight disease caused by *Fusarium equiseti* Corda Sacc. is very harmful to the plant. Number of workers studied the chemical management but frantically use of fungicides disturbs the ecological balance hence ecofriendly management gaining an importance. *Trichoderma virens* is a biocontrol agent present in the soil. *Trichoderma* are important plant growth promoter (Windham ;1986, Baker; 1988 and liu ; 1990). They shown antagonistic potential against various phytopathogens.

Corresponding Author
Email

swapnalishinde171988@gmail.com

Introduction

Polianthes tuberosa L. is an ornamental and medicinal plant cultivated in field , gardens. It belongs to family Amaryllidaceae. It is night blooming perennial herb, commonly known as Nishigandha. For cut flower trade and beautiful fragrance it is widely cultivated in our area.

It is diuretic and gonorrhoea. Flower extract of *Polianthes tuberosa* used as a raw material to produce high grade perfume. It's attractive and scented flowers has great potential for export. Flowers remains fresh for long time hence stands for long distance transportation. Such commercially important plant suffering from many fungal

diseases, among all blossom blight disease caused by *Fusarium equiseti* Corda Sacc. is very harmful to the plant. Number of workers studied the chemical management but frantically use of fungicides disturbs the ecological balance and creates the resistance power in pathogen (Waghmare and Kamble 2010), hence ecofriendly management gaining an importance.

Trichoderma virens is a biocontrol agent present in the soil. *Trichoderma* are important plant growth promoter (Windham ;1986, Baker; 1988 and liu ; 1990). They shown antagonistic potential against various phytopathogens (Chet *et al.* 1981). Therefore in the present study investigation has been made on effect of Liquid Culture filtrates of *Trichoderma virens* on *Fusarium equiseti* by food poisoning technique. orted that *Trichoderma* is best alternative to the fungicides (Eziashi *et al.* 2007).

Material and Methods

1. Isolation of pathogen (*Fusarium equiseti*)

Naturally infected blossom blight samples of *Polianthes tuberosa* were collected from Kolhapur district (Radhanagari (Rashiwade), Karveer (Haldi), Panhala, Kagal, Gaganbawada, Bhudargad, Shahuwadi, Hatkanangale and Shirol) during 2011-2012. Infected samples brought to the Botany laboratory of The New College, Kolhapur in the sterile polythene bags. Then surface sterilization of infected samples was made with 0.1% mercury chloride, washed the material with sterile distilled water and removed the traces of mercury chloride. Samples were cut into small pieces and cultured on the Czapek Dox Agar (CDA) medium. After 4-5 days different fungal colonies were observed in the petriplates. Pathogen was identified with the help of standard mycological literature (Bilgrami *et al.* 1981; Subramanian 1971) pure culture of *Fusarium equiseti* was maintained on Czapek Dox Agar medium in BOD incubator.

2. Isolation of *Trichoderma virens* J. Miller, Giddens and foster

Rhizosphere soils were collected from Kolhapur district. *Trichoderma virens* J. Miller, Giddens and foster was isolated by dilution plate technique (Johnson 1957). Isolate was grown on PDA medium (Ricker and Ricker 1936). The isolated species was identified (Kubicek and Harman 2002; Nagamani and Manoharachary 2002). Pure culture of *Trichoderma virens* was maintained on the PDA medium for further study.

3. Effect of liquid culture filtrates:

500 ml. liquid culture media was prepared in a conical flask. Then media was sterilized. Inoculated the 5 mm diameter disc of *Trichoderma virens* from the 7 days old culture . then conical flasks was placed on the thermostat culture shaker for 10-15 days at 28°C. Then filtrate was filtered through Whatman's no. 1 filter paper and also from 0.2 millipore filter paper. For further use it was stored at 4°C. The filtrate was added to sterilized water to make the concentrates (25%, 50%, 75%, 100%). Then the percent filtrate was added to 2X media and prepare the solidifying petriplates. 5 mm disc of fungal pathogen was placed on the petriplates and incubated for 7 days . Plates made from culter media without any filtrate used as control.

Percent inhibition was calculated by using following formula, (Edington *et al.*, 1971).

$$I = [(C_2 - C_1) / C_2] \times 100$$

Where,

I = percent inhibition of radial mycellial growth

C₂ = radial growth of pathogen in control plates

C₁ = radial growth of pathogen in treated plates



Table 1: Effect of LCF on Antagonistic potential of *Trichoderma virens* against *Fusarium equisetii*.

Sr.No.	Antagonistic isolates	LCF Percentage	Radial mycellial growth in mm	Percent inhibit growth
1.	<i>Trichoderma virens</i>	25%	47	47.77%
		50%	38	57.77%
		75%	30	66.66%
		100%	23	74.44%
2.	Control		90	00.00%

Result

In the present study effect of liquid culture filtrate on antagonistic potential of *Trichoderma virens* against *Fusarium equiseti* were studied. 100% culter filtrate shows higher (74.44%) antagonistic potential while 25% culture filtrate shows less (47.77%) antagonistic potential than 100% and more antagonistic potential than control (0.00%).

References

Bilgrami KS , Jamaluddin S and Rizwi MA (1981) Fungi of India Part II. List and References. *Today and Tomorrow's Printers and Publishers, New Delhi.*

Chet I, Harman GE and Baker R, (1981) *Trichoderma hamatum* : Its hyphal interactions with *Rhizoctonia solani* and *Pythium* spp. *Microbial Ecology.*, 7: 29-38.

Eziashi EI, Omamor IB and Odigie EE,(2007). Antagonism of *Trichoderma viride* and effects of extracted water soluble compounds from *Trichoderma* species and benlate solution on *Ceratocystis paradoxa*. *Afr. J. Biotechnol.*, 6(4): 388-392.

Johnson LA, (1957) Effect of antibiotics on the number of bacteria and fungi isolated from soil by dilution plate method. *Phytopathology*, 47: 21-22.

Kolli SC, Nagamani A and Rahel RY, (2012). Growth responce of *Trichoderma* isolates against varying pH levels .*International Journal of Environmental Biology*, 2(4) :180-182.

Kubicek CP and Harman GE, (2002). “Basic biology, taxonomy and genetics” (Taylor and Francis Ltd. London), Pp.14.

Manjunath Hubballi, Sevugapperumal Nakkeeran, Thiruvengadam Hiruvengadam Raguchander, Theerthagiri Anand and Ramasamy Samiyappan, (2010). Effect of environmental conditions on growth of *Alternaria alternata* causing Leaf blight of Noni. *World Journal of Agricultural Science*, 6(2): 171-177.

Miguel A, Moreno-Mateos MA, Delgado-Jarana J, Codon AC and Benitez T, (2007). pH and Pac 1 control development and antifungal activity in *Trichoderma harzianum*, *Fungal. Genetics. Biol.*, 44:1355-1367.

Nagamani A and Manoharachary C,(2002) Monographic Contribution on *Trichoderma*. Associated Publishing Company. New Delhi.

Ricker AJ and Ricker RS, (1936). Introduction to Research on Plant diseases John S. Swift Co., St. Louis, Pp 117.

- Rousk J, Brookes PC and Baath E, (2009).** Contrasting soil pH effects on fungal and bacterial growth suggest functional redundancy in carbon mineralization. *Appl. Environ. Microbiol.*, 75 :1589-1596.
- Subramanian CV, (1971).** Hypomyces an account of Indian species except Cercospora. Indian Council of Agricultural Research, New Delhi, Pp 810.
- Benitez T,(2004).** Increased antifungal and chitinase specific activities of *Trichoderma harzianum* CECT 2413 by addition of a cellulose binding-domain, *Appl. Microbiol. Biotechnol.*, 64:675-685.
- Waghmare MB Kamble and SS, (2010)** Efficacy of carbendazim against *Alternaria alternata* causing leaf spot of rose, *Bioinfolet.*, 7(3):241.
- Edington LV , Khew KL, Barron G ,(1971)** Fungitoxic spectrum of Benzimidazole compounds. *Phytopathology*, 61: 42-44.



Intellectual medicinal properties of *Withaniasomnifera*(L.) Dunal: a review

¹Nilofar Shaikh and ²Madhuri Walvekar

¹Assistant Professor, Department of Zoology, D.K.A.S.C. College, Ichalkarenji, Kolhapur.

²Assistant Professor, Department of Zoology, Shivaji University, Kolhapur

KEYWORDS

W. somnifera,
Chemical nature,
Medicinal properties

Corresponding Author
Email
nshaikh20@gmail.com

ABSTRACT

W. somnifera, commonly known as ashwagandha, is an important medicinal plant that has been used in ayurvedic and indigenous medicine. Ashwagandha has long been considered as an excellent rejuvenator, a general health tonic and a cure for a number of health complaints. It is a sedative, diuretic, anti-inflammatory and generally respected for increasing energy, endurance, and acts as an-adaptogen that exerts a strong immunostimulatory and ananti- stress agent. In view of its varied therapeutic potential, it has also been the subject of considerable modern scientific attention. Chemical constituents in *W. somnifera*, such as steroidal lactones, alkaloids, flavonoids, tannin etc. *W. somnifera*, Shows different medicinal properties as Antioxidant effect, Chronic stress (CS), Nootropic effect, Antiparkinsonian properties, Antivenom property, Anti-inflammatory property, Immunomodulation and hematopoiesis, Antitumor properties, Hypolipidemic effect, Antibacterial effect,

Introduction

Ashwagandha in Sanskrit means “horse’s smell” which resembles the smell of sweaty horse. The species name *somnifera* means “sleep inducing” in latin, indicating to its sedating properties. The Solanaceae family is comprised of 84 genera that include about 3,000 species, scattered throughout the world. The genera *Withania* and *Physalis* play an important role in the indigenous medicine of South East Asia, e.g. in the Unani and Ayurvedic systems. The twenty-three known *Withania* species are widely distributed in the drier parts of tropical and subtropical zones, ranging from the Canary Islands, the Mediterranean regions and northern Africa to Southwest Asia. (Schonbeck-Temesy et al. 1972; Hepperet al.1991; Warrieret al. 1996; Hunziker, 2001). Among them, only two species, *W. somnifera* and *W. coagulans*, are economically and medicinally significant,

being used and cultivated in several regions (Javanshir, 2000; Sharma, 2004; Panwar and Tarafdar, 2006).

Ashwagandha is a small, branched, evergreen perennial and woody shrub grows usually up to two feet in height. Because of its wide range of occurrence, there are considerable morphological and chemical variations in terms of local species. *W. somnifera*, commonly known as ashwagandha, is an important medicinal plant that has been used in ayurvedic and indigenous medicine for over 3,000 years. In view of its varied therapeutic potential, it has also been the subject of considerable modern scientific attention. Ashwagandha roots are a constituent of over 200 formulations in ayurvedha, Siddha and unani medicine, which are used in the treatment of various physiological disorders (Asthana and Raina, 1989; Singh and Kumar, 1989).

Withania appears in WHO monographs on Selected Medicinal Plants and an American Herbal Pharmacopoeia monograph is also forthcoming (Marderosian, 2001). Classification of Ashwagandha are as follows-

Botanical Name: *Withania somnifera*

Common Names: Ashwagandha, winter cherry

Parts commonly Used: Root (Dried)

Taxonomical classification

Kingdom : *Plantae;*

Subkingdom : *Tracheobionta, Vascular plants;*

Super division : *Spermatophyta, Seed plants;*

Division : *Angiosperma*

Class : *Dicotyledons*

Order : *Tubiflorae*

Family : *Solanaceae*

Genus : *Withania*

Species : *somnifera Dunal*

Chemical constituents:

The chemistry of *Withania* species has been extensively studied and several groups of chemical constituents such as steroidal lactones, alkaloids, flavonoids, tannin etc. have been identified, extracted and isolated (Kapoor, 2001; Choudary et al. 1996; Rastogi and Mehrotra, 1998; Bandyopadhyay et al. 2007). At present, more than 12 alkaloids, 40 withanolides, and several sitoindosides (a withanolide containing a glucose molecule at carbon 27) have been isolated and reported from aerial parts, roots and berries of *Withania* species. The major chemical constituents of these plants, glycowithanolides (WSG), are mainly localized in leaves, and their concentration usually ranges from 0.001 to 0.5% dry weight (DW) (Kapoor, 2001; Atalet al. 1975).

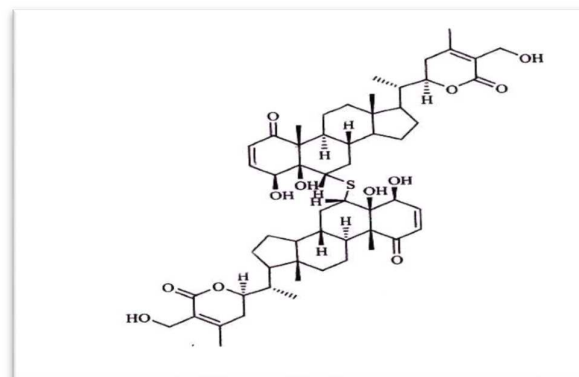


Fig- 1 Structure of Glycowithanolides

The biologically active chemical constituents are alkaloids (ashwagandhine, cuscohygrine, anahygrine, tropine etc), steroidal compounds, including ergostane type steroidal lactones, withaferin A, withanolides A, withasomniferin-A, withasomidienone, withasomniferols A-C, withanone etc. Other constituents include saponins containing an additional acyl group, and withanolides with a glucose at carbon 27 (sitoindoside IX and X) (Elsakka et al. 1990; Ganzer et al. 2003). Apart from these contents plant also contain chemical constituents like withaniol, acylsterylglucosides, starch, reducing sugar, hantreacotane, ducitol, a variety of amino acids including aspartic acid, proline, tyrosine, alanine, glycine, glutamic acid, cystine, tryptophan, and high amount of iron. Among these different constituents glycowithanolides (WSG) is the active principle of *W. somnifera* consisting of sitoindoside VII and X and withaferin A. (Bhattacharya et al. 1997). Glycowithanolides is the major bioactive chemical principle of *W. somnifera* (Ghosal et al. 1989). The purpose of this review is the study the different intellectual property of *W. somnifera*.

Medicinal values

This herb is considered an adaptogen which is a nontoxic herb that works on a nonspecific basis to normalize physiological function, working on the HPA axis and the neuroendocrine system. Ashwagandha is effective for insomnia but does not act as a sedative. Its rejuvenative and nerve properties produce energy which in turn help the body to settle and sleep.



Thus it helps the body to address a stress related condition rather than masking it with sedatives. A herb that rejuvenates the nervous system, erases insomnia and eases stress. Ashwagandha has also been shown to lower blood pressure and is highly effective in stopping the formation of stress induced ulcers. In arthritis, which involves joints that are painful, dry, swollen and inflamed, Ashwagandha would be the herb of choice. (Umadevi et al. 2012).

Medicinal Properties:

a) Antioxidant effect:

The brain and nervous system are relatively more susceptible to free radical damage than other tissues because they are rich in lipids and iron, both known to be important in generating reactive oxygen species. Free radical damage of nervous tissue may be involved in normal aging and neurodegenerative diseases, e.g., epilepsy, schizophrenia, Parkinson's, Alzheimer's, and other diseases. The active principles of WS, sitoindosides VII-X and withaferin A (glycowithanolides), have been tested for antioxidant activity using the major free-radical scavenging enzymes, superoxide dismutase (SOD), catalase (CAT), and glutathione peroxidase (GPX) levels in the rat brain frontal cortex and striatum. Decreased activity of these enzymes leads to accumulation of toxic oxidative free radicals and resulting degenerative effects. An increase in these enzymes would represent increased antioxidant activity and a protective effect on neuronal tissue. Active glycowithanolides of WS were given once daily for 21 days, dose-related increased in all enzymes were observed; the increases comparable to those seen with deprenyl (a known antioxidant) administration. This implies that WS does have an antioxidant effect in the brain, which may be responsible for its diverse pharmacological properties (Bhattacharya et al.1997). LPO blood levels were increased by lipopolysaccharides (LPS) from *Klebsiellapneumoniae* and peptidoglycans (PGN) from *Staphylococcus aureus*. Simultaneous oral administration of WS extract prevented an increase in LPO (Dhuley, 1998).

b) Chronic stress (CS):

Chronic stress (CS) can result in a number of adverse physiologic conditions including cognitive deficit, immunosuppression, sexual dysfunction, gastric ulceration, irregularities in glucose homeostasis, and changes in plasma corticosterone levels. In a rat model of chronic stress *Withaniasomnifera* and *Panax ginseng* extracts were compared for their ability to attenuate some effects of chronic stress. Both botanicals were able to decrease the number and severity of CS-induced ulcers, reverse CS-induced inhibition of male sexual behavior, and inhibit the adverse effects of CS on retention of learned tasks. In another study, *Withaniasomniferamethanolic* extract for 15 days significantly reduced the ulcer index, volume of gastric secretion, free acidity, and total acidity. A significant increase in the total carbohydrate and total carbohydrate/protein ratio was also observed. Study also indicated an increase in antioxidant defense, that is, enzymes SOD, CAT, and ascorbic acid, increased significantly, whereas a significant decrease in lipid peroxidation was observed. Bhatnagaret al.(2005) found that *Withaniasomnifera* inhibited stress-induced gastric ulcer more effectively as compared to the standard drug ranitidine. Bhattacharya et al.(2002) reported that chronic electroshock stress (14 days) significantly decreased the nor-adrenaline (NA) and dopamine (DA) levels in frontal Cortex, pons-medulla, hypothalamus, hippocampus and striatal, hypothalamal region, respectively, and increased the 5-hydroxytryptamine (5HT) level in frontal cortex, pons medulla, hypothalamus and hippocampus.

c) Nootropiceffect :

Effects of sitoindosides VII-X and withaferin isolated from aqueous methanol extract of roots of cultivated varieties of *Withaniasomnifera* were studied on brain cholinergic, glutamatergic and GABAergic receptors in rats. In a study by Zhao et al. (2002) Withanoside IV induced neurite outgrowth in cultured rat cortical neurons.

Oral administration of withanoside IV significantly improved memory deficits in Abeta-injected mice and prevented loss of axons, dendrites, and synapses. Withanoside IV may ameliorate neuronal dysfunction in Alzheimer's disease and that the active principle after metabolism is sominone. In another study reserpine treated animals also showed poor retention of memory in the elevated plus maze task paradigm. Naidu et al. (2006) evaluated that chronic *Withaniasomnifera* administration significantly reversed reserpine-induced retention deficits.

d) Antiparkinsonian properties

Kumar et al. (2006) demonstrated that *Withaniasomnifera* significantly inhibited haloperidol or reserpine-induced catalepsy and provide hope for treatment of Parkinson's disease. Antiparkinsonian effects of *Withaniasomnifera* extract has been reported due to potent antioxidant, antiperoxidative and free radical quenching properties in various diseased conditions. In another study, glycowithanolides (WSG) administered concomitantly with haloperidol for 28 days, inhibited the induction of the neuroleptic TD. Haloperidol-induced TD was also attenuated by the antioxidant, vitamin E, but remained unaffected by the GABA-mimetic antiepileptic agent, sodium valproate, both agents being administered for 28 days like WSG. Antioxidant effect of WSG, rather than its GABA-mimetic action reported for the prevention of haloperidol-induced TD (Bhattacharya et al.2002).

e) Antivenom property:

Venom hyaluronidases help in rapid spreading of the toxins by destroying the integrity of the extra-cellular matrix of the tissues in the victims. A hyaluronidase inhibitor WSG is purified from *Withaniasomnifera*. The glycoprotein inhibited the hyaluronidase activity of cobra (*Najanaja*) and viper (*Daboiarusselii*) venoms, which was demonstrated by zymogram assay and staining of the skin tissues for differential activity. Glycowithanolides (WSG) completely inhibited the activity of the enzyme at a concentration of 1:1

w/w of venom to WSG. External application of the plant extract as an antidote in rural parts of India to snakebite victims appears to have a scientific basis (Machiah et al.2006).

f) Anti-inflammatory property

The effects of *Withaniasomnifera*, as anti-inflammatory in a variety of rheumatologic conditions, have been studied by several scientists. *Withaniasomnifera* root powder also decreased air pouch granuloma induced by carrageenan on the dorsum of rats. *Withaniasomnifera* decreased the glycosaminoglycans content in the granuloma tissue more than hydrocortisone treatment. A study by Hindawiet al.(1992) found WSG inhibited the granuloma formation in cotton-pellet implantation in rats and the effect was comparable to hydrocortisone sodium succinate (5mg/kg) treatment.

g) Immunomodulation and hematopoiesis

In another study, glycowithanolides and a mixture of sitoindosides IX and X isolated from *Withaniasomnifera*, both produced statistically significant mobilization and activation of peritoneal macrophages, phagocytosis, and increased activity of the lysosomal enzymes. Ziauddin et al.(1996) found that root extract of *Withaniasomnifera* was tested for immunomodulatory effects in three myelosuppression models in mice: cyclophosphamide, azathioprin, or prednisolone. Significant increases in hemoglobin concentration, red blood cell count, white blood cell count, platelet count, and body weight were observed in *Withaniasomnifera* treated mice compared to untreated control mice. The authors also reported significant increases in hemolytic antibody responses toward human erythrocytes which indicated immunostimulatory activity. Rasool and Varalakshmi (2006) reported that immunosuppressive effect of *Withaniasomnifera* root powder could be a candidate for developing as an immunosuppressive drug for the inflammatory diseases.

h) Antitumor properties:

Withaniasomnifera is widely used in the



arthritis, asthma, and hypertension. *Withaniasomnifera* extracts may prevent or inhibit tumor growth in cancer patients and suggest a potential for development of new chemotherapeutic agents (Jayaprakasamet al.2003). In another study *Withaniasomnifera* was evaluated for its antitumor effect in urethane-induced lung adenomas in adult male albino mice. A significant increase in the life span and a decrease in the cancer cell number and tumour weight were noted in the tumour-induced mice after the treatment with *Withaniasomnifera*. The hematological parameters were also corrected by *Withaniasomnifera* in tumour-induced mice. These observations are suggestive of the protective effect of *Withaniasomnifera* in Dalton's Ascitic Lymphoma (Gupta et al.2001).

i) Hypolipidemic effect

Withaniasomnifera root powder decreased total lipids, cholesterol and triglycerides in hypercholesteremic animals. On the other hand, significantly increased plasma high density lipid (HDL)-cholesterol levels, HMG-COA reductase activity and bile acid content of liver. A similar trend also reported in bile acid, cholesterol and neutral sterol excretion in the hypercholesteremic animals with *Withaniasomnifera* administration. Further, a significant decrease in lipid-peroxidation occurred in *Withaniasomnifera* administered hypercholesteremic animals when compared to their normal counterparts. However, *Withaniasomnifera* root powder was also effective in normal subjects for decreasing lipid profiles (Visavadiya and Narasimhacharya, 2006). In another study with aqueous extract of fruits of *Withaniasomniferacoagulans* to high fat diet induced hyperlipidemic rats for 7 weeks, significantly reduced elevated serum cholesterol, triglycerides and lipoprotein levels. This drug also showed hypolipidemic activity in triton-induced hypercholesterolemia.

The histopathological examination of liver tissues of treated hyperlipidemic rats showed comparatively lesser degenerative changes compared with hyperlipidemic

controls. The hypolipidemic effect of *Withanicoagulans* fruits reported to be comparable to that of an ayurvedic product containing Commiphoramukkul (Hemalathaet al2006). Significant increase in urine sodium, urine volume, significant decrease in serum cholesterol, triglycerides, LDL (low density lipoproteins) and VLDL (very low density lipoproteins) cholesterol were observed indicating that root of WS is a potential source of hypoglycemic, diuretic and hypocholesterolemic agents (Andallu and Radhika, 2000).

j) Antibacterial effect

Both aqueous as well as alcoholic extracts of the plant (root as well as leaves) were found to possess strong antibacterial activity. Oral administration of the aqueous extracts successfully obliterated *Salmonella* infection in Balb/C mice as revealed by increased survival rate as well as less bacterial load in various vital organs of the treated animals (Owais et al2005).

k) Cardiovascular protection

Withaniasomnifera may be useful as a general tonic, due in part to its beneficial effects on the cardiopulmonary system. *Withaniasomnifera* showed strong cardioprotective effect in the experimental model of isoprenaline-induced myonecrosis in rats. Augmentation of endogenous antioxidants, maintenance of the myocardial antioxidant status and significant restoration of most of the altered haemodynamic parameters may contribute to its cardioprotective effect (Mohantyet al2004).

l) Ashwagandha rejuvenative and reproductive action

Increases libido and sexual function. Supports female reproductive system, and increases ovarian weight and folliculogenesis. Ashwagandha is approved as a greatest rejuvenative herb in Indian Herbal System. Useful in treating arthritis, diabetes and hypertension. Ashwagandha is a potent inhibitor of angiogenesis and it is respected for its phytochemical (Umadevi et al 2012).

Other importance

Ashwagandha improves energy and also memory by enhancing the brain and nervous function; shows anxiolytic effects, has hepatoprotective property, raises hemoglobin level and red blood cell count, improve energy level; has potent antioxidant activity, improve the cell-mediated immunity; promotes vigor and vitality along with cheerful sexual life and reproductive equilibrium and act as powerful adaptogen. Pharmacological research reports on *Ashwagandha* reveal its, Anti-tumor (Harikrishnan et al. 2008). Diseases like TB, chronic upper respiratory diseases and HIV have been added to the list of *Ashwagandha* due to its strong immunostimulatory activity, and it is recognized as a blood tonic, especially in gynecological disorders including anemia and irregular menstruation. Patients with anxiety can also benefit from *Ashwagandha* (Umadevi et al. 2012). Conservation and sustainability of *Ashwagandha* as a medicinal plant reported by (Shinde et al. 2015). Walvekar et al. (2013) studied the Effects of glycowithanolides on lipid peroxidation and lipofuscinogenesis in male reproductive organs of mice.

Conclusion

Present study concluded that *W. somnifera* showed most valuable medicinal properties and it is used in against different effective parameters of human health. *Ashwagandha* is an essential plant in various traditional system of medicine. This root is widely used in the Indian system of medicine as it is or combination with other plants and is used to treat fever, as diuretic, laxative, insomnia, lumbar pain, nervous disorders, asthma, cardiac disorders, psoriasis, marasmus of children, senile debility. Leaves are bitter and recommended in fever, painful swellings, and inflammation of eye. There is huge scope of further scientific research on various therapeutic aspect of this important medicinal plant.

References

- Atal, C. K., Gupta, O. P., Ranghunathan, K. and Dhar, K. L. (1975):** Central Council for Research in Indian Medicine and Homeopathy, New Delhi, India.
- Asthana, R. and Raina, M. K. (1989):** Pharmacology of *Withaniasomnifera*(L.) Dunal-a review. *Indian Drugs*. 26: 199-205.
- Andallu, B. and Radhika, B. (2000):** Hypoglycemic, diuretic and hypocholesterolemic effect of Winter cherry (*Withaniasomnifera*, Dunal) root. *Indian Journal of Experimental Biology*. 3: 607-609.
- Bandyopadhyay, M., Jha, S. and Tepfer D. (2007):** Changes in morphological phenotypes and withanolides composition of Ri-transformed roots of *Withaniasomnifera*. *Plant cell Rep*. 26: 599-609.
- Bhattacharya, S.K., Kalkunte, S.S., Ghoshal. S. (1997):** Antioxidant activity of glycowithanolides from *Withaniasomnifera*. *Indian journal of Experimental Biology*. 35: 236-239.
- Bhattacharya, A., Muruganandam, A. V., Kumar, V. and Bhattacharya, S. K. (2002):** Effect of poly herbal formulation, EuMil, on neurochemical perturbations induced by chronic stress. *Indian J. Exp. Biol.* 40 (10): 1161-1163.
- Bhatnagar, M., Sisodia, S. S. and Bhatnagar. R. (2005):** Antiulcer and Antioxidant Activity of *Asparagus racemosus* WILLD and *Withaniasomnifera* DUNAL in Rats. *Ann. N. Y. Acad. Sci.* 1056: 261-278.
- Chaudary, M. I., Abbas, S., Jamal. A. S. and Atta-ur-Rahman. (1996):** *Withaniaomnifera*- a source of exotic withanolides. *Heterocycles*. 42: 555-563.
- Dhuley, J. N. (1998):** Effect of *Ashwagandha* on lipid peroxidation in stress induced animals. *J. Ethnopharmacol.* 60(2): 173-178.
- Elsakka, M., Grigorescu, E., Stanescu, U., Stanescu, U. and Dorneanu. V. (1990):** New data referring to chemistry of *Withaniasomnifera* species. *Rev. Med. Chir. Soc. Med. Nat. Iasi.* 94(2): 385-387.



- Ghosal, S., Lal, J. and Srivastava, R. (1989):** Immunomodulatory and CNS effects of sitoindosides IX and X, two new glycowithanolides from *Withaniasomnifera*. *Phytotherapy Res.*3: 201-206.
- Gupta, Y. K., Sharma, S. S., Rai, K. and Katiyar. C. K. (2001):** Reversal of paclitaxel induced neutropenia by *Withaniasomniferain* mice. *Indian J. Physiol. Pharmacol.* 45(2): 253-257.
- Harikrishnan B, Subramanian P, SubashS. (2008).** Effect of *Withaniasomniferaroot* powder on the levels of circulatory lipid peroxidation and liver marker enzymes in chronic hyperammonemia. *E-J Chem.* 5:872-877.
- Hepper, F. N. (1991):** In Solanaceae III: taxonomy, chemistry, evolution; Eds. Hawkes, J. G., Lester, R.N., Nee, M., Estrada, E. Royal Botanic Gardens, Kew: UK. 211-227.
- Hemalatha, S., Wahi, A. K., Singh, P. N. andChansouria, J. P. (2006):** Hypolipidemic activity of aqueous extract of *Withaniacoagulans*Dunal in albino rats. *Phytother. Res.* 20 (7):614-617.
- Hindawi, S. H., Al-Khafaji. M. H., Abdul- Nabi. (1992):** Anti-granuloma activity of Iraqi *Withniasomnifera*. *J. Ethnopharmacol.* 37 (2): 113-116.
- Hunziker, A. T. (2001):**Genera Solanacearum: the genera of the Solanaceae illustrated, arranged according to a new system; GantnerVerlag: Ruggell, Liechtenstein.
- Javanshir, K. (2000):**Vegetation of Bashagerd. 156-162.University of Tehran Publication: Tehran, Iran.
- Naidu, P. S., Singh, A. and Kulkarni. S. K. (2006):** Effect of *Withaniasomniferaroot* extract on reserpine-induced orofacial dyskinesia and cognitive dysfunction. *Phytother. Res.*20(2): 140-146.
- Jayaprakasam, B., Zhang, Y., Seeram, N. and Nair, M. (2003):** Growth inhibition of tumor cell lines by withanolides from *Withaniasomniferaleaves*. *Life Sci.* 74(1): 125-132.
- Kapoor, L. D. (2001):**Handbook of Ayurvedic Medicinal Plants. CRC Press: London, UK. 337-338.
- Kumar, A. and Kulkarni S. K. (2006):** Effect of BR-16A (Mentat), a polyherbal formulation on drug-induced catalepsy in mice. *Indian J. Exp. Biol.* 44(1): 45-48.
- Machiah, D. K., Girish, K. S. and Gowda. T. V. (2006):** A glycoprotein from a folk medicinal plant, *Withaniasomnifera*, inhibits hyaluronidase activity of snake venoms. *Comp.Biochem. Physiol. C. Toxicol. Pharmacol.* 143(2): 158-161.
- Marderosion, A. D. (2001):**The Review of Natural Products, Facts and Comparisons; St. Louis, MI, USA. 630-632.
- Mohanty, I., Arya, D. S., Dinda, A., Talwar, K. K., Joshi, S. and Gupta, S. K. (2004):** Mechanisms of cardioprotective effect of *Withaniasomniferain* experimentally induced myocardial infarction. *Basic Clin. Pharmacol. Toxicol.* 94(4): 184-190.
- Owais, M., Sharad, K. S., Shehbaz, A. and Saleemuddin, M. (2005):** Antibacterial efficacy of *Withaniasomnifera*(ashwagandha) an indigenous medicinal plant against experimental murine salmonellosis. *Phytomedicine*12(3): 229-235.
- Panwar, J. and Tarafdar, J. C. (2006):** Distribution of three endangered medicinal plant species and their colonization with arbuscularmycorrhizal fungi. *J. Arid Environ.*65: 337-350.
- Rasool, M. andVaralakshmi. P. (2006):**Immunomodulatory role of *Withaniasomniferaroot* powder on experimental induced inflammation: An *in vivo* and *in vitro* study. *Vascul.Pharmacol.* 44(6): 406-410.
- Rastogi, R. P. and Mehrotra, B. N. (1998):**Compendium of Indian Medicinal Plants; Central Drug Research Institute: New Delhi, India.
- Schonbeck-Temesy, E. and Reching, K. H. (1972):** *Solanaceae*. In Flora Iranicaeds. Reching, K. H. 100:29-26 AkademischeDruck. Verlagsanstalt, Graz.
- Sharma, R. (2004):**Agro-Techniques of Medicinal Plants. 31-33.Daya Publishing House: New Delhi, India.

- Shinde A.** Gahunge P. Rahat R. (2015) Conservation and sustainability of Ashwagandha: a medicinal plant, journal of biological and scientific opinion. 3(2); 94-99.
- Singh, S. and Kumar, S. (1998):***Withaniasomnifera*: The Indian Ginseng Ashwagandha; Central Institute of Medicinal and Aromatic Plants: Lucknow, India.
- Umadevi M., Rajeswari R., Sharmila C. Pushpa R. , Sampath Kumar K.P., Debjit (2012)** The harma innovation traditional and medicinal uses of withania Somnifera ; 102.
- Visavadiya, N. P. and Narasimhacharya, A. V. (2006):** Hypocholesteremic and antioxidant effects of *Withaniasomnifera*(Dunal) in hypercholesteremic rats. *Phytomedicine*.
- Warrier, P. K., Nambiar, V.P.K. and Ramankutty, C. (1996):**Indian Medicinal Plants: A Compendium of 500 species. 5:409. Orient Longman: Hyderabad, India.
- Walvekar M, Shaikh N. Sarvalkar P. (2013)** Effects of glycowithanolides on lipid peroxidation and lipofuscinogenesis in male reproductive organs of mice, Iran J Reprod Med Vol. 11. No. 9. pp: 711-716
- Zhao, J., Nakamura, M., Hattori, N., Kuboyama, T., Tohda, C. and Komatsu, K. (2002):**Withanolide derivatives from the roots of *Withaniasomnifera*and their neurite outgrowth activities. *Chem. Pharm. Bull. (Tokyo)*. 50(6): 760-765.
- Ziauddin, M., Phansalkar, N., Patki, P., Diwanay, S. and Patwardhan. B. (1996):** Studies on the immunomodulatory effects of ashwagandha. *J. Ethnopharmacol.* 50(2): 69-76.



MSG (Monosodium Glutamate) induced male gonadal lesions and reproductive disabilities in vertebrate model *Mus musculus*.

¹Gondil K. A., ²Kusarkar S. P., ³Babar K. K., ⁴Kasar P. M., ⁵Bhivate S. B. and ⁶Kamble N. A.

^{1,2,3,4,5} Research student, Department of Zoology, Shivaji University, Kolhapur.

⁶ Associate Professor, Department of Zoology, Shivaji University, Kolhapur.

KEYWORDS

Mus musculus, Monosodium Glutamate, Reproductive system, Histology

Corresponding Author
Email

drkmitinkumar@ediffmail.com

ABSTRACT

Oral administration of Monosodium Glutamate (MSG) has been reported to have adverse effects on various organs of experimental animals and can lose appetite control. Since decades MSG was widely used as flavour enhancer especially in Chinese meal. Chronic consumption of MSG showed pathological disturbances along with some metabolic alterations. For present investigation the healthy animals were divided into 5 groups. Group 1st is control group, while remaining 4 groups were treated with MSG (80mg/100gmBW/day). Animals from all groups were sacrificed according to CPCSEA guideline and gonadal tissue was taken for histological investigation. Alterations and changes in male gonadal tissues were interpreted with reference to reproductive physiology and capacitation of sperm

Introduction

Monosodium glutamate (MSG) is known as sodium salt of glutamic acid (Eweka, 2007), commonly known as ajjinomoto. It was documented that ajjinomoto interfere in the metabolic reactions, (IFIC, 1994). In most of the cases MSG found to be in canned and packed food (John, 2006). Chemically MSG consisting of about 78% of glutamic acid and 22% of some ionic concentration as sodium and water (Samuels, 1999). Modern commercial MSG has its origin from most of fermented reaction which are carbohydrate oriented. Scientists have reported that excess utilization of MSG and MSG derived products leads to chronic or acute effect in animal cell (Egbuonu, 2009). Experimentally it was proved and documented that higher concentration of MSG can cause symptoms like numbness, sweating, dizziness and in acute conditions neurological problems also.

Biodunet et. al., (1993) has documented that MSG has severe toxicological impact regarding neuropathology in most of the vertebrate species including human being. According to Swelim (2004), MSG can cause photo degenerative ability in the retinal cells of the experimental animal with the relevant symptoms. Onakewhor, (1998), has reported that as per chronic or acute doses of MSG spermatogenic cells were destructed in male wistar rat. The infertility, degeneration of cells with haemorrhage in the gonadal cells was documented by Oforofuoet. et. al. (1997). Onakewhoret.et.al. (1998), documented azoospermic and aspermic condition caused due to higher accumulation of MSG in gonads of experimental animal. As reproduction is one of the important phenomenon in organisms, were functioning of male gonads critically responsible for spermatocytic activity, taking account of available literature and documentation, we have decided to find out the impact

of MSG on testicular content of male gonadal cells against experimental model as *Mus musculus*.

Material and Methods

For present case study 20 adult's experimental animal *Mus musculus* were selected. Animals breed and reared in the departmental animal house under maintained temperature (24-28°C) and humidity. The animals were kept in animal house. All the animals were feed by standard food pellets and provided with drinking water add libitum. All animals were kept in cleaned and aerated cages and standard protocols were adapted for to carry out experimental procedure.

After maturity of experimental animal *Mus musculus* (average 6 months period) healthy animals were segregated and selected. The adults were grouped in 5 groups as control and experimental 1, 2, 3 and 4 respectively. Controlled animals were feed and reared with normal diet and water. While experimental animals were treated against predetermined dose of MSG for 30 days, 45 days, 60 days and 75 days respectively.

After completion of exposure period and intoxication by respective dose animals from experimental groups were sacrificed by cervical dislocation. As the present investigation aimed for, find out testicular pathology, so testicular sac was dissected out and applied for normal histological technique. For histopathological assessment the testicular slides were subjected to standard Haematoxylene – Eosin staining technique. Slides were observed under the microscope. As per the dose dependent exposure period section were interpreted for testicular anomalies and reproductive inabilities. Finally results were comparatively interpreted in relation to find out attractions in physiology of reproduction and development.

Group	Control	Exp 1	Exp 2	Exp 3	Exp 4
No.of Animals	4	4	4	4	4
Dose	-	80mg/ 100gm /day	80mg/ 100gm /day	80mg/ 100gm /day	80mg/ 100gm /day

Result and Discussion

Ultrastructure of male gonadal cells in the control

Morphological study of male reproductive tract of experimental animals showed matured gonadal part as testes. Sectional view reviled normal architecture of seminiferous tubules. H.E. stained seminiferous tubules showed peripheral boundary tissue with basal lamina. Microscopically tubules were found lined with spermatogenic cells. In matured gonadal cells we found a differentiation of spermatocytic cells. Some of the cells were darkly stained and showed marked morphometric variation as globular and polygonal cells. We found some of the intratubular connective tissue in between the adjacent seminiferous tubules. Major microscopic observation noted were sequentially arranged male gamatogenic cells upto maturity of the spermatid. Histological spermatogenic cells were numerously arranged as, spermatocyte at the centre of tubule indicating active spermatogenesis in the non-treated animal. Similar kinds of observation were documented by Mohamed, (2012). Alalwani (2013) document normal spermatogenesis in the varied steps after maturity in the control animals.



Fig - A Testes of Mice

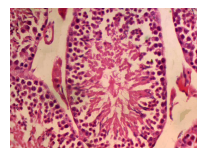


Fig- B (Control Section, H-E, X 400)

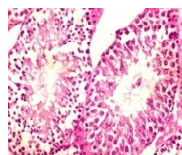


Fig - C (30 days, H-E, X 400)

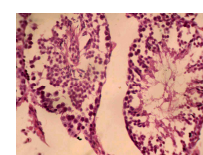


Fig -D (45 days, H-E, X 400)

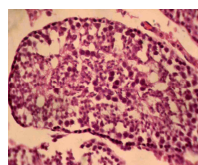


Fig - E (60 days, H-E, X 400)

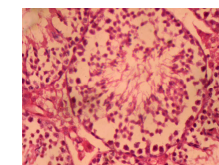


Fig - F (75 days, H-E, X 400)



Testicular pathology against MSG dose

In present investigation we found that male gonadal cells of experimental model *Mus musculus* showed deteriorating effect in MSG exposed animals up to 75 days. As per the exposure period 30, 45, 60 and 75 days we found sequential and stepwise degeneration of spermatocytes and ruptured basement membrane in the gonadal cells. Gonadal sections showed interrupted lining of connective tissue and interstitial cells. Marked changes were observed after 75 days exposed animals with damaged sertoli cells, degenerated leydigs cells. Germinal cells were found depleted with immature spermatid, spermatozoa in the tubular lumen fig. B, C, D, and E respectively. Similar kinds of results were documented by Das et.al, (2010). Our result coincides with Nayanatara et. al, (2008) where they documented severe damage and cellular necrosis in the gonadal cells. Mohamed (2012) documented that heavy damage in germinal cells against MSG dose applied for short and long term to assess male gonadal cells of rat. Farmobi et. al, (2006) also documented gamatogenic toxicity against MSG dose in gonadal cells of experimental rat.

With the above observation, we found that depending upon exposure period and induction of MSG the male gonadal cells of *Mus musculus* were became less potential regarding fertility. Animals were found less potential to fertilize ovum or egg as they have changed the mating behaviour. Experimentally conclude, that higher consumption of ajinomoto can alter and interfere the gametogenesis and maturation of sperm in experimental model of *Mus musculus*. The major change we found inactivity and sluggishness leading to harmful effect on the reproductive behaviour and potential of animals. Indicating MSG as a toxic component in the food content if gets abused.

Acknowledgement

We are thankful to the Head, Department of Zoology, Shivaji University, Kolhapur for providing facility to carry out present work.

References

- Eweka O. (2007).** Histological studies of the effects of Monosodium glutamate on the kidney of adult Wistar rats. *Internet J health*; 6:2.
- IFIC (1994),** Review of monosodium glutamate, examining the myths.
- Samuels S. (1999).** The toxicity/safety of MSG: a study in suppression of information. *Account Res*; 6(4):259-310.
- Moze S, Sefcikova L, Lenharde Z, Raek L. (2004).** Obesity and changes of alkaline phosphatase activity in the small intestine of 40-80 day old subjects to early postnatal overfeeding of Monosodium Glutamate. *Physiol Res*; 53:177-86.
- Ejbbuonu A, Obidoa O, Ezeokonkwo C, Ezeanyika L, Ejikeme P. (2009).** Hepatotoxic effects of low dose oral administration of Monosodium Glutamate in male albino rats. *Afr J Biotechnol*; 8:3031-5.
- Biodun D, Biodun A. (1993).** Spice or poison? Is Monosodium glutamate safe for human consumption. *Natl Concord*; 4:5.
- Onakewhor J, Oforofuo I, Singh S. (1998).** Chronic administration of Monosodium Glutamate induces oligozoospermia and glycogen accumulation in Wistar rat testes. *Afr J Reprod Health*; 2(2):190-7.
- Oforofuo O, Onakewhor J, Idaewor P. (1997).** The effect of chronic administration of MSG on the histology of adult Wistar rat testes. *Biosci Res Commun*; 9:2.
- DasR, Ghosh S. (2010).** Long-term effect of monosodium glutamate on spermatogenesis following neonatal exposure in albino mice- a histological study. *Nepal Med Coll J*; 12:149-53.
- Nayanatara A, Vinodini N, Damadar G, Ahemed B, RamaswamyC, Shabarinath M, Bhat M, (2008).** Role of ascorbic acid in monosodium glutamate mediated effect on testicular weight sperm morphology and sperm count in rat testis. *J Chain Clin Med*; 3:1-5.

Mohamed IK (2012). The effects of oral dosage of monosodium glutamate (MSG) applied for short- and long-term on the histology and ultrastructure of testes of the adult rats. *J Anim Vet Adv*; 11(1):124-33.

Farmobi E, Onyema O. (2006). Monosodium glutamate-induced oxidative damage and genotoxicity in the rat modulatory role of vitamin C, vitamin E and quercetin. *Hum Exp Toxicol*; 25:251-9.

Swelim (2004). MSG can cause photo degenerative ability in the retinal cells of the experimental animal with the above symptoms. *Egypt J Med Lab Sci*. Volume 13, 45-71.



Histopathological study of Etova P-400 on liver and kidney of *Mus musculus*

¹Tushar Kakade ²Sanindhar Gaikwad and ³Rajan More

¹Research Scholar, Department of Zoology, Yashwantrao Chavan Institute of Science, Satara- 415 001

^{2*}Assistant Professor, Department of Zoology, Eknath Sitaram Divekar College, Varvand-412 215

³Assistant Professor, Department of Zoology, Yashwantrao Chavan Institute of Science, Satara- 415 001

KEYWORDS

Etova P- 400,
Histopathology,
Mus musculus,
Liver, Kidney

Corresponding Author
Email

sanindhargaikwad@rediffmail.com

ABSTRACT

Etova P- 400 is one of the well-known drugs from NSAIDs. It acts as anti-inflammatory and pain relifant. However, it's over consumption or prolonged consumption showed severe histopathological conditions on the organism's body. So in order to build up reliable understanding about the impact of Etova P- 400 on the body of organism present investigation was carried out. It showed hampered liver and kidney cell architecture with number of histopathological conditions. It showed severe impact on the body physiology of the treated organisms.

Introduction

Non-steroidal anti-inflammatory drugs (NSAIDs) are widely used in treatment of minor pain and for the management of oedema and tissue damage resulting from inflammatory joint disease like Arthritis (Nikose et al., 2015). Etova P-400 is one of the well known non steroidal anti-inflammatory drug (NSAID) with combination of paracetamol i.e. diclofenac and paracetamol (Lapeyre, et al., 2006). It is widely used as an analgesic, antipyretic drug (Hargus et al., 1995).

The chief mechanism by which the NSAIDs reflect their therapeutic effects is inhibition of prostaglandin (PG) synthesis (Cooke and Scudamore, 1998). They competitively inhibit Cyclooxygenases (COXs), the enzymes that catalyse the synthesis of cyclic endoperoxides from arachidonic acid to form prostaglandins (Gulsen et al., 2003). Two COX isozymes have been well identified: COX-1 and COX-2 in this concern. COX-1 is continuously synthesized in body and present in all types of tissues and cells.

Thus it is important for the production of prostaglandins and helps in homeostatic maintenance (Zvaifler, 1988). Inhibition of COX-1 activity is considered a major contributor to NSAID GI toxicity (Ebaid, 2013). COX-2 is considered an inducible isozyme, and plays an important role in pain and inflammatory processes. So these drugs are very effective for treating the inflammatory and painful reactions in the organism's body.

However, drugs used as NSAIDs were well known to cause variety of adverse effects on body at long term exposure (E-Banhawy et al., 1993). They can causes severe histopathological effects like necrosis, vacuolation, enlargement of nucleus and shifting of nucleus etc. Several non steroidal anti-inflammatory drugs have been reported with liver and kidney damage (Hasan, 2015).

Similarly Etova P-400 is also assumed as one of the leading pain relifant, anti-inflammatory drug, but its overconsumption is considered to be disadvantageous.

It also causes severe pathological conditions like kidney and liver damage.

Therefore by keeping in view above scenario, the present investigation was carried out to assess histopathological effects of Etova P-400 on mice liver and kidney at chronic exposure level.

Material and Methods

For present investigation, healthy adult male mice of 22 weeks were used (Fig. 1). They made available from Arvind Gavali College of Pharmacy, Jaitapur, Satara (MS), India. For experimentation purpose mice were divided into three groups Viz; A, B and C. Group A was treated as Control group and remaining were treated as experimental ones. Dose concentrations of 10 and 20, mg/ml/mice were administered intra- peritoneally to B and C groups respectively. Experimentations were repeated for four weeks and then the animals were sacrificed.



Fig. 1: - Experimental animal *Mus musculus* with its Intraperitoneal region.

CAF was used for the fixation of tissue. Tissues were embedded in paraffin wax and used for sectioning. Sections of 5 micron were used for histological observations. Haematoxyline Eosin technique was used for the histopathological assessment. For better illustration slides were observed under light microscope at 10x and 45x Magnifications.

Result and Discussion

During experimentation Etova P-400 showed its

adverse histopathological effects over the liver and kidney tissues. In control group animals liver cells and kidney cells appears to be normal and healthy as mentioned in Plate 1.

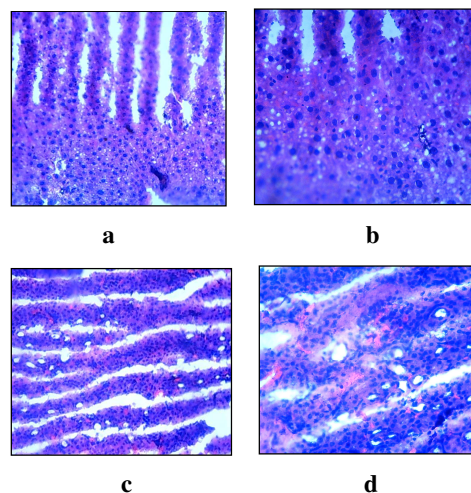


Plate 1- showing control group animal's histological sections with normal cellular architecture-

- Section of liver with 100 X magnification showing normal liver lobule
- Section of liver with 4000 X magnification showing central and small sized nucleus.
- Section of Kidney with 100 X magnification showing normal cell structure.
- Section of Kidney with 4000 X magnification showing central and small sized nucleus.

While experimental group showed altered histological sections with vacuolation, cell necrosis along with enlargement and shifting of nucleus from centre to the periphery.

According to experimentation it was noticed that administration of Etova P-400 for 10 mg/ml/mice showed histopathological changes like cell necrosis due to which cell death takes place. The nucleus is shrunk due to drug activity and is stained dark in color & appearance of shape is smaller. Formation of vacuole takes place in the tissue. Enlargement in nucleus is prominent, which may be due to condensation of chromatin material and formation of fragments. Shifting of nucleus takes place from centre to its periphery. There is condensation of chromatin with can undergo apoptosis, it is followed by Karyorrhexis (Plate 2).

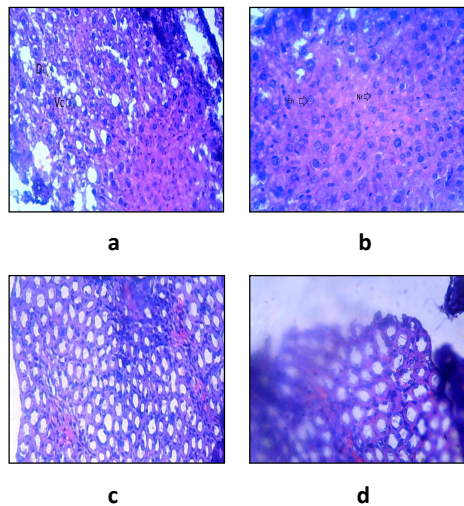


Plate 2- showing experimental group animal's histological sections treated with 10/mg/ml/mice dosage.

- Section of liver with 100 X magnification showing abnormal vacuolation.
- Section of liver with 4000 X magnification showing enlarged nucleus with cell necrosis.
- Section of Kidney with 100 X magnification showing enlarged vacuolation.
- Section of Kidney with 4000 X magnification showing displaced nucleus with necrosis. (En- Enlargement of Nucleus, Nr- Necrosis, Vc- Vacuolation, D- Displacement of Nucleus from periphery)

At 20 mg/ml/mice dosage the liver lobules showed major vacuolation with enlarged nucleus shifted towards the periphery. It may be followed by apoptosis. Kidney cells also showed similar line of cellular histopathology (**Plate 3**).

In this study, the effect of Etova p-400 on liver and kidney has toxic effect with increased period after the recommended dosage. The use of Etova p-400 for prolonged period causes necrosis. Similar lines of results were also noticed by Abdul et al., (2016) for Cranberry extract induction with Diclofenac sodium on rat liver and kidney. Vacuolation of the cytoplasm of the liver and kidney cells appeared at first in the hepatocytes of the peripheral zone of the hepatic lobules, extending gradually toward the center.

This may be due to the direction of the lobular blood supply as mentioned by Ramnathan et al., (2013) for Zaltoprofen induction to rat liver lobules. Amer et al., (1998) also mentioned similar histopathological observation for eimerian toxication to rabbit liver lobules. Nucleomegali i. e. Enlargement of nucleus and shifting of nucleus from centre to the periphery was also observed. Results confirm the toxicity of excessive consumption of Etova P- 400 for longer duration over the liver and kidney. So it must be utilized with safe exposure limit and for limited duration to avoid the chronic toxicity.

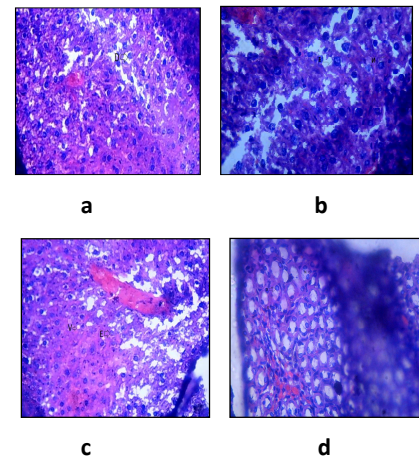


Plate 3- showing experimental group animal's histological sections treated with 20/mg/ml/mice dosage.

- Section of liver with 100 X magnification showing major vacuolation.
- Section of liver with 4000 X magnification showing enlarged nucleus with cell necrosis.
- Section of Kidney with 100 X magnification showing major vacuolation.
- Section of Kidney with 4000 X magnification showing displaced nucleus with necrosis. (En- Enlargement of Nucleus, Nr- Necrosis, Vc- Vacuolation, D- Displacement of Nucleus from periphery)

Conclusion

During experiment an adverse effect of Etova P-400 on liver & kidney of mice shows histopathological changes like Necrosis, Vacuolation, Nucleomegalii, Pyknosis which proves it as dreadful toxicant when consumed for prolonged duration at high dosage. However, a novel observation like shifting of nucleus from centre to periphery has been observed in this experiment, which can't be interpreted properly. So it requires more deep study and experimental work for determining the reasons for shifting of nucleus.

Acknowledgement

The authors are thankful to Principal and Head Department of Zoology, Y. C. I. S. Satara, Principal and Head Department of Zoology, E. S. Divekar College, Varvand for providing infrastructure and laboratory facilities for commencement of this work.

References

- Abdul-Maksoud A. H., Mohammed A. H., Naglaa A. E. K. G. and Mahmoud R. A., (2016):** Hepatoprotective Effects of Cranberry Extract against Diclofenac Sodium Induced Liver Toxicity in Rats, *Inter. J. Pharma. Sci.*, 6(2): 1447-1453.
- Amer M. A., Elewa F. H., El-Shershaby A. M. and Abdel-Azia A. M., (1998):** Histopathological and histochemical effects of eimerian infection on the host tissues: liver of rabbit, *Egypt. J. Zool.*, 31: 1-43.
- Cooke J. D. and Scudamore R. A., (1989):** Studies on the pathogenesis of rheumatoid arthritis. *Br. J. Rheumatol.*: 28: 243.
- E-Banhawy M. A., Sanad S. M., Sakr S. A., El-Elaimy I. A. and Mahran H. A., (1993):** Histopathological studies on the effect of the anticoagulant rodenticide "Brodifacoum" on the liver of rat, *J. Egypt. Ger. Soc. Zool.*: 12(C):185-227.
- Gulsen A., Alparsalan G., Meral O., Ekerem C., Nermin K. and Osman G., (2003):** Histopathologic Changes in Liver and Renal Tissues Induced by Different Doses of Diclofenac Sodium in rats, *Turk. J. Vet. Ani. Sci.* 27: 1131-1140.
- Hargus S. J., Martin B. M., George J. W. and Pohl L. R., (1995):** Covalent modification of rat liver dipeptidyl peptidase IV (CD 26) by the non-steroidal antiinflammatory drug Diclofenac, *Chem. Res. Toxicol.*: 88: 993-996.
- Hasan M. A. A., (2015):** Toxic And Histopathological Changes of harmful Effect of Diclofenac Sodium on Some Loose Organs in Albino Rats for Twelve Weeks, *J. Med. Sci. Chem. Res.*, 3(3): 4694-4702.
- Ebaid M. A D., Mohamed A. D., Amany T. and Mohamed G., (2013):** Piroxicam-induced hepatic and Renal Histopathological Changes in mice, *Libyan. J. Med.*: 82-88.
- Lapeyre M. M., De-Castro A. M., Bareille M. P., Del-Pozo J. G., Quejejo A. A., Arias L. M., Montastruc J. L. and Carvajal A., (2006):** Non-steroidal anti-inflammatory drug related hepatic damage in France and Spain: analysis from national spontaneous reporting systems, *Fundam. Clin. Pharmacol.*, 20(4): 391-395.
- Ramanathan S., Salem S. R. and Kazhumaram V. P., (2013):** Zaltoprofen induces histological changes in albino rat liver, *Eur. J. Anat.*, 17(2): 123-126.
- Nikose S., Arora M., Singh P. K., Naik S., Khan S. and Nikose S., (2015):** Hepatotoxicity and Changes in Liver Enzymes Due To Use Of Non-Steroidal Anti Inflammatory Drugs (NSAIDs) in Non-Traumatic Musculoskeletal Painful Disorders *PubMed Journals*, 1: 2-3.
- Zvaifler N. J., (1988):** New perspectives on the pathogenesis of rheumatoid arthritis. *Am. J. Med.*: 85:12.



Use of Agrochemicals in the Management of *Sesamum* Blight Caused by Bavistin Resistant *Alternaria sesami*

A. B. Patil and S. S. Kamble.

Mycology and Plant Pathology Research Laboratory,
Department of Botany, Shivaji University, Kolhapur. 416 004

KEYWORDS

Alternaria sesami, Bavistin, agrochemicals, resistant, *Sesamum indicum*.

Corresponding Author
Email

patilashvini1977@gmail.com

ABSTRACT

There was large variation in the MIC of bavistin among the 34 isolates of *Alternaria sesami* causing *Sesamum* blight on the Czapek Dox agar plates and also on *Sesamum indicum* plants. MIC on agar plates ranged from 18 to 51% while it was 10 to 25% on *Sesamum* plants. Isolate As-14 was highly resistant. Use of bavistin in mixture with agrochemicals, such as fungicides (Roko, Stargem, Tagron, Kocide and Caviet) controlled the growth of pathogen on agar plates and completely prevented the infection of pathogen on *S. indicum* plants suggesting the reduction in resistance. Among the fungicides used Stargem, Caviet and Kocide at 25 ppm along with Bavistin 25% gave 100% PCE.

Introduction

Sesamum indicum L. is ancient oil seed crop belongs to family pedaliaceae. It is having different vernacular names like gingelly, simsim, ajonjoly, sesamo and til. Sesame is originated in Africa and later on spread to West Asia to India, China and Japan. According to Agro crops reports (2016) India's annual average production covers 7,15,000 metric tons contributing around 23% of the world's total sesame production. In last decade production of sesame in India has been declining due to number of bacterial, fungal, mycoplasma and viral disease. Out of which leaf blight of sesame caused by *Alternaria sesami* is destructive one which causes the loss of yield up to 30-40% (Laj *et al.* 2007). Naik *et al.* (2003) reported that 80% loss of sesame yield by *Alternaria sesami* infection. In present investigation efforts were made to manage the disease by using bavistin but it required very large quantity. Therefore agrochemicals were

used to study on the development of bavistin resistance in *A. sesami*.

Material and Methods

Sensitivity of 34 isolates of *Alternaria sesami* to bavistin was determined by food poisoning technique (Dekkar and Gielink, 1979). Synergistic effects of agrochemicals on development of bavistin resistant *A. sesami* (As- 14) were studied by mixing different fungicides (Stargem, Roko, Tagron, Caviet and Kocide) with 4 different concentration (25,50,75, 100 ppm) with bavistin.

For *in vitro* studies fungicides were mixed with bavistin (51%) at different concentration in CDA medium. A 6 mm disc of resistant isolate As-14 was inoculated on the CDA plate and radial mycelial growth was measured after 15 days. Bavistin alone served as control. For *in vivo* studies above fungicides were applied on healthy *S. indicum* plants in different concentrations along with bavistin (25%). with bavistin served as control.

On these plants 10 ml mycelia suspension (10⁶ spores) of resistant isolate As-14 was inoculated. These plants were kept under observation for 10 days. The plants treated only with bavistin served as control.

Percentage Control Efficacy (PCE) of the agrochemicals was calculated by using following formula.

$$PCE = (1 - X / Y)$$

Where,

X- The diameter of the lesion on fungicides treated.

Y- The diameter of lesion on untreated control (without any fungicide / agrochemicals).

Results and Discussion

All fungicides controlled the growth of resistant pathogen As-14 at 100 ppm but stargem completely inhibited the growth of pathogen at 75 ppm concentration on agar plates. In *in vivo* studies showed that all fungicides except roko were effective against the disease and prevented As-14 infection on sesame plants (Table -1). From Table -2 it is clear that PCE of stargem was 100% at 75 ppm (*in vitro*). In *in vivo* bavistin (25 %) with stargem, caviet and kocide at 25 ppm gave 100 % PCE.

Table –1: Synergistic effect of other fungicides on the development of bavistin resistance in *A. sesami* (*in vitro* and *in vivo*).

Sr. No.	Fungicides with bavistin (51%)	Concentration (ppm)	Radial growth (mm)	Percentage of Infection
1.	Roko(Thiophanate methyl 70%)	25	19.66	20.00
		50	17.66	18.00
		75	17.00	10.00
		100	16.33	00.00
2.	Stargem(Mancozeb-88.23%)	25	14.33	00.00
		50	11.33	00.00
		75	00.00	00.00
		100	00.00	00.00
3.	Tagron(Metalaxyl-35%)	25	20.66	10.00
		50	16.66	00.00
		75	13.33	00.00
		100	10.00	00.00
4.	Kocide(Copper hydroxide -53.8%)	25	15.66	00.00
		50	12.66	00.00
		75	12.00	00.00
		100	09.33	00.00
5.	Caviet (Tebuconazole-25%)	25	15.66	00.00
		50	12.33	00.00
		75	12.00	00.00
		100	11.00	00.00
6	Control Bavistin alone (51%)		09.66	12.00

According to Grabski and Gisi (1987) synergistic interaction among fungicides is another way to reduce selection for fungicide resistant isolate. Couch and Smith (1991) reported that synergistic action of fungicides prevented the infection of *Pythium aphanidermatum* on perennial ryegrass.

More (2009) reported that Tilt with Mancozeb, Zineb,

Captan and Roko inhibited by *Phakopsora pachyrhizi* causing rust of soybean. Carbendazim along with other fungicides (Kavach, Mancozeb and Ridomil) completely inhibited growth of resistant isolate of *Alternaria alternata* (Fries) Keisler causing leaf spot of gerbera (Sutar, 2010). According to Bhale (2002) benomyl in combination with captan and carbendazim completely inhibited the growth of



Fusarium oxysporum causing wilt of spinach. Waghmare (2010) reported that carbendazim with other fungicides inhibited the growth of *Alternaria alternata* causing leaf spot of rose. Similar types of results were also reported by other workers in different pathogens (Bharade, 2002; Telmore, 2004; Patil, 2009 and Andoji, 2016).

Acknowledgment

Authors are grateful to Head, Department of Botany, Shivaji University, Kolhapur for providing necessary laboratory facilities.

Table –2: Percentage Control efficacy (PCE) of fungicides in controlling the bavistin resistant isolate of *A. sesami* (*in vitro* and *in vivo*).

Sr. No.	Fungicides with bavistin	Concentration (ppm)	PCE <i>in vitro</i>	PCE <i>in vivo</i>
1.	Roko	25	78.15	80.00
		50	80.37	82.00
		75	81.11	90.00
		100	81.85	100.00
2.	Stargem	25	84.07	100.00
		50	87.41	100.00
		75	100.00	100.00
		100	100.00	100.00
3.	Tagron	25	77.04	90.00
		50	81.48	100.00
		75	85.18	100.00
		100	88.88	100.00
4.	Kocide	25	82.6	100.00
		50	85.93	100.00
		75	86.66	100.00
		100	89.63	100.00
5.	Caviet	25	82.6	100.00
		50	86.00	100.00
		75	86.66	100.00
		100	87.77	100.00
6.	Control Bavistin alone		89.26	88.00

References

Muley DV, Mane UH (1987). Endosulfan induced changes in oxygen consumption in two species of freshwater lamellibranch molluscs. *J. Environ. Biol* 5(1): 28-33.

Andoji YS (2016) Management of chickpea Root Rot. Ph. D. Thesis, Shivaji University Kolhapur.

Bhale UN (2002) Studies on management of some important diseases of spinach in Maharashtra. Ph.D. Thesis, Dr. Babasaheb Ambedkar Marathawada University, Aurangabad.

Bharade SS (2002) Studies on management of fruit rot of pomegranate. Ph. D. Thesis, Dr. Babasaheb Ambedkar, Marathawada University, Aurangabad.

Couch HB, Smith BD (1991) Synergistic and antagonistic interactions of fungicides against *Pythium aphanidermatum* on perennial ryegrass. *Crop. Prot.* 10: 386-390.

Dekker J, Gielink AJ (1979) Acquired resistance to pimaricin in *Cladosporium cucumerinum* and *Fusarium oxysporum f. sp. narcissi* associated with decreased virulence *Nath. J. P 1. Path.* 85:67-73.

Grabski C, Gisi U (1987) Quantification of synergistic interactions of fungicides against *Plasmopora* and *Phytophthora*. *Crop. Prot.* 6:64-71.

More SB (2009) Studies on management of soybean rust
Ph.D.Thesis, Shivaji University, Kolhapur.

Patil VB (2009) Studies on management of charcoal rot of sweet potato. Ph.D. Thesis, Shivaji University, Kolhapur.

Sutar M (2010) Studies on chemical management of leaf spot of Gerbera. M. Phil Dissertation, Shivaji University, Kolhapur.

Telmore KM (2004) Studies on management of some important diseases of Betelvine. Ph. D. Thesis, Dr. Babasaheb Ambedkar Marathwada University, Aurangabad (M. S.).

Waghmare MB (2010) Studies on management of some important diseases of rose. Ph.D Thesis, Shivaji University, Kolhapur.



Effect different pH levels on the growth of *Colletotrichum capsici* (Syd E J Butler & Bisby) causing anthracnose disease

M.S.Sutare

YPSC Solankur Tal Radhanagari Dist Kolhapur

KEYWORDS

Anthracnose,
Colletotrichum capsici,
medicinal plant ,pH.

Corresponding Author
Email

raj_rbm_raj@yahoo.co.in

ABSTRACT

Effect of different pH levels were tested *in vitro* condition against the growth of pathogenic fungi *Colletotrichum capsici* causing anthracnose disease to medicinal plants. pH is important physical parameter affecting growth of fungi. Therefore, different pH levels were studied. Among the different media (PDA), with different pH levels, the host leaf supported the maximum growth and sporulation of fungal mycelium at pH 6. Whereas, most acidic and alkaline pH was found to be inhibitory for fungal mycelial growth.

Introduction

Several plants are the major source of natural medicines. They are used in various systems of medicines i.e. Ayurveda, Unani. But due to contamination fungal pathogens, these plants reduce their medicinal value. Kareppa BM (2004). Therefore, the pH as a physical factor responsible for the growth of fungal pathogens was studied.

Materials and methods

Effect of pH on growth of fungal pathogens: The effect of pH on growth of fungal pathogens was determined by the method given by Manjunath et al, (2010). In this method, Potato Dextrose Agar (PDA) media of seven different pH i.e. 4, 5, 6, 7, 8, 9 and 10 were prepared. The pH of media was adjusted by adding drops of 1 N hydrochloric acid (HCL) and 0.1 % sodium hydroxide (NaOH). The sterilized media of different pH levels were poured in sterilized petriplates in about 20 ml quantities and allowed to solidify in triplicate.

The 5 mm pure culture disc of pathogens i.e. *Alternaria alternata*, *Colletotrichum capsici*, *Colletotrichum dematium*, *Drechslera speciferum* and *Phoma vasicae* was inoculated with the help of cork borer of 5mm diameter in the center of solidified PDA media aseptically. These plates were incubated at room temperature for 9 days. The growth of fungal pathogens was measured in millimeter.

Experimental Results

The mycelial growth of *Colletotrichum capsici* (Syd E J Butler & Bisby) was measured up to 9th day of incubation period. There was no growth on 1st day of incubation from 4 to 10 pH. On 2nd, 3rd, 4th, 5th, 6th, 7th, 8th, 9th day mycelial growth was 2, 4, 7, 13, 20, 34, 43, and 49 mm respectively. The pH 5 shows mycelial growth on 2nd was 1 mm, on 3rd day– 4mm, on 4th day –9mm, on 5th day–24mm, on 6th day– 35mm, on 7th day – 48mm, on 8th day–58 mm and on 9th day–66 mm. The 6 pH shows mycelial growth on 2nd, 3rd, 4th, 5th, 6th and 7th day i.e. 8, 18, 38, 59, 78 and 90 mm

respectively. At 7 pH 00, 4, 10, 22, 30, 43, 58, 68 and 73 mm mycelial was observed on 1st, 2nd, 3rd, 4th, 5th, 6th, 7th, 8th and 9th day respectively. The pH 8 shows mycelial growth as on 2nd day it was 3 mm, on 3rd day-14 mm, 4th day-27 mm, 5th day-38mm, 6th day-45 mm, 7th day-58 mm, 8th day-63 mm and on 9th day it was 68 mm. The media of pH 9 shows mycelial growth on 2nd, 3rd, 4th, 5th, 6th, 7th, 8th and 9th day i.e. 00, 3, 9, 18, 24, 32, 41, 53 and 66 mm respectively. The mycelial growth was noted i.e., 3, 6, 13, 29, 39, 48, 55 and 65 mm on 2nd, 3rd, 4th, 5th, 6th, 7th, 8th and 9th day, respectively at pH 10.

The above results indicates that most favorable pH for the growth of *Colletotrichum capsici* was 6 pH. Below 6 and above 7 pH the growth of *Colletotrichum capsici* constantly decreased as shown in shown in table.

The above results clearly indicates that most favourable pH for growth of *Alternaria alternata* (Fr.Keissler) was 7. It also shows that the mycelial growth increased up to pH 7 and afterwards decreases up to pH 10. as shown in table 1.

Table 1: Effect of different pH values on the growth of *Colletotrichum capsici*.

pH	Growth (mm)								
	Incubation period (days)								
	1	2	3	4	5	6	7	8	9
Control	0	3	6	22	30	43	62	80	90
4.0	0	2	4	7	13	20	34	43	49
5.0	0	1	4	9	24	35	48	58	66
6.0	0	8	18	38	59	78	90	90	90
7.0	0	4	10	22	30	43	58	68	73
8.0	0	3	14	27	38	45	58	63	68

Discussion

Philomena (1980), studied the effect of pH and other parameters on the growth of fungi from Irish coastal waters. They reported that slightly acidic medium enhanced the growth of fungal pathogens viz. *Alternaria sp*, *Cladosporium herbarum*, *Dendryphiella saling*, *Monodictys pelagica*, *Stachybotrys atra* and *Zalerion maritimum*. Farooqi, et. al, (1985) also observed influence of pH on the growth of *Alternaria citri* on citrus fruit juice. They found that the fruit juice having pH 4 shows rapid growth of fungi i.e. *Alternaria citri*.

References

- Farooqi WA, Malik MA., Shaukat GA, MS Ahmad (1985).** Influence of pH on the growth of *Alternaria citri* on citrus fruit juice. Proc. Fla. State ort. Soc. 98: 214-215.
- Kareppa BM, (2004)** Studies on fungal diseases of cultivated medicinal plant in Marathwada region of Maharashtra. “National Conference on Biotechnological approaches towards the integrated management of crop diseases”, held at Dr. B.A.M. Uni. Aurangabad. 30 July, 2004. : 77.
- Manjunath,H, Nakkeeran S, Raguchander T, Anand, T, Samiyappan R (2010).** Effect of Environmental conditions on growth of *Alternaria alternata* causing leaf blight on Noni. World J. of Agri Sci. 6 (2): 171-177.
- Philomena, MTC (1980).** The effect of temperature, pH, light and dark on the growth of fungi from Irish coastal waters. J. Mycologia. 22 (2): 350-358.



Sustainable capability of carbendazim resistance *Alternaria alternata* causing leaf spot *Aloe vera* in the mixed population.

M.B.Waghmare

Department of Botany, The New College, Kolhapur

KEYWORDS

Alternaria alternata , *Aloe vera* , Carbendazim , Sustainable.

Corresponding Author
Email

drmahendrawaghmare@gmail.com

ABSTRACT

Aloe vera is commonly growing xerophyte .Now days it is affected by number of fungal diseases. Among all leaf spot is most common fungal disease caused by *Alternaria alternata* . In the present study investigation has been made on sustainable capability of carbendazim resistance of *Alternaria alternata* causing leaf spot of *Aloe vera* by counting the surviving colonies of the pathogen on *Aloe vera* . In the result it was found that the reproduction ratio always smaller on untreated plant than on the carbendazim treated plant.

Introduction

Aloe vera is succulent, evergreen perennial plant. It is widely grows in the tropical climates. In India it grows for the decorative purpose and medicinal uses. Medicinally its constituents used in the cosmetics, ointments hair wash, moisturizer, minor burns and sun burns. Such medicinally useful plant suffered heavy loss from leaf spot disease caused by *Alternaria alternata* . So for getting the quality juice and high yield it is necessary to control the pathogen. Therefore in the present study investigation has been made on sustainable capability of carbendazim resistance of *Alternaria alternata* causing leaf spot of *Aloe vera* by counting the surviving colonies of the pathogen on *Aloe vera* .this work will benefited to the new researchers which are in the study of fungicide resistance and in the disease management.

Material and Methods

Alternaria alternata identified as major pathogen causing leaf spot disease of *Aloe vera*. Naturally infected leaf samples of *Aloe vera* collected from Kolhapur and Sangli

districts. They were brought to the laboratory in clean, sterilized polythene bags, and isolated the pathogen on CDA medium. The fungi were identified with the help of relevant Mycological literature (Subramanian, 1972; Barnett and Hunter, 1972). Isolated four isolates from above districts and determined the MIC. From these four isolates , isolate (A3) was resistant to the carbendazim and isolate (A1) was sensitive to the carbendazim . To find out survival ability of carbendazim resistant isolate of *Alternaria alternata* causing leaf spot of *Aloe vera* in mixed population, mycelial suspension in sterile distilled water were prepared from 8 days old culture of carbendazim sensitive isolate *Alternaria alternata* (A1) and resistant isolates (A3). The mycelial suspension from these two isolates was mixed in following proportions.

Sensitive	:	Resistant
90	:	10
75	:	25
50	:	50

Clean, healthy treated carbendazim (5%) and untreated *Aloe vera* leaves were inoculated with the suspension of above three mixtures individually. After 15 days incubation period, mycelial suspension was prepared from infected plants separately. The suspension from each of the above mentioned mixture was used to inoculate second (next) passage of plants. Prior to inoculation at each passage 10 ml samples were taken from each mycelial suspension and were diluted with sterile distilled water to approximately 200 mycelial fragments per ml. one ml of each suspension was then pipetted out on the surface of 10 ml water agar plates 1 ml per plate and incubated for 8 days till the colonies is visible, out of which 100 colonies from each mixture were transferred onto the Czapek Dox Agar plates containing (2%) Carbendazim concentration lethal to sensitive isolate. These plates were incubated for four days. The surviving colonies were counted and were considered as resistant isolate. Same procedure was followed for four successive passages.

Results and Discussion

In the result it was found that the reproduction ratio always smaller on untreated plant than on the carbendazim treated plant. Results are in agreement with, (Bhale,2002;More, 2009; Patil, 2010; Jagtap, 2010 Waghmare, 2010 and Ramteke, 2011. These workers studied the survival ability of different pathogens on different plants.

Reference

Bhale U.N. (2002). Studies on management of some important diseases of Spinach in Maharashtra.Ph.D. Thesis Babasaheb Ambedkar Marathwada University, Aurangabad.

Jagtap, A.A. (2010) studies on management of rhizome rot of turmeric. Ph. D. Thesis, Shivaji University, Kolhapur.

More, S.B. (2010) studies on management of Soybean rust. Ph.D. Thesis, Shivaji University, Kolhapur.

P.K. Ramteke (2011) Studies on management of *Fusarium solani* rhizome rot of Ginger in Maharashtra. Ph.D. Thesis Shivaji University, Kolhapur.

Patil, V.B. (2010) Studies on management of charcoal rot of sweet potato. Ph.D. Thesis Shivaji University, Kolhapur.

Wadikar M.S. (2003). Studies on charcoal rot management of Pigeon pea. Maharashtra.Ph.D. Thesis Babasaheb Ambedkar Marathwada University, Aurangabad.



Seasonal Abundance of Mayflies (Ephemeroptera) In Kolhapur District

¹ Rohini Kamble and ² T.V. Sathe

¹Research Student, Department of Zoology, Shivaji University, Kolhapur

²Professor, Department of Zoology, Shivaji University, Kolhapur

KEYWORDS

Mayflies,
Ephemeroptera,
River, Seasonal
Abundance,
Kolhapur district

Corresponding Author
Email
rohistr36@gmail.com

ABSTRACT

A total of 10 species of Mayflies namely, *Sparsorythus gracilis* Sroka and Soldan, *Caenis nigrostriata* Navas, *Clypeocaenis bisetosa* Soldan, *Cloeon bicolor* Kimmins, *Cloeon kimminsi* Hubbard, *Cloeon marginale* Hagen, *Procloeon bimaculatum* Eaton, *Prosopistoma indicum* Peters, *Epeorus gilliesi* Braasch, *Povila corporaali* Lestage have been reported and seasonal abundance made from different study area of eight rivers of Kolhapur district at 15 days interval by one-man one-hour search method. Highest abundance found in Kasari River and lowest in Bhogavati River, indicating Kasari River is better than Bhogawati from the viewpoint of water pollution.

Introduction

Mayflies are hemimetabolic insects. They are being visualized as a potential food source for fishes and other aquatic organisms. Mayflies are important for the ecology of freshwater streams, ecocycles as well as food webs. They are excellent indicators of ecosystems health. Thus, they are good water pollution indicators. Mayflies (Ephemeroptera) play a crucial role in aquatic ecosystems by cycling nutrients and provide an important food source for fish, birds and other aquatic insects. They also have varying degrees of tolerance to natural and anthropogenesis disturbances, making them excellent indicators of pollution of ecosystems health. About 3000 species of 400 genera with 42 families of mayflies out of which 390 species in 84 genera and 20 families recorded in the Oriental region and 41 genera are endemic to the region (Barber-James *et al.*, 2008). In India 124 species have been recorded (Subramanian and Sivaramakrishnan, 2010). Mayflies are expanded group,

distributed in nearly all lentic and lotic ecosystem and are especially abundant in rivers and streams. They contribute significantly to ecological processes (You and Gui 1995). Seasonal abundance of mayflies has been studied in rivers of Kolhapur district. As Kolhapur region of India is gene rich area. Mayflies have an important role in both terrestrial and aquatic ecosystems in food webs. significant

Material and Methods

Mayflies were collected from different study spots by using insect collection. They are temporarily stored in plastic containers until reaching to the laboratory. The collected adults of mayfly killed by immersing in absolute alcohol and then passed into different grades of alcohol for dehydration. The permanent slide preparation of adults mayflies done by using xylene and DPX. Mayfly nymphs collected by immersing the insect collection net into the water. The nymphs of mayfly caught into the net then

separated and stored into the plastic containers. These collected nymphs of mayflies were along with water poured into the glass aquarium for their growth and hatching by providing appropriate air and temperature. The glass aquarium sealed by muslin cloth for to trap the hatched adults of mayflies.

On basis of a number of mayflies collected and availability of mayflies, distributional records made from various places of Kolhapur district at 15 days interval. One-man one-hour search method used for making distributional records in tehsils of Kolhapur district, Shahuwadi, Radhnagari, Karveer, Kagal, Hatkangale and Shirol selected.

Result and Discussion

A total of 10 species of Mayflies namely, *Sparsorythus gracilis* Sroka and Soldan, *Caenis nigrostriata* Navas, *Clypeocaenis bisetosa* Soldan, *Cloeon bicolor* Kimmins, *Cloeon kimmnsi* Hubbard, *Cloeon marginale* Hagen, *Procloeon bimaculatum* Eaton, *Prosopistoma indicum* Peters, *Epeorus gilliesi* Braasch, *Povila corporaali* Lestage. have been reported from different study area of eight rivers of Kolhapur district.

Seasonal abundance was maximum in month of May and minimum in month of February. During December to June, the mayflies are abundant. *Clypeocaenis bisetosa* species and *Procloeon bimaculatum* species was more abundant and *Caenis nigrostriata* species having lower abundance. Mayflies are more abundant in month of April to May. The species *Sparsorythus gracilis* was abundant in month of May and their number decreased at February, this species is medium abundant. *Caenis nigrostriata* was abundant in month of April and May.

Clypeocanis bisetosa species was more abundant in month of May and their number decreased at January. *Cloeon bicolor* species was abundant in month of March to June. *Cloeon kimmnsi* species was higher abundant in month of April. *Procloeon bimaculatum* species was abundant in month

of February to June; in the month of May, this species is more abundant. *Cloeon marginale* species was abundant in month of March to June. *Prosopistoma indicum* species was abundant in month of March to June. In month of June, this species is more abundant. *Epeorus gilliesi* was most abundant in month of April, May and June, in this month this species is higher in number while, *Povila corporaali* species was abundant in month of March to June.

Mayflies adult life was terrestrial and aquatic in the immature called naids (nymphs). The subimago was the early, reproductively immature adult and the mature ones are imago (<http://wgbis.ces.iisc.ernet.in>). The subimago molts within 24 hours and imago is the final reproductive stage. They are completed their life cycle within two years. (Ireland red list 7, 2012). Mayflies undergo an incomplete metamorphosis (Mayers, 2011). Adult Mayflies do not feed. According to Dubey *et al.*, (2013) mayflies were important fish food.

Mayflies were the important food source for aquatic ecosystems (Cummins, 1974) and provided food to fish, birds and other vertebrates (Healey, 1984). They were tolerant to natural and anthropogenesis disturbances, making them excellent indicators of ecosystem health (Healey, 1984).

Mayflies were the most important groups in the aquatic food web (Perez and Segnini, 2010). Seasonal fluctuation in the abundance of tropical insect population systematically investigated only in recent years. According to Landa (1969), mayfly nymphs feed on detritus material and were highly sensitive to toxic material entering the water. Most of the mayfly nymphs were low tolerant to pH, dissolved oxygen, substrate and temperature of the water. (Alhejoj *et al.*, 2014).

The nymphs of mayflies were associated with different organisms of running waters (Zelinka, 1977). Mayflies were very good indicators of conservation and they can be used to identify significant localities at much smaller scale than those identified by studies on vertebrates. The moulting of nymphs was dependent upon surrounding



Sr. No	Name of mayfly	Family	June	July	Aug	Sep	Oct	Nov	Dec	Jan	Feb	Mar	Apr	May
1.	<i>Sparsorythus gracilis</i>	Tricorythidae	-	-	-	-	-	-	-	-	+	+	+	+
2	<i>Caenis nigrostriata</i>	Caenidae	-	-	-	-	-	-	-	-	-	-	+	+
3.	<i>Clypeocaenis bisetosa</i>	Caenidae	+	-	-	-	-	-	+	+	+	+	+	+
4.	<i>Cloeon bicolor</i>	Baetidae	+	-	-	-	-	-	-	-	-	+	+	+
5.	<i>Cloeon kimminsi</i>	Baetidae	+	-	-	-	-	-	-	-	+	+	+	+
6.	<i>Procloeon bimaculatum</i>	Baetidae	-	-	-	-	-	-	+	+	+	+	+	+
7.	<i>Cloeon marginale</i>	Baetidae	+	-	-	-	-	-	-	-	-	+	+	+
8.	<i>Prosopistoma indicum</i>	Prosopistomati dae	-	-	-	-	-	-	-	-	-	+	+	+
9.	<i>Epeorus gilliesi</i>	Heptageniidae	+	-	-	-	-	-	-	-	-	+	+	+
10.	<i>Povila corporaali</i>	Polymtarcyida e	+	-	-	-	-	-	-	-	-	+	+	+

Table 1: Seasonal abundance of mayflies in Kolhapur district

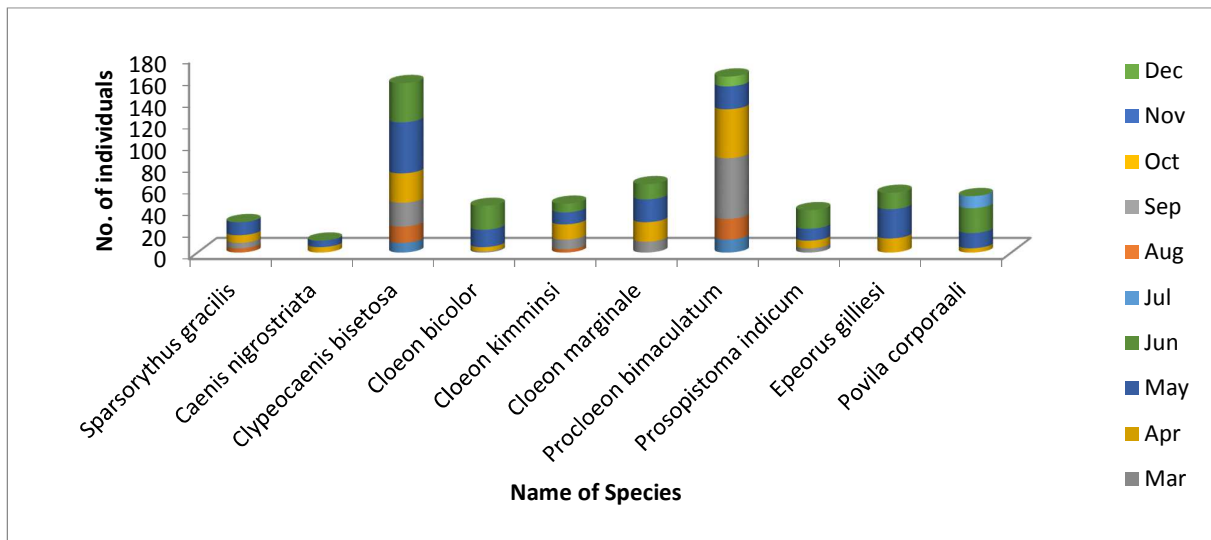


Fig.1: Seasonal abundance of mayflies.



Fig.- 2 Map of Kolhapur District showing study area.

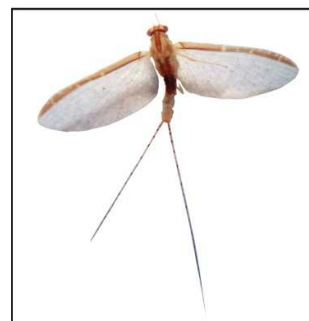


Fig. -3 Adult of *Cloeon marginale*.



Fig.- 4 Adult of *Procloeon bimaculatum*.

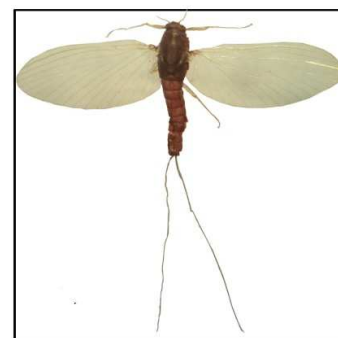


Fig.- 5 Adult of *Povila corporaali*.

References

- Alhejoj, I., Salameh, E and Bandel, K. 2014. An effective indicator of water conditions in Jordan. *Int. J. Sci. Res. Env. Sci.* 2(10):361-370.
- Barber-James, H. M., Gattolliat, J., Sartori, M and Hubbard, M. D. 2008. Global diversity of mayflies (Ephemeroptera:Insecta) in freshwater. *Hydr.*, 595:339-350.
- Bauernfeind, E and Moog, O. 2000. The assessment of ecological integrity of mayfly; a methodological approach. *Hydr.*, 422/423: 71-83.
- Brittain, J. E. and Sartori M. 2003. Ephemeroptera (Mayflies). *Enc. of Ins.*, 373- 380.
- Cummins, K. W. 1974. Structure and function of stream ecosystem. *Bioscience*, 2:631-641.
- Dubey, S., Sharma, S and Chaurasia, R. 2013. The insect diversity of River Kunda Khargone district M.P. (India). *Glo. J. bio*, 2(3):454-455.
- Healey, M. C. 1984. Fish predation on aquatic insects. 255-288.
- Landa, V. 1969. Comparative anatomy of mayfly larvae (Ephemeroptera). *Acta ent.* 66:289-316.
- Mayers, L., B. Kondratieff and Ruiter, D. 2011. The mayflies, stoneflies and caddisflies of the Adirondack park, New York State. *Trans. Ame. Ent. Soc.*, 137(1): 63-140.
- Perez and Segnini 2010. Seasonal variation of mayflies in tropical Andean head water stream. *Ecotrópicos*, 23(1):37-49.



Subramanian and Sivaramakrishnan 2010. Checklist of ephemeroptera of India, Zoological Survey of India.

You, D. S. and Gui, H. 1995. Economic insect fauna of China. Ephemeroptera. Beijing: Science Press, 48:15.

Zelinka, 1977. The production of Ephemeroptera in running waters. *Hydrobiologia*, 56(2): 121-125



A study of fitness performance and maximum oxygen consumption (VO₂ max) in the residential and non-residential school children's of Kolhapur District, MS, India

¹ Manjare K.G. ² Sanadi R.A. and ³ Jadhav A.D.

¹ Adarsh Gurukul Vidyalay & Junior College, Peth Vadgaons

² Research scholar, Department of Zoology, Shivaji University, Kolhapur- 416 004

² Assistant Professor, Department of Zoology, Shivaji University, Kolhapur- 416 004

KEYWORDS

Physical Fitness, BMI, VO₂ max, Physiological parameters, Residential school and Non-residential School Children's

Corresponding Author Email

reshmasaniadi09@gmail.com

ABSTRACT

Physical fitness is the most important for survival of the healthy life. It is a general state of health and well-being. Physical fitness is an individual depends on the amount of oxygen which can be transported by the body to working muscles, and the efficiency of muscles to use that oxygen. The acquaintance interaction of modern life style, we are neglecting the natural physical activities and increased the risks among the society for the chronic diseases exclusively from coronary heart diseases. Our aim to find fitness performance in residential and non-residential school children's age group of (15-16yrs) of, Peth Vadgaons village of Kolhapur district. The study was divided into two group Residential (n=50) and non-residential (n=50) school children's. Anthropological measurements like height (cm), weight (kg), BMI (kg/m²) was measured by standard protocol. Physical fitness index and VO₂ max calculated by Harvard Step Test and pulse rate per min was recorded from carotid pulse. Data was analyzed by using Microsoft Excel software. Our study revealed that, PFI and VO₂ max significantly higher in residential children's than non-residential children's. BMI of residential children's and non-residential children's were statistically significant. The present study concluded that residential school children's were more physically fit than the non-residential children's. Regular physical exercise was recommend to non-residential children's

Introduction

Physical fitness is the most important for survival of the healthy life (Khodnapur, *et.al.*, 2012; Das, 2001). It is a general state of health and well-being. Physical fitness is an individual depends on the amount of oxygen which can be transported by the body to working muscles, and the efficiency of muscles to use that oxygen. The acquaintance interaction of modern life style, we are neglecting the natural physical activities and increased the risks among the society for the chronic diseases exclusively from coronary heart diseases. Predominantly cardio respiratory fitness is dependent on physical fitness index. Poor physical fitness

is dependent on physical fitness index. Poor physical fitness showed a potent risk factor and stronger predictor of cardiovascular and causes morbidity and mortality than any other established risk factors (Castillo *et.al.*, 2005; Sengupta and Sahoo, 2011). Several factors like heredity, environment, socioeconomic status, regular exercise, diet and nutrition, and proper rest is important for physical fitness (Khodnapur, *et.al.*, 2012).

Several studies have established that physical fitness and health can assist in the prevention of chronic progressive diseases, accordingly to provide improved health status and quality of life.

A small increase in physical activity performances, mortality could be reduced by as much as 5-6% deaths per year (Powell and Blair, 1994). Increase in the level of intelligence, tolerance, activity and social behavior were the advantages of physical fitness (Pansare, 1986). Pratt *et.al.*, (2003) suggested for any age group physical activity measured by standard questionnaire was accepted worldwide. Kulinna (2003) especially studied for student physical activity pattern: grade, gender and activity influence.

Physical activity and health related physical fitness in public school children used statistical analysis with random selection of subjects (Wang and Pereira, 2003; Singh *et.al.*, 2015). Choudhary *et.al.*, (2002) examined respiratory pressure in residential and non-residential school children. Harvard step test was conducted to assess Physical Fitness Index (PFI) of residential sainik school children of age 12-14 years by Choudhary *et.al.*, (2002). Khodnapur *et.al.*, (2012) assessed the physical fitness status of Sainik residential school children. Khodanpur *et.al.*, (2012) found that, the effect of exercise and nutrition is important to the physical fitness of growing children's. They also found statistically significant higher values ($p=0.000$) of VO₂ max, PFI, FEV₁, PEF_R and MEP in residential school children compared to non-residential school children.

Exercise and nutrition are important for cardiopulmonary fitness. VO₂ max and PFI of in residential school children's was significantly higher than non-residential school children (Dhanakshirur *et.al.*, 2012).

In India non-residential schools, education is provided but regular exercises, Yoga and food does not monitored. Non-residential children's bring their own tiffin from home and play in recess and physical education lecture. Sometimes they forget to carry tiffin. In residential have executed regular exercise training, Yoga training by qualified trained persons for the students. The provided food for the students is nutritional and under the supervision of qualified dieticians. By considering all the above aspects, the present study is undertaken to study physical fitness index and Maximum oxygen consumption in Residential and Non-residential school children's.

Material and Methods

Study area

The present study was undertaken in Residential and Non-residential school, Adarsh Gurukul Vidyalya and Jr. College, Peth Vadgaon, from Kolhapur district of Maharashtra.

Selection of subjects

In this cross sectional descriptive study sample size was randomly selected (Carine *et.al.*, 2012). Subjects were enrolled after explaining the nature of the study and obtaining written informed consent from each participant of 15 to 16 yrs. age group and written consent of Principals also taken. The subject with previous medical history and subject who, declining to part of the study would be excluded from the study. The data was collected at the college campus during working hours and during resting period.

Method of collection of data

For assessment, we divided the students into two groups.

Group I: In group I 50 male willingly students are enroll from residential (Sainik) school of Adarsh Vidyniketan and Jr. College, Minche, from Kolhapur district of Maharashtra.

Group II: In group II 50 male willingly students are enroll from non-residential school of Adarsh Vidyniketan and Jr. College, Minche, from Kolhapur district of Maharashtra. tightly attached to the wall of trough and remain as it is (Fig-1 B).

1. Anthropological measurement

The height and weight of participants was measured with the help of measuring tape and weighing machine. The blood pressures were recorded by sphygmomanometer. The pulse rate/min of subject was recorded from carotid pulse.

1.1 Body Mass Index (BMI)

The body mass index (BMI) is measure of weight adjust for height (Must and Andersons 2006, Tehard *et.al.*, 2002). It was calculated by Quetelet Index, which is a statistical measure of the weight of a person scaled according to height. It was developed in 1832 by the Belgian polymath Adolphe Quetelet (Safrit MJ 1986). Body Mass Index (BMI) was calculated based on the formula-



$$BMI = \frac{\text{Weight in Kg}}{\text{Height in } m^2}$$

1.2 Physical Fitness Index (PFI)

The physical fitness can be defined as the quantitative expression of the physical condition of the workers. The Modified Harvard Step Test was used for assessment of physical fitness index (PFI) of randomly selected workers (Fox, 1973).

$$PFI = \frac{(\text{Duration of exercise in second} \times 100)}{(\text{pulse } 1 + 2 + 3)}$$

Procedure:

The subject was advised to step up on the modified Harvard steps of 33cms height once every two seconds (30 per minute) for 5 min., a total of 150 steps. At one, three and five minutes during the test, pulse rate was recorded from 1 to 1 ½, 2 to 2 ½, 3 to 3 ½ minutes during the recovery period and performance (physical fitness index, PFI) is assessed by duration of stepping and the sum of the 3 pulse count.

1.3 Maximum Oxygen Consumption (VO₂ Max)

Maximum oxygen consumption (VO₂ Max) was calculated by VO₂ Max (ml/kg/min) by Margaria's equation (Marquaria et.al., 1965) by using Modified Harvard Step Test (HST).

The VO₂ Max was calculated by using following formula-

$$VO_2 \text{ max} = 111.33 - (0.42 \times P\text{Max})$$

1. Physiological response

General physiological responses and anthropological measurement (blood pressure, pulse, temperature, weight, height,) were recorded by the standard technique of occupational safety and health (Kohn et.al., 1996).

2.1 Pulse Rate

The pulse rate per minute of the subjects were recorded from carotid pulse during the working condition.

Statistical Analysis

The statistical analysis like frequency, mean, standard deviation standard error of mean was done by using

Microsoft excel 2013 and SPSS software 20.

Result and Discussion

Table no. 1 revealed that anthropological measurements like height, weight and BMI of residential and non-residential school children's. The mean of height and weight does not show any significant difference in Group I and Group II. The mean BMI for Group I was 19.09±2.39 kg/m² and in Group II it was 18.35±3.36 kg/m². The BMI was significantly higher in group I than Group II.

The Table no. 2 showed the physiological responses and PFI percentage. The mean pulse rate in Group I was 73.14±4.9 and 70.88±2.06 bpm in Group II which was significantly less than Group I. The physical fitness index 118.52±10.53% and 103±14.66 % in Group I and Group II respectively. The Group I showed the significant difference of PFI than the Group I. The Table no. 3 revealed VO₂ Max in Group I was 60.93±3.3 ml/kg/min, which was significantly higher than Group II it was 48.33±6.65 ml/kg/min.

Figure no. 1 revealed that BMI range in Group I (residential) and Group II (non-residential) school children's. Group I showed the 46% Underweight category, 54% Normal category while, Group II contains 60% Underweight category, 38% Normal category and 2% Obese category. Group I (residential) significant difference in BMI category than the Group II (non-residential). Figure no. 2 showed the Physical fitness index (PFI) score in Group I (residential) and Group II (non-residential) school children's. Group I shows 100% excellent score, while Group II showed 64% excellent score, 24% good score and 12% average score. There is a significant difference in fitness score of Group I and Group II.

The regular exercise have a beneficial effect on the health. Several studies proved that physical fitness is necessary to carry out daily task. In school curriculum gymnastic activity was introduced by John Bernard (Choudhur et.al., 2002).

SR. NO.	PARAMETER	GROUP I (RESIDENTIAL) N=50			GROUP II (NON-RESIDENTIAL) N=50		
		MEAN	±SD	SE	MEAN	±SD	SE
1	Height in cm	163.98	5.16	0.73	162.5	6.65	0.94
2	Weight in kg	51.14	6.66	0.95	48.66	10.35	1.46
3	BMI kg/m ²	19.09	2.39	0.34	18.35	3.36	0.47

Table 1: Anthropological Measurements of Residential and Non-residential School Children'

SR. NO.	PARAMETER	GROUP I (RESIDENTIAL) N=50			GROUP II (NON-RESIDENTIAL) N=50		
		MEAN	±SD	SE	MEAN	±SD	SE
1	Pulse rate (bpm)	73.14	4.9	0.69	70.88	2.06	0.29
2	PFI (%)	118.52	10.53	1.49	103	14.66	2.073

Table 2: Physiological response of Residential and Non-residential School Children's Reveled the

SR.NO.	PARAMETER	GROUP I (RESIDENTIAL) N=50			GROUP II (NON-RESIDENTIAL) N=50		
		MEAN	±SD	SE	MEAN	±SD	SE
1	VO ₂ Max (ml/kg/min)	60.93	3.3	0.47	48.33	6.65	0.94

Table 3: VO₂ Max of Residential and Non-residential School Children's

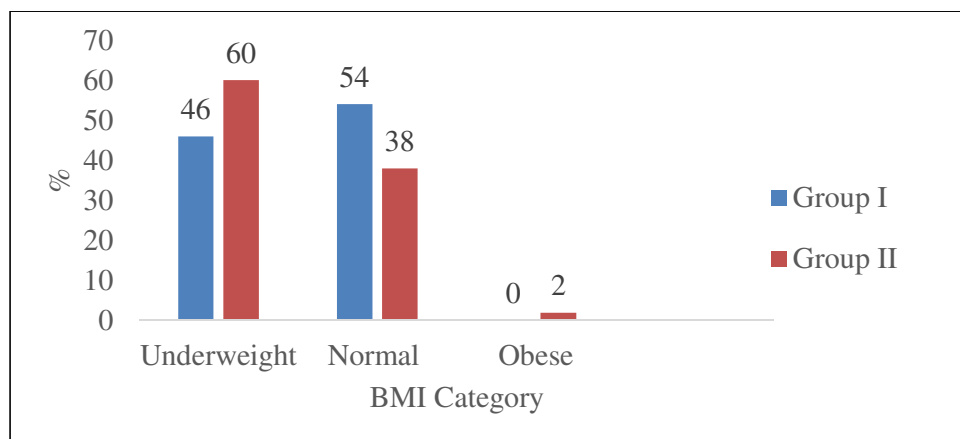


Fig.- 1: Body Mass Index of Residential and Non-residential School Children's.

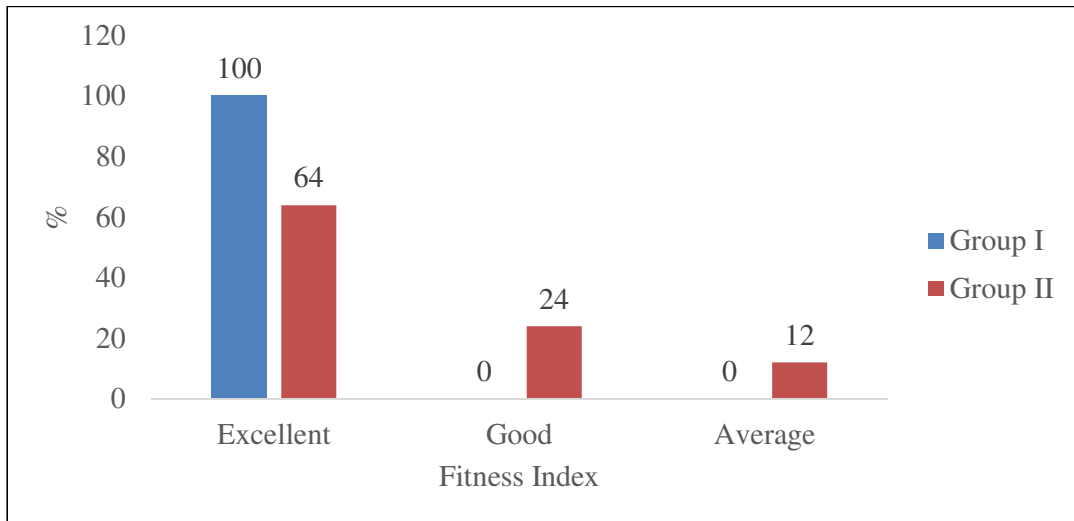


Fig.- 2: Physical Fitness Index Residential and Non-residential School Children's.

In India non-residential schools, education is provided but regular exercises, Yoga and food does not monitored. Non-residential children's bring their own tiffin from home and play in races and physical education lecture. Sometimes they forget to carry tiffin. In residential schools have executed regular exercise training, Yoga training by qualified trained persons for the students. The provided food for the students is nutritional and under the supervision of qualified dieticians. In non-residential schools, education is being provided but regular exercise are not supervised. The physical fitness is assessed by cardiopulmonary efficiency tests by PFI and VO_2 max. The mean BMI for Group I was 19.09 ± 2.39 and in Group II it was 18.35 ± 3.36 kg/m². The BMI was significantly higher in group I than Group II. The Table no. 2 showed the physiological responses and PFI percentage. The physical fitness index $118.52 \pm 10.53\%$ and $103 \pm 14.66\%$ in Group I and Group II respectively.

The Group I showed the significant difference of PFI than the Group I. The Table no. 3 revealed VO_2 max in Group I was 60.93 ± 3.3 , I was 60.93 ± 3.3 , which was significantly higher than Group II it was 48.33 ± 6.65 ml/kg/min. BMI is the most appropriate simple indicator by which weight-for-height can be related to health outcome, therefore, proposed the use of BMI to monitor both under nutrition and overweight

(WHO, 1997). There is significant difference between residential (trained) school children's students than non-residential (untrained) school children's due to regular physical activity and training may be one of the contributing factors in attainment of such growth (Sharman and Down, 1971). Fitness Index (PFI) is one of the important criteria to assess the cardiopulmonary efficiency of a subject (Sunil and Das, 1993). Chatterjee *et.al.*, (2001) showed higher PFI score in trained (athletics) than those of untrained (non-athletics) but comprising of female subjects only. Ara *et.al.*, (2007) observed that physically active children had significantly higher values of VO_2 max than that of non-physically active children. Decrease in pulse rate in residential school children may be attributed to increased parasympathetic discharge to heart and this is in turn due to regular exercise (Clarke, 1975).

Conclusion

Our study clearly showed that regular exercise and balanced nutrition will improve physical fitness. Our study also revealed effects of regular exercise improve VO_2 max and physical fitness index in growing children's. Consequently, regular physical exercise and yoga can be comprised as a part of curriculum for school going children's. The present study concluded that residential school children's

were more physically fit than the non-residential children's. Regular physical exercise was recommend to non-residential children's.

Acknowledgement

The authors are much thankful to Founder President Mr. D.S. Ghugare, Head Mistress Mrs. M. D. Ghugare and Residential and Non-Residential school children's Adarsh Vidnyketan and Jr. College, Peth Vadgaons, from Kolhapur district of Maharashtra.

References

- Ara I, Moreno LA, Gutin B and Casajus JA. (2007).** Adiposity, physical activity and physical fitness among children from Aragon, Spain. *J of Obesity* 15:1918 –1924.
- Carine AB, Bethany JF, and James AH and Preedy VR (2012)** .Handbook of Anthropometry: Physical Measures of Human Form in Health and Disease, Chapter 1 Calculating Sample Size in Anthropometry, Springer Science Business Media, 4-5.
- Castillo Garzon MJ, Ortega Porcel FB, Ruiz Ruiz J.(2005).** Improvement of physical fitness as Anti-aging intervention. *Med Clin (Barc)*. 124(4):146-55
- Chatterjee S and Mitra A. (2001).** The relation of physical fitness score with different morphological parameters and VO₂ Max on adult female Athletes and Non athletes. *Ind. J Physiol and Allied Sci*. 55(1): 7-11.
- Choudhari, D, Aithal M and Kulkarni, VA. (2002).** Maximal expiratory pressure in Residential and Non-Residential school children. *Indian J. Padiatrics*, 2002;69:229–232.
- Choudhari, D, Choudhari S, Kulkarni, VA. (2002).** Physical fitness: A comparative study between students of residential (saini) and non-residential schools (aged 12-14 years), *Indian J.Phy.and pharma*, 2002;46(3):328-332.
- Choudhur D, Choudhuri S, Kulkarni VA. (2002).** Physical fitness: A comparative study between students of residential and nonresidential schools (Aged 12-14 years). *Indian J Physiol Pharmacol*, 46(3):328-332.
- Clarke DH. (1975).** Exercise Physiology. Prentice Hall Inc, Englewood Cliffs, New Jersey.
- Das KK, Dhundasi SA. (2001).** Physical fitness: A longitudinal study among muslim children of Bijapur (Karnataka). *Indian J Physiol Pharmacol* 45(4):457-462.
- Dhanakshirur, GB, Khodnapur JP and Aithala M. (2012).** Role of Exercise and Nutrition on Cardiopulmonary Fitness, *Indian Medical Gazette*, 2012:6-9.
- Fox EL, Billings CE, Robert L, Bason R and Mathews D. (1973).** Fitness standards for college students. *Euro. J. of App. Physio. and Occu. Physio.*1973; 31(3): 231-236.
- Khodnapur, JP, Bagali SC, Mullur LM, Dhanakshiur GB and Aithala M.(2012).** Role of Regular Exercise On Vo₂ Max And Physiological Parameters Among Residential And onresidential School Children Of Bijapur *IJBAR*, 3(5):397: 400.
- Kohn J, Friend M and Winter BC and Rokville, (1996).** Fundamentals of Occupational Safety and Health. Govt. Institute Press.
- Marquaria R, Aghema P, Rovelli E. (1965).** Determination of maximal oxygen consumption in man. *J Appl Physiol* 20:1070-1073.
- Must, A and Anderson SE. (2006).** Body Mass Index in Children and Adolescents: Consideration for Population-based Applications. *Int. J. of Obesity*. 30:590-594.
- Pansare, MS. (1986).** Physiology of Fitness, Med. J.f Western India. 1986;14:18-20.
- Powell K.E. and Blair S.N. (1994).** The public health burdens of sedentary living habits: theoretical but realistic estimates. *Med.Sci.Sports Exerc*. 26:851.



- Pratt, M, Ekelund, U, Yngve, A, Sallis, JF and Ojha P. (2003).**International Physical Activity Questionnaire: 12-country reliability and validity, *Med.Sci.Sports Exerc*,5(8):1381-1395.
- Safrit MJ. (1986).** Introduction to Measurement in Physical Education and Exercise Science. Times Mirror Ed. Mosby College Publishing. 250.
- Sengupta P, Sahoo S. (2011).** Evaluation of Health Status of the fishers: prediction of cardiovascular fitness and anaerobic power. *WJLSMR*. 1(2):25-30.
- Sharman IM, Down MC. (1971).** The effect of Vit E and training on physiological function and athletes performance in adolescent swimmers. *Brit. J. Nutr.* (26):265-276.
- Singh, H, Shekhar C and Kumar S. (2015).** Assessment of Yoga on the Status of the Physical Fitness among children of Residential School, *IJTEMAS*; 16-20.
- Sunil KR and Das. (1993).** Determination of Physical Fitness Index (PFI) With Modified Harvard Step Test (HST) In Young Men and Women. *Ind. J Physiology & Allied Sci.* 47(2):73-76.
- Tehard, B, Van Liere M, Com Nougé C, Clavel-Chapelon FJ. (2002).** Anthropometric measurements and body silhouette of women: validity and perception of the American Dietetic Association, *Elsevier*. 102 (12):1779-84.
- WHO Physical Status: (1995).** The Use and Interpretation of Anthropometry. (Technical Report Series No. 854.) World Health Organization, Geneva.



Seasonal abundance of Ichneumonids from Western Maharashtra

¹ Sutar Mahesh and ² T.V.Sathe

¹Research student, Department of Zoology, Shivaji University, Kolhapur

² Professor, Department of Zoology, Shivaji University, Kolhapur

KEYWORDS

Ichneumonids,
Insect pest,
Host plant,
Biocontrol agent,
Western Maharashtra,

ABSTRACT

Ichneumonids are very potential biocontrol agents of lepidopterous pests. 30 species of Ichneumonids belonging to genera *Charops*, *Campoletis*, *Diadegma*, *Ecthomorpha*, *Eriborus*, *Enicospillus*, *Goryphus*, *Isotima*, *Netelia*, *Perilissus*, *Pristomerus*, *Xanthopimpla* and *Ichnojoppa* were prevalent in Western Maharashtra and found controlling lepidopterous pests. *Campoletis chloridae* and *Xanthopimpla spp.* were common in Kolhapur, Sangli and Satara districts. *Charops charukeshi* S. and D. was recorded on *Spilosoma obliqua* (Walk.) (Lepidoptera), *Thiocides postica* (Walk.) (Lepidoptera) and Lepidopteran semilooper (Unidentified). *Campoletis chloridae* Uchida was recorded on *Helicoverpa armigera* (Hubn.) (Lepidoptera), *Spodoptera litura* (Fab.) and *Spodoptera exigua* (Fab.). *Diadegma fenestralis* (Cameron) was recorded on *H. armigera*, *D. trichoptilus* (Cameron) on *H. armigera*, *Exelastis atomosa* (Wal.), *Diadegma surendrai* Gupta on *Phthorimaea operculella*, *D. trochanteratus* Morlay on *Diachrocrocis puntiferalis* (Guence), *D. vulgari* Morlay on *S. exigua*, *D. recini* R. and K on *D. puntiferalis*. *Enicospillus sp.* on *H. armigera* and *S. litura*. *Goryphus sp.* on *E. vitella*, *Netelia ephippata* Smith on *Achea janat*. *Perilissus cingulator* (Morlay) on *Athalia proxima* (Klug), *Pristomerus euzopherae* Viereck on *Euzophera perticella* Rag., *Pristomerus valnerator* Pan on *Phthorimaea operculella* Zaller. *Xanthopimpla cera* Cam. on *Scirpophaga nivella* Fab., *X. nursei* Cameron on *Sylepta derogata* Fab., *X. punctata* Fab. on *Chilo partellus* (Swin.). *Ichnojoppa sp.* on *Parnara mathias*.

Corresponding Author
Email
maheshstr36@gmail.com

Introduction

Ichneumonids are very potential biocontrol agents of lepidopterous and coleopterous pests. For sampling of parasitoids and predators basic knowledge is required. The parasitoids have host specificity as their hosts are related to one or closely related group of insects. Thus for sampling of parasitoids pest species of insects are needed. Parasitoids parasitize larval and pupal stages of pests mostly and cause mortalities in them. Therefore, Ichneumonids are widely used in biological control of insect pests in India and other countries (Debatch, 1964; Sathe and Bhoje, 2000). 60 percent successful programmes of biological insect pest control are designed with parasitoids. Since, rearing of parasitoid is

comparatively easy than predators. Therefore, hoping maximum utility of Ichneumonids in biological pest control the present work was carried out from Sangli, Satara and Kolhapur district. The review of literature indicates that biodiversity of Ichneumonids has been attempted by Morley (1913), Townes et al. (1961), Sathe et al. (1996), Sathe (1986a, 1987a, 1992a), Sathe et al. (2003), Sathe (2015) etc.

Material and Methods

Biodiversity of Ichneumonids has been studied by collecting insect pest stages (larvae & pupae) from collection spots at 15 days interval. The pest stages collected have been reared in the laboratory (24 ± 1° C, 75 % R. H.,

in the laboratory (24 ± 1° C, 75 % R. H., 12 Hr photoperiod) on their natural food for screening parasitoids. One man one hour search method was adopted for collection of Ichneumonids. The Ichneumonids have been identified by consulting appropriate literature (Townes *et al.*, 1961, Sathe *et al.*, 2003, Sathe 2015)

Result and Discussion

Results are recorded in table 1 and figs 1-8. The results indicated that *Campoletis chlorideae* and *Xanthopimpla* spp. were common in Kolhapur, Sangli and Satara districts. 30 species of Ichneumonids have been collected and identified on various insect pests. *Charops charukeshi* S. and D. was recorded on *Spilosoma obliqua* (Walk.) (Lepidoptera), *Thiocides postica* (Walk.) (Lepidoptera) and Lepidopteran semilooper (Unidentified). *Campoletis chlorideae* Uchida was recorded on *Helicoverpa armigera* (Hubn.) (Lepidoptera), *Spodoptera litura* (Fab.) and *Spodoptera exigua* (Fab.). *Diadegma fenestralis* (Cameron) was recorded on *H. armigera*, *D. trichoptilus* (Cameron) on *H. armigera*, *Exelastis atomosa* (Wal.), *Diadegma surendrai* (Gupta) on *Phthorimaea operculella* (Zeller), *D. trochanteratus* (Morlay) on *Diachrocrocis puntiferalis* (Guence), *D. vulgari* (Morlay) on *S. exigua*, *D. recini* R. and K on *D. puntiferalis*. *Enicospillus* sp. on *H. armigera* and *S. litura*. *Goryphus* sp. on *E. vitella*, *Netelia ephippata* Smith on *Achea janata* (Linnaeus). *Perilissus cingulator* (Morley) on *Athalia proxima* (Klug), *Pristomerus euzopherae* Viereck on *Euzophera perticella* (Rag.), *Pristomerus valnerator* Pan on *Phthorimaea operculella* (Zeller). *Xanthopimpla cera* (Cam.) on *Scirpophaga nivella* (Fab.), *X. nursei* (Cameron) on *Sylepta derogata* (Fab.), *X. punctata* (Fab.) on *Chilo partellus* (Swin.). *Ichnojoppa* sp. on *Parnara mathias* (Fabricious). Most of the above species were found in Kolhapur, Sangli Satara (Western Maharashtra).

Sathe (1986b) made survey of Hymenopterous parasitoids on *Chapra mathias* Fab., a paddy pest in Kolhapur. He reported three Hymenopterous parasitoids

namely *Apanteles baoris*, *Ichnojoppa* sp. and *Chalcid*. Further he reported that *A. baoris* appeared along with pest and about 5 per cent parasitism in the beginning was recorded, later it increased to 87 per cent. From a single host larva 20-53 adults were successfully developed. In 50 hosts average of 43 adults of *A. baoris* were recorded. High percentage of parasitism, good parasitoid range might be of help in checking pest population in field conditions.

Sathe (1986a) also made survey of natural enemies of *Exelastis atomosa* Wals. on pigeon pea in Kolhapur. He reported 3 parasitoid on *E. atomosa*, out of which *D. trichoptilus* (Cameron) was an Ichneumonid parasitizing about 15-18 per cent larvae. A survey of parasitoids of Ber hairy caterpillar *Thiocides postica* (Walk.) from Kolhapur was also made by Sathe (1987b). He reported 3 parasitoids namely *A. creatonoti* Viereck, *Charops* sp. (Ichneumonidae) and *Tachina (Exorista) faliar* Meigen (Diptera). The per cent parasitism in these parasitoids was 30 per cent, 15 per cent and 8 per cent respectively.

In a survey of *Spodoptera litura* (Fab.) from Kolhapur Sathe reported 10 hymenopterous parasitoids parasitizing *S. litura*. The highest parasitization (60 %) by *Campoletis chlorideae* Uchida was in the fields of groundnut. Early, second instar caterpillars were preferred for parasitization. *C. chlorideae*, *Enicospillus* sp. and *Ectromorpha* sp. were noted on *S. litura* as Ichneumonid parasitoids. On *Spodoptera exigua* (Fab.) 13 hymenopterous parasitoids have been recorded from Kolhapur. Maximum parasitization caused by *C. chlorideae* in regions was 35 per cent, 60 per cent and 71 per cent in high, medium and low rainfall respectively. The lowest parasitization, 3 per cent was recorded by *Ectromorpha* species.

Recently, Sathe (1992b) prepared index of hymenopterous parasitoids and pest insects from Maharashtra. Sathe *et al.* (2003) reported 13 species of Ichneumonids from Maharashtra. Similarly, Kavane *et al.* (2003) also reported two hymenopterous parasitoids namely *Xanthopimpla predator* (Ichneumonidae) and *A. angaleti* (Braconidae) from



Satara district during the years 2000 to 2003 on wild silkworm *Antheraea mylitta* (Drury). Sathe and Cougale (2006) reported 10 hymenopterous parasitoids on *H. armigera* (Hubn.). Out of which *C. chloridae* was dominant over the other parasitoids reported. The present work was the confirmation of previous work will be very good base line data for utilization of Ichneumonids in biological pest control programmes.

References

- Debatch P., 1964.** Biological control of insect pests and weeds Chapman and Hall Ltd., New Petter Lane Lon. pp. 1-843.
- Morley. C., 1913.** Fauna of British India including Ceylon and Burma. Hymenoptera, Vol, 3. pp. 1-531
- Sathe, T.V. 1986a.** New records of natural enemies of *Exelastis atomosa* Walsingham, a Pigeon pea pest in Kolhapur, India. *Oikoassay* 3 (1), 17.

Table. 1: District wise record of Ichneumonids with pest species and crop

Sr. No.	Species	Pest species	Crop	Disribution	Occurrence
1	<i>Banchopsis ruficronis</i> (Cameron)	<i>Helicoverpa armigera</i> (Hubn.)	Gram	Kolhapur	Rare
2	<i>Charops charukeshi</i> S. and D.	<i>Spilosoma obliqua</i> (Walk.)	Ber	Kolhapur, Sangli	Common
			<i>Punica granatum</i>	Sangli, Satara	Common
		<i>Thiocides postica</i> (Walk.)	Ber	Kolhapur, Sangli, Satara	Common
		Lepidopteran semilooper (Unidentified)	<i>Punica granatum</i>	Kolhapur, Sangli, Satara	Common
3	<i>Campoletis chloridae</i> Uchida	<i>H. armigera</i>	Groundnut	Kolhapur, Sangli, Satara	Common
			Gram	Kolhapur, Sangli, Satara	Common
		<i>Spodoptera litura</i> (Fab.)	Groundnut	Kolhapur, Sangli, Satara	Common
			Caster	Kolhapur, Sangli, Satara	Common
		<i>Spodoptera exigua</i> (Fab.)	Groundnut	Kolhapur, Sangli, Satara	Common
4	<i>Diadegma fenestralis</i> (Cameron)	<i>H. armigera</i>	Jowar	Kolhapur, Sangli, Satara	Common

5	<i>D. trichoptilus</i> (Cameron)	<i>H. armigera</i>	Jowar	Kolhapur, Sangli, Satara	Common
		<i>Exelastis atomosa</i> (Wals.)	Red Gram	Kolhapur, Sangli, Satara	Common
6	<i>Diadegma surendrai</i> Gupta	<i>Phthorimaea operculella</i> (Zeller)	Potato	Kolhapur	Common
7	<i>D. trochanteratus</i> (Morley)	<i>Diachrocrocis puntiferalis</i> (Guence)	Mulberry	Kolhapur, Sangli	Rare
8	<i>D. vulgari</i> (Morley)	<i>S. exigua</i>	Jowar	Kolhapur, Sangli, Satara	Common
9	<i>D. recini</i> R. and K	<i>D. puntiferalis</i>	Caster	Sangli, Satara, Kolhapur	Common
10	<i>Ecthromorpha</i> sp.	<i>Mythmna separata</i> (Walker)	Jowar	Sangli, Satara, Kolhapur	Common
11	<i>Eriborus</i> <i>trochanteratus</i> (Morley)	<i>H. armigera</i>	Jowar	Kolhapur, Sangli, Satara	Common
		<i>P. operculella</i> (Zeller)	Potato	Sangli, Satara, Kolhapur	Common
12	<i>E. sinicus</i> Holm.	<i>Tryporiza insertulus</i> (Wlk.)	Sugarcane	Kolhapur, Sangli, Satara	Common
13	<i>Enicospillus</i> sp.	<i>H. armigera</i>	Jowar	Kolhapur, Sangli, Satara	Rare
		<i>S. litura</i>	Groundnut	Kolhapur, Sangli, Satara	Rare
			Cow peas	Kolhapur, Sangli, Satara	Rare
14	<i>Goryphus nurseri</i> (Cam.)	<i>E. vitella</i>	Cotton	Sangli	Common



15	<i>Goryphus</i> sp.	<i>E. vitella</i>	Cotton	Kolhapur, Sangli	Rare
			Lady finger	Kolhapur, Sangli, Satara	Common
16	<i>Isotima javensis</i> Rohwer	<i>Acigona steniella</i> (Hmps.)	Sugarcane	Kolhapur, Satara	Common
17	<i>Netelia ephippata</i> Smith	<i>Achaea ianata</i> (Linnaeus)	Caster	Kolhapur, Sangli, Satara	Rare
18	Netelia sp.	<i>A. janata</i>	Caster	Kolhapur, Sangli, Satara	Rare
		<i>S. litura</i>	Groundnut	Kolhapur, Sangli, Satara	Rare
19	<i>Perilissus cingulator</i> (Morley)	<i>Athalia proxima</i> (Klug)	Mustard	Kolhapur	Rare
20	<i>Pristomerus testaceous</i> (Morlay)	<i>Leucinodous orbonalis</i> (Guenee)	Brinjal	Kolhapur, Sangli, Satara	Common
21	<i>Pristomerus euzopherae</i> Viereck	<i>Euzophera perticella</i> (Rag.)	Sweet potato	Kolhapur, Sangli	Rare
22	<i>Pristomerus valnerator</i> Pan.	<i>P. operculella</i>	Potato	Kolhapur	Rare
23	<i>Xanthopimpla cera</i> Cam.	<i>Scirpophaga nivella</i> (Fab.)	Sugarcane	Kolhapur, Sangli, Satara	Common
24	<i>X. nursei</i> Cameron	<i>Sylepta derogata</i> (Fab.)	Cotton	Sangli, Kolhapur	Common
25	<i>X. punctata</i> Fab.	<i>Chilo partellus</i> (Swin.)	Jowar	Kolhapur, Sangli, Satara	Common
26	<i>X. predator</i> (Linn.)	<i>C. partellus</i>	Jowar	Kolhapur, Sangli, Satara	Common
			Maize	Kolhapur, Sangli, Satara	Common

27	<i>X. stemator</i> Cameron	<i>C. partellus</i>	Jowar	Kolhapur, Sangli, Satara	Common
28	<i>Xanthopimpla</i> sp.	Paddy borers	Paddy	Kolhapur	Common
29	<i>X. transversalis</i> (Vollenhoven)	Jamun borer	Jamun	Kolhapur	Common
30	<i>Ichnojoppa</i> sp.	<i>Parnara mathias</i> (Fabricious)	Paddy	Kolhapur, Sangli, Satara	Rare



Fig. 1 Paddy field from study area.



Fig. 2 A field of Gram.



Fig. 3 *H. armigera* attacking gram.

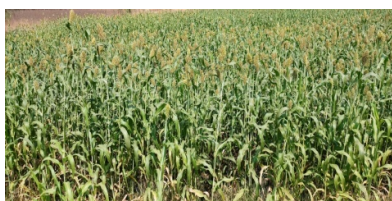


Fig. 4 Jowar Crop.



Fig. 5 Ground nut field



Fig. 6 *E. atomosa* larvae attacking chick pea



Fig. 7 Cocoon of *Diadegma* sp.



Fig. 8. Adult of *Diadegma* sp.



- Sathe, T.V. 1986b.** Parasitic complex associated with *Chapra mathais* Fab.(Lep. : Hesperidae), a paddy pest in Kolhapur. Geobios New Reports, 5, 59-60.
- Sathe, T.V. 1987a.** Life tables and intrinsic rate of natural increase of *Diadegma trichoptilus* (Cameron) (Hymenoptera : Ichneumonidae) population on *Exelastis atomosa* Wals. (Lepi. : Pterophoridae). J. Adv. Zool., 8(1) : 1-4.
- Sathe, T.V. 1987b.** New records of parasitoids of Ber hairy caterpillar *Thiocidas postica* Wlk. in Kolhapur, India. Sci. & Cult. 13, 185.
- Sathe, T.V. 1992 a.** A new species of the genus *Rhygoplitis* Gahan (Hymn. :Braconidae) in India. J. Zool. Res., 5, 13-16.
- Sathe, T.V. 1992b.** Natural enemies of some insect pests of economic importance. Oikoassay, 9, 15-17.
- Sathe T. V 2015.** Biological pests control through Ichneumonids. Daya Publ. House, New Delhi, Pp. 1-115
- Sathe T. V and Bhoje P. M., 2000.** Biological pests control. Daya Publ. House, New Delhi, Pp. 1-122.
- Sathe T.V. and T.M. Chougale, 2006.** Natural enemies of *Heliocoverpa armigera* (Hubn.) on pigeon pea from western Maharashtra. Indian. J. Environ. & Ecoplan. 12 (3), 657-659.
- Sathe, T.V., and Margaj G.S. 1996.** Mating behaviour in *Eriborus argenteopilosus* (Cameron), a parasitoid of *Heliothis armigera* (Hubn.). J. Karnat. Univ. (Special issue), 17-21.
- Sathe, T.V. and A.R. Pandharbale, 2003.** Biodiversity of Moths (Order : Lepidoptera) from Western Ghats of Satara district, India. Bull. Biol. Sci., 1, 81-88.
- Towens, H., Towens, M and Gupta, V.K. 1961.** A Catalogue and reclassification of the Indo-Australian Ichneumonidae. Mem, Amer, Ent. Inst. : 1-522



Application of Morphometrics to Reveal the Similarity Matrix and Distance Matrix among Closely Related *Cleome* L. Species from Kolhapur District

S. A. Deshmukh and D. K. Gaikwad*

Department of Botany, The New College, Kolhapur

*Department of Botany, Shivaji University, Kolhapur

KEYWORDS

Cleome, Morphometrics, Kolhapur, Similarity matrix

ABSTRACT

On the basis of various quantitative characters with the help of multivariate statistical analysis, six *Cleome* L. species from the Kolhapur district were morphometrically analyzed to reveal the similarity matrix among them. The principal component analysis and distance matrix revealed that the quantitative characters like capsule length, leaf breadth, inflorescence length, sepal length, sepal breadth, petal breadth, pistil length and anther length play very important and decisive role in segregation of these closely related taxa as a separate species while the quantitative characters like petiole length, leaf and leaflet number, leaf length, pod length and petal length are very important in grouping the taxa under single genus. Cluster analysis and dendrogram showed that the species *C. chelidonii*, *C. monophylla* and *C. simplicifolia* are closely related with each other while *C. viscosa*, *C. speciosa* and *C. gynandra* are forming similarity clade with each other.

Corresponding Author
Email
sageraea@gmail.com

Introduction

Cleome L. (spider flower) belongs to family cleomaceae consisting about 200 species distributed in tropical and subtropical parts of the world (Aparadh *et al.*, 2012). Seven species of *Cleome* are reported from Kolhapur district (Yadav and Sardesai, 2002). The genus has wide ethnobotanical importance and various species are implied to cure various diseases (Chatterjee and Prakash, 1991). As the species are closely related their proper identification is needed in the field of ethnobotany for proper treatment to cure particular disease. Morphometric studies reveal the similarity and distance matrix among the closely related species which facilitates distinct grouping and segregation among these species.

Material and Methods

Different *Cleome* L. species were collected from Kolhapur district during the year 2016-17 and were identified with the help of Flora of Kolhapur District (Yadav and Sardesai, 2002). Various quantitative characters viz. capsule length, petiole length, leaf length, leaflet length, leaf breadth, inflorescence length, pedicel length, sepal length, sepal breadth, petal length, petal breadth, number of seeds per pod, pistil length and anther length were measured and the mean values from the twenty five samples obtained was processed for principal component analysis and cluster analysis with the help of MVSP (Kovach, 1999).

	<i>C. viscosa</i>	<i>C. speciosa</i>	<i>C. gynandra</i>	<i>C. simplicifolia</i>	<i>C. chelidonii</i>	<i>C. monophylla</i>
Capsule length	6.6	4.7	5.9	3.1	6.5	8.5
Petiole length	2.78	6.83	2.97	1.9	7.23	1.6
Leaf/ leaflet number	3.91	5.21	5	1	5.12	1
Leaf length	3.94	9.76	3.89	2.18	5.15	3.64
Leaf breadth	1.28	3.24	1.95	0.98	1.54	3.11
Inflorescence length	6.18	15.59	14.15	13.58	13.16	9.84
Pedicle length	1.81	2.79	1.11	1.26	2.97	0.94
Sepal length	0.75	0.31	0.42	0.38	0.39	0.415
Sepal breadth	0.94	1.1	1.23	0.79	1.29	0.1
Petal length	1.24	2.68	1.39	1.1	1.54	0.87
Petal breadth	0.32	0.91	0.34	0.38	0.48	0.17
No. of seeds/ pod	34	22	17	28	45	35
Pistil length	0.72	0.98	1.1	8.23	1.15	6.14
Anther length	0.21	0.89	0.12	0.34	0.14	0.31

Table 2. Principal component analysis of *Cleome* L. species revealing similarity matrix.

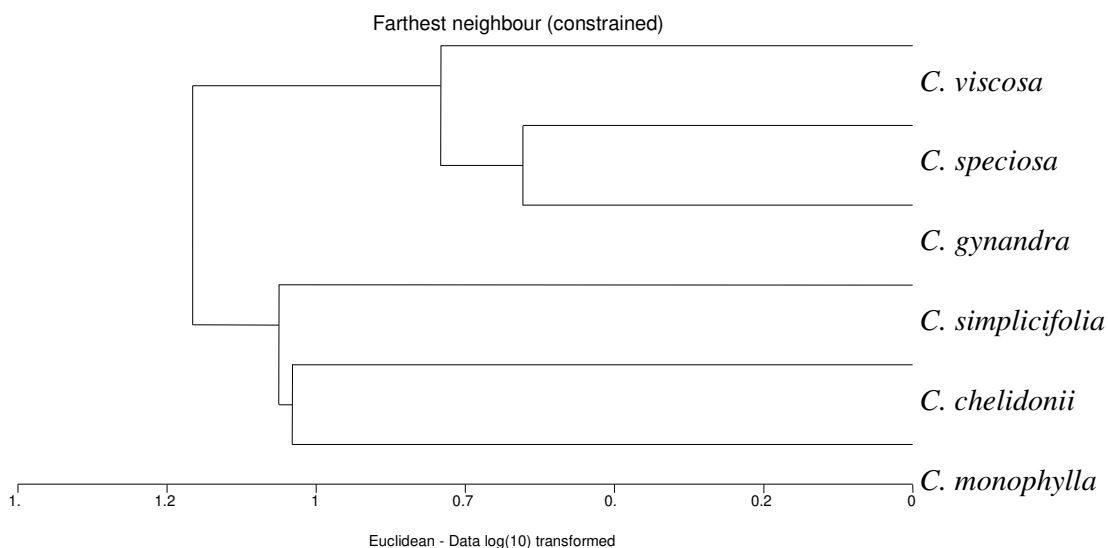
Capsule length	1.000													
Petiole length	-0.03	1.000												
Leaflet/ leaf number	0.141	0.807	1.000											
Leaf length	0.164	0.810	0.691	1.000										
Leaf breadth	0.449	0.191	0.105	0.657	1.000									
Inflorescence length	-0.49	0.414	0.154	0.291	0.246	1.000								
Pedicle length	-0.09	0.937	0.676	0.729	0.035	0.198	1.000							
Sepal length	0.345	-0.31	0.070	-0.29	-0.43	-0.93	-0.13	1.000						
sepal breadth	-0.38	0.699	0.814	0.344	-0.37	0.333	0.623	-0.01	1.000					
Petal length	-0.27	0.839	0.715	0.890	0.373	0.498	0.763	-0.39	0.620	1.000				
Petal breadth	-0.45	0.806	0.575	0.799	0.260	0.552	0.780	-0.46	0.595	0.970	1.000			
Seeds/pod	0.359	0.074	-0.22	-0.14	-0.24	-0.44	0.295	0.267	-0.27	-0.35	-0.27	1.000		
Pistil length	-0.28	-0.69	-0.96	-0.65	-0.09	0.111	-0.61	-0.31	-0.70	-0.61	-0.45	0.150	1.000	
Anther length	-0.36	0.302	0.012	0.633	0.551	0.347	0.347	-0.45	-0.06	0.679	0.73	-0.27	0.026	1.000



Table 3. Cluster analysis revealing distance matrix among the studied *Cleome* L. species.

Distance matrix						
<i>C. viscosa</i>	0.000					
<i>C. speciosa</i>	0.791	0.000				
<i>C. gynandra</i>	0.498	0.653	0.000			
<i>C. simplicifolia</i>	0.967	1.207	0.916	0.000		
<i>C. chelidonii</i>	0.538	0.556	0.601	1.062	0.000	
<i>C. monophylla</i>	0.880	1.165	0.901	0.598	1.040	0.000

Figure 1. Dendrogram on the basis of farthest neighbour and mean character difference among *Cleome* L. species



Results and Discussion

In the field of numerical classification, principal component analysis, similarity matrix, distance matrix and cluster analysis are widely employed (Sonibare *et al.*, 2004). Mean values of the quantitative characters are tabulated in Table 1. The results obtained on the basis of similarity matrix in between studied quantitative characters revealed significant correlation in between petiole length and leaf length, petiole length and pedicel length, petiole length and petal length, petiole length and petal breadth, leaf length and petal length, pedicel length and petal length, pedicel length

and petal breadth & petal length and petal breadth. The quantitative characters like capsule length and inflorescence length, capsule length and petal breadth, capsule length and anther length, petiole length and pistil length, leaf length and pistil length, leaf breadth and sepal length, inflorescence length and sepal length, pedicel length and pistil length showed distinct separation features. The distance matrix studies among the studied *Cleome* species revealed closeness among *C. gynandra* and *C. chelidonii*, *C. simplicifolia* and *C. monophylla* and farness among *C. viscosa* and *C. simplicifolia*, *C. viscosa* and *C. monophylla*, *C. speciosa* and *C. monophylla*, *C. gynandra* and .

C. simplicifolia, *C. gynandra* and *C. monophylla*. Dendrogram on the basis of farthest neighbour and constrained clustering strategy forms distinct two clades comprising three species each. *C. viscosa*, *C. speciosa* and *C. gynandra* form one clade and other species viz. *C. simplicifolia*, *C. chelidonii* and *C. monophylla* forms second clade.

Acknowledgements

Authors are thankful to Dr. P. D. Chavan, Dr. A. S. Nigwekar, Principal, The New College, Kolhapur and the Faculty, Department of Botany, The New College, Kolhapur for their guidance and support.

References

- Aparadh, V. T., Mahamuni, R. J. and Karadge, B. A. (2012).** Taxonomy and physiological studies in spider flower (Cleome species); A critical review. Plant science feed 2(3):25-46.
- Chatterjee, A. and Prakash, S. C. (1991).** The treatise on Indian Medicinal Plants, 2nd Eds., Vol.I. New Delhi Council for Scientific and Industrial Research, pp. 155.
- Kovach, W. L. (1999).** MVSP- multivariate statistical package of windows, version 3.1, Pentraeth Wales, Uk. Kovach computing services.
- Sonibare, M. A., Jayeola, A. A. and Egunyomi, A. (2004).** A morphometric analysis of the genus *Ficus* Linn. (moraceae). African Journal of Biotechnology, 3(4):229-235.
- Yadav, S. R. and Sardesai, M. M. (2002).** Flora of Kolhapur District. Shivaji University, Kolhapur.



Bio-control of *Fusarium udum*, the causal organism of pigeonpea wilt utilising *Trichoderma* spp.

U.A. Desai *, S. S. Kamble

Department of Botany, Shivaji University, Kolhapur

KEYWORDS

Trichoderma, *Fusarium udum*, Pigeonpea.

Corresponding Author
Email

desaiudaysingh@gmail.com

ABSTRACT

Collection of symptomatic samples of pigeonpea from different localities from Maharashtra and Karnataka state were done. The symptomatic region from the material was incorporated on Czapek Dox Agar medium and the isolated fungal mycelium was confirmed as *Fusarium udum*. Collection of soil samples were also done at exact location from where the samples of pigeonpea were collected and *Trichoderma* spp. was isolated from the soil samples. Both the fungal isolates were then studied for their antagonistic potential.

Introduction

India holds a major contribution of around 78% of the world's total pigeonpea production, becoming the largest importer (20%) and producer (25%). India engages an area of 3.73 million hectare with an annual production of 2.31 million tonnes with the production of 678 kg/ha (Anonymous, 2010). Pigeon pea is being developed in over 40 nations within, Caribbean, Africa, Asia and the Australia. Pigeon pea contributes to about 5% of the worldwide generation of pulses (Hillocks *et al.* 2000). Pigeonpea is cultivated as a forage crop in most of the countries and also inter-cropped with various crops like cotton, sorghum soybean and sugarcane. Apart from taking pigeonpea as a major crop it is also cultivated intercrop because of the cultivation period of the crop which is 6 -7 months compared with the other 3-4 months crops and also the space occupied by the crop is more compared to the major crop taken. The plant establishes soil productivity and increase fertility by fixing atmospheric nitrogen (Reddy *et al.*, 1990). Pigeon pea is a popular and commercially important

nutraceutical crop as it contains high level of amino acids proteins and vitamin B (Desai *et al.*, 2015). Such nutraceutical and commercially important crop is affected by various serious diseases and leads to heavy destruction (Patil *et al.*, 2012). Pigeon pea is bombarded by numerous bacteria, viruses and fungi but amongst them just a few create a negative impact on the plant.

The wilt caused by *Fusarium udum*, is one of the most destructive disease affecting the plant (Kannaiyan *et al.*, 1985; Desai *et al.*, 2016). Fungal pathogen, *Fusarium udum* is one of the main constraints in attaining the desired yield of the crop. Genus *Fusarium* account to the most significant group of ascomycetous fungi, whose members are liable for enormous economic loss causing depletion in yield, quality and quantity of pea (Nelson *et al.*, 1983; Leslie and Summerell, 2006). Several *Fusarium* species also cause catastrophic diseases on various cereal grains (White, 1980; Parry *et al.*, 1995; Nyvall *et al.*, 1999; Goswami and Kistler, 2004). Many members of *Fusarium* are known to produce type A and B trichothecene mycotoxins that cause toxicosis in humans and animals (Mali *et al.*, 2015).

Material and methods

Collection of material:

Fifteen isolates of infected pigeon pea plants were collected from Kolhapur, Sangli districts of Maharashtra and Dharwad, Vijapura (Bijapur) and, Belgavi (Belgaum) districts of Karnataka. The infected plant materials were brought to the laboratory in clean polythene bags, they were cut into small pieces (0.5-1.0cm length) along the symptomatic region of stem, root and leaves, they were subsequently surface sterilized by sequential dipping in 70% ethanol for 30 sec and in 0.1% HgCl₂ for 1 min and were later rinsed in sterilized distilled water, and then cultured on Czapek Dox agar (CDA) amended with 25 mg/l of streptomycin (Mali et al., 2016). Plates were incubated at 25± 2°C for 6 days (Jadhav et al., 2010). The plates were observed for fungal outgrowth through the symptomatic parts of plants. After a period of 5-6 days white cottony fungal mass was observed. On the basis of visual morphological and microscopic characters the fungal isolate was identified as *Fusarium udum* (Butler). *Fusarium udum* was consistently isolated from infected tissues which were purified by single-spore culture method (Mali et al., 2016). The sensitivity of *Fusarium udum* was carried out by using Food Poisoning Technique (Dekker and Gielink, 1979).

Dual culture method

Dual culture technique as described by Morton and Stroube (1955) was utilized for the method to test the antagonistic property of *Trichoderma harzianum* and *Trichoderma viride* against resistant isolate Fu-2 and sensitive isolate Fu-1 of *Fusarium udum*. Autoclaved at 15 lbs pressure, 20 ml Czapek Dox agar was poured in petriplates and was allowed to cool. 8mm diameter mycelial disc obtained with the help of cork borer from the actively growing margin region of the 7 day old *Trichoderma* spp. and equally old disc from the sensitive isolate Fu-1 and the resistant isolate Fu-2 of *Fusarium udum*. The discs were placed opposite to each other in equal distance from the periphery of the Petri plates. In the plate which were used as control i.e. without *Trichoderma* spp. a sterile agar

disc was kept at opposite of resistant and sensitive isolate of *Fusarium udum*. The plates were incubated at 28±2°C. The plates were maintained in triplicates for each resistant Fu-2 and sensitive Fu-1 isolate. After a interval of two, four, six and eight day's incubation period, radial mycelial growth fungal pathogen was measured and percent inhibition of radial growth was measured in relation with control, it was observed by the following the formula:

$$L = [(C-T)/C] \times 100$$

Where,

L is the inhibition of radial mycelial growth,

C is radial growth measurement of the pathogen in control,

T is radial growth of the pathogen in the presence of *Trichoderma* spp.

The fungal antagonist i.e. *Trichoderma* spp tried to inhibit the growth of fungal pathogen *Fusarium udum* (Table 1). The results thus prove that *Trichoderma* spp. acts as a very effective antagonistic agent in controlling the activity of *Fusarium udum*. The results shown thus prove that these antagonistic results are obtained due to mycoparasitism. The process of coil formation is the most common form of mycoparasitism and leads to the destruction of fungal pathogen *Fusarium udum*. *Trichoderma harzianum* showed a 2 mm inhibition zone of *Fusarium* spp. and eventually it overgrew the *Fusarium* spp. colony. Hence *Trichoderma harzianum* was found to be more effective in regard to the antagonistic property of the fungus against *Fusarium udum*.

Result

The antagonistic property of *Trichoderma harzianum* and *Trichoderma viride* against *Fusarium udum* as a biocontrol agent showed a very promising result. *Trichoderma harzianum* proved to be effective in controlling the growth of both the resistant and sensitive isolate of *Fusarium udum*. Hence *Trichoderma harzianum* was found to be a very effective antagonistic agent against soil borne pathogen *Trichoderma*.



Table 1. *In vitro* growth inhibition of sensitive and resistant isolates *Fusarium udum* in dual culture method.

Sr. No.	Antagonist	% Reduction of Mycelial Growth	
		Sensitive Fu-1	Resistant Fu-2
1.	<i>Trichoderma harzianum</i>	78.34	89.22
2.	<i>Trichoderma viride</i>	74.92	92.06

Fig. 1 *In vitro* growth inhibition of sensitive and resistant isolates *Fusarium udum* in dual culture method.

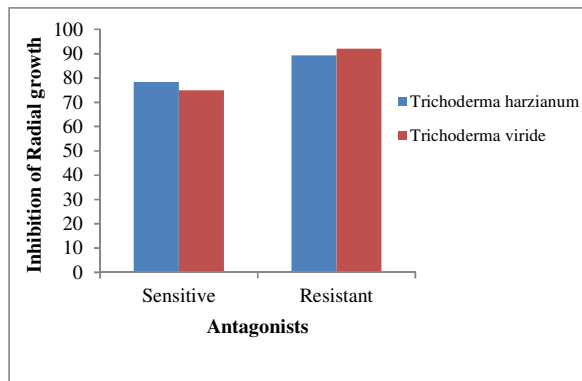
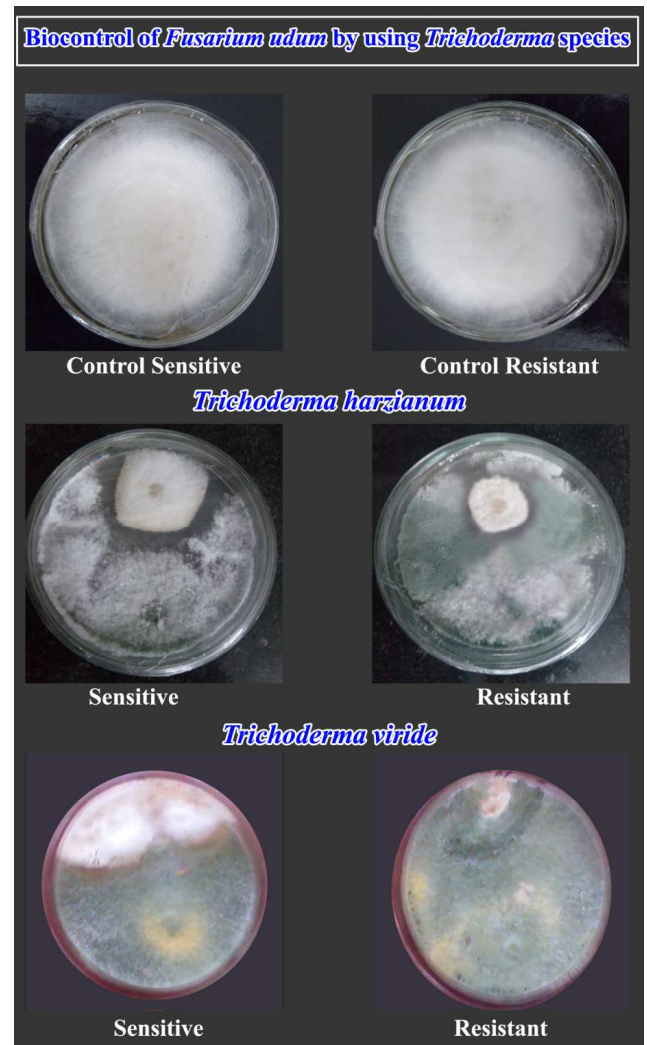


Fig. 2 Biocontrol of *Fusarium udum* by using *Trichoderma* species through *in vitro*



Discussion

Wilt caused by *Fusarium udum* is one of the biggest hurdles in the yield of Pigeon pea (*Cajanus cajan*) throughout the world. The pathogen is soil borne and hence many practices especially the use of chemicals in controlling the spread of wilt is less effective. Though the severity of disease varies in different climatic zones globally, wilt caused by *Fusarium udum* is one of the severest diseases affecting the crop. Many chemical practices help to a larger extent in containing the spread of the disease. Chemical practices involve use of various systemic and contact fungicides (Desai and Kamble, 2017). But, indiscriminate uses of fungicides of all kind including systemic, contact, etc. are not only harmful to environment but also show severe effect onto humans and animals equally, they can be flown down easily onto the

water table transferring it to other nearby areas and leaving a severe impact globally. Hence, employing certain bio-control agents is one of best alternative against the use of chemicals for the soil borne fungal pathogen like *Fusarium udum*.

Use of bio – control agents tends to be more environment friendly as well as they are safe and cost effective.

Acknowledgement

We thank the Head of the Department of Botany for providing necessary facilities to perform this experiment.

References:

- Anonymous. (2010).** Agriculture statistics at a glance, Department of Agriculture and Cooperation, Ministry of Agriculture, Govt. of India, New Delhi, 108-109.
- Dekker J and Gielink A J (1979).** Acquired resistance to pimaricin in *Cladosporium* f. sp. *Narcissi* associated with decreased virulence. *Neth. J. Pl. Pathol.* 85: 67-73
- Desai UA and Kamble SS (2017).** Effects of different fungicides on the growth of *Fusarium udum* a comparative study. *International journal of basic and applied research.* 7 (11):51-64.
- Desai UA, Andoji YS and Kamble SS (2015).** Effect of passage on the development of Benomyl resistance in *Fusarium udum* (Butler) causing wilt in Pigeon pea. *International Journal of Research in Botany.* 5(2): 27-30.
- Desai UA, Andoji YS and Kamble SS (2016).** Influence of temperature and different culture media on growth of *Fusarium udum* (Butler), causal organism of wilt of pigeonpea. *International Journal of Biological Research.* 4 (1): 42-45.
- Goswami RS and Kistler H C (2004).** Heading for disaster: *Fusarium graminearum* on cereal crops. *Molecular Plant Pathology* 5: 515-525.
- Hillocks RJ, Minja E, Silim SN and Subramanyam P (2000).** Diseases and pests of pigeonpea in eastern Africa. *International Journal of Pest Management* 46: 7– 18.
- International Journal of Tropical Medicine, 5(3):** 68-72. Host Specificity of pigeonpea wilt pathogen *Fusarium udum*. *Indian Phytopath.* 38: 553.
- Leslie JF and Summerell BA (2006).** The *Fusarium* laboratory manual. Blackwell Professional, Ames, Iowa
- Mali AM and Chavan NS (2016).** *In vitro* rapid regeneration through direct organogenesis and *ex-vitro* establishment of *Cucumis trigonus* Roxb. An underutilized pharmaceutically important cucurbit. *Industrial Crops and Products,* 83:48-54. <http://www.sciencedirect.com/science/article/pii/S0926669015306257>.
- Mali AM, Patil VB, Ade AB, Chavan NS and Kamble SS (2015).** First report of *Fusarium* sp. FIESC 17 on *Cucumis trigonus* in India. *Plant Disease,* 99, 1274, [http:// dx.doi.org/10.1094/PDIS-09-14-0881-PDN](http://dx.doi.org/10.1094/PDIS-09-14-0881-PDN).
- Mali AM, Patil VB, Pise NM and Ade AB (2016).** First Report of Leaf Spot Caused by *Fusarium* sp. NFCCI 2882 on *Angiopteris evecta*: A King Fern from Western Ghats, India. *Plant Disease,* 100 (3): 646. <https://apsjournals.apsnet.org/doi/full/10.1094/PDIS-04-15-0427-PDN>.
- Morton DT and Stroube N H (1955).** Antagonistic and stimulatory effects of microorganism upon *Sclerotium rolfsii*. *Phytopathology.* 45:419-420.
- Nelson PE, Toussoun TA and Marasas WFO (1983).** *Fusarium* Species: An illustrated manual for identification. Pennsylvania State University Press, University Park.



Parry DW, Jenkinson P and McLeod L (1995). Fusarium ear blight (scab) in small grain cereals – a review. *Plant Pathology* 44: 207-238.

Patil VB, Mali AM, Mahamuni RJ, Chavan NS and Kamble SS (2012). First report of leaf spot caused by *Phoma costrarcensis* on *Delphinium malabaricum* in Western Ghats of India. <https://apsjournals.apsnet.org/doi/abs/10.1094/PDIS-12-11-1012-PDN>.

Reddy MV, Nene YL, Kannaiyan J, Raju T N, Saka VN, Davor A T, Songa W P and Omanga P (1990). “Pigeonpea lines resistant to wilt in Kenya and Malawi”, *International Pigeonpea News letter*, Vol 6, 1990, p. 34.

White D G (1980). *Compendium of corn diseases*. APS, St. Paul, Minnesota.



Evaluation of Antimicrobial Properties and Phytochemical Content of Leaf and Fruit Peel Extract of *Capparis divaricata*

Manjunath Gopika, Vhanmane R. S, Vhankade A. M, Swami V. R.

Department Of Biotechnology

V. G. Shivdare College of Arts, Commerce and Science Solapur.

KEYWORDS

Capparis divaricata, antimicrobial, phytochemical analysis, fruit peel.

Corresponding Author
Email

manjunathags28@gmail.com

ABSTRACT

The use of plant as medicine is as old as human civilization of people of all ages. Both developing and developed countries use plant in an attempt to cure various diseases and get relief from physical suffering. The Indian subcontinent has a rich flora of various plant used in traditional medical treatments. *Capparis divaricata* is a drought resistant plant growing in dry region. *Capparis divaricata* (family –*Capparidaceae*) is found throughout India especially in Deccan peninsula from Maharashtra southwards to TamilNadu. It exhibits different uses as Herbal medicine. Therefore, the present study was undertaken with the objectives to assess the antimicrobial properties and phytochemical contents of the leaf and fruit peel extract of *capparis divaricata*. Results are analyzed and tabulated. In *E.coli*, *E.coli PUC18* and *Bacillus cereus* the extract of *capparis divaricata* at the concentration 100,200,300 mg were prepared zone of inhibition is calculated in mm. phytochemical analysis reveals the presence of alkaloids, tannins, saponins, and glycosides in sufficient amount.

Introduction

The use of plant as medicine is as old as human civilization. Medicinal plants are considered as a rich source of wide variety of ingredient which can be used for the development of drug. Specific plant knowledge may provide insight for strategic consumption and sustainable use. The continuous usage of herbal medicine by a large proportion of the population in the developing countries is largely due to the high cost of western pharmaceuticals and health care. The alternate medicine system is now gaining momentum with the knowledge of active principles identified from plant species.

Capparis divaricata is a drought resistant plant

growing in dry region. *Capparis divaricata* (family –*Capparidaceae*) is found throughout India especially in Deccan peninsula from Maharashtra southwards to TamilNadu. It exhibits different uses as Herbal medicine. Therefore, the present study was undertaken with the objectives to assess the antimicrobial properties and phytochemical contents of the leaf and fruit peel extract of *capparis divaricata*. No reports have been found concerning the pharmacological action of dry leaf and fruit peel of *capparis divaricata*. Therefore the present study was undertaken to evaluate the antimicrobial and phytochemicals of the aqueous and ethanolic extract of the aerial parts and fruit peel of *capparis divaricata*.

Material and Methods:

Source of plant material:

Leaves and fruit peel of *capparis divaricata* plant was obtained from Shingadgaon, solapur.

Preparation of leaf extracts:

The leaves of the plant were carefully removed and thoroughly washed with distilled water to remove dust particles. They were dried in shade and finely powdered using an electronic blender. Five grams of powdered material was subjected to cold extraction with ethanol and water separately. The extracts were centrifuged at 5000rpm for 30 min at 4°C and evaporated to dryness under controlled temperature (35-40°C). Each residue was reconstituted with 25 ml of respective solvent. These extract were used for antimicrobial assay and phytochemical analysis. Sample were kept in refrigerator until further use.

Source of microorganisms:

The test bacterial pathogens included *Escherichia coli*, *Bacillus cereus* and *Escherichia coli PUC 18*, was obtained from V.G. Shivdare college of Arts, Commerce and Science Solapur.

Assay of antibacterial activity:

Antibacterial activity of the extract was studied by agar well diffusion method. The bacterial from nutrient agar slants was transferred into Mueller Hinton broth and incubated at 37°C. Lawn cultures of the test pathogens were prepared by swabbing sterile Mueller Hinton agar plates with 24 hours old bacterial culture. Wells were punched with sterile cork borer (6mm internal diameter) 25µl of the extract with different concentration was added to each well. Control was maintained with respective solvent. Incubation was done at 37°C for 24 hours, diameter of the inhibitory zones were measured to the nearest millimeter (Table no.1).

Phytochemical assessment of leaf and fruit peel extract:

Qualitative screening for the presence of various phytochemical compounds was performed using the aqueous and ethanolic extract.

Qualitative analysis for phytochemical constituents:

Phytochemical screening procedure was carried out to determine the biologically active compound that contribute to the flavor, color, and other characteristic of leaves and fruit peel. (Table no: 3)

Test for alkaloid: About 2gm of ground sample were ponded separately on a mortar. 0.2g was boiled with 5ml of 2% hydrochloric acid on steam bath for 5 minutes the mixture was allowed to cool and filtered and filtrate treated was shared in equal proportion into 3 test tube and labeled A, B, C. 1ml of the filtrate was treated with 2 drops of the following reagent respectively with Dragendroff's reagent red precipitate was shown. With Mayer's reagent a creamy white colored precipitate indicated the presence of alkaloid.

Test for flavonoid: 0.5gm of the macerated sample of *capparis divaricata* was introduced into 10 ml of ethyl acetate and heated in boiling water for 1 minute. The mixture was then filtered and the filtrate used for the following test. 4ml of filtrate was shaken with 1ml of 1% aluminium chloride solution and kept. Formation of a yellow color in the presence of 1ml dilute ammonia solution indicated the presence of flavonoids.

Test for Saponins: 0.1g of the sample was boiled with 5ml of distilled water for 5 minutes. Mixture was filtered and the filtrate used for the following test. To 1ml of filtrates, 2 drops of olive oil was added, the mixture was shaken and observed for the formation of emulsion. 1ml of the filtrate was diluted with 4ml of distilled water. The mixture was vigorously shaken and then observed on a stand for stable froth.

Test for the tannins: Into 2g of the ground sample, 5ml of 45% ethanol was added and boiled for 5 minutes. The mixture was cooled and filtered. 1ml of the filtrate was added 3 drops



of lead sub acetate solution .A gelatinous precipitate was observed which indicates the presence of tannins. Another 1ml of the filtrate was added 0.5ml of bromine water. A pale brown precipitateswere observed indicate the presence of tannins.

Test for glycosides: 2g of the sample was mixed with 30ml of distilled water and it was heated for 5 min on a water bath, filtered and used as follows: 5ml the filtrate was added to 0.2ml of fehling solution A and fehling solution B until it turns alkaline and heated in a water bath for 2 min. A lightish blue coloration was observed (instead of brick red precipitate) which indicates the absence of glycosides. Final observation is tabulated.

Quantitative Analysis of Phytochemical Constituents:

Determination of alkaloids: 0.5gof the sample was dissolved in 96% ethanol and 20% H₂SO₄ (1:1) mixture. 1ml of the filtrate was added to 5ml of 60% tetraoxosulphate and allowed to stand for 5 min. then, 5ml of 0.5% formaldehyde was added allowed to stand for 3hrs. The reading was taken at absorbance of 565nm.

Determination of flavonoids: Flavonoid in the test sample was determined by the acid hydrolysis of spectrophotometric method .0;5g ofprocessed plant sample was mixed with 5ml dilute HCL and boiled for 30 min.the boiled extract was allowed to cool and filtered. 1ml of the filtrate was added to 5ml of ethyl acetate and 5ml of 1% NH₃.It was then scanned from 420nm-520nm for the absorbance.

Determination of saponins: 0.5 of the sample was added to 20ml of 1N HCL and boiled for 4 hr. after cooling it was filtered and 50ml of petroleum ether was added to the filtrate, for ether layer and evaporated to dryness. 5ml of acetone and ethanol was added to the residue. 0.4ml of each was taken into 3 different test tubes. 6ml of ferrous sulphate reagent was added into them followed by 2ml of concentrated H₂SO₄. It was thoroughly mixed after 10 min the absorbance was taken at 490nm.

Determination of tannins: 5g of the ground sample was shaken constantly for 1 min with 3ml of methanol in a test tube and then poured into a Buchner funnel with the suction already turned on. The tube was quickly rinsed with an additional 3ml of methanol and the contents poured at once into the funnel. The filtrate was mixed with 50ml of water and analyzed within an hour. For aqueous extraction,5ml of water was used for extraction and for the rinse and filtrate was added to 50ml of water. 3ml of 0.1 ml FeCl₃ in 0.1 NH₄Cl was added to 5ml of the extract and followed immediately by timed addition of 3ml of 0.008 ml K₂F₆(CN)₆ .the absorbance was taken at 720 nm spectrophotometrically. Obtained values are tabulated.

Result and Discussion

Medicinal plants have always been the source of biologically active compounds used for the treatment of various infectious diseases.

Antibacterial activity: From table 1 and 2 it is clear that the aqueous and ethanolic extract of *capparis divaricata* shows growth inhibition activity at 300mg. as concentration increases the zone of inhibition increases for *E.coli* and *B.cereus* but for *E.coli PUC18* as concentration increases zone of inhibition decreases.

Phytochemical analysis: Previous studies have reported that number of medicinal plants species tested has some active biological compound these biological compounds includes the phytochemicals. The Qualitative tests reveal the presence of alkaloids, flavonoids, tannins, Saponin and glycosides (Table no: 3). The quantitative analysis in aqueous extract of leaf shows the amount of tannins to be high followed by flavonoid, alkaloids and Saponin. In fruit peel amount of flavonoid is higher followed by Saponin, alkaloid, tannin and glycoside. (Table no: 4)

In ethanolic extract leaf has maximum amount of alkaloid followed by tannin, flavonoids, Saponin and glycosides. (Table no: 5) Tannin and flavonoids are organic compounds

Acknowledgment

consisting of complex mixture of polyphenolic compounds that are widespread in the plant, such as leaf, immature fruits etc. They help in preventing the microbial growth. The secondary metabolites help in management of diseases and oxidative stress which leads to cellular damage.

We wish to extend our sincere gratitude to Dr. Basutkar, Prof. M. B patil, Prof. Gopika Manjunath, for providing us the support and guidance for this research work. We are also thankful to entire supporting staff of the laboratory whose help has been invaluable for the successful completion of our research work.

Table 1: Antibacterial activity of aqueous extract of *capparis divaricata*

Aqueous extract	Concentration in mg	Diameter of the zone of inhibition(mm)		
		<i>E.coli</i>	<i>E.coli PUC 18</i>	<i>Bacillus cereus</i>
<i>Capparis Divaricata</i>				
	100mg	6 ±0.2	9 ± 0.2	5 ± 0.3
	200mg	8 ±0.3	8 ± 0.2	6 ± 0.2
	300mg	9 ± 0.4	7 ± 0.3	7 ± 0.4

Table 2: Antibacterial activity of ethanolic extract of *capparis divaricata*

Ethanolic extract	Concentration in mg	Diameter of the zone of inhibition(mm)		
		<i>E.coli</i>	<i>E.coli PUC 18</i>	<i>Bacillus cereus</i>
<i>Capparis Divaricata</i>				
	100mg	8±0.2	7± 0.3	7± 0.2
	200mg	9±0.3	6± 0.2	8± 0.4
	300mg	10±0.2	3 ± 0.3	9± 0.5

Table 3: Qualitative analysis of different extracts of *capparis divaricata* for phytochemical.

Sr.No	Name of the phytochemical	Different extract of <i>Capparis divaricata</i>			
		Aqueous		Ethanolic	
		Leaf	Fruit peel	leaf	Fruit peel
1.	Alkaloids	+ve	+ve	+ve	+ve
2.	Flavonoids	+ve	+ve	+ve	+ve
3.	Tannins	+ve	+ve	+ve	+ve
4.	Saponins	+ve	+ve	+ve	+ve
5	Glycosides	+ve	+ve	+ve	+ve

+ve = present, -ve= negative.



Table 4: Quantitative analysis of *Capparis divaricata* for phytochemical.

Sr. no	Name of phytochemical	<i>Capparis divaricata</i> (aqueous extract)	
		Leaf	Fruit peel
1.	Alkaloids (mg/100g)	44.80	69.56
2.	Flavonoids(mg/100g)	50.20	96.34
3.	Saponins(mg/100g)	42.86	72.24
4.	Tannins(mg/100g)	64.81	42.56
5.	Glycosides(mg/100g)	24.2	32.30

Table 5: Quantitative analysis of *Capparis divaricata* for phytochemical.

Sr. no	Name of phytochemical	<i>Capparis divaricata</i> (ethanolic extract)	
		Leaf	Fruit peel
1.	Alkaloids (mg/100g)	62.32	55.20
2.	Flavonoids(mg/100g)	52.2	44.33
3.	Saponins(mg/100g)	34.1	45.22
4.	Tannins(mg/100g)	53.3	49.22
5.	Glycosides(mg/100g)	21.1	36.2

References

Balladh B. and Chaurasia O.P (2007) traditional medicinal plant of cold desert Ladakh—used in treatment of cold, cough and fever, j. *Ethnopharmacol.*,112(2),341-349(2007).

Brain K R, and Turner TD(1975)The Practical Evaluation of Phytopharmaceuticals. Wright- Scientica, Bristol,;57-58.

Calis I, Kuruuzum-Uz A, Lorenzetto PA, et al. (2002) (6S)-Hydroxy-3-oxo- α -ionol glucosides from *Capparis spinosa* fruits. *J. Phytochemistry.*;59:451-457.

Capasso A, Piacente S, Pizza C. et al (1997)

Isoquinoline alkaloids from *Argemone mexicana* reduce morphine withdrawal in guinea pig isolated ileum. *Planta Medica*;63(4):326-8.

Ekramul Haque M, Mahmuda Haque, Mukhlesur rahman M, (2002) E-octadec-7en-5-ynoic acid from the roots of *Capparis zeylanica*. *J. Ethnopharmacology.*;108:208-211.

Gadgoli C. Mishra SH. (1999) Antihepatotoxic activity of p-methoxy benzoic acid from *Capparis spinosa*. *J. Ethnopharmacology.*;66(2):187-192.

Ghule BV, Muruganathan G, Nakhat PD (2006)
Immunostimulant effects of Capparis zeylanica Linn.
leaves. J. Ethnopharmacol.108(2):311-5.

Ghule BV, Muruganathan G. and Yeole PG (2007)
Analgesic and antipyretic effects of Capparis
zeylanica leaves. J. Fitoterapia.;78(5):365-9.

OECD guidelines, 2008.

Ram Nath Chopra SR. Poisonous Plants of India,
(1984)1:196-197

Samy R.P, Pushparaj P.N and Gopalakrishnakone P.A.
(2008) Compilation of bioactive compounds from
Ayurveda, *bioinformation*, 3, 100-110

Sarragiotoo MH, Nazari AS, Marcos Lins de Oliveira
(2004) Prolinebetäubem B-methylproline, 3-
carbomethoxy-N-methyloyridinium and kaempferol
3,7-dirhamnoside from Capparis humili. J.
Biochemical Systematics and Ecology.;32:505-507.

Sofowora A. (1993) Medicinal Plants and Traditional
Medicine in Africa. Spectrum Books Limited, Ibadan,
Nigeria.;151-153.

Trease G. and Evans WC. (1983)Textbook of
Pharmacognosy. 12th ed., Balliere, Tindall,
London.;343-383.

Turana M, Kordalib S, Zenginb H. (2003) Macro and Micro
Mineral Content of Some Wild Edible Leaves
Consumed in Eastern Anatolia, Acta Agriculturae
Scandinavica. J. Plant Soil Science.;53:129-137.



Histology of male reproductive system in longhorn beetle *Aeolesthes holosericea* Fabricius (Coleoptera: Cerambycidae).

Patil N. K.¹ and S. M. Gaikwad^{2*}

¹Assistant Professor, Department of Zoology, M. H. Shinde Mahavidyalya, Tisangi.

²Assistant Professor, Department of Zoology, Shivaji University, Kolhapur

KEYWORDS

Spermatogonia, vasa efference, vas deference, ejaculatory duct, *Aeolesthes holosericea*.

Corresponding Author
Email
namdevkpatil@rediffmail.com

ABSTRACT

Histology of male reproductive system in the adult of *Aeolesthes holosericea* was studied. Histologically, testis shows peritoneum, epithelium and various stages of the spermatogenesis like spermatogonia, spermatocytes, spermatids, sperm bundles and cysts and inter follicular septum. T. S. of vasa efference and seminal vesicle show peritoneum, circular muscles, epithelium and fluid in the lumen. T. S. of ejaculatory duct reveals the peritoneum, glandular coat, circular muscle, cuboidal epithelium, and intima. T. S. of all three accessory glands (A, B and C) shows somewhat similar structure like the circular muscle, basement membrane, columnar epithelium and secretion in the lumen. The aedeagus shows structures like the penis, tegmen, parameres, dorsal sturts, and musculature.

Introduction

In insects, reproductive organs exhibit the variety of forms, but there is a basic design and function of each component so that even the most aberrant reproductive system can be understood in terms of the generalized plan. The individual components of reproductive system can vary in shape (e.g. of gonads and accessory glands), position (e.g. of the attachment of accessory glands), and number (e.g. of ovarian and testicular tubes or sperm storage organs) between different insect groups and sometimes even between different species in the same genus (Gullan and Cranston 2010). The main reproductive function of a male is to produce and store the spermatozoa and transport it to the female reproductive tract. The studies on histomorphology of various systems in insect are essential to know the basic histological organization of various organs in an insect.

In the present investigation, efforts have been made to understand the histology of male reproductive system in the adult of *A. holosericea* which is a wood boring serious pest of so many plants.

Material and Methods

The adults obtained from laboratory culture as well from the field were used for the histomorphological investigation. They were dissected in chilled insect ringer solution (Ephrussi and Beadle 1936). Various parts of male reproductive systems were fixed in Bouin's fixative and Stieve's fixative for 24 hr. The tissue was washed under running tap water for 12 hr to remove excessive fixative and then gradual dehydration of tissue was carried out using ethyl alcohol. The tissue which was fixed in Stieve's – fixative were washed in 50% alcohol and post fixed transfe-

-rred to 70 % alcohol containing enough iodine for 5 to 8 hr) for removal of excess mercury as per Humason (1962). This step was followed by gradual dehydration as usual. After dehydration, the tissue was cleaned in xylene, infiltrated and embedded in molten paraffin wax (52°C - 54°C). The tissues were sectioned at 5-7 µm thickness. The sections were dewaxed and stained with Haematoxylin-Eosin (Humason1962). Histological observation of each reproductive organ was made and microphotography was done.

Results

Histological details of an adult male reproductive system of an insectan type in general and coleopteran type in particular with minor differences. Histologically, testicular follicle of the testis is lined with the thin layer of epithelium whose cells externally rest upon a basement membrane, outside of which there is a peritoneal coat of connective tissue. The transverse section of each follicle shows various septa as ingrowths of thin strands of connective tissue, from the periphery which converge towards the center from where the vas efference is originated (Fig.1&2). These intra follicular septa divide the substance of the follicle into 100-150 compartments. The follicular compartment shows a radial arrangement as usually observed in other forms of Coleoptera and contains a succession of zones in which the sex cells are in different stages of development. The arrangement of sex cells in the compartment is so systematically that represent entire process of spermatogenesis from apical to distal end of the tubules (Fig.3). Each compartment is divided into four zones viz. germarium with densely packed primordial germ cells (spermatogonia), the zone of growth containing spermatocytes in sperm cysts, the zone of maturation containing spermatids within cysts and zone of transformation showing mature spermatozoa in bundles. The spermatozoa are located at the posterior ends of the testicular compartments in the proximity of the vas efference. The entire process of spermatogenesis is seen in the peripheral region of the follicle and major central portion of the follicle is filled with spermatozoa covering, a middle circular muscle layer and

Internally a layer of cuboidal epithelium lined by the basement membrane (Fig.4). Posteriorly, the wall becomes thickened and cuboidal epithelial cells become tall columnar. The lumen of vas efference is filled with spermatozoa and secretory material. The vas deference shows thick walled tube with an inner lining of columnar epithelial cells rest on basement membrane surrounded by circular muscle layer and peritoneum (Fig.5). The posterior portion of the vas deference becomes distended forming the seminal vesicle. The histological details of the seminal vesicles are observed like that of vas deference. However, the lumen of the seminal vesicle is seen empty and the wall of the seminal vesicle is internally lined with an intimal layer (Fig.6). At the junction of seminal vesicle and the vas deference i.e. the anterior portion of vas deference, there is constriction provided with well-developed circular muscle fibers. The wall of ejaculatory duct consists outer peritoneum, thick layer glandular cells and several layers of circular muscle fibers with an inner epithelial layer. It is internally lined with a well-developed layer of chitinous cuticle i. e. intima hence it is ectadenia. The epithelial cells are cuboidal in nature and show stratified epithelium (Fig.7&8). There are three accessory glands named A, B, and C. All three accessory glands shows the inner layer of epithelium rest on basement membrane surrounded by a layer of circular muscle fibers. In transverse section, the wall of accessory gland A shows a layer of tall columnar epithelial cells (Fig.9a). The nuclei are placed central and apically epithelium show brush border with secretory globules. The epithelium of accessory gland B and C is made up of two layers of cuboidal epithelial cells with central nuclei (Fig.9b & c, Fig.10). The cytoplasm of epithelial cells seems to be granular and the lumen of all accessory glands is filled with secretory material.

Discussion

The anatomy of the male reproductive system in *A. holosericea* is studied by Gaikwad and Patil (2017) and the present study is the extension work to the male reproductive system of *A. holosericea*. The male reproductive organs in the *A. holosericea* consists of a pair of testes, 2 pairs of vasa



efferentia, a pair of vasa deferentia, seminal vesicle, ejaculatory duct, aedeagus and accessory glands (Gaikwad and Patil 2017). Each testis in *A. holosericea* consists of two follicles (Fig.1). Each follicle shows a thin layer of epithelium based on the basement membrane and externally covered with peritoneum. According to Imms (1963) and Snodgrass (1935), the sperm tubes or follicles are divided into a series of zones according to the state of development of the germ cells. They differentiate these zones as germarium containing primordial germ cells or spermatogonia, the zone of growth in which the spermatogonium enter a stage of multiplication and develop into spermatocytes, the maturation zone where spermatocytes undergo meiosis and give rise to spermatids and lastly zone of transformation where spermatids become transformed into spermatozoa. Each spermatogonial group in most insects soon becomes enclosed in a cellular envelope known as sperm cyst (Snodgrass 1935). A similar type of zonation is observed in the compartments of the testicular follicles of *A. holosericea* along with the sperm cysts. Edwards (1961) described the development of spermatozoa in Cerambycid beetle *P. reticularis* in which he mentioned the formation of cysts containing primary and secondary spermatocytes in the pupal stage. Ehara (1951), who examined the histology of adult testes of 41 species of Cerambycidae and distinguished Cerambycinae and Lepturinae and found only spermatozoa and spermatids from Lamiinae. According to Snodgrass (1935), Imms (1963), Escherich (1894), and Wigglesworth (1965) in the majority of insects, the vas deference consists of a narrow tube and its enlarged posterior seminal vesicle. According to Muir (1918) and Singh (1924), the vas deference of coleopteran is a secondary structure and is ectodermal in origin. However, Metcalfe (1932) has clearly mentioned that vas deference in Coleoptera is mesodermal in origin as it is an outgrowth of the testis. In the species under study, the posterior portion that is the region of the seminal vesicle is internally lined with intima and rest anterior part has no chitinous lining indicate that anterior region of vas deference is a mesodermal and posterior region of vas deference is ectodermal in origin. The histological details of the vasa

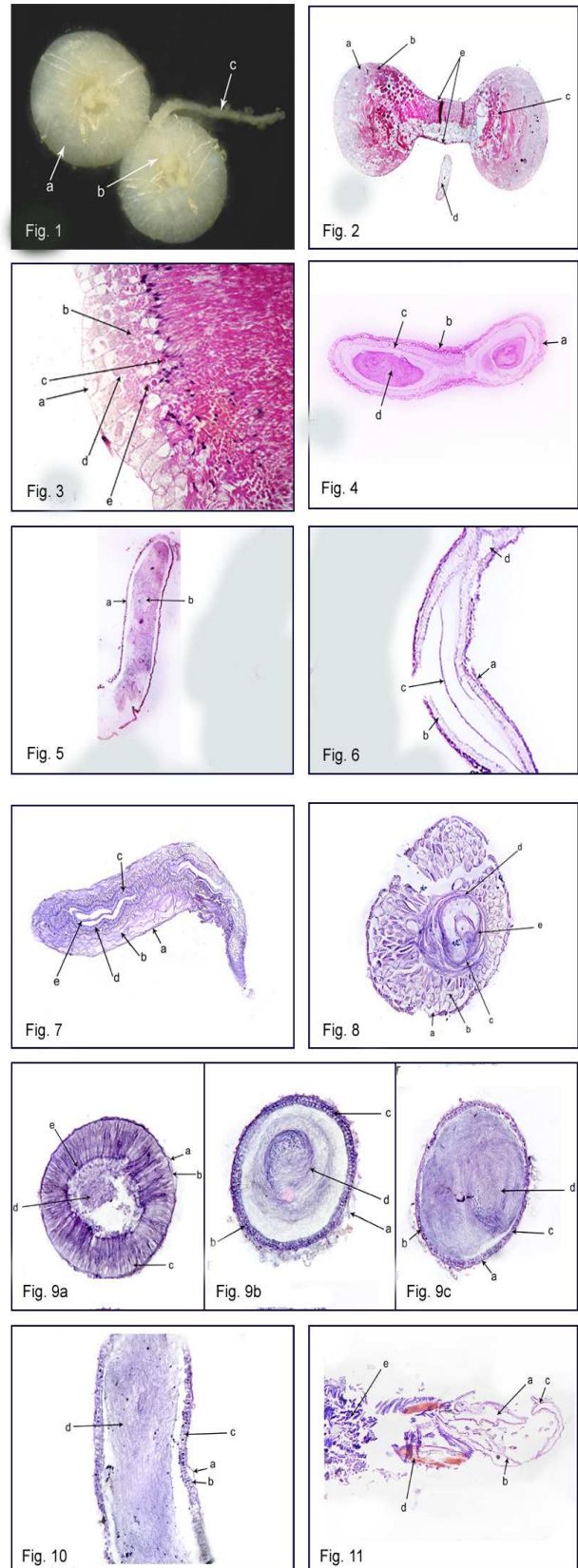


Fig. 1: Whole mount of testicular follicle, vasa-efferentia and vas- deference Note a: testicular follicle, b: vas-efference, c: vas-deference.

Fig.2. L.S.of testicular follicle (40X) Note a: peritoneum, b:epithelium, c:developing sex cells (spermatogenic cells) d: vas-efference, e: dorsal and ventral concavities in the follicle.

Fig.3. T.S. of testicular follicle (400X) depicts, a:spermatogonia, b: spermatocytes, c: spermatids, d:sperm bundle, e:cyst, f:inter follicular septum.

Fig.4 T. S. of vasa-efferentia junction (100X) shows a: peritoneum, b: circular muscle, c:epithelium, d: fluid containing spermatozoa.

Fig.5.L. S. of vas-efferens (100X) Note a: vas- efferens wall, b: lumen filled with secretion containing spermatozoa.

Fig.6. L. S. of seminal vesicle (100X) shows, a: circular muscles, b:epithelium c: intima ,d: constriction at the junction of seminal vesicle and vas-deference

Fig.7. L. S. of glandular ejaculatory duct (100X) Note a: peritoneum, b: glandular coat, c: circular muscle, d: cuboidal epithelium, e: intima.

Fig.8. T. S. of glandular ejaculatory duct (100X) depicts, a: peritoneum, b: glandular coat, c: circular muscle, d: cuboidal epithelium, e: intima

Fig. 9a T. S. of accessory gland A (400X) showing a: circular muscles, b:basement membrane, c:columnar epithelium, d: secretion in lumen, e:brush border

Fig.9b T. S. of accessory gland B(400X) showing a: circular muscle, b: basement membrane,c: cuboidal epithelium, d: lumen filled by secretion.

Fig.9c T. S. of accessory gland C(400X) showing a: circular muscle, b: basement membrane,c: cuboidal epithelium,d: lumen filled by secretion

Fig. 10 L. S. of accessory gland B (400X) depicts a: Circular muscle, b: basement membrane, c: epithelium d:secretion in lumen.

Fig. 11 Cross section of aedeagus (400X) . Note, a: penis, b: tegmen, c; parameres,d: dorsal sturts, e: musculature.

Conclusion

Results obtained in the present investigation may help to understand histology of male reproductive systems in adult *A. holosericea* and will help to design the regulatory mechanism to control the population of this serious pest.

Acknowledgements

The authors are also thankful to Head, Department of Zoology, Shivaji University, Kolhapur for laboratory facilities during work.

References

- Berberet R C, Helms T J (1972) Comparative anatomy and Histology of selected systems in larval and adult *Phyllophaga anxia* (Coleoptera: Scarabaeidae).AnnEntomolSoc Am 65 (5): 1026 -1053
- Chapman R F (1998) The insect structure and function,4th Edition, Cambridge University Press. pp 740
- Escherich K (1894) Anatomischestudien liber das mannlicheGenitalsystem der Coleoptera.Z WissZool 57: 620–641.
- Edmonds W D (1974) Internal anatomy of *Coprophanaeus lancifer* (L.) (Coleoptera: Scarabaeidae). International journal of insect morphology and Embryology 3(2):257-272
- Edwards J S (1961) On the reproduction of *Prionoplus reticularis* (Coleoptera: Cerambycidae) with general remarks on the reproduction in the Cerambycidae. Q j MicroscSci102(4):519-529
- Ehara S (1951) Histological structure of male gonads of some Cerambycid beetle with remarks on their systematic relationship. J FacSci Hokkaido Univ10:266
- Ephrussi B,Beadle GW (1936) Transplantation technique, *Drosophila*.Amer Naturalist 70:218-225
- Gillot C (1982) Entomology 3rdEdition,University of Saskatchewan, Saskatoon, Saskatchewan, Canada.pp729.
- Gaikwad S M, Patil N K (2017) Anatomy of the male reproductive system in *Aeolesthesholosericea* Fabricius,1787 (Coleoptera: Cerambycidae) Intl JResBiosci, Agri and Tech 5(3):304-307
- Gullan P J; Cranston P S (2010) The insects: an outline of entomology- 4th ed. Wiley- Blackwell Publication, New York. pp 565
- Humason GL(1962) Animal tissue techniques. W. H. Freeman and Co., San- Fransico, London. pp 468
- Imms A D (1963) *A general textbook of entomology*, 9th ed. revised by Richards OW and Davies RG. Asia Publishing House, Mumbai. pp 886



Inamdar R F; Joshi PV (1984) Histological studies of female reproductive system of *Platynotus punctatipennis* (Coleoptera: Tenebrionidae) J Morphol 181:1-8

Jacob R A (1989) Comportment de butinge de I abeille domestique et desabeilles savages dans vergers de prommiersenbelgique. Apidologie 20: 271-285

Metcalf M E (1932) The structure and development of the reproductive system in the Coleoptera with notes on its homologues. Quart J micr Sci 75: 49-130

Mani M S (1982) General Entomology 3rd and revised edition Oxford and IBH Publishing Co. New Delhi. pp 912

Muir F (1918) Notes on the ontogeny and morphology of the male genital tube in Coleoptera. Transactions of the Royal Entomological Society of London 223- 229.

Murad H, Ahmad I (1977) Histomorphology of the male reproductive organ of the red flour beetle, *Tribolium castaneum* L. (Coleoptera : Tenebrionidae). J Anim Morphol Physiol 24: 35-41

Slipinski A, Escalona H (2012) Generic revision and phylogeny of *Microheiseine* (Coleoptera: Coccinellidae). Systematic Entomology 37: 125-171

Singh P H (1924) The development of the ovipositor and efferent ducts of *Tenebrio molitor* L. (Coleoptera), with remark on the comparison of the latter organ in the two sexes Proceeding of the Zoological Society of London, Part III: 869-83

Snodgrass R E (1935) Principles of insect morphology. Tata McGraw-Hill Pub, Co., Ltd., New Delhi pp 667

Tembhare D B (2013) Modern Entomology, Himalaya Publishing House, Mumbai pp 506

Wigglesworth V B (1965) The principles of Insect Physiology. Dutton, New York, pp 427-497

Wigglesworth V B (1976) Evolution of insect wings and flight, Nature (London) 246: 127-129



Diversity of Bivalve Molluscs from Karanja Estuary, Uran Dist- Raigad (ms) - a systematic survey

Kamble S. P.

Assistant Professor, Department of Zoology, Mahatma Phule Arts, Science, Commerce College,
Panvel, Dist. Raigad (MS)

KEYWORDS

Karanja estuary, Bivalve molluscs, Systematic, Diversity.

**Corresponding Author
Email**

sam_kam23@rediffmail.com

ABSTRACT

The present work deals with the systematic survey of bivalve molluscs of Karanja estuary. The survey revealed a total 15 species of bivalve molluscs, these bivalves belonging to 4 families and 14 genera were recorded. The observation indicates the fragility and productivity of estuary.

Introduction

Being a very specialized environment, estuaries supports a wide assemblage of animal communities. It is the life habitats of many groups of animals which live entirely within. Many suspension feeding marine bivalve molluscs live in variable environments, such as estuaries and shallow coastal waters.

Many ecological and faunal survey studies have been carried out on the back waters and mangroves all over the world; some are Ganpati and Lakshmana Rao (1959) in the Godavari estuary. Berry (1964, 1972 and 1975) studied the distribution of molluscs in the Malaysian mangrove swamp, Macnae (1968) has described the general account of the fauna and flora of mangrove swamp and forests in Indo west pacific region, Subba Rao and Mookherjee (1975) in Mahanadi estuary Orissa, Hutchings and Recher (1982), Sasekumar (1981) has studied meiofauna of Malayan mangrove shore and Ashton (1999) studied biodiversity and community ecology of mangrove plants, molluscs and crustaceans in two mangrove forest in peninsular Malaysia. Subba Rao *et.al.* (1983) studied the malacofauna of Muriganga estuary, Sunderban.

Present work has been carried out with a view to catalogue the bivalve molluscs living in intertidal sandy and muddy region of the Karanja estuary.

Material and Methods

Samples of bivalve molluscs were collected at fortnight intervals during low tide period. The sampling procedure consist of placing series of quadrates of nylon rope of one meter square and one foot depth, by laying randomly just over the bed. The sand in the quadrates was dug out with the help of shovel and spade and sieved through different sieves having different mesh sizes for different animals.

They were thoroughly washed and passed with different grades of alcohol. Then they were preserved in 70% alcohol. Some animals were preserved in 10% formalin. Bivalve molluscs were identified according to Abbott, (1954); Macdonald, (1982), Gordon, (1990); Sowerby, (1996) and Apte, (1998).

Result and Discussion

order	Family	Genus	Species
I. Arcoidea	1. Arcidae	<i>Arca</i>	1) <i>granosa</i> (Linnaeus, 1758)
II. Eulamellibranchia	2. Veneridae	<i>Meretrix</i>	2) <i>meretrix</i> (Linne, 1758) 3) <i>casta</i> (Chemnitz) (Preston, 1915)
		<i>Katylsia</i>	4) <i>opima</i> (Gmelin)
		<i>Paphia</i>	5) <i>laterisulca</i> (Roding)
		<i>Gelonia</i>	6) <i>proxima</i> (Gmelin)
		<i>Sanguinolaria</i>	7) <i>diphos</i> (Linnaeus, 1758,1771)
		<i>Dosinia</i>	8) <i>prostata</i> (Linne, 1758)
		<i>Venerupis</i>	9) <i>microphylla</i> (Deshayes)
		<i>Gafrarium</i>	10) <i>divaricata</i> (Chemnitz)
	3. Ostreidae	<i>Crassostrea</i>	11) <i>gryphoides</i> var <i>cattuckensis</i> (Newton & Smith)
		<i>Saccostrea</i>	12) <i>cucullata</i> (Born, 1778)
III. Mytiloidea	4. Mytilidae	<i>Perna</i>	13) <i>viridis</i> (Linne)
		<i>Modiolus</i>	14) <i>metcalfei</i> (Hanley)
		<i>Pinna</i>	15) <i>succatta</i>

Table-1: Checklist of molluscan fauna (Bivalvia) from Karanja estuary.

Kingdom : Animalia
 Sub-kingdom : Invertebrata
 Phylum : Mollusca
 Class : Pelecypoda (Bivalvia)



Total 15 species of bivalves belonging to 4 families and 14 genera were recorded in survey viz. *Crassostrea cuttuckensis*, *Saccostrea cucullata*, *Meretrix meretrix*, *Meretrix casta*, *Katelysia opima*, *Paphia laterisulca*, *Gelonia proxima*, *Sanguinolaria diphos*, *Dosinia prostata*, *Venerupis microphylla*, *Gafrarium divaricata*, *Arca granosa*, *Perna Viridis*, *Modiolus metcalfei*, *Pinna sucatta* (Table-1). The abundance of bivalves indicates the rich productivity of estuary.

Most dominant macro faunal group recorded for Maharashtra coast are given molluscs group was represented by many important species of bivalves such as *Perna viridis*, *Crassostrea cucullata*, *Pinctada* sp. *Meretrix casta*, *M. Meretrix*, *Gafrarium* sp. etc. (Anon, 1984).

The bivalve molluscs play a vital role in converting the organic matter together meiobenthos into biomass which in turn is consumed by fishes. Thus the molluscs help in the secondary productivity and form an important component in the food web of the estuarine ecosystem (Durga Prasad *et al.* 2001). Due to a good food quality they are widely exploited by local fishermen's. Many factors, both natural and man-made have been responsible for limiting the distribution of bivalve species and causing them to become rare or even extinct.

References

- Abbott, R. T. (1954)** American Seashells. D. Van Nostrand Company, Inc.: Princeton, New Jersey. 541 pp.
- Anon, N.A. (1984).** The mangrove ecosystem: Research methods UNESCO, 251 p.
- Apte, D. (1998).** *The book of Indian shells.* (Bombay Natural History Society), Oxford University, Press, Delhi.
- Ashton, E.C. (1999).** Biodiversity and community ecology of mangrove plants, molluscs and crustacean in two mangrove forests in Peninsular Malaysia in relation to local management practices D Phil thesis University of New York U.K.
- Berry, A. J. (1964).** Faunal zonation in mangrove swamps. *Bull. Nat. Mus.* Singapore 32:90-98.
- Berry, A.I. (1972).** The natural history of west Malaysia mangrove faunas Malayan. *Nature Journal* 25: 135 – 162.
- Berry, A.I. (1975).** Molluscs colonizing mangrove trees with observations on *enignormia rosea* (Anomiidae), *Proceedings of the malacological society* 41: 589 – 600.
- Durga Prasad N. H. K., D. V. Rama Sarma and L. M. Rao (2001).** Molluscan fauna of Gosthani Estuary A systematic survey., *J. Aqua Biol.* Vo. 16 (1): 15 – 17.
- Ganapati, P.N. and M.V. Lakshman Rao (1959).** *Curr. Sci* 28: 232
- Gordon, N. R., (1990).** Seashells a Photographic Celebration. New York: Mallard Press, Hardcover. Color Photographs; Folio; 144.
- Hutchings, P.A. and Recher H.F. (1982).** The fauna Australian mangroves. *Proceedings of Linean society of NSW* 106 (1) 83 – 121.
- Macdonald. (1982).** The Macdonald Encyclopedia of Shells. *Macdonald and Co (Publishers) Ltd. London and Sydeny.*
- Macnae, E (1968).** A general account of the fauna and flora of mangrove swamps and forest in the Indo West Pacific Region, *Advances in Marine Biology*, 6: 73 – 270.
- Sasekumar, A (1981)** The ecology of meiofauna shore Ph.D. thesis Department of Zoology University of Malaysia Kuala Lumpur, Malaysia.
- Sowerby, G. B. (1996)** Shells of the World. London, Bracken Books. hardcover met stofomslag, 139 pp.
- Subba Rao, N.V. and Maokherjee H.P. (1975)** *Recent Researchers in Estuarine Biology* (ed.) R. Natarajan Hindustan Publ. Corp. (I.) Delhi (India).
- Subba Rao, N.V., Dey A and S. Barua (1983)** Studies on the malacofauna of muriganga estuary Sunderbans West Bengal *Bull. Zool. Surv. India* 5 (1): 47 – 56.



Acute toxic effect of sugar factory effluent on behavior and mortality in fresh water fish, *Labeo calbasu*

Vinod Kakade

Assistant Professor, Department of zoology, Eknath Sitram Divekar College Varvand,
Pune- 412 215 (MS) India.

KEYWORDS

Effluent,
Labeo calbasu,
Toxicity,
Mortality

Corresponding Author
Email

ybkakade156@gmail.com

ABSTRACT

Labeo calbasu was exposed to a lethal concentration of sugar factory effluent for respective hrs. The LC₅₀ value of the prepared concentration for 24, 48, 72 and 96 hrs were found at 11, 10.5, 10 and 9.5% respectively. At this concentration increase opercular movement, erratic swimming, loss of equilibrium, leaping out of water was observed during experiment

Introduction

Industrial development has been generally equated with ecological degradation which leads to environmental pollution. Every year, million tons of pollutants are introduced into environment by various routes. Any change in the aquatic medium causes behavioral changes in fish ultimately leading to physiological adjustment.

Brown (1976) listed twelve basic types of investigation in toxicity studies. According to him chief use of toxicity test is for preliminary screening and monitoring of chemicals and effluents to determine the extent of risk to aquatic organisms and to determine the component causing death. This has opened a field of experimental area for the ecologists concerned in evaluating the degree of damage to biota and suggesting necessary protective measures. Fish, serve as the most proteinous food available at the cheapest rate and hence has become a necessary ingredient or component of the national economy of the third world countries, particularly countries facing food problems. Acute toxicity tests are especially important in determining the effect of toxicant on organisms in a short period of time (Hagen, 1959).

The toxicity testing using fish as a model was reported as early in 1951 by Doudoroff et al., and latter several reports were added by others on various pesticides (Murthy, 1986; Murthy and Kondaiah, 1991).

The present study has been under taken to investigate the effect of sugar factory effluent on behavior and mortality of fresh water fish *Labeo calbasu* after acute (a relatively short term exposure with lethal concentration) treatment.

Material and Methods

Fish *Labeo calbasu* collected from river Bhima near Kangaon, Tal Daund, (Pune) having average weight (5-8 gm) and length (8-9 cm) and acclimatized for two weeks under laboratory conditions. A batch of ten fishes was introduced each prepared concentration at interval of 24hr, 48hr, 72hr and 96 hr to get exact LC₅₀ values. Toxicity was determined according to static bioassay method to estimate LC₅₀ values of the respective hrs (Sprague, 1970). A control group of same fish was also kept during experimentation. The water was renewed every 24 hours

Mortality at different time interval in the concentrations of sugar factory effluent was recorded and also observed changes in the behavior of fishes. The LC₅₀ values of the different time periods were calculated by regression analysis method (Finneys 1971).

Result and Discussion

Fish exposed to lethal concentration of sugar factory effluent showed highly excited state and seemed most affected. The fish showed irregular swift movements and erratic jumping in water and the loss of equilibrium and were found floating on the surface with an increased opercular beats and widen opercular flap, after a short interval the fish showed jerky movements and swimming without any direction, the highly affected fish died while less affected ones slowly re-gained their normal swimming activities. The LC₅₀ values of sugar mill effluent were assayed for 24, 48, 72 & 96hr are 11, 10.5, 10 and 9.5 % respectively (Table. 1).

Exposure period (hrs)	LC ₅₀ (%)	Log of conc.	Empirical probit	Expected probit	Calculate LC ₅₀
24	11	1.0413926	5	5	10.970925
48	10.5	1.0211892	5	5	10.484506
72	10	1.0	5	5	9.987242
96	9.5	0.97777236	5	5	9.470094

Table no-1 Probit regression line for LC₅₀ values in *Labeo calbasu* exposed to concentration of sugar factory effluent.

In Joshi and Rege (1980) studied toxicity of pesticides and other chemicals and demonstrated that toxicity increased with exposure time. Similarly, fish exposed to pesticides and industrial effluents show behavioral changes (Symons, 1973; Verma et al., 1977 and Bakthavathasalam and Reddy, 1981).

Summer (1980) reported that Diquat and Paraquat have low level of toxicity of perch, *Perca fluviatilis*, and roach, *Rutilus rutilus*.

Saksena (1987) studied the comparative toxicity of Mercuric chloride to freshwater teleost, *Clarias batrachus* and *Puntius ticto*.

The 96h LC₅₀ value of mercuric chloride to *Clarias batrachus* and *Puntius ticto* are 0.15 mg/l and 0.10 mg/l. Gupta et al., (1993) reported toxicity of Zinc to fresh water teleost *Notopterus notopterus* and *Puntius zavanicus*. Daud et al., (1998) reported the 6.6 mg/l unionised ammonia for 48hrs LC₅₀ in hybrid Tilapia species *Mossambicus niloticus*. Zyadh and Abdel (2000) studied toxicity and bioaccumulation of Copper, Zinc and Cadmium in some aquatic organism like fishes, crabs Mollusca etc.

Aziz et al., (1993) showed that *T. mossambica* exposed to weak and strong doses of CdCl₂ produced haematological abnormalities. Abou, et al., (1995) found organochlorine pesticides in fresh water and sediments of Nile River and some lakes. Durairaj and Salvarajan (1995) reported high toxicity of combined Quinalphos and Phenthoate on *O. mossambicus* than the individual pesticide. James et al., (1995) studied effect of Cu and Hg on *H. fossils* and found significant decrease in food consumption and growth. Kidd et al., (1995) reported high concentration of toxaphene and other organochlorine compounds in fish from subarctic lake. Sarkar and Konar (1995) studied effect of Thiodon, Cr and alkaline FI on *O. mossambicus*, *Cyclops viridis* and *Porandiarowerbyi* and found that there was no impact of pH, DO alkalinity and water hardness. The effect was toxic to plankton and additive and antagonistic on worm and fish.

Muniyan and Veeraraghavan (1999) while working on toxicity of Ethofenprox to *O. mossambicus* found erratic swimming, hyper and hypo-activity changes in opercular movement, loss of equilibrium, mucous secretion all over the body and chromatic changes on skin.



The fish *T. mossambica* was exposed to median lethal concentration (LC₅₀ for 24 hrs) for lead, zinc and copper were 0.073, 0.26 & 0.115µg/l respectively and showed characteristics changes in behavior, fishes survived rapidly in the experimental media and were trying to jump out of water at short intervals. Later fishes exhibited restlessness by erratic opercular movement, difficult in respiration, convulsions and short erratic jerky movements (Mazher Sultana and DawoodSharief 2004).

Patnaik and Patra (2006) reported the 96 hr LC₅₀ of sevin for *Clarias batrachus* at 15.3 mg/l. Kumar et al., (2006) reported the median lethal concentration for copper 3, 6, 12, 24, 48, 72 and 96 hrs at 99.59, 89.39, 66.74, 52.63, 44.26, 33.61 and 28.21 ppm. It is also reported that the treated fish, *C. mrigala* showed loss of equilibrium, changes in opercular movement, changes in orientation and locomotion, mucus coating on the body and erratic swimming.

Sudheer Kumar et al., (2006) reported the exposure of fish to different concentration of chlorpyrifos showed no mortality up to 0.1 ppm, but, found 50% mortality at 0.18 ppm and 100% mortality at 0.26 ppm. In case of azadirachtin no mortality was observed up to 3.4 ppm, 50% mortality at 4.2 ppm and 100% mortality at 5 ppm

Khillare (1985) studied toxicity of pesticide on fresh water fish *Barbus stigma*. Khillare and Wagh (1987) studied LC₅₀ of endosulfan to four species of fishes with variable conditions of temperature, water hardness and Ph. Khalaf (1990) studied acute and chronic toxicity of organochlorine, organophosphate and carbonate pesticide to fresh water fish *S. mossambicus*.

Jignasachhaya et.al. (1997) observed 1.72% as the 96 hr LC₅₀ value for textile and printing industry effluents in the mud skipper's *Periophthal musdipes*. Rana and Sudhir (1999) observed the acute toxicity of tannery and textile dye effluent on common teleost fish *Labeo rohita*, the LC₅₀ of textile dye effluents were 8.8, 8.4, 8.0, 7.2 mg/l for 24, 48, 72 & 96 hr

The 96hrs LC₅₀ of Endosulphan for the *Anabustudineus* was recorded at 16.91ppb. When *A. testudineus* was expose to Endosulfan, the fish exhibited a series of behavioral responses such as imbalanced and restlessness of movement, erratic swimming, tremor, flashing and lethargy (Bindu and Geeta, 2009).

During present study LC₅₀ of sugar factory effluent for different time periods (24, 48, 72 and 96h.) have been obtained at 11, 10.5, 10 and 9.5%, and showed increase in frequency of the opercular movements, loss of balance and attempts to escape from the aquarium were prominent, which are coreleted with work of earliar researcher, Khillare and Wagh (1988), Mazher Sultana and DawoodSharief (2004), Kumar et.al., (2006), Bindu and Geeta (2009).

References

- Abou Arab, A. K., Gomaa, M. N., Badawy, A and Naguib, K. (1995):** Distribution of organochlorin pesticides in the Egyptian aquatic ecosystem. Food Chem. Vol. 54, No. 2. pp. 141-146.
- Aziz, F., Amin, M. and Shakoori, A. R., (1993):** Toxic effects of DDT on the kidney of a freshwater fish, *Channa punctatus* (Bloch) Trends in Ecotoxicology, 257-262.
- Bakthavathsulam, R. and Reddy, Y. S. (1981):** Toxicity and behaviour responses of *Anabustesticines* (Bloch.) exposed to pesticides. Indian J. Environ. Hlth23 : 215-392.
- Bindu V. S. and P.R. Geetha (2009):** Acute toxicity, Behavioural Changes and Haemopoieic Alterations induced by endosulfan in the fresh water teleoast *Anabus testudineus*. Poll Res. 28 (1): 53-58 (2009).
- Brown V.M. (1976)** Advances in testing the toxicity of substances to fish chemistry Ind. 21:143-149.
- Dandoroff P., B.G. Anderson, G.E. Burdic, P.S. Galtsoff, W.B. Hart, R. Patric, E.R. Strong , E.W. Surber and W.M. and Van Horn (1951):** Bioassay

methods for evaluation of acute toxicity of industrial wastes of fish. *Sewage and Indust. Wastes*.23:1380-1397.

- Daud, S.K., Hosbollash, D., Law, A.T.C (1998):** Effect of unionized ammonia on Red *Tilapia mossambicus* O. niloticces Hybrid). The second international Symposium on Tilapia in aquaculture Bangkok, Thailand; 15: 411-413.
- Durairaj, S. and Selverajan, V. R., (1995):** Synergistic action of organophosphorus pesticides of fish, *Oreochromism ossambicus*. *J. Environ. Bio.*16(1) : 51-53.
- Finney, D. J., (1971):** Probit analysis, 3rd Edition, combridge University Press, London.
- Gupta, A.K. and Chakrabarti, P. (1993):** Toxicity of Zinc to fresh water teleasts. *Notopterus notopterus* (Pallas) and *Puntius javanicus* .*J. Freshwater. Biol.* 5(4) 359-363.
- Hagen, J.M. (1959):** Acute toxicity in “Appraisal of the safety of chemical in food, drugs and cosmetics” Association of food and drug officials of United States of America. 17-25.
- James, R., Sampath, K., Sivakumar, V. and Babu, S. (1995):** toxic effects of copper and mercury on food intake, growht and proximate chemical compsoition in *Heteropneustes fossilis*. *J. Environ. Biol.* 16(1): 1-6.
- Jignasachhaya., JayeshThaker., Mansuri, A.P; and RahulKunde (1997):** Textile dying and printing industry effluent induced changes in the activity of few ATPase in the gill and intestine of mudskipper, *Periophthal musdipes*. *Poll. Res.* Vol. 16(2): 93-97.
- Joshi, A. G. and Rege, M.S., (1980):** Acute toxicity of some pesticides and few inorganic salts to the mosquito fish, *Gambusiaaffinis*(Baird and Girard). *Indian J. Exp. Biol.* 18: 435-437.
- Khillare, Y. K. (1985):** Toxicological effect pesticide on fresh water fish *Barbus stigma* (Ham) Ph. D. Thesis, Dr B. A. M. University, Aurangabad
- .Khillare, Y. K. and Wagh, S. B., (1987):** Acute toxicity of the pesticide endosulfan to fish. *J. Environ, Ecol,* 5(4) : 805-806.
- Kidd, K. A., Schindler, D .W., Muir, D.C.G., Lockhart, W.L. and Hesseil, R.N. (1995):** High concentration of toxaphane in fishes from asubarctic lake. *Science Wash.* Vol. 267. No. 5221, Pp. 240- 242.
- Mazher, S. and Dawood, S. (2004):** Effect of heavy metals on the histopathology of gill and Brain of *Tilapia mossambicus*. *J. Aqua. Biol.* 19(1): 165-168.
- Muniyan, M and Veeraghavan, K., (1999):** Acute toxicity of ethofenprox to the freshwater fish, *oreochromic mossambicus* (Peters). *J. Environ. Biol.* 20 (2) : 153-155.
- Murthy, A.S. (1986):** Toxicity of pesitices to fish. *CRC Press, Florida.*Vol.141.
- Murthy, A.S. and K. Kondaiah (1991):** Standard test for firsh form India and the neighbouring countries. *Bull. Environ. Contam. Toxicol.*46 : 871-878.
- Patnaik and Patra, A.K. (2006):** Haemoatopoietic alterations induced by carbarlyin *Clarias batrachus* (LINN). *J. Appl. Sci. and Environ. Mangt.* Vol. 10, No. 3 pp, 5-7.
- Rana, K.S. and Raizada Sudhir (1999):** Acute toxicity of tannery and textile dye effluent on a common telecast *Labeo rohita*: Histological alternation in liver. *J. Environ. Biol;* 20(1): 33-36.
- Saksena, D.N. (1987):** On the comparative toxicity of mercuric chloride to two freshwater teleosts. *J. Hydrobiol.* Vol. 3 No.5pp. 29 to 32.
- Sarkar U.K. and Konar S.K. (1995):** The combined effects of pesticide thiodon, heavy metal chromium and detergents ekaline FI on and fish food Organisms. *J. Environ Bio.* 16 (1): 19-26.
- Sprague, J. B., (1970):** Measurement of pollutant toxicity to fish II. Utilizing and applying bioassy results. *Ibid.,* 4 : 3-32.



Sudheer Kumar, D.J., John Sushma, N. and Sivaiah, U.

(2006): Effect of chlorpyrifos and azadirachtin on Ach and AchE of fish, *Tilapia mossambica*. Aquacult. Vol. 7 (1), 87-91.

Summer L.A. (1980): The Bipyridinium Herbicides, New South Wales Australian Academic Press.

Symons, P. E. K. (1973): Behavior of young Atlantic Salmon (*Salmosalar*) exposed to forcefedfenitrathion, an organophosphate insecticide. J. Fish. Res. Board. Can. 30: 651 – 655.



Water quality assessment of takve lake of shirala taluka, Sangli district.

¹Shakila P. Maldar*, ²Niranjana S. Chavan.

¹Smt. Kasturbai Walchand College, Department of Botany, Sangli*

²Department of Botany, Shivaji University, Kolhapur

KEYWORDS

Physicochemical parameters, Water quality Index, Takve Lak

Corresponding Author
Email
drsunillondhe@gmail.com

ABSTRACT

The present study was attempted to calculate Water Quality Index of Takve Lake. Takve water body is located in Shirala Taluka of Sangli district, Maharashtra. In order to assess the status of quality of water the work is under taken. The present water body is selected as it is located in remote place. There are several ways to assess the quality of water as deemed fit for drinking, irrigation and industrial use. Water quality index, indicates the quality in terms of index number and offers a useful representation of overall quality of water for public .A number of parameters affect the usability of water for particular purpose. Thus water quality index was determined on the basis of various Physico-chemical parameters viz. Electric conductivity, pH, temperature, total hardness, total alkalinity, ammonia, dissolved oxygen, Biochemical oxygen demand, organic nitrogen, Total nitrogen, and Total phosphorus. The index value of water body during rainy season and summer season was found to be above 50 indicating poor quality status. But in winter index value is below 50 (41.17) indicating good water quality of water.

Introduction

The fresh water is of vital concern for mankind, since it is directly linked to human welfare .The surface water bodies are most important source of water for human activities are unfortunately under sever environmental stress .

The measurement of water quality index decide the water quality status .Water quality index of ponds and lakes have been studied by several workers. (Horton (1965) Shardendu and Ambasht (1988) Yogendra and Puttaiah (2008) Umamaheshwari (2010). Water quality index thus provides a single number that expresses over all water quality at a

certain locations and objective of water quality index to turn complex water quality data into information that is understandable and useable by the public.

Water Quality Index (WQI) is defined as a rating reflecting the composite influence of different water quality parameters as the overall quality of water. A single number cannot tell the whole story of quality; there are many other water quality parameters that are not included in the index. However water quality index based on important parameters can serve as simple indicator. In general water quality indices incorporate data from multiple water quality

parameters in to a mathematical equations that rates the health of water body with number.

Shirala taluka ,situated at the bank of Morna River which has numerous lentic water bodies .These water bodies are manmade(artificially constructed reservoirs) to provide water for irrigation purpose or domestic use. These water bodies reflect the society around them. The water quality of water body Takve has not been studied scientifically so far. Hence the present investigation is under taken: Shirala taluka experiences three distinct seasons, summer, rainy and winter. The WQI was calculated from the suitability of pond water for human consumption. The weights for various water quality parameters were assumed to be inversely proportional to the recommended standards which have been presented in respective table for the corresponding parameter. Takve water body is selected for assessing the quality of water. Because the water body practically receive domestic water and agricultural runoff throughout the year. Therefore to know the current status of the water body present work is attempted.

Material and Method

The water samples were collected at an interval of 30 days and analyzed for 12 physico-chemical parameters by following standard procedures. The parameters ,pH,electrical conductivity, and dissolved oxygen were monitored at the sampling sites and other parameters like total hardness, total alkalinity ,ammonia, total nitrogen ,organic nitrogen ,total phosphorus ,biological oxygen demand were analyzed in the laboratory as per the APHA (1995) and Trivedi and Goel (1984) during the year 2012-2013.

The WQI has been calculated by using the standards of drinking water quality recommended by World Health Organization (WHO), Bureau of Indian Standards (BIS) and Indian Council of Medical Research(ICMR) .The weighted arithmetic Index method has been used for the calculation of WQI of water body .The quality rating OR sub index (qn)was calculated using the following expressions.

$$q_n = 100(V_n - V_{io}) / (S_n - V_{io})$$

Where,

Q_n = Quality rating for the n^{th} water quality parameter

V_n = Estimated value of the n^{th} parameter at a given sampling stations

S_n = Standard permissible value of n^{th} parameter

V_{io} = Ideal value of the n^{th} parameters in pure water i.e. 0 for all other

Parameters except the parameters pH and Dissolved oxygen (7.0 and 14.6mg/l) respectively.

Unit weight was calculated by a value inversely proportional to the recommended standard value S_n of the corresponding parameter

$$W_n = K / S_n$$

Where,

W_n = Unit weight for the n^{th} parameter

S_n =Standard value for the n^{th} parameter

K = Constant of proportionality

The overall WQI level and status of water quality as suggested by Chatterjee and Raziuddin (2002) is given in Table-1

Table 1: Water Quality Index (WQI) level and status of water Quality

Water quality Index	Water Quality Status
$90 \geq$	Excellent
65 to 89	Permissible
39 to 64	Marginally suitable
11 to 34	In adequate for use
$0 \leq$	Totally Unsuitable



The drinking water standards as recommended by recommending agencies and unit weights are presented in Table .2

Table .2 Drinking water standards and unit weights

Parameters	Standards	Recommending Agency	Unit Weight
pH	6.5-8.5	ICMR/BIS	0.236
Electric conductivity (EC)	300	ICMR	0.371
Temperature	-----	-----	-----
Total alkalinity (TA)	120	ICMR	0.014
Total hardness (TH)	500	ICMR/BIS	0.003
Dissolved oxygen (DO)	5.0	ICMR/BIS	0.330
Biological oxygen demand(BOD)	5.0	ICMR/BIS	0.330
Ammonia	5.0	ICMR/BIS	0.12042
Total Nitrogen	-----	-----	-----
Organic Nitrogen	-----	-----	-----
Total Phosphorus	6.0	ICMR/BIS	0.10035

❖ All values except pH and Electric conductivity are in mg/l EC in mmhos/cm

Results and Discussion

The results of present investigations are depicted in Table 3 and 4. Water Quality Index of the lake Takve was calculated for seasons (Rainy, winter and summer season.)

Table 3:- Seasonal variation in Physico-chemical parameters

Sr. no.	Parameters	Rainy season	Winter season	Summer season
1	pH	7.5	6.46	7.96
2	Electrical conductivity	10.599	40.747	59.101
3	Total alkalinity (TA)	184.17	128.33	129.00
4	Total Hardness(TH)	156.42	114.33	139.00
5	Dissolved Oxygen(DO)	2.28	2.85	3.34
6	Biological Oxygen Demand(BOD)	1.63	0.43	1.79
7	Ammonia	8.15	0.52	3.03
8	Total Phosphorus	0.02	0.13	0.58

All values except pH and Electrical Conductivity are in mg/L, Ec expression in mmhos/cm

Table 4:- Water Quality Index calculated for Rainy season.

Sr.no.	Parameters	V _n	S _n	1/S _n	W _n	Q _n	W _n Q _n
1	pH	7.5	7	0.143	0.1547	50	7.735
2	EC	10.599	300	0.003	0.0032	3.533	0.0113
3	Total alkalinity (TA)	184.17	120	0.008	0.0086	153.48	1.320
4	Total Hardness(TH)	156.42	500	0.003	0.0032	31.284	0.1001
5	Dissolved Oxygen(DO)	2.28	05	0.200	0.2164	128.3	27.76
6	Biological Oxygen Demand (BOD)	1.63	05	0.200	0.2164	32.6	7.055
7	Ammonia	8.15	05	0.200	0.2164	163	35.27
8	Total Phosphorus	0.02	06	0.167	0.1806	0.333	0.0601
					∑W _n = 1.0	∑q _n = 562.53	∑W _n q _n = 79.312

Water Quality Index in Rainy season = $\frac{\sum q_n W_n}{\sum W_n}$

$$\boxed{WQI = 79.312}$$

Table 5:- Calculation of Water Quality Index calculated for in winter season.

Sr. no	Parameters	V _n	S _n	1/S _n	W _n	Q _n	W _n Q _n
1	pH	6.46	7	0.143	0.1547	36.00	5.5692
2	EC	40.747	300	0.003	0.0032	13.582	0.0435
3	Total alkalinity (TA)	128.33	120	0.008	0.0086	106.94	0.9197
4	Total Hardness(TH)	114.33	300	0.003	0.0032	38.11	0.1220
5	Dissolved Oxygen(DO)	2.85	05	0.200	0.2164	122.40	26.487
6	Biological Oxygen Demand (BOD)	0.43	05	0.200	0.2164	8.6	1.861
7	Ammonia	0.52	05	0.200	0.2164	10.4	2.251
8	Total Phosphorus	0.13	06	0.167	0.1806	2.167	0.391
					∑W _n = 1	∑Q _n = 338.20	∑W _n q _n = 37.644

Water Quality Index (WQI) in winter season = $\frac{\sum q_n W_n}{\sum W_n}$

$$= 37.644/1$$

$$\boxed{WQI = 37.644}$$



Table 6:- Calculation of Water Quality Index calculated in summer season.

Sr. no	Parameters	V _n	S _n	1/S _n	W _n	Q _n	W _n Q _n
1	pH	7.96	7	0.143	0.1547	64	14.016
2	EC	59.101	300	0.003	0.0032	19.700	0.0634
3	Total alkalinity (TA)	129.00	120	0.008	0.0086	107.5	0.9245
4	Total Hardness(TH)	139.0	300	0.003	0.0032	46.33	0.1483
5	Dissolved Oxygen(DO)	3.34	05	0.200	0.2164	117.29	25.382
6	Biological Oxygen Demand (BOD)	1.79	05	0.200	0.2164	35.8	7.7471
7	Ammonia	3.30	05	0.200	0.2164	60.6	13.114
8	Total Phosphorus	0.58	06	0.167	0.1806	9.67	1.7464
					∑W _n = 1	∑Q _n =460.89	∑W _n Q _n =88.55

Water Quality Index (WQI) in summer season = $\frac{\sum q_n W_n}{\sum W_n}$

$$= 88.55/1.58$$

Water Quality index of Takve was established by placing eight (8) important physicochemical parameters in three different seasons viz. Rainy, winter, and summer season. From the results it was observed that WQI of the lake was maximum during rainy seasons.

In rainy season the WQI was found to be 57.53 which indicates poor water quality. In winter season it is 41.175 which is good water quality. But again in summer it changes (56.04) is poor as per standard values. Based on the results, it is clear that water is not suitable for drinking in rainy and summer season. This water quality rating clearly expresses the status of the lake i.e. water is unsuitable for the human consumption.

In present investigation pH ranged between 6.46 to 7.96. In many of the collections the pH remained near neutral. However, when average values for three seasons are taken into account, the present water body found to be slightly alkaline. These findings are similar to the observations of Ambasht (1971), Peter (1975) Shardendu and Ambasht (1988) Swarnalata and Narasing Rao (1993), Sinha (1995) and Yogendra and Puttaiah (2008) who have also made similar observations in their studies on different water bodies. Maximum Ec found in summer season the concentration of dissolved oxygen regulates the distribution of aquatic flora and fauna. The present investigation indicated that the conc. of dissolved oxygen fluctuated between 2 to 3 mg/l in rainy season,

and in winter season while 3 to 4 mg/l in summer season. Seasonally, the concentration of dissolved oxygen was more during summer and least during rainy season. This observation is similar with observations of Poonam Bhadija and Ashokkumar vaghela (2013)

Biochemical oxygen demand is a parameter to assess the organic load in water body. The BOD concentration ranges between 1 to 3 mg/l. Present values summarize that there are fluctuations in the physicochemical parameters seasonally. However, during rainy season because of dilution, mixing and run off the water quality changes. The present piece of work suggests that the Takve lake water is not suitable for drinking purpose.

References

- Ambasht,R.S. (1971)** , Ecosystem study of a tropical pond in relation to primary production of different vegetation zones, *Hydrobiologia*,12:57-61.
- APHA, (1981)**, Standard methods for the Examination of water and waste water, APHA, Washington DC.USA.
- APHA, (1995)**, Standard methods for the Examination of water and waste water, 9thEdition, American Public Health Association, Washington D.C.
- Chatterjee,C.and Raziuddin, M. (2002)** , Determination of water quality Index (WQI) of a degraded river in Asanol Industrial area ,Ranging , Burdoan , West Bengal ,Nature, Environment and Pollution Technology, 1(2): 49-59 and 181-189.
- Petre,T.,(1975)** ,Limnology and Fisheries of Nymba Yamung, a manmade lake in Tanzania, *Journal of Tropical Hydrobiology, Fish*, 4:39-50.
- Shardendu and Ambasht ,R.S. (1988)** ,Limnological Studies of rural pond and an urban tropical ecosystem, ecosystem, oxygen in forms and ionic strength, *Journal of Tropical Ecology*.
- Sinha, S.K. (1995)** , Potability of rural ponds water at Muzaffarpur (Bihar) ,A note on water quality pollution *Research*,14 (1) : 135-140.
- Trivedi and Goel, (1984)**, Chemical and Biological methods or water pollution studies, Environment Publication, Karad.
- Uma Maheshwari,S, S, S.(2010)**, Water Quality Index of Temple pond at TalaKadu Karnataka, India, *Lake (2010)* ,Wetlands ,Biodiversity and climate change.
- Venkateshwarlu, V. (1993)** Ecological studies on the rivers of Andhra Pradesh with special reference to water quality and pollution, *Proceeding of Indian Academy of Science (Plant Science)* , 96: 495-508
- Yogendra, K and Puttaiah, E.T., (2008)** Determination of Water Quality Index and suitability of an Urban water body in Shimoga Town Karnataka. *Proceedings of Taal .2007. The 12th World Conference* ,:342-346 (Editors ,Sengupta)



Detection of seed mycoflora of some important oil seeds from Kolhapur

S.C.Vhandrao, J.D.Babar, G.B.Gosavi, R.K.Kamble, S.A.Magdum, S.L.Soudagar and S. S. Kamble.

Mycology and Plant Pathology Laboratory, Department of Botany, Shivaji University, Kolhapur. 416 004

KEYWORDS

Colletotrichum truncatum,
Rhizoctonia solani,
Aspergillus flavus and
Pythium sps, *Sclerotium rolfii*.

Corresponding Author
 Email

s20sk@yahoo.co.in

ABSTRACT

Samples of oil seeds (Groundnut, Soybean, Mustard and Sunflower) were collected from Kolhapur Grocery market, and examined for seed Mycoflora by following Blotter method (Doyer, 1938) and Agar plate method (Muskett and Malone, 1948). Seeds of Soybean showed presence of *Colletotrichum truncatum*, *Rhizoctonia solani*, *Aspergillus flavus* and *Pythium sps*; while seeds of Mustard showed presence of *Sclerotium rolfii*; seeds of Groundnut showed *Aspergillus flavus*; while seeds of Sunflower showed presence of *Rhizoctonia sps*.

Introduction

Microorganisms play important role in affecting the quality of seed of which fungi are the largest group. these fungi may decrease seed germinability, cause seed discoloration produce toxins that may be injurious to man and animals and may reduce seed weight also. (Neergard,1986)

In India soybean, groundnut, sunflower, mustard are most commonly used edible oils for preparing daily food. These oils are considered as healthy oils and they are obtained from their seeds. In present investigation efforts were made to determine seed mycoflora of soybean, groundnut, mustard and sunflower seeds.

Material and Method

Samples of oil seeds (Soybean, Groundnut, Mustard and Sunflower.) were collected from Kolhapur Grocery Market.

The collected seeds were surface disinfected with 0.1% HgCl₂ for 2 minute and then rinsed three times in sterile distilled water. Surface disinfected seeds were placed on water soaked blotters in petriplate. Plates were incubated for 12 hours at alternating cycle of light and darkness by following Blotter (Doyer, 1938) and Agar plate methods (Muskett and Malone, 1948).

Table: 1. Seed mycoflora of selected oil seeds

Sr. no.	Name of oil seed	Seed borne fungi detected
1.	Soybean	<i>Colletotrichum truncatum</i> , <i>Rhizoctonia solani</i> , <i>Aspergillus flavus</i> and <i>Pythium sps</i> .
2.	Groundnut	<i>Aspergillus flavus</i> .
3.	Mustard	<i>Sclerotium rolfii</i> .
4.	Sunflower	<i>Rhizoctonia sps</i> .

Results and Discussion

From table 1 it is clear that, Soybean seeds were infected by, *Colletotrichum truncatum*, *Rhizoctonia solani*, *Aspergillus flavus* and *Pythium sps.* Groundnut seeds were infected by *Aspergillus flavus*. Mustard seeds were infected by *Sclerotium rolfsii* and Sunflower seeds were infected by *Rhizoctonia sps.*

Popoola and Akueshi (1986) reported *Aspergillus niger*, *Colletotrichum sps.*, *Fusarium oxysporum*, *Fusarium solani* and *Penicillium sps.* on seeds of Soybean. Similarly, Agrwal and Gupta (1989) found that *Macrophomina phaseolina*, *Fusarium sps.*, and *Aspergillus sps.* dominantly occurred on Soybean seeds. Abdalla (1974) noted that, *Rhizopus sps.*, *Penicillium sps.*, *Sclerotium bataticola* and *Fusarium sps.* on groundnut seeds, similarly, Lumpungu and Bitigula (1989) reported, *Fusarium sps.* and *Sclerotium bataticola* on Groundnut seeds. Shrivastav, Singh and Pathak et al. (1980), reported, *Alternaria alternata*, *Aspergillus flavus*, *Aspergillus niger*, *Trichoderma viride*, on mustard seeds.

Vijaylakshmi and Rao (1950), observed *Alternaria alternata*, *Aspergillus flavus*, *Aspergillus niger*, *Penicillium citrinum*, *Rhizopus nigricans* on sunflower seeds; Afzal et al. (2010), reported *Alternaria alternata*, *Alternaria helianthi*, *Aspergillus flavus*, *Aspergillus niger*, *Fusarium solani*, *Penicillium* and *Rhizopus sps.* on sunflower seeds.

References

- Abdulla, M.H. (1974).** Mycoflora of groundnut kernels from the Sudan. Transaction of the British Mycological Society. 63(2):353-359.
- Afzal, R., Mughal, S.M, Munir, M., Sultan, K., Qureshi, R., Arshad, M. and Laghari, A.k. 2010.** Mycoflora associated with seeds of different sunflower cultivars and management. Pak. J. 42(1):435-445.
- Agrwal, S.C. and Gupta, R.K. (2007)** Fungal pathogens detected on soybean seeds grown in different localities. Seeds Res. 14(2):208-210.
- Lumpungu, K., Baelenge, B. and Bitijula, M. (1989).** The effect of groundnut seeds coat on the development of pathogenic fungi. Tropicitura. 7(4):128-131.
- Popoola, T.O.S and Akueshi, C.O. (1986).** Seedborne fungi and bacteria of soybean (*Glycin max L.*) in Nigeria. Seeds Res. 14(2):170-176.
- Shrivastava, K.K, V N Singh and K K Pathak (2006)** Seeds Mycoflora of Stored Mustard and its control by fungicide, Department of Botany, Banaras Hindu University, Varanasi 221005.
- Vijayalakshmi, M. and Rao, A S (1985).** Fungal infection of sunflower seeds under different conditions of storage. Indian Phytopath.. 38(2):315-318.



Zinc ferrite as efficient H₂S gas sensor

S. D. Jadhav^a, A.D.Pinjarkar^b, S.L.Pawar^b, R. P. Patil^{b*}

^aDepartment of Chemistry, Yeshwantrao Chavan Science College, Karad-415124, MH, India

^b Department of Chemistry, M.H. Shinde Mahavidyalaya, Tisangi - 416206, MH, India

KEYWORDS

Zinc ferrite,
Co-precipitation,
XRD, SEM,
Electrical resistivity,
Gas sensor.

Corresponding Author
Email
raj_rbm_raj@yahoo.co.in

ABSTRACT

ZnFe₂O₄ was synthesized by using co-precipitation method under stoichiometric conditions. The structure and the crystal phase of the powder were characterized on an X-ray diffractometer. The ferrite powder existed as single phase cubic spinel oxide and has a particle size of ~30nm. DC electrical resistivity of the prepared ferrite powder was studied by using two probe method and it indicates the semiconducting nature of prepared spinel ferrite. Gas sensing response of zinc ferrite was evaluated as a function of operating temperature for different test gases such as ammonia, chlorine, LPG, CO₂, Cl₂, hydrogen sulphide and H₂. ZnFe₂O₄ exhibit significantly high response towards H₂S gas at their 300 ppm concentration at 300^oC.

Introduction

Hydrogen sulphide gas is a colorless, corrosive, toxic and flammable gas, occurring naturally in crude petroleum, natural gas, volcanic gases, and hot springs with smell of rotten eggs. Combustions of petroleum and coal are the predominant sources of the gases containing sulfur. Hydrogen sulfide is considered a broad-spectrum poison, meaning that it can poison several different systems in the body, although the nervous system is most affected. The toxicity of H₂S is comparable with that of hydrogen cyanide. It forms a complex bond with iron in the mitochondrial cytochrome enzymes, thus preventing cellular respiration. Since hydrogen sulfide occurs naturally in the body, the environment and the gut, enzymes exist in the body capable of detoxifying it by oxidation to (harmless) sulfate. Hence, low levels of hydrogen sulfide may be tolerated indefinitely.

The gases containing sulfur can result in undesirable disastrous deformations such as infection to respiratory track and lung cancer [1, 2]. In last decade, remarkable efforts have been taken for the development of ferrite gas sensors in detection of toxic gas pollutants from vehicle exhaust, biological hazards, environment, and pollution monitoring [3]. Therefore, monitoring of traces of such gases has become prime research work [4]. Various oxide as well as dioxides has been well studied as a sensor material to detect most of the reducing gases [5-7]. Sensors based on semiconducting oxides like SnO₂, ZnO, and WO₃ have been widely studied, due to their distinct advantages, such as high response time and low cost [8-9]; however, selectivity remains the main challenge for such materials. But the major problem associated with this material is its total lack of selectivity. Several novel materials are being tried with distinct and extraordinary gas sensing capabilities.

It is observed that the gas sensitivity depends on kinds of semiconducting material, temperature, and test gases to be detected. Mixed-metal oxides are a family of oxides that play an important role in a wide variety of fields [10]. The basis for this wide range of applications is related to the variety of transition metal cations that can be incorporated into the lattice of the parent spinel structure. The parameters such as phase formation, crystallite size, particle size, grain size, dopants, surface area, sensitivity, selectivity, operating temperature, gas concentration, response time, and recovery time play an important role in development of ferrite gas sensors [3]. This semiconductor material has a normal spinel structure with tetrahedral sites occupied by Zn^{2+} ions and octahedral sites by Fe^{3+} ions [11, 12].

Earlier research extensively reviews the recent development of semiconductor metal oxide gas sensors for environmentally hazardous gases including NO_2 , NO , N_2O , H_2S , CO , NH_3 , CH_4 , SO_2 and CO_2 [13-14]. Zinc ferrite is a kind of well-known electronic and magnetic properties [15, 16]. Seki et. al. [17] have reported the utilization of ferrites for water vapors detection as humidity sensitive active elements. Because the zinc ferrite behaves as an n-type semiconductor, conductivity will be increased in the presence of water vapor. Vaingankar et al [18] have investigated the humidity sensitivity of Cu-Zn ferrite. The use of Mg ferrite as humidity sensor has been reported by Shimizu et al [19]. Hence, ferrites synthesized by the conventional ceramic routes have a limitation as a gas sensor. This involves high temperature firing of appropriate oxides and carbonates mixtures. Some of the reports on ferrite as a sensor reveal their response toward various gases, more specifically; Xinshu et al [20] synthesized zinc ferrite at $800^\circ C$, which exhibits a response toward chlorine, while Liu et al [21] reported doped noble metal nickel ferrite to be sensitive toward H_2S . Recently, Xiangfeng et al [22] synthesized nanotubes and nanorods of nickel ferrite using a hydrothermal method that were found to be sensitive toward triethylamine. Hence, there is always a search for a new gas sensor. In particular, H_2S detection is one of the major needs in the industrial area.

In this paper, we prepared Zinc ferrite co-precipitation method and investigated their gas sensing response under different conditions. We report our results on the sensing response of the synthesized zinc ferrite to hydrogen sulphide, a potentially toxic gas, and describe an attempt to fabricate H_2S sensor element from the zinc ferrite. Also paper deals with the sensing mechanism of H_2S sensor.

2. Experimental

The zinc ferrite has been synthesized by using co-precipitation technique. A. R. grade zinc sulphate and ferrous sulphate were dissolved in appropriate proportion. The metal salts were then precipitated as hydroxides using 10% NaOH solution maintaining 10pH. Hydroxides were then oxidized using 30% H_2O_2 (100Vml) solution. The precipitate was washed and filtered till it is free from sulphate and excess alkali. The precipitate was dried in vacuum cryostat at $110^\circ C$ to form dry powder. The above powder was sintered separately at different temperatures from $500-900^\circ C$ for 4 hour to optimize formation of spinel phase. The sintered powder was mixed with 2% polyvinyl alcohol as a binder and uniaxially pressed at a pressure of $8t/cm^2$ to form pellets.

X-ray powders diffraction patterns were recorded on a diffractometer (Philips PW 1730) with microprocessor controller, using $CrK\alpha$ radiation ($\lambda = 2.289\text{\AA}$). Scanning electron microscopic studies (JEOL JSM 6360) was carried out for evaluation of surface topography. The variation of DC resistivity with temperature (RT to $500^\circ C$) was measured by the two-probe method.

3. Gas sensing measurements

The gas sensing apparatus was fabricated in our laboratory as per the design [23]. The gas sensor was made by pressing the powder in the form of pellet. The gas sensing characteristics with reference to time at different operating temperatures and concentrations were recorded. The sensor sensitivity defined as the ratio of the change in electrical resistance in the presence of test gas and in presence of air.



The gas response (S) for a given test gas was calculated using following equation. $S = R_a / R_g$ (1)

Where, 'Ra' and 'Rg' are the resistance of the sensor in air and in the test gas, respectively.

4. Result and discussions

4.1. Structural Characterization

The X-ray diffraction patterns of ZnFe₂O₄ was indicate that a single phase cubic spinel structure (Fig.1). Further, the particle size was estimated using line broadening analysis of X-ray diffraction and it found particle size ~30 nm. Scanning electron micrograph of the sample is shown in Fig.2 and it indicates the formation of grains by aggregation of small crystallites. The average grain size was calculated by Cottrell's method and it lies in the range 0.5-1µm. The variations of DC resistivity with room temperature to 500°C were measured by the two-probe method. The graph of log ρ Vs 10³/T (Fig.3.) shows that resistivity decreases with rise in temperature. It indicates the semiconducting nature of this spinel ferrite.

4.2. Gas-Sensing Properties

Gas sensing performance of composition of the Zn-ferrite has been tested for various oxidizing and reducing gases viz. ethanol, LPG, H₂, Cl₂ CO₂ and ammonia gas. It is known that adsorbed oxygen species plays an important role in the detection of gases. The activity of the reducing gas "R" on the zinc ferrites surface can be described as follows

Initially, oxygen from the atmosphere adsorbs on the surface of the ferrite and extracts electrons from its conduction band to form O⁻ species on the surface, consequently decreasing the conductance. When reducing gas R is introduced, it reacts with O⁻(ads) to form RO, and electrons enter the conduction band of ZnFe₂O₄, leading to an increase in the conductance. In summary, H₂S reacts with adsorbed O⁻ on ZnFe₂O₄ and decomposes into gaseous SO₂ and water vapor with releasing electrons [24]. It is worth noting that ZnFe₂O₄ is known as an absorbent for H₂S and

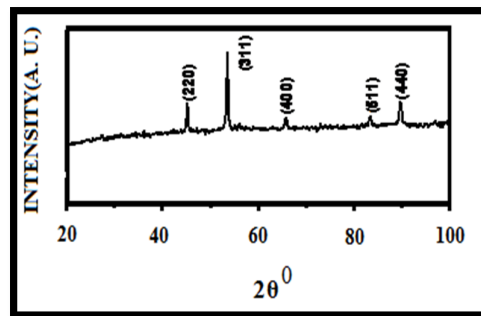


Fig. 1 X-ray diffraction pattern of ZnFe₂O₄ system

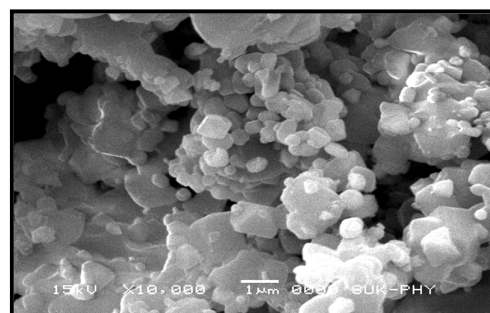


Fig. 2 SEM image of ZnFe₂O₄ sintered at 500°C.

oxidizes it to SO₂ and H₂O. Although the exact mechanism for the selectivity toward H₂S in ZnFe₂O₄ is not clear, it may be due to its favorable absorption configuration on ZnFe₂O₄ as compared with the other gases, making it selective toward H₂S.

The gas sensitivity of ZnFe₂O₄ towards LPG, NH₃, CO₂, Hydrogen sulphide, H₂ and Cl₂ at 300 ppm concentrations were depicted in (Fig.4.). As can be seen from the results, the response toward H₂S gas is more as compared with other gases such as NH₃, LPG, Cl₂ CO₂, and H₂, gases/vapours. This clearly indicates that ZnFe₂O₄ exhibits a selective response toward H₂S gas. To find the optimum operating temperature for 300 ppm of H₂S gas used as shown in (Fig. 5.).It indicates that 300°C Zinc ferrite gives maximum response and it indicates that quantity of adsorbed gas increases with increase in the operating temperature, because the gas sensing mechanism depends on the working temperature [4, 25, 26].

It is interesting to find that such a low temperature also provides sufficient excitation energy to show a significant response toward the test gas the ferrite-based sensors.

This low-temperature response in the undoped ferrite can be attributed to the active articles and their specific morphology obtained due to the co-precipitation method.

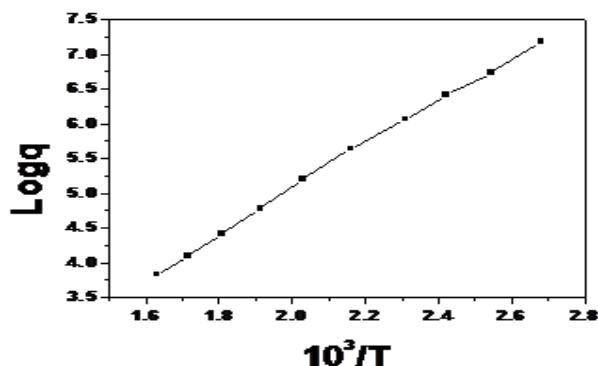


Fig. 3 Typical electrical resistivity plot for the ZnFe_2O_4

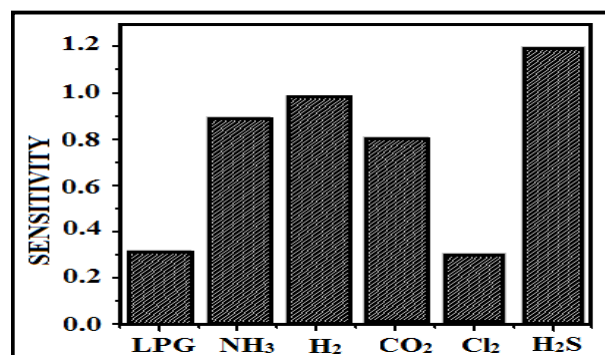


Fig. 4 Sensitivity of ZnFe_2O_4 for different gases/vapours at 300°C .

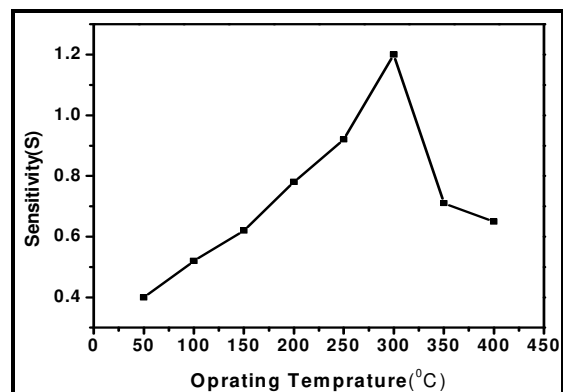


Fig.5 Sensitivity of ZnFe_2O_4 towards H_2S gas at 300 ppm

5. Conclusion

ZnFe_2O_4 was synthesized by co-precipitation route which shows n-type semiconducting behavior. This material was tested for its sensitivity to different gases/vapours. ZnFe_2O_4 is found to be selective for the detection of H_2S gas at an operating temperature of 300°C . These studies have only indicated that the need of ferrites for the detection of some of the toxic and hazardous gases.

References

- [1] G. S. Sodhi, Fundamental Concepts of Environmental Chemistry, first ed., Narosa Publishing House, New Delhi, 217–223, (2002).
- [2] G. Brawer, Handbook of Preparative Inorganic Chemistry, vol. II, second ed., Academic Press, New York, 1017–1347, (1965).
- [3] Gadkari, A.B. Shinde, T. J. Vasambekar, P.N. Sensors Journal, IEEE, Vol.11, Iss. 4, 849 – 861, (2011)
- [4] P. P. Hankare, S.D. Jadhav, U.B. Sankpal, R.P. Patil, R. Sasikala, I.S. Mulla, Journal of Alloys and Compounds, Vol.488, 1, 270- 272, (2009).
- [5] N. Yamzoe, Sens. and Actuators B 5, 7(1991).
- [6] W. Gopal and K. D. Schierbaum, ibid. 26(1-3)1 (1995).
- [7] G. Sbeveglieri (Ed.), “Gas Sensors: Principles, Operation Developments” (Kluwer, Dordrecht, 1992).
- [8] Y. Liu, E. Koep, M.L. Liu, Chem. Mater. 17 (2005) 3997–4000.
- [9] P. Feng, Q. Wan, T. H. Wang, Appl. Phys. Lett., 87 (2005) 213111.
- [10] P.P. Hankare, S.D. Jadhav, U.B. Sankpal, S.S. Chavan, K.J. Waghmare, B.K. Chougule, Journal of Alloys and Compounds, Vol. 475, 1-2, 926,(2009).
- [11] H. Deng, X.L. Li, Q. Peng, X. Wang, J.P. Chen, Y.D. Li, Angew. Chem. Int. Ed. 44, 2782-2785(2005).



- [12] K. Wetchakun, T. Samerjai, N. Tamaekong, C. Liewhiran, C. Siriwong, V. Kruefu, A. Wisitsoraat, A. Tuantranont, S. Phanichphant, *Sensors and Actuators B: Chemical*, Vol.160, Iss. 1, 580-591,(2011).
- [13] V.D. Kapse, S.A. Ghosh, F.C. Raghuwanshi, S.D. Kapse, U.S. Khandekar *Talanta*, Volume 78, Issue 1,19-2515, (2009).
- [14] Satyendra Singh, B.C. Yadav, Rajiv Prakash, Bharat Bajaj, Jae Rock lee *Applied Surface Science*, Vol. 257, Iss. 24, 10763-107701(2011).
- [15] J.F. Hochepped, P. Bonville, M.P. Pileni, *J. of Phys. and Chem.*104, 905 (2000)
- [16] K. Seki, J.I. Shida, H. Murakami, *IEE Trans. Instr. Meas.* 37, 3(1988).
- [17] A.S. Vaingankar, S.G. Kulkarni, M.S. Sagare, *Bordeaux, France*, 3-6, (1996)
- [18] Y. Shimizu, H. Arai, T. Seiyama *Sens. Actuators B*, 7, 11-22 (1985)
- [19] N. Xinsu, D. Weiping, and D. Weimin, *Sens. Actuators B*, 99, 2–3(2004).
- [20] Y. L. Liu, H. Wang, Y. Yang, Z. M. Liu, H. F. Yang, G. L. Shen, and R. Q.Yu, *Sens. Actuators B*, 102, 148-54 (2004).
- [21] C. Xiangfeng, J. Dongli, and Z. Chenmou, *Sens. Actuators B*, 123,793–97 (2007).
- [22] I. Yokota, *J. Phys. Sco. Japan*. 16 2213, (1961).
- [23] S. L. Darshane, R. G. Deshmukh, S. S. Suryavanshi, I. S. Mulla, *J. Am. Ceram. Soc.* 91, 8, 2724-2726, (2008).
- [24] A.B. Bodade, A.M. Bende, G.N. Chaudhari, *Vacuum*,



Effect of Sn doping on Structural Properties of Cobalt Ferrites Synthesized by Sol Gel Method

P. V. Gaikwad^{*1}, P.D. Kamble²

^{*1,2} Department of Chemistry, Balasaheb Desai College, Patan - 415206, MS, India

KEYWORDS

A. Ferrites,
B. Sol Gel Process,
C. X-ray diffraction,
D. SEM

Corresponding Author

Email

pratapsinghgaikwad@gmail.com

kamble_prakash59@rediffmail.com

ABSTRACT

Properties of Ferrites strongly depend on the chemical composition and the microstructure. Highly crystalline $\text{Co}_{1-x}\text{Sn}_x\text{Fe}_2\text{O}_4$ ($x=0.0,0.4$) powder was synthesized by using sol-gel method and subsequently sintered at 900 °C for 4 h. Monophasic nature of the sample was characterized using X-rays.

The influence of Sn doping on the structural properties of cobalt ferrite was observed by calculating various parameters. The crystallite size of prepared samples is calculated in nm range by XRD diffraction pattern, using Scherer

Introduction

Ferrite belongs to an important category of materials, because of their numerous practical applications ferrites largely used in magnetic devices in electronic, optical and microwave installations. Spinel ferrites, with the general formula of MFe_2O_4 , where M is a divalent cation, offer more interesting catalytic activities compared to the corresponding single component metal oxides [1–4]. On the contrary, CoFe_2O_4 nanoparticles have a remarkable chemical stability and have been used in various fields [5, 6].

Recently, considerable efforts have been made on the surface modifications and preparation of different types of metal oxides. Various methods are available for the synthesis of metal oxides, such as co-precipitation [7], sol–gel [8], hydrothermal [9], citrate–gel [10], etc. The selection of appropriate synthetic procedure often depends on the desired

properties and final applications. Out of these synthesis techniques, sol–gel auto combustion method has several advantages over others for preparation of metal oxides. Sol gel process begins with a relatively homogeneous mixture and involves low temperature conditions resulting in uniform ultrafine porous powders [11]. The size and shape of the ferrite particles depends on the synthetic process. Tin doped ferrites particles can be formed and their structural characterization viz. study of crystallinity, desired phases and particle size determination was done by x-ray diffraction [12].

In this paper we report Tin doped Cobalt Ferrite powder [$\text{Co}_{1-x}\text{Sn}_x\text{Fe}_2\text{O}_4$ ($x=0.0, 0.4$)] was synthesized by simplest sol gel technique and various parameters such as crystallite size, d-spacing, lattice constant were calculated by XRD diffraction pattern. Grain size was determined by SEM micrographs.

2. Experimental Technique

2.1 Synthetic Technique

The system $\text{Co}_{1-x}\text{Sn}_x\text{Fe}_2\text{O}_4$ ($x=0.0, 0.4$) was synthesized by sol-gel method. All reactants and template materials were chosen which are cheap, easily accessible & reasonably safe to work. A.R. grade ethylene glycol, cobalt sulphate ($\text{CoSO}_4 \cdot 7\text{H}_2\text{O}$), ferrous sulphate ($\text{FeSO}_4 \cdot 7\text{H}_2\text{O}$) and Tin sulphate (SnSO_4) were used as starting materials. Above sulphates were taken in appropriate proportions, dissolved into distilled water and mixed together. A solution of ethylene glycol was added slowly with constant stirring to the metal sulphate solution. The mixed solution was extracted using air condenser. Due to these sulphates get evolved which was tested by using blue litmus paper. After removing all sulphates, solution was heated on hot plate with continuous stirring at 180°C . During evaporation the solution become viscous and gets converted into gel. The formed gel was heated at 250°C when all remaining quantity of water was released from the mixture and loose powder was formed. This was crushed and then heated separately at 900°C for 4 hours to get final product. Fig 1 shows images of powders for CoFe_2O_4 (1) & $\text{Co}_{0.6}\text{Sn}_{0.4}\text{Fe}_2\text{O}_4$ (2)

2.2 Characterization

A computerized X-ray powder diffractometer (Siemens D-500 diffractometer) with $\text{Cu-K}\alpha$ radiation ($\lambda=1.5406 \text{ \AA}$) was used to identify the crystalline nature of the samples and to calculate lattice parameter and crystallite size. The lattice parameters were calculated for the cubic phase using following relation.

$$\frac{1}{d^2} = \frac{h^2}{a^2} + \frac{k^2}{b^2} + \frac{l^2}{c^2} \dots \dots \dots (1)$$

Where a, b and c are lattice parameters, (hkl) is the Miller indices and d is the interplanar distance.

From the X-ray diffraction peaks, crystallite size was estimated using Debye Scherer's formula [13].

$$t = \frac{0.9\lambda}{\beta \cos\theta} \dots \dots \dots (2)$$

Where, symbols have their usual meaning. The X-ray density (dx) was calculated using the following relation [14],

$$dx = \frac{8M}{Na^3} \dots \dots \dots (3)$$

Where N= Avogadro's number (6.023×10^{23} atom/mol), M= molecular weight, and a = lattice constant.

Scanning electron microscope (SEM) was used to study the morphology of the powders. The grain size of all the samples was calculated by Cottrell's method [15].

3. Results and discussion

3.1 XRD (X-ray Diffraction):-

The structure and phase purity of the product was confirmed by analyzing the observed powder X-ray diffraction patterns. The X-ray diffraction pattern of $\text{Co}_{1-x}\text{Sn}_x\text{Fe}_2\text{O}_4$ ($x=0.0, 0.4$) was as shown in Fig 2 (a, b). The inter planer distance for each diffraction peak was calculated and calculated 'd' values are given in Table 1 & 2. All XRD patterns were indexed using JCPDS data for $\text{Co}_{1-x}\text{Sn}_x\text{Fe}_2\text{O}_4$ ($x=0.0, 0.4$) ferrites (card no- 004-0836 & 22-1086 respectively) which reveals that the cubic spinel structure with (3 1 1) as most intense peak. Some extra peaks might be due to the formation of hematite Fe_2O_3 at 500°C temperature. Cobalt-Tin ferrite powder better crystalline sized at even the temperature of 500°C . It is well known that Co^{+3} ions responsible for distorting (Jahn-Teller) the lattice form cubic to tetragonal symmetry. Cobalt ferrite synthesized was cubic with lattice constant (a) 8.3715 \AA having cubic symmetry. The presence of cubic symmetry for CoFe_2O_4 suggests that the distorting Co^{+3} ions are not present only at one side i.e. tetrahedral or octahedral but they are distributed between two sites. If all Co^{+3} would have been either at tetrahedral or octahedral site the compound should have shown tetragonal symmetry. Therefore as a results of distribution of Co^{+3} ions between two sites there is a compensating effect of tetrahedral and octahedral distortions therefore CoFe_2O_4 shows cubic symmetry. The crystallite size was 6.90 nm and theoretical density 6.80 gm/cm^3 . However when Sn added into CoFe_2O_4 & $\text{Co}_{0.6}\text{Sn}_{0.4}\text{Fe}_2\text{O}_4$ synthesized. It was also cubic but decrease in lattice constant (a) 8.2914 \AA . $\text{Co}_{0.6}\text{Sn}_{0.4}\text{Fe}_2\text{O}_4$ crystallite size was 8.32nm and theoretical density 5.31 gm/cm^3 .



Fig. 1: Images of powders for CoFe_2O_4 (1) & $\text{Co}_{0.6}\text{Sn}_{0.4}\text{Fe}_2\text{O}_4$ (2)

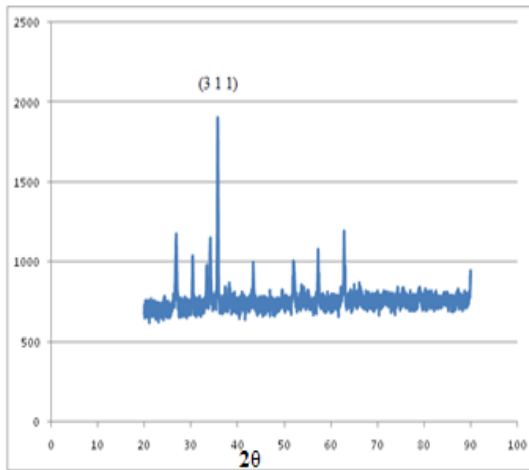
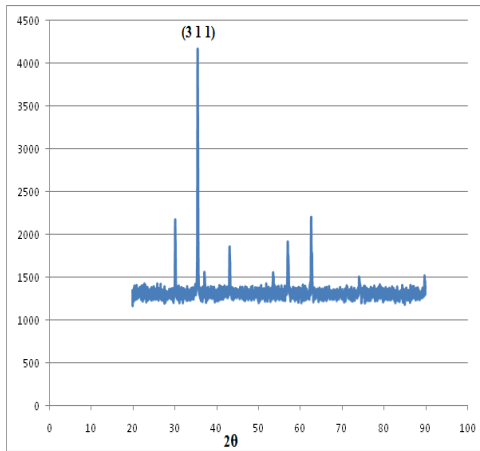
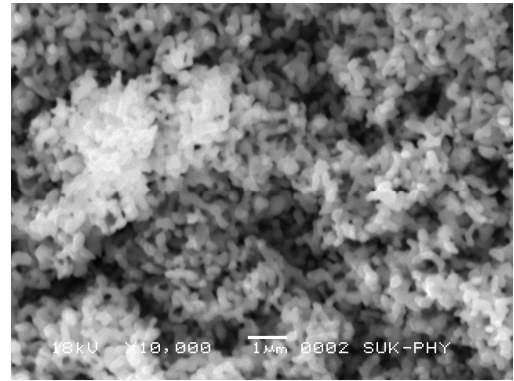
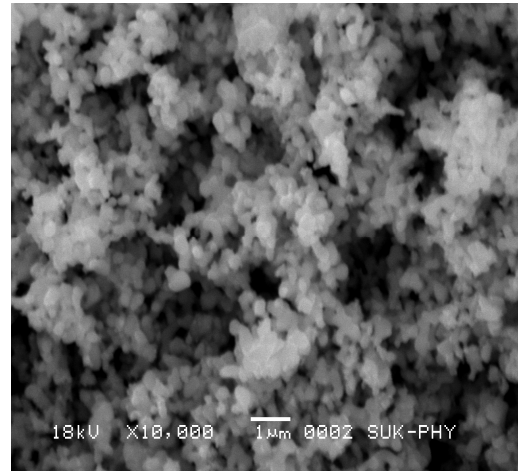


Fig. 2 (a, b) - XRD patterns of System $\text{Co}_{1-x}\text{Sn}_x\text{Fe}_2\text{O}_4$ ($x=0.0, 0.4$) powder sintered at 900°C



(a)



(b)

Fig. 3 (a, b) – SEM micrographs of system $\text{Co}_{1-x}\text{Sn}_x\text{Fe}_2\text{O}_4$ ($x=0.0, 0.4$)

3.2 Scanning Electron Microscopy:-

Fig.3 shows SEM micrographs of CoFe_2O_4 & $\text{Co}_{0.6}\text{Sn}_{0.4}\text{Fe}_2\text{O}_4$ with their bulk counterpart. SEM micrograph of CoFe_2O_4 exhibits bunch of several small particles while distribution of particles increases with addition of Sn. These micro-sized particles contain number of crystallites aggregated with each other as shown in Fig. 3(a, b). XRD is measuring size of crystallites only which is almost 8.32 nm & 6.90 nm respectively for CoFe_2O_4 & $\text{Co}_{0.6}\text{Sn}_{0.4}\text{Fe}_2\text{O}_4$; however size of aggregated entity is being measured by SEM which is of the order of several μm . Average grain size decreases with addition of Sn to CoFe_2O_4 which is given table 3.

Sr. No.	Peak	2 θ	d	d ²	h k l
1	2175	30.2179	2.9551	8.7326	(2 2 0)
2	4174	35.5693	2.5218	6.3594	(3 1 1)
3	1560	37.1707	2.4167	5.8409	(2 2 2)
4	1858	43.2113	2.0928	4.3798	(4 0 0)
5	1554	53.6101	1.7087	2.9196	(4 2 2)
6	1915	57.0966	1.6118	2.5978	(3 3 3)
7	2205	62.7116	1.4803	2.1912	(4 4 0)
8	1504	74.1446	1.2778	1.6327	(5 3 3)
9	1519	89.8132	1.0911	1.1904	(5 5 3)

Table 1– 2 θ , interplanar distance (d), Miller indices (hkl) of CoFe₂O₄ system

Sr. No.	Peak	2 θ	d	d ²	h k l
1	1175	26.89	3.3130	10.9759	(2 1 1)
2	1037	30.38	2.94	8.6436	(2 2 0)
3	1151	34.19	2.6204	8.8664	(3 1 0)
4	1905	35.77	2.5082	6.2910	(3 1 1)
5	998	43.37	2.0846	4.3455	(4 0 0)
6	1007	51.98	1.7576	3.089	(3 3 2)
7	1080	57.27	1.6076	2.5843	(3 3 3)
8	1193	62.87	1.4769	2.1812	(4 4 0)
9	946	89.97	1.0895	1.1870	(7 3 0)

Table 2– 2 θ , interplanar distance (d), Miller indices (hkl) of Co_{0.6}Sn_{0.4}Fe₂O₄ system

Sr. No.	Sample	Lattice Constant (a)	Crystal Size (nm)	X-ray density(X) gm/cm ³	Average Grain Size (μ m)
1	CoFe ₂ O ₄	8.3715	8.32	5.31	0.47
2	Co _{0.6} Sn _{0.4} Fe ₂ O ₄	8.2914	6.90	6.18	0.43

Table 3– Lattice constant (a), Crystallite size (t), Theoretical X-ray density (d_x), Average Grain size of system Co_{1-x}Sn_xFe₂O₄ (x=0.0, 0.4).



Conclusion:- Synthesis of $\text{Co}_{1-x}\text{Sn}_x\text{Fe}_2\text{O}_4$ ($x=0.0, 0.4$) powder was successfully done by sol-gel techniques. Single phase cubic Cobalt-Tin ferrite is formed having most intense peak (3 1 1). Variation in lattice constant is found when Sn doped into CoFe_2O_4 between 8.3715 Å to 8.2914 Å. Crystal sizes and theoretical density was found 8.32 nm & 5.31 gm/cm^3 respectively for CoFe_2O_4 . While crystal sizes and theoretical density of $\text{Co}_{0.6}\text{Sn}_{0.4}\text{Fe}_2\text{O}_4$ was found 6.90 nm & 6.18 gm/cm^3 respectively. SEM micrograph shows both contain number of crystallites aggregated and size of aggregated entity is in μm .

Acknowledgement-

One of the Author Dr.P. D. Kamble thanks to DST SERB for their financial assistance through Major research project dated 21/10/2016(DST NO - SB/EMEQ-347/2014 dated 21/10/2016.)

References:-

- [1] G Yan, Y Jiang, C Kuang, S Wang, H Liu, Y Zhang, J Wang (2010) *J Chem Commun* 46:3170–3172.
- [2] P P Hankare, P D Kamble, S P Maradur, M R Kadam, U B Sankpal, R P Patil, R K Nimat, P D Lokhande (2009) Ferros spinels based on Cu and Co prepared via low temperature route as efficient catalysts for the selective oxidation of alcohol. *Journal of Alloys and Compounds* 487:730–734.
- [3] S H Xiao, W F Jiang, LY Li, X Li (2007) Low-temperature auto-combustion synthesis and magnetic properties of cobalt ferrite nanopowder. *J Mater Chem Phys* 106:82–87.
- [4] Menini L, Pereira M C, Ferreira A C, Fabris J D, Gusevskaya E V (2011). *Appl Catal A* 392:151–157.
- [5] R S Turtelli, G V Duong, W Nunes, R Grossinger, M Knobel (2008) *J Magn Magn Mater* 320:339–342.

- [6] Nguyen Viet Long, Yong Yang, Toshiharu Teranishi, Cao Minh Thi, Yanqin Cao, Masayuki Nogami (2015) Related magnetic properties of CoFe_2O_4 cobalt ferrite particles synthesized by the polyol method with NaBH_4 and heat treatment: new micro and nanoscale structures. *RSC Adv* 5:56560–56569.
- [7] A S Albuquerque, J D Ardisson, W A A Macedo, J L Lopez, R Paniago, A I C Persiano (2001) Structure and magnetic properties of nanostructured Ni-ferrite. *J Magn Magn Mater* 226:1379-1381.
- [8] S Bhukal, M Dhiman, S Bansal, M K Tripathi, S Singhal (2016) Substituted Co–Cu–Zn nanoferrites: synthesis, fundamental and redox catalytic properties for the degradation of methyl orange. *RSC Adv* 6:1360–1375.
- [9] S Phumying, S Labuayai, E Swatsitang, V Amornkitbamrung, S Maensiri (2013) Nanocrystalline spinel ferrite (MFe_2O_4 , M = Ni, Co, Mn, Mg, Zn) powders prepared by a simple aloe vera plant-extracted solution hydrothermal route. *Materials Research Bulletin* 48:2060–2065.
- [10] P.P. Hankare, U.B. Sankpal, R.P. Patil, I.S. Mulla, P.D. Lokhande, N.S. Gajbhiye, (2009) Synthesis and characterization of $\text{CoCr}_x\text{Fe}_{2-x}\text{O}_4$ nanoparticles. *J Alloys Compd* 485:798-801.
- [11] J.A. Rodriguez, M. Fernandez-Garcia (2007) *Textbook of Synthesis, Properties and Applications of Oxide Nanomaterials*. Wiley Interscience, A John Wiley and Sons, Inc. Publication, p. 95.
- [12] H E Moussaoui, T Mahfoud, S Habouti, K E Maalam, M Ben Ali, M Hamedoun, O Mounkachi, R Masrour, E K Hlil, A Benyoussef (2015) Synthesis and Magnetic Properties of Tin Spinel Ferrites Doped Manganese. *J Magn Magn Mater* 405:181-186.
- [13] P P Hankare, M R Kadam, R P Patil, K M Garadkar, R Sasikala, A K Tripathi (2010) Effect of zinc substitution on structural and magnetic properties of copper ferrite. *J Alloys Compd* 501:37-41.

- [14] P.V. Gaikwad, P.D. Kamble, M.R. Kadam, S.D. Zimur (2017) Effect of Co Content on Structural & Magnetic Properties of Manganese Copper Ferrites Synthesized by Sol Gel Auto Combustion Method. Int J Current Engg Sci Res 4:61-67.
- [15] A Cottrell, (1967) An Introduction to Metallurgy, Edward Arnold, London.



Synthetic studies on 1, 2, 4-triazoles derivatives and biological evaluation as antifungal and antibacterial agents

^bSujatha.k, ^a A.M.A.Khader ^aBalakrishna Kalluraya

^aDepartment of studies in Chemistry, Mangalore University, Mangalagangothri-574199, Karnataka, India

^bDepartment of studies in Chemistry, Karnatak University, Dharwad-580003, Karnataka, India

KEYWORDS

Corresponding Author
Email
sujathak4@rediffmail.com

ABSTRACT

A novel series of 5-(*α*-aryloxy ethyl)-1,2,4 triazole were prepared and subjected to hydrazone reaction in the presence of catalytic amount of acid. Such reactions resulted in the formation of 3-aryloxyethyl-4-arylidene amino-5-mercapto-1,2,4-triazoles, The structures of new compounds have been established by spectral and analytical data. The new compounds have been tested for their antimicrobial activity.

Introduction

Triazoles are five membered heterocyclic ring. Triazoles and their derivatives are extensively studied because of their interesting antimicrobial activity, they exhibit broad spectrum of pharmacological activity¹⁻⁵ such as antifungal, antibacterial and antiinflammatory⁶ activities, therefore the development of antifungal agents targeting specific structures or functions is being actively pursued. These trends have emphasized on the need for more effective less toxic and safe antimicrobial agents. Itraconazole⁷⁻¹⁰, voriconazole¹¹, Ravuconazole¹² are significant antifungal agents presently available in the market for the treatment of fungal infections. Prompted by these observations, we planned to synthesize structurally modified triazoles (4) and studied their antibacterial and antifungal activity.

method and are uncorrected. IR spectra were obtained in KBr disc on a Shimadzu FT-IR 157 spectrophotometer. ¹H NMR spectra were recorded either on a Perkin-Elmer EM-390 or on a Bruker WH-200 (400 MHz) spectrometer in CDCl₃ or DMSO-d₆ as solvent, using TMS as an internal standard and chemical shifts are expressed in δ scale. Mass spectra were determined on a Jeol SX 102/Da-600 mass spectrometer/ Data System using Argon/Xenon (6kv, 10mA[°]) as the FAB gas. The accelerating voltage was 10kV and spectra are recorded at room temperature. The progress of the reactions was monitored by TLC on pre-coated silica gel plates.

MATERIALS AND METHODS

1.1 General Procedure

All the melting points were determined by open capillary

1.2 Chemistry:

The four differently substituted-3-aryloxyethyl-4-amino-5-mercapto triazoles were employed in the preparation of corresponding Schiff's bases. All of them were prepared starting from substituted phenols. Phenols on reacting with methyl 2-chloropropanoate in dry acetone in presence of anhydrous potassium carbonate gave α -methylaryloxypropanoates (**1**). Hydrazinolysis of these esters with hydrazine hydrate in absolute ethanol yielded α -aryloxypropano hydrazides (**2**). Potassium dithiocarbazates (**3**) were prepared by treating these hydrazides (**17**) with carbon disulphide in absolute ethanol in the presence of potassium hydroxide. Cyclisation of these potassium dithiocarbazates (**3**) with hydrazine hydrate yielded 3-aryloxyethyl-4-amino-5-mercapto-1,2,4-triazoles (**4a-d**). The synthetic route followed for obtaining title compound is outlined in **scheme 1.1**.

Similarly 3-[1-(1*H*-imidazol-1-yl)ethyl]-4*H*-1,2,4-triazol-4-amine (**5e**) was obtained by employing the same procedure. (**Scheme 1.2**) Condensation of 4-amino-5-(1-aryloxyethyl)-4*H*-1,2,4-triazole-3-thioles (**4a-d**) and 3-[1-(1*H*-imidazol-1-yl)ethyl]-4*H*-1,2,4-triazol-4-amine (**5e**) with appropriately substituted aromatic aldehydes in ethanol medium employing con. Sulphuric acid as catalyst gave the novel series of 3-aryloxyethyl-4-arylidene amino-5-mercapto-1,2,4-triazoles, 3-[1-(1*H*-imidazol-1-yl)ethyl]-4-[arylmethylene]amino-4*H*-1,2,4-triazole-5-thiol (Schiff's bases) (**6a-o**). (**Scheme 1.3**).

1.2.1 General synthetic procedure for compounds

General procedure for the synthesis of methyl aryloxypropanoate (**1**):-

A mixture of substituted phenol (0.2mol), methyl 2-chloropropanoate (0.2 mol) and anhydrous potassium carbonate (41.4g, 0.3mol) in dry acetone (500ml) was refluxed on water bath for 16 hours. The reaction mixture was filtered hot and the solvent was removed under reduced pressure, the crude methyl aryloxypropanoate ester was taken for next stage without any further purification.

General procedure for the synthesis of methyl aryloxypropanohydrazide (**2**):-

A mixture of methyl aryloxypropanoate (0.1mol) and 99% hydrazine hydrate 5ml (0.1mol) in ethanol 40ml was heated on a water bath for eight hours, the solution on cooling gave solid mass of aryloxypropanohydrazide which was collected by filtration and recrystallised from alcohol to get white crystals in good yield (86%).

General procedure for the preparation of aryloxypropano potassium dithiocarbazates (**3**):-

A solution of an appropriate aryloxypropanohydrazide (0.1mol) in ethanol (100ml) was added slowly to a solution of potassium hydroxide (0.15 mol) in ethanol (50ml). The resulting mixture was stirred well till a clear solution was obtained. Carbon disulphide (0.15mol) was added drop wise to it and stirred vigorously. The temperature was not allowed to rise above 30°C. Solid mass began to separate immediately. It was further stirred for 24 hours at room temperature. The resulting mixture was diluted with ether (100ml) and the precipitate formed was collected by filtration, washed with dry ether and dried at 65°C under vacuum. The salt obtained by this procedure was used for the next reaction without further purification.

General procedure for the preparation of substituted 4-amino-5-mercapto-1,2,4-triazoles (**4a-d**), (**5e**):-

Potassium dithiocarbazinate (0.1mol) and hydrazine hydrate (99%, 0.2 mole) and 2 ml water were gently heated so that it started to boil in about thirty minutes, diluted the reaction mass with water, and was neutralised with hydrochloric acid. The solid separated was collected by filtration, dried and recrystallised from ethanol.

4-amino-5-[1-(2,4-dichlorophenoxy)ethyl]-4H-1,2,4-triazole-3-thiol (4d)

IR: (KBr: : γ/cm^{-1}): 3300-3400 (NH₂), 1130-1180 (C=S stretching). ¹H-NMR (δ ppm, DMSO-d₆, 400 MHz): 1.54 (d, 3H, CH₃), 4.4 (q, 1H, OCH), 6.5-7.5 (m, 3H, Ar-H), 8.9 (br, 2H, NH₂)



4-amino-5-[1-(4-chlorophenoxy)ethyl]-4H-1,2,4-triazole-3-thiol (4b)

¹H-NMR (δ ppm, DMSO-d₆, 400 MHz): d 1.6(d, 3H, CH₃), 4.6 (q, 1H, OCH), 6.5-7.5 (m, 3H, Ar-H), 10.28. 8.9 (br, 2H, NH₂),

4-amino-5-[1-(2,6-dimethylphenoxy)ethyl]-4H-1,2,4-triazole-3-thiol (4c)

¹H NMR (δ ppm, DMSO-d₆, 400 MHz): δ, 1.4 (d, 3H, CH₃), 2.2 (s, 6H, 2X CH₃), 4.4 (q, 1H, O-CH), 6.7-7.5 (m, 3H, Ar-H), 10.1 (br, 2H, NH₂).

General procedure for the preparation of 3-aryloxyethyl-4-arylidene amino-5-mercapto-1,2,4-triazoles,

4-[[biphenyl-4-ylmethylene]amino]-5-[1-(2,4-dichlorophenoxy)ethyl]-2,4-dihydro-3H-1,2,4-triazole-3-thione (6g)

IR: (KBr: : γ/cm⁻¹): 1619 (C=N), ¹H NMR (δ ppm, DMSO-d₆, 400 MHz): δ, 1.49 (d, 3H, CH₃), 4.2 (q, 1H, O-CH), 7.4-7.5 (m, 12H, Ar-H), 8.47(s, 1H, N=CH).

4-[[biphenyl-4-ylmethylene]amino]-5-[1-(1H-imidazol-1-yl)ethyl]-4H-1,2,4-triazole-3-thiol (6m)

¹H NMR (δ ppm, DMSO-d₆, 400 MHz): δ, 1.9 (d, 3H, CH₃), 5.9 (q, 1H, NCH), 7.01-8.01 (m, 12H, aromatic and imidazole protons) 9.95 (s, 1H, N=CH), 14.12 (s, 1H, SH).

The structures of the newly synthesized triazoles (**4a-d**), (**5e**) and their Schiff bases were established on the basis of analytical and spectral data. The characterization data of these compounds are given in **Tables 3.1** and **3.2** respectively.

Antimicrobial studies:-

The newly synthesized compounds were screened for their antibacterial activity *invitro* against Gram-positive bacteria namely *Escherichia coli*, *Staphylococcus aureus*, and Gram-negative bacteria namely *Pseudomonas aeruginosa*, *Bacillus subtilis* and the fungus namely *Candida albicans*

by disc diffusion method. The test compounds were dissolved in N,N-dimethyl formamide (DMF) to obtain a solution of 10μg/ml concentration. The inhibition zones of microbial growth produced by different compounds were measured at the end of an incubation period of 48 hours at 37°C. DMF alone showed no inhibition zone. Penicillin and Flucanazole were used as reference standards to evaluate the potency of the tested compounds. The results are illustrated in the **Table-3**. This study reports the successful synthesis of the title compounds. The antimicrobial activity study revealed that few of the tested compounds showed significant antifungal activity.

RESULTS AND DISCUSSION

The compounds **6a-o** synthesized as per the outlined **scheme (1.3)** were purified by recrystallization and the purity was ascertained by TLC using Silica Gel G as stationary phase. The instrumental data suggested the formation of the compounds as desired. Antimicrobial screening of the compounds was performed using four different strains of bacteria and one strains of fungi. Compounds **6a**, **6f**, **6g**, **6j**, **6l**, **6m**, **6o** showed good activity against three different microbial strains (bacteria). The structural make up of the compounds were thought of to be responsible of their antimicrobial activities.

The compounds **6a,6b**, **6c**, **6e**, **6f**, **6g**, **6i,6j**, **6l,6m**, showed very good activity against microbial fungal strains even better than the standard The structural make up of the compounds were thought of to be responsible of their antimicrobial activities. Compound **6a,6b**, **6c** are having a phenoxy group as aromatic substituent and biphenyl, pyridyl, 4-chlorophenyl groups as R substituent attached to triazole. **6e**, **6f** are having 4-chlorophenoxy as Ar substituent and pyridyl, 4-chlorophenyl groups as R substituent attached to triazole. , **6g** **6i** are having 2,4-Dichlorophenoxy as Ar substituent and pyridyl, biphenyl groups as R substituent attached to triazole. **6j** **6l** are having 2,6-Dimethylol phenoxy as Ar substituent and pyridyl, biphenyl groups as R substituent attached to triazole.

due to the presence of phenoxy methyl group attached to 1,2,4-triazole nucleus. The phenoxy methyl group gives the compound extra stability while entering the bacterial cell membrane and the thiol group enhances penetration into fungal cell wall. Introduction of chloro (Cl) moiety at 4-position into the aromatic ring attached to the triazole nucleus resulted in poor antimicrobial activity with less antifungal activity, i.e. compound **6d** showed poor activity.

Further substituted phenoxy group as aromatic substitution attached to the triazole nucleus leads very good antimicrobial activity. Compound containing a pyridyl moiety attached to the triazole nucleus further enhances the lipophilicity of the molecule enabling it to penetrate the microbial cell more easily, thus showing good activity.

Table-1 Characterization data of 4-amino-5-(1-aryloxyethyl) (1-imidazolylethyl)-1,2,4-triazole-3-thiol (4a-d), (5e)

Compd No	Ar	M.P (°c) Yield	Colour and crystal forms	Elemental analysis		
				Found (Calc)		
				C	H	N
4a	4-Chlorophenyl	170 74%	Yellow crystalline	44.32 (44.22)	4.05 (4.06)	20.80 (20.68)
4b	Phenyl	122 68%	Pale yellow crystals	50.51 (50.84)	5.10 (5.17)	23.68 (23.67)
4c	2,6-DimethylPhenyl	150 60%	Yellow crystals	54.46 (54.47)	6.05 (6.06)	21.17 (21.18)
4d	2,4-DicloroPhenyl	165 65%	Light yellow crystals	32.32 (32.30)	3.28 (3.27)	6.04 (6.05)
5e	Imidazolyl	158 63%	Yellow crystals	37.18 (37.17)	4.47 (4.45)	37.19 (37.14)

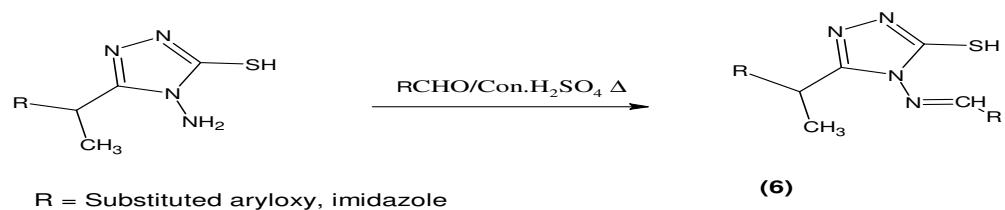
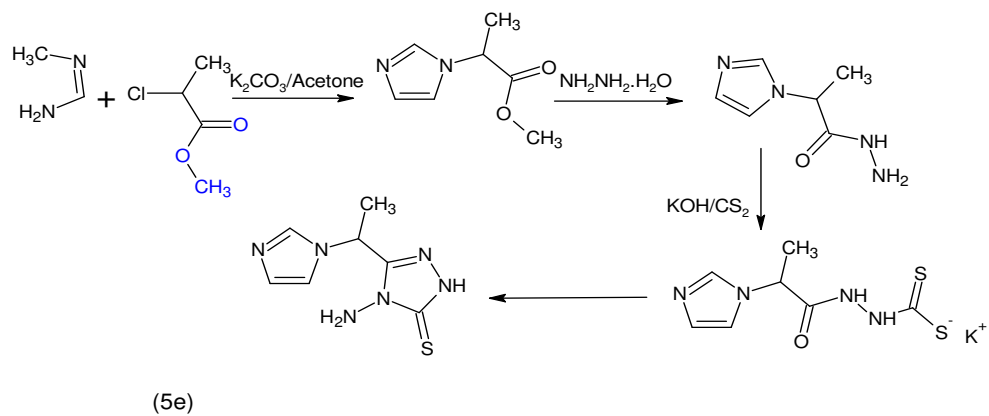
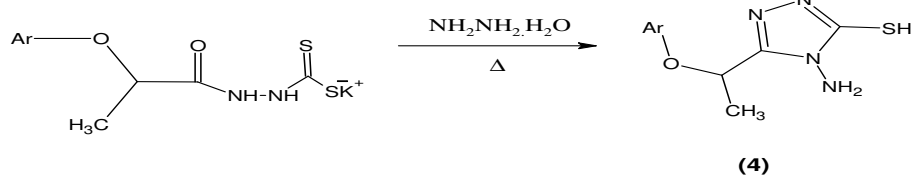
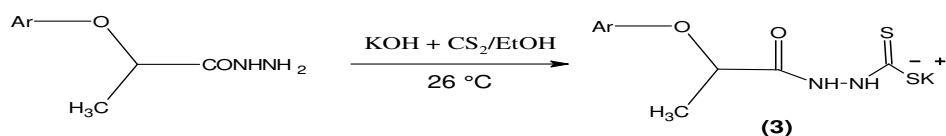
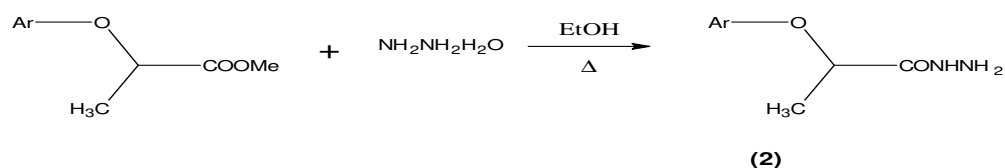
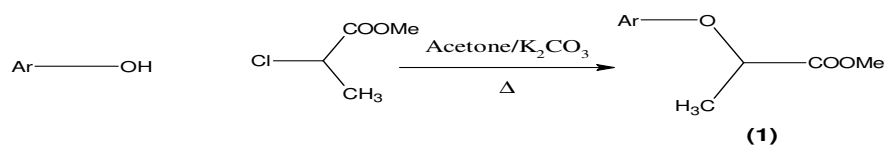
Solvent for recrystallisation: ethanol.



Table-2 Characterization data of 3-(1-arylethyl) / (1-imidazolylethyl) -4-arylidene amino-5-mercapto-1,2,4-triazoles (6a-o)

Compd No	Ar	R	Yield (%) M.P(°C)	Colour and Crystal form	Elemental analysis (Calc) Found		
					C	H	N
6a	Phenoxy	Biphenyl	55 170-72	Light yellow crystals	68.98 (68.99)	5.03 (5.04)	13.99 (13.98)
6b	Phenoxy	4-Chlorophenyl	58 142	Yellow crystals	56.90 (56.89)	4.25 (4.21)	15.61 (15.59)
6c	Phenoxy	Pyridyl	61 148-150	Pale yellow needles	59.06 (59.04)	4.65 (4.66)	21.52 (21.53)
6d	4-Chlorophenoxy	Biphenyl	54 106-08	Yellow needles	63.51 (63.50)	4.40 (4.39)	12.88 (12.89)
6e	4-Chlorophenoxy	4-Chlorophenyl	61 155-156	Pale yellow micro needles	51.92 (51.93)	3.59 (3.58)	14.25 (14.29)
6f	4-Chlorophenoxy	Pyridyl	53 256	Pale yellow crystals	53.41 (53.42)	3.92 (3.91)	19.46 (19.45)
6g	2,4- Dichlorophenoxy	Biphenyl	55 204	Light yellow crystals	58.85 (58.84)	3.87 (3.86)	11.94 (11.93)
6h	2,4- Dichlorophenoxy	4-Chlorophenyl	64 160	Yellow crystals	47.74 (47.75)	3.06 (3.05)	13.10 (13.11)
6i	2,4- Dichlorophenoxy	Pyridyl	54 289	Cream needles	48.74 (48.73)	3.32 (3.33)	17.76 (17.75)
6j	2,6- Dimethylphenoxy	Biphenyl	59 166-68	Pale yellow crystals	70.07 (70.08)	5.64 (5.66)	13.07 (13.05)
6k	2,6- Dimethylphenoxy	4-Chlorophenyl	57 160	Yellow crystals	58.98 (58.99)	4.95 (4.96)	14.48 (14.49)
6l	2,6- Dimethylphenoxy	Pyridyl	57 289	Yellow needles	61.17 (61.18)	5.42 (5.43)	19.81 (19.82)
6m	Imidazolyl	Biphenyl	46 135	Yellow crystals	61.52 (61.53)	4.65 (4.66)	21.52 (21.53)
6n	Imidazolyl	4-Chlorophenyl	54 157	Creamish yellow needles	48.51 (48.52)	3.76 (3.77)	24.09 (24.10)
6o	Imidazolyl	Pyridyl	45 159	Light brown Microcrystals	49.51 (49.53)	4.16 (4.17)	31.09 (31.10)

o Solvent for recrystallisation: ethanol.



Reaction scheme



Table-3 Antibacterial and antifungal data of Schiff's bases (6a-o).

Compd No	Antibacterial activity (MIC in µg/mL)				Antifungal activity (MIC in µg/mL)
	<i>E.coli</i>	<i>S.aureus</i>	<i>P.auriginosa</i>	<i>B.subtitis</i>	<i>C.albicans</i>
6a	6.25	6.25	3.12	3.12	3.12
6b	6.25	6.25	3.12	6.25	3.12
6c	6.25	3.12	6.25	12.5	3.12
6d	6.25	12.5	6.25	6.25	6.25
6e	3.12	6.25	3.12	12.5	3.12
6f	12.5	12.5	3.12	3.12	3.12
6g	6.25	6.25	3.12	3.12	3.12
6h	6.25	6.25	6.25	6.25	6.25
6i	6.25	12.5	3.12	12.5	3.12
6j	12.5	6.25	6.25	3.12	3.12
6k	6.25	6.25	6.25	12.5	6.25
6l	-	6.25	3.12	3.12	3.12
6m	6.25	3.12	6.25	3.12	3.12
6n	3.12	6.25	3.12	6.25	6.25
6o	3.12	6.25	3.12	3.12	6.25
Standard:Pencillin	0.12	0.12	0.12	0.12	---
Standard:Flucanazole	-	-	-	-	8.0
Control: DMF	-	-	----	---	---

References

- [1] B.S. Holla, R. Gonsalves, S. Shenoy, *Farmaco*, **1998**, *53*, 574–578.
- [2] B.S. Holla, B. Veerendra, M.K. Shivananda, N.S. Kumari, *Indian J. Chem.* **2003**, *42*, 2010–2014.
- [3] M. Ashok, B.S. Holla, *J. Pharmacol. Toxicol.* **2007**, *2*, 256–263.
- [4] D.J. Prasad, M. Ashok, P. Karegoudar, B. Poojary, B.S. Holla, N.S. Kumari, *Eur. J. Med. Chem.* **2009**, *44*, 551–557.
- [5] G. Turan-Zitouni, Z.A. Kaplancikli, M.T. Yildiz, P. Chevallet, D. Kaya, *Eur. J. Med. Chem.* **2005**, *40*, 607.
- [6] A. Almasirad, S.A. Tabatabai, M. Faizi, A. Kebriaeezadeh, N. Mehrabi, A. Dalvandi, A. Shafiee, *Bioorg. Med. Chem. Lett.* **2004**, *14*, 6057–6059.
- [7] A. Espinel-Ingroff, K. Boyle, D. Sheehan, J. *Mycopathologia* **2001**, *150*, 101–115.
- [8] M.M. Pearson, P.D. Rogers, J.D. Cleary, S.W. Chapman, *Ann. Pharmacother.* **2003**, *37*, 420–432.
- [9] E.K. Manavathu, J.L. Cutright, P.H. Chandrasekar, *Antimicrob. Agents Chemother.* **1998**, *42*, 3018.
- [10] E.M. Johnson, A. Szekely, D.W. Warnock, J. *Antimicrob. Chemother.* **1998**, *42*, 741–745.
- [11] J.C. Fung-Tomc, T.C. White, B. Minassian, E. Huczko, D.P. Bonner, *Diagn. Microbiol. Infect. Dis.* **1999**, *35*, 163–167.
- [12] D.S. Burgess, R.W. Hastings, *Diagn. Microbiol. Infect. Dis.* **2000**, *38*, 87–93.
- [13] M.A. Pfaller, S.A. Messer, R.J. Hollis, R.N. Jones, D. Diekema, *J. Antimicrob. Agents Chemother.* **2002**, *46*, 1723–1727.



Synthesis of Nanoropes, Nanorods, Nanodiscs and Nanoflowers of ZrO₂ Thick Films for various Applications and Their Characterizations

G. B. Shelke^a, D. R. Patil^b

^aDepartment of Physics, Nanasaheb Y. N. Chavan A. S. C. College Chalisgaon, 424101, India

^bBulk and Nanomaterials Research Lab, Department of Physics, R. L. College Parola, India

KEYWORDS

Characterizations,
Nanomaterials, Synthesis,
Thick films

Corresponding Author
Email

prof_drpatil@yahoo.in

ABSTRACT

It is observed that, pure stoichiometric ZrO₂ is expected to be insulating. However, the synthesized powder of ZrO₂ is not exactly stoichiometric and hence, is not insulating. So, nanostructured ZrO₂ powder was synthesized by disc type ultrasonicated microwave assisted centrifuge technique. Thick films of nanostructured pure ZrO₂ powder were fabricated by screen printing technique. These films were surface activated by bismuth chloride for different intervals of time followed by firing at 500°C for 30 min. The surface morphology, chemical composition and crystal structure of the unmodified and surface functionalized nanostructured ZrO₂ powder by Bi₂O₃ have been investigated by FESEM, E-DAX, XRD, etc.

1.0 Introduction

Zirconium dioxide (ZrO₂) sometimes known as zirconia is a white crystalline oxide of zirconium. The crystal structure of ZrO₂ is monoclinic. It's most occurring form, with a monoclinic crystalline structure having wide band gap of 5.8 eV. The band gap energy of ZrO₂ is dependent on the phase (cubic, tetragonal, monoclinic or amorphous) and preparation methods with typical estimates from 5-7 eV. ZrO₂ is one of the most studied ceramic materials. Pure ZrO₂ has a monoclinic crystal structure at room temperature and found transitions to tetragonal and cubic at increasing temperatures. Use of zirconia is in the production of ceramics with other uses including as a protective coating on particles of titanium dioxide pigments, as a refractory material, in insulation, abrasives and enamels. Stabilized zirconia is used in oxygen sensors [1-12] and fuel cell membranes because it has the ability to allow oxygen ions to move freely through the crystal structure at high temperatures. The high ionic

2. 2. SYNTHESIS OF NANOSTRUCTURED ZrO₂ POWDER

Nanostructured ZrO₂ powder was synthesized by disc type ultrasonicated microwave assisted centrifuge technique [13-14], by hydrolysis of AR grade zirconium oxychloride in aqueous-alcohol solution (Fig. 1). An initial aqueous-alcohol solution was prepared from distilled water and propylene glycol in the ratio of 1:1. This solution was then mixed with 1 M aqueous solution of zirconium oxychloride in the ratio 1:1. The special arrangement was made to add drop wise aqueous ammonia (0.1 ml / min.) with constant stirring until the optimum pH of solution becomes 7.9. After complete precipitation and centrifugation, the hydroxide was washed with distilled water until chloride ions were not detected by AgNO₃ solution. Then the precipitate in a glass beaker was placed in a microwave oven for 10 minutes with continuous on-off cycles, periodically, followed by calcination at 500°C for 2 hrs in muffle furnace. The dried precipitate was ground by agate pestle-mortar to ensure sufficiently fine particle size and re-calcined in a muffle furnace



Fig. 1: Disc type ultrasonicated microwave assisted centrifuge technique

at 500°C for 2 hrs, to eliminate the organic impurities, if present. The crystallite size of synthesized ZrO₂ powder was monitored by XRD analysis and confirmed on calculating by Scherer's formula. Thus, the dry white powder of nanostructured ZrO₂ has been prepared to use.

3. THICK FILM FABRICATION

The thixotropic paste was formulated by mixing the synthesized nanostructured powder of pure ZrO₂ with a solution of ethyl cellulose (a temporary binder) in a mixture of organic solvents such as butyl cellulose, butyl carbitol acetate and turpineol. While in formulating the paste, the ratio of inorganic to organic part was kept as 80:20. The thixotropic paste was screen printed on the glass substrates and the thick films of desired patterns were obtained [15-18]. Films prepared were dried at 80°C under an IR lamp, followed by firing at 500°C for 30 min. in ambient air. Silver contacts were made by vacuum evaporation for electrical measurements of thick films. Thus, the thick films of pure ZrO₂ are now ready to use in the desired applications.

4. SURFACE FUNCTIONALIZATION OF ZrO₂ THICK FILMS

Surface activation of as prepared thick films of pure ZrO₂ powder was achieved by dipping them into a 0.01 M aqueous solution of bismuth chloride, for different intervals of time viz. 5 min., 15 min., 30 min. and 45 min. and dried at 80°C under an IR lamp, followed by firing at 500°C for 30 min. in ambient air. The particles of bismuth chloride dispersed on the film surface would be transformed to bismuth oxide (Bi₂O₃) upon firing process.

Thus, the different mass % of Bi₂O₃ incorporated in to thick films of pure ZrO₂ was prepared.

5. MATERIALS CHARACTERIZATIONS

5.1 X-RAY DIFFRACTION STUDY

X-ray diffraction study of ZrO₂ powder was carried out using BRUKER AXSD 8 (Germany) advance model. X-ray diffraction with CuKα₁ (λ = 1.54060 Å) radiation is in 2θ range of 20° to 80°. Fig. 2 depicts the XRD pattern of pure ZrO₂ powder. The 2θ peaks observed at 23.96, 40.22, 44.60, 49.21, 54.93, 59.17, 61.79, 65.18, 70.78, 73.99 and 78.30 are correspond to the (011), (211), (112), (220), (113), (131), (312), (231), (004), (041) and (232) planes of reflections. The XRD spectrum reveals that, the material is polycrystalline in nature and monoclinic in structure. The observed peaks are matching well with JCPDS reported data of pure ZrO₂. The material was observed to be nanocrystalline in nature. The lattice parameters were found to be a = 5.21, b = 5.26 and c = 5.37. The unit cell volume was evaluated as 145.16 (JCPDS card no. Zr-002-0464).

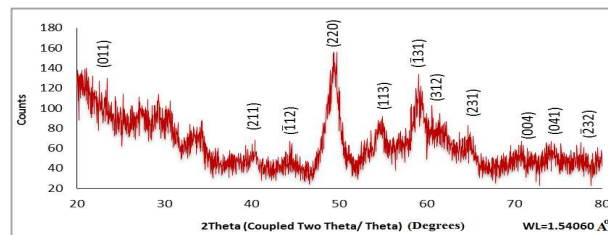


Fig. 2: XRD of pure ZrO₂ powder

It was also observed from XRD analysis that, the synthesized pure ZrO₂ powder has slightly less amorphous nature (46.5%) and slightly more crystallinity (53.5%).

5.2 QUANTITATIVE ELEMENTAL ANALYSIS-EDAX

The quantitative elemental composition of the pure ZrO₂ and Bi₂O₃ activated ZrO₂ thick films were analyzed using an energy dispersive spectrometer and mass % of Zr, O, ZrO₂, Bi, Bi₂O₃ and Bi₂O₃-ZrO₂ are represented in Table 1. The elemental analysis shows that, the synthesized powder of ZrO₂ is not exactly stoichiometric and hence is not insulating.



The prepared powder of pure ZrO_2 is excess in oxygen, which increases its p-typeness characteristic. This leads to semiconducting nature of the synthesized pure ZrO_2 . Excess or deficiency of the constituent material particles leads to the semiconducting nature of the material. Also, the mass % of Zr and O in each activated samples are not as per the stoichiometric proportion and all samples (except 15 min. sample) are observed to be oxygen deficient or excess in zirconium. So, the maximum numbers of electrons are free to conduct the current and the electrons behave as the majority current carriers. This enhances n-typeness of synthesized ZrO_2 .

Table 1: Quantitative elemental analysis of pure and Bi_2O_3 activated ZrO_2 films

Mass % of	Dipping time (min.)					
	0 (Pure) (Expected)	0 (Pure) (Observed)	5	15	30	45
Zr	74.03	72.75	87.49	43.47	37.09	22.10
O	25.97	27.25	08.36	26.41	16.53	08.99
ZrO_2	100.00	100.00	95.37	66.42	48.29	23.19
Bi	00.00	00.00	04.15	30.12	46.38	68.90
Bi_2O_3	00.00	00.00	04.63	33.58	51.71	76.81
Bi_2O_3 - ZrO_2	100.00	100.00	100.0	100.0	100.0	100.0

It is clear from Table 1 that, the mass % of Bi_2O_3 (ZrO_2) on the surface of the film increases (decreases) with dipping time, which may be attributed to the chemisorption of bismuth chloride particles on the surface of the thick films proving masking of the film during dipping process. Thus, dipping process is the simple and low cost technique to activate the surface of the film. This forms Bi_2O_3 - ZrO_2 interfaces on the surface of the film, leading to increase the resistivity.

5.3 MICROSTRUCTURAL ANALYSIS (FESEM)

5.3.1 UNMODIFIED (PURE) ZrO_2

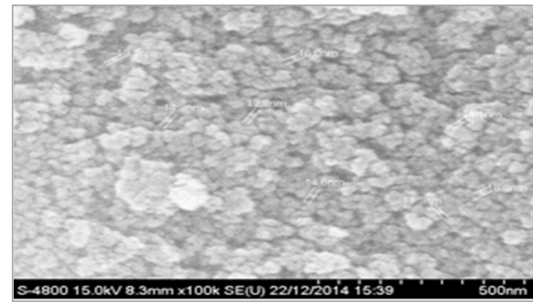
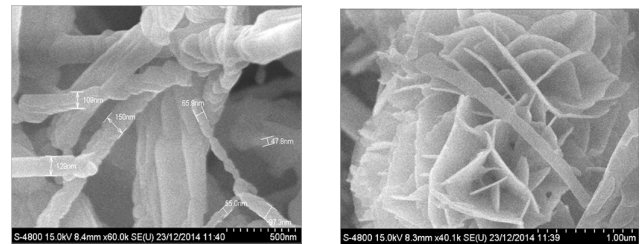


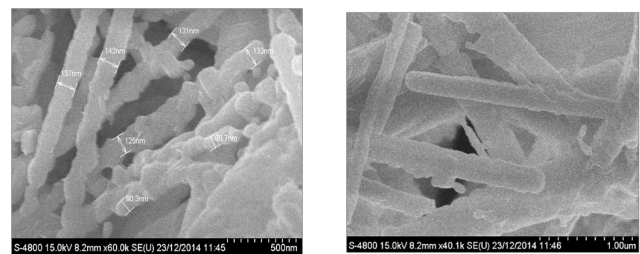
Fig. 3: Micrograph of unmodified (pure) ZrO_2 thick film

Fig. 3 depicts the SEM image of pure ZrO_2 thick film fired at $500^\circ C$ for 30 min. Pure ZrO_2 thick film consists of voids and a wide range of randomly distributed grains with sizes ranging from 10 nm to 20 nm distributed as smaller grains. The appearance of the film looks porous. The nanoscale grains exhibit high surface to volume ratio.

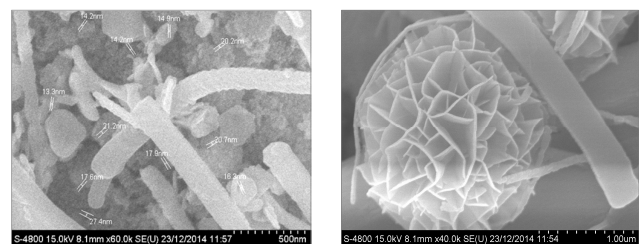
5.3.2 Bi_2O_3 ACTIVATED ZrO_2



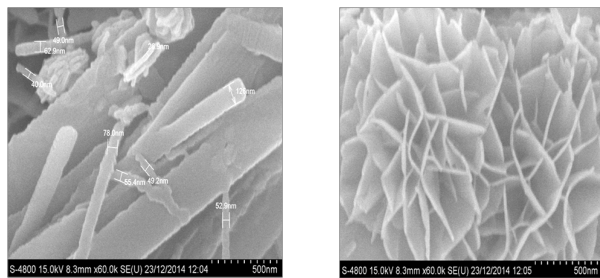
(a) 5 min.



(b) 15 min.



(c) 30 min.



(d) 45 min.

Fig. 4: Micrographs of Bi_2O_3 activated ZrO_2 thick films for different dipping times

Fig. 4 depicts the microstructure of Bi_2O_3 activated ZrO_2 samples for various dipping time viz. 5 min., 15 min., 30 min. and 45 min. and at two magnifications, each.

Fig. 4 (a) depicts the fabrication of Bi_2O_3 nano-rope and nano-discs on the ZrO_2 film, further forming nanoflowers. The average size of nano-rope is about 60 nm and the thickness of nano-discs is about 25 nm. The voids, nano-rope and nanoflowers are randomly distributed and even oriented on the film surface.

Fig. 4 (b) depicts the fabrication of Bi_2O_3 nanorods on the ZrO_2 film surface, distributed randomly with voids. The average size of Bi_2O_3 nanorods is about 100 nm.

Fig. 4 (c) depicts the nanorods and nanoflowers of Bi_2O_3 on the ZrO_2 grains. Film consists of voids and random distribution of nanorods on the film surface. The average size of Bi_2O_3 nanorods is about 25 nm and the thickness of nano-petals is about 20 nm.

Fig. 4 (d) depicts the formation of nanorods and nanoflowers of Bi_2O_3 on the ZrO_2 film surface. The marked region on the image shows the formation of nanopetals of nanoflowers and second image shows the complete nanoflower. The average size of Bi_2O_3 nanorods is about 76 nm. The thickness of nanopetals is about 12 nm in size.

CONCLUSIONS

1. Thick films of nanostructured ZrO_2 material can be fabricated by using simple and low cost screen printing mechanism.
2. Dipping process is one of the effective processes to modify the surface morphology of the thick films in order to enhance the conductivity of the samples.
3. Pure stoichiometric ZrO_2 is expected to be insulating.
4. Synthesized powder of ZrO_2 is not exactly stoichiometric and hence is not insulating.
5. The bulk ZrO_2 powder can be effectively transformed into nanostructured form by using disc type ultrasonicated microwave assisted centrifuge technique.

REFERENCES

1. B. Lei, Li Wang, H. Zhang, Y. Liu, H. Dong, M. Zheng, X. Zhou, Luminescent carbon dot assembled SBA-15 and its oxygen sensing properties, *Sens. Actuators B* 230 (2016) pp. 101-108.
2. J. Exner, M. Schubert, D. Hanft, T. Stocker, P. Fuierer, R. Moos, Tuning of the electrical conductivity of $\text{Sr}(\text{Ti},\text{Fe})\text{O}_3$ oxygen sensing films by aerosol co-deposition with Al_2O_3 , *Sens. Actuators B* 230 (2016) pp. 427-433.
3. Swagata Banerjee, O. V. Arzhakova, A. A. Dolgova, D. B. Papkovsky, Phosphorescent oxygen sensors produced from polyolefin fibers by solvent crazing method, *Sens. Actuators B* 230 (2016) pp. 434-441.
4. NoriaIzu, Sayaka Nishizaki, Woosuck Shin, Toshino Itoh, Maiko Nishibori, Ichiro Matsubara, Resistive O_2 sensor using Ceria-Zirconia sensor material and Ceria-Yttria temperature compensating material for Lean-Burn engine, *Sensors* 9 (2009) pp. 8884-8895.
5. NoriaIzu, Noriko Oh-hori, Woosuk Shin, Ichiro Matsubara, Norimitsu Murayama, Masaki Itou, Response properties of resistive O_2 sensors using $\text{Ce}_{1-x}\text{Zr}_x\text{O}_2$ thick films in propane combustion gas, *Sens. Actuators B* 130 (2008) pp. 105-109.



9. N. Izu, W. Shin, I. Matsubara, N. Murayama, N. O. Hori, M. Itou, Temperature independent resistive oxygen sensors using solid electrolyte zirconia as a new temperature compensating material, *Sens. Actuators B* 108 (1-2) (2005) pp. 216-222.
10. A. Rothschild, S. J. Litzelman, H. L. Tuller, W. Menesklou, T. Schneider, E. I. Tiffée, Temperature independent resistive oxygen sensors based on $\text{SrTi}_{1-x}\text{Fe}_x\text{O}_{3-\delta}$ solid solutions, *Sens. Actuators B* 108 (1-2)
11. N. Izu, N. O. Hori, M. Itou, W. Shin, I. Matsubara, N. Murayama, Resistive oxygen sensors based on $\text{Ce}_{1-x}\text{Zr}_x\text{O}_2$ nanopowder prepared using new precipitation method, *Sens. Actuators B* 108 (1-2) (2005) pp. 238-243.
12. Y. Hu, O. K. Tan, J. S. Pan, H. Huang, W. Cao, The effects of annealing temperature on the sensing properties of low temperature nanosized SrTiO_3 oxygen gas sensor, *Sens. Actuators B* 108 (1-2) (2005) pp. 244.
13. Wenqing Cao, Ooi Kiang Tan, W. Zhu, Jisheng S. Pan, Jiang Bin, Study of $x\alpha\text{-Fe}_2\text{O}_3\text{-(1-x)ZrO}_2$ solid solution for low temperature resistive O_2 gas sensors, *Sensors IEEE* 4 (2003) pp. 421-434.
14. P. Jasinski, T. Suzuki, H. Anderson, Nanocrystalline undoped ceria oxygen sensor, *Sens. Actuators B* 95 (1-3) (2003) pp. 73-77.
15. Papkovsky D. B., New oxygen sensors and their application to biosensing, *Sens. Actuators B* 29 (1-3) (1995) pp. 213-218.
16. Kapse S. D., Raghuvanshi F. C., Kapse V. D., Patil D. R., Characteristics of high sensitivity ethanol gas sensors based on nanostructured spinel $\text{Zn}_{1-x}\text{Co}_x\text{Al}_2\text{O}_4$, *J. Current Appl. Phys.* 12 (2012) pp. 307 – 312.
17. Khamkar K. A., Bangale S. V., Dhapte V. V., Patil D. R., Bamne S. R., A Novel Combustion Route for the Preparation of Nanocrystalline LaAlO_3 Oxide Based Electronic Nose Sensitive to NH_3 at Room Temperature, *Sens. Transducers* 146 (2012) pp. 145-155.
6. Patil D. R., Patil L. A., Patil P. P., Cr_2O_3 -activated ZnO thick film resistors for ammonia gas sensing operable at room temperature, *Sens. Actuators B* 126 (2007) pp. 368–374.
7. Patil D. R., Patil L. A., Ammonia sensing resistors based on Fe_2O_3 -modified ZnO thick films, *Sensors IEEE* 7 (2007) pp. 434-439.
8. Gawas U. B., Verenkar V. M. S., Patil D. R., Nanostructured ferrite based electronic nose sensitive to ammonia at room temperature, *Sens. Transducers* 134 (2011) pp. 45-55.



Photoelectrochemical applications of NiSe thin films prepared by Chemical bath deposition method

B.V. Jadhav*

*Department of Chemistry, Changu Kana Thakur A.C.S.College, New Panvel, Raigad 410206, Maharashtra, India

KEYWORDS

Chemical deposition;
photoelectrode; Power
output; Spectral response
Photoresponse.

Corresponding Author Email

bjadhav02@yahoo.com

ABSTRACT

Nickel selenide photoelectrodes have been synthesized by chemical bath deposition method onto stainless steel plate. The configuration of fabricated cell is $p\text{-NiSe|NaOH (1M)+ S (1M)+Na}_2\text{S (1M)|C}_{(\text{graphite})}$. The photoelectrochemical cell characterization of the photoelectrodes is carried out by studying current–voltage characteristics in dark, capacitance–voltage in dark, barrier-height measurements, power output, photoresponse and spectral response. The junction ideality factor was found to be 5.61. The flat band potential was found to be 304 mV. The barrier-height value was found to be 0.195 eV. The study of power output characteristic shows open circuit voltage, short circuit current, fill factor and efficiency was found to be 160 mV, $71\mu\text{A}/\text{cm}^2$, 41.89% and 0.11%, respectively. Photoresponse shows lighted ideality factor is 5.37. Spectral response shows the maximum current observed at 721 nm.

Introduction

Thin films of metal chalcogenide semiconductors are of considerable interest for their excellent optical properties in the visible range. In photoelectrochemical cells (PEC), the use is made of the interface which forms on mere dipping the semiconductor into electrolyte solution and the liquid junction potential barrier can be easily established. Polycrystalline semiconductor films can also be used without any drastic decrease in efficiency. This is probably due to the intimate and perfect contact of liquid electrolyte with the crystalline grains. Thus PEC cells provide an economic chemical route for trapping solar energy [1]. Along with PEC the semiconductor electrolyte interface may be used for photoelectrolysis, photocatalysis and photoelectrochemical power generation [2,3]. The properties of such systems are mainly dependent on the interface formed between the semiconductor electrode and electrolyte hence from material

point of view the microstructure of the photoelectrode surface is of main importance [4,5]. The advantage of PEC cells is simpler to make as compared to the p–n junctions which require highly pure semiconducting material.

In this paper, we report the study of the photoelectrochemical performance of chemically deposited NiSe photoelectrode. $I\text{-}V$, $C\text{-}V$ characteristics, barrier height measurements, power out curves, photoresponse and spectral response parameters are studied.

2. Experimental details

2.1. Reagents and preparation of solutions

All the chemicals used were analytical grade. It includes nickel sulphate octahydrate, tartaric acid, liquor ammonia, sodium sulphite, hydrazine hydrate and selenium powder. All the solutions were prepared in double distilled water. Sodium seleno sulphate (0.25M) was used as

selenium source for the deposition of cadmium selenide thin films. The solution was prepared by refluxing 5 g selenium powder with 15 g sodium sulphite in 200mL double distilled water for 9 h at 363 K. The solution was cooled, filtered to remove undissolved selenium and stored in an airtight bottle [6].

2.2. Deposition of photoelectrode

Nickel selenide thin films have been deposited on stainless steel substrates by using chemical bath deposition method. In actual experimentation, 10 mL (0.25M) nickel sulphate octahydrate solution was taken in 100 mL beaker. 4 mL (1M) tartaric acid, 15 mL ammonia, 25 mL (50%) hydrazine hydrate and 10 mL (0.25M) sodium selenosulphate were added in the reaction mixture at 278 K temperature. The temperature of the bath was maintained at 278K using ice bath. The stainless steel plates were clamped vertically on a specially designed substrate holder and rotated in the reaction mixture with a speed of 50 ± 2 rpm. The temperature of the bath was then allowed to increase upto 298 K slowly. After 3 hours, the stainless steel plates were removed washed several times with double distilled water. The photoelectrode was dried naturally and preserved in a dark dessicator over anhydrous calcium chloride. The resultant films were homogenous, well adherent to stainless steel substrate.

2.3. Fabrication of PEC cell

Three electrode configurations are used in experiment. NiSe as photoanode, CoS-treated graphite rod as a counter electrode. A saturated calomel electrode was used as reference electrode and sulphide-polysulphide as electrolyte.

2.4. Characterization of PEC cell

The area of illuminated electrode was 3.0cm^2 . The type of conductivity exhibited by the film is determined by noting the polarity of the emf developed in PEC cell under illumination. The current-voltage ($I-V$) characteristic in dark has been plotted. The junction ideality factor has been determined by plotting the graph of $\log I$ versus V .

The Mott-Schottky plot is used to determine the flat band potential. 1 kHz frequency is used to determine the flat band potential. The power output characteristic has been obtained for a PEC cell at a constant illumination of $30\text{mW}/\text{cm}^2$. The fill factor and power conversion efficiency of the cell is calculated from photovoltaic power output characteristics. The barrier-height was examined from temperature dependence of reverse saturation current at different temperature. Light ideality factor was measured from photoresponse. Spectral response was determined by measuring short circuit current as well as open circuit voltage as function of incident light wavelength (400-1000nm).

3. Results and discussion

3.1. Conductivity type

A PEC cell with configuration p-NiSe|NaOH (1M) + S (1M) + Na₂S (1M)|C_(graphite) was formed. Even in the dark, PEC cell shows dark voltage and dark current. The polarity of this dark voltage was positive towards semiconductor electrode. The sign of the photovoltage gives the conductivity type of NiSe. This suggests that NiSe is a p-type conductor.

3.2. $I-V$ characteristics in dark

Current-voltage ($I-V$) characteristics of PEC cell in dark have been studied at 303K and shown in Fig. 1. The characteristics are non-symmetrical indicating the formation of rectifying type junction. The junction ideality factor (n_d) can be determined from the plot of $\log I$ with voltage and the variation is shown in Fig. 2. The ideality factor was found to be 5.61, which is higher. The higher value of n_d suggests the dominance of series resistance as well as structural imperfection. It also suggests that average transfer across the semiconductor electrolyte interface with significant contribution from surface states and deep traps [7,8].

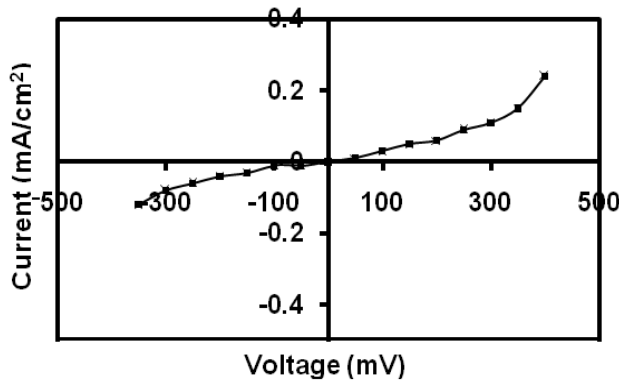


Fig. 1. *I-V* characteristics of NiSe photoelectrode (in dark)

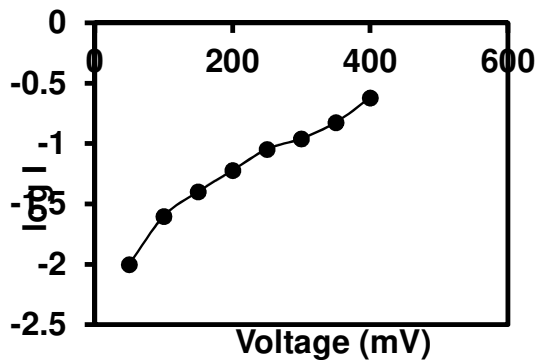


Fig. 2. Determination of junction ideality factor of NiSe photoelectrode.

3.3. *C-V* characteristics in dark

The measurements of capacitance as a function of applied voltage provided useful information such as type of conductivity, band bending depletion layer width and flat band potential (V_{fb}). The flat band potential of a semiconductor gives information of the relative position of the Fermi levels in photoelectrode as well as the influence of electrolyte and charge transfer process across the junction. This is also useful to measure the maximum open circuit voltage (V_{oc}) that can be obtained from a cell. Measured capacitance is the sum of the capacitance due to depletion layers and Helmholtz layer in electrolyte, which is neglected by assuming high ionic concentration [9].

Under such circumstances, V_{fb} can be obtained using Mott-Schottky relation by standardizing with saturated calomel electrode (SCE);

$$C^{-2} = [2 / q\epsilon_s\epsilon_0 N_d] (V - V_{fb} - kT / q) \quad (1.1)$$

where symbols have their usual meaning. The variation of C^{-2} with voltage for representative samples is shown in Fig. 3. Intercepts of plots on voltage axis determine the flat band potential value of the junction. The flat band potential value found to be 304 mV (SCE) for NiSe-polysulphide redox electrolyte, which is a measure of electrode potential at which band bending is zero. The non-linear nature of the graph is an indication of graded junction formation between NiSe and polysulphide electrolyte. Non-planar interface, surface roughness, ionic adsorption on the photoelectrode surface may be possible reasons for deviation from linearity in $C-V$ plot.

3.4. Barrier height measurements

The barrier height was determined by measuring the reverse saturation current (I_0) flowing through the junction at different temperature from 363 to 303K. The reverse saturation current flowing through junction is related to temperature as [10,11]

$$I_0 = AT^2 \exp(-\Phi_\beta / kT) \quad (1.2)$$

where A is Richardson constant, k is the Boltzmann constant, Φ_β is the barrier height in eV. To determine the barrier height of the photoelectrode, a graph of $\log(I_0/T^2)$ versus $1000/T$ was plotted. The plot of $\log(I_0/T^2)$ with $1000/T$ for representative sample is shown in Fig. 4. From the slope of the linear region of plot, the barrier height was determined. The barrier height value is found to be 0.195 eV.

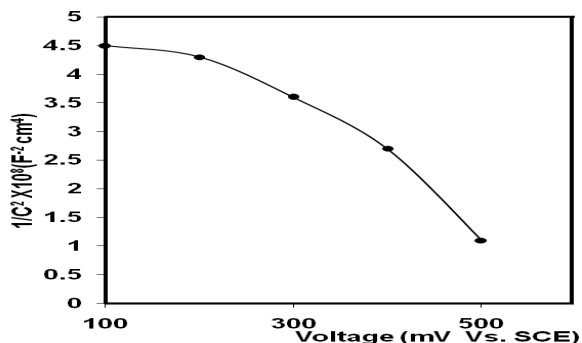


Fig. 3. C–V characteristics of NiSe photo electrode.

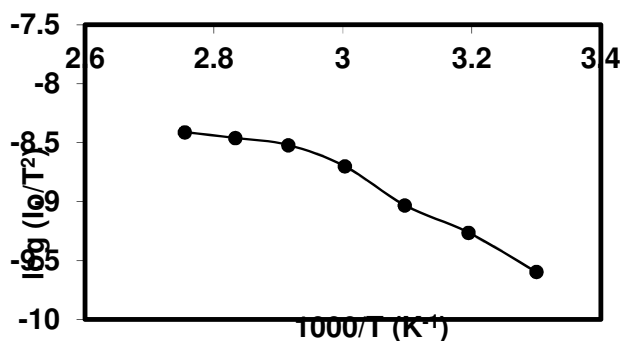


Fig. 4. Determination of barrier-height measurement of NiSe photoelectrode.

3.5. Power output characteristics

Fig. 5 shows the photovoltaic power putout characteristics for a cell recorded under 30 mW/cm² illumination intensity. The maximum power output of the cell is given by the largest rectangle that can be drawn inside the curve. The open circuit voltage and short circuit current are found to be 160 mV and 71μA/cm² respectively. The calculation shows that the fill factor is 41.89%. The power conversion efficiency is found to be 0.11%. The low efficiency may be due high series resistance and interface states which are responsible for recombination mechanism. The value of series resistance and shunt resistance were found to be 1287 Ω and 846 Ω, respectively. The main drawback in utilizing PEC cell is the absence of space charge region at the photoelectrode–electrolyte interface. In this situation, the photogenerated charge carriers can move in both the direction.

3.6 Photoresponse

To study, the response of the PEC cell towards light, the cell was illuminated with light of different intensity. The open circuit voltage and short circuit current were measured as a function of light intensity. Fig.6 shows variation of short circuit current (I_{sc}) as a function of light intensity, whereas, Fig.7 shows the variation of open circuit voltage (V_{oc}) as a function of light intensity. The photoresponse measurements showed a logarithmic variation of open circuit voltage with the incident light intensity. However, at higher intensities, saturation in open circuit voltage was observed, which can be attributed to the saturation of the electrolyte interface, charge transfer and non-equilibrium distribution of electrons and holes in the space charge region of the photoelectrode. But short circuit current follows almost a straight line path. The photoelectrode- electrolyte interface can be modeled as a Schottky barrier solar cell [12] and it is therefore possible to represent the current-voltage relationship as;

$$I = I_{ph} - I_d = I_{ph} - [I_o \exp (qV/n_dkT) - I] \quad (1.3)$$

Where, I is the net current density, I_{ph} is the photocurrent densities, I_d is the dark current density, I_o is the reverse saturation current density, V is the applied bias voltage and n_d is the junction ideality factor. In bias voltage condition $V > 3kT/q$ and at equilibrium open circuit conditions;

$$I_{ph} = I_d \text{ and } V = V_{oc} \text{ Thus,}$$

$$V_{oc} = (n_d kT/q) \ln (I_{sc}/I_o) \quad (1.4)$$

Where, V_{oc} is open circuit voltage, I_{sc} is short circuit current. As $I_{sc} \gg I_o$, a plot of $\log I_{sc}$ against V_{oc} should give a straight line and from the slope of the line the lighted ideality factor can be determined. The plot of $\log I_{sc}$ with V_{oc} for NiSe photoelectrode is shown in Fig.8. The lighted ideality factor was calculated and found to be 5.37

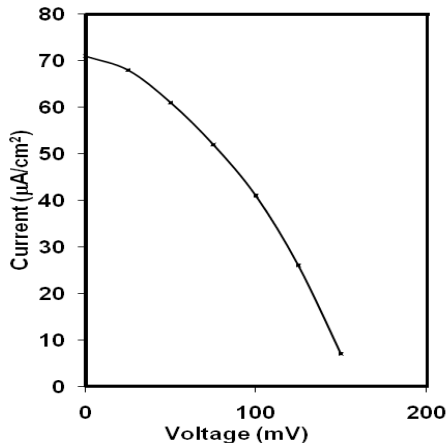


Fig. 5. Power output curves for NiSe photoelectrode.

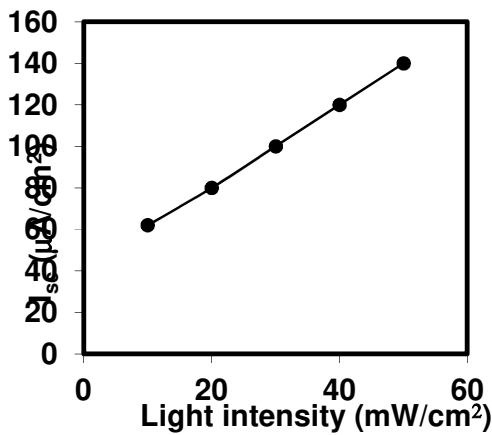


Fig.6. Photoresponse as a function of short circuit current for NiSe photoelectrode.

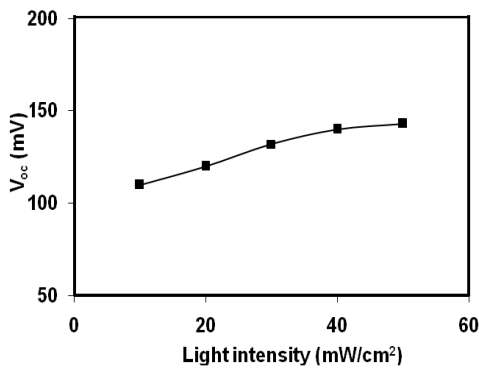


Fig.7. Photoresponse as a function of open circuit voltage for

NiSe photoelectrode

3.7 Spectral Response

The spectral response of photoelectrochemical cell is one of the most powerful techniques to measure the performance of the cell qualitatively. Therefore, the spectral response of a cell has been recorded in the 400-1000 nm wavelength range. The photocurrent action spectra were examined and are shown in Fig.9. It is seen that spectra attains maximum value of current at around wavelengths 721 nm and decreases with increase in wavelength. The decrease in current on shorter wavelength side may be due to absorption of light in the electrolyte and high surface recombination of photogenerated minority carriers. The decrease in current on longer wavelength side may be attributed to non-optimized thickness and transition between defect levels. The maximum current is obtained corresponding to $\lambda = 721$ nm gives band gap value 1.72 eV for agreeing with the results of optical absorption studies [2, 5].

The various cell characteristics such as V_{oc} , I_{sc} , η , $ff\%$, Φ_{β} , V_{fb} , R_s , R_{sh} , nL , nd are cited in Table 1 for nickel selenide photoelectrode.

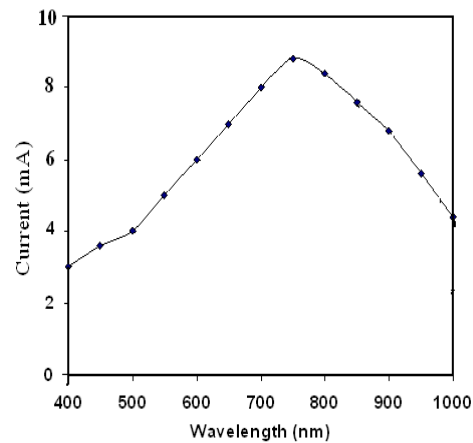


Fig. 9. Determination of spectral response for NiSe photoelectrode.

Table 1. PEC cell performance parameters of NiSe photoelectrode

Comp	V _{oc} (mV)	I _{sc} (μA/cm ²)	η %	ff %	Φ _β (eV)	V _{fb} (mV)	R _{sh} (Ω)	R _s (Ω)	n _L	n _d
NiSe	160	71	0.11	41.89	0.195	304	846	1287	5.31	5.61

4. Conclusion

Nickel selenide photoelectrode can be deposited by using nickel sulphate octahydrate, tartaric acid, ammonia, hydrazine hydrate and sodium selenosulphate onto stainless steel plate. The photoelectrochemical cell can be easily fabricated using NiSe photoanode, sulphide-polysulphide as electrolyte, CoS-treated graphite rod as a counter electrode. A saturated calomel electrode was used a reference electrode. The various performance parameters were determined for NiSe photoelectrode.

References

- [1] S. Chandra, Photoelectrochemical Solar Cells, Gordon and Breach, London, 1984.
- [2] V.V. Killedar, C.D. Lokande, C.H. Bhosale, Ind. J. Pure & Appl. Phys. 36 (1998) 643.
- [3] P.J. Holmes, The Electrochemistry of Semiconductors, Academic Press, 1992.
- [4] M.B. Bouroushian, D. Karoussos, T. Kosanovic, Solid State Ionics 177 (2006) 1855.
- [5] P.P. Hankare, P.A. Chate, S.D. Delekar, M.R. Asabe, I.S. Mulla, J. Phys. Chem. Solids 67 (2006) 2310.
- [6] P.P. Hankare, P.A. Chate, D.J. Sathe, M.R. Asabe, B.V. Jadhav, Journal of Alloys and Compounds 474 (2009) 347.
- [7] H.J. Lewerenz, H. Goslowsky, F. Thiel, Sol. Energy Mater. 9 (1983) 159.
- [8] A. Chemseddine, R. Morineau, J. Lirage, Solid State Ionics 9 (1983) 357.

- [11] A. Aruchami, G. Aravamudan, G.V. Subba Rao, Bull. Mater. Sci. 4 (1982) 483.
- [12] K. Rajeshwar, L. Thomson, P. Singh, R.C. Kainthala, K.L. Chopra, J. Electrochem. Soc. 128 (1981) 1744.



Simple Method for Synthesis of Pd Supported Nanoparticles and Its Applications in Organic Transformation

A. V. Mali^a, A. S. Tapase^c and P.P. Hankare^b

^aUG & PG Department of chemistry, Yashwantrao Chavan College of Science, Karad. Vidyanagar, Karad – 415 124 M.

^bDepartment of chemistry, Shivaji University, Kolhapur.

^cDattajirao Kadam Arts Science-Commerce college, Ichalkaranji -416115. Maharashtra, India.

KEYWORDS

Synthesis,
Characterization,
Catalytic application

Corresponding Author

Email

nkushvmali@gmail.com

ABSTRACT

Silica supported palladium nanoparticles were prepared by very simple solution reduction method using N-cetyl-N,N,N-trimethyl ammonium bromide (CTAB) as a capping agent and Sodium borohydride as a reducing agent. These synthesized materials are air and moisture stable used in open air. Crystalline nature and particle size of the material is characterized by powdered x-ray spectroscopy. The synthesized materials are used as heterogeneous catalyst in Heck coupling reaction with best results. This heterogeneous catalyst are separated from reaction mixture by simply filtration and repeatedly used without loss of activity. Crystalite size of Pd/SiO₂ was estimated to be 56 nm.

Introduction

The arylation and vinylation of alkene with aryl or vinyl halides was discovered independently by Heck and Mizoroki about 40 year ago [1-2]. Now a day it is universally known as Heck reaction. Palladium catalyzed Heck reaction between aryl halide and olefins is an important reaction in modern organic synthesis [3-5]. The reaction is generally catalyzed by either Pd (0) or Pd (II) complexes in solution [6-8]. In order to circumvent the problems, like catalyst recovery and air sensitivity associated with reactions under homogeneous condition, heterogeneous catalytic systems were developed. In recent years, Heck reaction has been catalyzed by palladium metal supported on charcoal, mesoporous Carbon, magnesium oxide, palladium/Nb-MCM-41, polymers, zeolites, polyionic resins [9-12]. Basic supports such as layered double hydroxide, basic zeolites,

alkaline exchanged sepiolites, mixed oxide, fluorapatite [13-17] have been used because Pd on these supports shows considerably higher activity towards Heck reaction. To our knowledge alumina supported palladium nanoparticles has not been prepared by reduction method using CTAB & Sodium borohydride as a reducing agent and has not been used in open air, as a heterogeneous catalyst for the Heck reaction. Herein, we report the synthesis and characterization of air and moisture stable silica supported palladium nanoparticles and it used as a heterogeneous catalyst for the Heck reaction. The catalyst is air stable, can be stored and handled in air, and after the reaction it can be recovered by simple filtration and reused without significant loss of activity.

2. EXPERIMENTAL SECTION

The melting point of product determined in open capillary tube are uncorrected. Infrared spectra were recorded using KBr pellets on a FT Perkin Elmer spectrometer. The ^1H NMR and ^{13}C NMR spectra were recorded in DMSO/ CDCl_3 on a Bocker-300 spectrophotometer. (Scheme No-1)

2.1 Catalyst preparation

Catalyst were prepared as, Solution A: - Silica and Sodium borohydride solution were taken in beaker and stirred for 10 min to obtain homogeneous 'Solution A' (details are given in Table 1). Solution B: - CTAB were added in distilled water and stirred for 30 min to obtained clear CTAB solution 'Solution B'

Solution A and Solution B were mixed and PdCl_2 was added drop wise in to the mixture of 'Solution A and Solution B' under constant stirring. (Details are given in Table 1) The resulting gel was stirred 1 hr for homogenization and was placed for 3 days. The above clear liquid was decanted and solid particles was washed repeatedly with water & acetone till the filtrate was neutral to litmus and dried.

Table 1. The preparation of Silica Supported Palladium Nanoparticles

Sr. No	% of Pd	Solution A in mL		Solution B in mL (CTAB 0.5M)	PdCl_2 in mL 1.56×10^{-3} M
		SiO_2 in mg	NaBH_4 (0.5M)		
1	1	500	50	50	50
2	2	500	100	100	100
3	3	500	150	150	150
4	4	500	200	200	200

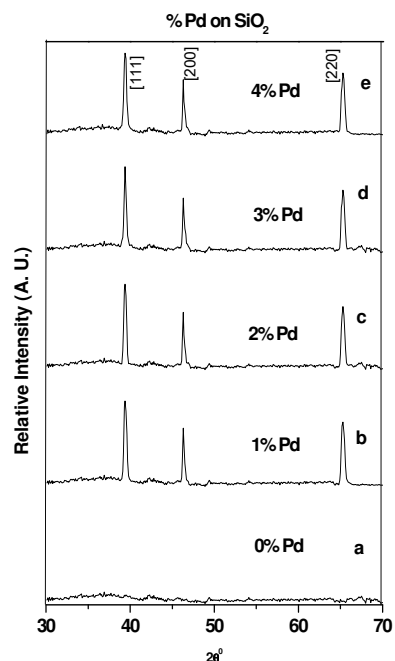
2.2 Catalyst Application

Heck reaction of bromobenzene with styrene was carried out using these catalyst after activation at 200°C for 4 hr (scheme. 1.) A typical reaction was carried out in open air, Bromobenzene 0.42 mL (4 mmol), styrene 0.68 mL (6 mmol), K_2CO_3 1.646 g (12 mmol), solvent DMF 5 mL and Pd/SiO_2 5wt% (0.074g) with respect to reactants was taken in 50 mL round bottom flask connected to water condenser and heated in oil bath at 130°C with constant stirring. The reaction was monitored time to time by TLC. After the 9 hr reaction was quenched with 5 mL of water and the catalyst was filtered. Next 50 mL of water was added to the filtrate and the product was extracted with ether. The product obtained after evaporation of the solvent was purified by column chromatography using silica gel (60-120 mesh) with petroleum ether as eluent. The results of the screening of the catalysts are presented in table 2.

3. RESULT AND DISCUSSION

3.1 X-ray Study:-

Fig 1. XRD of Pd/SiO_2 a- SiO_2 , b-1% Pd/SiO_2 , c-2% Pd/SiO_2 , d-3% Pd/SiO_2 , e-4% Pd/SiO_2 .



The structure and phase purity of the catalyst were confirmed by analyzing the observed powder X-ray diffraction patterns. Fig.1. The X-ray diffraction of SiO₂ and Pd/ SiO₂ catalyst shows three peaks around 39°, 46° and 67° respectively. These peaks corresponds to [111], [200] and [220] planes of a face centered cubic lattice, indicating the FCC structure with single phase nature. From the X-ray diffraction peaks, average particle size was estimated using Scherrer's formula. $D = 0.9\lambda/\beta\cos\theta$

Where β is the FWHM of the most intense peak, θ is the Bragg angle for the most intense peak, and λ is the wave length of $\text{CuK}\alpha = 1.54 \text{ \AA}$. From above equation the average crystallite size of X Pd/ SiO₂ (X =1% - 4%) was estimated to be 56 nm.

3.2 Heck Reaction:- Scheme No:-1

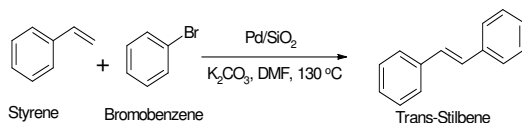


Table 2 Heck reaction over heterogeneous catalysts: Pd/ SiO₂

Entry	Alkyl Halide	Olefins	Catalyst	Yield %
1			-	00
2			PdCl ₂	37 ^a
3			1%	76
4			2%	79
5			3%	79
6			4%	80
7			2%	79 ^b
8			2%	78 ^c

Reaction Conditions:- Bromobenzene (4mmol), Styrene (6 mmol), K₂CO₃ (12mmol), Pd/ SiO₂ 5wt%, DMF 5 ml Temp 130°C Time 9 Hr

a Yield after first cycle, b Yield after second cycle. c Yield after third cycle,

3.2 Spectral Analysis:-

m.p. 124°C; IR (KBr): 2926, 1597, 1451, 962, 764, 692, 525; ¹H NMR (CDCl₃): δ 7.28 (t, 2H), δ 7.39 (t, 4H), δ 7.55 (d, 2H), δ 7.15 (s, 2H); ¹³CMR (CDCl₃): 78.7, 97.4, 129.6, 137.9.

4. CONCLUSION

Pure SiO₂ without Pd loading did not produce trans stilbene even after 18 hr. When the reaction was carried out with 0.1 mol% of PdCl₂ as the catalyst, the product yield was 37%. Surprisingly, the 2% loading of palladium is sufficient for the Heck reaction. In ethanol solvent no reaction was observed under reflux conditions.

The heterogeneous nature of the reaction over Pd/ SiO₂ was tested as follows. The catalyst Pd/ SiO₂, bromobenzene and K₂CO₃ (except the olefin) were mixed in dry DMF and heated at 130°C with constant stirring for 5 hr. The catalyst was filtered out quickly and styrene was added to the reaction mixture followed by 10 % more of the K₂CO₃ base and the reaction was continued for another 5 hr at 130°C. Analysis by GC did not reveal any product formation. This showed that the reaction did not proceed on the removal of the solid catalyst suggesting its heterogeneous nature. The catalyst could be recycled without any treatment, through some loss was noticed in the yield of trans stilbene from the reaction between bromobenzene and styrene using 2 % Pd/ SiO₂. In summary, alumina supported palladium nanoparticles has been successfully prepared in a stable form. This catalyst proves to be an excellent catalyst for Heck coupling reaction. A bromobenzene and styrene catalyzed by PdCl₂ and the Pd/ SiO₂ carried out in air. Excellent conversions and yields make this Pd/ SiO₂ catalyst is novel

and efficient catalytic system. These reactions take place at low as well as at elevated temperatures although, of course, the reactions require a longer time at a lower temperature. **5.**

ACKNOWLEDGEMENT:

This work has been supported by University Grant Commission New Delhi (UGC) for financial support. One of the Author A.V. Mali thanks UGC for sanctioning Minor Research Project. UGC letter No. 47-1979/11(WRO) dated 21st Feb 2012.

References:-

- [1] E. F. Heck, *Acc. Chem. Res.* **1979** (12) 146.
- [2] T. Mizoroki, K. Mori, A. Ozaki, *Bull. Chem. Soc. Jpn.* **1971** (44) 581.
- [3] R.F. Heck, *Palladium Reagents in Organic Synthesis*, Academic Press, London, 1985.
- [4] Zhang, N.; Xu, Y.-J. *Chem. Mater.* **2013** (25) 1979.
- [5] Wu, X.-F.; Anbarasan, P.; Neumann, H.; Beller, M. *Angew. Chem., Int. Ed.* **2010** (49) 9047.
- [6] Kumar, A.; Rao, G. K.; Kumar, S.; Singh, A. K. *Organometallics* **2014** (33) 2921.
- [7] Patel, H. H.; Sigman, M. S. *J. Am. Chem. Soc.* **2015** (137), 3462.
- [8] Liu, X.; Li, B.; Gu, Z. *J. Org. Chem.* **2015** (80) 7547.
- [9] Yu, L.; Huang, Y.; Wei, Z.; Ding, Y.; Su, C.; Xu, Q. *J. Org. Chem.* **2015** (80) 8677.
- [10] Bej, A.; Ghosh, K.; Sarkar, A.; Knight, D. W. *RSC Adv.* **2016** (6) 11446.
- [11] Shen, C.; Shen, H.; Yang, M.; Xia, C.; Zhang, P. *Green Chem.* **2015** (17) 225.
- [12] Elazab, H. A.; Siamaki, A. R.; Moussa, S.; Gupton, B. F.; El-Shall, M. S. *Appl. Catal., A* **2015** (491) 58.
- [13] Camp, J. E.; Dunsford, J. J.; Dacosta, O. S. G.; Blundell, R. K.; Adams, J.; Britton, J.; Smith, R. J.; Bousfield, T. W.; Fay, M. W. *RSC Adv.* **2016** (6) 16115.
- [14] Xu, T.; Zhang, Q.; Jiang, D.; Liang, Q.; Lu, C.; Cen, J.; Li, X. *RSC Adv.* **2014** (4) 33347.
- [15] Planellas, M.; Moglie, Y.; Alonso, F.; Yus, M.; Pleixats, R.; Shafir, A. *Eur. J. Org. Chem.* **2014** 3001.
- [16] Jiang, Z.-j.; Wang, W.; Zhou, R.; Zhang, L.; Fu, H.-y.; Zheng, X.-l.; Chen, H.; Li, R.-x. *Catal. Commun.* **2014** (57) 14.
- [17] Shah, D.; Kaur, H. *J. Mol. Catal. A: Chem.* **2016** (424) 171.



Comparative Study of Germination of Seed of *Vigna radiata* and *Vigna aconitifolia* by Treatment of Ultrasonic Wave using Sonicator

Avinash A Ramteke* and Shivaji R Kulal

*Department of Chemistry, Devchand College, Arjun Nagar-591237, Tal. Kagal, Dist. Kolhapur, (MS), India

Department of Chemistry, Raje Ramrao Mahavidyalaya, Jath-416004, Dist. Sangali, (MS), India

KEYWORDS

Ultrasonication,
Fertilisers,
Germination,
Plant growth regulator,
Crop plants.

Corresponding Author
Email
dravinash03@gmail.com

ABSTRACT

Now a day, the ultrasound has found of uses in engineering, science and medicine etc, therefore it has great importance. Recently the research work is still in progress to study the effect of ultrasonic waves in chemical, physical, biological, mechanical and industrial fields. Hence this paper is investigated the study of plant growth regulators of crop plants (*Vigna radiata* and *Vigna aconitifolia*) through germination. The growth parameters like germination, survival, seedling height, young leaf and root/shoot ratio etc were studied. The results thus found were used to assay the effect of ultrasonic waves on crop plants.

Introduction

Crop plants and human being have unique relationship since time immemorial and they are play a vital role in the human life. The population of India is increasing day to day, hence their food demand increases. Therefore, need to improve the yield of crop plants. To fulfil their demand, researchers and scientist search new application in agricultural field for increase the yield, currently, with the continuous application of fertilizers on plants to increase the yield. Actually, a plant's normal growth and function depend on relatively high intracellular water content. The important contributions of the nineteenth century, experimental plant physiology to agriculture was discovery that soil fertility and crop yields could be increased by adding several nutrients to

the soil. Germination is an economical and simple method for improving the nutritive value and several studies have reported [1-3] and it is used for higher yield and effective growth of plant and agricultural product. Therefore, it's using to increase the crop yield because the intensity of ultra wave is not so intense therefore it cannot be damage to the cell of plants as well as human being also. Now days, ultrasonic wave also used to synthesis of mono and bimetallic Au-Ag reduced graphene oxide based nanocomposites [4]. So, researchers and scientist purposely concentrating on the application of ultrasonic wave for the study of germination pattern of crop plants which are use in everyday life of human. Since, many years use of chemical fertilizers in the agriculture field to increase the yield of crop plants were reported [5, 6].

Hussain *et. al* [7] reported the vermicomposting eliminates the toxicity of Lantana (*Lantana camara*) and turns it into a plant friendly organic fertilizer that identified with IR spectra. Changed and induction of amino peptidase activities in response to pathogen infection during germination of pigeon pea (*Cajanas cajan*) seeds [8]. Seed dormancy is an important process in the germination and different methods have been applied to overcome the seed dormancy such as regulatory hormones [9], light and seed scarification [10], salinity, temperature and humidity [11], seed stratification [12]. A Physiological and antioxidant response of germinating mung bean seedlings to phthalate esters in soil has been studied by MA Ting-Ting *et.al* [13]. But the fertilizers used in the field are contains hazardous chemicals which is harmful to the soil, environment as well as human directly or indirectly. Ultimately the fertility of soil is decreases due to over use of chemical fertiliser. Therefore, the aim of this work was to study the effects of growth regulators and germination pattern of *Vigna radiata* and *Vigna aconitifolia* plants in presence of ultrasonic wave.

Material and Methods

To pass the ultrasonic wave through the seeds, which were taken to study for germination process and it compare with the control system (distilled water was used as a control and germination patterns were studied without presence of ultrasonic wave as well as fertiliser solution) and fertiliser solution system. The instrument ultra sonicator (Maxsell company, volume: 3.8 lit, dimension: L×W×D: 302×152×100 mm, frequency: 40 kHz, power: 100W, weight: 5Kg, size: 70×38×60) was used. The ten healthy seeds of *Vigna radiata* and *Vigna aconitifolia* of equal size were selected for germination study and thoroughly wash it by using doubly distilled water and it immersed in distilled water, fertiliser solution and ten healthy seeds were kept in ultra sonicator and note down the reading of germination patterns after 3 days, 6 days and 10 days. Three sets of the experiments were arranged for study the parameters. The average values of these parameters are presented in Table 1.

Results and Discussions

To understand the germination process of plants, use the PGR technique is most important to study the germination parameters such as percentage of germination, survival, seedling height, shoot length, root length and leaf area of young leaves. In the present paper, compared the study of germination effects of control system, fertiliser solution system with the ultrasonic wave system on *Vigna radiata* and *Vigna aconitifolia* plants in terms of PGR and their general order of plant growth regulators were found as

1. For *Vigna radiata* – Ultrasonic waves > Fertiliser > Control
2. For *Vigna aconitifolia* - Ultrasonic waves > Fertiliser > Control

Thus, the above obtained order of plant growth regulators which determined from the Table 1 and ultrasonic wave can functions as good plant growth regulators towards the selected (*Vigna radiata* and *Vigna aconitifolia*) crop plants. The Table 1 clearly shows that average value of parameters like, percent germination, survival, and seedling heights, shoot length is greater than root length and it is found higher in presence of ultrasonic wave treatment than control and fertiliser systems, Hence, it is indicated that ultrasonic wave treatment was found more effective technique to germinate the seeds of beneficial crop plants like *Vigna radiata* and *Vigna aconitifolia*.

Conclusion

The results thus obtained and it is represented in the table no.1 that shows the effect on parameters of plant growth regulator due to the seeds presence in different systems such as ultrasonic wave, fertiliser and control. Out of these systems the ultrasonic wave treatment shows greater positive effect than fertiliser and control on the parameters like percentage of seed germination, root length, shoot length and seedling height etc. But high response with ultrasonic wave was given by *Vigna radiata* crop plant rather than *Vigna aconitifolia*. Hence, the conclusion of this obtained results is, the ultrasonic wave treatment can functions as good plant growth regulators.



Table No.1 Comparison the effect of ultrasonic wave, fertiliser and control on germination patterns for *Vigna radiata* and *Vigna aconitifolia*.

*Plant Growth parameters		Seeds of <i>Vigna radiata</i> *			Seeds of <i>Vigna aconitifolia</i> *		
		Control	Ultrasonic wave	Fertiliser	Control	Ultrasonic wave	Fertiliser
No. of Seeds used for Germination		10	10	10	10	10	10
%Germination After 3 day		64 %	73%	67 %	73%	80 %	76%
% Survival	after 6 day	80%	90%	85%	86%	92%	90%
	after 10 day	97%	100%	99%	100%	100%	100%
Seedling Height in cm 6 day		0.7 cm	1.0 cm	0.9 cm	0.8 cm	1.2 cm	1.0 cm
Shoot Length in cm	after 6 day	2.2 cm	3.0 cm	2.4 cm	2.3 cm	3.5 cm	2.7 cm
	after 10 day	2.5 cm	3.5 cm	2.7 cm	2.6 cm	3.8 cm	3.0 cm
Root Length in cm	after 4 day	1.4 cm	2.5 cm	1.5 cm	1.6 cm	2.6 cm	1.8 cm
	after 10 day	2.2 cm	3.4 cm	2.4 cm	2.3 cm	3.6 cm	2.7 cm
Length of young leaf in cm	after 4 day	0.3 cm	0.5 cm	0.3 cm	0.4 cm	0.7 cm	0.4 cm
	after 10 day	0.6 cm	0.8 cm	0.6 cm	0.7 cm	0.9 cm	0.8 cm

‘*’=average values of the parameters which obtained from triplicate experiments done by authors.

‘Fertiliser’= 0.1 % solution of urea as fertiliser.

‘Control’= Double distilled water.

Acknowledgment:

We acknowledge and appreciate the help from B.Sc.III chemistry students, Devchand College, Arjunagar for this research work and also thankful to Department of Chemistry, Devchand College Arjunagar, Tal. Kagal, Dist. Kolhapur Maharashtra, India for providing the laboratory facilities.

References:

[1]U. Jain, B. Mishra, S. Gupta, Geobios, 2011, 38 (2), 214-215.
 [2] P.D.Shirgave and A.A.Ramteke, Advances in life sciences, 2012, 1(2), 145-146.
 [3]S.Ali, S.K.Ram, P.K.Yadav, A.Shffe, A.K.Verma, A.Tripathi, P.Mehta, P.Singh, Advances in Life Sciences, 2012, 1(2), 174-175.
 [4]B. Neppolian, C. Wang, M.A. kumar, Ultrasonics Sonochemistry, 2014, (21):1948-1953.
 [5]A.A.Ramteke, M.L.Narwade, A.B.Gurav, S.P.Chavan, A.G.Wandre, Der Chemica Sinica, 2013, 4(3):22-26.
 [6] A.A. Ramteke, P.D. Shirgave, J. Nat. Prod. Plant Resour, 2012, 2 (2):328-333

[7] N. Hussain, T. Abbasi, S.A. Abbasi, Journal of Hazardous Materials, 2015, (298):46-57.
 [8] P.R. Lomate, V.K. Hivrale, Journal of Plant Physiology, 2011, (168):1735– 1742.
 [9] G. Sozi, A.O. Chiesa, Scientia Horticulture, 1995, 62(4): 255-261.
 [10] R. Jun, L. Tao, Forest Ecology and Management, 2004, (195):291-300.
 [11] J.W. Bradbeer, Seed dormancy and Germination. Chapman and Hall, New York, USA, pp. 38-54, 1998 .
 [12] C.R. Lindig, S. Lara-Cabrera, Seed Science and Technology, 2004, 32(1):231-234.
 [13]M.A.Ting-Ting, P.Christie, Luo Yong-Ming, T.Ying, Pedosphere, 2014, 24(1):107-115.



Comprehensive Structural Investigations of Nanocrystalline MoO₃ thin films

S.V.Kite^{a,c}, P.A.Chate^b, K.M.Garadkar^c, U.B.Sankpal^d, Z.D. Sande^a, D.J.Sathe^{a*}

^a Dept. of Chemistry, KIT's College of Engineering, (Autonomous) Kolhapur, (M.S.) India.

^b Dept. of Chemistry, JSM College, Alibag-Raigad, (M.S.) India.

^c Dept. of Chemistry, Shivaji University, Kolhapur, (M.S.) India.

^d Dept. of Chemistry, Gogate-Jogalekar Arts, Science College, Ratnagiri, (M.S.) India.

KEYWORDS

Modify CBD polycrystalline, W-H plot, NRF plot

Corresponding Author
Email
djsathe07@yahoo.co.uk

ABSTRACT

The structural properties of MoO₃ thin films prepared by modify chemical technique with citric acid as a chelating agent is reported here. X-ray diffraction (XRD) patterns have confirmed phase formation and use for the calculation of cell lattice, volume, average crystallite size, microstain and dislocation density of thin films. The XRD pattern of thin films revealed that the MoO₃ are polycrystalline in nature and orthorhombic phase. The average crystallite size was obtained by using Scherrer's formula as well as Williamson- Hall (W-H) plot method which is obtained 23.28 nm and 27.54 nm respectively. The lattice parameter was found to be $a = 13.10 \text{ \AA}$, $b = 6.92 \text{ \AA}$, $c = 5.79 \text{ \AA}$ and volume of MoO₃ is 524.23 \AA^3 . Microstain of thin films was found to be 1.50×10^{-3} and dislocation density is $1.97 \times 10^{15} \text{ line/m}^2$. The crystallographic properties MoO₃ thin films are discussed from the point of applications based on achieving high performance devices.

Introduction

Now days considerably prominent research going on transition metal oxides (TMOs) Such as molybdenum oxide, vanadium oxide and tungsten oxide because of their wide range of stoichiometry [1]. Thin films of metal oxides and specifically those of Molybdenum have pulled in the consideration of mainstream researchers mainly due to their physical and compound properties. The surface of these materials has fascinating structural and electronic properties that support their utilization on various mechanical applications. For synthesis of MoO₃ thin film various techniques have been reported like Spray Pyrolysis [2], Spin Coating [3], Chemical Deposition [4], Liquid phase deposition [5], Reactive Pulsed-Laser Assisted Deposition [6],

Photochemical Metal-Organic Deposition [7], Sol-Gel [8] and Electrodeposition [9]. In between them, MoO₃ exhibits interesting structural, electrical and optical properties [10-12], which leads to the applications in gas sensing [13-15], solar cell [16], Microbatteries [17], catalyst, etc. Semiconductor metal oxide thin films have been broadly utilized for gas sensors as their conductivity changes because of connections with gas particles. Such sensors likewise offer minimal effort, simple manufacture and predictable execution regarding other kind of gas sensors.

As per as pervious literature on crystallographic data of material is not as much of. Henceforth, in this paper, we are main focusing on the synthesis of MoO₃ thin films and the detail study of X-ray

diffraction (XRD) parameters like phase confirmation, cell lattice, volume, average crystallite size, microstrain and dislocation density using various calculation and analytical techniques. The crystallographic properties MoO₃ thin films are discussed from the point of applications based on achieving high performance devices.

2. Experimental details

Each of the chemicals used for deposition of MoO₃ thin films is analytical grade. The substrate which was washed with series of chromic acid, detergent, acetone, distilled water to remove impurities and proper nucleation.

For the deposition of MoO₃ thin films, take a mixture of 15 ml 0.1 M ammonium molybdate as a source of molybdenum, 15 ml 10% hydrazine hydrate as reducing agent, 12 ml 0.1 M citric acid as a complementary complexing agent, and 15 ml 0.25 N KOH solutions. The total volume of mixture made 150 ml by adding distilled water and stir solution continuously for few minutes then put the glass substrate into the bath solution for 4 hours. The temperature of bath was 298 K, Speed of rotation of substrate between 40± 5 rpm, speed of stirrer near about 40± 5 rpm, set on to the Modified –Chemical Bath Deposition Unit Fig.1. After 4 hours glass substrates was removed and annealed at 773 K for 3 hours to form white coloured MoO₃ thin films which are used for further characterizations.



Fig.1. Automatic Chemical Bath Unit (A-CBD unit)

3. Results and discussion

Thickness measurement of molybdenum oxide thin films by gravimetric technique. Thin Film thickness was estimated by weighing method using the formula,

$$t = w/A\rho$$

Where, 't' is the thickness of the film, 'w' is the weight gain, A is the area of the coated film and ρ is the density. Density of molybdenum oxide is 4.69 gm/cm³. Thickness measurement of molybdenum oxide thin films by the mass difference method listed in table 1.

The X-ray diffraction measurements were obtained using a Philips diffractometer. A Cu Kα1 (λ = 1.54060 Å) radiation tube with line focus was operated at X-ray 40kV/40mA. The X-ray powder diffraction patterns were obtained in the range of 5-70 °, in steps of 0.01. X-ray powder diffraction analysis of the molybdenum oxide thin films was carried out to determine the type of crystal system, lattice parameters, cell volume, crystallite size, microstrain, dislocation density.

Fig. 2 shows X-ray diffraction patterns of as deposited thin film. It is clearly seen that the deposited thin films were amorphous since XRD profiles showed no diffraction peaks. Fig.3 shows X-ray diffraction patterns of (MoO₃) thin films after annealed at 773 K for 3 hours.

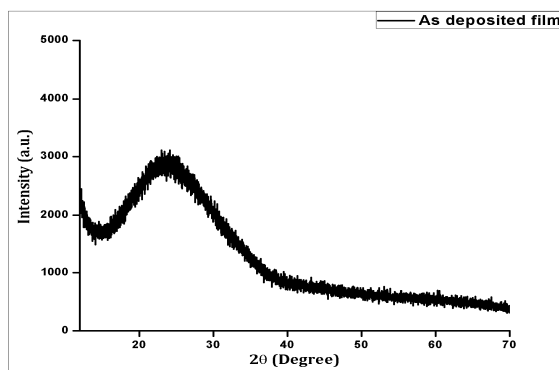


Fig. 2. X-ray diffraction pattern of as-deposited MoO₃ thin films



Annealing Temp. (K)	Mass of the substrate in 'gm'		Mass of the material in 'gm' W=(m ₂ -m ₁)	Dimensions of the films in 'cm'		Thickness of the films (t) in 'μm'
	Before deposition(m ₁)	After deposition(m ₂)		Length (l)	Breath (b)	
773 K	5.7441	5.7467	0.00265	5	2.3	0.24585

Table 1. Thickness measurement of **MoO₃ thin films**

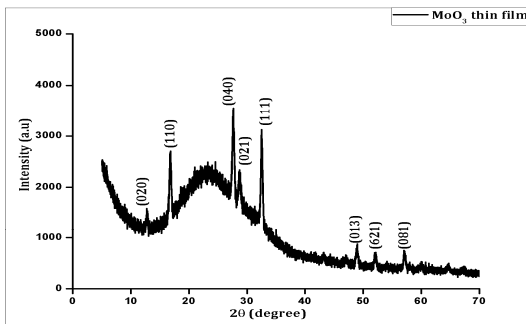


Fig. 3. X-ray diffraction pattern of **MoO₃ thin films**

The XRD patterns indicates that the crystallization of film transformed from amorphous to polycrystalline in nature with orthorhombic phase by comparing data with X pert high score software and JCPDS card no 05-508. The peaks were also observed (020), (110), (040), (021), (111), (013), (621), (081) at 2θ = 12.7647, 16.7576, 27.6079, 28.6965, 32.5462, 48.9315, 52.1602 and 57.1844 respectively are shown in Table 2. The distance between adjacent planes in the Miller indices (hkl) calculated from the Bragg Equation;

$$n\lambda = 2d \sin\theta$$

The observed 'd' values and JCPDS card no 05-508 are exactly matched which indicates synthesized material in orthorhombic phase. The unit cell lattice parameters of orthorhombic system by calculated following relation

$$\frac{1}{d^2} = \frac{h^2}{a^2} + \frac{k^2}{b^2} + \frac{l^2}{c^2}$$

The lattice constant found to be a = 13.10 Å, b = 6.92 Å, c = 5.79 Å which is the well agreement with the previous literature values and volume of MoO₃ is 524.23 Å³.

The crystallographic data of the each Miller indices (hkl) have calculated and obtained from X- pert high score software are highlighted in Table 2.

The full width at the half- maximum (FWHM) of the diffraction peaks obtained from the refinement was used to calculate the crystallite size (D) using Scherrer's equation;

$$D = 0.9\lambda/\beta \cos\theta$$

The microstrain (ε) developed in the films were calculated by using equation;

$$\epsilon = \beta \cos\theta/\lambda$$

Also dislocation density (δ) is calculated by using the relation;

$$\delta = n/D^2$$

Where n is the factor which is equal to unity for minimum dislocation density . The exact values of the lattice parameter have been calculated by plotting the graph of the lattice parameter (a) versus Nelson-Riley Function (NRF) for each plane it is seen that in Fig. 4.

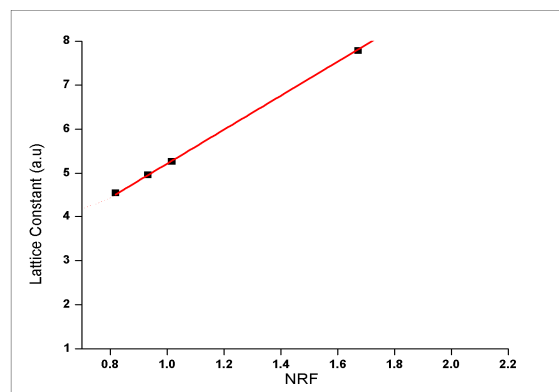
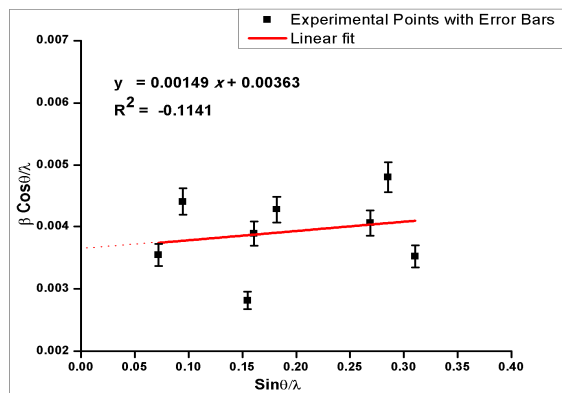


Fig. 4. Typical Nelson-Riley plot for lattice parameter of **MoO₃ thin films**

2θ	FWHM (β)	d-spacing [Å]	hkl	Crystalline size (nm)	Dislocation Density (δ) (* 10 ¹⁵) Line/m ²	Microstrain (ε) (* 10 ⁻³)	Lattice parameter (Å)	Cell volume (Å ³)
12.76	0.0055	6.935	020	25.103	1.58	1.365	a= 13.10 b= 6.92 c= 5.79 (Orthorhombic phase)	524.23
16.75	0.0069	5.290	110	20.175	2.45	1.699		
27.60	0.0045	3.231	040	31.625	0.99	1.083		
28.69	0.0062	3.110	021	22.894	1.90	1.497		
32.54	0.0069	2.751	111	20.792	2.31	1.648		
48.93	0.0069	1.861	013	21.928	2.07	1.563		
52.16	0.0082	1.753	621	18.519	2.91	1.850		
57.18	0.0062	1.610	081	25.26	1.56	1.357		

Table 2.

The microstrain (ε) and crystallite size (D) also obtained from Williamson- Hall plot method Figure 5 by plotting $\sin\theta/\lambda$ versus $\beta \cos\theta/\lambda$. The slope of the graph gives the microstrain and reciprocal of intercept gives crystallite size which is found to be 1.49×10^{-3} and 27.54 nm respectively. The all experimental points do not lie on a linear fitted straight line due to strain present in polycrystalline material. The compare results of crystallite size (Scherer's Formula and Williamson-Hall Plot Method) and microstrain (by calculation and Williamson- Hall Plot) are displayed in Table.3



Conclusion

Summarizing, we have synthesized MoO₃ thin films by simple, low cost, Automatic-Chemical bath deposition method. The structural properties result shows that MoO₃ thin films are in polycrystalline nature with average crystallite size 23.28 nm. The crystal system is orthorhombic phase. These crystallographic calculations and graphical methods of MoO₃ material may be useful for researcher. On the basis of crystallographic data MoO₃ thin films can be constructive for various applications.

Acknowledgements

Authors are thankful to SERB-DST, New Delhi for the financial support under project No.SB/FT/CS-018/2013.



Sample	Crystalline size (D) (nm)		Microstrain (ε)		Dislocation Density (δ) Line/m ²
	Scherer's Formula	Williamson-Hall Plot Method	$\beta \cos\theta/4$	Williamson-Hall Plot Method	
MoO ₃ Thin Films	23.28	27.54	1.50×10^{-3}	1.49×10^{-3}	1.97×10^{15}

References

- 1) A.Arfaoui, B.Ouni, S.Touihri, A.Mhamdi, A.Labidi, T.Manoubi, Effect of annealing in a various oxygen atmosphere on structural, optical, electrical and gas sensing properties of MoxOy thin films, *Optical Materials*, 45, 109–120(2015).
- 2) H.M. Martinez, J.Torres, M.E.Rodriguez-Garcia, L.D.Lo pez Carreno, Gas sensing properties of nanostructured MoO₃ thin films prepared by spray pyrolysis, *Physica B*, 407, 3199–3202 (2012).
- 3) Loundja Chibane, Mohamed Said Belkaid, Marcel Pasquinelli, Hassina Derbal-Habak, Jean-Jacque Simon , Dallila Hocine, Development of Molybdenum Trioxide (MoO₃) by Spin Coating Method for Photovoltaic Application, *Journal of Materials Science and Engineering B*, 3 (7), 418-422 (2013).
- 4) Metodija Najdoski, Toni Todorovski, Julijana Velevska ,Molybdenum oxide thin solid films prepared with a new chemical bath deposition method, *Physica Macedonica*, 56, 57-62(2007).
- 5) Shigehito Deki,Alexis Bienvenu Beleke, Yuki Kotani,Minoru Mizuhata, Liquid phase deposition synthesis of hexagonal molybdenum trioxide thin films,*Journal of Solid State Chemistry*,182, 2362–2367 (2009).
- 6) C.V. Raman, C.M. Julien,Chemical and electrochemical properties of molybdenum oxide thin films prepared by reactive pulsed-laser assisted deposition,*Chemical Physics Letters*, 428(1–3), 114–118 (2006).
- 7) G.E. Buono-Core, G. Cabello, A.H. Klahn, A. Lucero, M.V. Nuñez, B. Torrejón, C. Castillo, Growth and characterization of molybdenum oxide thin films prepared by photochemical metal–organic deposition (PMOD), *Polyhedron*, 29(6), 1551–1554(2010).
- 8) Sun Jiebing, Xiong Rui ,Wang Shimin , Tang Wufeng, Tong Hua, Shi Jing, Preparation and Characterization of Molybdenum Oxide Thin Films by Sol-Gel Process,*Journal of Sol-Gel Science and Technology*, 27 (3), 315–319 (2003).
- 9) Nobuyoshi Baba, Shigeyoshi Morisaki, Naoki Nishiyama,Preparation of Electrochromic MoO₃ Thin Films on ITO Glasses by Electrodeposition,*Japanese Journal of Applied Physics*, 23(2)(1984).
- 10) S. Krishnakumar,C. S. Menon, Electrical and optical properties of molybdenum trioxide thin films, *Bulletin of Materials Science*, 16(3), 187–191(1993).

- 11) Antonella M. Taurino, Angiola Forleo, Luca Francioso, Pietro Siciliano Michael Stalder , Reinhard Nesper, Synthesis, electrical characterization, and gas sensing properties of molybdenum oxide nanorods, *Applied Physics Letters*, 88(15),(2006).
- 12) R.S. Patil, M.D. Uplane, P.S. Patil, Structural and optical properties of electrodeposited molybdenum oxide thin films, *Applied Surface Science*, 252(23), 8050–8056(2006).
- 13) Jaswinder Kaur, V. D. Vankar, M. C. Bhatnagar, Gas Sensing Properties of MoO₃ doped SnO₂ thin Films, *World Academy of Science, Engineering and Technology*, 43, 322-324(2008).
- 14) M.B. Rahmani, S.H. Keshmiri, J. Yu, A.Z. Sadek, L. Al-Mashat, A. Moafi, K. Latham, Y.X. Li, W. Wlodarski, K. Kalantar-zadeh, Gas sensing properties of thermally evaporated lamellar MoO₃, *Sensors and Actuators B*, 145, 13–19 (2010) .
- 15) M. C. Rao, Vacuum Evaporated MoO₃ Thin Films for Gas Sensing Application, *Physics*, 3(4),417-418(2013).
- 16) Y. Boutaleb, R. Rehamnia, Y. Berredjem and J.C. Bernède, Nanostructured solar cells based on MoO₃ film deposition, *Revue des Energies Renouvelables*, 18, 193–198(2015).
- 17) Rao M.C., Ravindranadh K, Kasturi A. and Shekhawat M.S., Structural Stoichiometry and Phase Transitions of MoO₃ Thin Films for Solid State Microbatteries, *Research Journal of Recent Sciences*, 2(4), 67-73(2013).



Effect Of Tin (Sn) Substitution On The Structural Properties Of Co Ferrite Nano Particle Synthesized Via Sol-gel Route.

S.D. Zimur, P.D. Kamble ,M.R. Kadam , P.V. Gaikwad.

Balasaheb Desai College Patan.

KEYWORDS

Ferrites ,
Nano particles ,
X-ray diffraction,
Lattice Constant

Corresponding Author
Email

ABSTRACT

Tin Substituted Co Ferrite nanoparticles ($\text{Co}_{1-x}\text{Sn}_x\text{Fe}_2\text{O}_4$, with $X= 0, 0.25, 0.50, 0.75$ and 1) were prepared by Sol-Gel auto combustion route and the effect of Tin concentration on Lattice Constant, Particle size and Powder density were investigated. X-ray Diffraction analysis confirms the formation of ferrites in Cubic nano phase. The Results show that the Particle size decreased from (17.65) to (8.72) nm with increasing the concentration of tin to the ($X=1$). The Lattice Constant increased from (8.3698) to (8.7395) \AA^0 with increasing concentration of Tin to ($X=1$), while the theoretical powder density decreased from (5.72) to (5.30) g/cm^3 by increasing tin ion concentration to value at ($X=1$).

Introduction

Nanocrystalline ferrites are currently the subject of interest because of its wide applications in industrial as well as research areas. They are attractive because of their importance in ferrofluids , magnetic drug delivery ,hyperthermia for cancer treatment etc[1]. These materials are called as ferrites which have general formula MFe_3O_4 , where M is divalent ion like Zn^{++} , Mn^{+} . This is the ferrite ceramics and heterogeneous materials consists of oxides with of different iron oxide as the basic composed and the fall in this category of soft and hard ferrites.

CoFe_2O_4 has inverse spinel structure with Co^{2+} ions in octahedral sites and Fe^{3+} equally distributed between tetrahedral and octahedral sites whereas SnFe_2O_4 has a normal spinel with Sn^{4+} in tetrahedral and Fe^{3+} in octahedral sites [2]. Therefore , Tin substitution in Cobalt ferrite may have some distorted spinel structure depending upon the concentration of the precursor solutions.

Novel properties and numerous applications of nanophase materials, especially ceramic powders, have encouraged many researchers to invent and explore the methods, both chemical and physical by which such materials can be prepared. Cobalt ferrite is synthesized by variety of methods including solid state reaction method, high energy ball milling [3], co-precipitation [4], sol-gel [5], RF sputtering and microemulsion method [6].

To study the crystalline structures of solids, X-ray diffraction is the most widely used and the least ambiguous method for the precise determination of positions of atoms in all kinds of matter ranging from fluids and powders .It is non-destructive techniques that provided detailed information about the materials. Through x-ray diffraction information is provided for characterization of crystalline materials represented crystal structures, phase, preferred crystal orientation ,and other structural parameters such as Lattice parameters, crystallite sizes ,

crystallinity, strain and crystal defects. To find the crystal structures we need to determine lattice constant, particle size and x-ray density.

2 Experimental:

2.1 Materials and methods-

Ferrite powder were prepared by Sol-gel auto combustion method. In this method, Cobalt nitrate, ferric nitrate, Tin chloride, Citric acid, Ammonia solution were used as a starting raw materials.

2.2. Instrument Used.

We have used in this work a set of devices for the purpose of testing physics that were conducted in this research work and these devices are :

2.2.1. Mass measurement instrument.

We have been using a sensitive balance of a high degree of sensitivity of four decimal degrees.

2.2.2. Magnetic Stirrer.

Is a laboratory device that employs a rotating magnetic field to cause a stir bar immersed in a liquid to spin very quick, for obtained homogenous mixture between atoms and liquid particles.

2.2.3 X-ray Diffractometer.

The X-ray diffraction pattern was recorded using a Bruker D8 Focus powder diffractometer with Cu K α radiation at a wavelength of 0.15406 nm.

2.3. Preparation Methods.

After the weights of metal salts, appropriate amounts of distilled water was added to them, according to the percentage standard stoichiometric weight: two moles of ferric nitrate, one mole of metal salts (Cobalt and Tin) and one mole of Citric acid (the mole ratio of metal salt to citric acid is 1:1) to provide increased fuel to the mixture of ferrite series (Co_{1-x}Sn_xFe₂O₄), where X =0,0.25,0.50 0.75 and 1). All these are collected in a glass beaker to become a total solution and mixed well at room temperature by magnetic stirrer with high velocities and after a short period of time until solution becomes smooth and slimy red coloured. Ammonia solution was slowly added in the form of drops in the mixture of

solution to control its pH until reach the value of (8.5 to 9), with continuous stirring.

It was subsequently raise the temperature of the solution to 60⁰C for a period of one hour and then increases the temperature 80⁰C. After that the size of solution in the beaker glass be less with high viscosity and after 30 minutes, the solution viscosity is very high, hence the beginning of gel formation on the surface of other solution.

After the completion of the solution turned to gel, the temperature drops to the room temperature and this gel becomes dry and dark brown. Then put inside the oven at a temperature 120⁰C for 3 hours to become a dry gel. On further heating the dried gel burnt in a self propagating combustion manner till whole quantity of gel get completely converted to a floppy loose powder. Later burnt precursor powder was sintered at 870⁰c for 4 hours. The Sol gel auto combustion has various advantages such as simple, inexpensive, quick synthesis and does not required any vacuum process or sophisticated instrumentation.

3. Result and Discussion-

The polycrystalline Co_{1-x}Sn_xFe₂O₄ have been investigated by X- ray diffraction techniques are shown in fig.(1). All the compositions of Co-Sn ferrites could be indexed in terms of a single phase cubic structures. It can seen from figures that all ferrites powders consisted of well crystalline phase. The intensity of main diffraction peak of a spinel ferrite at the (311) plane was considered as a measure of its degree crystallinity. An increase in concentration of tin in the Co-Sn ferrite resulted in the measurable shift in 2 θ towards the smaller angles as a mechanical stress within the crystals as shown in table no. (1)

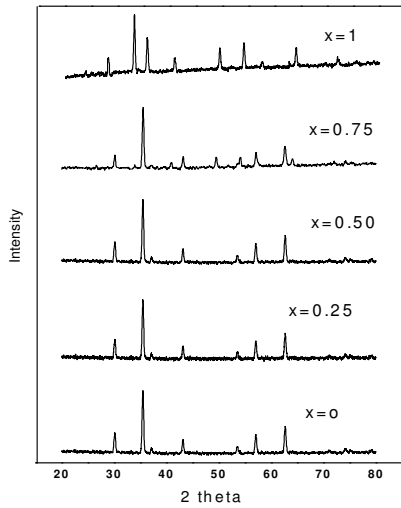


Fig.1 XRD Pattern of Ferrite Powder X= 0, 0.25, 0.50, 0.75 and 1.

3.1. Crystallite Size.

The Sherrer formula [7] relates the thickness of crystallite to the width of its diffraction peaks, and is widely used to determine particle size. The Sherrer Formula is given by ;

$$D = k \lambda / \beta \cos \theta \dots\dots\dots (1)$$

Where D is crystallite size, β is the broadening of diffraction line measured at half its maximum intensity (FWHM), k is the shape factor (k=0.9) , λ is the wavelength of X-ray. The crystallite size of the ferrite powders was determined using formula (1) and table (1) show that the crystallite size decreases from 17.65 to 8.72 nm with increasing Sn⁴⁺ ion concentration as shown in fig. (2). The decrease in particle size with Sn ion content may be explained by the electronic configuration of Co²⁺ (3d⁷) and its more tendency to interact with ligands and oxygen anions, as compared to Sn⁴⁺ (4d¹⁰), which has a complete electronic configuration [8].

The lack of d-electrons is important because there are very little covalent interaction and tendency toward extension between Sn⁴⁺ and its ligands, furthermore ,it

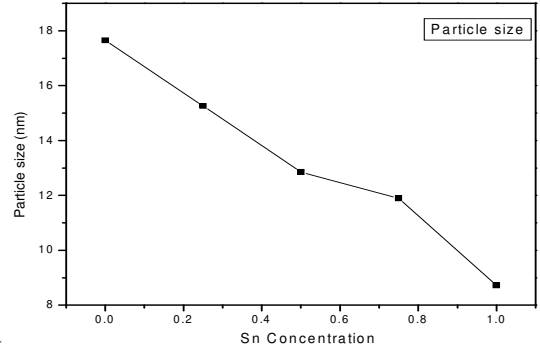


Fig. No.2. Change in Particle size with the degree of Sn substitution in Co_{1-x}Sn_xFe₂O₄.

3.2 Lattice Constant.

A parameter defining the unit cell of a crystal lattice is the length of one of the edges of the cell or the angle between edges. It is also known as lattice parameters or lattice constant. Lattice constant refers to constant distance between the lattice points. It is calculated using of relate to the inter – planer spacing for the d_{hkl} planes in the cubic structure as,

$$a = \lambda (h^2+k^2+l^2)^{1/2} / 2 \sin \theta \dots\dots\dots (2)$$

Braggs condition demands that a proper combination of θ and λ is found for efficient reflection.

Lattice parameter of the ferrite was calculated using equation (2) and table (1) show that the lattice parameter increases from 8.3698 Å⁰ to 8.7395 Å⁰ with Sn⁴⁺ ion increase. It is seen in Fig (3) that the lattice parameter increases with Sn⁴⁺ ion concentrations, the ionic radius of Sn⁴⁺ can be presented for this effect. Tin ions have a strong tendency to be arranged at tetrahedral sites. The addition of Sn⁴⁺ ions into Co-Ferrite structure causes migration of Fe³⁺ ions from the A site to the B site. Sn⁴⁺ ions (0.82) owns a larger cations ,as compared to Fe³⁺ ions (0.64 Å⁰) and Co²⁺ ions 0.78Å⁰), thus the lattice expands [9].

Table No.1 Lattice constant, Particle size, X-ray density and cell volume.

X	2θ	D (nm)	d (nm)	a (Å)	V (Å ³)	Dx (g/cm ³)
0	35.51	17.65	2.4545	8.3698	584.28	5.72
0.25	35.26	15.26	2.4557	8.3761	588.435	5.56
0.50	35.10	12.85	2.4567	8.3777	590.783	5.41
0.75	34.84	11.89	2.4587	8.4127	594.703	5.36
1	33.15	8.72	2.4606	8.7395	621.09	5.30

3.3. X-ray density.

The values of X ray density (dx) is calculated from the XRD data using the relation given by Smita and Wing [10].

$$Dx = 8M / N_a a^3 \text{ (g/cm}^3\text{)} \dots\dots\dots(3).$$

Where dx is the x-ray density (g/cm³), Z is the number of molecules per formula unit (Z=8 for spinnel system), M is the molecular weight of the samples, N_a is the Avogadro's number, and "a" is the lattice constant.

The X ray density (dx) of the ferrite nanopowder was determined using the relation (3), is given in the table (1), which decreased its value from 5.72 to 5.30 g/cm³ and their density depend upon the lattice constant. Table (1) show that the lattice constant increases with increase in Sn ion concentration, so that the X-rays density decreased with increase in Sn ion concentration as shown in fig. (4).

Conclusion

X-ray Diffraction analysis confirms the formation of ferrites in Cubic nano phase. The Results show that the Particle size decreased from (17.65) to (8.72) nm with increasing the concentration of tin to the (X=1). The Lattice Constant increased from (8.3698) to (8.7395) Å with increasing concentration of Tin.

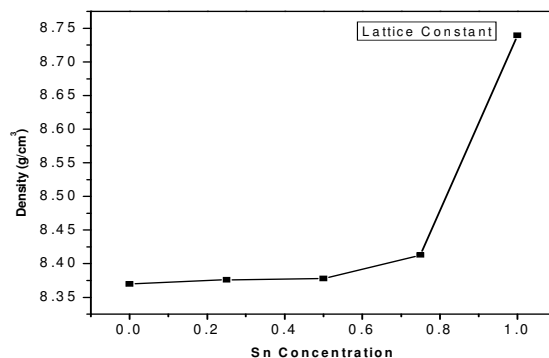


Fig.3 Change in Lattice Constant with Sn Substitution in Co-Sn Ferrites.

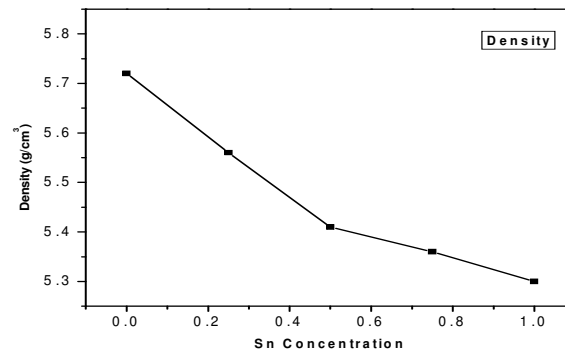


Fig.4. Change in X-ray Density with Sn substitution in Co-Sn ferrites.



Acknowledgement-

One of the Author Dr.P. D. Kamble thanks to DST SERB for their financial assistant through Major research project dated 21/10/2016(DST NO - SB/EMEQ-347/2014 dated 21/10/2016.)

References:

- [1] Koch, C.C. Nanostructured materials: processing, properties and potential application William Andrew Publishing, Norwich, New York, USA, 2002; pp ix-xii.
- [2] Ozin, G.A; Arsenault, A.C. Nanochemistry: A chemical approach to nanomaterials, The Royal Society of Chemistry, UK, 2005; pp v-ix.
- [3] Burda, C; Chen, X; Narayana, R.;E1-Sayed, M.A. Chem. Rev. 2005, 105, 1025.
- [4] Wang, C. Y.; Jiqnq, W.Q.; Zhou, Y.; Wang, Y.N.; Chen, Z.Y. Mater. Res. Bull. 2000, 35, 53.
- [5] G .Vaidyanathan, S. Sendhilmathan, R. Arulmurugan, Structural and magnetic properties of $\text{Co}_{1-x}\text{Zn}_x\text{Fe}_2\text{O}_4$ nanoparticles by Co-precipitation method, Journal of Magnetism and Magnetic Materials 313 (2007) 293-299.
- [6] Wang, Y.; Tang, X.; Yin, L.; Huang, W.; Gedanken, A. Adv.Mater.2000, 12,1137.
- [7] A. Navrotsky, O .J. Kleepa, Thermodynamics of formation of simple spinel, Journal of Inorganic and Nuclear Chemistry 30 (1968)479-498.
- [8] S.Kumar, V. Singh, S. Aggarwal, U. K. Mandal, R.K. Kotnala, Influence of processing methodology on magnetic behaviour of multicomponent ferrite nanocrystals, Journal of Physics and Chemistry C 114 (2010) 6272-6280.
- [9] H. Gleiter , Nanocrystalline materials, Progress in Material Science 33 (1989) 223-315.
- [10] B.D. Cullity, Elements of X-Ray Diffraction , second ed., Addison-Wesley Publishing Company ,Inc ,United States Of America, 1978, p.89.



Synthesis and Electrical, Magnetic studies of $\text{Cu}_{1-x}\text{Co}_x\text{Fe}_2\text{O}_4$ Ferrite

M R. Kadam^{1*} P.D.Kamble¹, S. A. Shivade²,

^{1*} Department of Chemistry, B.D. College, Patan, Satara, India.

²Department of Chemistry, KMC, College, Khopoli, Raigad 410203, India.

KEYWORDS

Molluscan Species,
Behavior,
Heavy metal

Corresponding Author
Email

ABSTRACT

The Cu-Co mixed ferrite viz. $\text{Cu}_{1-x}\text{Co}_x\text{Fe}_2\text{O}_4$ ($x= 0, 0.25, 0.50, 0.75$ and 1.0 M) were synthesized by the oxalate co-precipitation method. Formation of the cubic ferrite phase was confirmed by X-ray diffraction studies. Microstructural and compositional features were studied by scanning electron microscopy and energy dispersive X-ray analysis technique. Increasing activation energy with cobalt were studied by electrical resistivity. Thermoelectric power measurements showing the negative slope indicate that all the samples are n-type semiconductors and magnetization measurements were made by using a high field hysteresis loop tracer.

Introduction

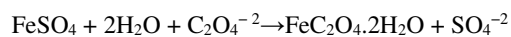
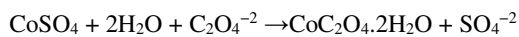
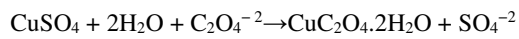
Spinel structures with AB_2O_4 ferrite shows enormous structural, electrical and magnetic properties and have been investigated by number of researchers [1]. The physical and chemical properties depend upon factors such as sintering temperature, sintering time, rate of heating and rate of cooling which changes the nature of ions and their site distribution amongst tetrahedral and octahedral sites. In this research area there is growing interest due to its technological applications such as magnetic resonance imaging, magnetic drug delivery, magnetic recording media, magnetic storage fluids, sensors, pigments [2]. The spinel ferrites are effective catalysts for the number of industrial processes. These applications mainly depend upon microstructure and surface properties of the fine powders which depend upon the method of preparation [3]. Literature report's on mixed metal oxides are prepared by various methods such as ceramic, sol-gel, hydrothermal, citrate precursor, co-precipitation and combustion, etc. [4].

In the present investigation an attempt has been made to establish a new chemical route which is both affordable and versatile for the synthesis of fine mixed metal oxide powders, where oxalate precipitation method was used to prepare ferrite compounds. The prepared compounds were physically characterized by XRD, SEM, EDAX, electrical resistivity, magnetic hysteresis.

2. Experimental

2.1. Sample preparation

The various compounds of the system $\text{Cu}_{1-x}\text{Co}_x\text{Fe}_2\text{O}_4$ were prepared by oxalate co-precipitation method. The high purity AR grade copper sulphate, cobalt sulphate and ferrous sulphate were carefully dissolved in doubly distilled water. The precipitation was carried out by adding oxalic acid maintaining pH at 4.7. The chemical reactions proceed as follows:



The precipitate was washed thoroughly with distilled water to remove the sulphate and filtered through the Whatmann filter paper no. 41. The absence of sulphate ions in the filtrate was confirmed with the barium chloride test. The precipitate was dried to obtain the powder, The above powders were heated separately at 900°C for 6 hours to get final product. The granulated powders were pressed into pellets of 1.04 cm diameter under a pressure of 10 tons per cm² and thickness was adjusted to about 0.3 cm.

2.2. Characterization:

The powder X-ray diffraction patterns were recorded on Philips PW-1710 X-ray diffractometer by using CuK α radiation. The lattice parameters were calculated using high angle reflection of XRD by using the following formula,

$$\frac{1}{d^2} = \frac{h^2 + k^2 + l^2}{a^2} \quad \text{----- 1}$$

Crystallite size (t) was calculated by using the Scherrer's formula,

$$t = \frac{0.9 \lambda}{\beta \cos \theta} \quad \text{----- 2}$$

The percentage porosity was calculated by using the formula

$$P = \frac{dx - d_B}{dx} \times 100 \% \quad \text{----- 3}$$

where, the notations are their usual meaning.

The SEM micrographs of the samples were obtained using the scanning electron microscope (Model LICER steroscan 440). The grain size of all the samples was calculated by Cottrell's method. Elemental analysis was carried out by using the energy dispersive X-ray spectroscopy equipped with SEM. The two probe method was used to measure the d. c. resistivity of the materials by using the relation,

$$\rho = \left(\frac{\pi d^2}{4t} \right) R \quad \text{----- 4}$$

The activation energies were calculated from the curve of log ρ Vs 1000/T in between the temperature range of 300K to 773K. The graph of ΔV Vs ΔT (temperature difference) was plotted and the value of Seebeck or thermoelectric coefficient (α) was calculated from the slopes. The temperature range used for the measurements was between 300K and 473K. The magnetization measurements were made by using a high field hysteresis loop tracer. The magnetic hysteresis studies were carried out at 300 K using a field of 4KOe.

3. Results and discussion:

3.1. XRD analysis:

Fig.1 shows XRD pattern of prepared ferrite Cu_{1-x}Co_xFe₂O₄ where x = 0.0, 0.25, 0.5, 0.75 and 1.0. All compound shows polycrystalline nature. The observed 'd' values were matches well with standard 'd' values of JCPDS file No. 77-0010 CuFe₂O₄ and CoFe₂O₄, JCPDS file No. 22-1086) both showing cubic crystal structure. The absence of extra peak in the pattern confirms the single phase formation of samples. For all spinel ferrites shows strong orientation along (311) plane.

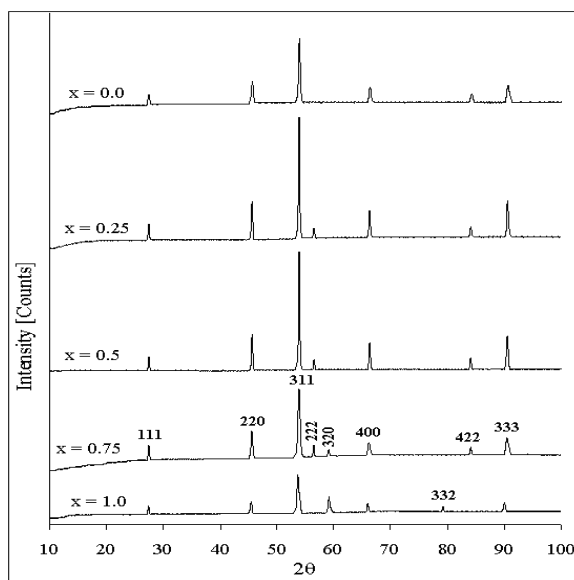


Fig. 1. XRD Patterns of Cu_{1-x}Co_xFe₂O₄ system.



The increase in lattice parameter on the addition of Co is due to the fact that as the concentration of Co^{2+} increases. Since the ionic radius of Co^{2+} (0.74\AA) is greater than Cu^{2+} (0.70\AA), it is expected that the lattice parameter should increase with Co^{2+} content in the ferrite samples as shown in Fig.1.1a) and also similar reported [5]. The crystallite size, X-ray density, physical density and percentage porosity has been listed in the table. The crystallite size lies in the range 31.06 to 47.31 nm and it shows nonlinear behavior with increasing cobalt content. X-ray density (d_x) decreases from $x= 0.0$ to $x = 1.0$ and lies between the range 5.437 and 5.2669 gm/cm^3 while the physical density (d_B) increases up to $x= 0.25$ and later on decreases with cobalt content, it varies in the range 4.686 to 4.841 gm/cm^3 . The porosity lies in the range of 9.97 to 13.95% for the present samples. According to mangal raja et.al. [6], typical porosity range for ferrite is 7-25 %. But others [29, 30] show different results. The porosity decreases up to $x = 0.5$ and later on increases.

Table1. Lattice constants, Crystallite size, X-ray density, physical density and Porosity for $\text{Cu}_{1-x}\text{Co}_x\text{Fe}_2\text{O}_4$ System

Sr. No.	Compound	Lattice Constants (\AA)	Crystal lite Size (nm)	X-ray density (d_x)	Physical Density (d_B)	Porosity (P) (%)
1	$x = 0.0$	8.3607	37.34	5.437	4.678	13.95
2	$x = 0.25$	8.3693	47.31	5.394	4.841	10.25
3	$x = 0.5$	8.3784	46.64	5.374	4.838	9.97
4	$x = 0.75$	8.3818	31.06	5.3412	4.799	10.15
5	$x = 1.0$	8.3973	31.54	5.2629	4.686	11.03

3.2. Scanning Electron Microscopy:

The Fig.2(a-e) represents the SEM micrographs of $\text{Cu}_{1-x}\text{Co}_x\text{Fe}_2\text{O}_4$ (where $x = 0.0, 0.25, 0.5, 0.75$ and 1.0) powder. The average grain size was measured by Cottrell's method [8]. SEM micrographs reveal that all samples show fine grains with varying porosity. The average grain size lies in the range 0.289 to 1.15 μm . The average grain size increases up to $x = 0.5$ with increasing cobalt content and later on decreases up to $x = 1.0$.

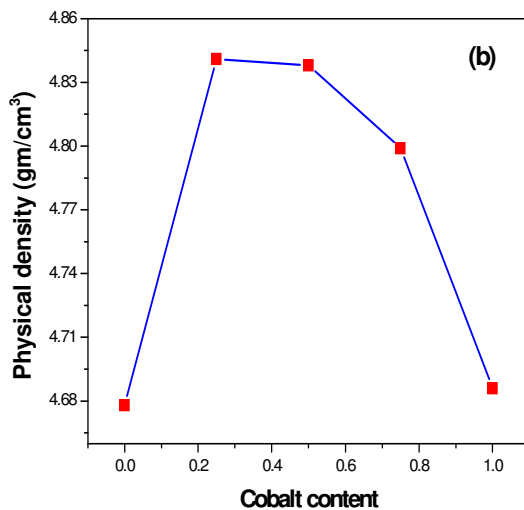
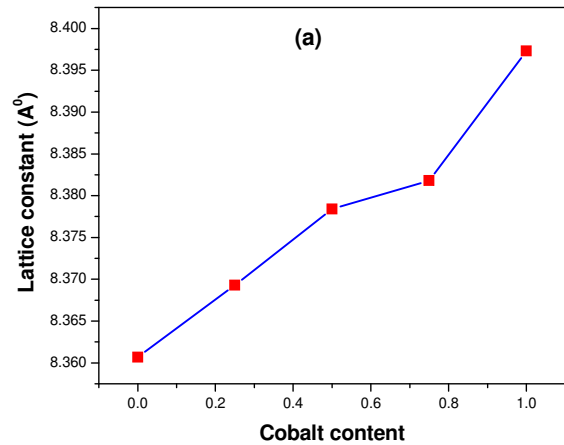
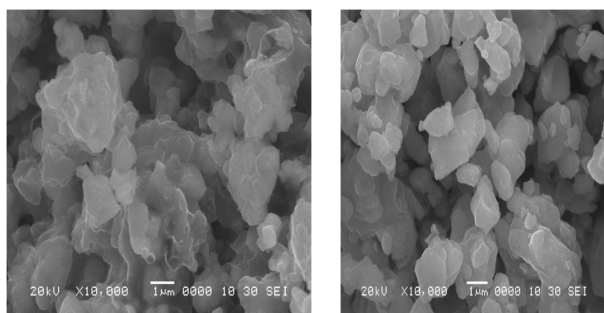


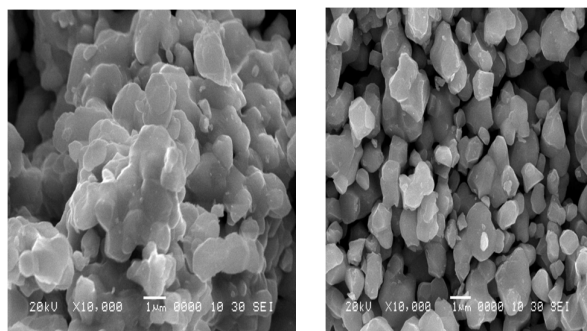
Fig.1.1a) Variations of lattice parameters with cobalt content
 b) Variations of physical density with cobalt content

The segregation of impurity phase is observed. This indicates that the complete solid solubility is obtained with substitution of Co^{2+} in the present samples. From the micrograph it is further observed that the porosity decreases with increasing grain size.



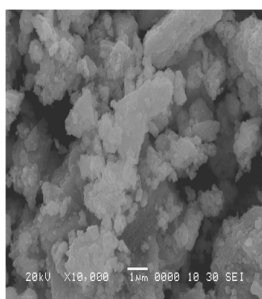
a) $x = 0.0$

b) $x = 0.25$



c) $x = 0.5$

d) $x = 0.75$

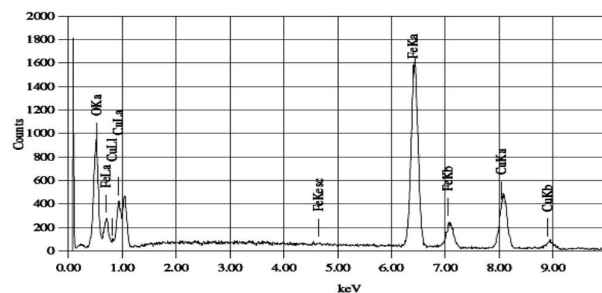


e) $x = 1.0$

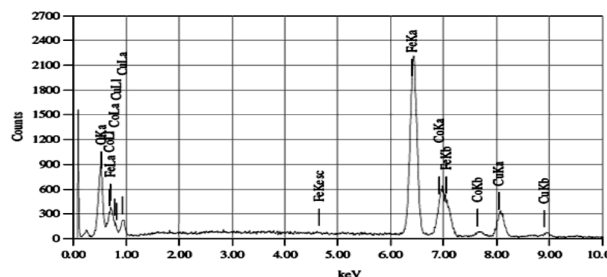
Fig.2 Scanning Electron Micrographs of $\text{Cu}_{1-x}\text{Co}_x\text{Fe}_2\text{O}_4$ system

3.3. Energy Dispersive X-ray Spectroscopy:

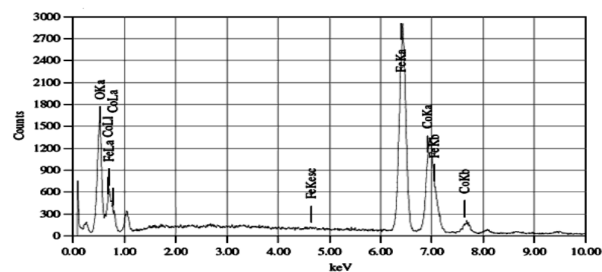
The EDAX (energy dispersed analysis by X-rays) spectra for the elemental analysis of $\text{Cu}_{1-x}\text{Co}_x\text{Fe}_2\text{O}_4$ system with $x = 0.0, 0.5, 1.0$ are shown in the Fig.3. The atomic ratios of Cu/Fe and Co/Fe were calculated theoretically from the spectra and are listed in the Table.



(a)



(b)



(c)

Fig. 3. Energy Dispersive Spectra of $\text{Cu}_{1-x}\text{Co}_x\text{Fe}_2\text{O}_4$ System

Composition (x)	Theoretical Ratio		Ratio From EDAX	
	Cu / Fe	Co / Fe	Cu / Fe	Co / Fe
0.0	0.5	-	0.452	-
0.5	0.25	0.25	0.238	0.225
1.0	-	0.5	-	0.504

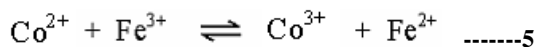
Table 2. Elemental analysis with EDAX of the $\text{Cu}_{1-x}\text{Co}_x\text{Fe}_2\text{O}_4$ System



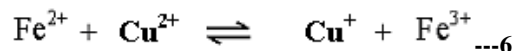
3.4. Electrical Resistivity:

The plots of $\log \rho$ vs. $10^3/T$ for the system $\text{Cu}_{1-x}\text{Co}_x\text{Fe}_2\text{O}_4$ with $x = 0.0, 0.25, 0.5, 0.75$ and 1.0 is shown in Fig.4. According to Jonkar [9] the semiconduction in the ferrite system

$\text{Co}_{1-x}\text{Fe}_x\text{O}_4$ takes place due to the presence of cobalt on octahedral site which favours the conduction mechanism [10].



According to Selvon (38), the semiconduction in the CuFe_2O_4 takes place through the hopping mechanism.



The d.c. resistivity of the $\text{Cu}_{1-x}\text{Co}_x\text{Fe}_2\text{O}_4$ compounds was measured in the temperature range 100 to 500°C which varied between 10^8 – $10^2 \Omega\text{-cm}$. The observed activation energies are listed in the Table 4. This table reveals that the activation energy values for different compositions varied between 0.583 – 0.800eV . The activation energy values increase with increasing cobalt content. All the compounds showed linear nature indicating Wilsons law is obeyed [11]

$$\rho = \rho_0 \exp(\Delta E/kT)$$

It has been observed that electrical resistivity in transition metal oxides is low if the material contains the cations of the same elements but their valency differing by unity are situated at similar sites in the lattice. The low activation energies and low resistivity values are observed for the CuFe_2O_4 as compared to the CoFe_2O_4 . This is probably may be due to the hopping centers in CuFe_2O_4 are more according to reaction (6) than the hopping centers in CoFe_2O_4 according to the equation (5) because Cu^{2+} oxidation state is less stable than Co^{2+} .

3.5. Thermoelectric power measurements:

The compositional variation of ΔV vs ΔT for the $\text{Cu}_{1-x}\text{Co}_x\text{Fe}_2\text{O}_4$ spinels with $x = 0.0, 0.25, 0.5, 0.75$ and 1.0 is shown in the Fig.5. From this figure it is observed that all the samples shows similar thermal variation.

Composition	Grain Size (μm)	Activation Energy ΔE (eV)
CuFe_2O_4	0.95	0.583
$\text{Cu}_{0.75}\text{Co}_{0.25}\text{Fe}_2\text{O}_4$	1.092	0.643
$\text{Cu}_{0.5}\text{Co}_{0.5}\text{Fe}_2\text{O}_4$	1.15	0.693
$\text{Cu}_{0.25}\text{Co}_{0.75}\text{Fe}_2\text{O}_4$	0.92	0.745
CoFe_2O_4	0.289	0.800

Table 4. Grain Size from SEM and Energy of activation from Resistivity of the $\text{Cu}_{1-x}\text{Co}_x\text{Fe}_2\text{O}_4$ system.

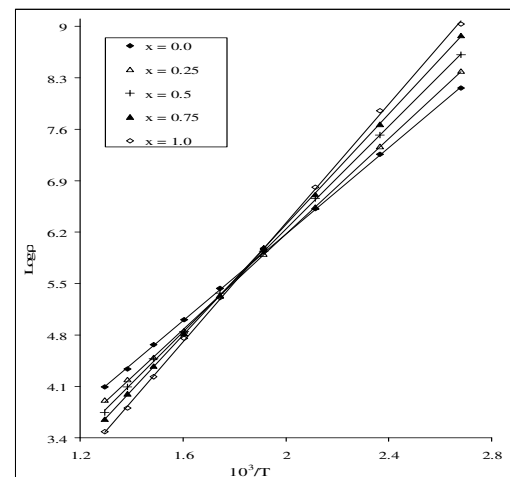


Fig. 4. Variation of $\log \rho$ with $10^3/T$ for $\text{Cu}_{1-x}\text{Co}_x\text{Fe}_2\text{O}_4$ System.

The curves for all the samples in this figure are with negative slope indicating that all the samples are n-type semiconductors. The Cu rich samples showed more n-type behavior as compared to Co rich samples

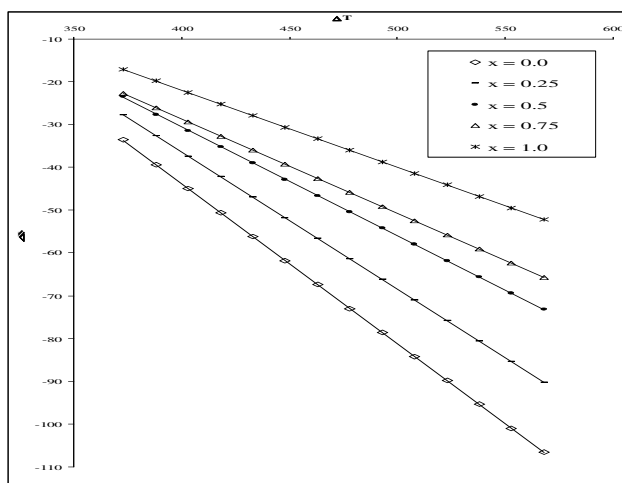


Fig. 5. Plots of ΔV Vs ΔT for the $\text{Cu}_{1-x}\text{Co}_x\text{Fe}_2\text{O}_4$ system

3.6. Magnetic hysteresis:

The measurements of saturation magnetization (M_s), remanent magnetization (M_r) and coercive field (H_c) are made by replacing the standard nickel sample with our samples. The hysteresis loop for the samples in the system $\text{Cu}_{1-x}\text{Co}_x\text{Fe}_2\text{O}_4$ ferrites (where $x = 0.0, 0.25, 0.5, 0.75, 1.0$) are shown in Fig.6. The variation of magnetic moment (μ_B) saturation magnetization (M_s), remanent magnetization (M_r) and coercive field (H_c) is given in Table 5. The initial increase of the saturation magnetization can be attributed to the improved grain size which increases with the Co substitution because the product powder becomes the mixture of magnetic spinel phase. The saturation magnetization tends to decrease gradually after the composition $x = 0.5$ in which coexisting cubic Co phase is ferromagnetic. It is observed that when the Co^{3+} ion is substituted for the Cu^{2+} ion in the lattice, the magnitude of the B site moment increases, which results in an increase in the μ_B value. The slight variation in μ_B values observed for the system may be due to the presence of a small canting of the B site moment with respect to the direction of the A site moment and may also be due to other magnetic interactions such as A-A or B-B interactions [12]. The added Co^{2+} in the CuFe_2O_4 replaces Cu^{2+} from the octahedral sites which increases the spin than the Cu^{2+} therefore, saturation

magnetizations (M_s) and thus magnetic moment increases with increasing content of cobalt. In present of saturation magnetization increases from CuFe_2O_4 (8.90emu/gm) to CoFe_2O_4 (29.76emu/gm) as shown in Fig.7. Similarly magnetic moment (μ_B) also increases from 0.38BM to 1.25 BM. The remanent magnetization of ferrites increases from CuFe_2O_4 to CoFe_2O_4 [13]. The values varies from 1.89 – 6.74 emu/gm are attributed to the fact that the saturation magnetization of pure CoFe_2O_4 is larger than that of the pure CuFe_2O_4

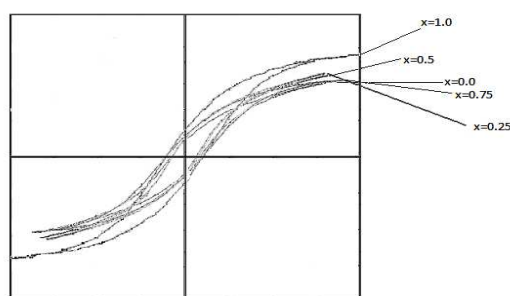


Fig.6 Hysteresis loops of $\text{Cu}_{1-x}\text{Co}_x\text{Fe}_2\text{O}_4$ system

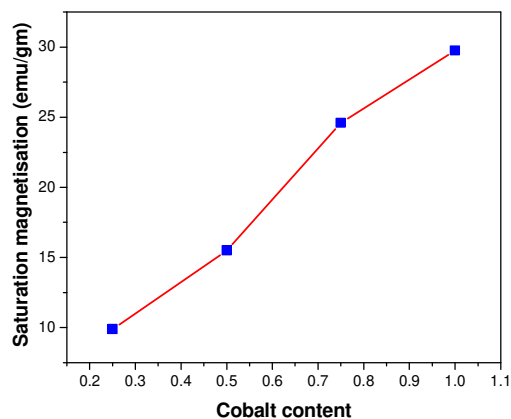


Fig.7. Variation of saturation magnetisation (M_s) with cobalt content.



Table 5. Magnetic Hysteresis for $\text{Cu}_{1-x}\text{Co}_x\text{Fe}_2\text{O}_4$ system.

Sr. No.	Compound	Saturation Magnetization (Ms) at 250k emu/gm	Coercive Field (Hc) Oe	Remanent Magnetization (Mr) emu/gm	Magnetic Moment (μ_B)
1	CuFe_2O_4	8.90	225.3	1.89	0.38
2	$\text{Cu}_{0.75}\text{Co}_{0.25}\text{Fe}_2\text{O}_4$	9.88	188.06	2.11	0.42
3	$\text{Cu}_{0.5}\text{Co}_{0.5}\text{Fe}_2\text{O}_4$	15.5	174.45	2.62	0.66
4	$\text{Cu}_{0.25}\text{Co}_{0.75}\text{Fe}_2\text{O}_4$	24.6	287.21	4.3	1.04
5	CoFe_2O_4	29.76	295.35	6.74	1.25

4. Conclusion:

In the system $\text{Cu}_{1-x}\text{Co}_x\text{Fe}_2\text{O}_4$, all the samples showed single cubic phase, as observed by X-ray powder diffraction technique. The crystallite size varied between 0.289 and $1.15\mu\text{m}$. Scanning electron micrographs indicated that grains are uniformly distributed. EDAX measurements show that all the samples are fairly stoichiometric. Electrical resistivity measurements indicates that all the samples are semiconductors (ΔE varies between 0.583 and 0.800 eV) while thermo emf measurements show that all the compositions are n-type indicating the electrons are the majority charge carriers. Magnetic hysteresis measurements indicated that all the compositions are ferrimagnetic. Saturation magnetization, magnetic moment, and remanent magnetization increases with increase in cobalt content.

References:

- [1] T. Mathew, B. S. Rao and C. S. Gopinath, J. Catalysis, 210, 405 (2002)
- [2] G. Cainelli, G. Cardillo, Chromium Oxidation in Organic Chem. Springer Verlag, Berlin (1984)
- [3] B. K. Das Preparation and Characterization of Mater. (Ed) J. M Honing. And C N R Rao, New York, Academic Press, (1981)
- [4] S. Sunder, B. K. Srivastava And D. Krishnamurthy, Ind. J. Pure and Appl. Phys. 42,366(2004)
- [5] R. D. Shannon and C. T. Prewitt. Acta Crystallogr. B26, 1076 (1970)
- [6] R. V. Mangalaja, S. Ananta Kumar and P. Manohar, Mater. Lett., 58, 593 (2004)
- [7] D. Ravinder, Materials Letters, 40(4), 198 (1999)
- [8] S. L. Kadam, K. K. Patankar, V. L. Mathe, M. B. Kothate, R. B. Kate And B. K. Chougale, J. Electro. Ceram. Soc. 10, 47 (2003)
- [9] G. H. Jonkar, J. Phys. Chem. Solids 9, 165(1959)
- [10] R. Satyanarayana, S. Ramana Murthy, T. Seshagiri Rao and S. M. D. Rao, J. Less. Com. Mat. 86, 115(1982)
- [11] K. S. Rane, M. S. Vernekar and P. Y. Sawant, Bull. Mater. Sci., 5,323 (2001)
- [12] M. Guyot and V. Cagan, J. of Mag. and Magnetic Mat. 27, 202 (1982)
- [13] P. J. Van der Zaag, P. J. Van der valk and M. Th. Rekveldt, Applied Phys. Letters 69 (11), 2927 (1996)



Application of Pomegranate Albedo for Biosorption of Methylene Blue Dye

Prakash Patil^{1,2}, Bharat Pawar¹ and Sunil Mirgane^{2*}

¹Department of Chemistry, Sangola, College Sangola, Kadlas Road Sangola, MS, India – 413307.

²Department of Chemistry, J E S College Jalana, MS, India– 416004.

KEYWORDS

Methylene blue dye,
Pomegranate albedo,
FTIR

Corresponding Author
Email
mirganesunil@gmail.com

ABSTRACT

This study offers the removal of methylene blue dye with biosorbent prepared from waste albedo of Pomegranate. The dried albedo were ground prior to their activation by carbonization in muffle furnace at 800°C for 1 hours. These carbonized pomegranate albedo (CPA) used as low-cost, and environment-friendly adsorbents as a new source for active carbon, for the removal of dyes. The Characterisation of biosorbent was made by Fourier transform infrared Spectroscopy (FTIR) and Scanning Electron Microscopy (SEM). Activated carbon used for the study of Methylene blue (MB) dye removal with help of spectrophotometer. P^H and conductivity were also studied in aqueous solution of activated carbon.

Introduction

In India, pomegranate is considered as a crop of the arid and semi arid regions because it withstands different soil and climate stresses. It thrives best under hot dry summer and cold winter provided irrigation facilities are available [1]. Owing to its low maintenance cost, tolerant to biotic and abiotic stresses, high yielding potential, better keeping quality and higher nutraceutical fruit value, popularity of pomegranate is increasing among the growers and consumers worldwide [2]. Causes discharge of wastewater containing dyes into surface or subsurface water resources due to problems in degrading processes. Malachite green (MG) is a cationic dye primarily used for colouring materials like cotton, silk, paper, wool and leather, beside its use as a biocide and disinfectant [3].

Since MG is a carcinogenic and mutagenic dye which is harmful for human and animal cells, its discharge through wastewater creates major environmental problems [4]. Adsorption is accepted as the most efficient technique for removing pollutants from wastewater among many other methods thanks to its characteristics such as simplicity of design, high efficiency and economic feasibility [5]. Activated carbon is the most widely used adsorbent in adsorption processes; however, it is costly and but has adsorption capacity. Due to this research scientist have concentrated on finding alternative natural adsorbents to activated carbon. Natural adsorbents are preferred for their biodegradable, non-toxic nature, low commercial value.

Experimental

A typical process involves 500 gm pomegranate peel were taken then they were cut into small peaces washed and dried

Result and Discussion

The concentration of MB solution before and after adsorption were estimated by measuring absorbance at 665 nm with help of spectrophotometer. 0.250 gm amount of from waste albedo of Pomegranate adsorbent was placed in 50 ml flasks containing 6.25, 5.25, 4.25, 3.25, 2.25 mg/L concentration of dye solution of corresponding pH ranging from 5.5 to 6.0.



Fig:1 Diluted pomegranate albedo sample for absorption study

Then flasks were shaken thoroughly with hand for 5 minutes, After filtration final concentration of dye solution were analyzed by spectrophotometer. The amount of equilibrium uptake of dye is calculated by using equation $q_e = (C_0 - C_e) V / W$

Q_e - is the dye up taken by adsorbent mg/g, C_0 - is the initial MB concentration, C_e - is the MB concentration (mg/l) after the batch adsorption process, W - is the Mass of adsorbent (gm), V is the Volume of dye solution

Absorbance of Pure dye	Absorbance of Pure dye + non Pomegranate Albedo sample	Absorbance of Pure dye + Activated Pomegranate Albedo
1.74	1.70	1.00
1.69	1.63	0.90
1.63	1.30	0.70
1.54	1.01	0.28

From table shows that on dilution Abs value decreases it show that the activated pomegranate albedo the degrades the MB dye. It was also found that dye uptake capacity changes as dye concentration capacity changes as shown in table 1. The interaction between dye molecule and adsorbent is basically a combined result of charges on dye molecules and adsorbent is basically a combined result of charges on dye molecules and the surface of the adsorbent.

Conclusion

The purpose of this work to use economic and environmental –friendly adsorbents has been considered as a new source of active carbon. The study offers the removal of harmful dye with carbonized pomegranate albedo. To consider the potential application of waste pomegranate albedo to removal methylene blue dye. This will useful for the farmers to use waste pomegranate albedo to grow economy of farmer.

Refrences.

- Saxena AK, Manan JK, Berry SK (1987) Pomegranate post harvest technology chemistry and processing. Indian Food Packer 41: 43-60.
- NHBMA (2010) Indian Horticulture Database-2009. National Horticulture Board Ministry of Agriculture Govt of India.
- [3] S. Banerjee, G.C. Sharma, R.K. Gautam, M.C. Chattopadhyaya, S.N. Upadhyay, Y.C.Sharma, Removal of Malachite Green, a hazardous dye from aqueous solutions using Avena sativa (oat) hull as a potential adsorbent, J Mol Liq, 213 (2016) 162-172.
- [4] Y.H. Song, S.G. Ding, S.M. Chen, H. Xu, Y. Mei, J.M. Ren, Removal of malachite green in aqueous solution by adsorption on sawdust, Korean J Chem Eng, 32 (2015) 2443-2448.
- [5] M.A. Ahmad, R. Alrozi, Optimization of preparation conditions for mangosteen peel based activated carbons for the removal of Remazol Brilliant Blue R using response surface methodology, Chem Eng J, 165 (2010) 883-890.



Development of growth charts for 5-10 year aged children

S.S.Shinde^{a,b}, S. V. Kakade^{b*}

^aDepartment of Statstics, M.H.Shinde Mahavidyalaya,Tisangi - 416206, MH,India

^bDepartment of Community Medicine, Krishna Institute of Medical Sciences,
Karad-415124, MH, India

KEYWORDS

Hight for age,
weight for age,
BMI for age, Growth curves
for 5-10 year age group.

Corresponding Author
Email

ABSTRACT

India is a diversified country and hence growth pattern of indian children has changed over different areas. Thus it is necessary to produce local updated growth references for any perticular area. These growth charts were prepared by collecting data from english medium schools in kolhapur district. We considered that children going to english medium school are from well-to-do family & are healthy. So the growth charts being standard & healthy growth charts. The study aim was to construct the standard growth charts for 5-10 years old childs.The number of boys and girls enrolled in this study are 777 and 465 respectively,lying in age 5-10 years.The growth refereces are being constructed for weight for age,Height for age separatly for boys & girls.

Introduction

Growth is an integral part of childhood & growth monitoring is critical for the assessment of health & disease in an individual child & the community as a whole (1) child growth charts are among the most commonly used tools for assessing the general well being of children(2). Growth patterns differ amongst different populations especially in children above the age of 5 years, as nutritional, environmental & genetic factors. Hence it is necessary to have region-specific growth charts to monitor growth of children bet 5-10 years.

Reference centile curves are used widely in medical practice as a screening tool. The need for centile curves, rather than a simple reference range arises when the measurement is strongly dependent on some covariate, often age. So that the reference range changes with the covariate.

The case for making the centiles curves smooth is to some extent cosmetic. The centiles are more pleasing to the eye when smoothed appropriately(3).

According to above references it is clear that the pattern of growth of population changes with time and place. Hence it is essential to undate growth charts regularly.

Objectives

- ❑ To assess growth parameters for 5-10 years age group children.
- ❑ To develop growth curves for the same age group separately for boys and girls.

A cross-sectional study was conducted in Kolhapur district. A prior permission for the study was taken from the Educational Department, Zilla Parishad, Kolhapur. English medium school (EMS) children from both genders in the age group of 5-10 years were enrolled in the study considering representative of the healthy growth. From every taluka one EMS was selected randomly. Each & every student, except physically & mentally abnormal in the age group of 5-10 year from the selected school was assessed. Height was measured using modern well developed digital height measuring machine with the subject standing straight. Subject's weight without foot wares & with light cloths was measured using digital weighing machine.

Statistical Analysis

The individual child data, demographic and anthropometric, was recorded on predesigned proforma. Recorded data was classified according to age, sex & Taluka. There were ten age groups 5-5.5 yr., 5.5-6 yr., 9.5-10 yr. Minimum sample size criteria (atleast 26) was determined for each age group sexwise for height, weight and BMI on the basis of findings of Vaman Khadilker at al^R(4). Using sample size determination method $n=(Z_{1-\alpha/2}^2 * SD^2) / (\text{Median} * \epsilon)^2$, taking $\epsilon =$ precision of 10%. The data was further cleaned by removing outliers. Talukawise equality in genderwise proportion was assessed by applying Chi-square test. ANOVA revealed no significant difference in talukawise height and weight for each study age group. On the basis of the ANOVA result, agewise data of all study talukas were clubbed into single data set as a representative of whole district.

Descriptive statistics Mean, S.D. & percentiles for anthropometric variables were calculated to summarize the data.

Because of statistical variation in the reference sample empirical percentile curves are generally irregular, some type of smoothing over weight or height was required to apply. To achieve this purpose various regression models were applied on study data. SPSS ver.20 used to analyse the data.

Total 777 boys of different ages studying in EMSs were enrolled in the study. Table I to III depicts mean, SD and various percentiles of height, weight and BMI for age of these boys, respectively. With very less proportion of exception, all these anthropometric parameters showed increasing trend with increasing age.



Results

TableI: Mean & Percentiles of Height for age of Boys

Age_ Gr	N	Mean	SD	3	10	25	50	75	90	97
5-5.5 yrs	70	107.949	4.698	99.913	101.54	105	107	111.25	115.45	116.487
5.5-6 yrs	95	110.644	4.1874	102.164	106	108.4	110.2	112.8	116.2	121.036
6-6.5 yrs	95	113.698	4.5915	106.28	108	110.4	113.5	116.6	118.76	124.872
6.5-7 yrs	75	116.651	4.8648	106.616	109.6	113.5	116.9	120	122.8	126.136
7-7.5 yrs	91	120.401	4.6815	112.476	114.9	117.3	119.7	123.2	126.78	131.408
7.5-8 yrs	68	122.607	4.6701	113.056	116.5	120.05	122	125.375	128.06	132.73
8-8.5 yrs	73	125.926	5.868	115.888	118.44	121.6	125.4	129.95	134.5	138.326
8.5-9 yrs	80	128.393	5.6327	119.172	121.06	123.85	128	132.525	135.87	141.585
9-9.5 yrs	67	130.921	5.475	119.064	122.94	126.6	132.1	134.6	137.42	139.576
9.5-10 yrs	63	132.349	6.2572	118.336	125.2	128.2	132	136.4	139.92	146.424

TableII: Mean & Percentiles of Weight for age of Boys

Age_ Gr	N	Mean	SD	3	10	25	50	75	90	97
5-5.5 yrs	70	16.761	2.4557	13.378	14.3	15.1	16.5	18.05	19.59	22.009
5.5-6 yrs	95	17.259	2.7284	13.5	14.56	15.9	16.8	18	20.49	23.1
6-6.5 yrs	95	18.388	2.5843	14.628	15.3	16.6	18.3	19.5	21.24	25.396
6.5-7 yrs	75	19.38	2.8993	15.028	16.18	17.5	18.8	20.6	23.74	27.132
7-7.5 yrs	91	20.434	2.8482	16.456	17.2	18.4	20.1	21.8	23.9	27.7
7.5-8 yrs	68	21.571	2.9904	16.784	18.5	19.425	21.3	22.85	24.9	32.057
8-8.5 yrs	73	22.832	3.6811	17.498	18.6	20.35	22.4	24.65	27.62	32.518
8.5-9 yrs	80	24.413	3.3967	18.943	20.34	21.725	24.15	26.35	28.3	32.014
9-9.5 yrs	67	27.019	5.9775	19.164	21.4	23.4	25.1	29.1	34.86	41.172
9.5-10 yrs	63	26.583	6.02	18.912	20.74	22.6	25.4	28.8	35.58	43.324

TableIII: Mean & Percentiles of BMI for age of Boys

Age_ Gr	N	Mean	SD	3	10	25	50	75	90	97
5-5.5 yrs	70	14.3208	1.2256	12.0972	13.2837	13.6618	14.1184	14.8971	15.3024	16.6941
5.5-6 yrs	95	14.0412	1.4803	12.1153	12.732	13.1016	13.9643	14.6251	15.6684	16.8372
6-6.5 yrs	95	14.1722	1.2859	12.3858	12.8981	13.3929	14.03	14.6281	15.4587	18.0057
6.5-7 yrs	75	14.1701	1.2409	12.2094	12.8784	13.4657	13.9727	14.6353	15.9331	17.6433
7-7.5 yrs	91	14.0474	1.3024	12.0215	12.6732	13.1268	13.888	14.6319	15.6602	16.7437
7.5-8 yrs	68	14.2994	1.2704	12.5899	12.9887	13.386	14.1946	14.8251	15.8288	17.5056
8-8.5 yrs	73	14.3511	1.6843	12.0142	12.3658	13.1484	14.1345	15.3173	16.4414	18.4931
8.5-9 yrs	80	14.7559	1.3019	12.5949	13.2571	13.7879	14.6824	15.3807	16.109	18.3394
-9.5 yrs	67	15.6498	2.5934	12.4105	13.149	13.9021	14.787	16.9166	19.2525	22.741
9.5-10 yrs	63	15.0535	2.5207	12.1285	12.8688	13.352	14.7498	15.7874	18.6084	23.6089

Curve Estimation

TableIV:Characterstics of curves developed for Height for age of boys applying various models.

Model	3 rd Percentile		97 th Percentile	
	R ²	trend	R ²	trend
Quadratic	0.972	stable	0.976	stable
Compound	0.937	upword	0.971	upword
Growth	0.937	upword	0.971	upword
Logerithmic	0.928	stable	0.913	stable
Cubic	0.983	declining	0.976	stable
S	0.733	stable	0.714	stable
Exponential	0.937	upword	0.971	upword
Logistic	0.937	upword	0.971	upword

TableV:Characterstics of curves developed for weight for age of boys applying various models.

Model	3 rd Percentile		97 th Percentile	
	R ²	trend	R ²	trend
Quadratic	0.969	stable	0.947	upword
Compound	0.961	upword	0.949	upword
Growth	0.961	upword	0.949	upword
Logerithmic	0.883	stable	0.749	stable
Cubic	0.985	declining	0.956	upword
S	0.659	stable	0.577	stable
Exponential	0.961	upword	0.949	upword
Logistic	0.961	upword	0.949	upword

TableVI:Characterstics of curves developed for BMI for age of boys applying various models.

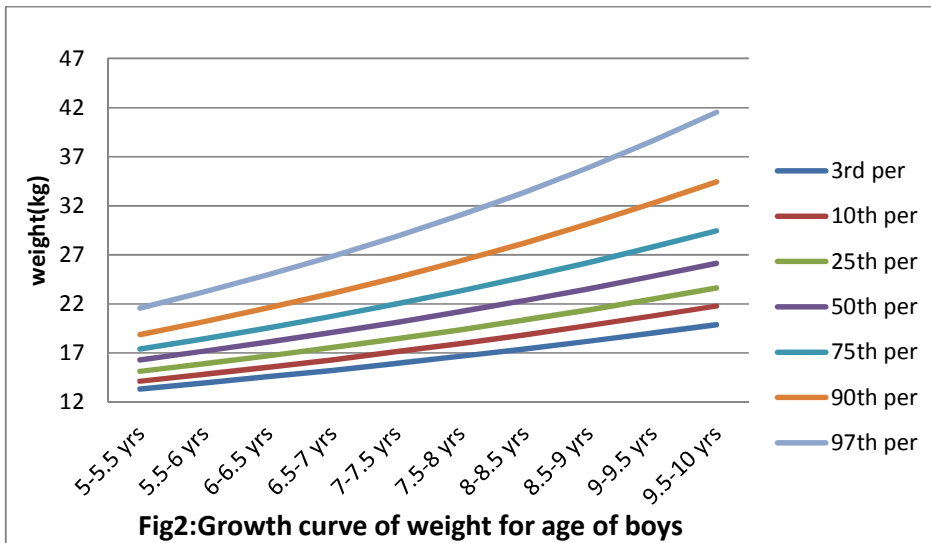
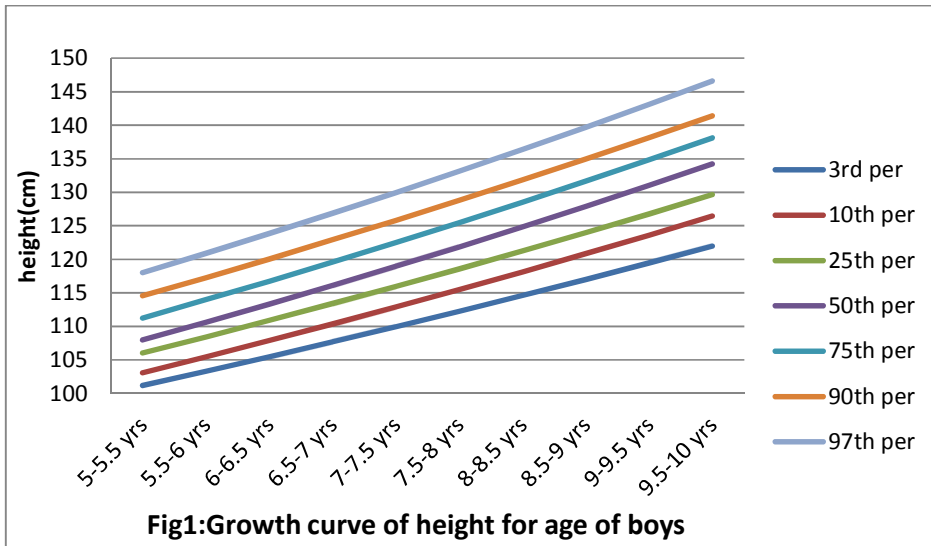
Model	3 rd Percentile		97 th Percentile	
	R ²	trend	R ²	trend
Quadratic	0.127	stable	0.862	upword
Compound	0.077	upward	0.667	upward
Growth	0.077	upward	0.667	upward
Logerithmic	0.103	stable	0.440	stable
Cubic	0.158	declining	0.917	upward
S	0.103	stable	0.262	stable
Exponential	0.077	upword	0.667	upward
Logistic	0.077	upward	0.667	upward

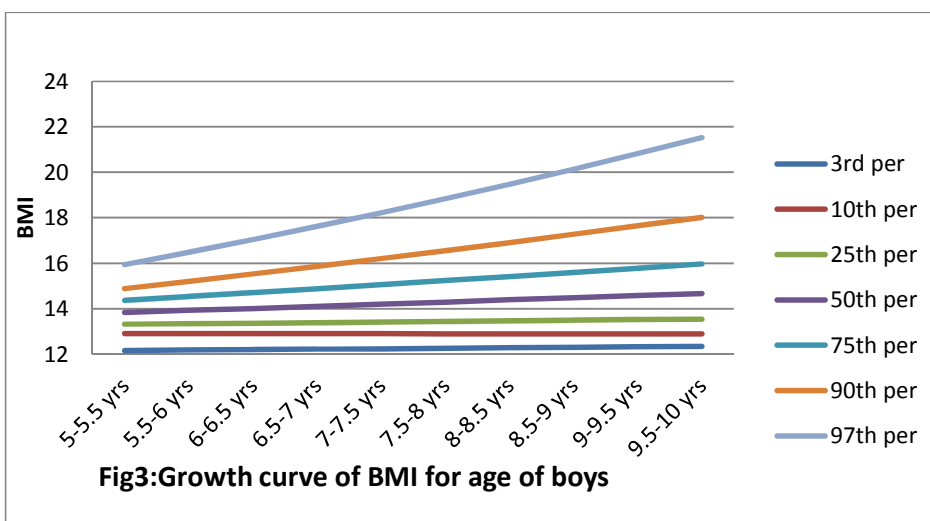


As per R^2 – value and nature of the curve that expected for study age group of observations Compound, Growth, Exponential and Logistic models were favourable to our study data (Table IV,V,VI). But exponential models are often used with population growth. So we select exponential regression in our study.

$$Y=ae^{bx}$$

All observed percentile values (3rd to 97th) for various ages were used to estimate respective values by using Exponential Regression model. These estimates of height, weight and BMI were used to generate the smooth curves (Fig.1 to 3).





TableVII: Mean & Percentiles of Height for age of Girls

Age _ Gr	N	Mean	SD	3	10	25	50	75	90	97
5-5.5 yrs	45	107.369	3.9688	98.796	101.78	104.6	106.9	110	113.26	115.492
5.5-6 yrs	58	109.528	4.0297	101.794	103.92	107.3	109.6	112.9	115.01	116.723
6-6.5 yrs	53	112.715	5.2548	102.17	105.88	109.6	111.4	115.2	120.16	125.532
6.5-7 yrs	56	115.836	5.1665	104.946	109.48	113.5	114.7	119.05	122.65	127.947
7-7.5 yrs	55	117.907	5.4421	107.892	109.66	115.4	117.7	120.2	125.64	131.6
7.5-8 yrs	56	122.65	6.1172	110.67	115.05	118.1	122.15	127.25	130.5	134.959
8-8.5 yrs	36	124.625	6.1111	112.195	117.21	121.075	123.55	128	132.3	143.312
8.5-9 yrs	38	129.545	6.6957	116.585	121.1	125.575	129	133.15	140.75	143.996
9-9.5 yrs	33	130.718	5.8091	118.074	123.32	125.95	131.2	135.55	138.22	142.92
9.5-10 yrs	35	133.457	6.5723	122.264	124.92	128.5	132.7	137.5	142.08	149.964

TableVIII: Mean & Percentiles of Weight for age of Girls

Age _ Gr	N	Mean	SD	3	10	25	50	75	90	97
5-5.5 yrs	45	16.224	2.0812	12.938	13.34	14.75	16	17.85	19.12	21.044
5.5-6 yrs	58	16.534	1.8465	12.531	14.48	15.125	16.4	18.125	19.1	19.723
6-6.5 yrs	53	17.66	2.967	12.662	14.3	15.5	17.5	19.6	21.76	25.036
6.5-7 yrs	56	18.443	2.6825	14.871	15.24	16.525	18	19.3	21.88	25.895
7-7.5 yrs	55	19.68	2.7096	15.812	16.6	17.7	19.1	20.8	23.38	26.796
7.5-8 yrs	56	21.85	3.9757	16.2	17.11	18.575	21.25	24.55	27.96	30.887
8-8.5 yrs	36	23.528	4.5691	17.766	18.44	20.05	22.1	26.8	30.79	34.234
8.5-9 yrs	38	25.221	6.04	14.631	18.48	20.1	24.5	28.7	32.35	42.428
9-9.5 yrs	33	25.636	5.6323	18.516	19.72	21.15	24.7	28.3	33.58	43.39
9.5-10 yrs	35	26.789	4.6285	18.664	21.86	23.6	25.9	28.8	34.28	41.288



TableIX: Mean & Percentiles of BMI for age of Girls

Age _ Gr	N	Mean	SD	3	10	25	50	75	90	97
5-5.5 yrs	45	14.028	1.1723	11.6224	12.5423	13.4064	13.8317	14.5962	15.8538	16.8132
5.5-6 yrs	58	13.7578	1.0939	11.4455	12.3504	13.0633	13.8157	14.2766	15.1794	16.1447
6-6.5 yrs	53	13.8396	1.6146	10.5899	12.0607	12.667	13.4773	15.021	16.212	17.2891
6.5-7 yrs	56	13.708	1.4247	11.7879	12.3374	12.7113	13.4982	14.2278	15.0902	17.9943
7-7.5 yrs	55	14.1461	1.5712	11.2983	12.5328	13.0321	14.1431	14.7938	16.5604	18.0994
7.5-8 yrs	56	14.4224	1.631	11.9146	12.4079	13.1885	14.4172	15.18	16.7092	18.5204
8-8.5 yrs	36	15.0536	2.0443	12.2073	12.7675	13.5513	14.6994	15.8728	19.1152	20.2442
8.5-9 yrs	38	14.8789	2.4754	8.816	12.5105	13.4976	14.5673	15.8057	18.3087	20.8661
9-9.5 yrs	33	14.8562	2.1314	12.1342	12.5509	13.5686	14.175	15.8024	17.846	21.2507
9.5-10 yrs	35	14.9937	2.0383	12.3681	13.0577	13.69	14.334	15.6168	18.5466	21.4103

Total 465 girls of different ages studying in EMSs were enrolled in the study. Table VII to IX depicts mean, SD and various percentiles of height, weight and BMI for age of these girls, respectively. With very less proportion of exception, all these anthropometric parameters showed increasing trend with increasing age.

TableX:Characterstics of curves developed for Height for age of girls applying various models.

Model	3 rd Percentile		97 th Percentile	
	R ²	Trend	R ²	Trend
Quadratic	0.993	upword	0.971	stable
Compound	0.990	upword	0.957	upword
Growth	0.990	upword	0.957	upword
Logerithmic	0.851	stable	0.957	upword
Cubic	0.993	upword	0.971	stable
S	0.609	stable	0.703	stable
Exponential	0.990	upword	0.957	upword
Logistic	0.990	upword	0.957	upword

TableXI:Characterstics of curves developed for Weight for age of girls applying various models.

Model	3 rd Percentile		97 th Percentile	
	R ²	trend	R ²	trend
Quadratic	0.748	stable	0.890	upword
Compound	0.743	upword	0.920	upword
Growth	0.743	upword	0.920	upword
Logerithmic	0.682	stable	0.726	stable
Cubic	0.754	stable	0.920	declining
S	0.485	stable	0.536	stable
Exponential	0.743	upword	0.920	upword
Logistic	0.743	upword	0.920	upword

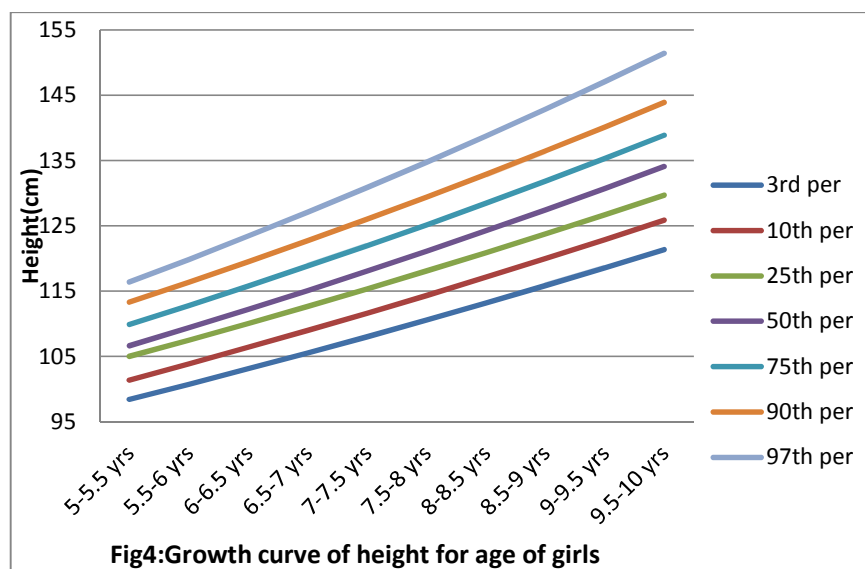
TableXII: Characteristics of curves developed for BMI for age of girls applying various models.

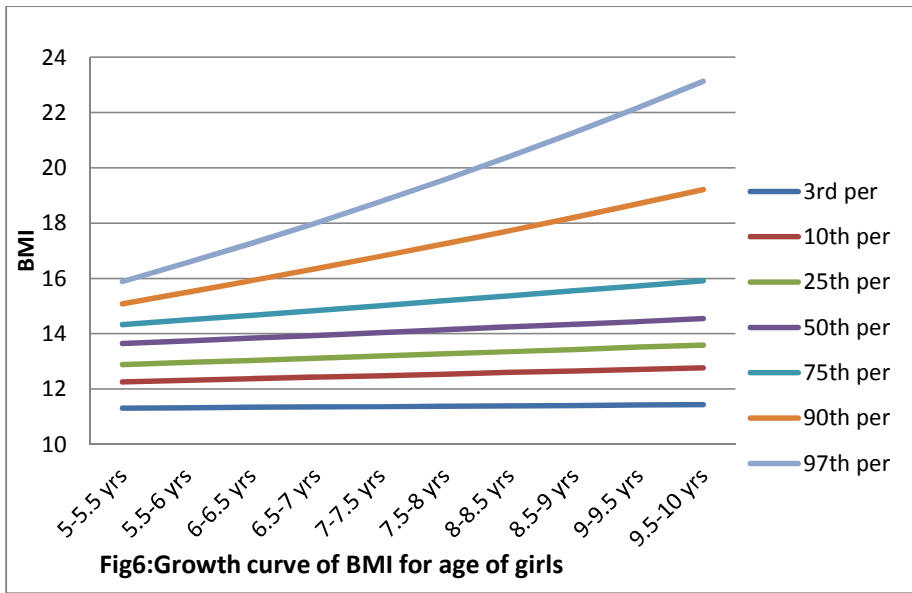
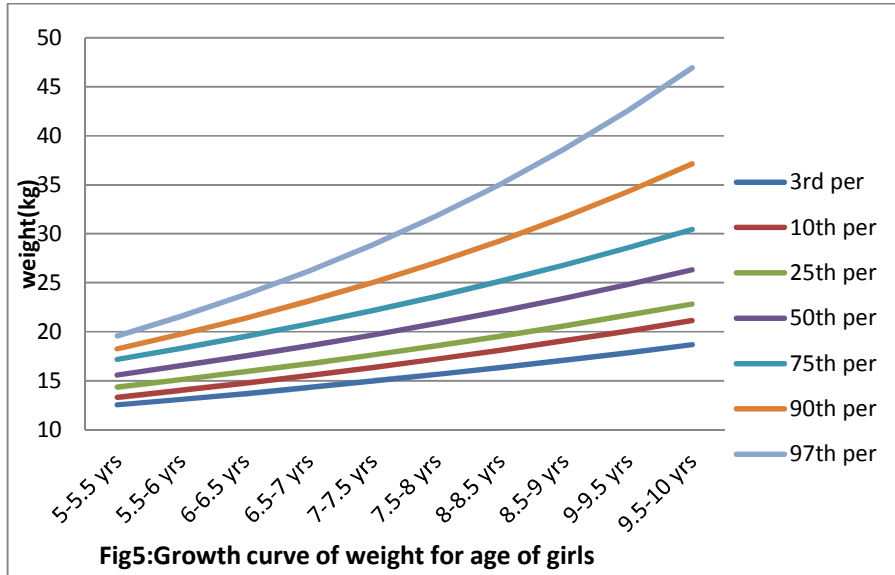
Model	3 rd Percentile		97 th Percentile	
	R ²	trend	R ²	trend
Quadratic	0.042	stable	0.946	upward
Compound	0.001	upward	0.940	upward
Growth	0.001	upward	0.940	upward
Logerithmic	0.001	stable	0.785	stable
Cubic	0.089	stable	0.967	declining
S	0.002	stable	0.510	stable
Exponential	0.001	upward	0.940	upward
Logistic	0.001	upward	0.940	upward

As per R² – value and nature of the curve that expected for study age group of observations Compound, Growth, Exponential and Logistic models were favourable to our study data (Table X,XI,XII). But exponential models are often used with population growth. So we select exponential regression in our study.

$$Y=ae^{bx}$$

All observed percentile values(3rd to 97th) for various ages were used to estimate respective values by using Exponential Regression model.These estimates of height,weight and BMI were used to generate the smooth curves (Fig.4 to 6).





Conclusion

The growth curves developed in the present study are based on children attending English medium school hence considering them to be from well-to-do families. These will help in identifying those who are not having good health at respective age in the community. Hence these growth curves will help as path of good health and growth of the child in 5 to 10 years age.

References

1. Revised IAP Growth Charts for Height, Weight and Body Mass Index for 5- to 18-year-old Indian Children
Vaman Khadilkar, Sangeeta Yadav, Kk Agrawal, Suchit Tamboli, Monidipa Banerjee, Alice Cherian, Jagdish P Goyal, Anuradha Khadilkar, V Kumaravel, V Mohan, D Narayanappa, I Ray And Vijay Yewale
2. Construction of the World Health Organization child growth standards: selection of methods for attained growth curves
E. Borghi, M. De Onis, C. Garza, J. Van den Broeck, E. A. Frongillo, L. Grummer-Strawn, S. Van Buuren, H. Pan, L. Molinari, R. Martorell, A. W. Onyango And J. C. Martines.
3. T.J Cole, P.J.Green Smoothing Reference Centile Curves: The LMS Method and Penalized Likelihood. *Stat Med* 1992;11:1305-19.
4. Vaman Khadilkar, Sangeeta Yadav, KK Agrawal, et al. Revised IAP Growth Charts for Height, Weight and Body Mass Index for 5-to 18-year-old Indian Children. *Indian Pediatrics*. Volume 52, January 15, 2015.
K Park. Park's Textbook of Preventive and Social Medicine. 23rd Edition, published by Bhanot, P:541-549.
5. Stuart H. C. and Stevenson S. S. (1959), In: Nelson, W. E. ed "Textbook of Paediatrics" 7th Ed., Saunders.
6. WHO (1978), A Growth Chart for International Use in MCH care.
7. WHO (1983), Measuring Changes in Nutritional Status.
8. ICMR (1984), Growth and Development of Indian Infants, TRS No. 18
9. ICMR (1976), ICMR Bull 6 (3) 1.
10. Gueri, M. et al (1980) *Bull WHO*, 58 (5) 773-777.
11. WHO Child Growth Standards. *Acta Paediatr Supplement*, 2006;450:5-101.
12. Brooks, G.D. (1982) Growth assessment in childhood and adolescence, Oxford.
13. Tanner, J. M. (1978) In : Textbook of Paediatrics, Forfav, J.O., Arneil G. C., eds, 3rd Ed. Churchill Livingston.
14. Rigby RA, Stasinopoulos DM. Smooth centile curves for skew and kurtotic data modeled using the Box-Cox power exponential distribution. *Stat Med* 2004;23:3053-76.
15. Mercedes de Onis, Adelheid W Onyango, Elaine Borghi, et al. Development of a WHO growth reference for school-aged children and adolescents. *Bulletin of the World Health Organization*. Sept 2007, 85(9).
16. Cole, T.J. Fitting smoothed centile curves to reference data. *Journal of the Royal Statistics Society, Series A, General* 151, 385-526. (1988)
17. Box, G.E.P. AND D.R. Cox, (1964) An analysis of Transformations, *J.Royal Stat.soc.(B)*, (1964) 26, 211-252.
18. Koenkar, R. (2005), *Quantile Regression*, Cambridge U. Press.
19. J. Harine Sargunam, M.A.S. Haseen FATHIMA, Dr. M.I. Fazal Mohamed. A Study on Growth Parameters and Prevalence of Overweight And Obesity Among School Going Children (5-10 Years) In Tirunelveli District. *IOSR Journal of Nursing and Health Science*, Volume 3, Issue 2, Ver. II (Mar-Apr. 2014) PP 07-14.
20. Katherine M Flegal. Curve smoothing and transformations in the development of growth curves. *Am J Clin Nutr* 1999;70(suppl):163S-5S.



Degradation of methyl orange by using ternary TiO₂/SnO₂/WO₃ nanocomposite as an efficient visible light active photocatalyst

Satish M. Patil^{a, b}, Shamkumar P. Deshmukh^{a, c}, and Sagar D. Delekar^{a*}

^aDepartment of Chemistry, Shivaji University, Kolhapur – 416004 (MS), India.

^bDepartment of Chemistry, Karmaveer Hire Arts, Science, Commerce and Education College, Gargoti, Tal: - Bhudargad, Dist: - Kolhapur – 416209 (MS), India.

^cDepartment of Chemistry, D. B. F. Dayanand College of Arts and Commerce Solapur – 413002 (MS), India.

KEYWORDS

Methyl orange, Ternary metal oxides, PL spectra, Photocatalysis, TiO₂/SnO₂/WO₃ nanocomposites

Corresponding Author
Email

sddelekar7@rediffmail.com

ABSTRACT

Ternary mixed-metal oxide semiconductors (MOS) proved to be efficient photocatalysts for the degradation of hazardous organic moieties present in industrial waste water. Herein, we have synthesized ternary TiO₂/SnO₂/WO₃ nanocomposites (NCs) by using sol-gel wet impregnation method and used as photocatalyst for the removal of methyl orange dye under visible light irradiation. UV-visible spectrophotometer was used to monitor degradation process of dye with regular time intervals. Ternary MOS NCs were well characterized by using sophisticated instrumental methods to explore various physico-chemical properties. It was revealed that, ternary NC with 1:1:1 composition of TiO₂, SnO₂ and WO₃ nanoparticles respectively (TSW-1) showed highest catalytic activity towards degradation of methyl orange (MO) dye. Almost complete degradation of MO dye was achieved within 120 min by using TSW-1 NC photocatalyst at ambient temperature and moderate experimental conditions.

Introduction

Variety of organic dyes have been used to impart colors to the objects in textile, paper and paint industries [1, 2]. For environmental safety removal of these dyes from water sources is an essential task before scientific community. In tropical countries like India, solar energy is abundantly available and its utilization for the photocatalytic purification of water is one of the promising strategy. This process of purification is economically and technologically best for the developing countries [3]. Other methods for the purification of water are also available such as UV-light treatment, sorption by activated carbon, flocculation, redox detoxification etc. [4];

but these methods are inefficient on the grounds of economical and workability aspects. In literature, the single TiO₂ nanoparticles (NPs) [5] or binary or ternary mixed metal oxide nanocomposites (MOS NCs) containing TiO₂ NPs as base materials [6, 7] were reported as excellent photocatalysts for removal of organic dyes. TiO₂ is ubiquitous material used for photocatalysis because of its interesting band gap structure. The conduction band potential of TiO₂ is more negative (~ -0.48 V) as compared to potential of water reduction reaction (~ 0 V) with respect to normal hydrogen electrode (NHE). On the contrary, its valence band potential is more positive (~ 2.8 V) than

potential of water oxidation reaction (~ 1.25 V) with respect to NHE [8]. Thus, it is possible to use TiO_2 as a good photoreductive and photooxidative material in the degradation of dyes. Furthermore, it is low cost, non-toxic and photoelectrochemically stable material than any other transition metal oxide. But, it is UV active only and unable to absorb light in the visible region of electromagnetic spectrum, which is one of the serious limitation of TiO_2 as a single photocatalyst [9, 10]. The inability of visible absorptivity of TiO_2 may be attributed to its wide optical band gap (~ 3.2 eV). In addition to that, there is fast recombination of photogenerated electron-hole pairs. TiO_2 material is therefore needed to be modified by using different strategies and then this modified TiO_2 materials found effective in large number of applications including photodegradation, photocatalytic organic transformations, etc. Doping of TiO_2 with metals or non-metals and forming its composite in nano-dimension with other materials, particularly, metal oxide semiconductor/s to form binary or ternary mixed metal oxide nanocomposites are the two most used strategies by workers [11].

In this work, we have successfully carried out synthesis of ternary $\text{TiO}_2/\text{SnO}_2/\text{WO}_3$ NCs by simple wet impregnation method. The as prepared materials were characterized by using various techniques to explore their physico-chemical properties. Finally, these ternary NCs were tested for their photocatalytic performance by monitoring degradation process of Methyl Orange (MO) as a model dye.

1.0 Experimental section

1.1 Chemicals and reagents

Titanium (IV) isopropoxide (TTIP), acetyl acetone (AcAc), isopropyl alcohol, stannous chloride dihydrate, NH_3 solution, tungstic acid, hydrochloric acid etc. were purchased from Sigma Aldrich. All chemicals and reagents were of AR grade and used without purification. Deionized water (18 $\text{m}\Omega\cdot\text{cm}$) was used in all the experiments.

2.2 Synthesis of bare TiO_2 , SnO_2 , WO_3 and their binary counterparts

This can be done by using our previous method [6].

2.3 Synthesis of ternary $\text{TiO}_2/\text{SnO}_2/\text{WO}_3$ NCs

Sonochemically assisted wet impregnation method was employed to prepare ternary nanocomposites. In this method, the desired amount of WO_3 NPs was dispersed in 25 mL of deionized water and sonicated for 15 min by using a probe sonicator. This dispersed WO_3 NPs solution was dropped into dispersed $\text{TiO}_2/\text{SnO}_2$ nanocomposites solution and sonicated for 15 min to assure thorough intermixing of WO_3 NPs with $\text{TiO}_2/\text{SnO}_2$ nanocomposites. The pale yellow product was dried at 110°C and finally calcined at 450°C for 3 h to obtain pale yellow ternary $\text{TiO}_2/\text{SnO}_2/\text{WO}_3$ nanocomposites. For sake of simplicity, the various ternary NCs prepared with different weight % of $\text{TiO}_2/\text{SnO}_2/\text{WO}_3$ like 1:1:1, 1:0.25:0.25, 1:0.4:0.2 and 1:0.6:0.4 respectively are labeled as TSW-1, TSW-2, TSW-3 and TSW-4 respectively.

2.4 Characterization

The crystallographic details of as prepared materials were studied by powder X-ray diffraction (XRD) spectroscopy using Ni-filtered $\text{Cu K}\alpha$ radiation at 1.54056 \AA (X'pert PRO, Philips, and Eindhoven). UV-visible (UV-Vis) diffuse reflectance spectra (DRS) and the time-dependent degradation spectra were recorded for MO dye using a LabIndia 3092 UV-visible spectrophotometer. The photoluminescence spectra of samples were recorded using a PL spectrophotometer (PL4450, Japan).

2.5 Photocatalytic studies

In a typical procedure, 50 mg of ternary TSW-1 NC photocatalyst was dispersed in 100 mL of aqueous MO dye solution (20 ppm). In order to establish adsorption-desorption equilibrium between the dye molecules and the catalyst surface, solution was stirred for 60 min in the dark. A Photo Chemical Reactor System (Lelesil Innovative Systems, Thane, India) was used with high-pressure lamp with 250 W power illuminating visible light in the wavelength between 400-750 nm. After every 15 min aliquots were withdrawn from the reactor to monitor the progress of the degradation process. The aliquots were centrifuged and their corresponding UV-Vis spectra were obtained using an UV-Visible spectrophotometer.

3.0 Results and discussion

3.1 XRD analysis

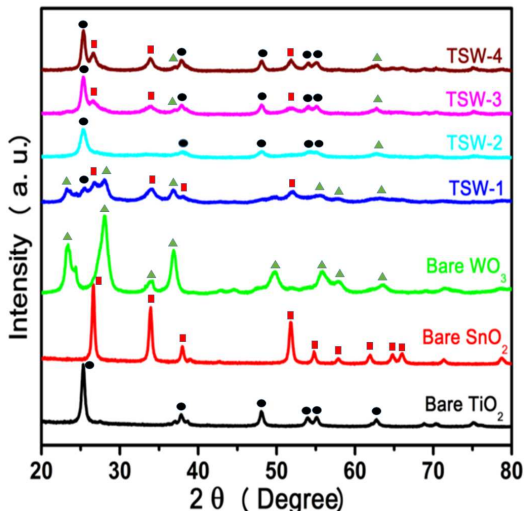


Figure 1. Powder X-ray diffraction patterns of bare tetragonal anatase TiO_2 (●) (JCPDS # 21-1272), bare tetragonal cassiterite SnO_2 (■) (JCPDS # 41-1445), and bare hexagonal WO_3 (▲) (JCPDS # 75-2187) and their ternary TSW-1, TSW-2, TSW-3, and TSW-4 NCs.

The structural properties of bare metal oxide NPs, and their ternary NCs were studied by powder X-ray diffraction (XRD) method. In Fig. 1, various XRD patterns of bare TiO_2 , bare SnO_2 , bare WO_3 NPs, and their ternary counterparts were given. The reflections of XRD patterns of bare NPs are well matched with tetragonal anatase phase of TiO_2 (●, JCPDS #21-1272), tetragonal cassiterite phase of SnO_2 (■, JCPDS #41-1445) and hexagonal phase of WO_3 (▲, JCPDS #75-2187). In all the composites, emergence of all characteristic peaks of TiO_2 , SnO_2 and WO_3 well revealed that, the formation of intermixed ternary NCs with appropriate weight percentage of bare individual NPs took place. The peak intensities of WO_3 decrease with a decrease in its weight %. On the contrary, peak intensities of TiO_2 and SnO_2 NPs increase with increase in their weight % in the composite.

3.2 UV-visible diffused reflectance spectroscopy (DRS) analysis

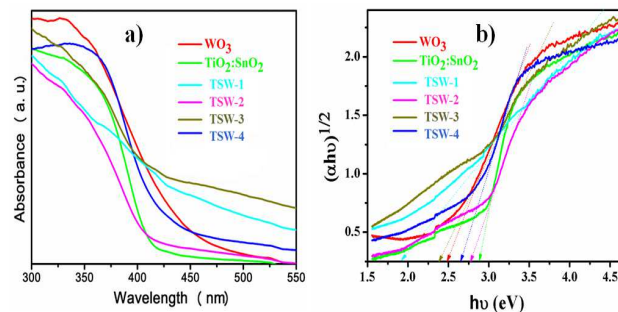


Figure 2. a) The diffused reflectance UV-visible spectra (DRS) of various samples and b) The plot of transformed Kubelka-Munk function $(\alpha hc)^{1/2}$ versus the energy of light (eV) for various samples.

Figure 2 represents the diffused reflectance UV-visible (DRS) spectra of as prepared samples. It has been clearly evidenced that, ternary TSW-1 NC has the lowest optical band gap ($\sim 1.92\text{eV}$) than any other material and thus it absorbs light in a visible region (red shift) of the electromagnetic spectrum. The optical band gap values for bare WO_3 , binary $\text{TiO}_2:\text{SnO}_2$ NC, ternary TSW-2, TSW-3, and TSW-4 NCs are $\sim 2.47\text{ eV}$, 2.87 eV , 2.77 eV , 2.38 eV , and 2.66 eV respectively. Thus, TSW-1 NC with the highest visible light absorption ability should be a potential efficient photocatalyst for the removal of methyl orange dye from the test solution.

3.3 Photoluminescence (PL) analysis

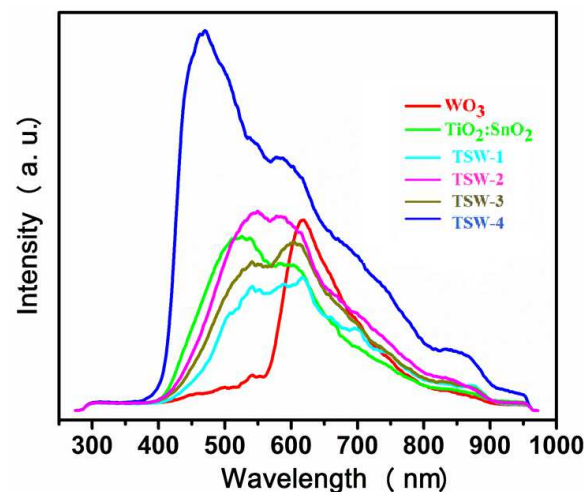


Figure 3. PL spectra of nanoparticles with the excitation wavelength of 350 nm.

The photocatalytic activity of a metal oxide semiconductor has characteristic intrinsic relationship with its photoluminescence (PL) spectrum. In PL spectrum, when band intensities are lower, it will be the good sign of higher separation rate of photo-induced electron-hole pairs. Subsequently, if separation rate of charge carriers is high in the material, its photocatalytic activity is also high [12].

Fig. 3 indicates the PL spectra of all as prepared materials. The PL spectrum of bare WO_3 shows single exciton peak at the region 617 nm which is in line with previous reports [13]. But, the higher intensity of this peak reveals higher rate of electron-hole pair recombination and thus this material was not fitted for photocatalytic applications. Similarly, other binary and ternary NCs shown their corresponding PL bands at characteristic wavelength regions. Among all those PL spectra, the band intensities of ternary TSW-1 NC PL spectrum are weak. This indicated higher separation rate of photo-induced charges in case of TSW-1 NC and therefore its highest photocatalytic activity.

3.3 photocatalytic studies of ternary TSW-1 NC

On the basis of various characterizations, it has been revealed that, the ternary TSW-1 NC possess best potential to use as photocatalyst for the removal of hazardous organic moieties present in the waste water. Thus, further degradation studies were conducted by using this material as visible light active catalyst. The methyl orange (MO) dye was selected as a model dye for degradation studies. All experimental conditions such as pH, catalyst amount, and dye concentration were optimized to evaluate photocatalytic activity of the ternary TSW-1 NC. It was found that, pH = 7, catalyst amount = 50 mg and dye concentration 20 ppm were good for degradation studies. The photocatalytic performance of TSW-1 NC under visible light irradiation was examined by monitoring the photodegradation of MO dye at ambient temperature ($25 \text{ }^\circ\text{C} \pm 2 \text{ }^\circ\text{C}$). Fig. 4 shows UV-visible absorption spectra obtained for the MO aqueous solution (initial concentration 20 ppm) in presence of TSW-1 NC with respect to time under visible light irradiation.

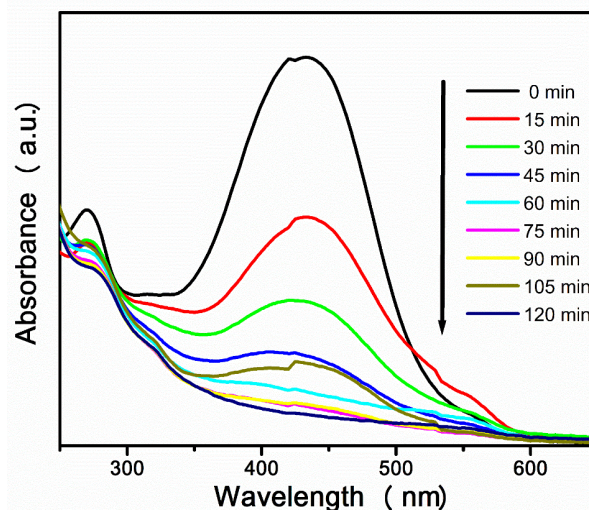


Figure 4. Time-dependent absorption spectra changes in CR aqueous solution in the presence of TSW-1 NC photocatalyst.

The maximum absorption peak at 435 nm and another less intense absorption peak at 270 nm were due to azo bonds and the naphthalene ring structure of MO. The absorption intensities of both these peaks were decreased with respect to time in the presence of TSW-1 NC as catalyst. This clearly indicated the breakage of the azo links and aromatic rings in the structure and thus removal of MO dye from aqueous solution by means of its degradation [14]. Only 120 min were required for almost complete degradation of MO dye, which is solid evidence of superior photocatalytic activity of ternary TSW-1 NC material.

For a good photocatalyst, its stability and therefore recyclability is an important criteria. We have ascertained recyclability of TSW-1 NC photocatalyst by using same catalyst for five consecutive degradation cycles of MO dye. After first use the catalyst was recovered by centrifugation and filtration method, it was then dried at 110°C for the removal of organic moieties and surface adsorbed water molecules and then it was used for next cycle of degradation. The same protocol was repeated for further consecutive cycles and results obtained are shown in Figure 5.

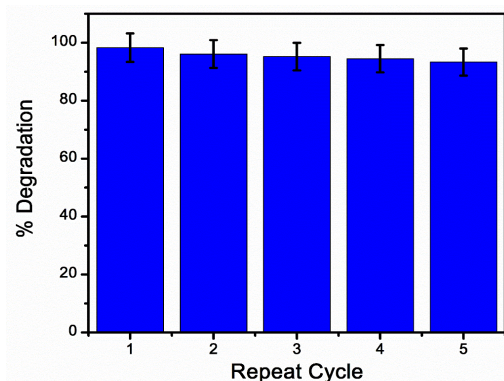


Figure 5. Recyclability of TSW-1 NC with MO after consecutive five cycles of the continuous photodegradation process. No significant loss in catalytic activity was observed. But, there is slight decrease in % degradation was evidenced. This may be due to the loss of catalyst during recovery process and also due to adsorption dye molecules on its surface.

Conclusions

In this work, we synthesized ternary $\text{TiO}_2/\text{SnO}_2/\text{WO}_3$ NCs using a simple sol-gel wet impregnation method. XRD analysis of the annealed samples indicated the formation of intermixed ternary NCs. Further, UV-visible spectroscopic analysis showed that the optical band gap of TSW-1 NC is lower than any other material. Thus, TSW-1 NC has its absorption band edge in the visible region of electromagnetic spectrum and proved good photocatalyst for dye degradation study. The activity of TSW-1 NC was also supported by PL spectroscopic studies where it shows weak absorption band intensities. Lower intensities of absorption bands in PL spectrum proved higher separation rate of photo-generated charge carriers and thus higher photocatalytic activity of TSW-1 NC. In degradation of MO dye this TSW-1 NC showed excellent photocatalytic activity and degradation of dye required 120 min under visible light irradiation. Thus, we have established an efficient and easy strategy for the preparation of TiO_2 -based ternary MOS NCs and their utilization in photocatalytic applications.

Acknowledgements

SMP is thankful to the University Grants Commission, New Delhi, India for financial assistance under the award of UGC-FIP [F. No. 36-40/14 (WRO)], which is gratefully acknowledged.

References

- [1] M. Aboulhassan, S. Souabi, A. Yaacoubi, M. Baudu, Improvement of paint effluents coagulation using natural and synthetic coagulant aids, *Journal of hazardous materials*, 138 (2006) 40-45.
- [2] V. Gupta, Application of low-cost adsorbents for dye removal—A review, *Journal of environmental management*, 90 (2009) 2313-2342.
- [3] C.E. Tyner, Application of solar thermal technology to the destruction of hazardous wastes, *Solar energy materials*, 21 (1990) 113-129.
- [4] P. Kumar, M. Govindaraju, S. Senthamilselvi, K. Premkumar, Photocatalytic degradation of methyl orange dye using silver (Ag) nanoparticles synthesized from *Ulva lactuca*, *Colloids and surfaces B: biointerfaces*, 103 (2013) 658-661.
- [5] I.K. Konstantinou, T.A. Albanis, TiO_2 -assisted photocatalytic degradation of azo dyes in aqueous solution: kinetic and mechanistic investigations: a review, *Applied Catalysis B: Environmental*, 49 (2004) 1-14.
- [6] S. Patil, A. Dhodamani, S. Vanalakar, S. Deshmukh, S. Delekar, Multi-applicative tetragonal $\text{TiO}_2/\text{SnO}_2$ nanocomposites for photocatalysis and gas sensing, *Journal of Physics and Chemistry of Solids*, 115 (2018) 127-136.
- [7] H. Kim, J. Kim, W. Kim, W. Choi, Enhanced photocatalytic and photoelectrochemical activity in the ternary hybrid of $\text{CdS}/\text{TiO}_2/\text{WO}_3$ through the cascaded electron transfer, *The Journal of Physical Chemistry C*, 115 (2011) 9797-9805.
- [8] M. Grätzel, Photoelectrochemical cells, *nature*, 414 (2001)
- [9] R.P. Barkul, M.K. Patil, S.M. Patil, V.B. Shevale, S.D. Delekar, Sunlight-assisted photocatalytic degradation of textile effluent and Rhodamine B by using iodine doped TiO_2 nanoparticles, *Journal of Photochemistry and Photobiology A: Chemistry*, 349 (2017) 138-147.

- [10] S.A. Vanalakar, S.M. Patil, V.L. Patil, S.A. Vhanalkar, P.S. Patil, J.H. Kim, Simplistic eco-friendly preparation of nanostructured $\text{Cu}_2\text{FeSnS}_4$ powder for solar photocatalytic degradation, *Materials Science and Engineering: B*, 229 (2018) 135-143.
- [11] S. M Patil, S. P Deshmukh, A. G Dhodamani, K. V More, S. D Delekar, Different Strategies for Modification of Titanium Dioxide as Heterogeneous Catalyst in Chemical Transformations, *Current Organic Chemistry*, 21 (2017) 821-833.
- [12] J. Liqiang, Q. Yichun, W. Baiqi, L. Shudan, J. Baojiang, Y. Libin, F. Wei, F. Honggang, S. Jiazhong, Review of photoluminescence performance of nano-sized semiconductor materials and its relationships with photocatalytic activity, *Solar Energy Materials and Solar Cells*, 90 (2006) 1773-1787.
- [13] L. Tao, S. Zhao, P. Miao, J. Yu, X. Wang, Y. Wang, Z. Liu, B. Li, Y. Wang, Y. Sui, Tunable Photoluminescence in WS_2/WO_3 Monolayer/Nanoparticles Hybrid Structure, *physica status solidi (RRL)-Rapid Research Letters*.
- [14] C. Hu, C.Y. Jimmy, Z. Hao, P.K. Wong, Photocatalytic degradation of triazine-containing azo dyes in aqueous TiO_2 suspensions, *Applied Catalysis B: Environmental*, 42 (2003) 55.



Use of some agrochemicals in the management of leaf spot of ginger caused by *Phyllosticta zingiberi* resistant to carbendazim

J. M. Gorule and S. S. Kamble

Mycology and Plant Pathology Laboratory, Department Of Botany, Shivaji University, Kolhapur. 416004.

KEYWORDS

Carbendazim, Ginger, Isolate, Resistant, Fungicides, Herbicides.

Corresponding Author
Email
jvotigorule5@gmail.com,

ABSTRACT

There was variation in the minimum inhibitory concentration of carbendazim among the 13 isolates of *Phyllosticta zingiberi* Ramkr. causing leaf of ginger, on the agar plates and on ginger plants. MIC on agar plates ranged from 2 to 9 % while it was 2 to 8 % on ginger plants. Isolate Pz-11 was highly resistant with resistance factor 4. Use of carbendazim in mixture with some agrochemicals such as, fungicides (kocide, aliette, bordeaux mixture and dhanuka) and herbicides (matin, aandhi and 2,4-D) inhibited the growth of the pathogen both on plates and on ginger plants. There was cent percent control of disease, showing 100% control efficacy on ginger plants by using mixture of above said fungicides.

Introduction

Ginger (*Zingiber officinale*) is a herbaceous perennial, belonging to family Zingiberaceae. Rhizome of ginger is known as *Sunthi* in Ayurveda and description of the plant appears in the old text like *Charaka*, *Sushruta*, *Vagbhatta* and *Chakra-dutta*. It is medicinal plant that has been widely used all over the world. The plant is erect, has many fibrous roots, aerial shoots (pseudostem) with leaves, and the underground stem (rhizome). It is widely used to cure stomach problems, diarrhoea, nausea, chest pain, low back pain, stomach pains, etc. It is used as flavouring agent in food and beverages. Ginger oil is used in soaps and cosmetics for fragrance. Such important plant is attacked by no. of diseases but *Phyllosticta* leaf spot caused by *Phyllosticta zingiberi* causes major loss to ginger. Leaf spot disease of ginger leads to heavy reduction in rhizome yield through the destruction of chlorophyllous tissue (Ramakrishnan, 1941) resulting 13 to 66 percent yield losses (Sarma et al., 1994).

The disease starts as water soaked, oval to elongated spots and later turn as whitish spots surrounded by dark brown margin with yellowish halo. The lesions enlarge and adjacent lesions coalesce to form necrotic areas. (Ramakrishnan, 1941).

Carbendazim was used to control the disease, but, there was increase in carbendazim resistance in the pathogen. Therefore, the aim of the present investigation was to examine the effect of agrochemicals on the development of carbendazim resistance in *Phyllosticta zingiberi*.

Material and Method

Thirteen samples exhibiting leaf spot of ginger were collected from different districts of Maharashtra and their sensitivity to carbendazim was different both *in vitro* and *in vivo*. MIC on agar plates ranged from 2 to 9 % while it was 2 to 8 % on ginger plants. From the results of MIC, it was observed that isolate Pz-11 was highly resistant with resistance factor 4, hence synergistic effect of some

fungicides and herbicides on isolate Pz-11 was carried out.

In vitro studies

For this, different fungicides (Bordeaux mixture, dhanuka, kocide and aliette) and herbicides (matin, aandhi and 2,4-D) were mixed in combination (10, 25, 50, 75 and 100 mg/ml) with carbendazim (8%) to find out their synergistic effect. Resistant isolate (Pz-11) was grown on the medium containing resistant dose of carbendazim (8%). Medium containing carbendazim alone was treated as control. An increase in radial mycelial growth over control was considered as increase in resistance, whereas decrease in growth was considered as decrease in resistance. (Waghmare, 2010).

Table1:-Synergistic effect of fungicides on the development of carbendazim resistance in *Phyllosticta zingiberi*. (In vitro)

Sr. No.	Fungicides with Carbendazim (8%)	Concentration of fungicides (mg/ml)	Radial mycelial growth (mm)
1	Kocide	10	00
		25	00
		50	00
		75	00
		100	00
2	Aliette	10	00
		25	00
		50	00
		75	00
		100	00
3	Bordeaux mixture	10	00
		25	00
		50	00
		75	00
		100	00
4	Dhanuka	10	00
		25	00
		50	00
		75	00
		100	00
5	Carbendazim 8% alone		11.67

In vivo studies

For *in vivo* studies, healthy ginger leaves were used. The fungicides (bordeaux mixture, dhanuka, kocide and aliette) and herbicides (matin, aandhi and 2,4-D) were mixed in combination (10, 25, 50, 75 and 100 mg/ml) with carbendazim (8%). For this studies, wild resistant isolate Pz-11 was selected. The fungicides at different concentrations were mixed with carbendazim having concentration of 8%. These solutions were sprayed on healthy ginger plants. After 24 hrs. 10 ml of mycelial suspension (331×10^4 spores/ml) made from actively growing mycelium of *Phyllosticta zingiberi* was inoculated on the ginger plants with sprayer. These plants were covered with polythene bags to maintain the relative humidity and to avoid other contamination. The plants which were sprayed with carbendazim 8% were considered as control. After 10 days of inoculation, results were taken by using 0-4 scale and compared with control.

Table 2:- Synergistic effect of fungicides on the development of carbendazim resistance in *Phyllosticta zingiberi*. (In vivo)

Sr. No.	Fungicides with Carbendazim (8%)	Concentration of fungicides (mg/ml)	Percentage of infection
1	Kocide	10	0
		25	0
		50	0
		75	0
		100	0
2	Aliette	10	0
		25	0
		50	0
		75	0
		100	0
3	Bordeaux mixture	10	0
		25	0
		50	0
		75	0
		100	0
4	Dhanuka	10	0
		25	0
		50	0
		75	0
		100	0
5	Carbendazim 8% alone		0



Fig. 1:- Synergistic effects of fungicides on the development of carbendazim resistance in *Phyllosticta zingiberi*. (In vitro)

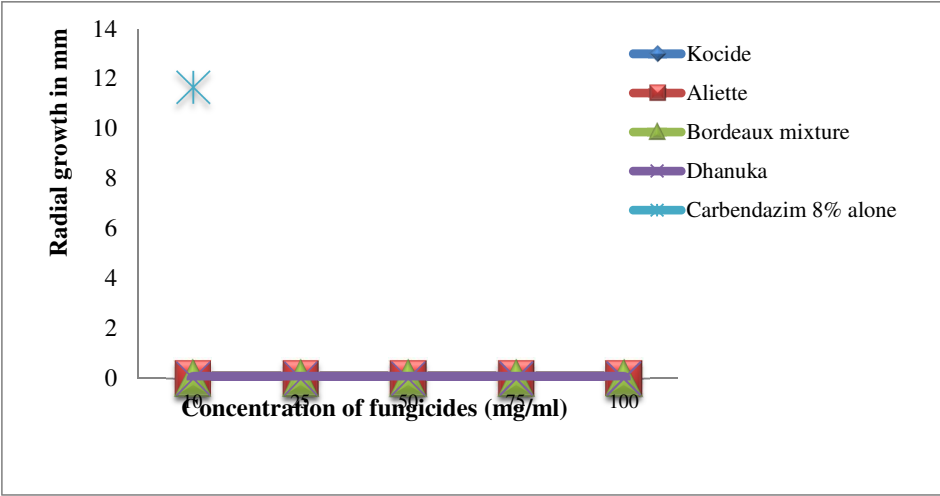


Fig. 2:- Synergistic effect of fungicides on the development of carbendazim resistance in *Phyllosticta zingiberi*. (In vivo)

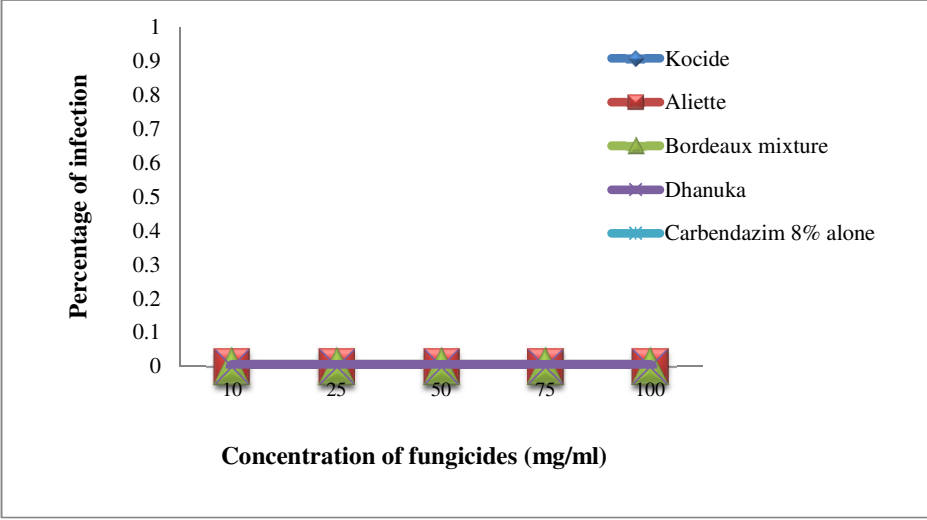


Table 3:- Synergistic effect of herbicides on the development of carbendazim resistance in *Phyllosticta zingiberi*. (In vitro)

Sr. No.	Herbicides with Carbendazim (8%)	Concentration of herbicides (mg/ml)	Radial mycelial growth in mm
1	Matin	10	14.33
		25	12.00
		50	9.67
		75	9.00
		100	8.00
2	Aandhi	10	13.33
		25	11.67
		50	10.33
		75	8.33
		100	8.00
3	2,4-D	10	12.67
		25	12.00
		50	9.67
		75	9.00
		100	8.00
4	Carbendazim 8% alone		11.67

Table 4:- Synergistic effect of herbicides on the development of carbendazim resistance in *Phyllosticta zingiberi*. (In vivo)

Sr. No.	Herbicides with Carbendazim (8%)	Concentration of herbicides (mg/ml)	Percentage of infection
1	Matin	10	0
		25	0
		50	0
		75	0
		100	0
2	Aandhi	10	0
		25	0
		50	0
		75	0
		100	0
3	2,4-D	10	0
		25	0
		50	0
		75	0
		100	0
4	Carbendazim 8% alone		0

Fig. 3:- Synergistic effect of herbicides on the development of carbendazim resistance in *Phyllosticta zingiberi*. (In vitro)

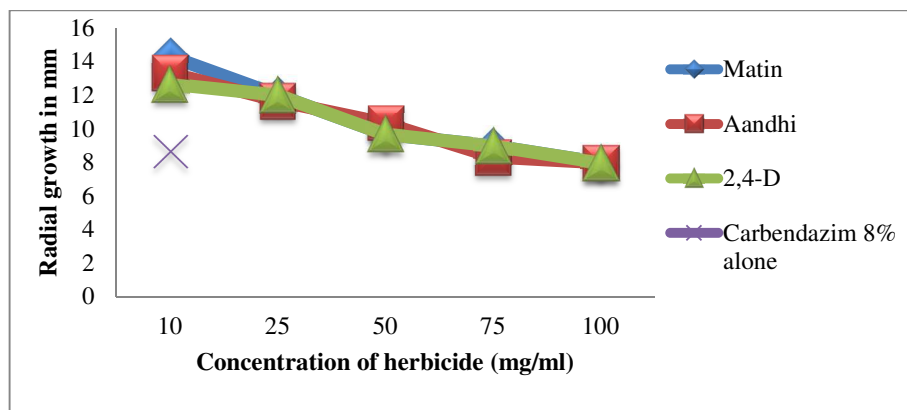
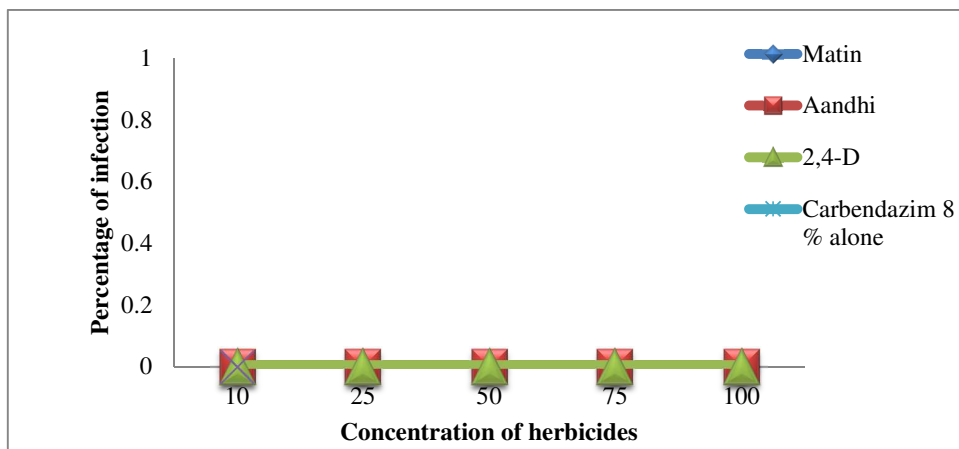


Fig. 4:- Synergistic effect of herbicides on the development of carbendazim resistance in *Phyllosticta zingiberi*.

(In vivo)



Results and discussion:

In case of fungicides (bordeaux mixture, dhanuka, kocide and aliette) there was complete inhibition of the growth of resistant isolate of *Phyllosticta zingiberi*, both *in vitro* and *in vivo* whereas in case of herbicides (matin, aandhi and 2,4-D) there was inhibition of the growth of resistant isolate of *Phyllosticta zingiberi*, as the concentration increases from 10 to 100 µg/ml. There was cent percent control of disease, showing 100% control efficacy on ginger plants by using mixture of above said herbicides.

According to Dalavi (2016), ridomil with fungicides (roko, kavach, carbendazim and benomyl) and herbicides (matine, aandhi-71%, 2-4-D and atrazine) reduced development of ridomil resistance in *Rhizopus artocapi* causing fruit rot of jackfruit.

According to Andoji (2016) fungicides (kocide, kavach, dhanuka, bavistin, ridomil and roko) used in mixture with benomyl, inhibited the growth of resistant isolate of *Fusarium solani* causing chickpea root rot.

Mishrakoti (2015) concluded that benomyl, dhanuka and kocide inhibited the growth while roko reduced the growth of *Alternaria dauci* causing blight of carrot, as the concentration of fungicides increases, as compared to carbendazim in control. In case of herbicides like aandhi 71, feroxone and matin prevented the infection at 75µg/ml concentration while tohfa prevented the infection at 50 µg/ml

feroxone and matin prevented the infection at 75µg/ml concentration while tohfa prevented the infection at 50 µg/ml concentration.

Fungicide mixtures of mancozeb with dicarboximide fungicide, iprodione or vinclozolin, are effective in commercial control of *Botrytis* leaf blight of onion caused by *Botrytis squamosa*. (Lorbeer, 1994)

References:

- Andoji YS (2016)** Management of chickpea root rot, Ph.d. thesis, Shivaji University, Kolhapur.
- Dalavi RB (2016)** Studies on management of fruit rot of jackfruit, Ph.d. thesis, Shivaji University, Kolhapur.
- James W, Lorbeer (1994)** Synergism, Antagonism, and Additive Action of Fungicides in Mixtures, Presented at the 86th Annual Meeting of The American Phytopathological Society, August 9, 1994, Albuquerque, NM.
- Loebeer JW (1990)** Efficacy of dicarboximide fungicides and fungicide combinations for control of *Botrytis* leaf blight of Onion in New York, Plant disease, Vol. 73 (3), 235-237.
- Mishrakoti MS (2015)** Studies on leaf blight management of Carrot, Ph.d. Thesis, Shivaji University, Kolhapur.

Ramkrishnan TS (1941) A leaf spot disease of *Zingiber officinale* caused by *Phyllosticta zingiberi* N. SP., Proceedings of the Indian Academy of Sciences - Section B.15(4), pp: 167-171.

Sarma YR, Anand RM and Venugopal MN (1994) Diseases of Spice Crops. pp. 1015-1057. In: Advance in Horticulture – Plantation and Spice Crops, Part 2 (1994) Vol. 10 (K.L. Chadha and P. Rethinam, eds.) Malhotra Publishing House, New Delhi.

Waghmare MB (2010) Studies on management of some important diseases of rose. Ph. D Thesis, Shivaji University, Kolhapur.



Effect of interactions between symbiotic VAM fungus and diazotrophic bacteria, *Rahnella* on carbohydrate and mineral contents of non-leguminous plant, *Abelmoschus esculents* (L.) Moench.

¹D. D. Gharge* and ²B. A. Karadge

^{a*}Department of Botany, Yashwantrao Chavan College of Science, Vidhyanagar, Karad-415 124, Maharashtra, India.

^bDepartment of Botany, Shivaji University, Kolhapur, 416 004, Maharashtra, India.

KEYWORDS

Mycorrhiza, *Glomus*, *Rahnella*, 16S RNA, synergism.

ABSTRACT

It is perhaps for the first time that the symbiotic nitrogen fixing bacterium, *Rahnella* has been reported from the non-leguminous plant, 'bhindi' (*Abelmoschus esculents* (L.) Moench.) in this study. The bacterium has been identified as *Rahnella aquatilis* strain DDG1 as confirmed by 16S RNA technique. The *Rahnella* has formed nodule like structures, referred here as protuberances, on the roots of the plants. As bhindi plant also has an abundance of vesicular arbuscular mycorrhizal fungi (VAMF) in rhizosphere, the interactions between *Glomus ambisporum*, Smith & Schenck and the *Rahnella* with reference to the carbohydrate and mineral contents of both root and leaves of this plant have been studied. The seeds were treated with *Rahnella* and *Glomus* alone as well as in combination of both and the plants were grown in sterilized soil. Inoculation of bhindi with *Glomus* increased the carbohydrate and mineral contents of the root and leaves. However, the inoculation of *Glomus* in combination with *Rahnella* resulted in significant enhancement in carbohydrate and mineral contents of the root and leaves. It appears that *Rahnella* displays a synergistic effect with *Glomus* in bhindi.

Corresponding Author
Email
botanyrtps@gmail.com

Introduction

In the life of bhindi plant, there are many challenges, as many of the commercial plantations of this highly nutritive tropical fruit vegetable plant are in soils with low fertility. So, the major problem for bhindi plants is the deficiencies of essential nutrients necessary for proper growth and development. These deficiencies can not only be caused by the lack of nutrients in the soil, but also if the nutrients needed for plant growth exceeds the roots ability to uptake nutrients.

nutrients. It has been known for a long time that beneficial microorganisms within the soil form symbiotic relationships with the roots of plants, which in turn, enhance the uptake of essential nutrients by plants. The mycorrhizal fungi also have the ability to uptake more nutrients, as they act as extensions of the roots. The occurrence of endomycorrhizal fungi in soil, their association with both forest plants and agricultural crops, and its role in improving the quality of plant has been well

Kaushik *et al.*, 1992; Ortas, 2003; Boureima *et al.*, 2007). Mycorrhizal infection has a particular value for legumes because nodulation and symbiotic nitrogen fixation by rhizobia require an adequate phosphorus supply (Carling *et al.*, 1978). Various researchers have made efforts to increase the quality of legume plants through the inoculation of mycorrhizal strain alone or in combination with *Rhizobium* sp. (Stancheva *et al.*, 2006; Yanjun *et al.*, 2010; Arumugam *et al.*, 2010). But non-leguminous plants are not more known to dual association of bacteria and mycorrhizal fungi. Thus, hardly any work has been done (Servín, 2014) to improve the yield and quality of non-leguminous plants by dual inoculation of VAM fungi and *Rahnella*. Experiment was conducted to study the possible contribution of endophytes (endomycorrhizal fungi and *Rahnella*) in association with each other, on carbohydrate and mineral content of *Abelmoschus esculentus* (L.) Moench.

Material and Methods

Native VAM fungus *Glomus ambisporum*, Smith and Schenck; was isolated from the rhizosphere of *Abelmoschus esculentus* (L.) Moench. by the wet sieving and decanting method (Gerdemann and Nicolson, 1963). *Rahnella aquatilis* DDG1 was also isolated from root protuberances of *A. esculentus* (L.) Moench. The mycorrhizal inoculum was mass produced on onion (*Allium cepa* L.). The *Rahnella aquatilis* DDG1 inoculum was mass produced on yeast extract mannitol agar (YEMA) medium. Locally collected seeds were used to raise the seedlings of *A. esculentus*. Seeds, free from physical defects and uniform size were surface sterilized (with 5% v/v H₂O₂) and put for germination in polythene bags, each containing 3 kg of sterilized soil.

Inoculation experiment was designed in single and double combinations. The seeds treated with *Rahnella aquatilis* DDG1, mycorrhiza, *Rahnella aquatilis* DDG1 combined with mycorrhiza, mycorrhiza inoculated onion crush and root protuberance crush, separately, were grown further upto 50 days from the emergence. The experiment was carried in six replicates. In control set no inoculum was added.

. Various inorganic constituents like Ca, Na, Mg, K,

Fe, Mn, Zn, and Cu of root and leaves of bhindi were estimated from oven dried plant material following the acid digestion method described by Toth *et al.* (1948). Phosphorus was determined from the same acid digest following the method described by Sekine *et al.* (1965). Nitrogen was determined by following the method described by Hawk *et al.* (1948).

Results and Discussion

Plants inoculated with *G. ambisporum*, either alone or in combination with *Rahnella*, brought about significant change in reducing sugars, total sugars, starch and total carbohydrate contents. The maximum carbohydrate content was noticed in dual inoculated plants followed by inoculation of VAM fungus alone (Table 1). Symbiotic association of mycorrhizal fungus alone recorded 38% increase of total carbohydrates in the root while 40% in the leaves over control and dual inoculation of mycorrhizal fungus and bacteria enhanced it by 48% in the root and 33% in the leaves over mycorrhiza inoculated plants.

Al-Garni (2006) studied the effect of dual inoculation of an arbuscular mycorrhizal fungi and nitrogen-fixer *Rhizobium* on cowpea with respect to physiological indices and reported that microsymbionts significantly increased (5.74%, over control) total carbohydrate content. Iman *et al.* (2008) carried out pot experiments to investigate the influence of single (VAM fungi) or dual (*Bradyrhizobium* and VAM fungi) inoculation as biofertilizer, on the growth and nutrient uptake of peanut (*Arachis hypogaea* L.) plants in virgin sandy soil amended with either rock phosphate or super phosphate and reported the significant increase in total carbohydrate content due to the single or dual inoculations of bio-fertilizers. Nemeč and Guy (1982) recorded greater amounts of total soluble sugars, sucrose, reducing sugars, starch and total nonstructural carbohydrates in citrus root stocks inoculated with *Glomus* spp.

The results indicated that the reducing sugars and total sugar content contents were higher in the leaves of bhindi than in the roots while starch and carbohydrate



The results indicated that the reducing sugars and total sugar content were higher in the leaves of bhindi than in the roots while starch and total carbohydrate contents were greater in the roots than that of in the leaves (Table 1). Maximum reducing sugars ($0.17\text{g } 100^{-1}\text{g dry tissue}$) and total sugar ($0.59\text{g } 100^{-1}\text{g dry tissue}$) were recorded in the leaves of bhindi. Generally, low sugar status enhances photosynthesis, reserve mobilization, and export, whereas the abundant presence of sugars promotes growth and carbohydrate storage (Koch, 1996). Thamizhiniyan *et al.* (2009) carried out experiment to investigate changes in starch content of *Coleus aromaticus* Benth. associated with mycorrhizal fungus and bacteria (*Azospirillum*) and observed a significant increase in the starch content compared to control plants. Increase in 'P' is always associated with an increase in 'N' accumulation. Photosynthetic 'N' use efficiency was enhanced by increased 'P' supply due to AMF. Thus, plants with the nitrogen fixer bacteria and AMF symbiotic associations had higher photosynthetic rates per unit leaf area (Yinsuo *et al.*, 2004). Talaat and Abdallah (2008) studied the effect of seed inoculation with *Rhizobium* and/or soil inoculation with the vesicular-arbuscular mycorrhizal fungus, (*Glomus mosseae*) on growth and total carbohydrate content of faba bean (*Vicia faba* L.) and reported that dual inoculation was of significant importance and resulted in increased growth and total carbohydrate content compared to uninoculated plants. According to Mathur and Vyas (1995), mycorrhizae (*Acaulospora morrowae*, *Gigaspora margarita*, *Glomus deserticola*, *G. fasciculatum*, and *Scutellospora calospora*) inoculated with *Ziziphus mauritiana* Lam. showed increase in net photosynthesis by increasing total chlorophyll and carotenoid contents, ultimately increasing the carbohydrates level. Singh *et al.* (2008) used mycorrhizal strains *Acaulospora laevis*, *Acaulospora scrbiculata*, *Glomus fasciculatum* and mixed AMF strains for inoculation of tissue culture raised *Chrysanthemum* plantlets and reported maximum increase in reducing sugar content in mixed AMF associated plantlets while non reducing and total sugar

contents were maximum in plants inoculated *Acaulospora laevis*. Semra (2004) reported increase in amounts of some reducing sugars (12-47%) (Fructose, α glucose and β glucose) and sucrose and total sugars of pepper (*Capsicum annum* L. cv Cetinel-150) inoculated with *Glomus intraradices*. Charest *et al.* (1993) studied the effect of vesicular-arbuscular mycorrhizae inoculation and chilling on growth and carbohydrate content of *Zea mays* L. and reported increase in growth and higher carbohydrates level in mycorrhizal than in nonmycorrhizal plants. Mathur and Vyas (2000) reported mycorrhizae (*Gigaspora margarita*, *Glomus constrictum*, *G. fasciculatum*, *G. mosseae*, *Sclerocystis rubiformis* and *Scutellospora calospora*) inoculated plants of *Ziziphus mauritiana* Lam. showed increased accumulation of sugars as compared with non-mycorrhizal plants.

Glomus ambisporum either individually or in combination with *Rahnella* significantly increased the Ca, Mg, Na, K, P, Fe, Mn, Zn, Cu and N contents of the root and leaves of bhindi (Table 2). Results indicated that Na, Mg, K, P, Zn, Cu and N contents were higher in the leaves compared to that of root while Na, Fe and Mn were more in the root. Mycorrhiza helps the plant to acquire mineral nutrients from the soil, especially immobile elements such as phosphorus, zinc, and copper and mobile elements such as calcium, potassium, iron, magnesium, manganese and nitrogen as well as it binds heavy metals into roots that restricts their translocation into shoot tissues (Srinivasagam *et al.*, 2013). Wu and Zou, (2009) observed mycorrhizal (*Glomus versiforme*) seedlings of citrus (*Poncirus trifoliata*) exhibited greater growth characteristics with higher concentration of P, K, Ca in the leaves and Fe in the roots. Plants with symbiotic association of mycorrhiza alone accumulated more N than control while dual inoculated plants accumulated N in still higher concentrations. Mycorrhizal colonization had a significant positive impact on the rate of nitrate-N accumulation. The results are consistent with the finding of Tobar *et al.* (1994a; 1994b) that mycorrhizal colonization increased plant nitrate-N uptake. Bacterium - mycorrhizal fungus -bhindi, tripartite symbiosis showed better nitrogen

fixation than that of mycorrhizal-bhindi symbiosis and it is consistent with the finding of Iman *et al.* (2008). This may be due to the fact that there may be a potential in tripartite symbiosis for improving N supply to plants through fixation of atmospheric N (Iman *et al.*, 2008). The result indicated that mycorrhiza colonized roots had 33% higher N than that of nonmycorrhizals while dual inoculation recorded 48% increase in N content over that of control plants. The combined inoculation of mycorrhiza and bacteria increased 11% N content of root over the plant with mycorrhiza alone.

Bloss and Peiffer (1983) reported that guayule (*Parthenium argentatum* Gray.) inoculated with two *Glomus* species had greater concentrations of Ca, Mg, Mn and Fe than in uninoculated plants. Smith and Roncadori (1986) reported all mycorrhizal plants of cotton had increased leaf tissue concentrations of P, Cu, Zn, and Mn with concentrations of Cu, Zn, and Mn being the highest in plants with symbiotic association with *Glomus ambisporum*. Abd El-Raheem *et al.* (1989) showed that the inoculation of tomato plant with *Azotobacter* or *Glomus* either individually or in combination increased the nutrient content (Na, K, Ca, Mg and Fe) of the root, shoot and whole plant. Jiang *et al.* (2008) observed higher absorption of N, P and K by mycorrhizal seedlings of tomato inoculated at sowing, among the inoculations at different stages such as fourth leaf and rooting stage. Amaya-Carpio *et al.* (2009) found that higher levels of P, N, Fe, Cu, and Zn in the leaves of *Ipomoea carnea -fistulosa* inoculated with *Glomus intraradices*. The accumulation of minerals may be attributed to the secretion of growth regulators which accelerate the uptake of minerals in accordance with Nickell (1982) who stated that uptake of K by wheat is accelerated by gibberellic acid. Clear evidence for mycorrhizal involvement in uptake of nutrients other than phosphate is scanty.

Vahdettin *et al.* (2010) carried out the study to determine the effects of three different mycorrhizal fungi (*Glomus mosseae*, *Glomus intraradices* and *Glomus fasciculatum*) on the growth and nutrient contents of four bean cultivars (Onceler, Seker, Terzibaba and Sehirali) which were sown in the growth medium inoculated with mycorrhizal

spores and reported that the mycorrhizal fungi had positive effects on the plant growth and nutrient (N, P, K, Ca, Mg, Fe, Cu, Mn, and Zn) uptake. Hashem *et al.* (2016) reported that inoculation treatments of *Bacillus subtilis* combined with AM fungi enhanced the N, P, K, Mg, and Ca contents in *Acacia gerrardii* tissues.

Significant increase in the mineral nutrient levels in the root and leaves due to dual inoculation of mycorrhizal fungus and bacteria indicates that there is a synergistic or additive beneficial effect of these two organisms on the growth bhindi plant. Bagyaraj and Menge (1978) and Redente and Reeves (1981) recorded a synergistic effect of mycorrhizal fungus *Glomus fasciculatum* and nitrogen fixing *Azotobacter* or *Rhizobium* on nitrogen fixation rates of tomato and sweetvetch (*Hedysarum boreale* Nutt.). Tripartite symbiosis of chickpea with mycorrhizal fungi (*G. intraradices*, *G. mosseae* and *G. etunicatum*) and rhizobia (six strains of *Mesorhizobium ciceri*) was studied by Alireza *et al.* (2011) and they reported that dual inoculation with arbuscular mycorrhizal fungi and bacteria enhanced the nitrogen, phosphorus, zinc, iron and copper content of plants. Tahira *et al.* (2012) reported significant increase in nitrogen and phosphorus contents of *Vigna radiata* inoculated with combination of mycorrhizal fungus and *Agrobacterium* sp. Increase in P is always associated with an increase in N accumulation. Photosynthetic N use efficiency was enhanced by increased P supply due to AMF. Thus, plants with the *Rhizobium* and AMF symbiotic associations had higher photosynthetic rates per unit leaf area (Yinsuo *et al.*, 2004). Results are supported and confirmed by the findings reported by Okon (2014) in *Abelmoschus esculentus* (L.) Moench.



Table 1: Effect of bacteria, mycorrhiza, their combination, mycorrhiza inoculated onion crush and root protuberance crush on carbohydrate content* of *Abelmoschus esculentus* (L.) Moench.

Treatment	Reducing sugars	Total sugars	Starch	Total carbohydrates
	Root			
Control	0.04	0.07	10.66	10.73
Bacteria	0.03	0.06	9.33	9.39
Mycorrhiza	0.07	0.14	14.67	14.81
Bacteria + Mycorrhiza	0.1	0.2	20	20.2
Onion crush	0.07	0.11	12.44	12.55
Protuberance crush	0.1	0.19	21.78	21.97
	Leaf			
Control	0.1	0.32	8.1	8.42
Bacteria	0.1	0.24	7.67	7.91
Mycorrhiza	0.13	0.48	11.35	11.83
Bacteria + Mycorrhiza	0.17	0.59	14.29	14.88
Onion crush	0.13	0.46	10.24	10.7
Protuberance crush	0.15	0.56	15.15	15.71

*Values are in g 100⁻¹g dry tissue.

Table 2 :Effect of bacteria, mycorrhiza, their combination, mycorrhiza inoculated onion crush and root protuberance crush on the mineral content*of *Abelmoschus esculentus* (L.) Moench.

Treatment	Mineral content (g 100 ⁻¹ g dry tissue)									
	Root									
	Ca	Mg	Na	K	P	Fe	Mn	Zn	Cu	N
Control	0.72	0.52	0.012	0.96	0.046	0.062	0.0025	0.0022	0.0015	2.73
Bacteria	0.62	0.59	0.01	0.9	0.054	0.045	0.0022	ND	0.0015	2.85
Mycorrhiza	1.53	0.63	0.016	1.4	0.088	0.125	0.0039	0.01	0.0017	3.55
Bacteria+ Mycorrhiza	1.77	0.82	0.022	2.34	0.185	0.147	0.006	0.015	0.0019	4.03
Onion crush	1.59	0.76	0.018	1.26	0.079	0.1	0.0047	0.0078	0.0018	3.63
Protuberance crush	1.86	0.88	0.026	2.42	0.181	0.163	0.0089	0.016	0.0022	3.74
	Leaf									
Control	0.9	0.76	0.006	1.06	0.062	0.028	0.0023	0.0073	0.0017	3.2
Bacteria	0.82	0.78	0.006	1.02	0.06	0.047	0.0021	0.0072	0.0017	3.38
Mycorrhiza	1.67	0.8	0.008	1.56	0.131	0.096	0.0028	0.023	0.0019	5.47
Bacteria+ Mycorrhiza	1.8	0.99	0.008	2.46	0.196	0.014	0.0032	0.028	0.0024	7.13
Onion crush	1.73	0.82	0.008	1.48	0.177	0.111	0.0028	0.026	0.0021	5.18
Protuberance crush	1.94	1.04	0.01	2.53	0.215	0.154	0.0032	0.031	0.0033	6.77

*Values are in g 100⁻¹ g dry tissue

ND- Not detected.

Conclusion

The present study clearly demonstrated the benefits of vesicular-arbuscular mycorrhizal fungus and *Rahnella* for enhancing the growth of *Abelmoschus esculents* (L.) Moench. Mycorrhizal infection often results in increased root respiration and mycelial biomass which could explore a larger soil volume for nutrients, consequently resulting in their higher uptake rates. In dual inoculation with the *Glomus ambisporum* + *Rahnella* sp. had a higher growth effect than the other treatments. This is due to the mutual positive action of *Rahnella* sp. and VAM fungus that helped in uptake of nutrients which ultimately enhanced the carbohydrate content of the plants.

Acknowledgement

First author is grateful to the college authority and Department of Botany, Shivaji University, Kolhapur, for the permission and facilities provided to complete this work.

References

- Abd El-Raheem, R., El-Shanshoury, M.A., Hassan, M.A. and Abdel-Ghaffar, B.A. (1989).** Synergistic effect of vesicular-arbuscular-mycorrhizas and *Azotobacter chroococcum* on the growth and the nutrient contents of tomato plants. *Phyton.*, (Austria). 29(2): 203-212.
- Al-Garni, Saleh M. Saleh. (2006).** Increased heavy metal tolerance of cowpea plants by dual inoculation of an arbuscular mycorrhizal fungi and nitrogen-fixer *Rhizobium* bacterium. *African Journal of Biotechnology.*, 5(2):133 -142.
- Alireza Tavasolee, Nasser Aliasgharzad, Gholamreza SalehiJouzani, Mohsen Mardi and Ahmad Asgharzadeh. (2011).** Interactive effects of arbuscular mycorrhizal fungi and rhizobial strains on chickpea growth and nutrient content *African Journal of Biotechnology.*, 10(39):7585-7591.
- Amaya-Carpio, L., Davies, F.T., Fox and T He C. (2009).** Arbuscular mycorrhizal fungi and organic fertilizer influence photosynthesis, root phosphatase activity, nutrition, and growth of *Ipomoea carnea* ssp *fistulosa*. *Photosynthetica.*, 47(1):1-10.
- Arumugam, R., Rajasekaran, S. and Najarajan, S.M. (2010).** Response of arbuscular mycorrhizal fungi and *Rhizobium* inoculation on growth and chlorophyll content of *Vigna unguiculata* L. Walp Var. Pusa 151. *J. Appl. Sci. Environ. Manage.*, 14(4):113 – 115.
- Bagyaraj, D.J. and Menge, J.A. (1978).** Interaction between a VA mycorrhiza and *Azotobacter* and their effects on rhizosphere microflora and plant growth. *New Phytologist.*, 80:567-573.
- Bloss, H.E. and Pfeifer, C.M. (1983).** Latex content and biomass increase in mycorrhizal guayule (*Parthenium argentatum* Gray.) under field conditions. *Annual Applied Biology.*, 104:175-183.
- Boureima, S., Dioef, M., Dioef, T.A., Dietta, M., Leye, E.M., Ndiaye, M. and Seck, D. (2007).** Effects of AM inoculation on the growth and development of sesame (*Sesamum indicum* L.). *African Journal of Agricultural Research.*, 3:234–238.
- Carling, D.E., Richle, N.E. and Johnson, D.R. (1978).** Effect of VAM on nitrate reductase and nitrogenase activity in nodulation and non-nodulating soybean. *Phytopathology.*, 68:1590–1596.
- Charest, C., Dalpe, Y., Brown, A. (1993).** The effect of vesicular-arbuscular mycorrhizae and chilling on 2 hybrids of *Zea mays* L. *Mycorrhiza.*, 4(2):89-92.



- Gerdemann, J.W. and Nicolson, T.H. (1963).** Spores of mycorrhizal *Endogone* species extracted from soil by wet sieving and decanting. *Transactions of the British Mycological Society.*, **46**:235.
- Gill, T.S. and Singh, R.S. (2002).** Effect of *Glomus fasciculatum* and *Rhizobium* inoculation on VA mycorrhizal colonization and plant growth of chickpea. *Journal of Mycology and Plant Pathology.*, **32**:162–167.
- Hashem, A., Abd, Allah E.F., Alqarawi, A.A., Al-Huqail, A., Wirth, S. and Egamberdieva, D.(2016).** The interaction between arbuscular mycorrhizal fungi and endophytic bacteria enhances plant growth of *Acacia gerrardii* under salt stress. *Frontiers in Microbiology* doi:10.3389/fmicb.01089.
- Hawk, P.B., Oser, B.L. and Summerson, W.H. (1948).** Practical physiological chemistry. The Blakiston Company, U.S.A.
- Iman, M., El-Azouni, Yasser, Hussein and Lamis, D. Shaaban. (2008).** The Associative effect of VA mycorrhizae with *Bradyrhizobium* as biofertilizers on growth and nutrient uptake of *Arachis hypogaea*. *Research Journal of Agriculture and Biological Sciences.*, **4**(2):187-197.
- Jiang Lang, Li ZhuMei, Huang JianGuo, Yuan Ling, Wu Hong Tian and Liang YongJiang. (2008).** Influences of arbuscular mycorrhizal fungi on growth and selected physiological indices of tobacco seedlings. *Plant Nutrition and Fertilizer Science.*, **14**(1):156-161.
- Kaushik, A., Dixon, R.K. and Mukerji, K.G. (1992).** Vesicular arbuscular mycorrhizal relationships of *Prosopis juliflora* and *Zizipus jujuba*. *Phytomorphology.*, **42**:133–147.
- Koch, K.E. (1996).** Carbohydrate modulated gene expression in plants. *Annu. Rev. Plant Physiol. Plant Mol. Biol.*, **47**:509–540.
- Mathur, N. and Vyas, A. (1995).** Influence of VA mycorrhizae on net photosynthesis and transpiration of *Ziziphus mauritiana*. *Journal of Plant Physiology.*, **147**(3-4):328-330.
- Mathur, N. and Vyas, A. (2000).** Influence of arbuscular mycorrhizae on biomass production, nutrient uptake and physiological changes in *Ziziphus mauritiana* Lam. Under water stress. *Journal of Arid Environments.*, **45**(3):191-195.
- Nelson, N. (1944).** A photometric adaptation of the Somogyi's method for the determination of glucose. *J. Biol. Chem.*, **153**:375-380.
- Nemec, S. and Guy, G. (1982).** Carbohydrate status of mycorrhizal and nonmycorrhizal citrus rootstocks. *Journal of the American Society for Horticultural Science.*, **107**(2):177-180.
- Nickell, L.G. (1982).** Plant Growth Regulators-Agricultural Uses. Pp.59-62. Springer-Verlag Berlin, Heidelberg, New York.
- Okon, I. E. (2014).** Growth response of okra (*Abelmoschus esculentus* (L.) Moench) to arbuscular mycorrhizal fungus inoculation in sterile and non-sterile soil. *International Journal of Research in Humanities, Arts and Literature.*, **2**(11):31-38.
- Ortas, I. (2003).** Effect of selected mycorrhizal inoculation on phosphorus sustainability in sterile and non-sterile soils in the Harrain plains in south Anatolia. *Journal of Plant Nutrition.*, **26**:1–17.
- Rani, P., Aggarwala, A. and Mehrotra, R.S. (1999).** Growth responses in *Acacia nilotica* inoculated with VAM fungus (*Glomus mosseae*), *Rhizobium* sp. and *Trichoderma harzianum*. *Indian Phytopathology.*, **52**:151–153.
- Redente, E.F. and Reeves, F.B. (1981).** Interactions between vesicular-arbuscular mycorrhizae and *Rhizobium* and their effect on sweetvetch growth. *Soil Sei.*, **132**:410 -415.

- Sekine, T., Sasakawa, T., Morita, S., Kimura, T. and Kuratom, K. (1965).** A laboratory manual for physiological studies of Rice (Eds.).
- Semra, DEMIR. (2004).** Influence of arbuscular mycorrhiza on some physiological growth parameters of pepper. *Turk J Biol.*, **28**:85-90.
- Servín, P. M. (2014).** Development of an inoculant of phosphate rock-solubilizing bacteria to improve maize growth and nutrition. Thèse Paola Magallón Servín Doctorat en microbiologie agroalimentaire - Philosophiae doctor (Ph.D.) Québec, Canada ©.
- Singh, Kanwar P., Kumar, K., Ravindra, Prasad, K.V., Pal, Madan and Raju D.V.S. (2008).** Influence of VAM inoculation on root colonization, survival, physiological and biochemical characteristics of *Chrysanthemum* plantlets. *Indian Journal of Horticulture.*, **65**(4):461-465.
- Smith, G.S. and Roncadori, R.W. (1986).** Responses of three vesicular-arbuscular mycorrhizal fungi at four soil temperatures and their effects on cotton growth. *New Phytol.*, **104**:89-95.
- Srinivasagam Krishnakumar, Natarajan Balakrishnan, Raju Muthukrishnan and Selvan Ramesh Kumar. (2013).** Myth and mystery of soil mycorrhiza: A review. *African Journal of Agricultural Research.*, **8**(38):47064717.-
- Stancheva, I., Geneva, M., Zehirov, G., Tsvetkova, G., Hristozkova, M. and Georgiev, G. (2006).** Effects of combined inoculation of pea plants with arbuscular mycorrhizal fungi and *Rhizobium* on nodule formation and nitrogen fixation activity. *Gen. Appl. Plant physiology, Special Issue.*, Pp. 61-66.
- Tahira Yasmeen, Sohail Hameed, Mohsin Triq and Javed Iqbal. (2012).** *Vigna radiate* root associated mycorrhizae and their helping bacteria for improving crop productivity. *Pak. J. Bot.*, **44**(1):87-94.
- Talaat N. B and Abdallah, A. M. (2008).** Response of faba bean (*Vicia faba* L.) to dual inoculation with *Rhizobium* and VA Mycorrhiza under different levels of N and P fertilization. *Journal of Applied Sciences Research.*, **4**(9):1092-1102.
- Thamizhiniyan, P., Panneerselvam, M. and Lenin, M. (2009).** Studies on the growth and biochemical activity of *Coleus aromaticus* Benth. As influenced by AM fungi and *Azospirillum*. *Recent Research in Science and Technology.*, **1**(6):259–263.
- Tobar, R.M., Azcon, R. and Barea, J.M. (1994a).** Improved nitrogen uptake and transport from ¹⁵N-labelled nitrate by external hyphae of arbuscular mycorrhiza under water-stressed conditions. *New Phytologist.*, **126**:119–122.
- Tobar, R. M., Azcon, R. and Barea, J.M. (1994b).** The improvement of plant N Acquisition from an ammonium-treated, drought-stressed soil by the fungal symbiont in arbuscular mycorrhizae. *Mycorrhiza.*, **4**:105–108.
- Toth, S.J., Prince, A.L., Wallace, A. and Mikkenlsen, D.S. (1948).** Rapid quantitative determination of eight mineral elements in plant tissue. Systematic Procedure involving use of a flame photometer. *Soil Sci.*, **66**:459-466.
- Vahdettin Ciftci1, Onder Turkmen, Ceknas Erdinc and Suat Sensoy. (2010).** Effects of different arbuscular mycorrhizal fungi (AMF) species on some bean (*Phaseolus vulgaris* L.) cultivars grown in salty conditions. *African Journal of Agricultural Research.*, **5**(24):3408-3416.
- Wu Qiang Sheng and Zou Ying Ning. (2009).** Mycorrhizal influence on nutrient uptake of citrus exposed to drought stress. *Philippine*



Agricultural Scientist., 92(1):3338.-

YanJun Guo, Yu Ni and Jianguo Huang. (2010).

Effects of *Rhizobium*, arbuscular mycorrhiza and lime on nodulation, growth and nutrient uptake of lucerne in acid purplish soil in China. *Tropical Grasslands.*, 44:109–114.

Yinsuo Jia, Vincent Myeles Gray and Colin John

Straker. (2004). The influence of *Rhizobium* and arbuscular mycorrhizal fungi on Nitrogen and Phosphorus accumulation by *Vicia faba* L. *Annals of Botany.*, 94(2):251-258.



Effect of NaCl on growth and development, polyphenol content and proline accumulation in the leaves of *Trianthema portulacastrum* L. grown in sand and soil culture.

J.M. Patil* and ¹B. A. Karagade

*Doodhsakhar Mahavidyalaya, Bidri.

¹Department of Botany, Shivaji University, Kolhapur.

KEYWORDS

Growth, Polyphenols, Proline, salinity, *Trianthema*.

Corresponding Author
Email
shubhangijmp@gmail.com

ABSTRACT

The effect of NaCl salinity (sand and soil culture) on root length, shoot length, total length (height of plant), biomass (fresh and dry wt.), moisture percentage, polyphenol content and proline accumulation in a sodium loving plant, *Trianthema portulacastrum* L. has been investigated. The plant exhibited better performance in growth and development under low salinity (100 mM) level, 300 mM salt concentration was harmful. Polyphenol content was decreased due to NaCl salt stress in sand and soil culture. Proline accumulation was significant under increasing NaCl salinity levels in both culture media.

Introduction

Salinization of agricultural soils is a worldwide concern, especially in irrigated lands. Saline soil is characterized by the presence of toxic levels of sodium and its chlorides and sulphates. Salt induces osmotic stress by limiting absorption of water from soil and ionic stress resulting from high concentrations of toxic salt ions within plant cells. Plants have evolved a variety of protective mechanisms for survival and growth under these unfavorable environmental conditions. The accumulation of ions and osmolytes such as proline prevents water loss and ion toxicity. Another most important factor of salt tolerance mechanisms is the ability of plant cells to adjust osmotically and to accumulate organic solutes. These accumulated compounds are important for cell osmoragulation and protection of subcellular structure (Munns, 2002). Salinity tolerance is defined as the ability of plants to continuously grow under salt

stress conditions (Munns, 2002). According to Maggio *et al.* (2010) high salinity levels can cause water deficit, nutrient deficiency and ion toxicity leading to molecular damage and finally plant death.

The present study was made to investigate the effect of NaCl on growth and development, polyphenol content and proline accumulation in *Trianthema portulacastrum* L. grown in sand and soil culture.

Material and Methods

The plants were raised from seeds in acid free silica sand with Hoagland nutrient medium as well as in soil culture, and treated with 0.00 (Control), 100, 200 and 300 mM NaCl for two months. The treatments were given twice a week, alternating with water to check the loss of water from pots and to avoid excess accumulation of salts in the pots. Drainage of the water and salt solution was

well maintained. Two months after the growth in saline media the plants were analysed for different parameters.

1) Growth analysis:

For growth analysis 5 plants from every treatment pot were carefully uprooted and washed with water. Water drops from the plant surface were removed using blotting paper. Each plant was then analysed.

a) Root Length:

Root length of each plant was measured with thread and meter scale. The average and standard deviation were calculated.

b) Shoot Length:

Shoot length of each plant was also measured as above and the data was statistically analysed.

c) Total Length:

The root length and shoot length of respective plant were added together to find out height (total length) of the plant. Average and standard deviation were also calculated.

d) Fresh weight per plant:

The fresh weight of each plant from each treatment was measured and average fresh weight per plant and standard deviation were calculated.

e) Dry weight per plant:

After recording fresh weight the respective plants were kept in oven separately at 60°C until they gave constant dry weight, which was recorded. Then the average dry weight per plant and standard deviation were calculated.

f) Moisture %:

With the help of dry weight and fresh weight values for plants, the moisture percentage was calculated by using the formula-

$$\text{Moisture percentage} = \frac{\text{fresh wt} - \text{dry wt}}{\text{fresh wt}} \times 100$$

All the results were statistically analysed.

2) Polyphenols:

Polyphenols were estimated from fresh leaves according to Folin and Denis (1915). The polyphenol content is expressed as mg 100⁻¹ g fresh tissue.

3) Proline:

Free proline content of the leaves was estimated following the method by Bates *et al.* (1973). The proline content is expressed as mg 100⁻¹ g fresh tissue.

Result and discussion

It is evident from Tables 1 and 2, that NaCl salinity caused an increase in the root length, shoot length, total length, fresh weight, dry weight and moisture content under low (100 mM NaCl) level of salinity. The plants exhibited better performance in growth and development under low salinity levels in both culture conditions. On the other hand, growth and development of this plant was affected at the higher salt concentration (300 mM NaCl). It is interesting to note that even though there was decrease in the growth of the plants (under higher level of salinity i.e. 300 mM), these were not only surviving but also growing well except that there was stunted growth. These results are in accordance with Salunkhe and Karadge (1989) in *Dodonaea viscosa* L. and Patil (2014) in *Prosopis juliflora*.

The effect of NaCl salinity on polyphenols content of the leaves of *Trianthema portulacastrum* L. grown in sand and soil culture is shown in Fig.1. It is evident that the total polyphenols content was decreased by about 22 to 39 % over the control in sand culture under saline conditions. However, in case of soil culture polyphenols content was slightly increased under low concentration only (100mM) and then decreased under higher concentrations of NaCl.

Reduction in polyphenol content due to salinity has also been noticed by different workers in different plants. Karadge (1981) observed a linear decrease in polyphenol content of leaves of *Portulaca oleracea* with increasing concentrations of NaCl in the rooting medium. Giannakoula *et al.* (2012) noticed a reduction in the phenolic content (Resveratrol, P-coumaric acid, Gallic acid, Kaempferol, Quercetin, Catechin, Epicatechin, Rutin) of lentil seeds due to NaCl salt stress. Patil (2014) also reported a decrease in total polyphenols content of the leaves of *Prosopis juliflora* by about 23 to 53% over the control due to NaCl salinity stress.



NaCl Treatment (mM)	Root length (cm)	Shoot length (cm)	Total length (cm)	Biomass plant ⁻¹ (g)		Moisture %
				Fresh wt.	Dry wt.	
0.00 (Control)	8.12 ± 1.67	39.40 ± 8.20	47.52 ± 9.65	16.56 ± 9.58	1.84 ± 1.07	88.88 ± 0.53
100	9.17 ± 1.71 (+12.93)	52.50 ± 7.85 (+33.24)	61.67 ± 9.5 (+29.77)	23.19 ± 10.59 (+40.03)	2.50 ± 1.27 (+ 35.86)	89.21 ± 0.70 (+ 0.37)
200	7.90 ± 1.53 (-2.70)	49.60 ± 7.56 (+25.88)	57.54 ± 8.33 (+21.08)	20.67 ± 9.96 (+ 20.81)	2.44 ± 1.09 (+32.60)	88.19 ± 0.26 (-0.77)
300	7.50 ± 0.91 (-7.63)	35.10 ± 5.11 (-10.91)	42.60 ± 5.64 (-10.35)	11.38 ± 5.43 (-31.28)	1.50 ± 0.64 (-18.47)	86.49 ± 3.37 (-2.68)
MSI	302.58	348.22	340.50	333.57	350.00	296.90

Table2. Effect of NaCl salinity on growth and development of *Trianthema portulacastrum* L. grown in soil culture.

NaCl Treatment (mM)	Root length (cm)	Shoot length (cm)	Total length (cm)	Biomass plant ⁻¹ (g)		Moisture %
				Fresh wt.	Dry wt.	
00 Control	9.26 ± 0.55	24.00 ± 1.32	33.62 ± 1.55	9.05 ± 0.14	1.34 ± 0.07	85.19 ± 0.83
100	12.80 ± 1.22 (+38.22)	33.66 ± 3.51 (+40.80)	46.46 ± 3.52 (+38.19)	12.18 ± 1.46 (+34.58)	1.79 ± 0.16 (+33.58)	85.30 ± 1.05 (+0.13)
200	11.50 ± 1.00 (+24.19)	27.80 ± 4.91 (+15.83)	39.30 ± 4.91 (+16.89)	9.97 ± 0.94 (+10.16)	1.53 ± 0.14 (+14.17)	84.65 ± 0.12 (-0.64)
300	7.40 ± 0.12 (-20.08)	16.60 ± 1.22 (-30.83)	24.00 ± 1.10 (-28.61)	4.34 ± 0.24 (-52.04)	0.70 ± 0.05 (-47.76)	83.87 ± 0.39 (-1.54)
MSI	109.07	108.41	325.19	97.56	100.00	99.31

Fig.1. Effect of NaCl salinity on polyphenols concentration in the leaves of *Trianthema portulacastrum* L. grown in sand and soil culture.

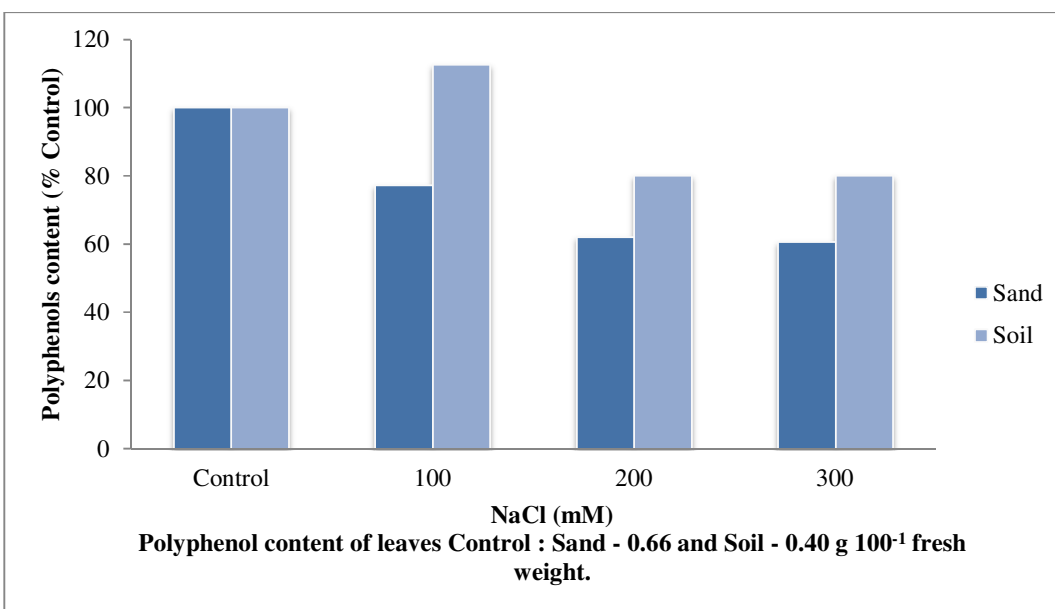
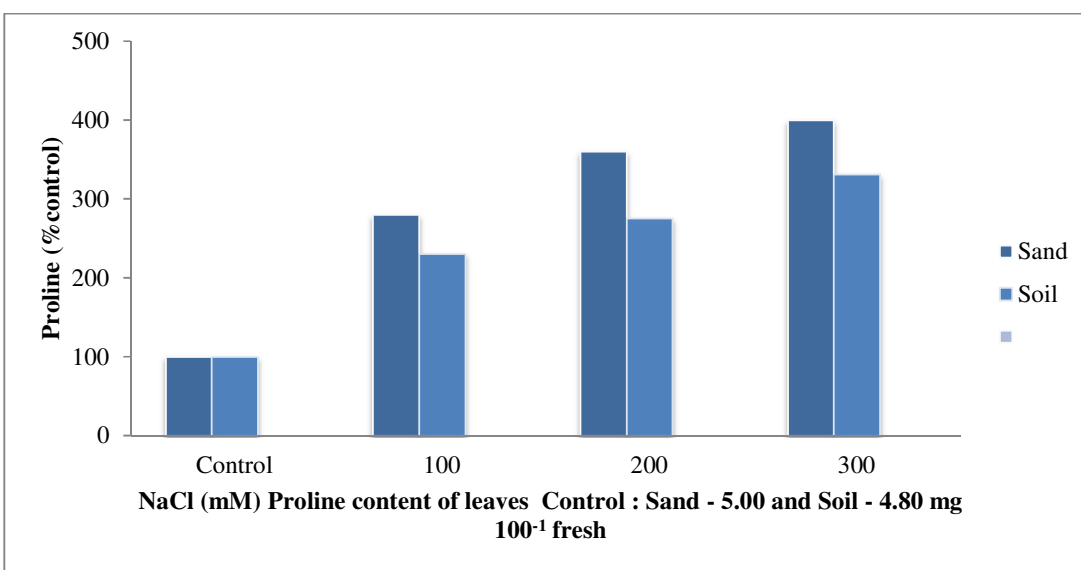


Fig.2. Effect of NaCl salinity on Proline concentration in the leaves of *Trianthema portulacastrum* L. grown in sand and soil culture.



The effect of NaCl salinity on proline concentration in the leaves of *Trianthema portulacastrum* L. grown in sand and soil culture is represented in Fig. no.2. From the results it is clear that the level of proline in the leaves of this plant was increased with increasing NaCl salinity levels in sand and soil

culture. Proline is an important secondary amino acid. Generally it is accumulated in the tissue of plants growing under salt stress. The accumulated proline helps in osmotic adjustment of such plants. It acts as an enzyme protector. The accumulation of osmolytes such



proline is a well known adaptive mechanism in plants against salt stress conditions. It has also been suggested that pro-accumulation can serve as a selection criterion for the tolerance of most species to stressed conditions (Parida and Das, 2005; Ashraf and Foolad, 2007). According to Liang *et al.* (2013) the amino acid proline is utilized by different organisms to offset cellular imbalance caused by environmental stress. Proline as a stress adaptor molecule indicates that proline has a fundamental biological role in stress response.

Many research workers have confirmed the role of proline as a compatible osmolyte, osmoprotectant and its role in salt stress tolerance. According to Tripathi *et al.* (2007) proline helps in osmotic adjustment under salt stress. They observed increase in proline content in *Najas gramenia* and *Najas indica* in response to the salt treatments. Accumulation of proline in *H. strobilaceum* allows seedlings to maintain a lower internal osmotic potential than that of the growth medium, which is necessary for water uptake in saline soils (Juan *et al.*, 2001). From the present investigation, it is clear that an increase in proline content in the leaves of *Trianthema portulacastrum* grown in sand and soil culture might be for osmotic adjustment under NaCl salinity stress.

Acknowledgement

Authors are thankful to the Head department of Botany, Shivaji University, Kolhapur (MS), India for his valuable suggestions.

References

Asharf M and Foolad MR (2007) Roles of glycinebetaine and proline in improving plant abiotic stress resistance. *Environ. Exp Bot.* **59** (2) : 206-216.

Bates LS, Waldren RP and Teare ID (1973) Rapid determination of free proline for water stress studies. *Plant and Soil.* **39** :205-207.

Folin O and Denis W (1915) A colorimetric estimation of phenols (and phenol derivatives) in urine. *J. Biol. Chem.* **22** :305-308.

Glannakoula A, Ilias IF, Dragisicmaksimov JJ, Maksimovic VM and Zivanovic BD (2012) Does overhead irrigation with salt affect growth, yield, and phenolic content of lentil plants? *Arch. Biol. Sci. Belgrade.* **64** (2) : 539-547.

Juan AP, Jose FC and Luis RD (2001) Seed germination, growth and osmotic adjustment in response to NaCl in a rare succulent halophyte from southeastern Spain, *Wetlands.* **21**(2) :256-264.

Karadge BA (1981) Physiological studies in succulents. A Ph. D. Thesis submitted to Shivaji University, Kholapur, (India).

Liang X, Zhang L, Natarajan SK and Becker DF (2013) Proline mechanism in stress survival. *Antioxid Redox Signal.* **19** (9) : 998-1011.

Maggio A, Barbieri G, Raimondi G and De Pascale S (2010) Contrasting effects of GA₃ treatments on tomato plants exposed to increasing salinity. *J Plant Growth Regul.* **29** :63-72.

Munns R (2002) Comparative physiology of salt and water stress. *Plant Cell Environ.* **25**: 239-250.

Parida AK and Das AB (2005) Salt tolerance and salinity effects on plants. a review. *Ecotoxicol Environ Saf.* **60** (3) :324-349.

Patil AV (2014) Influence of salt and water logging stress on physiology of *Prosopis juliflora* (SW)DC. A thesis submitted to Shivaji University, Kolhapur, (India).

Salunkhe SS, Karadage BA (1989) Influence of salinity and water stress on growth and constituents of *Dodonaea viscosa* L. *Geobios.* **16**:252-258.

Tripathi SB, Gurumurthi K, Panigrathi AK and Shaw BP

(2007) Salinity induced changes in proline and betaine contents and synthesis in to aquatic macrophytes differing in salt tolerance. *Biologia Plantarum*. 51(1):110-115.



Floristic Diversity of Wild Relatives of Grain Legumes from Nashik District

¹Mayur S Patil and ²Sanjay G Auti

¹KKHA Arts, SMGL Commerce and SPHJ Science College, Chandwad-423101, India

²HPT Arts and RYK Science College, Nashik 422005, India

KEYWORDS

Wild relatives of Grain Legumes, Floristic Diversity, Leguminosae Phytogeography, etc.

ABSTRACT

Wild relative of plants have always been considered for crop improvement. Wild relatives show some unique features viz. drought resistance, growth without fertilizers, growth with minimal use of water, etc. Such characters will have a greater impact on crop improvement qualitatively and quantitatively, if we are able to introduce it in the cultivated varieties. Wild relatives grow in extreme conditions in forest regions without any supplement of fertilizers and with minimum water supply. Leguminosae is the economically very important family as all the pulses and other economically valued plant belong to this family. Pulses are very rich source of dietary proteins especially for vegetarian peoples. Recent studies in pulses show declining trend. It may be due to vagaries of monsoon, untrained agricultural practices, etc. Wild relatives of pulses or grain legumes being having unique characters can be used for breeding practices with cultivated varieties. Present investigation deals with floristic studies of wild relatives of grain legumes from Nashik district.

Corresponding Author
Email

mayurpatil149@gmail.com

Introduction

Wild plants have been used since ancient times during civilization of India. Use of various wild and domestic plants is also mentioned in ayurveda as medicine. Plants have always been inevitable part of human life. Ancient peoples use plants to treat the disease. Plants fulfil all the basic needs of human life viz. food, shelter and clothing. Leguminosae is one of the most important economically valuable families in the plants. Leguminosae has economically important members like pulses, vegetables, etc. Pulses (grain legumes) are very important source of protein, especially, for vegetarian peoples. They are rich in number of essential amino acids. Wild plants

have always been important in breeding practices so as to incorporate desirable characters in cultivars. Wild relatives shows some unique characteristics like drought resistance i.e. ability to grow in scarcity of water, ability to grow without the help of fertilizers, etc. Such characters can be introduced in cultivated varieties to get the improved varieties.

Our study area Nashik district is very rich in plant diversity. It is gifted with the parts of Northern Western ghat which ranges from Kalsubai peak (Bhandardara) up to the Salher- Mulher (Satana). It includes phytodiversity rich regions like Anjaneri plateau, Brahmagiri (Tryambakeshwar), Nanduri (Vani), Harsul, Peth, Surgana, Mangi-Tungi, Goldari, Chandwad, etc. For the present



a. *Vigna sublobata*



b. *Vigna trilobata*



c. *Vigna vexillata*



d. *Vigna sahyadriana*



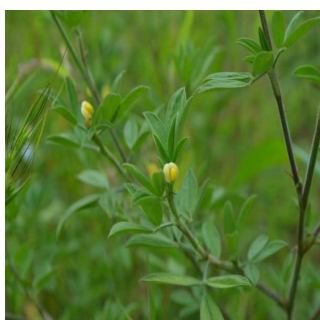
e. *Macrotyloma Uniflorum*



f. *Vigna unguiculata*



g. *Canavalia spp.*



h. *Lathyrus spp. (wild pea)*



investigation on floristic diversity, the region of western ghat of Nashik district was explored many times during monsoon and winter season.

Results and Discussion

During field visits, above mentioned wild relatives of grain legumes such as *Vigna sublobata*, *Vigna trilobata*, *Vigna umbellata*, *Vigna sahyadriana*, *Vigna unguiculata*, *Macrotyloma uniflorum*, *Lathyrus Species*, *Canavalia species*, *Phaseolus species*, etc. were found. The phytogeographical location for *Vigna sublobata* is Padli near Ghoti, Igatpuri in Maharashtra. *Vigna trilobata* and *Macrotyloma uniflorum* were found near Chandwad, Nashik. *Lathyrus Species*, *Canavalia species* and *Phaseolus species* were found near Goldari, Vani, Nashik. *Vigna sublobata* and *Vigna trilobata* were found at Igatpuri, Nashik. *Vigna sahyadriana* was found near Bhandardara.

Pods were collected and photographs were taken for identification. Plants were identified with help of "Genus *Vigna savi* in India -Illustrated guide for species identification and with the help of flora of Nashik District by Lakshminarsimhan".

Taken in to account the above work, it is concluded that, the Nashik district in Maharashtra is very rich as far as phytodiversity, more specifically; the diversity of wild relatives of grain legumes is concerned. Nashik district has a part of north western ghat which is declared as the hotspot of biodiversity as there are number of endemic plants are present on western ghat.

The above study regarding floristic diversity will be useful to find out any variation in the morphology of wild relatives of Grain legumes.

References

Anuja Bhat, et al., Wild relatives of crop plants in India, National bureau of plant genetic resources, Agro- biodiversity, PGR-41.

S. R. Yadav, M. M. Aitwade, K. V. Bhat, S. Ramarao.

Genus *Vigna Savi* in India: an illustrated guide for species identification, National bureau of plant genetic resources, New Delhi, pp. 19-31.



Effect of Foliar Acetyl Salicylic Acid Application on Total Nitrogen and Soluble Nitrogen Fractions of Groundnut

S H Jadhav

P. G. Department of Botany, Plant Physiology Section, Krishna Mahavidyalaya, Rethare, Satara - 415 110, (MS) India

KEYWORDS

Acetyl salicylic acid, groundnut, nitrogen content, nitrate, soluble proteins.

Corresponding Author
Email
jsunita1210@gmail.com

ABSTRACT

A field experiment was conducted to understand the influence of foliar acetyl salicylic acid (ASA) application on nitrogen content and soluble nitrogen fractions of groundnut plants. In the study, leaf and root nitrogen content, leaf nitrate content and soluble protein contents of leaves and seeds were determined. Groundnut plants were treated with foliar ASA application at different concentrations (5, 50, 100 and 200 ppm). The results showed decreased nitrate content in leaves and increased total nitrogen content as well as soluble proteins in leaves and seeds. It appeared that ASA could help to diminish the adverse effect of nitrate accumulation in groundnut plant whereas increased soluble protein contents might be involved in improving nutritive quality of groundnut. According to our results, the application of 100 ppm ASA should be recommended to improve nutritive quality of groundnut seeds.

Introduction

The groundnut is a major oilseed legume crop of India. Groundnut seeds are rich source of edible oil and proteins. Several workers reported health benefits of groundnut seeds consumption such as control of weight, prevention of Alzheimer cardiovascular disorders and cancer inhibition (Awad et al. 2000; Peanut Institute 2002). The main agenda before plant scientists is to develop high yielding and disease resistant varieties. In case of oilseed crops the main challenge is to develop strategies to improve nutritive quality. Several evidences recognized influence of climate, irrigation, fertilizers and plant growth regulators on the yield, protein, amino acid content and oil content of groundnut (Verma et al. 2008; Jadhav and Bhamburdekar, 2014). Salicylic acid is an endogenous growth regulator of phenolic nature and is considered as a potent plant hormone due to its role in plant

metabolism (Hayat et al. 2010). Salicylic acid and its analogs have been reported to induce significant effects on various physiological aspects in plants. It has been recognized that salicylic acid is required in the signal transduction for the induced systemic acquired resistance against some pathogenic infections (Sayeed, et al. 2011; Idress, et al. 2011). Acetyl salicylic acid (ASA) is one of the acetyl derivative of salicylic acid. Several studies documented influence of ASA on flowering, stomatal conductance, plant productivity, fatty acid composition and post harvest physiology (Tuna et al. 2007; Jadhav and Bhamburdekar, 2012 and 2014). Keeping the above points in view, the present research was undertaken to understand the effect of ASA applied as foliar spray on the soluble nitrogen fractions of groundnut plants.

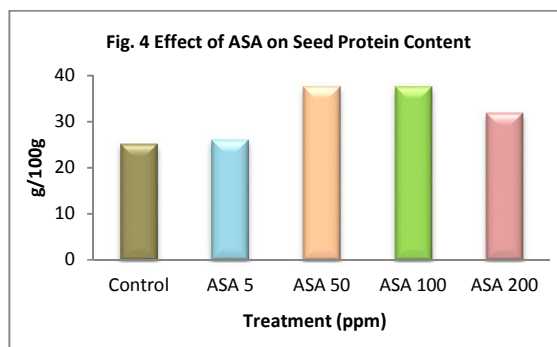
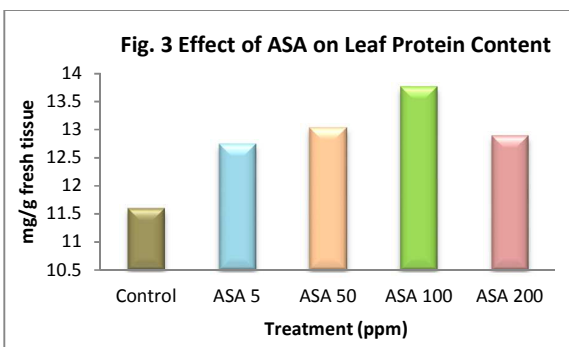
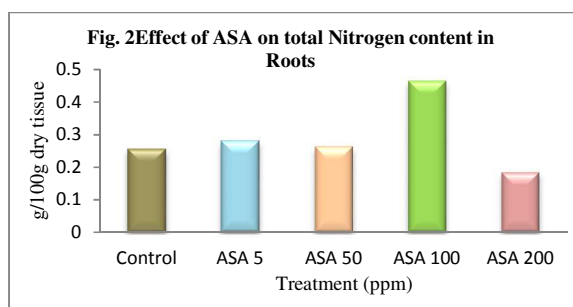
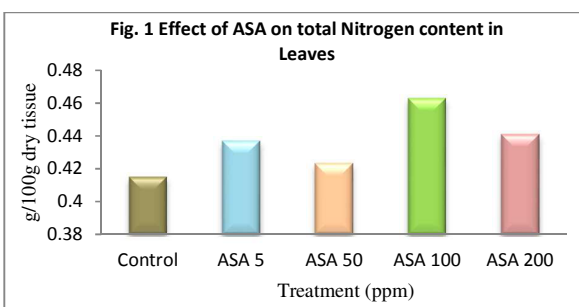
seeds were sterilized with 0.01% mercuric chloride solution and sown in 5×3 m field plots in complete randomized block design.

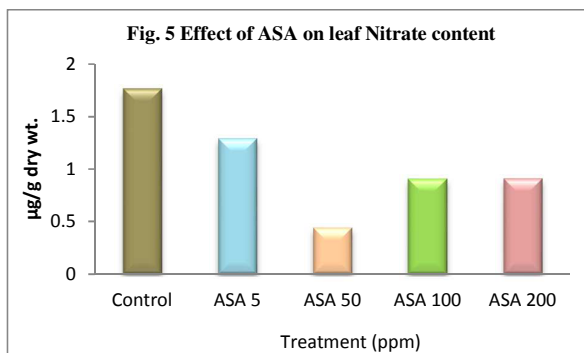
Material and Methods

The certified seeds of groundnut cultivar SB-11 were purchased from agricultural research station, Karad. The seeds were sterilized with 0.01% mercuric chloride solution and sown in 5×3 m field plots in complete randomized block design. At the age of 30 days after sowing, the foliage was sprayed uniformly with different concentrations of ASA (5, 50, 100 and 200 ppm) in 3 equal doses by keeping 4 days interval. The plants receiving foliar sprays of distilled water served as control. The following parameters were analyzed at the end of treatments:

Soluble Nitrogen Fractions: Oven dried 500 mg leaf material was homogenized in 20 ml 80% alcohol and filtered through Whatman No. 1 filter paper using Buchner’s funnel. The filtrate was then condensed on boiling water bath upto 1-2 ml. To this about 10 ml of distilled water were added and mixed well. All the washings and the filtrate were collected and final volume was made to 100 ml with distilled water. From this nitrate content and soluble proteins were estimated.

Nitrate (NO₃⁻) and Soluble Protein Content: The nitrate content was determined by the treatment of Kolhoff and Noponen (1933) whereas the soluble proteins of leaves were determined following the method by Lowry et al. (1951). Protein content of seeds of ASA treated groundnut plants was determined by using the Kjeldahl N analysis method (Nelson and Sommers 1980).





Results and Discussion

The results stated that the foliar spray of all the applied concentrations of ASA effectively enhanced the total leaf and root nitrogen content as well as leaf and seed protein contents. In particular the treatment of 100 ppm ASA noticeably increased nitrogen and soluble protein contents in groundnut (Fig. 1-4). In contrast to it, decreased leaf nitrogen content was recorded over control with all the concentrations of ASA (Fig. 5). The nitrogen requirement of groundnut is much more than cereals, as it contains high proteins. Our results show close conformity with the findings reported by Tuna et al. (2007) in Maize. They stated SA and related compounds mediated induction in nitrogen contents. The reduced nitrate content with ASA in present study is in agreement with the results reported by El-Khallil (2009). He noticed correlation in decrease nitrogen content and increased Ca^{2+} which has shown to increase the activity of nitrate transporter. Several reports have been recognized positive effect of SA and its analogs on protein contents of plants. The findings of present work pertinent to enhancement in protein levels show conformity with those of Paul and Sharma (2002).

It is clear from the present study that increased 'N' content due to ASA may possibly favors the uptake of other minerals as indicated by Moussa (2000). Higher nitrogen contents in roots might be involved in induction of nodule development of leghemoglobin content. Decreased nitrate content could help to diminish the adverse effects of nitrate accumulation in plants.

Conclusion

As groundnut is legume crop and rich source of protein, ASA mediated noticeable enhancement in nitrogen content and soluble proteins may prove effectual to improve nutritive quality of groundnut seeds. ASA upregulate the protein content which also beneficial in immune response in groundnut crop against adverse biotic and abiotic conditions.

References

- Awad AB., Chan KC, Downie AC, Fink CS (2000)** Peanuts as a source of B-sitosterol, a sterol with anticancer properties. *Nutrition and Cancer* 36: 238-241.
- El-Khallal SM, Hathout TA, Ratheim AA, Abd-Almalik AK (2009)** Brassinolide and salicylic acid induced growth, biochemical activities and productivity of maize plants grown under salt stress. *Research Journal of Agriculture and Biological Sciences* 5(4): 380-390.
- Hayat Q, Hayat S, Irfan M, Ahmad A. (2010)** Effect of exogenous salicylic acid under changing environment: A review. *Environmental and Experimental Botany* 68: 14–25.
- Hawk PB, Oser BL., Summeson WH (1984)** *Practical Physiological Chemistry* Pb. The Blakiston Co., USA.
- Idrees M, Naeem N, Aftab T, Khan MM, Moinuddin (2011)** Salicylic acid mitigates salinity stress by improving antioxidant defense system and enhances vincristine and vinblastine alkaloids production in prewinkle (*Catharanthus roseus* (L) G. Don). *Acta Physiol. Plant* 33: 987 - 999.
- Jadhav SH, Bhamburdekar SB (2012)** Effect of acetyl salicylic acid on growth and biochemical attributes of *Arachis hypogaea* L. *Proceedings of state level*

seminar, Recent Innovative Trends in Plant Mahatma Phule A.S.C. College, Panvel pp. 160-164.

Jadhav SH, Bhamburdekar SB (2014) Effect of acetyl salicylic acid on fatty acid composition of Groundnut (*Arachis hypogaea* L.) seeds. World Journal of Pharmacy and Pharmaceutical Sciences 3(2): 1968-1975.

Kolhoff IM, Noponen GE (1933) Diphenylamine sulfonic acid as a reagent for the colorimetric determination of nitrates. J Am Chem Soc 55, 1448-53.

Lowry OH, Rosenbrough NJ, Furr AL, Randall RJ (1951) Protein measurement with folin phenol reagent. J. Biol. Chem 193: 262-263.

Moussa BIM (2000) Effect of nitrogen source, rate and magnesium on yield, oil, protein content and mineral nutrition of peanut. Egyptian Journal of Soil Science 40 (4): 495-511.

Nelson DW, Sommers LE (1980) Total nitrogen analysis of soil and plant tissues. J. AOAC 63: 770-779.

Paul PK, Sharma P D (2002) *Azadirachta indica* leaf extract induces resistance in barley against leaf stripe disease. Physiology and Molecular Plant Pathology 61: 3-13.

Sayeed S, Anjum NA, Nazar R, Iqbal N, Masood A, Khan NA (2011) Salicylic acid-mediated changes in photosynthesis, nutrients content and antioxidant metabolism in two mustard (*Brassica juncea* L.) cultivars differing in salt tolerance. Acta Physiol. Plant 33: 877-886.

Tuna AL, Kaya C, Dikilitas M, Yokas I, Burun B, Altunlu H (2007) Comparative effects of various salicylic acid derivatives on key growth parameters and some enzyme activities in salinity stressed maize (*Zea mays* L.). Plants Pak J. Bot 39 (3): 787-798.

Verma A, Malik CP, Sinsinwar YK, Gupta VK (2008) Role of some Growth Regulators on Crop Physiology Parameters Influencing Productivity in Peanut. *J. Plant Sc. Res.*, 24: 1670-70.



Biopotential of *Trichoderma sp.* against *Fusarium oxysporum f.sp. dianthi* causing wilt of carnation in the presence of micronutrients

¹R. M.Waghmare, ²M. B.Waghmare , ¹S.K Mengane,¹ D.S Pawar, ³S.S. Kamble

¹ Department of Botany, M.H. Shinde Mahavidyalaya, Tisangi

²Department of Botany, The New College, Kolhapur

³Department of Botany, Shivaji University, Kolhapur

KEYWORDS

Fusarium oxysporum f.sp. dianthi *Trichoderma sp.*
Micronutrients.

Corresponding Author
Email

waghmaremahendra@gmail.com

ABSTRACT

Micronutrients are the key elements for the proper growth and development of the living organisms. Their deficiency inhibits the growth of microorganism. Therefore in the presence study investigation has been made on the antagonistic potential of *Trichoderma sp.* against *Fusarium oxysporum f.sp. dianthi* causing wilt of carnation in presence of different micronutrients. In this study two micronutrients were taken to study the antagonistic potential of *Trichoderma* species against *Fusarium* at 0.01, 0.02, 0.03 and 0.04 µg/ml. copper and zinc in the medium increased the antagonistic potential of *Trichoderma* species against *Fusarium oxysporum f. sp.dianthi*.

Introduction

Dianthus chinensis L. is an important ornamental plant cultivated in the gardens. It increases the aesthetic value of garden as well as house. It is small herbaceous plant having very attractive flowers. It belongs to the family Caryophyllaceae, It is anthelmintic, antibacterial, antichloristic, diaphoretic, diuretic, febrifuge and haemostatic. The old leaves are crushed and used for clearing the eyesight (Duke and Ayensu, 1985) . Such economically important medicinal and ornamental plant suffered from the wilt disease caused by *Fusarium oxysporum f.sp. dianthi*. Therefore for the high yield it is necessary to control the disease, but there are number of side effects reported in the chemical method of disease management. Hence in the present study different *Trichoderma sp.* used

against the pathogen in the presence of different micronutrients.

Material and Methods

Naturally infected wilt samples of carnation brought to the Botany laboratory of Shivaji University, Kolhapur in the sterile polythene bags. Surface sterilization of infected samples was made with 0.1% mercury chloride, washed the material with sterile distilled water and removed the traces of mercury choride. Samples were cut into small pieces and cultured on the Czapek Dox Agar (CDA) medium. After 4-5 days different fungal colonies were observed in the petriplates. Pathogen was identified with the help of standard mycological literature(Subramanian,1971) Pure culture of *fusarium oxysporum f.sp. dianthi* was maintained on Czapek Dox Agar medium in BOD incubator for further study.

In this study effects of micronutrients on antagonistic potential of *Trichoderma* species were studied. For this study micronutrients (copper, zinc,) were mixed in combination (0.01, 0.02, 0.03 and 0.04 µg/ml).to find out the antagonistic potential of *Trichoderma* species against *Fusarium oxysporum* f. sp. *dianthi* by Vincent, (1947).

Isolation of *Trichoderma* sp.

Rhizosphere soils were collected from Kolhapur and *Trichoderma* sp. were isolated by dilution plate technique (Johnson,1957) Both isolates were grown on CDA medium (Ricker and Ricker, 1936). The isolated species were identified (Kubicek and Harman, 2002; Nagamani and Manoharachary, 2002) . Pure cultures of *Trichoderma* were maintained on the CDA medium for further study in BOD Incubator .

Screening of *Trichoderma* sp. against *Fusarium oxysporum* f.sp. *dianthi* by dual culture method :

Antagonistic potential of *Trichoderma* spp. was evaluated against *Fusarium oxysporum* f.sp. *dianthi* by dual culture technique Followed (Morton and Stroube,1955). The growth inhibition was calculated by using the formula (Vincent ,1947)

Results and Discussion

Antagonistic potential of all *Trichoderma* species against *Fusarium oxysporum* f.sp. *dianthi* at 0.01, 0.02, 0.03 and 0.04 µg/ml increased the antagonistic potential of *Trichoderma* species. (Table 1and 2). These results are supported by the earlier workers (waghmare and Kamble, 2011; Hesamadin ,2010; Kumar et.al.,2007.)

Table 1. Effect of Zinc on the antagonistic potential of *Trichoderma* species against *Fusarium oxysporum* f. sp. *dianthi* causing wilt of carnation (in *Vitro*).

<i>Trichoderma</i> species	Antagonistic potential in %				
	Concentration of Micronutrients (Zn) in µg/ml				
	0.01	0.02	0.03	0.04	Control
<i>T. harzianum</i>	63.33	64.44	65.55	66.66	63.33
<i>T. koningii</i>	65.55	66.66	68.88	70.00	64.44
<i>T. pseudokoningii</i>	53.33	55.55	57.77	58.88	52.22
<i>T. virens</i>	58.88	61.11	63.33	66.66	57.77
<i>T. viride</i>	62.22	65.55	68.88	70.00	60.00

Table 2. Effect of Copper on the antagonistic potential of *Trichoderma* species against *Fusarium oxysporum* f. sp. *dianthi* (Fo- 2) causing wilt of carnation (in *Vitro*).

<i>Trichoderma</i> species	Antagonistic potential in %				
	Concentration of Micronutrients (Cu) in µg/ml				
	0.01	0.02	0.03	0.04	Control
<i>T. harzianum</i>	64.44	66.66	67.77	70.00	63.33
<i>T. koningii</i>	64.44	65.55	66.66	67.77	64.44
<i>T. pseudokoningii</i>	52.22	53.33	54.44	55.55	52.22
<i>T. virens</i>	58.88	60.00	61.11	62.22	57.77
<i>T. viride</i>	58.88	63.33	66.66	68.88	60.00
Mean	59.772	61.774	63.328	64.884	59.552
± SE	2.261	2.398	2.509	2.690	2.183



References

- Duke, J. A. and Ayensu, E. S. (1985).** *Medicinal Plants of China*.
- Eziashi , E. I., Omamor, I. B. and odigie, E. E. (2007) .** Antagonism of *Trichoderma viride* and effects of extracted water soluble compounds from *Trichoderma* species and benlate solution on *Ceratocystis paradoxa*. *Afr. J. Biotechnol.* 6(4): 388-392.
- Hesamadin Ramezani (2010).** Antagonistic effects of *Trichoderma* spp. against *Fusarium oxysporum* f.sp. *lycopersici* causal agent of tomato wilt. *Jr . of plant protection*, 2 (1):167-173.
- Incent , J. M. (1947).** Distortion of fungal hyphae in the presence of certain inhibitors. *Nature* 150:850.
- Johnson, L.A., (1957).** Effect of antibiotics on the number of bacteria and fungi isolated from soil by dilution plate method. *Phytopathology*, 47: 21-22.
- Kubicek , C. P. and Harman, G. E., (2002) .** “Basic biology, taxonomy and genetics” (Taylor and Francis Ltd. London).pp.14.
- Kumar, P., Mishra , A. K. and Panday , B. K., (2007).** *In vitro* evaluation of *Trichoderma* spp against vegetative mango malformation pathogen *Fusarium moniliformae* var *subglutinas*. *J. Eco-Friend Agri.* 2:187-189.
- Morton , D. J. and Stroube , W .H. (1955) .** Antagonistic and stimulating effects of soil micro-organism of *Sclerotium*. *Phytopathol.*, 45, 417-420.
- Nagamani , A. and Manoharachary, C. (2002) .** Monographic Contribution on *Trichoderma*. Associated Publishing Company. New Delhi.
- Ricker , A. J. and Ricker , R. S., (1936).** Introduction to Research on Plant diseases John S. Swift Co., St. Louis, pp 117.
- Subramanian, C. V., (1971) .** Hypomyces an account of Indian species except *Cercospora*. Indian Council of Agricultural Research, New Delhi, pp 810.
- Waghmare, M.B. and Kamble , S.S. (2011).** Efficacy of carbendazim against *Botrytis cinerea* causing leaf blight of rose. *Bioinfolet*, 8 (2): 157.



Qualitative analysis of secondary metabolites from some phytofungicidal plants

Dhanaji pawar¹, Mengane S.K¹ Waghmare R.M¹ and B. J. Patil^{2*}

Dept. of Botany

¹M. H. Shinde Mahavidyalaya Tisangi, Gaganbavada Dist- Kolhapur

Dept. of Botany & Plant Protection

^{2*}Sadguru Gadge Maharaj College, Karad, Dist. Satara 415 125.

Maharashtra State-India

KEYWORDS

Secondary metabolites, phytochemicals, phytofungicidal, drugs.

Corresponding Author
Email
dr,dp77@rediffmail.com

ABSTRACT

The Western Ghats of India is well known for its biodiversity. This paper deals with qualitative analysis of secondary metabolites from some plants. Different plants part having the different chemical compounds. Parts of *Parthenium hysterophorus*, *Pongamia glabra*, *Tridax procumbens*, *Nerium oleander*, *Lantana camara*, *Ipomoea carnea*, *Datura stramonium* and *Clerodendron inerme* were screened for phytochemicals studies. Alkaloids, Flavonoids, Saponnins, Steroids and Tannins were found to be present in selected plant. Some of these secondary metabolites are useful in different drugs as well as phytofungicidal or phytoinsecticides which are ecofriendly in controlling of fungal diseases and insect pest of crops.

Introduction

Number of chemical compounds present in plants. Drugs from the plants are easily available, safe, efficient, less expensive and rarely have side effects (Thite *et.al* 2013). The presence of antifungal compounds in higher plants has long been recognized in disease resistance (Mahadevan, 1982). Such compounds being biodegradable and selective in their toxicity are considered valuable for controlling plant diseases (Singh and Dwivedi; 1987). The analysis of plant material for secondary metabolites was carried out (Harbone, 1988, Wagner and Baldt 1996) using Thin Layer Chromatography (TLC) technique.

Phytochemical analysis of the extracts to detect alkaloids, flavonoids, phenols, saponnins, tannins, cardiac glycosides and terpenoids was done (Trease and Evans 1985). The *Lantana* and *Parthenium* exhibited the presence, saponnins, cardiac glycosides and steroids. Presence of

tannins, alkaloids, terpenes, flavonoids, glycosides, steroids etc in these weeds have been reported earlier (Mahadevappa *et.al* 2001, Singh *et.al*; 1990, 1991, 1996. Yadav and Tripathi 2000, 2003). *Parthenium hysterophorus* is a well known medicinal plant widely used traditionally in the treatment of various diseases and as a constituent of various drugs and in phytotherapy (Bakhtiar Muhammad *et.al* 2012).

According to De.*et.al* (2009) and Lutterodt *et.al* (1991) secondary metabolites play an important role in defense mechanism against microorganism. Number of plant species has been reported to have antifungal and antinsecticidal properties which will be useful to control disease and insect pest of crops.

Material and Methods

The extract or powder of each plant was taken for phytochemical analysis as per the qualitative chemical tests

mentioned by Parekh and Chanda (2007) and Bot. *et.al* (2007). For this qualitative analysis extraction method was used. Fresh parts of selected plants like, *Parthenium hysterophorus*, *Pongamia glabra*, *Tridax procumbens*, *Nerium oleander*, *Lantana camara*, *Ipomoea carnea*, *Datura stramonium* and *Clerodendron inerme* were collected from agricultural fields. About 20 grams of plant parts like root, stem, leaf and flower etc. were weighted and washed with running water for several times and then weep with blotting paper. They were crushed in a mortar and pestle with 20 ml distilled water. The extract was filtered through four layered muslin cloth and filtrate was then passed through what man's filtrate paper no.3. Filtrate centrifuge at 1600 rpm for five minutes. This filtrate was used for further analysis.

The phytoconstituents were investigated by performing following methods-

Alkaloids- Dragendroff's reagent, Mayer's reagent, Wagner's reagent, Tannic acid reagent (Homersleg, 1950 and Cromwell, 1955), Flavonoids- Shinoda test (Fransworth, 1960), Saponnins- Foam test, Haemolysis test (Fransworth, 1960). Steroids- Salkowaski test, Lieberman's test, Liberman-Burchard test (Fransworth, 1960), Tannins- Ferric chloride test, Lead acetate test, Potassium dichromate test, Gelatin solution test, Bromin water test (Trease and Evans, 2002). The results were tabulated.

Result and Discussion

Plants have the ability to produce a large variety of secondary metabolites. The results on phytochemical analysis are presented in table no.1. Wide variation in occurrence of phytochemicals, in different species and plant parts was reported. Alkaloides were present in all parts of *Tridax procumbens* and *Datura stramonium*. Flavonoides were present in all parts of *Nerium oleander* and *Ipomoea carnea*. Saponnins was found to be present in all parts of *Tridax procumbens*, *Lantana camara* and *Datura stramonium*. Steroides were present in root, stem and leaf of *Parthenium hysterophorus* and *Nerium oleander*. Tannins were found to be present in all parts of *Pongamia glabra*. Saponnins were highly present in different plant species than other secondary

metabolites. However it is concluded that selected plant species are phytochemically rich and diverse.

In present investigation selected plants are screened to find out chemical compounds. These plants may be a good source of phytochemicals than chemical fungicides that greatly reduces the soil fertility and also affects the food chain. From the above study it is concluded that these selected plants containing some important secondary metabolites and it increases the value of plants in case of phytofungicidal activity.

Acknowledgement

The authors express their sincere thanks to Principal and Head of the Department of Botany M. H. Shinde Mahavidyalaya, Tisangi for providing necessary laboratory facilities and cooperation during this research work.

References

- Bakhtiar Muhammad *et.al* (2012)** *African Journal of Biotechnology* Vol II (55),PP.11857-11860.
- Bot,Y.S; Mgbojikwe,L.O; Nwosu Chika, Abimiku Alash'le, Demas (2007).** *African Journal of Biotechnology*. 6(1):47.
- Cromwell, B.T(1955).** The alkaloid in modern methods of plant analysis. Springer Verlag, 4(1) : 19-21.
- De,N; Maori, L and Ardo,H (2009)** *J. Medicinal plant research*.3(3):116.
- Fransworth, B;(1960).** *Hanbuch der drogenkunde*, Wilhem Maudrich Verlag, Wein Band, V: 297-298.
- Harbone,J.B (1998)** "*Phytochemical Methods : A guide to modern techniques to plant analysis.*" Chapman and Hall London, UK.
- Homersleg, F.E; (1950).** The technology and Chemistry of alkaloids.D.Van.Nostrand Company, Inc.New.York.
- Lutterodt,G,D; Ismail, A.Basheer,R. H; and Baharudin,H.M.(199).** *Malaysium J. Med. Sci*; 6 (2):17.
- Mahadevan,A.(1982)** "*Bio-chemical aspects of plant diseases resistance part-I; performed inhibitory substances prohibitins.*" Today and Tomorrows Printers and



Publishers, New Delhi.PP.425-431.

Mahadevappa, M; Das, T.K. and Kumar A (2001)

Parthenium: A curse for natural herbs. Paper presented at National seminar on Herbal Conservation, Cultivation, Marketing and Utilization with special Emphasis on Chhattisgarh, “The Herbal State.” Srishti Herbal Academy and Research Institute and Chhattisgarh State Minor Forest Produce Trading and Dev.Co-op.Fed.Ltd; Raipur, India.

Parekh, J. and Chanda,S. (2007) *Turk J. Biol* 31:53.

Singh, R.K and Dwivedi (1987): *Ind. J. Phytochem.* 29: 3360.

Singh, S.K, Tripathi,V.J and Finzi,P.V(1996)

*Ind.Chem.Soc.*73(10):547.

Singh, S.K, Tripathi,V.J and Singh, R.H (1991) *J. Natural products.*54.755.

Thite, S.V, Chavan, Y.R, Aparadh, V.T and Kore B.A (2013) Preliminary phytochemical screening of some medicinal plants *IJPCBS.* 3(1):87-90.

Trease,G.E and Evans,W.C (1985).“Pharmacognocny” 12th ed. English Language Book Society, Bailliere Tindall, London.PP.394.

Trease,G.E and Evans,W.C (2002). Trease and evans pharmacognosy, 15th ed. W.B. Saunders Edinburgh London, New York, Philadelphia, St. Louis Sydney, Toronto: 3-4, 528-533, 538-547.

Wagner,H and Baldt,S.(1996) “*Plant Drug Analysis:A Thin Layer Chromatography Atlas.*” 2nd eds. Springer-Verlag Publication Berlin,Germany.

Yadav,S.B and Tripathi,V.J (2000). *Indian J.Heterocyclic Chemistry* 10:71.

Yadav,S.B and Tripathi,V.J (2003). *Fitoterapia* 74(3):320.

Secondary Metabolites	Preliminary distribution of various phytochemicals in different plant parts.																															
	<i>Parthenium hysterophorus</i>				<i>Pongamia glabra</i>				<i>Tridax procumbens</i>				<i>Nerium oleander</i>				<i>Lantana camara</i>				<i>Ipomea carnea</i>				<i>Datura stramonium</i>				<i>Clerodendron inerme</i>			
	R	S	L	F	R	S	L	F	R	S	L	F	R	S	L	F	R	S	L	F	R	S	L	F	R	S	L	F	R	S	L	F
Alkaloids	-	+	+	-	-	-	+	+	+	+	+	+	-	-	+	-	+	-	+	-	-	-	+	+	+	+	+	+	-	-	+	+
Flavonoids	+	-	-	-	-	+	+	+	+	+	+	-	+	+	+	+	+	-	+	-	+	+	+	+	+	-	+	+	+	+	+	-
Sapponins	-	-	+	-	-	+	+	+	+	+	+	+	-	-	-	-	+	+	+	+	+	+	+	-	+	+	+	+	-	-	+	+
Steroids	-	+	+	+	-	-	+	+	-	+	-	-	-	+	+	+	+	-	+	+	+	-	+	+	-	-	+	+	-	+	+	-
Tannins	-	-	+	-	+	+	+	+	+	-	+	+	-	+	+	+	+	-	+	+	+	-	+	+	-	-	+	+	-	-	+	+

Table no.1- Preliminary distribution of various phytochemicals in different plant parts.

KEY: + = Present, - = Absent , R = Root, S = Stem, L = Leaf, F = Flower.



Effect of interactions between symbiotic VAM fungus and nitrogen fixing bacteria, *Rahnella* on growth and chlorophyll content of non-leguminous plant, spinach (*Spinacia oleracea* L.)

*¹Gharge D. D. and ²Karadge B. A.

¹Department of Botany, Yashwantrao Chavan College of Science, Vidhyanagar, Karad-415 124, Maharashtra, India.

²Department of Botany, Shivaji University, Kolhapur, 416 004, Maharashtra, India.

KEYWORDS

Mycorrhiza, *Glomus*,
Rhizobium, 16S RNA,
synergism

ABSTRACT

The tripartite interaction between plant, mycorrhizal fungus and associated bacteria in legumes is well studied but very little work is on non-leguminous plants. The plant of spinach (*Spinacia oleracea* L.) is with vesicular arbuscular mycorrhizal (VAM) fungi in rhizosphere. Besides, the nitrogen fixing bacterium, *Rahnella* is also symbiotically associated with the spinach forming the nodule like structures referred here as protuberances, on the roots of the plant. The interactions between mycorrhizal fungus (*Glomus ambisporum*, Smith & Schenck) and the *Rahnella* with reference to the growth and chlorophyll content of spinach were studied in the present study. The bacterium has been identified as *Rahnella aquatilis* strain DDG3 (Acc. No. LC075773) as confirmed by 16S RNA technique.

The spinach plants were grown in sterilized soil. The seeds were treated with *Rahnella* and *Glomus* alone as well as in combination of both. Inoculation of spinach with spores of *Glomus*, obtained from the rhizosphere of the spinach plant, resulted in stimulated plant growth and increased chlorophyll content of leaves. Similarly, the inoculation of *Glomus* in combination with *Rahnella*, obtained from the protuberances of spinach root, resulted in enhancement in root infection and highest growth and chlorophyll content of leaves. In the same way almost similar results were obtained when onion crush, obtained from the onion bulbs inoculated with *Glomus*, and root protuberance crush of spinach for *Rahnella* + mycorrhiza inoculation as source of natural population. It can be concluded from the study that *Rahnella* displays synergistic effect on growth and chlorophyll content of spinach with *Glomus* by enhancing VAM fungus infection.

Corresponding Author
Email
botanyrtps@gmail.com

Introduction

The commercial cultivation of leafy vegetable crop plant spinach is usually in the soils with low fertility. So, the major problem for spinach plants is the deficiencies of essential nutrients necessary for proper growth and development. These deficiencies can not only be caused by the lack of nutrients in the soil, but also if the nutrients needed for plant growth exceeds the roots ability to uptake nutrients. It has been known for a long time that beneficial microorganisms within the soil form symbiotic relationships with the roots of plants, which in turn, enhance the uptake of essential nutrients by plants. The mycorrhizal fungi also have the ability to uptake more nutrients, as they act as extensions of the roots.

The occurrence of endomycorrhizal fungi in soil, their association with both forest plants and agricultural crops, and its role in improving the quality of plant has been well recognized (Rani *et al.*, 1999; Gill and Singh, 2002; Kaushik *et al.*, 1992; Ortas, 2003; Boureima *et al.*, 2007). Mycorrhizal infection has a particular value for legumes because nodulation and symbiotic nitrogen fixation by rhizobia require an adequate phosphorus supply (Carling *et al.*, 1978). Various researchers have made efforts to increase the quality of legume plants through the inoculation of mycorrhizal strain alone or in combination with *Rhizobium* sp. (Stancheva *et al.*, 2006; Yanjun *et al.*, 2010; Arumugam *et al.*, 2010). But non-leguminous plants are not more known to dual association of diazotrophic bacteria and mycorrhizal fungi except certain reports (Rik *et al.*, 2011). Thus, hardly any work has been done to improve the yield and quality of non-leguminous plants by dual inoculation of VAM fungi and nitrogen fixing bacteria. Experiment was conducted to study the possible contribution of endophytes (endomycorrhizal fungus and *Rahnella*) in association with each other, on growth and chlorophyll content of *Spinacia oleracea* L.

Materials and Methods

Glomus ambisporum, Smith and Schenck.

a native VAM fungus; was isolated from the rhizosphere of *Spinacia oleracea* L. by the wet sieving and decanting method (Gerdemann and Nicolson, 1963). *Rahnella* sp. was also isolated from the root protuberance of *Spinacia oleracea* L. The mycorrhizal inoculum was mass produced on onion (*Allium cepa* L.). The *Rahnella* inoculum was mass produced on yeast extract mannitol agar (YEMA) medium. Locally collected seeds were used to raise the seedlings of *Spinacia oleracea* L. Seeds free from physical defects and uniform size were surface sterilized (with 5% v/v H₂O₂) and put for germination in the polythene bags, each of containing 3 kg sterilized soil.

Inoculation experiment was designed in single and double combinations. The seeds treated with bacterium (*Rahnella* sp.), mycorrhizal fungus (*Glomus ambisporum*), bacterium combined with mycorrhizal fungus, mycorrhizal fungus inoculated onion crush and host root protuberance crush, separately, were grown up to 50 days from the emergence. The experiment was carried in six replicates. In control set no inoculum was added.

The plants were harvested from each replication, 50(±2) days after emergence for analysis. Plant shoot height and root length, dry weight, leaf area and mycorrhizal root colonization percentage (Philips and Hayman, 1970) of spinach were calculated at 50th day after emergence. Chlorophyll content from the leaves was determined following the method by Arnon (1949).

Results and Discussion

The plants (*Spinacia oleracea* L.) inoculated either with VAM fungus or mycorrhizal fungus inoculated onion crush showed significant increase in the root length, shoot height, dry weight and leaf area compared to inoculation of *Rahnella* alone or control plants (Table 1). The inoculation of VAM fungus (*G. ambisporum*) combined with *Rahnella* sp. or host root protuberance crush showed maximum values for the above growth parameters than plants inoculated with VAM fungus alone (Table 1).



Table 1

Effect of bacteria, mycorrhiza, their combination, mycorrhiza inoculated onion crush and host root protuberance crush on growth and chlorophyll content of *Spinacia oleracea* L.

Parameters	Control	<i>Rhizobium</i>	VAMF	<i>Rhizobium</i> + VAMF	Onion crush	oot protuberance crush
Root length (cm)	14.60 (±2.85)	14.38 (±1.50)	17.72 (±1.73)	20.54 (±2.45)	17.04 (±2.35)	21.86 (±1.98)
Shoot height (cm)	6.68 (±0.65)	6.00 (±0.94)	7.54 (±1.07)	8.20 (±0.92)	6.56 (±1.21)	8.94 (±0.56)
Dry weight (g)	00.0414	00.0553	00.106	00.204	00.083	00.276
Leaf area cm ² /plant	17.177	12.06	24.34	58.52	26.39	53.83
Mycorrhizal Colonization (%)	00	00	47	71	36	76
Chl. a (mg/100 g)	26.93	23.64	30.1	39.48	31.51	51.74
Chl. b (mg/100 g)	7.76	6.62	8.63	10.43	8.98	13.58
Ratio a/b	3.54	3.57	3.49	3.79	3.51	3.81
Total chl. (mg/100 g)	34.53	30.26	38.71	49.9	40.48	65.31

The inoculation of VAM fungus (*G. ambisporum*) combined with *Rahnella* sp. or host root protuberance crush showed maximum values for the above growth parameters than plants inoculated with VAM fungus alone (Table 1). In agreement with above results Aguilera-Gomez *et al.* (1999) reported inoculation of endomycorrhizal fungus (*Glomus intraradices*) increased leaf area, shoot and root mass of *Capsicum annum* L. compared to control. Zai *et al.* (2007) observed greatest dry weight of root and shoot, height of plant and largest total leaf area in beach plum (*Prunus maritime*, Marshall.) inoculated with *Glomus mosseae*, while the greatest root length of it with inoculation of *G. etunicatum*. Aher (2009) demonstrated that the inoculation of *Glomus fasciculatum* improved plant growth, shoot and root dry weight of *Arachis hypogea* more than uninoculated plants. Similarly, Kadian *et al.* (2013) evaluated the effect of two mycorrhizal fungi, *Funneliformis mosseae*, *Acaulospora laevis* alone and/or in combination with *Trichoderma viride*

and *Bradyrhizobium* sp. on symbiotic potential and various growth parameters of cluster bean [*Cyamopsis tetragonoloba* (L.) Taub]. The results revealed that the positive interaction among rhizospheric microorganisms leading to healthy and vigorous growth of the plants. Bagyaraj *et al.* (1979) studied interaction between *Glomus fasciailatiis* and *Rhizobium japonicum* and their effects on soybean (*Glycine max* L.) and reported that the dual inoculation with both the symbionts increased significantly the dry weight of shoot over single inoculation with either *Glomus* or *Rhizobium*. Ramaraj and Sharmugam (1990) have reported combined inoculation of *Rhizobium* and *Glomus etunicatum* to cowpea (*Vigna unguiculata* L.) in sterilized and unsterilized soils increased the biomass to the greater extent than either *Rhizobium* or mycorrhiza alone. Martha *et al.* (2016) studied the effect of inoculation with arbuscular mycorrhizal fungi (*Claroideoglomus etunicatum* and *Acaulospora* sp.) and plant growth-promoting rhizobacteria (*Rhizobium* sp. and *Burkholderia* sp.) on growth

of *Schizolobium parahyba* var. *amazonicum* under field conditions and reported increased total height and biomass over control. Jalaluddin (2005) also reported the dual inoculation of symbiotic VAM-fungi (*G. macrocarpum* and *G. warcupii*), and root nodule bacteria *Bradyrhizobium japonicum* increased fresh and dry weight as well as VAM colonization of *Glycine max* L. Raja (2008) treated the seeds of *Jatropha curcas* L. with biofertilizers viz. vesicular arbuscular mycorrhizal fungi, *Azospirillum*, *Azotobacter* and phosphate solubilizing bacteria and tested under field conditions, he observed significant increase in leaf area, root and shoot length, fresh and dry weight of shoot and root of all treated plants compared with untreated.

As given in Table 1; the plants inoculated with both *Rhizobium* and *G. ambisporum* together recorded a higher percentage (76%) of mycorrhizal infection than those inoculated with *G. ambisporum* alone. Similar influence of dual inoculation with mycorrhizal fungi (*Glomus mosseae* and *Glomus intraradices*) and *Rhizobium leguminosarum* bv. *viciae*, was reported by Geneva *et al.* (2006) in *Pisum sativum*. Manjunath *et al.* (1984) reported dual inoculation with both the organisms (*Rhizobium* and *Glomus fasciculatum*) improved mycorrhizal colonization of *Leucanea leucocephala* (Lam.) de Wit. roots. While Arumugam *et al.* (2010) indicated that the *Rhizobium* enhanced infection of mycorrhizal fungus in *Vigna unguiculata* L. Similar interactions have been observed between *Rhizobium* and VAM fungi in *Glycine max* L. by Jalaluddin (2005).

Plants inoculated with VAM fungus alone or in combination with *Rhizobium* showed significant changes in chlorophyll *a*, *b* and total chlorophyll content. The effect of interaction between mycorrhizal fungus and host plant on leaf chlorophyll content was significant. Sole mycorrhizal application resulted in higher amount (40.48mg/100 g fresh tissue) of chlorophyll content over inoculation of bacteria alone or control plants. In agreement with above results Jiang *et al.* (2008) reported inoculation of mycorrhizal fungus

(*Glomus intraradices*) at the stage of sowing of tobacco plant resulted in higher root infection rates and significant increase in chlorophyll content of leaves. Similar increase in level of chlorophyll content was observed in *G. fasciculatum* inoculated papaya plant by Shivaputra *et al.* (2004b). The interaction effect of bacteria and mycorrhizal fungus on leaf chlorophyll content was also significant. Dual inoculation of spinach with *G. ambisporum* and *Rhizobium* compared with mycorrhizal fungus alone had increased the chlorophyll content. The most amount of leaf chlorophyll of 65.31 mg/100 g fresh tissue was obtained by co-application of bacteria and mycorrhizal fungus (Table 1). The interactive effects were synergistically significant following inoculation of *G. ambisporum* and *G. ambisporum* with *Rhizobium*, which improved the photosynthetic pigment by 17% and 89%, respectively, relative to the control. The results are supported by other studies also. Mehrvarz *et al.* (2008) found that the dual inoculation with mycorrhizal fungus and bacteria caused significant increase in the chlorophyll content of *Hordeum vulgare* L. Arumugam *et al.* (2010) reported inoculation with mycorrhizal fungus, either alone or in combination with *Rhizobium*, brought about significant changes in chlorophyll *a*, chlorophyll *b*, and total chlorophyll contents of *Vigna unguiculata* L. Amira *et al.* (2012) also recorded enhanced chlorophyll content in *Acacia saligna* Labill. inoculated with *Sinorhizobium teranga* (R) in combination with mycorrhizal fungus. In dual inoculated spinach plants chlorophyll *a* content was more than all other treatments. This is evident from the chlorophyll *a:b* ratio (Table 1), which is always higher in dual inoculated plants than mycorrhizal fungus alone or control. Such an increase in chlorophyll content may lead to an increase in the rate of photosynthesis and transpiration caused increased growth (Sampathkumar and Ganeshkumar, 2003, Hayman, 1983). Result (Table 1) indicated that spinach inoculated with mycorrhiza alone showed increase in dry weight, leaf area and photosynthetic pigments but significant increase in these growth parameters was observed in plants inoculated with mycorrhiza in combination with *Rhizobium*. Dry weight is reliable parameter to know the



quantitative growth performance of the plant. Enhancement in dry weight indicates the positive effect of interactions between both the endosymbionts. Several studies indicated that the chlorophyll content is higher in the leaves of resistant varieties than in those of the susceptible ones as biochemical characters like phenols, proteins, and chlorophyll may play a vital role in making plants resistant to pathogens (Bhavani *et al.*, 1998, Charitha Devi and Reddy, 2001). Thus, the present study clearly reveals that increase in all studied growth parameters is because of the synergistic effect of association of VAM fungus, *Rahnella* and the host plant.

Conclusion

The present study clearly demonstrated the benefits of vesicular arbuscular mycorrhizal fungus and *Rahnella* for enhancing the growth of non-leguminous plant *Spinacia oleracea* L. Mycorrhizal infection often results in increased allocation of C to the root system, it implies increased root biomass, increased root respiration and mycelial biomass which could explore a larger soil volume for nutrient, consequently resulting in higher uptake rates. In dual inoculation of *Glomus ambisporum* and *Rahnella* sp. had a higher growth effect than the other treatments. This is due to the mutual positive action of *Rahnella* and VAM fungus that helped in uptake of nutrient content.

Acknowledgement

First author is grateful to the college authority and Department of Botany, Shivaji University, Kolhapur for the permission and facilities provided to complete this work.

References

- Aguilera-agomez, L., Davies, F. T. Jr., Olalde-Portugal, V., Duray, S. A. and Phavaphutanon, L. (1999). Influence of phosphorus and endomycorrhiza (*Glomus intraradices*) on gas exchange and plant growth of chile ancho pepper (*Capsicum annuum* L. cv. San Luis). *Phorosynthetica*. **36** (3): 441-445.
- Aher, R. K. (2009). Effect of AM fungi on mycorrhizal colonization, growth and nutrition of *Arachis hypogea* L. *International Journal of Agricultural Sciences*. **4** (1): 245-247.
- Amira, Sh. Soliman, Nermeen T. Shanan, Osama N. Massoud and Swelim, D.M. (2012). Improving salinity tolerance of *Acacia saligna* Labill. plant by arbuscular mycorrhizal fungi and *Rhizobium* inoculation. *African Journal of Biotechnology*. **11**(5): 1259-1266.
- Arnon, D. I. (1949). Copper enzymes in isolated chloroplasts. polyphenoloxidase in *Beta vulgaris*. *Plant Physiol*. **24**: 1-15.
- Arumugam, R., Rajasekaran, S. and Najarajan, S. M. (2010). Response of Arbuscular mycorrhizal fungi and *Rhizobium* inoculation on growth and chlorophyll content of *Vigna unguiculata* L. Walp Var. Pusa 151. *J. Appl. Sci. Environ. Manage*. **14** (4): 113 – 115.
- Bagyaraj, J., Manjunath, A. and Patil, R. B. (1979). Interaction between a vesicular-arbuscular mcorrhiza and *Rhizobium* and their effects on soybean in the field. *New Phytol*. **82**: 141-145.
- Bhavani, U., Venkatasubbaiah, K., Sudhakar, Rao A. and Saigopal, D. V. R. (1998). Studies on mosaic disease of sunflower: biochemical changes and growth parameters. *Indian Phytopathology*. **51**: 357-358.
- Boureima, S., Dioef, M., Dioef, T. A., Dietta, M., Leye, E. M., Ndiaye, M. and Seck, D. (2007). Effects of AM inoculation on the growth and development of sesame (*Sesamum indicum* L.). *African Journal of Agricultural Research*. **3**: 234-238.
- Carling, D. E., Richle, N. E. and Johnson, D. R. (1978). Effect of VAM on nitrate reductase and nitrogenase activity in nodulation and non-nodulating soybean. *Phytopathology*. **68**: 1590-1596.

- Charitha, Devi M. and Reddy, M. N. (2001).** Growth response of groundnut to VAM fungus and *Rhizobium* inoculation. *Plant Pathology Bulletin* **10**: 71–78.
- Geneva, M., Zehirov, G., Djonova, E., Kaloyanova, N., Georgiev, G. and Stancheva, I. (2006).** The effect of inoculation of pea plants with mycorrhizal fungi and *Rhizobium* on nitrogen and phosphorus assimilation. *Plant Soil Environ.* **52** (10): 435–440.
- Gerdemann, J. W. and Nicolson, T. H. (1963).** Spores of mycorrhizal *Endogone* species extracted from soil by wet sieving and decanting. *Transactions of the British Mycological Society.* **46**: 235.
- Gill, T. S. and Singh, R. S. (2002).** Effect of *Glomus fasciculatum* and *Rhizobium* inoculation on VA mycorrhizal colonization and plant growth of chickpea. *Journal of Mycology and Plant Pathology.* **32**: 162–167.
- Hayman, D. S. (1983).** The physiology of vesicular arbuscular endomycorrhizal symbiosis *Canadian Journal of Botany.* **61**: 944–963.
- Jalaluddin, M. (2005).** Effect of inoculation with VAM fungi and *Bradyrhizobium* on growth and yield of soybean in Sindh. *Pak. J. Bot.* **37** (1): 169–173.
- Jiang Long, Li ZhuMei, Huang JianGuo, Yuan Ling, Wu HongTian, and Liang Yong Jiang. (2008).** Influences of arbuscular mycorrhizal fungi on growth and selected physiological indices of tobacco seedlings. *Plant Nutrition and Fertilizer Science.* **14**(1): 156-161.
- Kaushik, A., Dixon, R.K. and Mukerji, K.G. (1992).** Vesicular arbuscular mycorrhizal relationships of *Prosopis juliflora* and *Zizipus jujuba*. *Phytomorphology.* **42**: 133–147.
- Manjunath, A., Bagyaraj, D. J. and Gopala, Gowda H. S. (1984).** Dual inoculation with VA mycorrhiza and *Rhizobium* is beneficial to *Leucaena*. *Plant and Soil.* **78** (3): 445–448.
- Martha, V. T., Cely, Marco A., Siviero, J. E., Flavia, R., Spago, Vanessa F., Freitas, Andre R.,**
- Barazetti, Rrika T., Goya, Gustavo de Souza Lamberti, Ig M.O. dos Santo, Admilton G., De Oliveira, ai Galdino Andrade. (2016).** Inoculation of *Schizolobium parahyba* with mycorrhizal fun and plant growth-promoting rhizobacteria increases wood yield under field conditions. *Front Plant Sci* doi: 10.3389/fpls.2016.01708
- Mehrvarz, S., Chaichi, M. R. and Alikhani, H. A. (2008).** Effects of phosphate solubilizing microorganisms and phosphorus chemical fertilizer on yield and yield components of barely (*Hordeum vulgare* L.). *American-Eurasian Journal of Agricultural and Environmental Science.* **3**(6): 822-828.
- Nisha Kadian , Kuldeep Yadav and Ashok Aggarwal. (2013).** Significance of bioinoculants in promoting growth, nutrient uptake and yield of *Cyamopsis tetragonoloba* (L.) “Taub.” *European Journal of Soil Biology.* **58**: 66–72.
- Ortas, I. (2003).** Effect of selected mycorrhizal inoculation on phosphorus sustainability in sterile and non-sterile soils in the Harrain plains in south Anatolia. *Journal of Plant Nutrition.* **26**:1–17.
- Philips, J. M. and Hayman, D. S. (1970).** Improved produces for clearing roots and staining parasitic and VAM fungi for rapid assessment of infection. *Transaction British Mycology Society.* **55**:158–161.
- Raja, G. (2008).** Effect of biofertilizers on *Jatropha curcas* L. under tropical conditions. *Asian Journal of Environmental Science.* **3**(1): 66-71.



- Ramaraj, B. and Sharmugam, N. (1990).** Interaction of vesicular-arbuscular mycorrhiza (*Glomus etunicatum*) and *Rhizobium* in cowpea. Conference paper Trends in mycorrhizal research. Proceedings of the National Conference on Mycorrhiza, held at Haryana Agricultural University, Hisar, India. pp. 107-108.
- Rani, P., Aggarwala, A. and Mehrotra, R. S. (1999).** Growth responses in *Acacia nilotica* inoculated with VAM fungus (*Glomus mosseae*), *Rhizobium* sp. and *Trichoderma harzianum*. *Indian Phytopathology*. **52**:151–153.
- Rik Op den Camp, Arend Streng, Stéphane De Mita, Qingqin Cao, Elisa Polone, Wei Liu, Jetty S. S. Ammiraju, Dave Kudrna, Rod Wing, Andreas Untergasser, Ton Bisseling and René Geurts. (2011).** LysM-Type mycorrhizal receptor recruited for *Rhizobium* symbiosis in non-legume *Parasponia*. *Science*. **331**(6019): 909-912.
- Sampathkumar, G. and Ganeshkumar, A. (2003).** Effect of AM fungi and *Rhizobium* on growth and nutrition of *Vigna mungo* L. and *Vigna unguiculata* L. *Mycorrhiza News*. **14**(4):15–18.
- Shivaputra, S. S., Patil, C. P., Swamy, G. S. K. and Patil, P. B. (2004b).** Cumulative effect of VAM fungi and vermicompost on nitrogen, phosphorus, potassium, and chlorophyll content of papaya leaf. *Mycorrhiza News*. **16**(2): 15-16.
- Stancheva, I., Geneva, M., Zehirov, G., Tsvetkova, G., Hristozkova, M. and Georgiev, G.(2006).** Effects of combined inoculation of pea plants with arbuscular mycorrhizal fungi and *Rhizobium* on nodule formation and nitrogen fixation activity. *Gen. Appl. Plant physiology*, Special Issue. pp. 61-66.
- Sukhada Mohandas. (1992).** Effect of VAM inoculation on plant growth, nutrient level and root phosphatase activity in papaya (*Carica papaya* cv. Coorg Honey Dew). *Nutrient Cycling in Agroecosystems*. **31**(3): 263-267.
- YanJun Guo, Yu Ni and Jianguo Huang. (2010).** Effects of *Rhizobium*, arbuscular mycorrhiza and lime on nodulation, growth and nutrient uptake of lucerne in acid purplish soil in China. *Tropical Grasslands*. **44**: 109–114.
- Zai, XM., Qin, P., Wan, SW., Zhao, FG., Wang, G., Yan, DL. and Zhou, J. (2007).** Effects of arbuscular mycorrhizal fungi on the rooting and growth of beach plum (*Prunus maritima*) cuttings. *Journal of Horticultural Science & Biotechnology*. **82**(6): 863-866.



Bioefficacy of plant extracts on *Macrophomina phaseolina* (Tassi) Goid causing charcoal rot of maize

¹S.G.Jagtap, T.R.Kavale* and ¹S.S. Kamble

¹Department of Botany, Shivaji University, Kolhapur-416009 (M.S).

*Ajara Mahavidyalaya, Ajara, Tal. Ajara, Dist.Kolhapur-416505 (M.S).

KEYWORDS

Plant extract, charcoal rot.

Corresponding Author
Email

Jagtap.sajav@gmail.com

ABSTRACT

Charcoal rot is an important disease of maize causing significant reduction in yield. In present study, the pathogenic fungus was isolated from stem of infected plants of maize. The in vitro efficacy of different plant extracts viz., *Azadirchta indica* L., *Adhatoda vasica* L., *Cynodon dactylon* L., *Pongamia glabra* Vent. and *Cassia fistula* L. were tested against charcoal rot of maize. Different concentrations 20, 40, 60, 80 and 100% of plant extracts were used in the study. All the plant extracts showed significant reduction in the growth of pathogen. Among the different extracts 80% aqueous extract of *Adhatoda vasica* L. was found most effective followed by *Azadirchta indica* L., *Cynodon dactylon* L., *Pongamia glabra* Vent. and *Cassia fistula* L.

Introduction

Maize (*Zea mays* L.) is a large grain plant domesticated by indigenous people in Mesoamerica in prehistoric time. It is the best grown in warm, tropical regions as it requires warm soil to develop optimally. It is an annual grass belonging to Poaceae and is a staple food crop grown all over the world. It is also commonly grown as a feed for livestock.

Such an important crop suffers from many fungal diseases, such as common smut caused by *Ustilago maydis* (de Candolle) Corda, head smut caused by *Sphacelotheca reiliana* (Kunhn) Clinton, brown rot caused by *Physoderma zeae maydis* F. J. Shaw, rust caused by *Puccinia sorghi* Schw., leaf blight caused by *Exserohilum turcicum* (Pass.) Leonard et rot caused by *Macrophomina phaseolina* (Tassi.) Goid. Among

Suggs. Seedling blight and wilt caused *Fusarium moniliforme* top rot caused by *Giberella zeae* (Schwein) Petch, Charcoal rot caused by *Macrophomina phaseolina* (Tassi.) Goid. Among these charcoal rot caused by *Macrophomina phaseolina* (Tassi.) Goid. is very serious.

Materials and Methods

The stems were collected from infected plants showing characteristic symptoms of charcoal rot, from the field from Songoan, Taluka: phaltan, Dist: Satara. The infected plant parts were cut in to pieces (2-3 mm), surface sterilized with 0.1% mercuric chloride solution for 30 seconds. The isolation was made from stems of maize plants. The infected portion from xylem region showing black brown shredding was washed three times with sterilized distilled water and then were transferred

aseptically on Czapek Dox Agar (CDA) media. The inoculated plates were incubated at room temperature ($30 \pm 2^\circ\text{C}$) and observations were made daily for emergence of culture.

Fresh leaves were washed through under tap water followed by sterilized water, the leaves were air dried and were grinded with the help of pestle and mortar by taking (1:1 w/v) one gram of extract was added in 1 ml distilled water separately for each plant extract and filtered through Muslin cloth and 100% plant extract solution was prepared. The extracts were poured in the flasks plugged with cotton and heated at 100°C for 10 minutes to avoid contamination (Madhavi and Singh). The plant extracts of *Azadirachta indica* L., *Adhatoda vasica* L., *Cynodon dactylon* L., *Pongamia glabra* Vent. and *Cassia fistula* were used by food poisoning technique (Nene and Thapilyal). Different concentrations of plant extracts (20, 40, 60, 80 and 100%) were incorporated to Czapek Dox Agar medium for inoculation of the test pathogen in sterilized petridishes. The isolated pathogen was grown on CzapekDox Agar and a disk of 6 mm was taken with the help of cork borer and it was placed aseptically at the center of petridishes (keeping upside down) containing different concentration of the poisoned medium and incubated at $30 \pm 2^\circ\text{C}$ for 5 days. Radial growth (mm) of fungus was measured after inoculation till 5 days at an interval of 24 h. The Data recorded during the course of investigation has been subjected to three-way classification. The conclusion was drawn on the basis of analysis of variance.

Results

Adhatoda vasica L. leaf extract inhibited the growth of fungus in all treatments within five days after inoculation (Table 1). The extracts at 80% concentration were effective in reducing growth (36.79 mm average) as compared to as compared to T₃, T₂, T₁ and control T₀. *Adhatoda vasica* extract inhibited the fungal growth in all treatments and minimum growth was recorded in T₄ 80% (31.33 mm) as compared untreated control. Results obtained with *Azadirachta*

indica leaf extract on radial growth of *Macrophomina phaseolina* (Tassi)Goid indicated that it was effective in reducing growth of fungus (37.39%). *Cynodon dactylon* inhibited the growth of fungus in 80% and 100% concentration. The maximum mycelial growth was observed in control agents (untreated).

Discussion

The inhibitory effect of the plant extracts might be attributed to the presence of antifungal compounds viz., Azadirachtin in *Azadirachta indica*, vasicine in *Adhatoda vasica* L. protocatechuic, ellagic and gallic acids in *Pongamia glabra* and anthraquinones, coumarin, saponins in *Cassia fistula*. and Saponins, Tannins, steroids and flavonoids in *Cynodon dactylon* and *Ocimum sanctum* against *Drechslera sorokiniana* were also reported (Verma et. al.). Natural chemicals and their use for integrated protection is one of the focuses of research workers all over the world (Kiran et. al). These results of the present investigation are clear indication for the potential of plant extracts to control fungal pathogens and these compounds can be used. It is evident from the results that all the plant extracts significantly inhibited the radial growth of isolated fungus. Amongst the plant extracts used *Adhatoda vasica* L was found most effective at 80% concentration followed by *Azadirachta indica*, *Pongamia glabra*, *Cynodon dactylon* and *Cassia fistula*. Plant extracts belonging to twelve families (Russel and Mussa) and *Prosopis juliflora* (Raghavendra et.al.) were used to control *Fusarium*. An antifungal property of *Polyalthia longifolia* extracts against *Macrophomina phaseolina* has been reported *Cassia fistula*. (Datar). Aqueous leaf extracts of *Allium sativum*, *Azadirachta indica*, *Eucalyptus globulus*, *Lowsonia inermis* and *Gungellylaleae* were effective against damping off of chilli (Kuruchave, and Padmavati). Among the alcoholic and aqueous leaf extracts of *Azadirachata indica*, *Polyalthia longifolia*, *Hyptis suaveolens*, *Mentha spicata*, and *Ocimum sanctum*, the alcoholic and aqueous leaf extract of *Azadirachata indica* proves best in managing soybean rust caused by *Phakopsora pachyrhizi* (Mengane and Kamble).



Table 1: Efficacy of plant extracts against *Macrophomina phaseolina* (Tassi.) Goid.

Conc.of treatment	<i>Adhatoda vasica</i>	<i>Azadirchta indica</i>	<i>Pongamia glabra</i>	<i>Cassia fistula</i>	<i>Cynodon dactylon</i>
T ₀ (control)	90.00	87.33	90.33	88.66	89.33
T ₁ (20%)	45.66	55.66	52.66	56.33	41.66
T ₂ (40%)	43.66	55.66	47.33	52.33	39.33
T ₃ (60%)	38.33	45.66	42.33	50.66	34.33
T ₄ (80%)	31.33	36.66	36.33	48.33	31.33
T ₅ (100%)	00.00	32.66	32.66	42.66	28.66

Application of these plant extracts which are easily available for controlling Panama wilt of banana are non-pollutive, cost effective non hazardous and do not disturb ecological balance. Thus it can be recommended that the use of *Azardiachta indica*, *Eucalyptus globulus*, *Artemisia annua*, and *Ocimum sanctum* against *Fusarium oxysporum* f.sp. *ubense* to give better results as they are biologically based and environmental safe alternatives. It is from the reports that plant extracts and plant essential oils are effective antimicrobial agents for soil born fungi, food spoilage fungi, foliar pathogens and nematodes and do not produce any residual effects.

References

Datar, V.V.(1999) Bioefficacy of plant extracts against caused by *Macrophomina phaseolina*(Tassi) Gold, the incitant of charcoal rot of sorghum. J. Mycol. P. Pathol.29: 251-253.

Kiran, K., S. Linguraju and S. Adiver. (2006) Effect of plant extract on *Sclerotium rolfsii*, the incitant of stem rot of ground nut. J. Mycol. Pl. Pathol., Pathol.; 36: 77-79.

Kuruचेve, V. and Padmavati, R.(1998) Management of damping off of chillies with plant products. Indian Phytopath.; 51 (3): 379-381.

Madavi, S. and R.P. Singh.(2005) Management of mushroom pathogens through botanicals. Ind. Phyto. Pathol.; 58: 189-193.

Mengane S.K. and S.S.Kamble.(2013) Efficacy of various phytoextracts on *Phakopsora pachyrhizica* causing rust of soybean. Geobios.; 40:58-60.

Nene, Y. and L. Thapilyal. (2000) Poisoned food technique of fungicides in plant disease control.; 3rd Edn. Oxford and IBH Publishing Company, New Delhi.

Raghavendra, M.P., S. Satish and K.A. (2002) Raveesha. *Prosopis juliflora* Swartz: A Potential plant for the management fungal diseases of crops. In: Asian Cong. Mycol. Pl. Pathol., Indian Soc. Mycol. Pl. Pathol. University of Mysore (Abst). Oct.1-4, pp: 136.

Russel, P.E. and M. Mussa. (1977) The use of garlic extracts to control foot rot of *Phaseleous vulgaris* caused by *Fusarium solanif. sp. phaesoli*. Ann Appl Biol.; 86: 369-372.

Varma, K.P. Yashoda, R. Hegde and S. Kulkarni.(2006) In vitro evaluation of phytoextracts and biocontrol agents against *Drechslera sorokiniana* In: Asian Cong. Mycol. Pl. Pathol., Indian Soc. Mycol. Pl. Pathol.



Synergistic effect of herbicides on the development of carbendazim resistance in *Alternaria dauci* causing leaf blight of carrot

M. S. Mishrakoti and S. S. Kamble

Mycology and Plant Pathology Laboratory, Department of Botany, Shivaji University, Kolhapur, Maharashtra

KEYWORDS

Synergistic, *Alternaria dauci*

Corresponding Author
Email

meerashravani30@gmail.com

ABSTRACT

Synergistic effect of herbicides may develop resistance in the pathogen. The synergistic effect of herbicides on development of carbendazim resistance in *Alternaria dauci* causing leaf blight carrot (Ad-2) were studied. In *in vitro* and *in vivo* studies, concentration of herbicides increases the growth of pathogen decreases.

Introduction

In agriculture, use of agrochemicals has become an important practice in control of diseases. Among fungal diseases, the leaf blight caused by *Alternaria dauci* (Kuhn) Groves & skollo is very common in carrot (*Daucus carota*). It is important pathogen of carrot in most 'production' areas of the world (Hooker, 1944; Netzer and Kenneth 1969; Scott and Wenham 1973; Strandberg, 1992b and Tahvonen, 1978). It incites leaf blight, a foliage blight that reduces photosynthetic area and can reduce yield. Synergistic effect of herbicides may develop resistance in the pathogen. In this view, the synergistic effect of herbicides was studied *in vitro* and *in vivo*.

Materials and methods

Synergistic effects of agrochemicals on development of carbendazim resistance in *Alternaria dauci* were studied *in vitro* and *in vivo*. The resistant isolate Ad-2 was selected for this study and herbicides (Aandhi 71%, Fernoxone, Matin, Tohfa) were used for the study.

In vitro studies:

Resistant isolate was grown on the medium containing resistant dose of carbendazim (20%) and above mentioned

herbicides at various (25, 50, 75 and 100 µg/ml) concentrations. Medium containing carbendazim alone was treated as control. An increase in radial mycelial growth over control was considered as increase in resistance, whereas decrease in growth was considered as decrease in resistance.

In vivo studies:

For *in vivo* studies, healthy carrot plants were used. Effect of above mentioned herbicides on the development of resistance in *Alternaria dauci* was studied. These above mentioned herbicides with carbendazim were mixed in combination (18%). For these studies, wild resistant isolate Ad-2 was selected. The agrochemicals at different concentrations were mixed with carbendazim having concentration of 18%. These solutions are sprayed on healthy carrot plants. After 24 hrs. a suspension made from actively growing mycelium of *Alternaria dauci* was above mentioned inoculated on the carrot plants with Camel hair brush. These plants were covered with polythene bags to maintain the relative humidity and other contamination.

mentioned inoculated on the carrot plants with Camel hair brush. These plants were covered with polythene bags to maintain the relative humidity and other contamination.

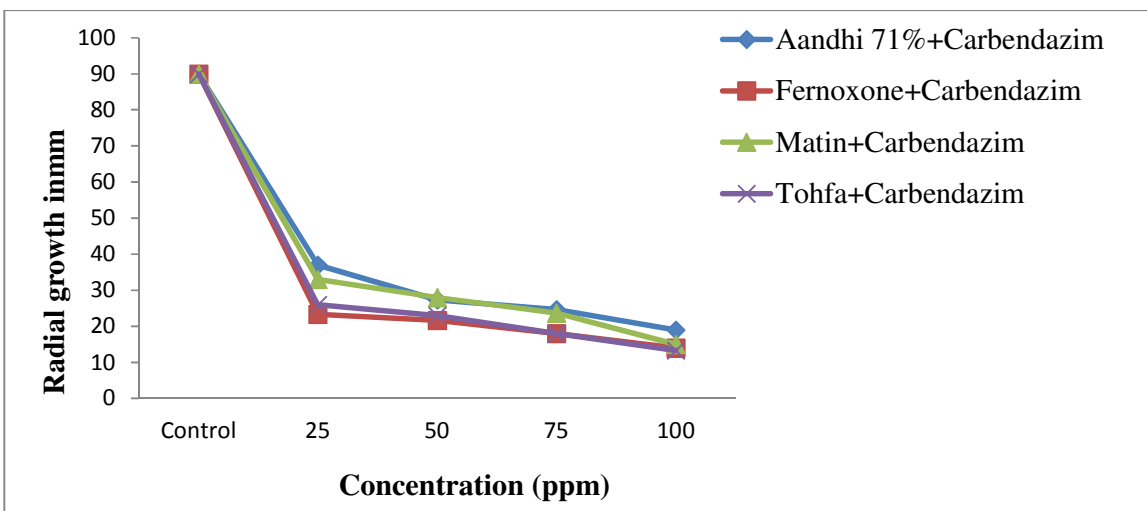


Fig.1: Synergistic effect of herbicides on the development of carbendazim resistance in *Alternaria dauci* (in vitro) causing leaf blight of carrot

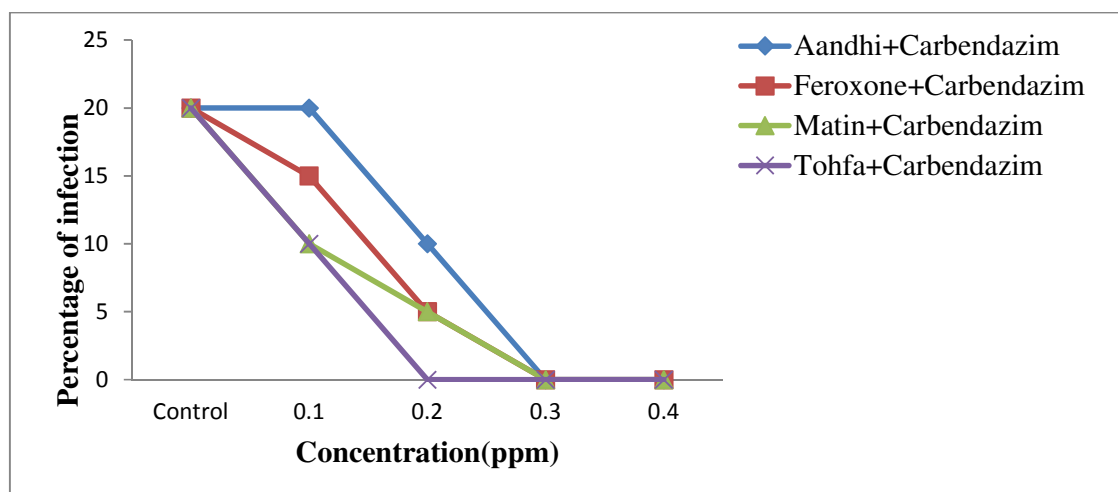


Fig 2.: Synergistic effect of herbicides on the development of carbendazim resistance in *Alternaria dauci* (in vivo) causing leaf blight of carrot.

Result and discussion

The results are illustrated in fig. 1 and fig.2. In *in vitro* studies, as the concentration of herbicides like Aandhi71, Feroxone, Matin and Tohfa increases, the growth of the pathogen decreases. In *in vivo* studies, Aandhi 71, Feroxone and Matin prevented the infection at 75µg/ml concentration while Tohfa prevented the infection at 50 µg/ml concentration. Herbicides like Aandhi-71, Feroxone, Matin and Tohfa decreases growth of pathogen *in vitro* while

Aandhi-71, Feroxone, Matin prevented infection to carbendazim at higher concentration and Tohfa prevented the infection of carrot at quite less concentration *in vivo* studies.

According to Kamble (1991), application of carbendazim with weedicides (gramoxone and atrazine), According to Bhale(2009), Benomyl in combination with captan, 2, 4-D, inhibited the mycelial growth of *Fusarium oxysporum f. spinaceae* causing wilt of spinach. He also observed



reduction in growth of resistant isolate of *Alternaria tenuissima* causing leaf spot of spinach when carbendazim used in combination with stomp.

References

- Bhale UN, Rajkonda JN and Sarwade PP (2009)** Evaluation of botanicals against *Alternaria spinaceae* causing leaf spot of spinach (*Spinacea oleracea L.*). Geobios 36:125-128.
- Hooker WJ (1994)** Comparative studies of two carrot leaf diseases. Phytopathology 34:606-612.
- Kamble SS (1991)** Studies on fungicide resistance in late blight and charcoal rot of potato. Ph. D. Thesis, Marathwada University, Aurangabad.
- Netzer D and R G Kenneth (1969)** Persistence and transmission of *Alternaria dauci* (Kuhn) Groves and Skolko in the semi arid conditions of Israel. Ann. Appl. Biol. 63:289-294.
- Scott DJ and HT Wenham (1973)** Occurrence of two seed borne pathogens *Alternaria radicina* and *Alternaria dauci* on important carrot seed in New Zealand. N. Z.J. Agr. Res. 6: 247-250.
- Strandberg J O (1992b)** Evaluations of plant introductions of *Daucus* sps. For tolerance to *Alternaria dauci* and some other horticultural characteristics. Univ. of Fla. Central Fla. Res. Educ. Ctr. Res. Rpt. SAN. 93-03.
- Tahvonen R (1978)** Seed borne fungi on parsley and carrot : *Alternaria dauci*, *Stemphylium radicinum*, *Septoria petroselini*. J. Sci. Agr. Soc. Finland 50: 91-102.



Effect of biofertilizers on growth of paddy (*Oryza sativa* L.) CV. JAYA.

N.B. Pawar^{1*}, N.S. Suryawanshi² and A.G. Rokade³

¹Department of Botany, Mahatma Phule A. S. C. College, Panvel, Dist Raigad M.S. India.410206,

²Department of Botany, K. V. Pendharkar College, Dombivali M.S. India.421203

³Department of Zoology, Mahatma Phule A. S. C. College, Panvel, Dist Raigad M.S. India.410206

KEYWORDS

Biofertilizers, Growth and yield parameters, Paddy (*Oryza sativa* L. cv. Jaya).

ABSTRACT

The present investigation was carried out in kharif season, during 2015 and 2016 at research farm, 'RayatShikshanSanstha's, M.P.A.S.C. College Panvel, District- Raigad (Maharashtra), India, to observe the effect of different biofertilizers on growth and yield parameters on Paddy (*Oryza sativa* L. cv. Jaya).The experimental farm was geographically situated at 18°, 59' 40' N latitude and 73°, 06' 50' E longitude at an altitude of 28 meters above mean sea level.The experiment was laid out in RBD replicated thrice with twelve treatments i.e.(T0) Control (without fertilizer), (T1)Chemical fertilizer(19:19:19,) (T2) Blue green algae,(T3) *Azospirillum brasilense*,(T4)*Bacillus megaterium*,(T5)*Trichoderma viride*,(T6)*Mycorrhizae*,(T7)*Pseudomonas aeruginosa*,(T8)T2+T7,(T9)T2+T6,(T10)T3+T4, and (T11)T3+T4+T7.RDC fertilizer was applied in three splitted doses. The first dose, consisting of 1/3 the normal dose, was applied before transplantation; the second 1/3 at the time of tillering; and the last 1/3 at the panicle initiation phase.

The study revealed the growth parameters like shoot length, root length, and dry matter production at various stages of growth in Paddy (*Oryza sativa* L.) cv. Jaya were favorably influenced by biofertilizers treatment. Overall results suggest that combine effect of Biofertilizers improves vegetative and reproductive growth of Paddy (*Oryza sativa* L. cv. Jaya)".

Corresponding Author
Email

nbpawar01@gmail.com

Introduction

Paddy (*Oryza sativa* L.) is most important staple food crop in the world and is grown under a broad range of environmental conditions. India is second largest producer and consumer of rice in the world after China. At national level, area under cultivation is 42.5 million hectares with the production of

152.6 million tones and average productivity is of 3.5 tones per hectares. At global level, paddy is cultivated under 158.4 million hectares area with annual production of around 697.2 million tones and average productivity of 2.85 tones per hectares (Sarvan et al,2016). Fertilizers come in two types - they are either chemical or biofertilizers. Increasingly high inputs of chemical fertilizers during last

fertilizers during last 150 years have not only left soils degraded, polluted and less productive but have also posed severe health and environmental hazards. Organic farming methods (such as the use of biofertilizers) would solve these issues and make the ecosystem healthier. Biofertilizers play a very significant role in improving soil fertility by fixing atmospheric nitrogen, both, in association with plant roots and without it, solubilise insoluble soil phosphates and produces plant growth substances in the soil. They are in fact being promoted to harvest the naturally available, biological system of nutrient mobilization (Venkatashwarlu, 2008). The role and importance of biofertilizers in sustainable crop production has been reviewed by several authors (Biswas et al. 1985; Wani and Lee, 1995; Katyaj et al. 1994).

Biofertilizers are becoming increasingly popular in many countries and for many crops. They are defined as products containing active or latent strains of soil microorganisms, either alone or with albae or fungi that increase plant availability and uptake of mineral nutrients (Vessey et al.,2006)571-586.Bio-fertilizers containing beneficial bacteria and fungi improve soil chemical and biological characteristics, phosphate solutions and agricultural production (El- Habbasha et al., 2007; Yosefi et al., 2011). Microbiological fertilizers are important to environment friendly sustainable agricultural practices (Bloemberg et al., 2000.) The Biofertilizer includes mainly the nitrogen fixing, phosphate solubilizing and plant growth promoting microorganisms (Goel et al., 1999).

Materials and Methods

Collection of seeds and raising seedlings:

Paddy (*Oryza sativa* L. cv. JAYA) seeds were collected from the Kharland research station Panvel, Dist Raigad.Jaya is a medium duration high yielding variety of rice. It is recommended for both crop seasons. The variety is known for its greater yield potential. The grains are long and white with good cooking quality.

Transplanting of paddy seedlings:Twenty one days old paddy seedlings were transplanted at 20 cm x 15 cm spacing

during both the seasons with five seedlingsper hill. Gap filling was carried out twelve DAT in order to ensure uniform plant population.

Experimental site:

This investigation was carried out at research farm of RayatShikshanSanstha'sMahatmaPhuleA.S.C.College, Panvel, Dist.Raigad (Maharashtra). The experimental farm is geographically situated at 18°, 59' 40' N latitude and 73°, 06' 50" E longitude at an altitude of 28meters above mean sea level.The experiment was conducted on the same site and layout during both the years. The study area is representative of the agro-ecological sub-region 19.3 coveringnorth Konkan coastal zone of Maharashtra(Sehgal *et. al.*, 1992),which comprises of Thane & Raigad districts.

Collection of experimental data:

a) Growth parameters-

Three hills per plot were selected randomly from each plot for recording for following observations at four stages (30th, 60th, 90th day after transplanting and at harvest).

- i)Shoot and root length (cm.)
- ii) Dry matter production hill⁻¹ At 30, 60, 90 DAT and at harvest

Dry matter accumulation/hill (g)- Dry matter accumulation per hill was recorded at 30, 60, 90 days after transplanting (DAT) and harvest. Plants uprooted from sample rows of two hills were taken after washing and cleaning the roots. After air drying, the samples were placed in an oven at 65 0C temperature, till their constant weights were obtained.

b) Yield parameters

- i)Panicle length (cm) –
The length of twenty panicles was measured in centimetre from the neck to the tip of the panicle and mean was taken as length of the panicle.
- ii) Weight of panicle(gm.)
- iii)No. of Spikelet'sperpanicle
- iv)Wt. of 1000Seeds (gm.) One thousand grains were drawn randomly from the bulk grain yield of net plot and their weight was recorded in gram.
- v)Grain yield (q./ha.)-The produce of each net plot was threshed, cleaned and the grain yield was recorded in kilogram



kilogram net per plot and converted on q./ hect.basis.

vi) Straw yield(q./ha.)- The weight of the straw harvested from the net area in each treatment was recorded after five days sun drying in the field and then converted onq/ha

Statistical Analysis-Pooled data was used for analysis. Duncan's multiple range test (DMRT) was performed to determine the significant difference between treatments (Gomez and Gomez, 1984).

Experimental details-	
Type of Soil	Sandy clay
Name of the Method:	RBD-Split plot design
No. of Treatments	12
No. of Replications	3
No. of Sub plots	12 x3= 36
Size of plot	1x1 m ²
Distances between two plots	25 cm.
No. of Plants per hill	5
Treatment details-	
Notation for treatment	T
T0	Control
T1	*Chemical fertilizer(19:19:19)
T2	<i>BGA</i>
T3	<i>Azospirillum brasilense</i>
T4	<i>Bacillus megaterium</i>
T5	<i>Trichoderma viride</i>
T6	<i>Mycorrhizae</i>
T7	<i>Pseudomonas aeruginosa</i>
T8	<i>BGA+ pseudomonas aeruginosa</i>
T9	<i>BGA+ Mycorrhizae</i>
T10	<i>Azospirillum brasilense +Bacillus megaterium</i>
T11	<i>Azospirillum brasilense +Bacillus megaterium</i> <i>+Pseudomonas aeruginosa</i>

*Nitrogen was applied in three splitted doses. The first dose, consisting of 1/3 the normal dose, was applied before transplantation; the second 1/3 at the time of tillering; and the last 1/3 at the panicle initiation phase.

Results and Discussion

Data on mean values of growth parameters pertaining to different treatments are presented in Table 1 TO 9. The good results were observed in biofertilizer treated plants in all respects and the results suggested that the treatment of biofertilizers in single, dual and multiple combination enhance the growth of paddy plants when compared to chemical fertilizer treated plants and control. The results on yield attributes such as Panicle length, weight of panicle, no. of Spikelet's per panicle, wt. of 1000 Seeds, Grain yield (q./ha.) and Straw yield (q./ha) showed a favorable influence during the entire study period (Table 2).

Combined application of *Azospirillum brasilense* + *Bacillus megaterium* + *Pseudomonas aeruginosa* recorded significantly higher growth parameters compared to single application. The results are in conformity with earlier reports (Nanda et al., 2016). Growth parameters viz. plant height, number of tillers hill⁻¹ and dry matter production hill⁻¹ were significantly affected by bio-fertilizers. Combined application of *Azospirillum brasilense* + *Bacillus megaterium* + *Pseudomonas aeruginosa* recorded significantly higher growth parameters compared to single application. The results of the present experiment confirmed the findings of Murthy *et al.* (2015). Increase in yield components, grain and straw yield might be due to higher photosynthetic activity because of increased leaf area index, which ultimately promoted dry matter production resulted in higher grain and straw yield. These results confirmed the findings of Davari and Sharma (2010) and Singh *et al.* (2013).

CONCLUSIONS

It can be seen from the above data that all the treatments were significantly higher than each other. The treatments T8 (*BGA* + *pseudomonas aeruginosa*), T9 (*BGA* + *Mycorrhizae*), T10 (*Azospirillum brasilense* + *Bacillus megaterium*) and T11 (*Azospirillum brasilense* + *Bacillus megaterium* + *Pseudomonas aeruginosa*) was significantly higher than all other treatments in growth and yield parameters. Based on these reports, it can be assumed that biofertilizers could offer an opportunity

for rice farmers to increase yields, productivity, and resource use efficiency.

Acknowledgments

The author is thankful to Prin. DR. G. A. Thakur M.P.A.S.C. College, Panvel, and thanks are due to my Supervisor DR. N. S. Suryawanshi, Department of Botany, K. V. Pendharkar College, Dombivali for providing laboratory facilities.

References

- Biswas, B.C. Yadav, D.S., and Satish Maheshwari, 1985.** Bio-fertilizers in Indian Agriculture. Fertilizer News 30(10): 20-28.
- Bloembergen GV, Wijfijes AHM, Lamers GEM, Stuurman N and Lugtenberg BJJ (2000).** Simultaneous imaging of *Pseudomonas fluorescens* WCS 3655.
- Gomez, K.A.; Gomez, A.A. (1984)** Statistical Procedures for Agricultural Research, 2nd ed.; John Wiley & Sons: New York, NY, USA, p. 680.
- Goel AK, Laura RDS, Pathak G, Anuradha G and Goela (1999).** Use of bio-fertilizers: potential, constraints and future strategies review. International Journal of Tropical Agriculture 17 1-18.
- Davari, M. R., Sharma, S. N. (2010):** Effect of different combinations of organic materials and biofertilizers on productivity, grain quality and economics in organic farming of basmati rice (*Oryza sativa*). – Indian Journal of Agronomy 55(4): 290-294.
- Dawari. R and Sharma. N (2011)** Effect of organic manures on basmati rice (*Oryza sativa* L) under organic farming of rice – wheat cropping system. Int., Journal of Agricultural and crop sciences. 3(3): 76-84.
- El-Habbasha SF, Hozayn M, Khalafallah MA (2007).** Integration effect between phosphorus levels



- and biofertilizers on quality and quantity yield of faba bean(*Vicia faba* L.) in newly cultivated sandy soils. Research Journal of Agriculture and Biological Science 3(6) 966-971.
- Katyal, J.C., Das, S.K., Korwar, G.R. and Osman. M (1994).** Technology for Mitigation stresses: Alternate land uses. Stressed Ecosystems and Sustainable Agriculture eds. Pp. 291-305
- Murthy KMD, Rao AU, Vijay D, Sridhar TV (2015)** Effect of levels of nitrogen, phosphorus and potassium on performance of rice. Indian Journal of Agriculture Research. ; 49(1):83-87.
- Nanda, G., Sravan, U.S., Singh, A. and Singh, S.P. (2016).** Effect of NPK Levels and Bio-Organics on Growth, Yield and Economics of Basmati Rice (*Oryza sativa* L.) cv. HUBR 10-9. Environ. Ecol., 34: 1530-1534.
- Sarvan, T., Jaiswal, H.K., Showkat, A.W. and Kumari, P. (2016).** Heterosis for yield and yield attributes in rice (*Oryza sativa* L.). Journal of Applied and Natural Science, 8(2): 622- 625
- Venkatashwarlu, B. (2006).** Role of bio-fertilizers in organic farming:Organic farming in rain fed agriculture: Central institute for dry land agriculture, Hyderabad.pp. 85-95.
- Vessey, J.K. (2003)** Plant growth promoting rhizobacteria as biofertilizers. Plant Soil, 255,571–586.



Effect of *Trichoderma koningii* culture filtrate on seed germination and growth of some vegetables (in vitro)

Prajakta Patil , Sneha Devardekar, Ragini Patil, Manali Jadhav, Supriya Patil, Snehal Patil, Trupti Ghadge ,
Swapnali Shinde*, M. B. Waghmare
The New College , Kolhapur.

KEYWORDS

Hibiscus cannabinus,
Trichoderma koningii,
Trigonella foenum, growth
rate, germination
percentage.

Corresponding Author Email

swapnalishinde171988@gmail.com

ABSTRACT

Vegetables are most important to increase the economy of the country. Delayed and erratic germination is one of the reasons of low yield which caused problem in fertilizer utilization, weed control, and uniform harvesting (Standifer *et al.*, 1989). Water soaked seeds leads suffocation and hence germination rate becomes low (Heydecker,1977). So in present study investigation has been made on to increase germination percentage and growth rate of some widely used vegetables by using LCF of *Trichoderma koningii*.

In present study seeds of 2 different vegetables viz. *Trigonella foenum* (Methi), *Hibiscus cannabinus* (Ambadi) were selected to study the effect of Culture filtrate on seed germination and growth rate. In the result it was found that in both treated seeds 100% seed germination and fast growth rate was observed as compare to control.

Introduction

Vegetables are most important to increase the economy of the country. Delayed and erratic germination is one of the reasons of low yield which caused problem in fertilizer utilization, weed control, and uniform harvesting (Standifer *et al.*, 1989). Water soaked seeds leads suffocation and hence germination rate becomes low (Heydecker,1977). To increase yield farmer use chemicals. Which are harmful for the nature and also for human health, therefore use of bioagents gaining an importance. *Trichoderma* is biocontrol agent. *Trichoderma* are filamentous saprophytic fungi present in soil. It contain the anatagonistic potential to control several phytopathogens also it helps in seed

also it helps in seed gemination (Koch, 1999;Spiegel and Chet, 1998; Barker and Paulitz, 1996;Harman and Hadar, 1983).. *Trichoderma* strains contain growth promoting properties like germination enhancement, root and shoot length, vigour index it helps to improve nutrient uptake. *Trichoderma* strain treatment to seed giving best results. So in present study investigation has been made on to increase germination percentage and growth rate of some widely used vegetables by using LCF of *Trichoderma koningii*.

In present study seeds of 2 different vegetables viz. *Trigonella foenum* (Methi), *Hibiscus cannabinus* (Ambadi) were selected to study the effect of Culture filtrate on seed germination and growth rate.

Materials and Methods

Isolation of *Trichoderma koningii* Oudemans

From Kolhapur district Rhizospheric soil were collected and brought to the lab. By soil dilution technique *Trichoderma koningii* Oudemans was isolated (Johnson, 1957). Identify the isolate (Kubicek and Harman, 2002; Nagamani and Manoharachary, 2002). Isolates of *Trichoderma* was grown on PDA medium (Ricker; Ricker, 1936). For further study pure culture of *Trichoderma koningii* was maintained on the PDA medium.

Preparation of spore suspension of *Trichoderma koningii*

Trichoderma koningii spore suspension was prepared by 3-4 days old culture of inoculated to liquid medium. Placed this for 5-6 days. Filtered through Whatmans filter paper. Under a light microscope concentration of spore suspension was adjusted to 10^8 conidia / ml by use of a hemacytometer

Seed selection and treatment

for the seed treatment we used one year old seed. Seeds standard germination was 60%. Seeds with no cracks selected and surface sterilization was takes place with 1% sodium hypochlorite solution for 15 minutes . Then seeds was rinsed three times with sterile distilled water and air dried. Starch was used as an adhesive A seed treatment takes place with spore suspension supplemented with 2% of starch. Then seeds were dipped in spore suspension . For untreated control seeds were dipped in 2% starch suspension and for water control seeds were dipped in water. Then seeds were dry with air and placed in sterile petriplates which contain Whatman filter paper soaked in sterile distil water. Ten seeds were placed in each petriplate. Germination and growth of coated seeds was compared with untreated control and to a water control Germination of seeds and growth was recorded daily for 10 days. Germination percentage of seeds were calculated as:

$$\text{Germination (\%)} = \frac{\text{Number of germinated seeds} \times 100}{\text{Total number of seeds}}$$

Total number of seeds

Result and Discussion:

In the result it is found that all vegetable seeds shown above 80% of seed germination when treated with spore suspension of *Trichoderma koningii* while in starch control above 65 % of seed germination observed and below 60% seed germination were found in the water control.

Table:1. Effect of spore suspension on seed germination of different vegetables

Sr. No.	Name of the vegetable	Germination in spore suspension treated seeds	Germination in starch treated seeds	Germination in water treated seeds
1.	<i>Trigonella foenum</i> (Methi)	100%	75%	60%
2.	<i>Hibiscus cannabinus</i> (Ambadi)	90%	65%	60%

Table: 2. Effect *Trichoderma koningii* LCF on growth of the plant after 10 days

Sr. No.	Name of the plant	Growth of the plant in LCF treated petriplates (mean in mm)	Growth of the plant in starch treated petriplates (mean in mm)	Growth of the plant in control petriplates (mean in mm)
1.	<i>Trigonella foenum</i> (Methi)	55.1 mm	40.3 mm	35.4 mm
2.	<i>Hibiscus cannabinus</i> (Ambadi)	70.4 mm	52.1 mm	40.2 mm



Acknowledgement

Authors are thankful to DBT, new delhi for finalcial assistance under “Star College Scheme” and the principal New college Kolhapur.

Reference

- Barker R, Paulitz TC (1996).** Theoretical basis for microbial interactions leading to biological control of soil borne plant pathogens. In: Hall R (Ed). Principals and practice of managing soil borne plant pathogens. Ann. Phythopathol. Soc. St. Paul, Mn. pp.50-79
- Harman GE, Hadar Y (1983).** Biological control of *Pythium* species. Seed Sci. Technol. 11: 893-906.
- Heydecker W, 1997.** Stress and seed germination and agronomic view. In the physiology and biochemistry of seed dormancy, A A Khan, ed. Amsterdam: North Holland publishing company.
- Johnson LA, 1957.** Effect of antibiotics on the number of bacteria and fungi isolated from soil by dilution plate method. *Phytopathology*, **47**: 21-22.
- Koch E (1999).** Evaluation of commercial products for microbial control of soil borne plant disease. Crop Prod. 18: 119-125.
- Kubicek CP and Harman GE, 2002.** “Basic biology, taxonomy and genetics” (Taylor and Francis Ltd. London), Pp.14
- Nagamani A and Manoharachary C, 2002.** Monographic Contribution on Trichoderma. Associated Publishing Company. New Delhi.
- Ricker AJ and Ricker RS, 1936.** Introduction to Research on Plant diseases John S. Swift Co., St.



Influence of plant growth regulators on total alkaloids content of *Amaranthus gangeticus* L. under salt stress.

¹Priyanka P. Jadhav and ²D. K. Gaikwad

¹Department of Botany, SSCM, Kolhapur, 416002, (MS) India

²Department of Botany, Shivaji University, Kolhapur.416004, (MS) India

KEYWORDS

Putrescine, GABA, Bionics, Alkaloids

ABSTRACT

Today's world is facing a problem of salinity stress. Plant growth regulators are widely used to prevail biotic stresses including salinity stress in plants. *Amaranthus gangeticus* L. belonging to the family Amaranthaceae and it is used as leaf and stem vegetable. The exogenous applications of plant growth regulators like Putrescine, SA, GABA, and Biotonic under the NaCl salinity stress (50, 100 mM) on the alkaloid content of *A. gangeticus* was studied. Total alkaloids content is increased with increasing salinity treatments in leaf and stem tissue of *A. gangeticus* as compared to unstressed control. The alkaloid content was increased by foliar application of SA, Putrescine, GABA and Biotonic in leaf and stem tissue of *A. gangeticus* under saline condition this might be helpful to increase salt tolerance potential of *A. gangeticus*.

Corresponding Author
Email

jpriyanka0510@gmail.com

Introduction

In many plants alkaloids are regarded part of constitutive chemical defence system (Croteau *et al.*, 2000). *Amaranthus* is an important leaf and stem vegetable crop as well as the seeds are used as an important source of critical amino acids. Formation of saline soil is a major problem of modern agriculture, which reduces the growth and productivity of major crop plants. Thus, the application of various growth regulators (SA, Putrescine, GABA and Biotonic formulation) ameliorate the salt stress. It is found beneficial for growth and development of this crop under saline condition. The various organic and inorganic constituents are considerably altered due to stress and further these are maintained due to foliar application of SA, Putrescine, GABA and Biotonic

Putrescine, GABA and Biotonic formulation. In many plants alkaloids are regarded part of constitutive chemical defence system (Croteau *et al.*, 2000).

Salinity treatments and foliar application of plant growth regulators :-

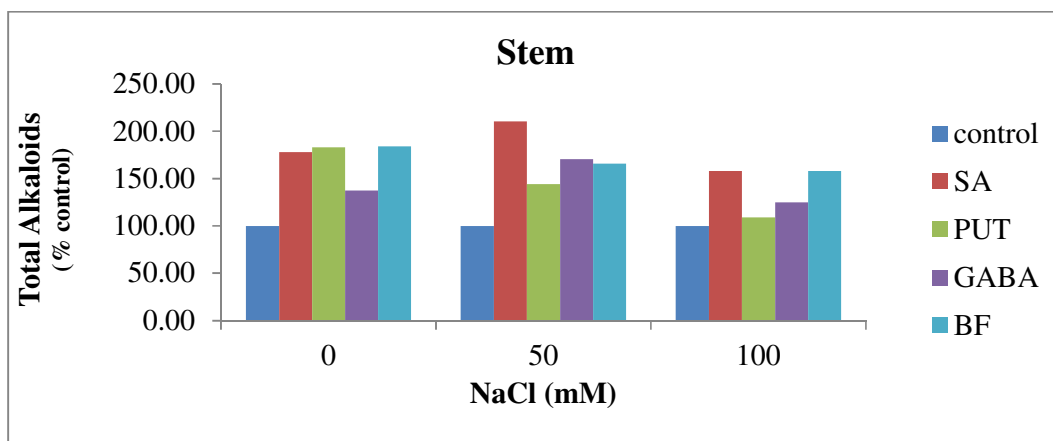
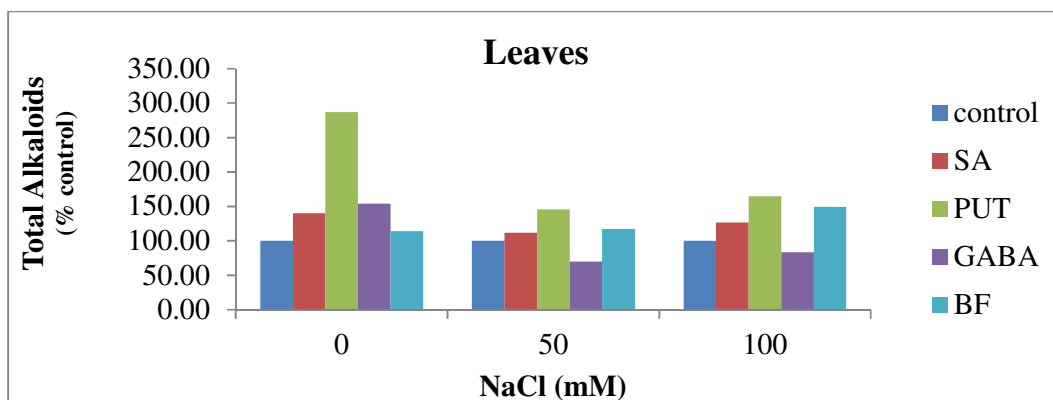
A. gangeticus Seeds were sown in earthen pots filled with garden soil containing farm yard manure in the proportion of 3:1. Pots were watered twice a week and every care was taken to raise healthy and vigorously growing plants in each pot. 30 days old seedlings were irrigated with equal volume of the saline water (50 and 100 mM NaCl) twice a week alternating with water. After two successive salinity treatments spray of respective plant growth regulators such as SA (50 ppm), Putrescine (10 ppm), GABA (10 ppm) and Biotonic formulation was given. (Biotonic formulation is a compound mixture of amino acids (Cystein, Methionine,

mixture of amino acids (Cystein, Methionine, Lysine, Valine and GABA), vitamins (Riboflavin B2 and Nicotinic acid B3), Saccharides (Myo-inositol), cytokinin (6BA) and protein (albumin), each compound dissolved separately and then all the compounds were mixed together to make the final volume 100 ml with DW to achieve 100 ppm concentration. This is the stock solution of biotonic formulation. 0.5 ml of stock solution was added in 1000 ml DW and used for foliar application) and spraying was repeated after one week from the first spray. After such two sprays the plants were used for analysis. The weed control of plant was done by hand weeding.

Total alkaloid: The total alkaloid content in the leaves and stem of *A. gangeticus* (from all the treatments and control)

was determined using 1,10-phenanthroline method described by Singh *et al.* (2004) with modification. The extracts were obtained by homogenizing 0.5 g plant material in 10 ml 80% ethanol. This was filtered through muslin cloth and centrifuged at 5000 rpm for 10 min. Supernatant was used for the further estimation. The reaction mixture consisted of 1ml plant extract, 1ml of 0.05 M solution of 1, 10- phenanthroline in ethanol and 1 ml of 0.025 M FeCl₃ in 0.5 M HCl. The reaction mixture was incubated for 30 minutes in water bath maintained at 70 ± 2^oC. The absorbance of red coloured product was measured at 510 nm against reagent blank. Alkaloid contents were estimated and it was calculated with the help of standard curve of colchicines. The values were expressed as g 100⁻¹ g of dry weight.

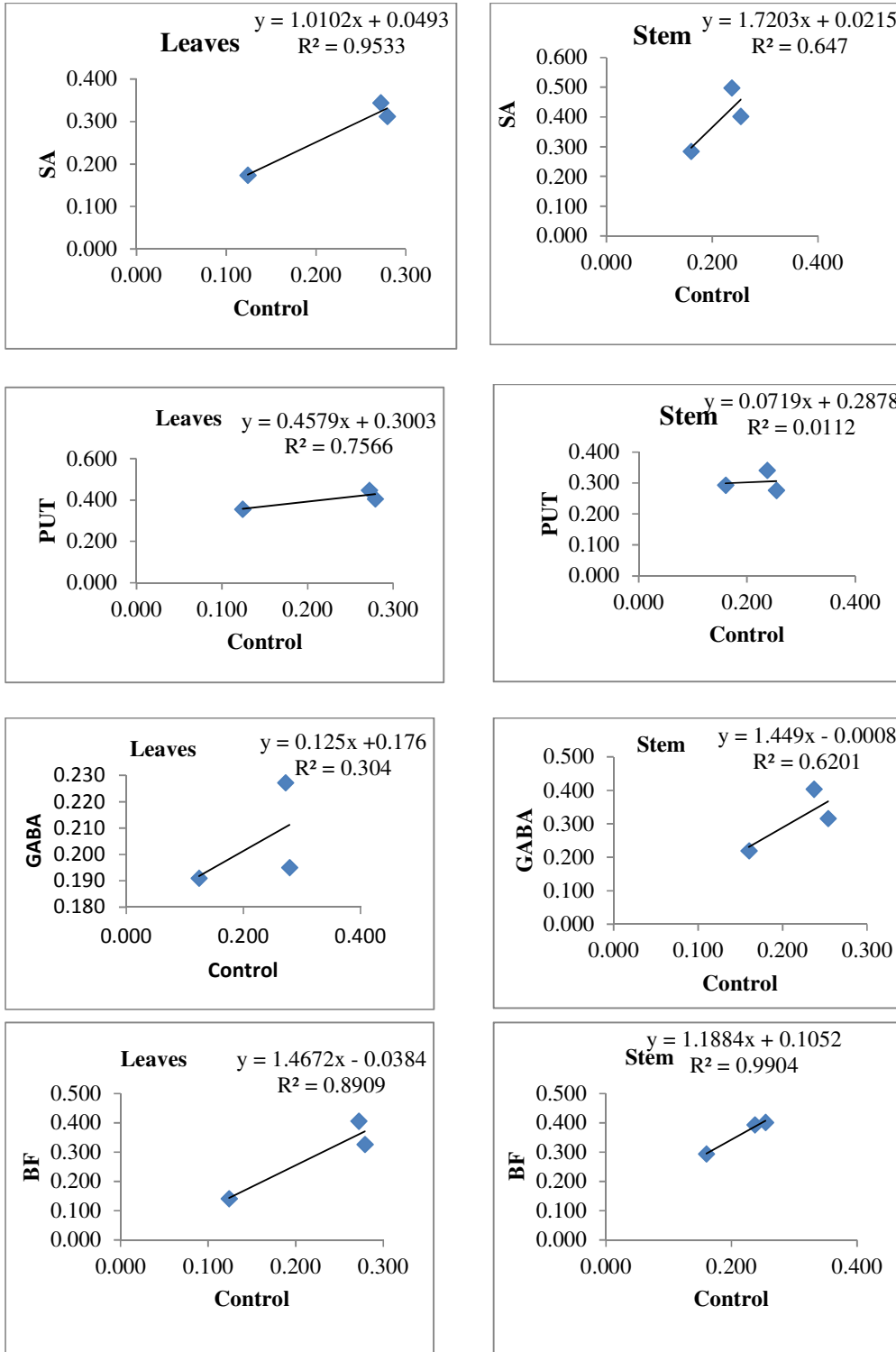
Fig.1.Effect of foliar application of plant growth regulators on total Alkaloids content of the leaves and stem of *A. gangeticus* L. grown under NaCl salinity stress.



Alkaloid (g 100⁻¹ g dry Wt.)



Fig.2. Relationship between plant growth regulators and different salinity treatment on total Alkaloid content of the leaves and stem of *A. gangeticus* L.



Result and discussion

Effect of foliar application of SA, Putrescine, GABA and Biotonic formulation on alkaloids content of the leaf and stem tissue of *A. gangeticus* grown under saline condition is shown in Figure 1. It is evident from the results that total alkaloids content is increased with increasing salinity treatments in leaf and stem tissue of *A. gangeticus* as compared to unstressed control. While the foliar application of SA, Putrescine, GABA and Biotonic formulation results in elevation in the alkaloid content in leaf and stem tissue than unsprayed stressed control and sprayed unstressed control. The linear regression analysis method of determining the R^2 (0.897) on alkaloids content Fig. 2 indicates that SA, Putrescine and biotonic formulation exhibits a positive correlation with different salinity stress treatment in the leaves and biotonic formulation in the stem of *A. gangeticus*.

Jaleel *et al.* (2007) reported that content of alkaloid increased with increase in salinity treatment in *Catharanthus roseus*. Nikam (2007) found that alkaloid content in leaf tissue of *Chlorophytum borivilianum* reduced under salinity treatments while only marginal changes found in the tuber tissue. Nivedithadevi and Somasundaram (2012) reported that content of alkaloid was increased by application of SA in *Solanum trilobatum* than as compare to control. Awate and Gaikwad (2014) found that foliar application of SA on medicinally important plant *Simarouba glauca* increases content of alkaloid in leaves. Application of SA to *Catharanthus roseus* increases alkaloid content in salt stressed and unstressed plants (Misra *et al.*, 2014). Foliar application of Putrescine to periwinkle (*Catharanthus roseus*) plant significantly increases total alkaloids content as compare to control (Talaat *et al.*, 2005). Ali (2000) found that content of alkaloid was increased in *Atropa belladonna* seedling by application of Putrescine.

The alkaloid content was increased by foliar application of SA, Putrescine, GABA and Biotonic in leaf and

stem tissue of *A. gangeticus* under saline condition this might be helpful to increase salt tolerance potential of *A. gangeticus*.

Conclusions

In the present study the alkaloid content increased due to foliar application of SA, Putrescine, GABA and Biotonic in leaf and stem tissue of *A. gangeticus* under saline condition, this might be helpful to increase bioactive potential of *A. gangeticus* under saline condition.

Reference

- Ali, R.M. (2000).** Role of putrescine in salt tolerance of *Atropa belladonna* plant. *Plant Science.*, **152**(2): 173–179.
- Awate, P. D. and Gaikwad, D. K. (2014)** Influence of Growth Regulators on Secondary Metabolites of Medicinally Important Oil Yielding Plant *Simarouba glauca* DC. under Water Stress Conditions. *Journal of Stress Physiology and Biochemistry*, **10**: 222-229
- Croteau, R., Kutchan, T.M. and Lewis, N.G. (2000).** Natural Products (Secondary metabolites). In: *Biochemistry and Molecular Biology of Plants*. (eds.) Buchanan, B., Gruissem, W. and Jones, R. (Publ.) American Society of Plant Physiologists: pp- 1250-1318.
- Jaleel, C.A., Manivannan P. and Sankar, B. (2007).** Water deficit stress mitigation by calcium chloride in *Catharanthus roseus*: Effects on oxidative stress, proline metabolism and in dole alkaloid accumulation. *Colloids Surf.B: Biointerfaces.*, **60**: 110-111.
- Misra, N., Misra. R., Mariam A., Yusuf K. and Yusuf L. (2014).** Salicylic Acid alters antioxidant and phenolics metabolism in *catharanthus roseus* grown under salinity stress. *Afr J Tradit Complement Altern Med.*, **11**(5): 118-125.
- Nivedithadevi, D. and Somasundaram, R. (2012). Secondary metabolites content Variations in *Solanum trilobatum*



- Nikam, V. K. (2007).** Physiological studies in a medicinal plant *Chlorophytum borivilianum* Ph. D. Thesis submitted to Shivaji University, Kolhapur (MS) India.
- Nivedithadevi, D. and Somasundaram, R. (2012).** Secondary metabolites content Variations in *Solanum trilobatum* (L.) under treatment with plant growth regulators. *International Journal of Pharmaceutical and Biological Archives.*, **3**(6): 1437-1444.
- Singh, D.K. , Srivastava, B. and Sahu, A. (2004).** Spectrophotometric determination of *Rauwolfia* alkaloids, estimation of Reserpine in pharmaceuticals. *Analytical Sci.*, **20**: 571-573.
- Talaat, I. M., Bekheta M. A. and Mahgoub, M. M. (2005).** Physiological response of periwinkle plants (*Catharanthus roseus* L.) to tryptophan and putrescine. *Int.J.Agric.Biol.*, **7**: 210-213.



Water quality assessment of takve lake of shirala taluka, Sangli district.

¹Shakila P. Maldar*, ²Niranjana S. Chavan.

¹Smt. Kasturbai Walchand College, Department of Botany, Sangli*

²Department of Botany, Shivaji University, Kolhapur

KEYWORDS

Physicochemical parameters, Water quality Index, Takve Lak

Corresponding Author
Email
drsunillondhe@gmail.com

ABSTRACT

The present study was attempted to calculate Water Quality Index of Takve Lake. Takve water body is located in Shirala Taluka of Sangli district, Maharashtra. In order to assess the status of quality of water the work is under taken. The present water body is selected as it is located in remote place. There are several ways to assess the quality of water as deemed fit for drinking, irrigation and industrial use. Water quality index, indicates the quality in terms of index number and offers a useful representation of overall quality of water for public .A number of parameters affect the usability of water for particular purpose. Thus water quality index was determined on the basis of various Physico-chemical parameters viz. Electric conductivity, pH, temperature, total hardness, total alkalinity, ammonia, dissolved oxygen, Biochemical oxygen demand, organic nitrogen, Total nitrogen, and Total phosphorus. The index value of water body during rainy season and summer season was found to be above 50 indicating poor quality status. But in winter index value is below 50 (41.17) indicating good water quality of water.

Introduction

The fresh water is of vital concern for mankind, since it is directly linked to human welfare .The surface water bodies are most important source of water for human activities are unfortunately under sever environmental stress .

The measurement of water quality index decide the water quality status .Water quality index of ponds and lakes have been studied by several workers. (Horton (1965) Shardendu and Ambasht (1988) Yogendra and Puttaiah (2008) Umamaheshwari (2010). Water quality index thus provides a single number that expresses over all water quality at a

certain locations and objective of water quality index to turn complex water quality data into information that is understandable and useable by the public.

Water Quality Index (WQI) is defined as a rating reflecting the composite influence of different water quality parameters as the overall quality of water. A single number cannot tell the whole story of quality; there are many other water quality parameters that are not included in the index. However water quality index based on important parameters can serve as simple indicator. In general water quality indices incorporate data from multiple water quality

parameters in to a mathematical equations that rates the health of water body with number.

Shirala taluka ,situated at the bank of Morna River which has numerous lentic water bodies .These water bodies are manmade(artificially constructed reservoirs) to provide water for irrigation purpose or domestic use. These water bodies reflect the society around them. The water quality of water body Takve has not been studied scientifically so far. Hence the present investigation is under taken: Shirala taluka experiences three distinct seasons, summer, rainy and winter. The WQI was calculated from the suitability of pond water for human consumption. The weights for various water quality parameters were assumed to be inversely proportional to the recommended standards which have been presented in respective table for the corresponding parameter. Takve water body is selected for assessing the quality of water. Because the water body practically receive domestic water and agricultural runoff throughout the year. Therefore to know the current status of the water body present work is attempted.

Material and Method

The water samples were collected at an interval of 30 days and analyzed for 12 physico-chemical parameters by following standard procedures.The parameters ,pH,electrical conductivity, and dissolved oxygen were monitored at the sampling sites and other parameters like total hardness, total alkalinity ,ammonia, total nitrogen ,organic nitrogen ,total phosphorus ,biological oxygen demand were analyzed in the laboratory as per the APHA (1995) and Trivedi and Goel (1984) during the year 2012-2013.

The WQI has been calculated by using the standards of drinking water quality recommended by World Health Organization (WHO), Bureau of Indian Standards (BIS) and Indian Council of Medical Research(ICMR) .The weighted arithmetic Index method has been used for the calculation of WQI of water body .The quality rating OR sub index (qn)was calculated using the following expressions.

$$qn=100(Vn-Vio)/(Sn-Vio)$$

Where,

Qn= Quality rating for the nth water quality parameter

Vn= Estimated value of the nth parameter at a given sampling stations

Sn= Standard permissible value of nth parameter

Vio= Ideal value of the nth parameters in pure water i.e. 0 for all other

Parameters except the parameters pH and Dissolved oxygen (7.0 and14.6mg/l) respectively.

Unit weight was calculated by a value inversely proportional to the recommended standard value Sn of the corresponding parameter

$$Wn= K/Sn$$

Where,

Wn= Unit weight for the nth parameter

Sn =Standard value for the nth parameter

K= Constant of proportionality

The overall WQI level and status of water quality as suggested by Chatterjee and Raziuddin (2002) is given in Table-1

Table 1: Water Quality Index (WQI) level and status of water Quality

Water quality Index	Water Quality Status
90≥	Excellent
65 to 89	Permissible
39 to 64	Marginally suitable
11 to 34	In adequate for use
0 ≤	Totally Unsuitable



The drinking water standards as recommended by recommending agencies and unit weights are presented in Table .2

Table .2 Drinking water standards and unit weights

Parameters	Standards	Recommending Agency	Unit Weight
pH	6.5-8.5	ICMR/BIS	0.236
Electric conductivity (EC)	300	ICMR	0.371
Temperature	-----	-----	-----
Total alkalinity (TA)	120	ICMR	0.014
Total hardness (TH)	500	ICMR/BIS	0.003
Dissolved oxygen (DO)	5.0	ICMR/BIS	0.330
Biological oxygen demand(BOD)	5.0	ICMR/BIS	0.330
Ammonia	5.0	ICMR/BIS	0.12042
Total Nitrogen	-----	-----	-----
Organic Nitrogen	-----	-----	-----
Total Phosphorus	6.0	ICMR/BIS	0.10035

❖ All values except pH and Electric conductivity are in mg/l EC in mmhos/cm

Results and Discussion

The results of present investigations are depicted in Table 3 and 4. Water Quality Index of the lake Takve was calculated for seasons (Rainy, winter and summer season.)

Table 3:- Seasonal variation in Physico-chemical parameters

Sr. no.	Parameters	Rainy season	Winter season	Summer season
1	pH	7.5	6.46	7.96
2	Electrical conductivity	10.599	40.747	59.101
3	Total alkalinity (TA)	184.17	128.33	129.00
4	Total Hardness(TH)	156.42	114.33	139.00
5	Dissolved Oxygen(DO)	2.28	2.85	3.34
6	Biological Oxygen Demand(BOD)	1.63	0.43	1.79
7	Ammonia	8.15	0.52	3.03

8	Total Phosphorus	0.02	0.13	0.58
---	------------------	------	------	------

All values expect pH and Electrical Conductivity are in mg/L, Ec expression in mmhos/cm

Table 4:- Water Quality Index calculated for Rainy season.

Sr.no.	Parameters	V _n	S _n	1/S _n	W _n	Q _n	W _n Q _n
1	pH	7.5	7	0.143	0.1547	50	7.735
2	EC	10.599	300	0.003	0.0032	3.533	0.0113
3	Total alkalinity (TA)	184.17	120	0.008	0.0086	153.48	1.320
4	Total Hardness(TH)	156.42	500	0.003	0.0032	31.284	0.1001
5	Dissolved Oxygen(DO)	2.28	05	0.200	0.2164	128.3	27.76
6	Biological Oxygen Demand (BOD)	1.63	05	0.200	0.2164	32.6	7.055
7	Ammonia	8.15	05	0.200	0.2164	163	35.27
8	Total Phosphorus	0.02	06	0.167	0.1806	0.333	0.0601
					∑W _n = 1.0	∑q _n = 562.53	∑W _n q _n = 79.312

Water Quality Index in Rainy season = ∑q_nW_n / W_n

$$WQI = 79.312$$

Table 5:- Calculation of Water Quality Index calculated for in winter season.

Sr. no	Parameters	V _n	S _n	1/S _n	W _n	Q _n	W _n Q _n
1	pH	6.46	7	0.143	0.1547	36.00	5.5692
2	EC	40.747	300	0.003	0.0032	13.582	0.0435
3	Total alkalinity (TA)	128.33	120	0.008	0.0086	106.94	0.9197
4	Total Hardness(TH)	114.33	300	0.003	0.0032	38.11	0.1220
5	Dissolved Oxygen(DO)	2.85	05	0.200	0.2164	122.40	26.487
6	Biological Oxygen Demand (BOD)	0.43	05	0.200	0.2164	8.6	1.861
7	Ammonia	0.52	05	0.200	0.2164	10.4	2.251
8	Total Phosphorus	0.13	06	0.167	0.1806	2.167	0.391
					∑W _n = 1	∑Q _n = 338.20	∑W _n q _n = 37.644

Water Quality Index (WQI) in winter season = ∑q_nW_n / ∑ W_n

$$= 37.644/1$$



WQI = 37.644

Table 6:- Calculation of Water Quality Index calculated in summer season.

Sr. no	Parameters	V _n	S _n	1/S _n	W _n	Q _n	W _n Q _n
1	pH	7.96	7	0.143	0.1547	64	14.016
2	EC	59.101	300	0.003	0.0032	19.700	0.0634
3	Total alkalinity (TA)	129.00	120	0.008	0.0086	107.5	0.9245
4	Total Hardness (TH)	139.0	300	0.003	0.0032	46.33	0.1483
5	Dissolved Oxygen (DO)	3.34	05	0.200	0.2164	117.29	25.382
6	Biological Oxygen Demand (BOD)	1.79	05	0.200	0.2164	35.8	7.7471
7	Ammonia	3.30	05	0.200	0.2164	60.6	13.114
8	Total Phosphorus	0.58	06	0.167	0.1806	9.67	1.7464
					∑W _n = 1	∑Q _n =460.89	∑W _n Q _n =88.55

Water Quality Index (WQI) in summer season = $\frac{\sum q_n W_n}{\sum W_n}$

Water Quality index of Takve was established by placing eight (8) important physicochemical parameters in three different seasons viz. Rainy, winter, and summer season. From the results it was observed that WQI of the lake was maximum during rainy seasons.

In rainy season the WQI was found to be 57.53 which indicates poor water quality. In winter season it is 41.175 which is good water quality. But again in summer it changes (56.04) is poor as per standard values. Based on the results, it is clear that water is not suitable for drinking in rainy and summer season. This water quality rating clearly expresses the status of the lake i.e. water is unsuitable for the human consumption.

In present investigation pH ranged between 6.46 to 7.96. In many of the collections the pH remained near neutral. However, when average values for three seasons are taken into account, the present water body found to be slightly alkaline. These findings are similar to the observations of Ambasht (1971), Peter (1975) Shardendu and Ambasht (1988) Swarnalata and Narasing Rao (1993), Sinha (1995) and Yogendra and Puttaiah (2008) who have also made similar observations in their studies on different water bodies. Maximum Ec found in summer season the concentration of dissolved oxygen regulates the distribution of aquatic flora and fauna. The present investigation indicated that the conc. of dissolved oxygen fluctuated between 2 to 3 mg/l in rainy season,

and in winter season while 3 to 4 mg/l in summer season. Seasonally, the concentration of dissolved oxygen was more during summer and least during rainy season. This observation is similar with observations of Poonam Bhadija and Ashokkumar vaghela (2013)

Biochemical oxygen demand is a parameter to assess the organic load in water body. The BOD concentration ranges between 1 to 3 mg/l .Present values summarize that there are fluctuations in the physicochemical parameters seasonally. However, during rainy season because of dilution, mixing and run off the water quality changes. The present piece of work suggests that the Takve lake water is not suitable for drinking purpose.

References

- Ambasht,R.S. (1971)** , Ecosystem study of a tropical pond in relation to primary production of different vegetation zones, *Hydrobiologia*,12:57-61.
- APHA, (1981)**, Standard methods for the Examination of water and waste water, APHA, Washington DC.USA.
- APHA, (1995)**, Standard methods for the Examination of water and waste water, 9thEdition, American Public Health Association, Washington D.C.
- Chatterjee,C.and Raziuddin, M. (2002)** , Determination of water quality Index (WQI) of a degraded river in Asanol Industrial area ,Ranging , Burdoan , West Bengal ,Nature, Environment and Pollution Technology, 1(2): 49-59 and 181-189.
- Petre,T.,(1975)** ,Limnology and Fisheries of Nymba Yamung, a manmade lake in Tanzania, *Journal of Tropical Hydrobiology, Fish*, 4:39-50.
- Sinha, S.K. (1995)** , Potability of rural ponds water at Muzaffarpur (Bihar) ,A note on water quality pollution Research,14 (1) : 135-140.
- Shardendu and Ambasht ,R.S. (1988)** oxygen in forms an ionic strength ,*Journal of Tropical,Limnological Studies of rural pond and an urban tropical ecosystem, ecosystem, oxygen in forms and ionic strength, Journal of Tropical Ecology.*
- Sinha, S.K. (1995)** , Potability of rural ponds water at Muzaffarpur (Bihar) ,A note on water quality pollution Research,14 (1) : 135-140.
- Trivedi and Goel, (1984)**, Chemical and Biological methods or water pollution studies, Environment Publication, Karad.
- Uma Maheshwari,S, S, S.(2010)**, Water Quality Index of Temple pond at TalaKadu Karnataka, India, *Lake (2010) ,Wetlands ,Biodiversity and climate change.*
- Venkateshwarlu, V. (1993)** Ecological studies on the rivers of Andhra Pradesh with special reference to water quality and pollution, *Proceeding of Indian Academy of Science (Plant Science)* , 96: 495-508
- Yogendra, K and Puttaiah, E.T., (2008)** Determination of Water Quality Index and suitability of an Urban water body in Shimoga Town Karnataka. *Proceedings of Taal .2007. The 12th World Conference, :342-346 (Editors ,Sengupta)*



Kinetics and Mechanism of Oxidation of Maltose by keggin type 12-tungstocobaltate (III) in hydrochloric acid Medium

Sunil N. Zende

Department of Chemistry, Doodhsakhar Mahavidyalya Bidri, Dist: Kolhapur, Maharashtra, India.

KEYWORDS

ABSTRACT

Kinetics and Mechanism of Oxidation of Maltose by keggin type 12-tungstocobaltate (III) in acidic medium has been investigated at 25°C for the first time. The value of pseudo-first-order rate constant remains constant with variation of Keggin type 12-tungstocobaltate (III) clearly indicating the order of reaction with respect to $[\text{Co}^{\text{III}}]$ is unity. First-order rate constant values were found to be increased with increase in $[\text{Maltose}]$ and $[\text{H}^+]$. The order with respect to maltose concentration was found to be one each. Variations in ionic strength (μ) and dielectric constant (D) of the medium have not influenced the oxidation rates. The proposed mechanism, involving most reactive activated complex formed as a result of interaction between the Keggin type 12-tungstocobaltate (III) and maltose is supported by kinetic orders, Michaelis-Menten plot and the main oxidation products of the reaction was identified as formic acid.

Corresponding Author
Email

sunil.zende018@gmail.com

Introduction

Carbohydrates are the fuel of life, being the main energy source for living organisms and the central pathway of energy storage and supply for most cells. The study of the carbohydrates and their derivatives has greatly enriched chemistry, particularly with respect to the role of molecular shape and conformation in chemical reactions [1]. These biological and economic importances of the carbohydrates and especially the monosaccharides and disaccharides have been largely responsible for the interest in the study of their biological and physiochemical properties along with reactivities [2]. The kinetics of oxidation of sugars by a variety of oxidants has been reported [3-4] in both acidic and alkaline media. Several different mechanisms showing the importance of enediols, cyclic forms of sugars, etc. have been established.

The oxidations of different substrates by KMnO_4 in acidic medium are reported [5, 6]. N-Bromosuccinamide is reported for oxidation of [7-11] sugar (a biologically important substrate). These reports and recent publications concerning the oxidation of sugars by organic halo amines have prompted us to use the heteropolyoxometalate for the oxidation of maltose in perchloric acid medium. The oxidation kinetics of maltose in alkaline[12] and ammoniacal[13] media have been described, but few studies in acidic media have been reported. The kinetics of oxidation of maltose by thallium (III), in the presence of sulphuric acid, in aqueous acetic acid was reported [14]. Studies involving the oxidation of the sugars by polyoxometalates are scarce, therefore we have undertaken the study of oxidation of maltose sugar by showing the importance of enediols, cyclic forms of sugars, etc. have

N-Bromosuccinamide is reported for oxidation of [7-11] sugar (a biologically important substrate). These reports and recent publications concerning the oxidation of sugars by organic halo amines have prompted us to use the heteropolyoxometalate for the oxidation of maltose in perchloric acid medium. The oxidation kinetics of maltose in alkaline [12] and ammoniacal [13] media have been described, but few studies in acidic media have been reported. The kinetics of oxidation of maltose by thallium (III), in the presence of sulphuric acid, in aqueous acetic acid was reported [14]. The first direct measurements of self exchange rates for electron transfer between POM anions in water using $[\text{Co}^{\text{II}}\text{W}_{12}\text{O}_{40}]^{6-}$ and its one electron oxidized derivative $[\text{Co}^{\text{III}}\text{W}_{12}\text{O}_{40}]^{5-}$ first synthesized and characterized by Baker and co-workers [4] has been extensively used as an oxidant both for organic and inorganic substrates [5]. The potential utility of $[\text{Co}^{\text{III}}\text{W}_{12}\text{O}_{40}]^{5-}$ as a well defined probe for determining the nature of outer-sphere oxidations of alkyl aromatic hydrocarbons [6]. When it is complexed with polytungstate ions $[\text{Co}^{\text{III}}\text{W}_{12}\text{O}_{40}]^{5-}/[\text{Co}^{\text{II}}\text{W}_{12}\text{O}_{40}]^{6-}$ which is attributed to the distribution of the charge density of the cobalt ion over a large area. The complex of transition metal ions with polyoxoanions like polytungstates are well known outer-sphere electron transfer reagent [7]. The redox reaction of $[\text{Co}^{\text{III}}\text{W}_{12}\text{O}_{40}]^{5-}$ have been recently revived [4,5]. Among various heteropolyacids structural classes the keggin type heteropolyacids have been widely used as homogeneous and heterogeneous catalysts for acid-base and oxidation reactions[8].The studies involving the oxidation of the sugars by polyoxometalates are scarce, therefore we have undertaken the study of oxidation of maltose sugar by 12-tungstocobaltate (III) in perchloric acid medium.

Materials and methods:

All the solutions were prepared in doubly distilled water. The solution of Maltose was prepared by dissolving D-maltose (SD Fine) in water. 12-tungstocobaltate (III) was prepared, by reported method.

Kinetic Measurements:

The reaction between $[\text{Co}^{\text{III}}\text{W}_{12}\text{O}_{40}]^{5-}$ and maltose was studied under pseudo-first-order conditions at a constant temperature of $25.0 \pm 0.1^\circ\text{C}$. The reaction was initiated by mixing the previously thermostated solutions of maltose and $[\text{Co}^{\text{III}}\text{W}_{12}\text{O}_{40}]^{5-}$ which also contained the requisite amount of perchloric acid, and doubly distilled water. The reaction was followed by determining the concentration of remaining $[\text{Co}^{\text{III}}\text{W}_{12}\text{O}_{40}]^{5-}$ spectrophotometrically at 624 nm. The sample run is given in Table 1 and the graph of $\log(a/a-x)$ versus 't' is shown in Fig 1. Ionic strength was maintained using NaClO_4 and to vary hydrogen ion concentrations HClO_4 (BDH) was used. The pseudo-first-order rate constants were determined from the plots of $\log [[\text{Co}^{\text{III}}\text{W}_{12}\text{O}_{40}]^{5-}]$ against time and the rate constants were reproducible within $\pm 4\%$.

Test for free radicals:

The reaction was also studied in presence of added acrylonitrile to understand the intervention of free radicals [15, 16] in the reaction. There was no effect of added acrylonitrile on the reaction and also no precipitate due to the polymerization of the added acrylonitrile was observed thus confirming the absence of any free radical formation in the reaction.

Results and discussion:

Stoichiometry and product analysis:

The stoichiometry was studied by keeping concentration of $[\text{Co}^{\text{III}}\text{W}_{12}\text{O}_{40}]^{5-}$ constant at $3 \times 10^{-3} \text{ mol dm}^{-3}$ and varying concentration of maltose from 0.2×10^{-3} to $3.0 \times 10^{-3} \text{ mol dm}^{-3}$. Different reaction mixtures containing varying concentration of maltose were prepared, which also contained required amount of perchloric acid. The concentration of unreacted $[\text{Co}^{\text{III}}\text{W}_{12}\text{O}_{40}]^{5-}$ was determined spectrophotometrically at 624 nm after 24 hours. The stoichiometry was found to be one mole of maltose per two mole of $[\text{Co}^{\text{III}}\text{W}_{12}\text{O}_{40}]^{5-}$. The main oxidation product, formic acid was detected [17] by TLC and spot test methods [18, 19].



Reaction order:

The reaction was carried out under pseudo-first-order conditions, keeping the concentration of perchloric acid constant at 0.3 mol dm⁻³ and varying either maltose from 0.01 to 0.1 mol dm⁻³ at constant [one mole of [Co^{III}W₁₂O₄₀]⁵⁻ (1.0 x 10⁻³ mol dm⁻³) or [one mole of [Co^{III}W₁₂O₄₀]⁵⁻ from 2.2 x 10⁻⁴ to 1.8 x 10⁻³ mol dm⁻³ at constant maltose (3.0 x 10⁻² mol dm⁻³). The pseudo-first-order rate constants were found to be increased with increase in the concentration of the maltose and the order was found to be 0.88 as determined by plot of log (k_{obs}) against log [maltose]. The order in oxidant concentration was found to be unity as the pseudo-first-order plots were found to be linear and the pseudo-first-order rate constants were fairly constant as the concentration of oxidant is varied (Table 2).

The effect of hydrogen ion concentration on the reaction was studied to know probable prior protonation equilibria of either the oxidant or the substrate and to identify the active reactant species. The concentration of H⁺ ion was varied from 0.1 to 0.5 mol dm⁻³ keeping all other concentrations constant. It was found that the reaction rate increases with the concentration of H⁺ ions (Table 2) and the order in [H⁺] was determined from the plot of log k_{obs} against log [H⁺] and was found to be 0.91.

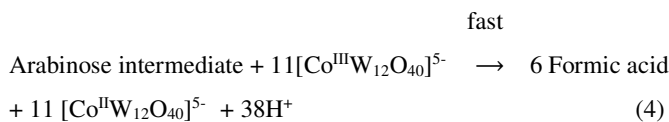
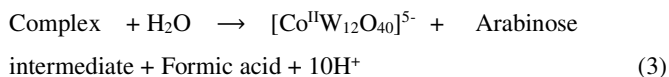
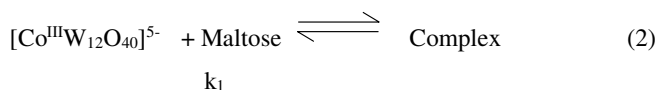
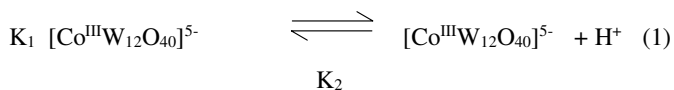
Effect of solvent polarity and ionic strength:

The effects of ionic strength and solvent polarity were studied keeping concentration of [Co^{III}W₁₂O₄₀]⁵⁻, methionine and perchloric acid constant at 1.0x 10⁻³ mol dm⁻³, 0.03 mol dm⁻³ and 0.35 mol dm⁻³ respectively at 25°C. Sodium perchlorate and acetonitrile were used to vary the ionic strength and solvent polarity, respectively. The rate of the reaction was unaffected by increasing ionic strength from 0.40 to 0.90 mol dm⁻³.

Mechanism and rate law:

The mechanism according to Scheme 3 proceeds with the

formation of a complex between the maltose and [Co^{III}W₁₂O₄₀]⁵⁻ in a prior equilibrium which then decomposes to give Arabinonic Acid, Formic acid and [Co^{III}W₁₂O₄₀]⁸⁻ in a rate determining step. Arabinonic Acid reacts with five molecules of oxidants in fast step to give the product formic acid.



$$\text{Rate} = \frac{k_1 K_2 [H^+] [\text{maltose}] [Co^{III}W_{12}O_{40}]^{5-}}{([H^+] + K_1)(1 + K_2 [\text{maltose}])} \quad (5)$$

$$k_{obs} = \frac{k_1 K_2 [H^+] [\text{maltose}]}{([H^+] + K_1)(1 + K_2 [\text{maltose}])} \quad (6)$$

Conclusions:

Kinetics of oxidation of maltose by protonated 12-tungstocobaltate (III) has been investigated at 25°C. Almost constant values of pseudo-first-order rate constant obtained during the variation of oxidant, 12-tungstocobaltate (III) clearly reveal that order of reaction with respect to [Co^{III}] is unity. First-order kinetics with respect to [Maltose] and [H⁺] is evident from the observed values of rate constants. Variations in ionic strength (μ) and dielectric constant (D) do not affect the rate of reaction. Protonated 12-tungstocobaltate (III) and unprotonated maltose have been postulated as the reactive species during the reaction. The main oxidation product of the reaction was identified as formic acid.

Table 1: Sample run for oxidation of maltose by 12-tungstocobaltate (III) in perchloric acid medium at 25°C .

$[\text{HClO}_4] = 0.3 \text{ mol dm}^{-3}$, $[\text{Co}^{\text{III}}] = 1 \times 10^{-3} \text{ mol dm}^{-3}$, $[\text{Maltose}] = 0.1 \text{ mol dm}^{-3}$, $I = 0.4$.

Time in min	Absorbance at 624 nm	Log(a/a-x)
0	0.284	-
2	0.261	0.036678
4	0.226	0.09921
6	0.193	0.167761
8	0.163	0.241131
10	0.137	0.316598
12	0.114	0.396413
14	0.095	0.475595
16	0.077	0.566828
18	0.064	0.647138
20	0.053	0.729042

Table 2: Effect of concentration of maltose, perchloric acid and 12-tungstocobaltate (III) ion, on the reaction between maltose and 12-tungstocobaltate (III) at 25°C

$10^3[\text{Co}^{\text{III}}\text{W}_{12}\text{O}_{40}]^{5-}$ mol dm ⁻³	10[HClO ₄] mol dm ⁻³	10[Maltose] mol dm ⁻³	$10^3 k_{\text{obs}}$ s ⁻¹
0.2	3.0	1.0	1.20
0.4	3.0	1.0	1.10
0.6	3.0	1.0	1.12
0.8	3.0	1.0	0.99
1.0	3.0	1.0	1.23
1.0	1.0	1.0	0.43
1.0	2.0	1.0	0.90
1.0	3.0	1.0	1.23
1.0	4.0	1.0	1.86
1.0	5.0	1.0	2.30
1.0	3.0	0.1	0.16
1.0	3.0	0.3	0.56
1.0	3.0	0.5	0.85
1.0	3.0	0.7	1.05
1.0	3.0	1.0	1.23



Fig:1 Pseudo first order plot for oxidation of maltose by 12-tungstocobaltate (III) in perchloric acid. (Conditions as in table 1)

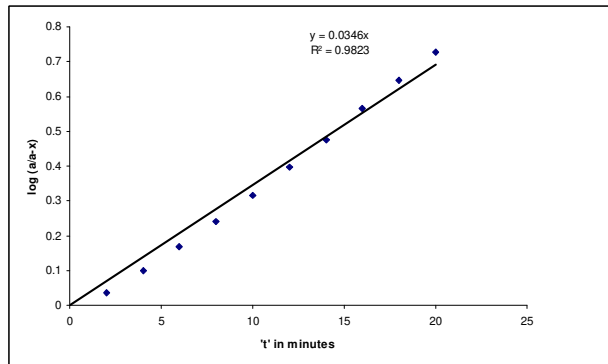


Fig: 2 Michaelis-Menten plot for oxidation of maltose by 12-tungstocobaltate (III) in perchloric acid. (Conditions as in table 2)

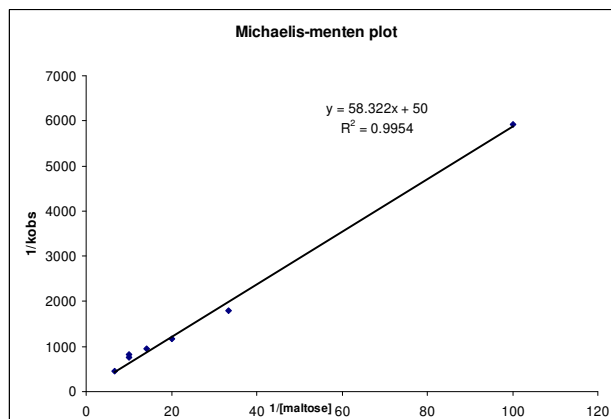
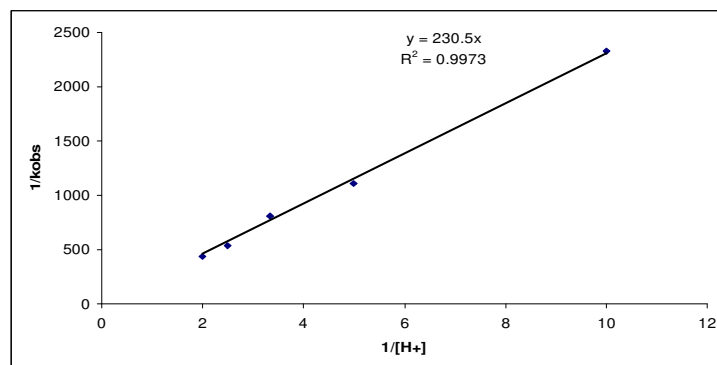


Fig. 3 Verification of rate law (Plot of 1/k_obs versus 1/[H⁺])





Ecofriendly Solvent Free Synthesis of Dihydropyrimidine Derivatives by Biginelli Reaction

A. C. Bhosale^a, S. A. Kenawade^b

Department of Chemistry, M. H. ShindeMahavidyalaya, Tisangi

Department of Chemistry, Devchand College, Arjunagar

KEYWORDS

Zinc ferrite,
Co-precipitation,
XRD, SEM,
Electrical resistivity,
Gas sensor.

Corresponding Author
Email

amarbhosalemsc@gmail.com

ABSTRACT

This work involves synthesis of dihydropyrimidine 4(a-f) derivatives from various substituted benzaldehyde, ethyl acetoacetate and urea/thiourea. After completion of the reaction products obtained 4(a-f) was confirmed by spectroscopy. Library of such dihydropyrimidine 4(a-f) derivatives has been generated and the structures were subjected to PASS for their probabilities of being biologically active. Biological prediction study of the library was done to find out most active molecules. Computer programme PASS predicted for three activities with top probability for compound 4(a-f) as- 1. Mucomembranous protector, 2. Arylacetonitrilase inhibitor, 3. Macrophage elastase inhibitor.

Introduction

Multicomponent reactions (MCRs) are of increasing importance in organic and medicinal chemistry^{1,2}. In times where a premium is put on speed, diversity, and efficiency in the drug discovery process, MCR strategies offer significant advantages over conventional linear-type syntheses. In such reactions, three or more reactants come together in a single reaction vessel to form new products that contain portions of all the components. MCRs can provide products with the diversity needed for the discovery of new lead compounds or lead optimization employing combinatorial chemistry techniques^{3,4}. The search and discovery for new MCRs on one hand, and the full exploitation of already known multicomponent reactions on the other hand, is therefore of considerable current

interest. One such MCR that belongs in the latter category is the venerable Biginellidihydropyrimidine synthesis^{5,6,7}.

In 1893, Italian chemist Pietro Biginelli reported⁸ on the acid catalyzed cyclocondensation reaction of ethyl acetoacetate (1), benzaldehyde (2), and urea (3). The reaction was carried out by simply heating a mixture of the three components dissolved in ethanol with a catalytic amount of HCl at reflux temperature. The product of this novel one-pot, three-component synthesis that precipitated on cooling of the reaction mixture was identified correctly by Biginelli as 3,4-dihydropyrimidin-2(1H)-one. Apart from a series of publications by the late Karl Folkers in the mid 1930s, the "Biginelli reaction" or "Biginelli condensation" as it was henceforth called was largely ignored in the early part of the 20th century.

The synthetic potential of this new heterocycle synthesis therefore remained unexplored for quite some time.

pharmacological efficiency

In the past decades, a broad range of biological effects, including antiviral, antitumor, antibacterial, and anti-inflammatory activities, has been ascribed to these partly reduced pyrimidine derivatives.

PASS is a software application that predicts 565 possible biological activities of a user selected (set of) compound(s). Using PASS predictions, novel pharmaceutical agents have been discovered with anxiolytic, anti-inflammatory, antihypertensive, anticancer and other activities. PASS is applicable to chemical libraries containing millions of compounds. Due to this significance of PASS, it is used in the present study as a tool to design the drug with highest probable activity.

Materials and methods:

All chemicals and solvents were reagent grade and used as purchased without any further purification. Analytical thin layer chromatography was performed on percolated silica gel 60-F 254 plates. IR spectra on KBr disks were recorded on a Shimadzu IR - 470 FT-IR spectrophotometer. The routine nuclear magnetic resonance spectra were taken in DMSO-CDCl₃ using a Bruker 300 MHz spectrophotometer with TMS as an internal standard. Chemical shift δ was given in ppm relative to TMS. The data found were in consistent with the proposed structure. Elemental analysis was done using EURO Vector Elemental Analyzer. Melting points are determined in an open capillary tube and are uncorrected.

In this paper, we prepared Zinc ferrite co-precipitation method and investigated their gas sensing response under different conditions. We report our results on the sensing response of the synthesized zinc ferrite to hydrogen sulphide, a potentially toxic gas, and describe an attempt to fabricate H₂S sensor element from the zinc ferrite. Also paper deals with the sensing mechanism of H₂S sensor. Synthetic Procedure for 5-ethoxycarbonyl-4-phenyl-6-methyl-3,4-dihydropyrimidine-2-(1H)-one 4(a):

Spectral Data and Elemental Analysis

6-Methyl-2-oxo-4-phenyl-1,2,3,4-tetrahydro-pyrimidine-5-carboxylic acid ethyl ester 4(a)

Molecular Formula: C₁₄H₁₆N₂O₃

Molecular Composition =C 64.60% H 6.20% N 10.76% O 18.44%

¹H NMR (DMSO, 400 MHz): δ 1.09 (t, 3H, -OCH₂CH₃) 2.25(s, 3H, CH₃), 3.97(q, 2H, -OCH₂CH₃), 5.05 (s, 1H, -CH), 7.28 (m, 5H, Ar-H), 7.75 (s, 1H, NH), 9.20 (s, 1H, NH).

6-Methyl-4-(3-nitro-phenyl)-2-oxo-1,2,3,4-tetrahydro-pyrimidine-5-carboxylic acid ethyl ester 4(b)

Molecular Formula =C₁₄H₁₇N₃O₅

Molecular Composition =C 54.72% H 5.58% N 13.67% O 26.03%

¹H NMR (DMSO, 400 MHz): δ 1.19 (t, 3H, -OCH₂CH₃) 2.30 (s, 3H, CH₃), 3.99 (q, 2H, -OCH₂CH₃), 5.15 (s, 1H, -CH), 7.35 (m, 4H, Ar-H), 8.75 (s, 1H, NH), 9.25 (s, 1H, NH).

4-(4-Hydroxy-phenyl)-6-methyl-2-oxo-1,2,3,4-tetrahydro-pyrimidine-5-carboxylic acid ethyl ester 4(c)

Molecular Formula =C₁₄H₁₆N₂O₄

Molecular Composition =C 60.86% H 5.84% N 10.14% O 23.16%

¹H NMR (DMSO, 400 MHz): δ 1.10 (t, 3H, -OCH₂CH₃) 2.05 (s, 3H, CH₃), 3.90 (q, 2H, -OCH₂CH₃), 5.05 (s, 1H, -CH), 6.05 (s, 1H, -OH), 7.15 (m, 4H, Ar-H), 7.60 (s, 1H, NH), 9.10 (s, 1H, NH).

6-Methyl-4-phenyl-2-thioxo-1,2,3,4-tetrahydro-pyrimidine-5-carboxylic acid ethyl ester 4(d)

Molecular Formula =C₁₄H₁₆N₂O₂S

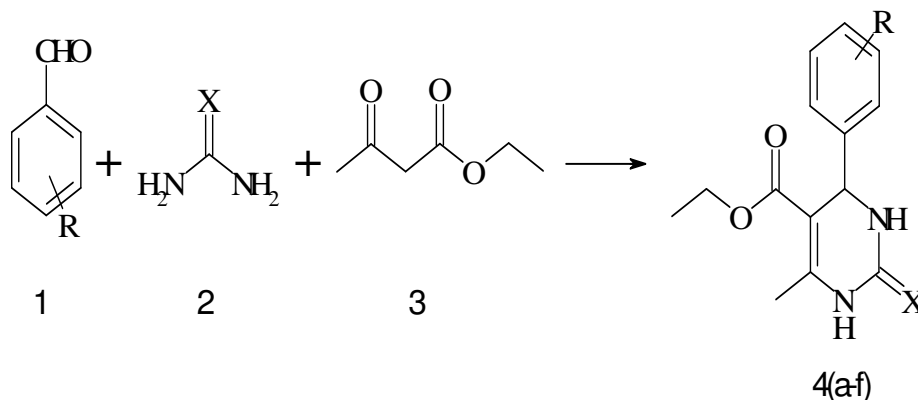
Molecular Composition =C 60.85% H 5.84% N 10.14% O 11.58% S 11.60%

¹H NMR (DMSO, 400 MHz): δ 1.09 (t, 3H, -OCH₂CH₃) 2.30 (s, 3H, CH₃), 3.95 (q, 2H, -OCH₂CH₃), 5.05 (s, 1H, -CH), 7.38 (m, 5H, Ar-H), 7.80 (s, 1H, NH), 9.40 (s, 1H, NH).

6-Methyl-4-(3-nitro-phenyl)-2-thioxo-1,2,3,4-tetrahydro-pyrimidine-5-carboxylic acid ethyl ester 4(e)

Molecular Formula =C₁₄H₁₇N₃O₄S

Molecular Composition = C 52.00% H 5.30% N 12.99% O 19.79% S 9.92%



4-(4-Hydroxy-phenyl)-6-methyl-2-thioxo-1,2,3,4-tetrahydro-pyrimidine-5-carboxylic acid ethyl ester 4(f)

Molecular Formula =C₁₄H₁₆N₂O₃S

Molecular Composition =C 57.52% H 5.52% N 9.58% O 16.42% S 10.97%

¹H NMR (DMSO, 400 MHz): δ 1.10 (t, 3H, -OCH₂CH₃), 2.20 (s, 3H, CH₃), 3.90 (q, 2H, -OCH₂CH₃), 5.05 (s, 1H, -CH), 6.25 (s, 1H, -OH), 7.28 (m, 4H, Ar-H), 7.79 (s, 1H, NH), 9.10 (s, 1H, NH).

Table – Physical characteristics of reaction

Compd	X	R	Reac ⁿ Time in hrs	Yield %	M. P. °C
4(a)	O	C ₆ H ₅	1	70	210
4(b)	O	3-NO ₂ -C ₆ H ₄	3	65	228
4(c)	O	4-OH-C ₆ H ₄	1.30	75	198
4(d)	S	C ₆ H ₅	1	75	200
4(e)	S	3-NO ₂ -C ₆ H ₄	2.50	60	220
4(f)	S	4-OH-C ₆ H ₄	1.35	60	210

Activity of compounds	Mucomembranous protector	Arylacetonitrilase inhibitor	Macrophage elastase inhibitor
4(a)	0.805	0.880	0.850
4(b)	0.608	0.554	0.570
4(c)	0.770	0.680	0.665
4(d)	0.901	0.790	0.900
4(e)	0.665	0.560	0.555
4(f)	0.775	0.600	0.647

Results and discussion

The confirmed structures were subjected to computer programme PASS for the prediction of their biological activities. Compound 4(a-f) were predicted for three activities with top probability.

1. Mucomembranous protector,
2. Arylacetonitrilase inhibitor,
3. Macrophage elastase inhibitor.

Conclusion

In conclusion, we have illustrated a new efficient procedure for the modified Biginelli reaction by heterocyclic EAA, aldehydes and thiourea within 1-3 hrs. The reaction proceeds briskly under solvent- free condition and work up is equally rapid and green approaches. The application of this method provides a simple powerful tool for the synthesis of a large number of pyrimidine derivatives.

References

11. Abramovitch R.A., Applications of Microwave Energy in Organic Chemistry. A review. *Org. Prep. Proc. Int.*, **23**, 683711(1991)
12. Strauss C.R. and Trainor R.W., Development in Microwave Assisted Organic Chemistry, *Aust. J. Chem.*,**48**, 1665-1692 (1995)
13. ThamaraiSelvi S., Nadaraj V., Mohan S., Sasi R. and Hema M., Solvent free Microwave Synthesis and Evalutation of Antimicrobial activity of Pyrimido[4,5-*b*]- and Pyrazolo[3,4-*b*]quinolines, *Bioorg. Med. Chem.*, **14**,3896-3903 (2006)
14. Nadaraj V., ThamaraiSelvi S. and Sasi R., Microwaveassisted Synthesis of Quinoline Alkaloids: 4-Methoxy-1- methyl-2-quinolinone and its Analogs, *Arkivoc*, 82-86 (2006)
15. Savalia R.V., Patel A.P., Trivedi P.T.1, Gohel H.R. and KhetaniD.B.Rapid and Economic Synthesis of Schiff Base of Salicylaldehyde by Microwave Irradiation, *Res. J. Chem. Sci.*, **3**, 97-99 (2013)
6. Varma R.S., Solvent-free Organic Syntheses, using supported Reagents and Microwave Irradiation, *Green Chemistry*, 43-55 (1999)
7. Gedye R.N., Smith F., Westaway K., Ali H., Baldisera L.,Laberge L. and Rousell J., The use of Microwave ovens for Rapid Organic Synthesis, *Tetrahedron Lett.*, **27**, 279-282 (1986)
8. Ahmed K.A., El-Molla M.M., Abdel-Mottaleb M.S.A., Mohamed S. Attia and El-Saadany S., Synthesis and Evaluation of Novel Fluorescent Dyes using Microwave Irradiation, *Res. J. Chem. Sci.*, **3**, 3-18, (2013)
9. Jeeva J. and Ramachandramoorthy T., Microwave Assisted Synthesis and Characterisation of Diamagnetic Complexes, *Res. J. Chem. Sci.*, **3**, 69-76 (2013)
10. Nadaraj V., ThamaraiSelvi S., Mohan S. and Daniel Thangadurai T., *Med. Chem. Res.*, **21**, 2911-2919 (2012)



Manganese doped Co-Zn Ferrite Nanoparticle Synthesis and Characterization; Effects of Annealing Temperature on the Size of nanoparticles.

Bhagvan V. Jadhav¹, Sajid F. Shaikh², Rajendra P. Patil³

¹Department of Chemistry, C.K.T. College, New Panvel (M.S.), India. 410206.

²Department of Chemistry, Anjuman Islam Janjira Degree College of Science, Murud-Janjira (M.S.), India.402201

³Department of Chemistry, M.H. Shinde Mahavidyalaya, Tiasangi, Kolhapur (M.S.), India. 416206.

KEYWORDS

Manganese doped
Co-Zn ferrite
nanoparticles,
sol-gel technique, XRD,
FT-IR

Corresponding Author
Email
bjjadhav02@yahoo.com

ABSTRACT

Manganese doped Co-Zn ferrite nanoparticles have been synthesized by sol-gel auto combustion method from nitrate salts of respective metal ions. The nanoparticles synthesized were annealed at different annealing temperatures of 873K, 973K, 1073K, 1173K and 1273K. The size of nanoparticles was also analyzed at a constant annealing temperature for different duration of time. X-ray diffraction pattern confirmed the formation of single-phase nanoparticles of Manganese doped Co-Zn ferrite. Fourier transform infrared study was performed to ascertain the structure of the nanoparticles. FT-IR studies also supported the trend of increasing size as shown by XRD results. The study revealed that crystallinity enhanced and size of the nanoparticles increased with increasing annealing temperature due to coercivity.

Introduction

Polycrystalline spinel ferrites are widely used in many electronic devices. They are preferred because of their high permeability in the radio- frequency (RF) region, high electrical resistivity, mechanical hardness and chemical stability. Ferrite nanoparticles are under intense research because of their unique chemical, mechanical, structural magnetic and electric properties.(1,2) Ferrite nanoparticles have versatile application in catalysis, electronics, photonics, sensors and Ferro fluids.(3) Ferrite nanoparticles are also used in biomedical sciences. Due to their unique size and shape, they can easily reach to the body parts where other conventional drugs find hard to reach.

Cobalt ferrite (CoFe₂O₄) is a well-known hard magnetic material with high coercivity and moderate magnetization. These properties, along with their great physical and chemical stability, make CoFe₂O₄ nanoparticles

suitable for magnetic recording applications (4). Many efforts have been made to improve the basic properties of these ferrites by substituting or adding various cations of different valence states depending on the applications of interest. Among spinel ferrites, Zn²⁺ substituted CoFe₂O₄ nanoparticles exhibit improved properties such as excellent chemical stability, high corrosion resistivity, magnetocrystalline anisotropy, magnetostriction, and magneto-optical properties (5-7).

Size of the particles depends mostly on the preparation method and conditions. In The literature, there are a number of methods like as hydrothermal synthesis, mechanical Milling and hydrolysis of metal carboxylate in organic solvent (8-9), sol-gel pyrolysis method (10),the microwave hydrothermal method (11), template-assisted hydrothermal method (12), and combustion technique are used to prepare ferrites nanoparticles. However sol-gel auto

combustion method is considered as an economical way of producing fine particles. Every method has the merits and demerits regarding the control of particles size and durability.

In the current study, focus was placed on the $\text{Co}_{0.4}\text{Zn}_{0.4}\text{Mn}_{0.2}\text{Fe}_2\text{O}_4$ nanoparticles prepared via sol-gel auto combustion method. The dependence of the morphology on annealing temperatures are investigated taking into account that mixed ferrites chosen here are highly sensitive to temperature (6).

2.1 MATERIALS:

Metal nitrates and chelating agent used for synthesis were A.R. grade. Iron nitrate nonahydrate $\text{Fe}(\text{NO}_3)_3 \cdot 9\text{H}_2\text{O}$, Zinc nitrate hexahydrate $\text{Zn}(\text{NO}_3)_2 \cdot 6\text{H}_2\text{O}$, Cobalt nitrate hexahydrate $\text{Co}(\text{NO}_3)_2 \cdot 6\text{H}_2\text{O}$, Manganese Nitrate and citric acid used were of purity 98-99%. The chemicals were used without further purification.

2.2. EXPERIMENTAL PROCEDURE:

$\text{Co}_{0.4}\text{Zn}_{0.4}\text{Mn}_{0.2}\text{Fe}_2\text{O}_4$ nanoparticles were synthesized by sol-gel auto combustion method, using starting material of high purity AR grade metal nitrate and citric acid. The metal nitrate solutions were mixed in the required stoichiometric ratios in minimum quantity of distilled water. The solutions will be mixed on a magnetic stirrer at 353K. The pH of the solution was maintained between 9 and 9.5 using ammonia solution. The solution mixture was slowly heated around 373K with constant stirring to obtain a fluppy mass. On further heating, colored powder will obtained. The powder will cooled for some time. The obtained powder nanoparticles were annealed at different temperatures of 873K, 973K, 1073K, 1173K and 1273K for 4 hours.

Synthesized nanoparticles was analyzed by X-ray diffraction technique (XRD) for structure and crystallinity. The formation of mixed metal ferrite nanoparticles was confirmed by Fourier transform infrared (FT-IR) studies. X-ray diffraction (XRD) data was collected at room temperature. Crystallographic properties e.g. phase of the material and crystal structure was determined using the same data.

3. RESULTS AND DISCUSSION

3.1. X-RAY DIFFRACTION (XRD) ANALYSIS:-

X-ray diffraction (XRD) patterns for the as prepared and annealed polycrystalline $\text{Co}_{0.4}\text{Zn}_{0.4}\text{Mn}_{0.2}\text{Fe}_2\text{O}_4$ ferrite powders are presented in Figure 1. The XRD spectra showed all the characteristics peaks corresponding to the characteristic planes (311), (511) and (440) appear at 35° , 57° and 64° on comparing with the patterns of all the investigated samples with that of standard JCPDS card, a single phase $\text{Co}_{0.4}\text{Zn}_{0.4}\text{Mn}_{0.2}\text{Fe}_2\text{O}_4$ has formed with no extra peaks. At 973K fully crystallized $\text{Co}_{0.4}\text{Zn}_{0.4}\text{Mn}_{0.2}\text{Fe}_2\text{O}_4$ has formed with sharp peaks indexed as (220), (311), (400), (422), (500) planes of spinel structure. In the present work, Figure 1 reveals the presence of the spinel structure for the as prepared $\text{Co}_{0.4}\text{Zn}_{0.4}\text{Mn}_{0.2}\text{Fe}_2\text{O}_4$, and the noticed broadening in the peaks of the as prepared sample could be attributed to the formation of ferrite particles in nano range. The sharpness of the peaks is also a good indicator for the increased size of the nanoparticles, as the particle size is increased by increasing the sharpness of the peak. The peak width decreases with the increase of annealing temperature which reflects the coarsening of particles. By increasing the annealing temperature, the diffraction peaks become sharper and narrower and increase in intensity. This is because of the amplification in crystallinity that leads to the increased particle size of the nuclei. It is evident from the XRD Pattern that crystallinity of ferrite nanoparticles is increased by increasing the annealing temperature.

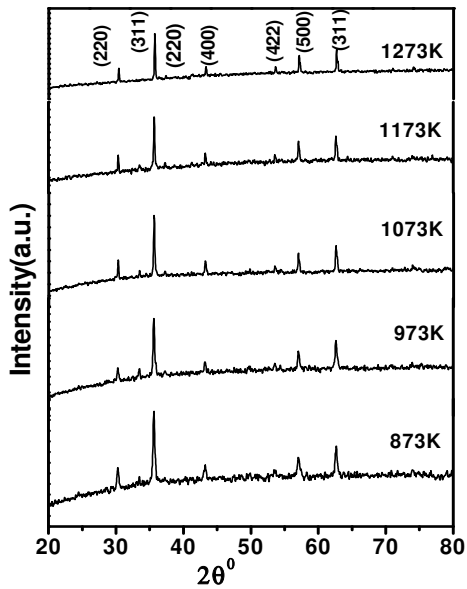


Figure 1. The X-ray diffraction (XRD) patterns for the polycrystalline $\text{Co}_{0.4}\text{Zn}_{0.4}\text{Mn}_{0.2}\text{Fe}_2\text{O}_4$ ferrites powders as prepared and that was annealed at different temperatures (873K-1273K)

3.2. PARTICLE SIZE CALCULATION OF ZINC FERRITE NANOPARTICLES BY SCHERER FORMULA:

The sizes of the nanoparticles at different annealing temperatures have been determined using Scherer equation from the Full width at Half Maximum (FWHM) value of [311] diffraction peak.

$$D = 0.9\lambda/\beta \cos \theta$$

Where D is the particle size, λ is the X-ray wavelength (1.5418), θ is the Bragg angle and β is the half maximum width.

The size of nanoparticles obtained at different annealing temperature was measured as 11.6 nm, 15.7 nm, 18.8 nm, 23.6 nm and 26.5 nm for 873K, 973K, 1073K, 1173K and 1273K annealing temperature for 4 hours respectively.

The particle size increases from 11.6 nm to 26.5 nm with the systematic variation of annealing temperature calculated by Scherer formula as shown in Figure 2.

3.3. FOURIER TRANSFORM INFRARED (FT-IR) STUDIES:

IR spectrum is considered an important tool to get information about the structure and the positions of ions in the crystal through the crystal's vibration modes (15). The formation of spinel $\text{Co}_{0.4}\text{Zn}_{0.4}\text{Mn}_{0.2}\text{Fe}_2\text{O}_4$ structure in the calcined zinc ferrite nanoparticles is further supported by FT-IR spectra shown (Figure 2-4). The peaks at 556 cm^{-1} correspond to the metal-oxygen (Fe-O) stretching vibrations and it is the characteristic peak of the spinel structure of $\text{Co}_{0.4}\text{Zn}_{0.4}\text{Mn}_{0.2}\text{Fe}_2\text{O}_4$ nanoparticles. The peak at 3450 corresponds to the vibration of O-H and the light band at 1640 could be attributed to the adsorbed water or humidity. This was further supported by disappearance of these bands at higher temperature. The strong absorption band at 426 cm^{-1} is described as the stretching modes of Zn-O (16).

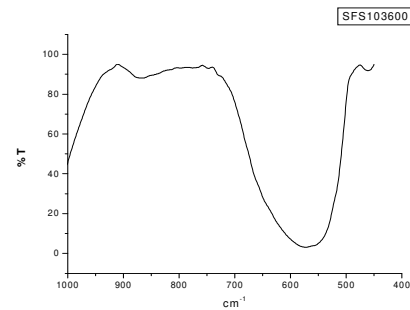


Figure2. The FTIR spectra for the polycrystalline $\text{Co}_{0.4}\text{Zn}_{0.4}\text{Mn}_{0.2}\text{Fe}_2\text{O}_4$ ferrites powders as prepared and that was annealed at 873K.

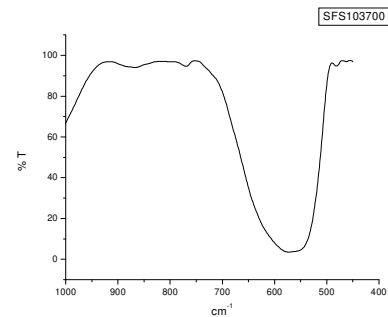


Figure3. The FTIR spectra for the polycrystalline $\text{Co}_{0.4}\text{Zn}_{0.4}\text{Mn}_{0.2}\text{Fe}_2\text{O}_4$ ferrites powders as prepared and that was annealed at 973K.

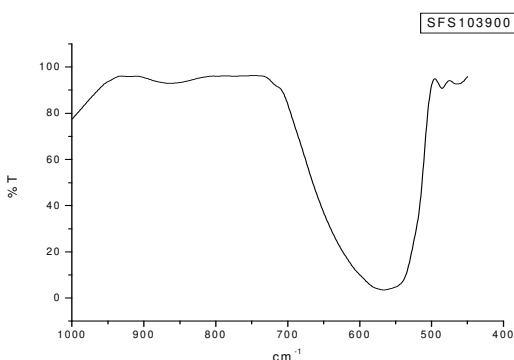


Figure3. The FTIR spectra for the polycrystalline $\text{Co}_{0.4}\text{Zn}_{0.4}\text{Mn}_{0.2}\text{Fe}_2\text{O}_4$ ferrites powders as prepared and that was annealed at 1173K.

4. CONCLUSION:

Nanosized $\text{Co}_{0.4}\text{Zn}_{0.4}\text{Mn}_{0.2}\text{Fe}_2\text{O}_4$ particles were synthesized by sol-gel autocombustion methods at different annealing temperatures to analyze the effect of annealing temperature on the particle size of the compound. The structure of the compounds was confirmed by XRD. FT-IR analysis supported the formation of spinel structure of $\text{Co}_{0.4}\text{Zn}_{0.4}\text{Mn}_{0.2}\text{Fe}_2\text{O}_4$ nanoparticles. The FT-IR spectra showed two characteristic metal oxygen vibrational bands, a Fe-O band, and Zn-O band. Scherer formula was used for the estimation of size of the $\text{Co}_{0.4}\text{Zn}_{0.4}\text{Mn}_{0.2}\text{Fe}_2\text{O}_4$ nanoparticles. Particles size of 11.6 nm, 15.7 nm, 18.8 nm, 23.6 nm and 26.5 nm were found at annealing temperature of 873K, 973K, 1073K, 1173K and 1273K respectively. The study shows that the particle size increases with increasing annealing temperature.

5. REFERENCES:

1. Dariel, M., L.H. Bennett, D.S. Lashmore, P. Lubitz, M. Rubinstein, W.L. Lechter, M.Z. Harford, 1987. Properties of electrodeposited CoCu multilayer structures J. Appl. Phys., 61: 4067.
2. El-Shabasy M. (1997). DC electrical properties of Zn-Ni ferrites. J. Magn. Magn. Mater, 172:188.

3. Guo, R., L. Fang, W. Dong, F. Zheng, M. Shen, 2010. Enhanced photocatalytic activity and ferromagnetism in Gd doped BiFeO_3 nanoparticles. J. Phys. Chem. 114: 21390.
4. Skomski R. (2003). Nanomagnetism. J. Phys.: Condens. Matter. 15: R1-R56.
5. Vaidyanathan.G and Sendhilnathan.S (2008). Characterization of $\text{Co}_{1-x}\text{Zn}_x\text{Fe}_2\text{O}_4$ nanoparticles synthesized by co-precipitation method. Physica B. vol. 403.no. 13-16: 2157–2167.
6. Vaidyanathan.G, Sendhilnathan.S, Arulmurugan.R.(2011). Structure and magnetic properties of $\text{Co}_{1-x}\text{Zn}_x\text{Fe}_2\text{O}_4$ nanoparticles by co-precipitation method. J. Magn. Mater. 313 :293–299.
7. AktherHossain.A. K. M., Tabata.H, and T. Kawai. (2008). Magnetoresistive properties of $\text{Zn}_{1-x}\text{Co}_x\text{Fe}_2\text{O}_4$ ferrites. J. Magn. Mater. 320:1157–1162.
8. Hadjipanayis, G.C., R.W. Siegel (Eds.), 1994. Nanophase Materials—Synthesis-Properties-Applications, Kluwer Academic Publishers, Dordrecht,
9. Mojumdar, S.C., J. Miklovic, A. Krutořková, D. Valigura and J.M. Stewart, 2005. Furopyridines and furopyridine-Ni(II) complexes Synthesis, thermal and spectral characterization J. Therm. Anal. Cal., 81: 211.
10. Lee.J. G., Minlee.H., Kim.C.S. (1998). Magnetic properties of CoFe_2O_4 powders and thin films grown by a sol-gel method. J. Magn. Mater. 90 :177.
11. Kim .C. K., Lee J. H., Katoh.S, Murakami.R, and Yoshimura.M. (2001). Synthesis of Co-Co—Zn and Ni—Zn ferrite powders by the microwave-hydrothermal method. Materials Research Bulletin.vol. 36.no. 12 :2241–2250.
12. He.H.Y. (2011). Magnetic Properties of $\text{Co}_{0.5}\text{Zn}_{0.5}\text{Fe}_2\text{O}_4$ Nanoparticles Synthesized by a Template-Assisted Hydrothermal Method. Journal of Nanotechnology .Article ID 182543.
13. M.M. Eltabey, N.Aboufotouh Ali, Effect of Annealing Temperature on Structural and Magnetic Properties of Co-Zn Ferrite Nanoparticles, International Journal of Advanced Research (2014), Volume 2, Issue 6, 184-192 185.



14. IsrafUd Din, S. Tasleem, A. Naeem, Maizatul S. Shaharun, Ghassan M.J. Al. Kaisy, Zinc Ferrite Nanoparticle Synthesis and Characterization; Effects of Annealing Temperature on the Size of nanoparticles, Australian Journal of Basic and Applied Sciences, 7(4): 154-162, 2013 ISSN 1991-8178.
15. Sattar.A.A., El-Sayed. H.M., El-Shokrofy.K.M., El-Tabey.M.M. (2005). —Improvement of the Magnetic Properties of Mn-Ni-Zn Ferrite by the Non-magnetic Al-Ion Substitution J. Appl. Sci. 5 (1) :162–168.
16. Lepot, N., M.K. Van Bael, H. Van den Rul, J. D'Haen, R. Peeters, D. Franco, J. Mullens, 2007. synthesis of ZnO nanorods from aqueous solution. Mater. Lett., 61: 2624.
17. Mary kutty Thomas, S.K., K.C. Ghosh, 2002. George, Mater. Lett., 56: 386.





GREEN SYNTHESIS AND CHARACTERISATION OF SILVER NANO-PARTICLES

Apoorva U.¹ Sammitha D.Hebbar² Leena Hublikar*
P.C.Jabin Science College Hubballi ^{1,2}

KEYWORDS

Nanotechnology,
Nanoparticles (NPs),
Ag NPs, synthesis,
applications

Corresponding Author
Email

shruthi.jamanoor@gmail.com

ABSTRACT

Nanotechnology is an important field of modern research dealing with design, synthesis, and manipulation of particle structures ranging from approximately 1-100 nm. Nanoparticles (NPs) have wide range of applications in areas such as health care, cosmetics, food and feed, environmental health, mechanics, optics, biomedical sciences, chemical industries, electronics, space industries, drug-gene delivery, energy science, optoelectronics, catalysis, single electron transistors, light emitters, nonlinear optical devices, and photo-electrochemical applications, etc. Silver nanoparticles possess unique properties which find myriad applications such as antimicrobial, anticancer, larvicidal, catalytic, and wound healing activities. Biogenic syntheses of silver nanoparticles using plants and their pharmacological and other potential applications are gaining momentum owing to its assured rewards. We are aimed at providing an insight into the phytomediated synthesis of silver nanoparticles and its characterization.

On the view of the above literature surveys on Nano-Chemistry, its preparation and their application, we made our sincere effort for the preparation and characterisation of Silver (Ag)NPs in our chemistry laboratory.

Introduction

The ideas and concepts behind nanoscience and nanotechnology started with a talk entitled "There's Plenty of Room at the Bottom" by physicist Richard Feynman at an American Physical Society meeting at the California Institute of Technology (CalTech) on December 29, 1959, long before the term nanotechnology was used. In his talk, Feynman described a process in which scientists would be able to manipulate and control individual atoms and molecules. Over a decade later, in his explorations of ultraprecision machining, Professor Norio Taniguchi coined the term nanotechnology. It wasn't until 1981, with the development of the scanning microscope that could "see" individual atoms, that modern

nanotechnology began.

Nowadays, there is a growing need to develop eco-friendly processes, which do not use toxic chemicals in the synthesis protocols. Green synthesis approaches include mixed-valence polyoxometalates, polysaccharides, Tollens, biological, and irradiation method which have advantages over conventional methods involving chemical agents associated with environmental toxicity. Selection of solvent medium and selection of eco-friendly nontoxic reducing and stabilizing agents are the most important issues which must be considered in green synthesis of NPs. The green synthesis of metallic nanoparticles (NPs) has attracted tremendous attention in recent years because these protocols are low cost

and more environmentally friendly than standard methods of synthesis.

Synthesis of silver NPs

1. MATERIALS AND METHODS

Materials

Fresh leaves of *Morinda citrifolia* and *Phyllanthus emblica* were collected from P.C. Jabin Science College, Hubballi. Silver nitrate obtained from Department of Chemistry, P.C.Jabin Science College, Hubballi. The required materials such as beakers, distilled water, microwave oven and other equipments were used and the experiment was carried out at Department of Material Science, BVBCET, Hubballi and at P.C. Jabin Science College, Hubballi. This work is based on the comparative study on Ag nano particles synthesis by *Morinda citrifolia* and *Phyllanthus emblica*.

1.2 Synthesis of silver nano particles

The fresh leaves of *Morinda* and *Gooseberry* are thoroughly washed and cut into fine pieces of leaves. These leaves are separately measured using an electronic weighing machine and noted i.e, 5g. Now to prepare the plant extract, two beakers with 100mL of distilled water should be taken. The cut pieces of leaves need to be added to the beakers and boiled in a microwave oven for 2 min. Now the plant extract in two separate beakers need to be filtered through Whatman filter paper with two different funnels. The plant extract need to be stored in a brown bottle so that the extract doesn't show reactions on exposure to the sunlight. It is stored at -15 °C and could be used within 1 week. Now equal volume of two filtrates are taken i.e, 10 mL each in a beaker and mixed thoroughly. The mixture was treated with aqueous 0.1N AgNO₃ solution and mixed thoroughly. Now, at room temperature, the change in colour of the mixture is observed as the times passes on. The colour changes from light red to brownish red. This colour change indicates the formation of silver nano particles. It showed that silver ions could be reduced by aqueous extract of plant parts to generate extremely stable silver nano particles in water.

Calculation and preparation of 0.1N AgNO₃ solution:

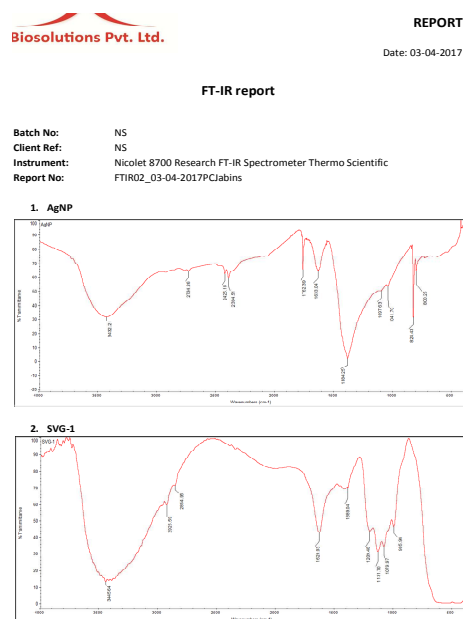
Prepare 100 mL of 0.1N AgNO₃ solution, (molecular weight of AgNO₃ is 169.87g)

169.87g ----- 1N -----1000mL

16.987g----- 1N -----100mL

1.6987g----- 0.1N -----100mL

Therefore, 1.6987g of AgNO₃ is added to 100 mL of distilled water to prepare 0.1N AgNO₃ solution.



Conclusion:

Chemistry-enabled nanotechnology has the potential to solve the environmental crisis due to the increasing consumption of non-renewable resources such as oil, natural gas, coal, and uranium to make energy and goods. A rapid method of synthesizing NPs have been developed by using the fresh leaf extract and was found that the extract is a potential reducing agent to produce stable NPs. The research provides a new input to the development and advancement of nanochemistry and furthermore their applications in our day today life.

Source (plant part) Chemical constituent References

Leaves **Tyrosine**Dittmar (1993), Elkins (1998) Leaves **Ursolic acid** Sang et al. (2002), Cardon (2003), Elkins (1998), Wang et al. (2002) Leaves **Valine**Dittmar (1993), Elkins (1998) Plant 2-methyl-3,5,6- trihydroxyanthraquinoneCardon (2003), Inoue



Synthesis, Characterization and gas sensing study of Cd-Mn Ferrite

N. M. Patil*, R. P. Patil^{b*}

Bhogawati Mahavidyalaya, Kurukali, Tal- Karveer, Dist. – Kolhapur 416001.

^bDepartment of Chemistry, M.H. Shinde Mahavidyalaya, Tisangi - 416206, MH, India

KEYWORDS

Cd-Mn Ferrite,
XRD, SEM,
Electrical
magnetic study,
Gas sensing performance.

Corresponding Author
Email
nmp_1@rediffmail.com

ABSTRACT

Hydroxide precursor method has been used for the synthesis of Nano-crystalline of Cd-Mn Ferrite material. The characterization of synthesized material was carried out by using X-ray diffraction (XRD), scanning electron microscopy (SEM), and IR spectroscopy. X-ray analysis revealed that all the compositions are in cubic phase. Homogenous grain structure was observed from SEM. FT-IR spectral studies indicate two absorption bands, one around 600cm^{-1} (Tetrahedral) and the other weak around 500cm^{-1} (Octahedral). The electrical dc resistivity measurement reveals the semiconducting nature of synthesized material where as the ferrimagnetic behavior has been confirmed by Magnetic study. Gas sensing performance of system $\text{Cd}_{1-x}\text{Mn}_x\text{Fe}_2\text{O}_4$ tested for various gases. The composition $\text{Cd}_{0.25}\text{Mn}_{0.75}\text{Fe}_2\text{O}_4$ is seen to be more selectivity and maximum response towards NH_3 gas at 30°C operating temperature.

Introduction

With the rapid development of information technology and mobile communication, the electronic components with small size, high efficiency, and low cost are urgently demanded [1,2]. Multilayer Chip Inductor (MLCI) is such a component, widely used in electronic products, such as cellular phone, notebook computer, and video cameras [3]. Up to now, ferrites have been the dominant materials for MLCI due to their better magnetic properties at high frequency and low sintering temperature [4,5]. Ferrite is also a pertinent magnetic material for wide applications owing to its high resistivity, high Curie temperature and environmental stability [6]. Materials with high permeability are required for reducing the number of layers in MLCI and realizing the better miniaturization.

Along with these properties ferrites are having wide range of applications such as in drug delivery system, photocatalysis and gas sensors.

The properties of ferrite material depend on preparation methods. The conventional way of producing these materials is by the solid-state reaction of oxide/carbonate and calcination at high temperature. The solid-state reaction method has some inherent disadvantages such as chemical inhomogeneity, coarser particle size, and introduction of impurities during ball milling [7]. The new chemical wet methods overcome these problems. Ferrites are prepared by various methods such as sol-gel [8], co-precipitation [9], citrate precursor [10], solvent evaporation [11] and hydrothermal [12].

In the present investigation, the co-precipitation method has been employed to synthesize Mn substituted Cadmium ferrite particles. The co precipitation method has overriding advantages over other methods, like usage of cheaply available raw materials as well as formation of more homogeneous, fine and reproducible products. The synthesized material was characterized by XRD, FT-IR, SEM, EDX, thermal analysis, electrical resistivity, magnetic hysteresis. Gas sensing performance of these ferros spinels was also studied for various oxidizing and reducing gases at different operating temperature. The photocatalytic degradation of congo red dye was investigated with respect to time.

2 Materials and Methods

The various compositions of the system $Cd_{1-x}Mn_xFe_2O_4$ ($x = 0.0, 0.25, 0.5, 0.75$ & 1.0) were prepared by co-precipitation method [13]. To prepare spinel compounds the high purity, water soluble sulphates such as manganese, cadmium and iron sulphates were dissolved separately. Mixture of these solutions together was taken in 1000ml beaker with constant stirring. Then they were precipitated as hydroxides using 10% NaOH solution by maintaining pH at 9.5-10. The hydroxides were then oxidized using 30% H_2O_2 (100vol.) solution and were digested in water bath for 4 hours at $90-95^\circ C$. Then precipitate was washed thoroughly with distilled water to remove the sulphates and excess alkali and filtered through the Whatman filter paper No. 41. The precipitate was dried in oven at $110^\circ C$. The dried powder was then heated at different temperatures to get resulting mixed-metal oxides. The above powders were heated separately at $900^\circ C$ for 4 hrs to get the final product.

The spinel powders were then mixed with binder (2% PVA in acetone) and pressed into pellets of the size 1 cm in diameter and about 0.3 cm thickness under a pressure 10000 psi. The pellets were initially heated at $450^\circ C$ for 6 hrs to remove binder. These pellets were then used for determination of various properties.

3 Results and Discussion

3.1 X-ray diffraction studies

The crystalline phase identification of system $Cd_{1-x}Mn_xFe_2O_4$ ($x = 0.0, 0.25, 0.5, 0.75$ & 1.0) was carried out by using a computerized X-ray powder diffractometer. The X-ray diffraction patterns of all the samples of system, sintered at $900^\circ C$ are shown in Fig.1.

The various crystallographic parameters such as d interplanar distance, lattice constant, crystallite size and h,k,l planes were determined from the X-ray diffraction pattern. The lattice parameters were calculated for the cubic phase using following relations.

$$a) \text{ for cubic phase } 1/d^2 = h^2 + k^2 + l^2 / a^2 \text{ ----- 1}$$

where, a = Lattice parameter,

(hkl) = Miller indices,

d = interplanar distance.

The crystallite size of sintered ferrites was calculated from the full width at half maxima of the most intense (311) peak by using Scherrer's formula.

$$t = 0.9\lambda / \beta \cos\theta \text{ ----- 2}$$

Where, symbols have their usual meaning.

The X-ray density was calculated according to the formula

$$d_x = 8M/N a^3 \text{ ----- 3}$$

where, N = Avagadros number (6.023×10^{23} atom/mole)

M = Molecular weight, and

a = lattice constant which was calculated from the X-ray diffraction pattern.

X-ray density is sometimes also called 'theoretical density'. XRD patterns show the reflections of the planes (111), (220), (311), (222), (400), (422), (511), out of these (311) is most intense peak. It reveals the formation of single phase cubic spinel, showing well defined reflections of allowed planes. The various crystallographic parameters of the samples are listed in Table 1.



Lattice parameter 'a' in Å of system goes on decreasing with content of Mn. Crystallite size lies between range 18.36 to 39.18 nm.

Table 1. Lattice constants, Crystallite size, X-ray density for Cd_{1-x}Mn_xFe₂O₄ system

Sample	Lattice parameter 'a' Å ⁰	Crystallite size nm	X-ray density gm/cc
CdFe ₂ O ₄	8.408	18.36	5.873
Cd _{0.75} Mn _{0.25} Fe ₂ O ₄	8.3585	25.73	6.2263
Cd _{0.5} Mn _{0.5} Fe ₂ O ₄	8.3403	39.18	6.0203
Cd _{0.25} Mn _{0.75} Fe ₂ O ₄	8.3297	25.64	5.5882
MnFe ₂ O ₄	8.3256	25.81	5.2431

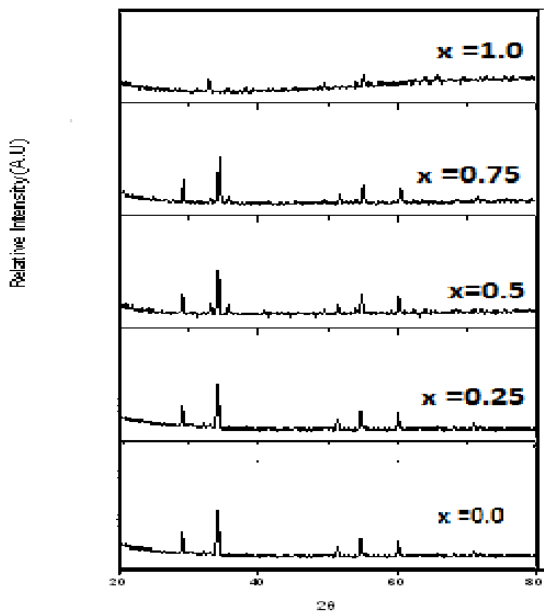


Fig. 1 XRD diffraction patterns for Cd_{1-x}Mn_xFe₂O₄ system (0 ≤ x ≤ 1).

3.2 Scanning Electron Microscopy

The particle surface morphology of Cd_{1-x}Mn_xFe₂O₄ system (0 ≤ x ≤ 1.0) was studied using Scanning Electron Microscopy technique (JEOL JSM 6360). The average grain size was measured by Cottrell's method [14].

The studies from the micrographs reveal that all samples show fine grains with varying porosity. The average grain size of ferrite decreases with increasing Ni content (0.5-0.3 μm). The grain size depends upon the interaction of grain boundary and porosity along with the sintering temperature [15-16]. Fig 2 shows SEM images of selected samples of Cd_{1-x}Ni_xFe₂O₄ System

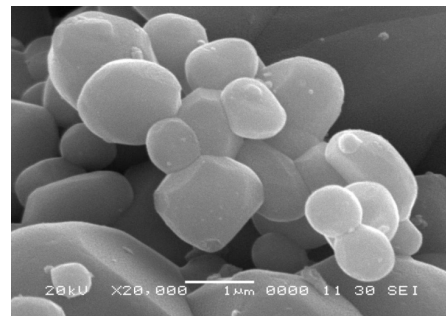


Fig. 2 SEM Image

3.3 Fourier transfer Infra-red spectroscopy

The FT-IR spectra of all sintered compositions of Cd_{1-x}Mn_xFe₂O₄ System (0 ≤ x ≤ 1.0) are shown in Fig 3 Waldron *et al.* [17] have reported the two main broad metal-oxygen bonds in the region 400 – 800 cm⁻¹ observed in normal ferrites. Both the absorption bands depend on the nature of octahedral M-O stretching vibration and nature of tetrahedral M-O stretching vibration. The highest ν₁ generally observed in the range of 700-550cm⁻¹, corresponds to intrinsic stretching vibrations of the metal at the tetrahedral site, M_{tetra} - O, whereas the ν₂, lowest band usually observed in the range 450 – 385 cm⁻¹ is assigned to octahedral -metal stretching, M_{octra} - O.

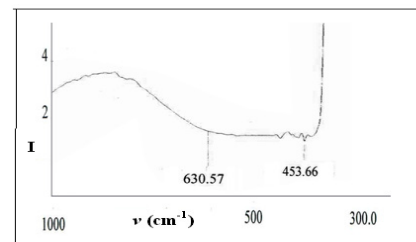


Fig. 3 IR spectra of the Cd_{1-x}Mn_xFe₂O₄ system

3.4 Electrical Resistivity

Electrical properties of $Cd_{1-x}Mn_xFe_2O_4$ system were studied by measuring the resistivity with respect to temperature. The temperature range from 100 to 500 °C. Fig 4 gives correlation between $\log \rho$ Vs $1000/T$. From this figure it is clear, that $\log \rho$ decreases with increasing temperature, which is a normal characteristics of semiconductor ferrites. The increase in conductivity with increasing temperature may be related to the increase in the drift mobility of the charge carriers, which are localized at ions or vacant sites. Moreover due to the lattice vibrations, the ions occasionally come close enough for the transfer of charge carriers and the conduction is also induced by the lattice vibrations. The temperature dependance conductivity may be explained on the basis of the conductivity in ferrites which occurs as a result of electron hopping between ions of the same element existing in different valence states on equivalent lattice sites [18-19]. The probability of electron hopping between Fe^{2+} and Fe^{3+} states is greater at the B sites due to the smaller distances between the metallic ions at these sites. From the figure it is also seen that conductivity increases with content of Mn. The conduction mechanism in ferros spinels was explained by Verway and de-Bohr [20], which involves exchange of electrons between the ions of same elements having variable oxidation states. e.g. $Fe^{2+} \leftrightarrow Fe^{3+}, Mn^{3+} \leftrightarrow Mn^{2+}$. The activation energy of electrical conduction was found to decrease with increasing Mn ion content

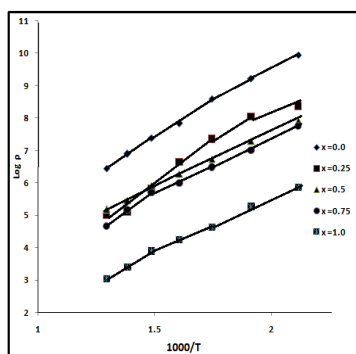


Fig. 4 Variation of $\log \rho$ with $10^3/T$ for $Cd_{1-x}Mn_xFe_2O_4$ System.

3.5 Magnetic Hysteresis

Magnetic hysteresis loop gives proof for determining the ordering of spins in magnetic materials. Fig. 5 shows the room temperature hysteresis loops for $Cd_{1-x}Mn_xFe_2O_4$ compositions. The shape of curves exhibit ferromagnetic behaviour of the investigated samples. The magnetic properties such as saturation magnetization (M_s), magnetic remanent (M_r), and coercivity (H_c) magnetic moment (μ_B) in Bohr magneton were elucidated from the hysteresis data and tabulated in Table 6.14. It can be seen from the figure that, both magnetization and magnetic remanent increase with increasing Mn content. This can be explained on the basis that A site preferential energy of non magnetic Cd^{2+} ions is greater than Mn^{2+} hence Cd^{2+} ion occupies A site, replaces Mn^{2+} ions. At low temperature in ferrite, the magnetic moment of the tetrahedral and octahedral sites points in opposite direction due to that observed magnetization is the difference between magnetisation of octahedral and tetrahedral site.

$$M_s = M_B - M_A$$

When the concentration of Cd^{2+} has higher value (i.e $x \leq 0.5$), the A-B interactions are much weaker than B-B interactions. The weakening of interactions of octahedral and tetrahedral site, canted the magnetic moment. Hence decrease in saturation magnetization observed.

Also at higher concentration of Mn, some amount Mn^{2+} occupies B sites because ionic radius of Mn^{2+} (0.083 nm) is greater than Fe^{3+} (0.055 nm). Subsequent decrease in Cd concentration does not change cation distribution of B site. Hence saturation magnetization increases with content of Mn. This behavior agrees well with previous results reported in the literature.

Table.2. All Magnetic parameters of $Cd_{1-x}Mn_xFe_2O_4$ system $x = 0.0, 0.50 \text{ \& } 1.0$

Sample	M_s emu/gm	M_r emu/gm	H_c Oe	μ_B
$CdFe_2O_4$	0.7755	0.0077	562.68	0.0400
$Cd_{0.5}Mn_{0.5}Fe_2O_4$	5.3132	2.8756	344.00	0.2467
$MnFe_2O_4$	17.374	5.4735	466.25	0.7174

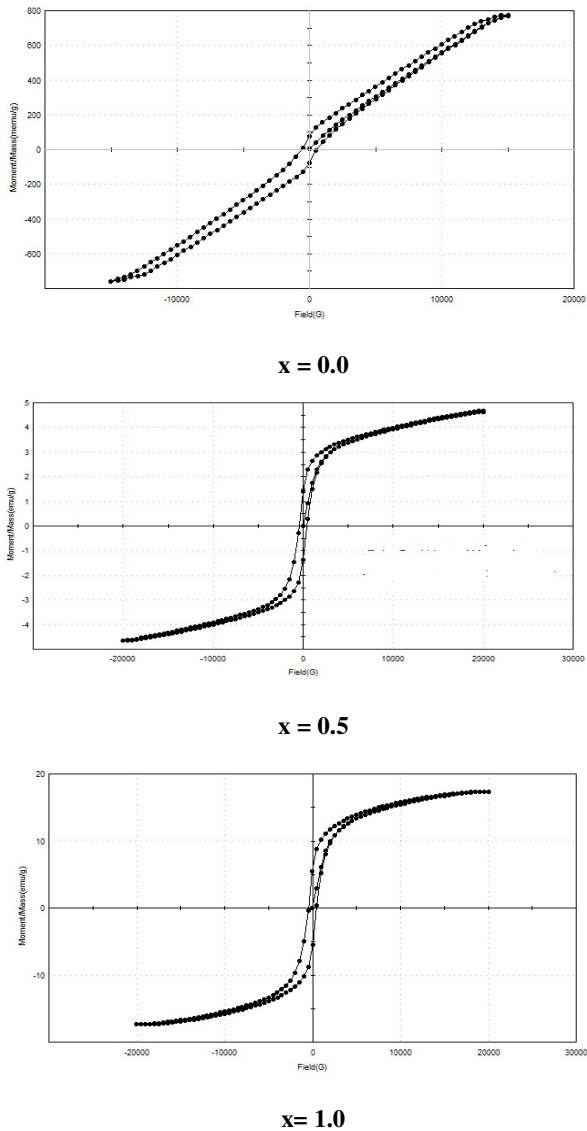


Fig.5. Hysteresis loops of $Cd_{1-x}Mn_xFe_2O_4$ system $x = 0.0, 0.5$ & 1.0

3.6 Gas Sensing Property

Gas sensing performance of each composition of the Mn-substituted Cadmium ferrite system has been tested for various oxidizing and reducing gases viz. Ammonia, H_2 , Ethanol, CO_2 , Cl_2 , H_2S and LPG. The response of gas was studied by using special assembly in which change in resistance of sample in presence of air and testing gas is measured. The gas response (%S) is calculated as follows:

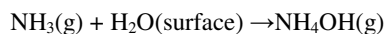
$$\%S = (R_a/R_g)100$$

where, R_a = resistance of the sample in air, R_g = resistance of the sample in the test gas.

Response of sample for testing gas depends on number of factors such as phase formation, crystallite size, particle size, grain size, dopants, surface area, sensitivity, selectivity, operating temperature, gas concentration, response time and recovery time. Nowadays, ferrite materials are used as gas sensors because they show more selectivity and stability for a particular gas than n-type semiconducting oxides. The specific surface plays important role in gas sensors. A large surface area gives high sensitivity within certain limits. Selectivity is an ability of a sensor to respond to certain gas in the presence of other gases. It is closely connected with operating temperature [21]. Sandu et al.[22] found that the Co-Mn ferrite is sensitive to CO gas. Tianshu et al. [23] prepared cadmium ferrite and tested for C_2H_5OH , CO, H_2 and C_4H_{10} reported that material is sensitive for C_2H_5OH . Rezlescu et al. [24] reported that copper ferrite shows sensitivity to LPG at an operating temperature of $350^{\circ}C$. Zinc ferrites were prepared by the hydrothermal method by Chu et al. [25]. The sensor shows maximum sensitivity for C_2H_5OH at operating temperature $180^{\circ}C$. In the present study, it is observed that the $Cd_{1-x}Mn_xFe_2O_4$ system shows maximum sensitivity towards NH_3 gas. The response of NH_3 at $30^{\circ}C$ was very high. The composition $Cd_{0.25}Mn_{0.75}Fe_2O_4$ shows maximum response.

The selective ammonia response of the sensor at room temperature can be explained by the surface reaction processes. On the surface of sample there are grain boundaries which leads to the formation of barrier height among the grains and hence increases the resistance in the absence of target gas. A few moles of H_2O from air (moisture) could be expected to adsorb on the surface of the film at room temperature. Upon exposure to ammonia, a remarkable decrease in the resistance of the sensor was observed, which may be due to the surface reaction of ammonia with physisorbed H_2O or by proton conductivity via NH_4^+ cations.

Oxide is well known to generate the solid acidity. The solid acidity on the sensor surface would form NH_4^+ cations, which constitutes the proton conductivity leading to a crucial decrease of the resistance. This would decrease the barrier height among grains:



Ammonium hydroxide NH_4OH produced during the surface reaction is volatile in nature. The high volatility of NH_4OH explains the quick response and fast recovery of the sensor.[27].

The $\text{Cd}_{1-x}\text{Mn}_x\text{Fe}_2\text{O}_4$ system also shows response to H_2S gas at different operating temperatures.

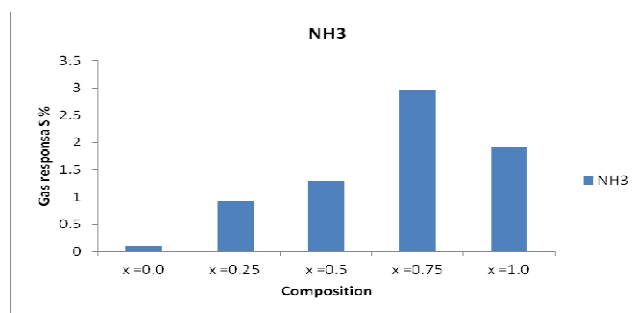


Fig.6. Sensitivity of $\text{Cd}_{1-x}\text{Mn}_x\text{Fe}_2\text{O}_4$ towards NH_3 gas at 30°C operating temperature

References:

- [1] P.K. Roy, J. Bera, J. Magn. Mater., 298 (2006) 38.
- [2] X. Qi, J. Zhou, Z. Yue, et al., Key Eng. Mater., 224 (2002) 593.
- [3] Bo Li, Zhen-Xing Yue, Xi-Wei Qi, Ji Zhou, Zhi-Lun Gui, Long-Tu Li, Mater. Sci. Eng., B 99 (2003) 252.
- [4] T. Nakamura, J. Magn. Mater., 168 (1997) 285.
- [5] J.H. Jean, C.H. Lee, W.S. Kou, J. Am. Ceram. Soc., 82 (2) (1999) 343.
- [6] Xi-Wei Qi, Ji Zhou, Zhenxing Yue, Zhi-Lun Gui, Long-Tu Li, J. Magn. Mater., 251 (2002) 316.
- [7] P.S. Anil Kumar, J.J. Shrotri, S.D. Kulkarni, C.E. Deshpande, S.K. Date, Mater. Lett., 27 (1996)
- [8] P. Lavela, J. L. Tirado, J. of Powder Sources., 172, I-1 (2007) 379.
- [9] B.A. Mulla and V. S. Darshane, Indian J. Chem., 22(A) (1983) 143.
- [10] M. C. Dimri, A. Verma, S.C. Kashyap, D. C. Dube, O. P. Thakur, C. Prakash, Mat. Sci. and Engg.:B., 133,(2006) 42.
- [11] M. Lal, D. K. Sharma, M. Singh, Indian J. Pure Appl. Phys., 43(2005) 291.
- [12] K. Wetchakun, T. Samerjai, N. Tamaekong, C. Liewhiran, C. Siriwong, V. Kruefu, A. Wisitsoraat, A. Tuantranont, S. Phanichphant, Sensors and Actuators B: Chemical, Vol.160, Iss. 1, 580-591,(2011).
- [13] V.D. Kapse, S.A. Ghosh, F.C. Raghuvanshi, S.D. Kapse, U.S. Khandekar Talanta, Volume 78, Issue 1, 19-2515, (2009).
- [14] Satyendra Singh, B.C. Yadav, Rajiv Prakash, Bharat Bajaj, Jae Rock lee Applied Surface Science, Vol. 257, Iss. 24, 10763-107701(2011).
- [15] J.F. Hochepped, P. Bonville, M.P. Pileni, J. of Phys. and Chem.104, 905 (2000)
- [16] K. Seki, J.I. Shida, H. Murakami, IEE Trans. Instr. Meas. 37, 3(1988).
- [17] A.S. Vaingankar, S.G. Kulkarni, M.S. Sagare, Bordeaux, France, 3-6, (1996)
- [18] Y. Shimizu, H. Arai, T. Seiyama 7, 11-22 (1985)
- [19] N. Xinsu, D. Weiping, and D. Weimin, Sens. Actuators B, 99, 2-3(2004).
- [20] Y. L. Liu, H. Wang, Y. Yang, Z. M. Liu, H. F. Yang, G. L. Shen, and R. Q. Yu, Sens. Actuators B, 102, 148-54 (2004).
- [21] C. Xiangfeng, J. Dongli, and Z. Chenmou, Sens. Actuators B, 123, 793-97 (2007).
- [22] I. Yokota, J. Phys. Sco. Japan. 16 2213, (1961).
- [23] S. L. Darshane, R. G. Deshmukh, S. S. Suryavanshi, I. S. Mulla, J. Am. Ceram. Soc. 91, 8, 2724-2726, (2008).
- [24] A.B. Bodade, A.M. Bende, G.N. Chaudhari, Vacuum, Vol. 82, Iss. 6, 588-593, (2008).
- [25] A.V. Kadu, S.V. Jagtap, G.N. Chaudhari, Current Applied Physics, Vol. 9, Iss.6, 1246-1251, (2009).



Analysis of habitable site of M. cymbalaria. Hook. f.

S.V.Madhale

Asst. Professor, Department of Botany, Shri. Yashwantrao Patil Science College, Solankur, (Radhanagari), India

KEYWORDS

Habitable site, soil, EDX, *M. cymbalaria*

Corresponding Author
Email
svmadhale@yahoo.com

ABSTRACT

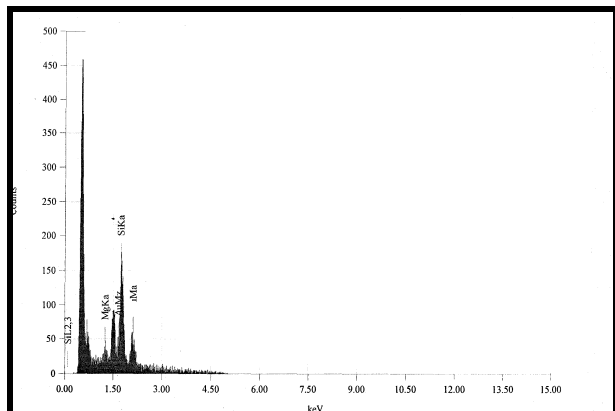
Soil is general term, habitat is slightly specific, while habitable site or niche is specific term. Rarity or abundance of a species depends upon the interaction between the characteristics of habitable site and the organism. Soil is the concept which is complex one, it refers to anchorage, water relations, mineral supply, aridity, fertility etc. Therefore, evaluation of some basic qualitative characters in relation to individual species from different location may provide us a profile of soil qualities which can support the species under study positively.

Introduction

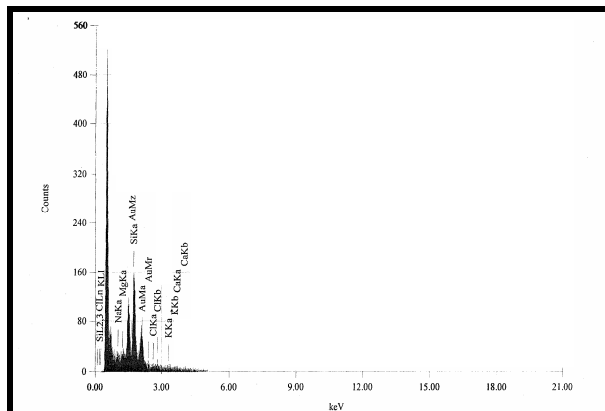
Habitat is the complex of geographical situation, climate, soil, and biological associate of the plant species. Soil is a mixture of different compounds including dead organic matter as well as biological entities. Generally it is considered as habitat. But habitat represents a particular set of environmental conditions i.e. the environmental complex in which soil is one of the component. The geographical foundation of soil prevailing in Solapur district is mainly of Deccan trap of volcanic origin. The district has soils with low water holding capacity. Therefore, crops in this area suffer the most during the draught conditions (Legros and Smith, 1994; Lee *et al.*, 2004). Basic soil properties are also worked out from different locations. Therefore, evaluation of some basic qualitative characters in relation to individual species from different location may provide us a profile of soil qualities which can support the species under study positively. Therefore, in the present piece of work some of the basic properties of soil are evaluated using EDX to study minerals.

Materials and methods:-

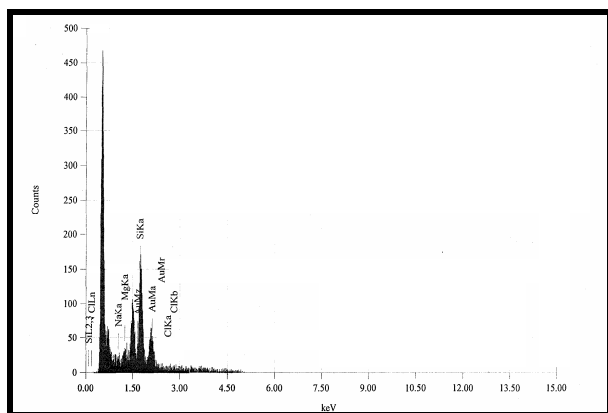
Soil samples were collected from different locations of Solapur districts. The geographical foundation of soil prevailing in Solapur district is mainly of Deccan trap of volcanic origin. For this purpose one line was considered passing from the center of population and four pits (15-15-15cm) were made in zigzag manner aside to the considered line. The soils from four pits were mixed thoroughly and brought to the laboratory and air dried and subjected to further analysis. Clay minerals were studied through EDX technique on scanning electron microscope (SEM – JEOL model along with Oxford Inca energy dispersive X- ray fluorescence spectrophotometer- EDX).



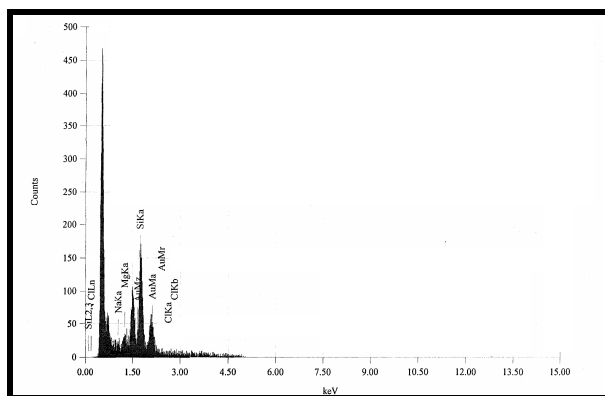
EDX peaks for clay minerals for Shetaphal



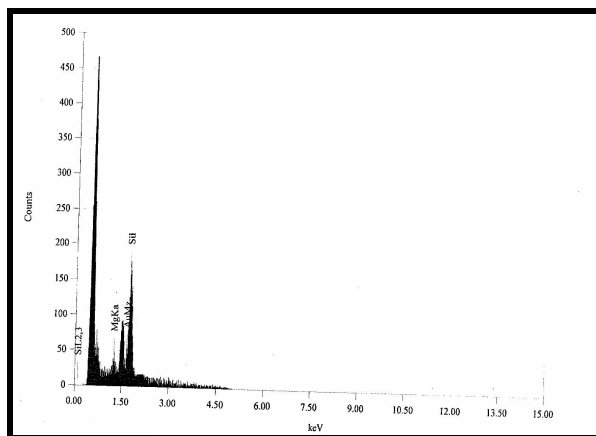
EDX peaks for clay minerals for Mangalwedha



EDX peaks for clay minerals for Ujani



EDX peaks for clay minerals for Papanus



EDX peaks for clay minerals for Barshi

Table No. 1: Percentage of minerals in the form of oxide in the soils of Solapur district.

Soil samples	Na ₂ O	MgO	K ₂ O	CaO	SiO ₂
Shetaphal	4.58	9.63	---	---	85.80
Mangalwedha	2.05	7.38	1.67	0.93	81.30
Ujani	8.48	5.40	---	---	76.40
Papnus	6.41	8.10	0.50	1.10	78.30
Barshi	---	11.25	---	---	72.17

--- Not detectable



Results and discussions:-

The minerals may be present in the form of oxides, chlorides, carbonates, sulphates etc. During the present work, attempt has been made to know the behaviour of each mineral in oxide form from different sites of Solapur district (Mitchell, 1964; Tindal, 1983). The technique used for the purpose is ZAP method for standard quantitative analysis of oxides. Including chloride, six minerals were detected. Some of the mineral were not detected because the concentration was below the detectable level. Calcium, Magnesium levels are comparatively higher than Potassium. Strikingly calcium in oxidized form is not detected to Shetaphal, Ujani and Barshi site. As well as potassium is also not detectable to Shetaphal, Ujani and Barshi site. Among all the minerals as oxides, the contribution of silicon is highest to all the sites. Chlorides detected from Mangalwedha and Ujani site. Similar observation was done by Mulimani (2007) for Bijapur district of Karnataka. The results reveal that clay minerals from different sites of *M. cymbalaria* are represented by Na₂O, MgO, K₂O, CaO, SiO₂, chloride. A trace of Au is also detected. (Table No. 1)(Fig. no.-I)

References :-

- Lee, S. H., Singh, A. P., Chung G. C. (2004). Rapid accumulation of hydrogen peroxide in cucumber roots due to exposure to low temperature appears to mediate decreases in water transport. *J. Exp. Bot.* 55:1733-1741.
- Legros, T., Smith D. L. (1994). Root zone temperature sensitivity of nitrogen fixing and nitrate supplied soyabean (*Glycine max* (L.) Merr.cv.Maple Arrow) and lupine (*Lupinus albus* L. cv. Ultra) plants. *Environ Exp Bot* 34:117-127.
- Mitchell, R. L. (1964). Trace elements in soil. In : *chemistry of soil*, F. A. Bear (ed) Oxford and IBH (Publ) : 320-366.
- Mulimani, M.B. (2007). Studies on economically important wild cucurbits of Bijapur district. Ph.D. thesis, Shivaji Univ., Kolhapur.

Tindall, H. D. (1983). *Vegetables in the Tropics*, Macmillan Press, London.



A comparative study of different compatibilisers on thermoplastic polyurethane/polyolefin blends.

Atul Dinkar Kamble^{@1}, Merlin Thomas², Neetha John³

^{@1}Shri Yashwantrao Patil Science College, Solankur, Tal- Radhanagri, Dist- Kolhapur, MH, India

²Institute of Science and Technology for advanced Studies and Research, V.V.Nagar, Dist- Anand, Gujarat, India

³Centre for Biopolymer Science and Technology (CBPST), CIPET, Kochi, Kerala, India

KEYWORDS

**Compatibilizer;
polyurethane blends;
SEM, DSC**

**Corresponding Author
Email
atulkamble02@gmail.com**

ABSTRACT

Thermoplastic polyurethane (TPU) and polyolefins blends have been prepared using different compatibilizers such as of polypropylene copolymer (PPCP), TPU-g-MA and TPU-g-AA in a melt screw extruder. Dispersion and the miscibility of the polymer matrix was characterized by Scanning electron microscope (SEM) and the interaction of compatibilisers with polymer matrix was revealed by Fourier transform infrared spectroscopy (FT-IR). It has been found that the formation of chemical bonding during melt blending may be enhanced the interaction. This compatibilized polymer blends exhibits better thermal stability, revealed by Thermogravimetric analysis (TGA) and Differential scanning calorimetric (DSC) results. Mechanical properties like tensile strength, impact strength, flexural strength and hardness were also studied using Universal Testing Machine (UTM). The results show that the blends having 20% loading of polyolefins (PO) with compatibilizers gives excellent performance in all aspects.

Introduction

Blends of TPU and PO are highly incompatible because of large difference in polarities and high interfacial tension. Blending of polymers is an economically attractive approach to development of new materials since it combines the desirable properties of more than one polymer [1]. Physical mixer of polyolefins (PO) with TPU is most versatile commodity polymers because of its excellent chemical and moisture resistance, superior ductility and stiffness, and fine manufacturability [2].

As the immiscible blends are thermodynamically unstable, compatibiliser must be added to stabilize the morphology. This process of stabilizing polymer blends is commonly called compatibilisation[3]. Polymers are considered miscible when specific attractive interactions among the functional groups of the macromolecules occur. The specific interactions include donor-acceptor, dipole-dipole, hydrogen-bonding, ion-ion, acid-base, and ion-dipole interactions. The techniques used for the detection of

polymer-polymer miscibility can be of several kinds, such as DSC, neutron scattering, morphology studies by optical and electron microscopy, dynamic mechanical measurements, IR spectroscopy, ultrasound and viscometry[4]. Copolymers are often used to compatibilize immiscible polymer blends, functioning as macromolecular surfactants to modify interfacial properties. Generally, there are two ways to incorporate block copolymers, adding premade copolymers or in situ formation[5-7]. In the first method, the block copolymers are synthesized in a separate step and then dispersed into the blend components. Theoretically, block copolymers should seek the interfaces during melt mixing to decrease unfavorable interactions[8,9]. In reactive compatibilization, functional polymers are added to (or just a natural part of) each blend component. During processing, complementary functional groups in each polymer react at the interfaces and form copolymers, which act as surfactants and compatibilize the blend. Both methods of compatibilization have been studied extensively[10-16].

In this research work, studies were done with blends of TPU/polyolefins using different compatibilisers in various proportions of polyolefins (5, 10, 15, 20, 25, 30%) the blends. Blends of TPU/polyolefins were prepared with various compatibilisers such as PPCP, TPU-g-MA and TPU-g-AA. Various properties of all the blends were examined and compared with conventional TPU/polyolefins blends.

EXPERIMENTAL

Material and Characterisation:

Low-density polyethylene (LDPE) (Grade: 24FS040) high density polyethylene (HDPE) (Grade: MA60200), polypropylene (PP) (Grade: H110MA) were supplied by Reliance India Ltd, Baroda. Thermoplastics polyurethane (TPU) prepared from aliphatic isocyanate (aliphatic grade), 85 shore A hardness, (Grade: W DP85085A), was supplied by Bayer India. Engage: Polyolefin elastomer (Grade 8402) purchased by DuPont Dow Elastomers, USA, ethylene vinyl acetate copolymer (EVA) and PPCP (Grade: MI 1530) supplied by IPCL, Baroda, India, Baroda. Xylene,

isopropanol, methanol, dimethyl formamide (DMF), benzoyl peroxide (BPO), maleic anhydride and acrylic acid etc. were laboratory grade.

Synthesis of compatibilizers[17-21]

Compatibilisers were prepared in laboratory as per the formulation given in Table 1. Polymer like TPU or PE 50 gm was dissolved in 200 ml of solvent in a three neck flask equipped with inert atmosphere. Solution of 5gm of grafting agent dissolved in a solvent and mixed with 0.4g initiator and added drop wise in to the three neck flask, temperature was then raised to 100⁰ C and stirring continued for the 3 to 4 hrs. The viscous liquid was precipitated in methanol and repeatedly washed with methanol to remove unreacted grafting agent. The compatibilisers synthesised were dried in vacuum oven at 80⁰ C. Structural characterisation of the above compounds, PE-g-MA, TPU-g-MA and TPU-g-AA were carried out using the Perkin-Elmer, spectrum GX FTIR spectrometer.

Blending Process

The polyolefins and Thermoplastic Polyurethane (TPU) were preheated for three hours at 80⁰ C. Pellets of TPU and each of the PO's with and without compatibilisers at different weight ratios were mixed on two roll mill and then extruded in a single screw extruder. The various compositions of blends of TPU/PO's with compatibilisers were prepared. Specimens for different mechanical testing were prepared from Injection moulding machine and compression moulding machine.

Mechanical properties

The tensile strength test of all the blends were carried out at room temperature according to ASTM D-638. The flexural strength tests of blends were done according to ASTM D-790. The izod impact strength test of all the blends were carried out at room temperature according to ASTM D-256. Surface and volume resistivity test of the blends TPU/PO's were carried out according to ASTM D 257.



TABLE 1 FORMULATION FOR COMPATIBILIZER SYNTHESIS

Ingredients	Name of Compatibilizer			Amount
	LDPE-g-MA	TPU-g-MA	TPU-g-AA	
Polymer	LDPE	PU	PU	50 gm.
Solvent	Xylene	Dimethyl formamide (DMF)	Dimethyl formamide (DMF)	400ml
Initiator	Benzoyl peroxide (BPO)	Benzoyl peroxide (BPO)	Benzoyl peroxide (BPO)	0.4gm
Grafting agent	Maleic anhydride	Maleic anhydride	Acrylic acid	5gm
Solvent for grafting agent	Isopropanol	Dimethyl formamide (DMF)	No solvent	20ml

Thermal and morphological properties

Thermal properties of the blends were studied using with Perkin-Elmer, DSC-PYRIS-I differential scanning electron (DSC) machine and Perkin-Elmer TGA-7 thermo gravimetric analysis (TGA). The fracture surface of the blend samples were analyzed with a Philips, Scanning Electron Microscope (SEM). The surface morphology of the TPU/PO's blends with or without compatibiliser was examined in scanning electron microscopic in the inert atmosphere of nitrogen gas.

RESULTS AND DISCUSSION

Characterisation of synthesized compatibilisers:

Three graft copolymers were synthesised in the laboratory and used as compatibilisers in the PO's/TPU blends. Figure 1(a) and 1(b) shows the FTIR spectrum of thermoplastic polyurethane and all three compatibilisers namely PE-g-MA (AK-1), PU-g-MA (AK-2), PU-g-AA (AK-3) respectively. In the FTIR spectra of PE-g- MA (AK-1), the characteristic absorption band due to C-H stretch of alkanes was present at 2800cm⁻¹, 1700cm⁻¹ for C=O stretch and absorption band at 1466 cm⁻¹ is of C-H deformation. In the FTIR spectra of PU-g-MA (AK-2), the characteristic absorption band due to

CO-NH stretch was present at 3430 cm⁻¹,1731 cm⁻¹ for C=O stretch, 2958 cm⁻¹ absorption band of C-H stretching. In the FTIR spectra of PU-g-AA (AK-3),the characteristic absorption band due to CO-NH stretch was present at 3351 cm⁻¹,1727cm⁻¹for the C=O,2959 cm⁻¹is for C-H stretching etc. The grafting reaction takes place via initiation of the labile methylene hydrogen of both the LDPE and TPU (aliphatic grade) using BPO as an initiator. The transfer radical produced generally propagates, and the growing chain may terminate or undergo second chain transfer shown in reaction scheme 1[22].

Figure 2 shows the GPC chromatograms of the thermoplastic polyurethane and maleic anhydride grafted thermoplastic polyurethane. The chromatograms were observed to be narrow and monomodal⁴¹. This separation process is well suited to the determination of the MWD of linear polymers. However in the case of branched polymers, for a given hydrodynamic volume, branched molecules has higher molecular weights than linear ones but are eluted at the same time⁴². GPC chromatogram data shows that the molecular weight of the TPU is 22348. After grafting, the molecular weight of TPU-g-MA was found to be 83060 which confirm

the grafting took place via cross-linking reaction. The FTIR spectrum and GPC data confirms the successful characterisation and identification of the chemical linkages present in the compounds.

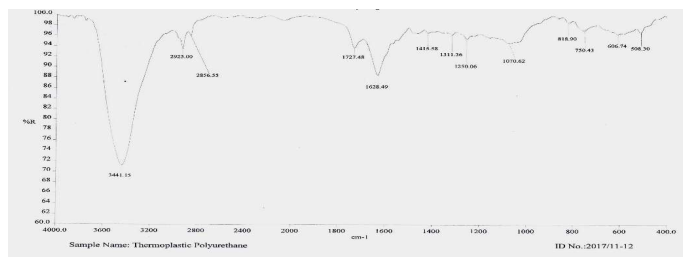


Figure 1(a): FTIR of TPU

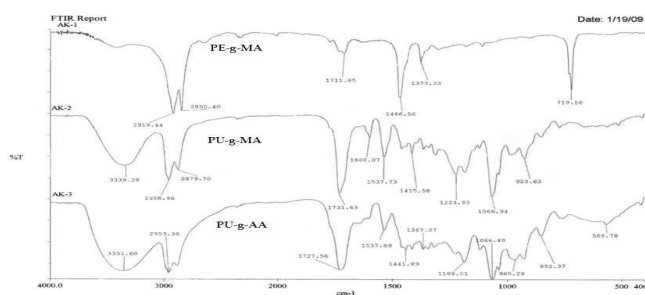


Figure 1(b).FTIR of grafts PE-g-MA (AK-1), PU-g-MA (AK-2), PU-g-AA (AK-3).

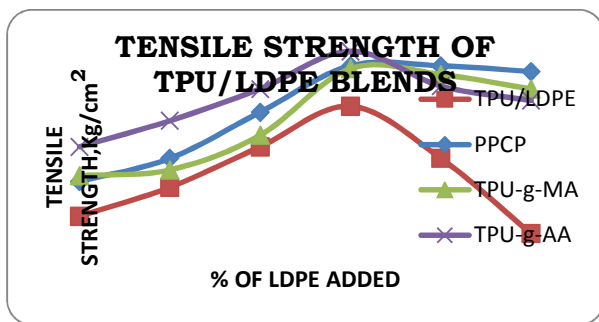


Figure 3(a)

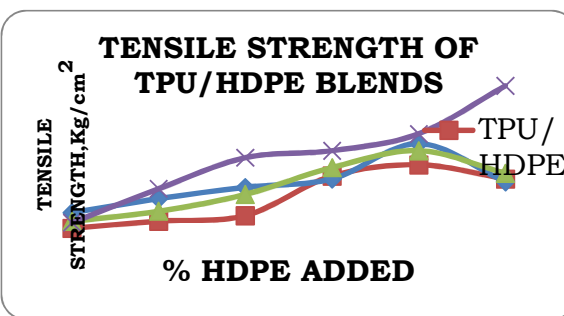


Figure 3(b)

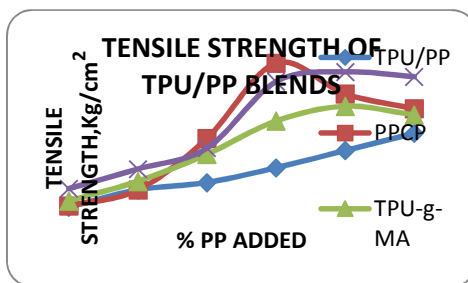


Figure 3(c)

Figure 3: Tensile strength of a) TPU/LDPE, b)TPU/HDPE, TPU/PP blends with and without compatibiliser.



Tensile strength of TPU/PO's blends with or without compatibilisers are shown in Figure 3. The figure 3(a), 3(b) and 3(c) show the tensile strength of the TPU/HDPE, TPU/HDPE and TPU/PP with and without compatibiliser respectively. Compatibilisers such as PPCP, PU-g-MA, and PU-g-AA were used for improving the properties. The tensile strength increases with increasing percentage of polyolefin in the blends. Incorporation of compatibilizer such as PPCP, TPU-g-AA and PU-g-MA in the TPU/Polyolefins blends further increased the tensile strength as compared to blends without compatibiliser. Compatibilisers such as PPCP, PU-g-MA and PU-g-AA show superior properties than convention blend due to the presence of PU phase and acidic polar phase which support the miscibility.

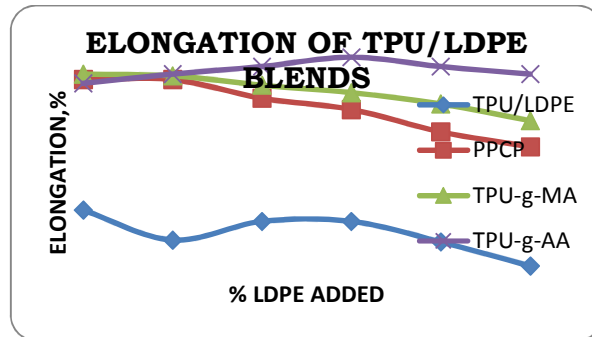


Figure 4(a)

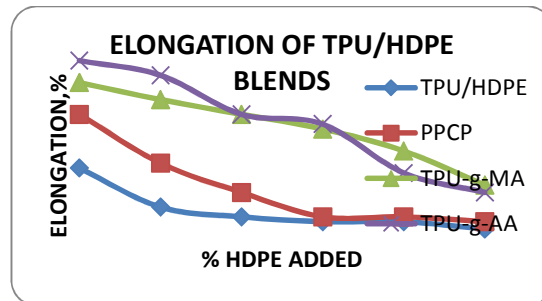


Figure 4(b)

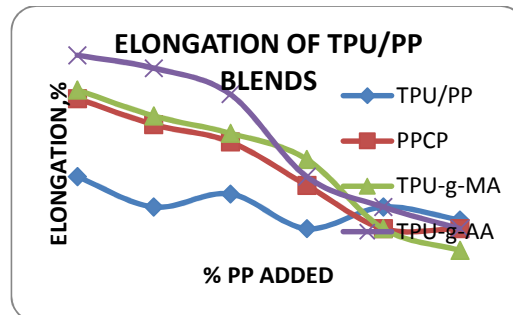


Figure 4(c)

Figure 4: % elongation of a) TPU/LDPE, b) TPU/HDPE, TPU/PP blends with and without compatibiliser

Figure 4 shows percentage elongation of TPU/Polyolefins blends with and without compatibilisers. Figure 4(a), 4(b) and 4(c) show the percentage elongation of TPU/LDPE, TPU/HDPE and TPU/PP blends with and without compatibiliser respectively. In each case of blends such as TPU/LDPE, TPU/HDPE, TPU/PP, percentage elongation increase with addition of compatibiliser as compared with blends of TPU/PO's without compatibiliser. Percentage elongation decreases with increasing polyolefin content in each blend. Increase in the percentage elongation of the blend is due to good adhesion between the two polymers after the addition of the compatibiliser into the blend.

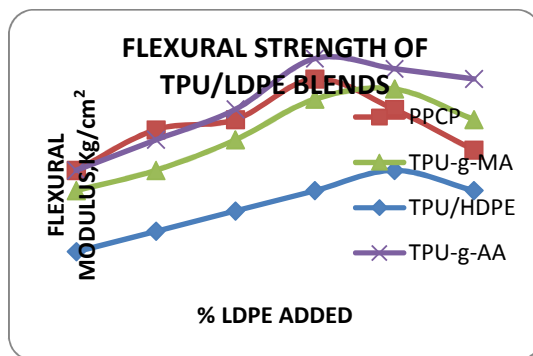


Figure 5(a)

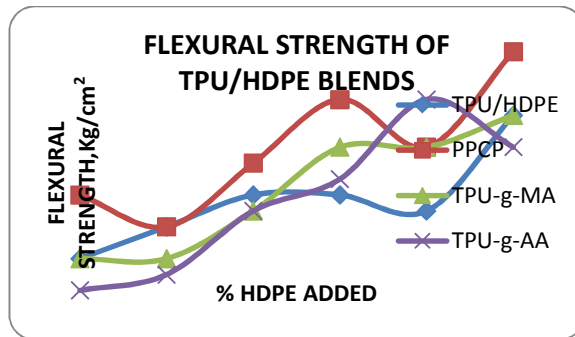


Figure 5(b)

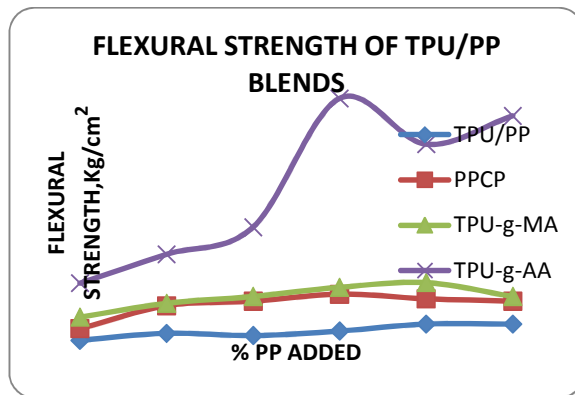


Figure 5(c)

Figure 5: Flexural strength of a) TPU/LDPE, b)TPU/HDPE, TPU/PP blends with and without compatibiliser.



Flexural strength of the TPU/PO's blends with and without compatibilisers are shown in Figure 5. Similar to other properties, flexural strength also increases with addition of compatibiliser into polymer blends compared with blends without compatibiliser. Flexural strength increases with increasing the percentage of the polyolefins as shown in figure 6. The extent of increase in flexural properties may be due to the blends morphology, the addition of compatibiliser increase miscibility of two polymers and hence, finer dispersity showing higher properties¹.

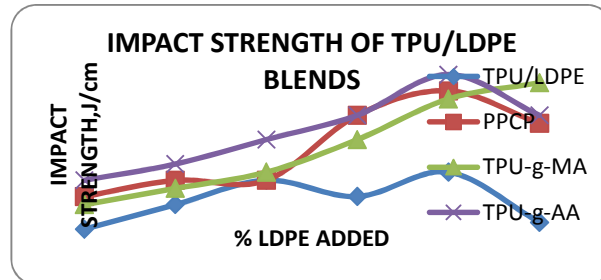


Figure 6(a)

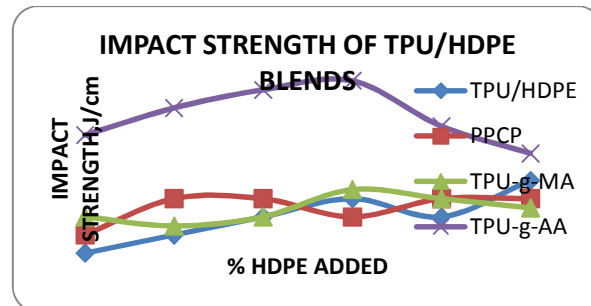


Figure 6(b)

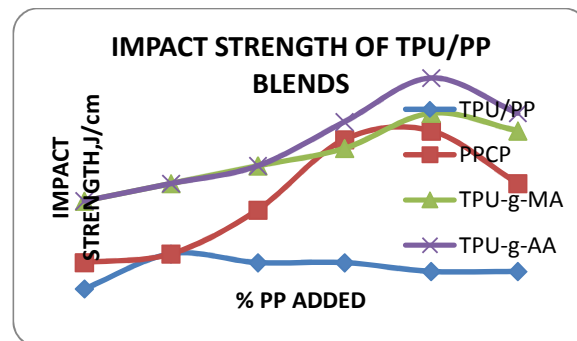


Figure 6(c)

Figure 6: Izod impact strength of a) TPU/LDPE, b) TPU/HDPE, TPU/PP blends with and without compatibiliser
The impact strength of various TPU/Polyolefins blends with and without compatibilizers is shown in Figure 6. Figure 6(a), 6(b) and 6(c) shows the TPU/LDPE, TPU/HDPE and TPU/PP blend with and without compatibiliser respectively. An addition of compatibilisers such as PPCP, PU-g-MA, and PU-g-AA into the TPU/PO's blends increases the impact strength as compare with blend without compatibiliser. Thus, increase in the impact strength may be due to addition of compatibiliser, compatibiliser increases the blend miscibility and toughness of the matrix compared to immiscible blends of the TPU/PO's blends.

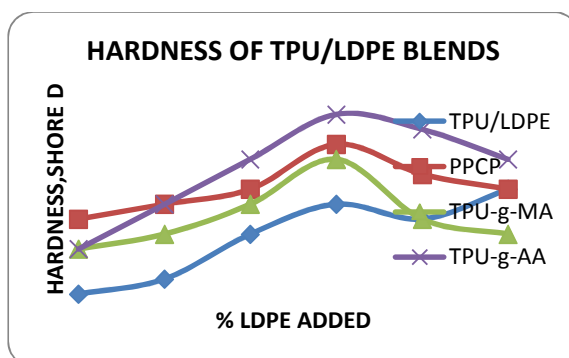


Figure 7(a)

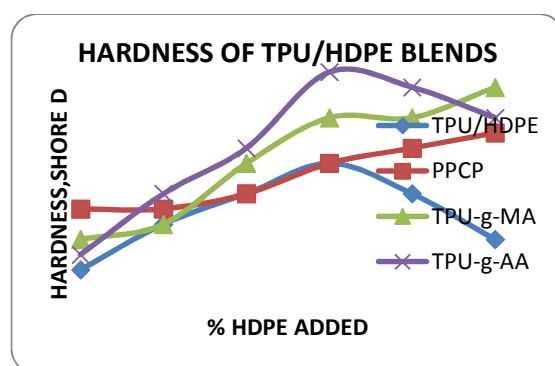


Figure 7(b)

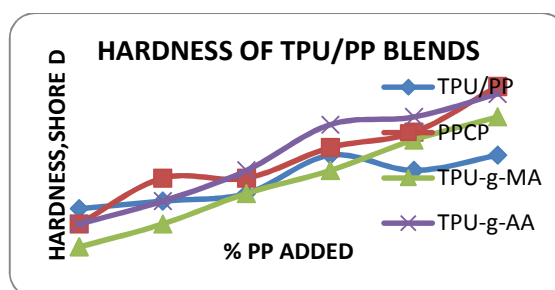


Figure 7(c)

Figure 7: Hardness of a) TPU/LDPE, b) TPU/HDPE, c) TPU/PP blends with and without compatibiliser.

Hardness of the TPU/LDPE, TPU/HDPE and TPU/PP blends with and without compatibiliser shown in the figure 7(a), 7(b) and 7(c) respectively. All the blends with compatibiliser show increase in hardness along with increasing percentage of polyolefin. TPU/PP blend show the highest Shore D hardness among the TPU/LDPE and TPU/HDPE blends with compatibiliser.

Morphology of TPU/PO blends

A SEM images of TPU/LDPE, TPU/HDPE, and TPU/PP blends with and without compatibiliser are shown in figure 8, 9 and 10 respectively. The passing of fracture through along the boundaries indicate the immiscibility of the two



polymers TPU and PO's when used without any compatibiliser. When compatibilisers PPCP, PU-g-MA, and PU-g-AA were added into the TPU/PO's blends, the blends of TPU/PO's display significantly finer morphology. Compatibiliser such as PPCP, PU-g-MA, PU-g-AA show excellent morphological behavior among all the blends. It gives the evidence that the above three compatibilisers give better results for miscibility of the TPU/PO's blends.

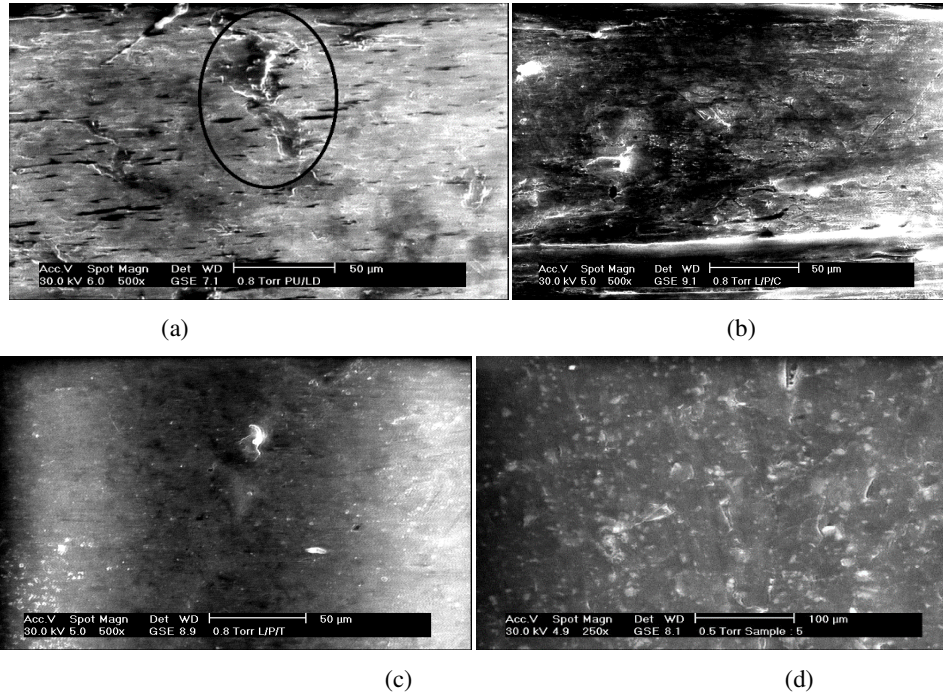


Fig.8: SEM images of a) TPU/LDPE, b) TPU/LDPE/PPCP, c) TPU/LDPE/TPU-g-MA, d) TPU/LDPE/TPU-g-AA

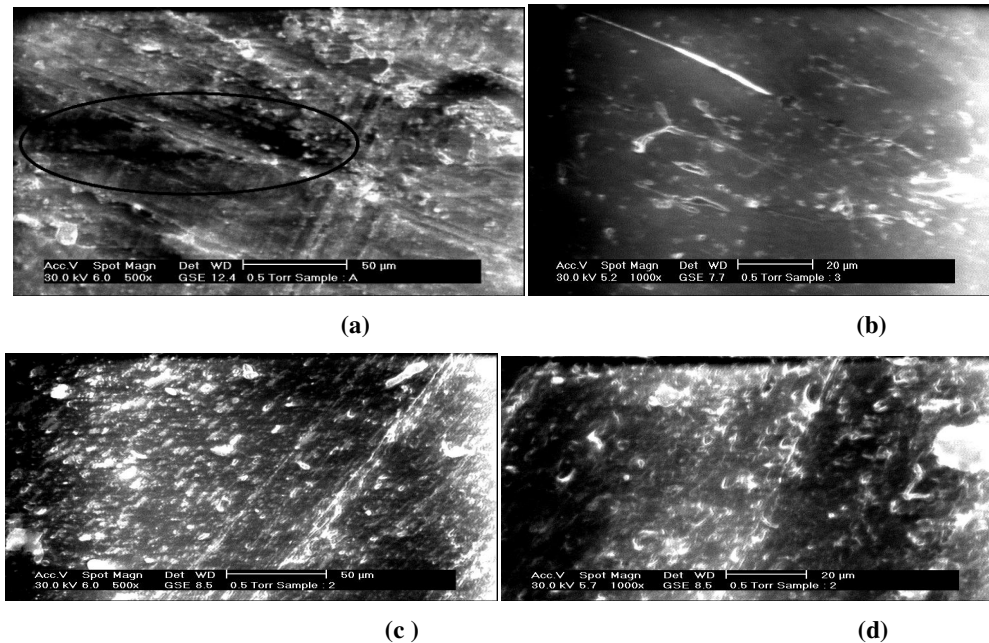


Figure 9: SEM images of a) TPU/HDPE, b) TPU/HDPE/PPCP, c) TPU/HDPE/TPU-g-MA, d) TPU/HDPE/TPU-g-AA.

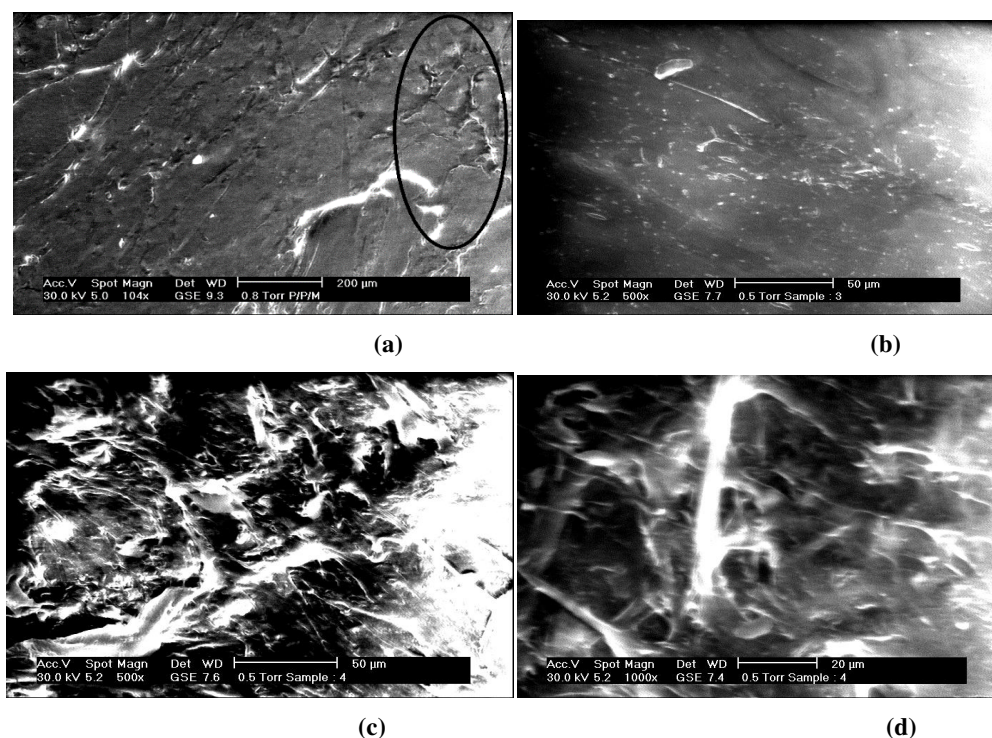


Figure 10: SEM images of a) TPU/PP, b) TPU/PP/PPCP, c) TPU/PP/TPU-g-MA, d) TPU/PP/TPU-g-AA.

CONCLUSIONS

TPU/PO's blends were successfully prepared by melt mixing technique with and without compatibiliser. SEM images show that the addition of small quantity of compatibilisers such as PPCP, TPU-g-MA, and TPU-g-AA improves the miscibility of all TPU/PO's immiscible polymer blends. Mechanical properties of the blends were increased with the addition of compatibiliser compared to conventional blends. PPCP and PU-g-AA was found to be good compatibilisers for the TPU/PO's blends.

REFERENCES

9. Yali Di, Maoqing Kang, Yuhua Zhao, Shirun Yan and Xinkui Wang, *Journal of Applied Polymer Science*, **99**, 875-883, 2006.
10. Rodriguez-Perez M.A. *Polymer Testing*, **28(2)**,188, (2009).

3. Kader M.A., Bhowmick A.K., *J ApplPolym Sci.*,**90**,278-286, (2003).
- 4.CemilAlkan, NebahatYurtseven, Leyla Aras, *Turk J Chem.*,**29**, 497 – 506, (2005).
- 5.Paul DR, Bucknall CB. *Polymer blends*. New York, Wiley, 2000.
- 6.Datta S, Lohse D. *Polymeric compatibilizers: uses and benefits in polymer blends*. New York: Hanser; 1996.
- 7.Koning C, Van Duin M, Pagnoulle C, Jerome R.,*ProgPolymSci*, **23**, 707, 1998.
8. Leibler L.,*Macromolecules*, **15**, 1283, 1982.
- 9.Noolandi J and Hong M.,*Macromolecules*, **15**, 482, 1982
- 10.Locke C, Paul D., *J ApplPolymSci*, **13**, 2957,1973
11. Epstein B. US patent **4,174**, 358, 1979.



- 12 Fayt R, Teyssie P., *Macromolecules*, **19**:2077, 1986
13. Hobbs S, Dekkers M, Watkins V., *J Mater Sci* **24**, 2025, 1989;
- 14 Fayt R, Jerome R and Teyssie P., *J Polym Sci, Polym Phys* **27**, 775, 1989.
- 15 Xanthos M and Dagli S., *Polym Eng Sci*, **31**, 929, 1991
- 16 Macosko C, Guegan P., Khandpur K, Nakagawa Y, Marechal P, Inoue T. *Macromolecules*, **29**, 5590, 1996
- 17 Ghaemy M and Roohina S., *Iranian polymer journal* **12**(1), 21, 2003
- 18 Bhattacharyya A and Misra B.N, *Prog Polym Sci*, **29**, 767, 2004
- 19 Al-Malaika S. and Eddiyanto E, *Polymer Degradation and stability*, **95**, 353, 2010
- 20 Maolin Z, Hasegawa S, Chen J and Maekawa Y, *Journal of Fluorine Chemistry*. **129**



Investigation of structural and magnetic properties of TiO₂ supported Zinc ferrite

R.P.Patil^{a*}, B. L. Shinde^b, M. N. Gadsing^c, R. K. Dhokale^d

^aM.H.Shinde Mahavidyalaya, Tisangi- 416206 (MH) India.

^bP.D.E. As.Waghire College, Saswad

^cJawahar Arts, Science and Commerce College, Anadur-413 603 (MS) India.

^dArts, Science and Commerce College, Naldurg-413 602(MS) India

KEYWORDS

Nanocomposite,
XRD,
TEM,
Magnetism,

Corresponding Author
Email
raj_rbm_raj@yahoo.co.in

ABSTRACT

Nanocrystalline TiO₂ loaded ZnFe₂O₄ was synthesized by wet chemical process. Phase formation study was carried out by using x-ray diffraction technique and it's reveals that TiO₂ properly supported on the surface of zinc ferrite. Nano sized two different layers such as cubic zinc ferrite and TiO₂ were confirmed by transmission electron microscopy technique. Magnetic data for all samples indicates that ferromagnetism was decreases with increasing non magnetic titania. In this manuscript detailed study of structural and magnetic properties of TiO₂ supported Zinc ferrites nanocomposites samples were investigated.

Introduction

Mixed-metal oxides having general formula AB₂O₄, where A is divalent metal ion, B is trivalent metal ion and O²⁻ is oxide ion. In these mixed-metal oxides Iron is main element, therefore this materials is called as ferrites. In our earlier research work, we have synthesized various mixed-metal oxides or ferrites such as Li_{0.5}Fe_{2.5}O₄, Li_{0.5}Mn_{2.5}O₄, CoFe₂O₄, ZnTiFeO₄ and ZnCrFeO₄ [1-5]. The structural, magnetic and electrical properties of these ferrites were based on method of preparation, sintering temperature, atmospheric conditions, complexing agent and purity of metal salts.

Several researchers have prepared different nano-sized ferrites by physical and chemical methods such as co-precipitation [6], sol-gel [7], microemulsion method [8], hydrothermal [9], spray pyrolysis [10], reverse micelle [11],

precursor [12], combustion synthesis [13] etc. Out of all methods, our interest only in citrate-gel method because this method is superior than others, not require any sophisticated instrument, obtained homogenous uniform grains and require low sintering temperature.

In this article, we have synthesized 10, 20 and 30% TiO₂ supported zinc ferrite by citrate-gel and impregnation method. After synthesis, structural properties of all samples were characterized by XRD and TEM analysis. Magnetic study was carried out by using Vibrating sample magnetometer. This research work was already published in one reputed journal [14] but dielectric permittivity study for 10, 20 and 30% TiO₂ supported zinc ferrites nanocomposite samples are not available in literature.

Therefore, our interest was synthesizing such type of nanocomposites and study their structural and magnetic properties are investigated in this manuscript.

2. Experimental

Crystalline zinc ferrite was synthesized by citrate gel auto-combustion method. High purity (AR grade) ferric citrate, zinc nitrate, citric acid were used as raw materials. The stoichiometric amounts of individual metal nitrates and metal citrate were dissolved in doubly distilled deionized water to get a clear, transparent solution. The solution of citric acid was added to separate metal nitrate solutions to form metal-citrate complex. The above solutions were mixed together with constant stirring to get a homogeneous mixture. The mixture was heated slowly upto 373 K to obtain a fluffy mass and combusted to get the dry powder. This sample was further annealed at 973 K for 4h. TiO₂ coating was done by sol-gel hydrolysis of titanium isopropoxide (Ti (OC₃H₇)₄) on ferrite nanoparticles followed by calcination treatment. Zinc ferrite nanoparticles were dispersed in titanium isopropoxide-isopropanol mixture (1:1 molar ratio). Water was slowly added to the above suspension under constant stirring. The resulting material was dried and calcined at 873K for 4h in air. Different concentrations of TiO₂ were loaded on zinc ferrite (10 to 30% by weight) to find out the optimum concentration of TiO₂ required.

X-ray diffractometer (Philips model PW-1710) was used to identify the phases and the crystalline nature of the samples using Cr K α radiation. Particle size was measured using a transmission electron microscope (TEM) (Philips, CM200, Operating voltages 20-200kv). The high field vibrating sample magnetometer (VSM) (LAKESHORE-Model: 7404) at a maximum applied field of 15KOe was used to measure the saturation magnetization, coercivity and remnant magnetization of all the samples.

3. Results and discussion

3.1 XRD studies

10, 20 and 30 percentage of TiO₂ on ZnFe₂O₄ nanoparticles. The diffraction pattern of ZnFe₂O₄ shows peaks corresponding to planes (111), (220), (311), (222), (400), (422) and (333) confirming the formation of spinel zinc ferrite (JCPDS Patterns No. 22-1086). Diffraction peaks corresponding to planes (101), (020) and (200) of anatase titanium oxide besides that of ZnFe₂O₄, are seen in the TiO₂ coated samples indicating the biphasic nature of the samples.

3.2 Transmission Electron Micrographs Study

Fig. 2 (a and b) depict the transmission electron micrographs of zinc ferrite and TiO₂ on ZnFe₂O₄ samples. It is evident from **Fig 2a** that the average particle size of zinc ferrite is around 80 nm. The superimposition of the bright spot with Debye ring pattern seen in the SAED pattern indicates polycrystalline nature of the sample. Formation of a single phase of zinc ferrite can be further confirmed from the SAED pattern of this sample. **Fig 2b** clearly shows the presence of a dispersed phase of TiO₂ on ZnFe₂O₄. The particle size of TiO₂ is estimated to be around 10 nm.

3.3 Magnetic study

Magnetic properties of the uncoated and anatase TiO₂ coated zinc ferrite as measured by VSM are shown in **Fig. 3**. From this figure, it can be seen that all samples showed two magnetic components. At low applied fields, a ferromagnetic behaviour is seen whereas at higher applied fields, a conversion to paramagnetism is observed. The magnetic parameters such as coercivity and remanent magnetization have very low values indicating that these are soft magnetic materials.

Conclusions

A composite of TiO₂-ZnFe₂O₄ ferrites of nanocrystalline nature were synthesized by sol-gel method. Phase formation was studied by using x-ray diffraction analysis. Transmission electron micrographs indicated the presence of a dispersed phase of TiO₂ on ZnFe₂O₄. As the samples have ferromagnetic properties at low applied fields.

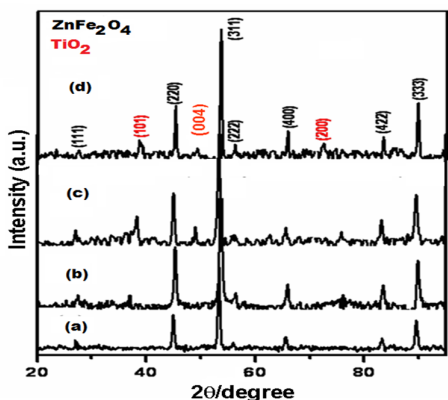


Fig 1. Powder XRD patterns of (a) $ZnFe_2O_4$ (b) 10% TiO_2 - $ZnFe_2O_4$ (c) 20% TiO_2 - $ZnFe_2O_4$ & (d) 30% TiO_2 - $ZnFe_2O_4$

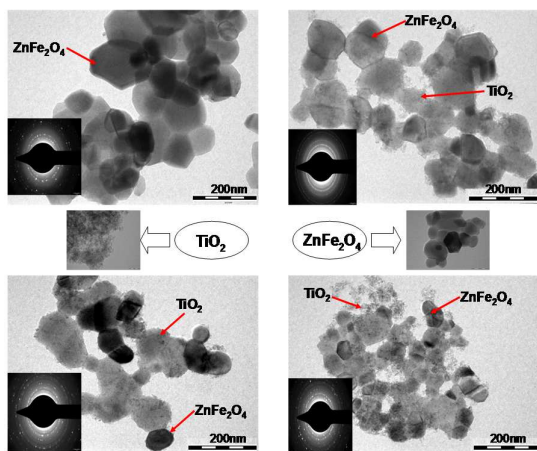


Fig 2. TEM micrographs of $ZnFe_2O_4$ and TiO_2 - $ZnFe_2O_4$

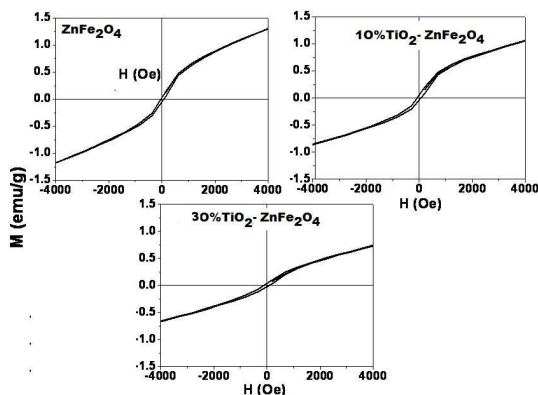


Fig 3. Magnetization as a function of applied magnetic field for (a) $ZnFe_2O_4$ (b) 10% TiO_2 - $ZnFe_2O_4$ & (c) 30% TiO_2 - $ZnFe_2O_4$

References

- [1] Hankare P.P., Patil R.P., Sankpal U.B., Jadhav S.D., Lokhande P.D., Jadhav K.M., Sasikala R., J. Solid State Chem. 182(2009)3217.
- [2] P.P. Hankare, U.B. Sankpal, R.P. Patil, I.S. Mulla, P.D. Lokhande, N.S. Gajbhiye, J. Alloys Compd. 485 (2009) 798.
- [3] P.P. Hankare, R.P. Patil, U.B. Sankpal, S.D. Jadhav, I.S. Mulla, K.M. Jadhav, B.K. Chougule, J. Magn. Mater. 321 (2009) 3270.
- [4] P. P. Hankare, R. P. Patil, K. M. Garadkar, R. Sasikala, and B. K. Chougule, Mater. Res. Bull. 46(2011)447.
- [5] R.S. Pandav, D.R.Patil, R.P.Patil, P.P.Hankare, J. of Magn.Magn.Mater. 05(2016)259–263.
- [6] T. J. Shinde, A. B. Gadkari P. N. Vasambekar, J. Magn. Magn. Mater., 333(2013)152-155.
- [7] R.P. Patil, N.M. Patil, R. Sasikala, P.P. Hankare, S.D. Delekar, Materials Research Bulletin 48 (2013) 1791–1795.
- [8] V.Pillai, P. Kumar, M. S. Multani, D. O. Shah, Colloid. Surface A80 (1993) 69.
- [9] X. Jiao, D. Chen, and Y. Hu, Mater. Res. Bull. 37 (2002) 1583.
- [10] A. Sutkaa, J. Zavickis, G. Mezinskisa, D. Jakovlevs, J. Barloti, Sen. Actu. B, 176 (2013) 330–334.
- [11] S.Thakur, S.C.Katyral and M. Singh, J. Magnetism Magnetic Materials 321 (2009)1.
- [12] P. P. Sarangi , S. R. Vadera, M. K. Patra and N. N. Ghosh, Powder Tech. 203 (2010) 348.
- [13] A. Sutka, G. Mezinskis, G. Strikis, A. Siskin, Energetika, 58 (2012) 166-172.
- [14] P.P. Hankare, R.P. Patil, A.V. Jadhav, K.M. Garadkar, R. Sasikala, Applied Catalysis B: Environmental, 107(2011)333-339.



Synthesis and characterization of Zn-Cr ferrite

S. B.Patil^a, N.M.Patil^b A.J.Davari^c, M.N.Patil^d, R. P. Patil^{e*}

^aKrantisinh Nana Patil College Walwa, Sangli-416313, MH, India.

^bBhogawati Mahavidyalaya, Kurukali, Tal- Karveer, Dist. – Kolhapur 416001

^cM.T.Yadav(Patil) Jr, College of Science Khanapur, MH, India

^dShri.Padmaraje Vidyalay Jr, College of Science Shirol, MH, India

^eM.H. Shinde Mahavidyalaya, Tisangi - 416206, MH, India

KEYWORDS

Zinc ferrite,
Co-precipitation,
XRD, SEM,
Electrical resistivity,
Gas sensor.

Corresponding Author

Email

raj_rbm_raj@yahoo.co.in

ABSTRACT

Nanocrystalline ZnCrFeO₄ ferrite has been synthesized. Formation of single phase cubic spinel structure was confirmed from their X-ray diffraction pattern. These ferrite sample existed as crystalline nanoparticles of about 30-40 nm size as observed from Transmission Electron Microscopy technique. Infrared spectra showed two main absorption bands in the range 400-800 cm⁻¹ arising due to tetrahedral (A) and octahedral (B) stretching vibrations. The sample was found to be ferromagnetic.

Introduction

Spinel nanoparticles have been intensively studied in the last decade for their unusual physical and chemical properties owing to their extremely small size, large specific surface area and number of promising applications. Among various classes of nanomaterials, spinels oxides are very common, most diverse and possess richest class in terms of physical, chemical and structural properties. In spinel structure, the oxygen atoms are closely packed in face centered lattices, into the interstices of which the metal ions are distributed. The unit cell of spinel contains 8 molecules (8 × FeFe₂O₄). There are 32 divalent oxygen ions, 16 trivalent iron ions and 8 divalent iron ions per unit cell. When the oxygen atoms arrange themselves in FCC structure, there are 8 occupied tetrahedral voids called the A and 16 occupied octahedral voids called the B sites.

Various methods are available for the synthesis of metal oxides, such as microwave refluxing [1], sol-gel [2-3], hydrothermal [4-5], co-precipitation [6-7], citrate-gel [8] and spray pyrolysis [9] etc. The selection of appropriate synthetic procedure often depends on the desired properties and final applications. Among these synthesis techniques, sol-gel autocombution method has several advantages over others for preparation of nanosized metal oxides as the process begins with a relatively homogeneous mixture and involves low temperature conditions and results a uniform ultrafine porous powders [10]. This method was employed by us to obtain improved powder characteristics, better homogeneity and narrow particle size distribution, thereby influencing structural, electrical and magnetic properties of spinel ferrites [11-13]. Spinel ferrites find potential applications in electrical components, memory devices,

magnetostrictive and microwave devices over a wide range of frequencies because of their high resistivity and low losses [14–18]. The field of ferrites is well explored, due to their potential applications and the interesting physics involved in them.

In the present work, we report the synthesis, characterization and catalytic activity of a magnetically separable sol-gel synthesized nanosized Zn-Cr ferrite. It is a simple process, which offers a significant saving in time and energy consumption over the traditional methods, and requires lower sintering temperature. This method was employed to obtain improved powder characteristics, more homogeneity and narrow particle size distribution, thereby influencing their structural, electrical and magnetic properties. The structural, electrical and magnetic properties were investigated by X-ray diffraction (XRD), TEM, SAED.

2.0 Synthesis Technique

Analytical grade chromium nitrate [$\text{Cr}(\text{NO}_3)_3 \cdot 9\text{H}_2\text{O}$], iron nitrate [$\text{Fe}((\text{NO}_3)_3 \cdot 9\text{H}_2\text{O})$], zinc nitrate [$\text{Zn}(\text{NO}_3)_2 \cdot 6\text{H}_2\text{O}$] and citric acid [$\text{C}_6\text{H}_8\text{O}_7 \cdot \text{H}_2\text{O}$] were used to prepare ZnCrFeO_4 by sol-gel method. Metal nitrates and citric acid were dissolved in minimum quantity of deionized water with 1:1 molar ratio. The pH of the solution was adjusted to about 9.0 to 9.5 using ammonia solution. The solution was transformed to dry gel on heating to 353K. On further heating the dried gel burnt in a self propagating combustion manner until all the gel completely converted to a floppy loose powder. The as burnt precursor powder was then sintered at 973 for 8 h for confirmation of phase formation. The sintered powders were granulated using 2 % polyvinyl alcohol as a binder and uniaxially pressed at a pressure of 8 ton / cm^2 to form pellets. These pellets were gradually heated to about 773K to remove the binder material.

The phase formation of the sintered samples was confirmed by x-ray diffraction studies using a Philips PW-1710 x-ray diffractometer with $\text{CrK}\alpha$ radiation ($\lambda=2.2897\text{\AA}$) in a θ – 2θ geometry at standard atmospheric

conditions. FTIR study was used to indicate the vibrational modes in the samples. The FTIR spectra were recorded using Perkin Elmer FTIR in KBr pellets. Particle size was measured using a transmission electron microscope (TEM) (Philips, CM200, operating voltages 20–200 kV).

3.0 Results and Discussion

3.1 X-ray diffraction study

The structure and phase purity of the products were confirmed by analyzing the X-ray diffraction patterns. **Fig.1.** depicts the XRD pattern of the different ZnCrFeO_4 composition and all x-ray parameters are summarized in **Table 1.** All the observed reflections could be assigned to cubic spinel lattice indicating their single phase nature. Unit cell parameters were determined by indexing the diffraction peaks in the XRD patterns.

3.2 FT-IR study

The Infra-red spectra of the sample were shown in **Fig.2.** It can be seen that the two main absorption bands in the range 400–800 cm^{-1} arising due to tetrahedral (A) and octahedral (B) stretching vibrations. Such absorption bands can be attributed to the statistical distribution of Fe at A-(tetrahedral) and B-(octahedral) sites. Waldron [36] ascribed the ν_1 band to the intrinsic vibration of the tetrahedral group (594 cm^{-1}) and ν_2 to octahedral group (487 cm^{-1}). The vibrational frequencies depend on cation mass, cation – oxygen distance and the bonding force. The BET surface area of ZnCrFeO_4 is found to be 8 $\text{m}^2 \text{g}^{-1}$.

3.3 Transmission electron micrograph

Fig.3 depicts transmission electron micrograph (TEM) of ZnCrFeO_4 sample. The corresponding selected area electron diffractograms (SAED) are given as inset in Figure. It is evident from this micrograph that the It is evident from this micrograph that the synthesized sample has spherical particles ranging from 30 to 40 nm.



The superimposition of the bright spot with Debye ring pattern indicates crystalline nature of the samples. Both the figures confirm that most of the particles are of size about 30 nm. This is in close agreement with the average crystallite size obtained from XRD (Table-1)

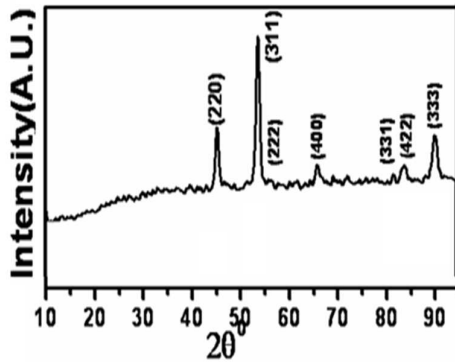


Fig.1.XRD

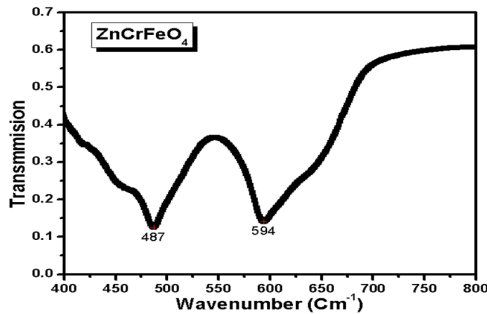


Fig.2.FTIR

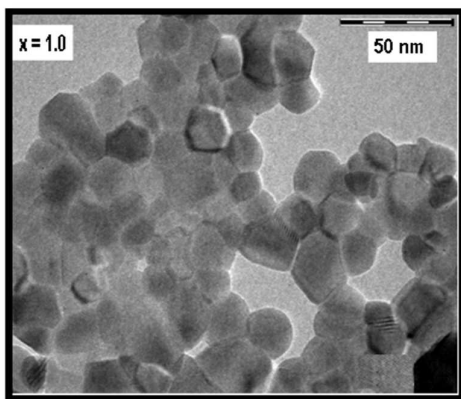


Fig.3.TEM

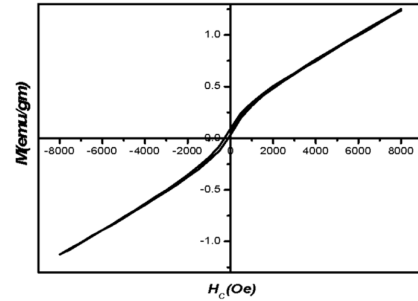


Fig. 4 VSM

3.5 Magnetic Study

Magnetic measurements of ZnCrFeO₄ system were carried out by using vibrating sample magnetometer (VSM) and they are depicted in Fig.4. The samples show typical S-type shape in M–H curve, though the coercive fields are very small. The magnetization rises very sharply as the applied field increases from zero in either direction and then slowly approaches saturation. This is the typical behavior of nanosized magnetic material where residual superparamagnetic relaxation leads to slow rise in the wings and ferrimagnetic part contributes to hysteresis loop with small coercive field. The magnetic data for the samples reveals that, it is ferrimagnetic in nature. The magnetic parameters such as saturation magnetization (M_s), remanant magnetization (M_r), and coercive field are summarized in Table 1.

4.0 Conclusions

Chromium-substituted nanocrystalline Zn-Cr ferrite sample was synthesized by sol-gel method. X-ray diffraction studies confirm the cubic spinel structure formation of the samples. FTIR spectral studies indicate two absorption bands, one around 600 cm⁻¹ (Tetrahedral) and the other around 500 cm⁻¹ (Octahedral). Transmission electron microscopy data revealed that the ferros spinels synthesized by autocombustion method are in nanocrystalline range (~30- 40nm) of the ferrite. The sample was found to be ferromagnetic.

Reference

- [1] J. Giri, T. Sriharsha, D. Bhadur, J. Mater. Chem. 14 (2004) 875.
- [2] M. George, A.M. John, S.S. Nair, P.A. Joy, M.R. Anantharaman, J. Magn. Mater. 302 (2006) 190.
- [3] S. Giri, S. Samanta, S. Maji, S. Gangli, A. Bhaumik, J. Magn. Mater. 288(2005) 296.
- [4] S. Thompson, N.J. Shirtcliffe, E. O'keefe, S. Appleton, C.C. Perry, J. Magn. Mater. 292 (2005) 100.
- [5] J. Wang, Mater. Sci. Eng., B 127 (2006) 81.
- [6] A.S. Albuquerque, J.D. Ardisson, W.A.A. Macedo, J.L. Lopez, R. Paniago, A.I.C. Persiano, J. Magn. Mater. 226 (2001) 1379.
- [7] P.P. Hankare, V.T. Vader, N.M. Patil, S.D. Jadhav, U.B. Sankpal, M.R.Kadam, B.K. Chougule, N.S. Gajbhiye, Mater. Chem. Phys. 113 (1) (2009) 233.
- [8] P.P. Hankare, U.B. Sankpal, R.P. Patil, I.S. Mulla, P.D. Lokhande, N.S. Gajbhiye, J. Alloys Compd. 485 (2009) 798.
- [9] S.Z. Zhang, G.L. Messing, J. Am. Ceram. Soc. 73 (1990) 61.
- [10] J.A. Rodriguez, M. Fernandez-Garcia, Textbook of Synthesis, Properties and Applications of Oxide Nanomaterials, Wiley Interscience, A John Wiley and Sons, Inc., Publication, 2007, p. 95.
- [11] A.T. Raghavender, D. Pajic, K. Zadro, T. Milekovic, P. Venkateshular Rao, K.M. Jadhav, D. Ravinder, J. Magn. Mater. 316 (2007) 1–7.
- [12] P.P. Hankare, R.P. Patil, U.B. Sankpal, S.D. Jadhav, P.D. Lokhande, K.M. Jadhav, R. Sasikala, J. Solid State Chem. 182 (2009) 3217.
- [13] P.P. Hankare, R.P. Patil, U.B. Sankpal, S.D. Jadhav, I.S. Mulla, K.M. Jadhav, B.K. Chougule, J. Magn. Mater. 321 (2009) 3270.
- [14] T. Nakamura J. Magn. Mater. 168 (1997) 285
- [15] R. C. Kambale, P. A. Shaikh, C. H. Bhosale, K. Y. Rajpure, Y. D. Kolekar, Smart Mater. Struct., 18 (2009) 85014.
- [16] P.P.Hankare, U.B. Sankpal, R.P. Patil, A.V.Jadhav, K.M.Garadkar, B.K.Chougule, J. Magn. & Magn. Mat., 323 (2011) 389.
- [17] P.P.Hankare, R.P.Patil, U.B.Sankpal, I.S.Mulla, K.M.Garadkar, R.Sasikala, A.K.Tripathi, J. Magn. & Magn. Mat., 322 (2010) 2629.
- [18] A. M. Shaikh, C.M.Kanmadi, B.K.Chougule, J.Mater.Chem.Phys, 93(2005) 548.



Synthesis, characterization and catalytic application of Cr substituted Zinc Manganese Ferrite

A.S.Chavan^b, C. F. Rajemahadik^c, R.S.Pandav^d, R. P. Patil^{a*}

^aDepartment of Chemistry, M.H.Shinde Mahavidyalaya, Tisangi 416234, MH, India

^bDepartment of Chemistry, Thakur College of Science and Commerce, Kandivali (E), Mumbai, MH 400101, India

^cDepartment of Civil engineering, Sanjay Ghodawat Polytechnic, Atigre-416118, India.

^dY.C.W.M.Warananagar, Maharashtra, India

KEYWORDS

Ferrites,
Sol-gel method,
XRD, SEM,
Catalysis

Corresponding Author
Email
raj_rbm_raj@yahoo.co.in

ABSTRACT

Nanocrystalline $ZnMn_{1-x}Cr_xFeO_4$ ($1.0 \geq x \geq 0$) ferrites were prepared by sol-gel route. The synthesized material was characterized by various physicochemical methods. X-ray diffraction (XRD) method was used to confirm the formation of single phase cubic spinel lattice for all the composition. Lattice parameter shows a decreasing trend with an increase in Cr content in the compositions. Formation of spherical nanoparticles was revealed by scanning electron microscopy (SEM) analysis. Photocatalytic activity studies for thymol blue degradation indicate an enhanced activity for the composites when the maximum chromium is present in $ZnMnFeO_4$. The detailed results of physicochemical properties and photocatalytic application have been discussed so as to bring out the role of chromium substitution in determining structural and photocatalytic application of Zn-Mn ferrites.

Introduction

Mixed-metal oxide nanoparticles have been intensively studied in the last decade for their unusual physical and chemical properties owing to their extremely small size, large specific surface area and number of promising applications. Among various classes of nanomaterials, metal oxides are very common, most diverse and possess richest class in terms of physical, chemical and structural properties. The result and prospects of numerous applications of metal oxides, such as fabrication of microelectronic circuits, sensors, piezoelectric devices, fuel cells, dielectrics, lasers, magnets and catalysts have been discussed in literature [1-13].

Recently, considerable effort has been made on the preparation of surface modified nanoparticles of different types of metal oxides. Various methods are available for the synthesis of metal oxides, such as microwave refluxing [14], sol-gel [15-16], hydrothermal [17-18], co-precipitation [19-20], citrate-gel [21] and spray pyrolysis [22] etc. The selection of appropriate synthetic procedure often depends on the desired properties and final applications. Among these synthesis techniques, sol-gel autocombustion method has several advantages over others for preparation of nanosized metal oxides as the process begins with a relatively homogeneous mixture and involves low

temperature conditions and results a uniform ultrafine porous powders [23]. This method was employed by us to obtain improved powder characteristics, better homogeneity and narrow particle size distribution, thereby influencing structural, electrical and magnetic properties of spinel ferrites [24-26]. Spinel ferrites find potential applications in electrical components, memory devices, magnetostrictive and microwave devices over a wide range of frequencies because of their high resistivity and low losses [27-31]. The field of ferrites is well explored, due to their potential applications and the interesting physics involved in them.

In this article, we report preparation of nanosized chromium substituted Zn-Mn ferrites by sol-gel method. It is a simple process, which offers a significant saving in time and energy consumption over the traditional methods, and requires lower sintering temperature. This method was employed to obtain improved powder characteristics, more homogeneity and narrow particle size distribution, thereby influencing their structural, electrical and magnetical properties.

2.0 Materials and Methods

2.1. Synthesis Technique

Analytical grade chromium nitrate [Cr (NO₃)₃.9H₂O], iron nitrate [Fe ((NO₃)₃.9H₂O)], zinc nitrate [Zn (NO₃)₂.6H₂O], manganese nitrate [Mn (NO₃)₂.4H₂O] and citric acid [C₆H₈O₇.H₂O] were used to prepare ZnMn_{1-x}Cr_xFeO₄ (where x = 0.0, 0.25, 0.50, 0.75 and 1.0) by sol-gel method and flow diagram for autocombustion technique is shown in **Fig.1**. Metal nitrates and citric acid were dissolved in minimum quantity of deionized water with 1:1 molar ratio. The pH of the solution was adjusted to about 9.0 to 9.5 using ammonia solution. The solution was transformed to dry gel on heating to 353K. On further heating the dried gel burnt in a self propagating combustion manner until all the gel completely converted to a floppy loose powder. The as burnt precursor powder was then sintered at 973K for 8 h for confirmation of phase formation. The sintered powders were granulated using 2 % polyvinyl alcohol as a binder and

uniaxially pressed at a pressure of 8 ton /cm² to form pellets. These pellets were gradually heated to about 773K to remove the binder material. These pellets were gradually heated to about 773K to remove the binder material. The phase formation of the samples calcined at different temperature was confirmed by X-ray diffraction studies using Philips PW-1710 X-ray diffractometer with CuK α radiation ($\lambda=1.54056\text{\AA}$). The lattice parameters were calculated for the cubic phase using following relations.

$$a) \text{ for cubic phase } a = d (h^2 + k^2 + l^2)^{1/2} \text{ ----- } 1.0$$

where, a and c = Lattice parameter, (hkl) = Miller indices

d = interplanar distance

The crystallite size of sintered ferrites was calculated from the full width at half maxima of the most intense (311) peak by using Scherrer's formula.

$$t = 0.9\lambda / \beta \cos \theta \text{ ----- } 2.0$$

Where, symbols have their usual meaning.

The X-ray density was calculated according to the formula

$$dx = 8M/Na^3 \text{ ----- } 3.0$$

where, N = Avagadros number (6.023 X 10²³ atom/mole)

M = Molecular weight, and

a = lattice constant which was calculated from the X-ray diffraction pattern. X-ray density is sometimes also called 'theoretical density'.

The SEM micrograph of the samples was obtained using scanning electron microscope (JEOL JSM 6360).

Photocatalytic performance studied by using hazardous dyes like Thymol blue. Thymol blue is a well known dye and is considered as a model of a series of commonly used dyes in the industry. The photocatalytic activity of the samples was studied for Thymol blue dye in presence of Ultra-violet light with different times of exposure. The role of chromium in modifying structural and photocatalytic properties of these ferrites has been explained.

3.0 Results and Discussion

3.1 X-ray diffraction study

The structure and phase purity of the products were confirmed by analyzing the X-ray diffraction patterns. **Fig.2.** depicts the

XRD patterns of the different $ZnMn_{1-x}Cr_xFeO_4$ compositions and all x-ray parameters are summarized in **Table 1**. All the observed reflections could be assigned to cubic spinel lattice indicating their single phase nature. Unit cell parameters were determined by indexing the diffraction peaks in the XRD patterns. The variation of unit cell parameter with chromium content is shown in **Fig.3**. It is observed that the unit cell parameter gradually decreases with increasing Cr content in the composition obeying Vegard's law. The slow linear decreasing trend in the lattice parameter is attributed to the replacement of Mn^{3+} (0.65\AA) ions by Cr^{3+} ions, a slightly smaller ion (0.62\AA), in the system [32]. From the X-ray diffraction peaks, average particle size was estimated by using Scherrer's formula. The crystallite size decreases with increase in Cr content as shown in **Fig. 4** and it is observed to vary in the range of 30-25nm. The slow decreasing trend of unit cell parameter due to incorporation of lighter Cr^{3+} ion in place of Mn^{3+} leads to a gradual decrease in the x-ray density with increase in chromium content (**Fig.5**). The x-ray density (ρ_x), lattice constant (a) and crystallite size (t) of the compositions are given in **Table.1**.

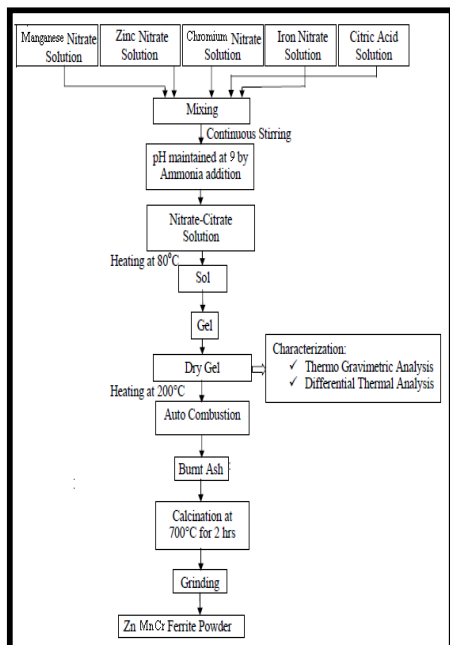


Fig.1. Flow diagram for sol-gel autocombustion

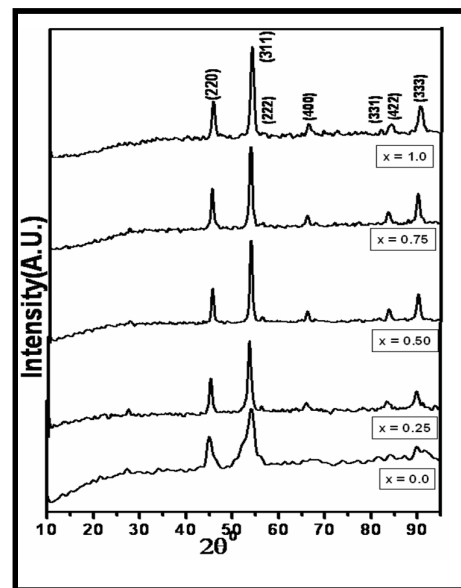


Fig.2 X-ray data for the system $ZnMn_{1-x}Cr_xFeO_4$

3.2. Scanning Electron Microscopy

The SEM images of chromium substituted Zn-Mn ferrites are shown in the **Fig.6(a-d)**. It is observed that the average grain size goes on decreasing with substitution of Cr content. The average grain size is smaller than $0.1\mu m$ for all the compositions. It can be seen that the grain size and crystallinity decrease significantly with increasing chromium content since the ionic radius of chromium is smaller than the ionic radius of manganese. The particle size becomes more uniform at higher chromium concentration.

3.3. Photocatalytic application

In recent years, the wide spread presence of chemicals such as heavy metals, herbicides, pesticides, aliphatic and aromatic detergents, arsenic compounds, solvents, degreasing agents, volatile organics, and chlorophenols pose a serious threat to the environment. When such chemicals contaminate water sources, they become really hazardous. For instance, waste waters produced from textile and dyestuff industrial processes contain large quantities of azo dyes. It is estimated that 15% of the total

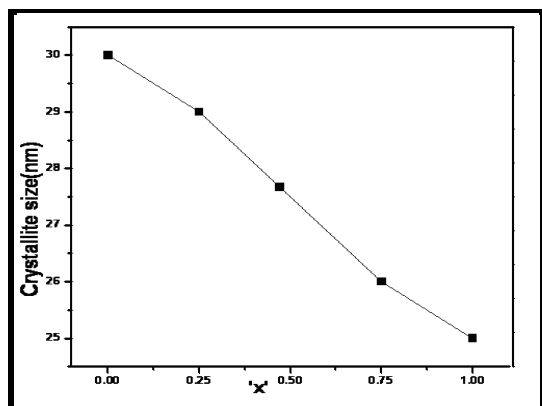


Fig.4 Variation of crystallite size with x in $ZnMn_{1-x}Cr_xFeO_4$ ferrites

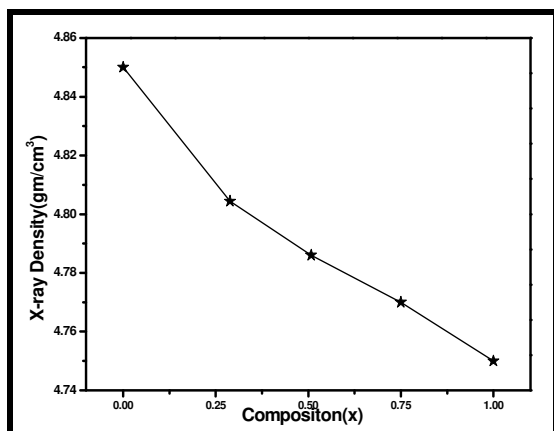
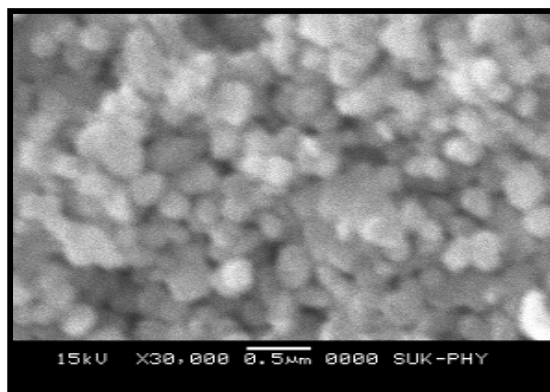
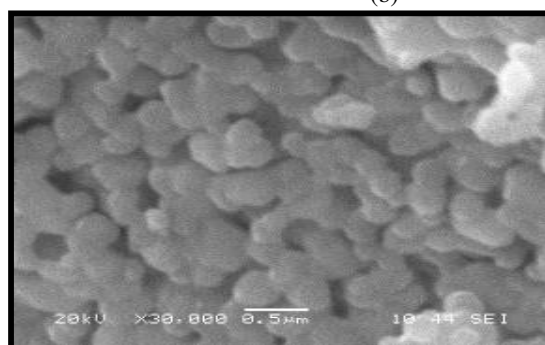


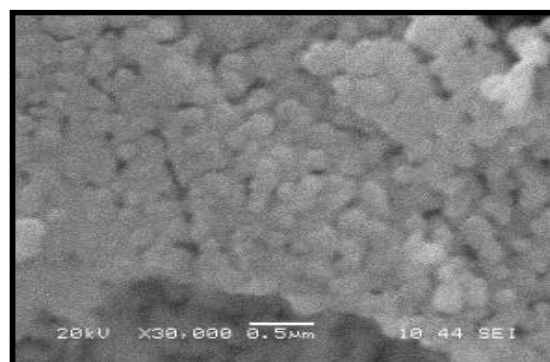
Fig.5 Variation of X-ray density with x in $ZnMn_{1-x}Cr_xFeO_4$ ferrites



(b)

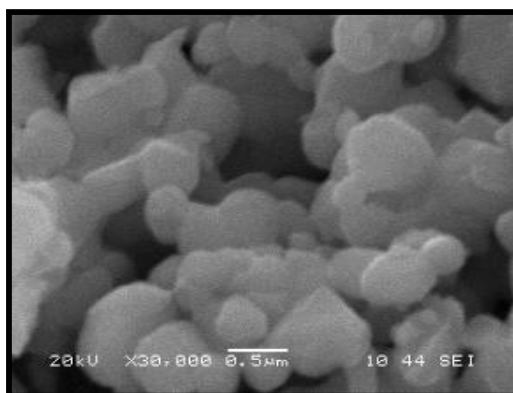


(c)



(d)

Fig.6 SEM micrographs for the system $ZnMn_{1-x}Cr_xFeO_4$
a) x = 0.0, b) x = 0.25, c) x = 0.75 and d) x = 1.0



(a)



released in waste waters. Oxidation of these organic pollutants at the surface of different metal oxides catalyst is an important photocatalysis application.

Heterogeneous photocatalysis is a process in which a combination of photochemistry and catalysis are operating together. It implies that both light and catalyst are necessary to bring out the chemical reaction. UV light illumination over a semiconductor like metal oxides produces electrons and holes. The valence band holes are powerful oxidants (+1 to+3.5V versus NHE depending on the semiconductor and pH), while the conduction band electrons are good reductants (+0.5 to -1.5V versus NHE). In 1977, Frank and Bard examined the possibilities of decomposing cyanide in water by Titania. Since then there is an increasing interest in semiconductor-mediated photo-oxidative processes.

There are number of different semiconducting materials which are readily available, but only few are suitable for sensitizing the photo-mineralization of wide range of pollutants. The semiconductor to be used as photocatalyst for photo-mineralization of wide range of organic pollutants must be (i) photoactive (ii) able to utilize visible and or near UV light (iii) biologically & chemically inert and (iv) photo-stable. It is generally found that only n-type semiconductor oxides are stable towards photo-anodic corrosion, although such oxides usually have bandgaps sufficiently larger than the semiconductors only absorb UV light.

The textile dyes and dye intermediates with high aromaticity and low biodegradability have emerged as major environmental pollutants and nearly 10-15% of the dye is lost in the dyeing process and is released in the wastewater which is an important source of environmental contamination. Considerable amount of water is used for dyeing and finishing of fabrics in the textile industries. The wastewater from textile mills causes serious impact on natural water and land in the surrounding area. As dyes are designed to be chemically and photolytically stable, they are highly persistent in natural environments.

The improper handling of hazardous chemicals in textile water also has some serious impact on the health and safety of workers putting them into the high-risk bracket for skin diseases like chemical burns, irritation, ulcers, etc. and respiratory problems.

The catalytic activity study of the Cr substituted Zn-Mn ferrite photocatalyst was carried by photodegradation rate of thymol blue. The experiment of photocatalytic reaction was conducted in a 100-ml Pyrex glass vessel with magnetic stirring and a UV lamp (8W) with the main wavelength of 253.7 nm. The as-prepared ferrite was used as photocatalyst during the study. It was, therefore, concluded that enhanced photodegradation is directly related to the reduced particle size of the ferrites, which implies photosensitization as the primarily involved process. It is seen from **Fig.7** that photocatalytic activity increasing with the increasing substitution of Cr- content. ZnCrFeO₄ shows better photocatalytic activity towards Thymol blue as compared to other Cr substituted ZnMn ferrites.

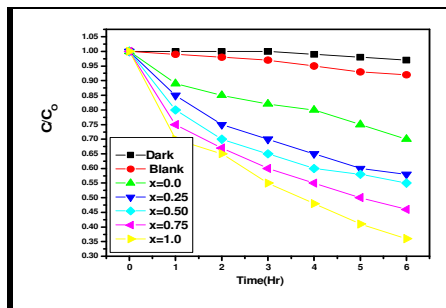


Fig.7. Photocatalytic study ZnMn_{1-x}Cr_xFeO₄ for system

3.4 Conclusions

Chromium-substituted nanocrystalline Zn-Mn ferrite samples were synthesized by sol-gel method. X-ray diffraction studies confirm the cubic spinel structure formation of the samples. The lattice constant and crystallite size decrease with increase of Cr content. Scanning Electron micrographs indicate the formation of uniform and fine grained samples. The photocatalytic degradation of thymol blue indicates that ZnCrFeO₄ powders can effectively photodegrade thymol blue under ultraviolet plus visible light irradiation.

Table. 1 Data on lattice parameter, crystallite size, x-ray density, Physical density, Porosity of $ZnMn_{1-x}Cr_xFeO_4$ ferrite samples.

Composition (x)	Lattice constant (a) nm	Crystallite size (t) nm	X-ray density(dx gm/cm ³)	Physical density (da gm/cm ³)	Porosity
0.0	0.841	30	4.85	4.95	4.89
0.25	0.839	29	4.80	4.87	5.21
0.50	0.836	28	4.78	4.83	5.67
0.75	0.833	26	4.77	4.82	5.97
1.0	0.831	25	4.75	4.78	6.23

References

- [1] M.H. Sousa, F. Atourinho, J. Depeyrot, G.J. da Silva, M.C. Lara, *J. Phys. Chem. B* 105 (2001) 1168.
- [2] K. Raj, R. Moskowitz, R. Casciari, *J. Magn. Magn. Mater.* 149 (1995) 174.
- [3] T. Hyeon, Y. Chung, J. Park, S.S. Lee, Y.W. Kim, B.H. Park, *J. Phys. Chem. B* 6 (2002) 6831.
- [4] R.V. Mehtha, R.V. Upadhyay, B.A. Dasanacharya, P.S. Goyal, K.S. Rao, *J. Magn. Magn. Mater.* 132 (1994) 153.
- [5] M.H. Kryder, *Mater. Res. Soc. Bull.* 21 (17) (1996) 184.
- [6] D.G. Mitchell, *J. Magn. Reson. Imaging* 7 (1997) 1.
- [7] P.P. Hankare, P.D. Kamble, S.P. Maradur, M.R. Kadam, U.B. Sankpal, R.P. Patil, K. Nimat, P.D. Lokhande, *J. Alloys Compd.* 487 (2009) 730.
- [8] T. Mathew, K. Sreekumar, B.S. Rao, C.S. Gopinath, *J. Catal.* 210 (2002) 405.
- [9] G. Blasse, *Philips Res. Rept. (Netherlands)* 20 (1965) 528.
- [10] J.B. Goodenough, *Magnetism and the Chemical Bond*, John Wiley, New York, 1966.
- [11] J. Smit, *Magnetic properties of materials*, in: *Intra-University Electronics Series*, vol. 13, 1971, p. 89.
- [12] G.R. Dube, V.S. Darshane, *Bull. Chem. Soc. Jpn.* 64 (1991) 2449.
- [13] V.A. Chaudhary, I.S. Mulla, K. Vihaymohanan, *Sens. Actuators, B* 55 (1999) 127.
- [14] J. Giri, T. Sriharsha, D. Bhadur, *J. Mater. Chem.* 14 (2004) 875.
- [15] M. George, A.M. John, S.S. Nair, P.A. Joy, M.R. Anantharaman, *J. Magn. Magn. Mater.* 302 (2006) 190.
- [16] S. Giri, S. Samanta, S. Maji, S. Gangli, A. Bhaumik, *J. Magn. Magn. Mater.* 288(2005) 296.
- [17] S. Thompson, N.J. Shirlcliffe, E. O'keefe, S. Appleton, C.C. Perry, *J. Magn. Magn. Mater.* 292 (2005) 100.
- [18] J. Wang, *Mater. Sci. Eng., B* 127 (2006) 81.
- [19] A.S. Albuquerque, J.D. Ardisson, W.A.A. Macedo, J.L. Lopez, R. Paniago, A.I.C. Persiano, *J. Magn. Magn. Mater.* 226 (2001) 1379.
- [20] P.P. Hankare, V.T. Vader, N.M. Patil, S.D. Jadhav, U.B. Sankpal, M.R. Kadam, B.K. Chougule, N.S. Gajbhiye, *Mater. Chem. Phys.* 113 (1) (2009) 233.
- [21] P.P. Hankare, U.B. Sankpal, R.P. Patil, I.S. Mulla, P.D. Lokhande, N.S. Gajbhiye, *J. Alloys Compd.* 485 (2009) 798.
- [22] S.Z. Zhang, G.L. Messing, *J. Am. Ceram. Soc.* 73 (1990) 61.
- [23] J.A. Rodriguez, M. Fernandez-Garcia, *Textbook of Synthesis, Properties and Applications of Oxide Nanomaterials*, Wiley Interscience, A John Wiley and Sons, Inc., Publication, 2007, p. 95.



- [25] P.P. Hankare, R.P. Patil, U.B. Sankpal, S.D. Jadhav, P.D. Lokhande, K.M. Jadhav, R. Sasikala, J. Solid State Chem. 182 (2009) 3217.
- [26] P.P. Hankare, R.P. Patil, U.B. Sankpal, S.D. Jadhav, I.S. Mulla, K.M. Jadhav, B.K. Chougule, J. Magn. Magn. Mater. 321 (2009) 3270.
- [27] T. Nakamura J. Magn. Magn. Mater. 168 (1997)285
- [28] R. C. Kambale, P. A. Shaikh, C. H. Bhosale, K. Y. Rajpure, Y. D. Kolekar, Smart Mater. Struct., 18 (2009) 85014.
- [29] P.P.Hankare, U.B. Sankpal, R.P. Patil, A.V.Jadhav, K.M.Garadkar, B.K.Chougule, J. Magn. & Magn. Mat., 323 (2011) 389.
- [30] P.P.Hankare, R.P.Patil, U.B.Sankpal, I.S.Mulla, K.M.Garadkar, R.Sasikala, A.K.Tripathi, J. Magn. & Magn. Mat., 322 (2010) 2629.
- [31] A. M. Shaikh, C.M.Kanmadi, B.K.Chougule, J.Mater.Chem.Phys, 93(2005) 548.
- [32] A. R. Denton and N. W. Ashcroft 1990 Phys. Rev. A 43, 3161.



Electrochemical synthesis of $\text{Mn}(\text{OH})_2$ and $\text{Co}(\text{OH})_2$ thin films for supercapacitor electrode application

N. C. Maile, S. D. Ghongade, S. K. Khare, H. B. Kamble and V. J. Fulari

Holography and Materials Research Laboratory,

Department of Physics, Shivaji University, Kolhapur- 416004 (M.S.) India.

KEYWORDS

Electrochemistry,
Cobalt hydroxide,
Manganese hydroxide,
Nanoflakes,
Supercapacitor.

ABSTRACT

The $\text{Mn}(\text{OH})_2$ and $\text{Co}(\text{OH})_2$ has been successfully synthesized by electrochemical method. The simple cathodic nitrate reduction reaction has been carried out to electrochemically deposit the $\text{Mn}(\text{OH})_2$ and $\text{Co}(\text{OH})_2$ on cost effective stainless steel substrate. The three electrode configuration has been utilized in which, stainless steel used as working electrode, graphite used as counter electrode and saturated calomel electrode used as reference electrode. The structural and morphological characterizations of $\text{Mn}(\text{OH})_2$ and $\text{Co}(\text{OH})_2$ were carried out by XRD, FESEM, EDS and etc. Observations reveals that, the deposition of uniform nanoflakes of $\text{Mn}(\text{OH})_2$ and $\text{Co}(\text{OH})_2$ are grown successfully on conducting stainless steel. The nanoflakes of $\text{Mn}(\text{OH})_2$ exhibit maximum specific capacitance value of 147 F g^{-1} for 0.6 mA cm^{-1} current density value in $2 \text{ M Na}_2\text{SO}_4$. Also, nanoflakes of $\text{Co}(\text{OH})_2$ exhibits a maximum specific capacitance value of 456 F g^{-1} at a scan rate of 5 mVs^{-1} in 1 M KOH

Corresponding Author
Email
vjiavfulari@gmail.com

Introduction

Supercapacitors are unique energy-storage devices because of their high power density and their capability to quickly charge and discharge, which are favorable characteristics of devices that were used in hybrid vehicles, backup energy systems, and portable electronics (Dubal, Wu, & Holze, 2016; Shinde, Dubal, Ghodake, Kim, & Fulari, 2014). Homogeneous surface morphologies are of interest to form different functional coatings. Supercapacitors store energy in the form of a double layer or in the form of a redox reaction involving a change in oxidation state during charging and discharging process (Zhang & Pan, 2015). For both mechanisms, functional electrode materials are crucial for the conversion and storage of energy, makes them as an essential component of the supercapacitor. Among different methods

of fabrication for functional electrode materials, electrochemical deposition is simple, binder free, low-cost method as compared to evaporation, sputtering, chemical vapor deposition (CVD), etc.

For supercapacitor, transition metal oxides and hydroxides were considered to be most promising electrode materials. The high cost RuO is not commercial even it gives high specific capacitance (Dubal, Chodankar, Holze, Kim, & Gomez-Romero, 2017). Previously, attempts has been made in order to study the hydroxides $(\text{Ni-Co})(\text{OH})_2$ (Gong, Cheng, Liu, Zhang, & Zhang, 2014), conducting polymer such as polypyrrole (Thombare, Fulari, Rath, & Han, 2012) and carbon nanotubes (Fayazfar, Dolati, & Ghorbani, 2011) etc. Observations has been established the crucial morphology dependence properties for these mat-

erials towards electrochemical storage. Among the other, Mn(OH)_2 and Co(OH)_2 considered being promising electrode material due to its hexagonal structure as well as layered structure with large interlayer spacing (Anandan, Gnana Sundara Raj, Lee, & Wu, 2013; Bae, Cha, Lee, & Jung, 2015; Kong et al., 2011; Liu, Hu, Chuang, & Huang, 2013). The supercapacitance study of, Mn(OH)_2 and Co(OH)_2 has to been done collectively.

In this work, the nanoflakes of Mn(OH)_2 and Co(OH)_2 were successfully grown on the stainless steel substrate by simple potentiostatic electrochemical deposition method. The synthesized films were characterized for their structural and morphological study by X ray diffraction (XRD) study, field effect scanning electron microscope (FESEM) study and energy dispersive spectroscopy (EDS) study, etc. The electrochemical measurements of electrodeposited Mn(OH)_2 and Co(OH)_2 were performed by cyclic voltammetry (CV) and galvanostatic charge-discharge (GCD) study.

1. Experimental

1.1 Chemicals

All analytical grade chemicals were used for the synthesis. So, no any further purification was required. The cobalt (II) nitrate hexahydrate [$\text{Co(NO}_3)_2 \cdot 6\text{H}_2\text{O}$], Manganese(II) nitrate tetrahydrate [$\text{Mn(NO}_3)_2 \cdot 4\text{H}_2\text{O}$], potassium hydroxide [KOH], and sodium sulfate [Na_2SO_4] were obtained from Thomas Baker India Pvt. Ltd.(Mumbai).

1.2 Synthesis of Mn(OH)_2 and Co(OH)_2 thin films

The Mn(OH)_2 and Co(OH)_2 were deposited on stainless steel (grade 304,) substrate by potentiostatic mode of electrodeposition, from electrolyte bath (30 mL) containing 0.1 M of $\text{Mn(NO}_3)_2 \cdot 4\text{H}_2\text{O}$ for Mn(OH)_2 and $\text{Co(NO}_3)_2 \cdot 6\text{H}_2\text{O}$ for Co(OH)_2 at room temperature (300 K). Initial pH of the solution was ~ 6 . The three electrode configuration in which stainless steel (SS) of dimension $1 \times 5 \times 0.03 \text{ cm}^3$ as working electrode, graphite plate (G) with dimension $1.5 \times 6 \times 0.2 \text{ cm}^3$

as counter electrode and saturated calomel electrode (SCE) as reference electrode were used. The SS and G were kept suspended in electrolyte solution from 1 cm apart. Prior to deposition all the electrodes were washed and cleaned with double distilled water. The SS electrode polished with zero grade polish paper. To remove any remaining surface contamination, cleaned substrates were etched in 10% H_2SO_4 for 2 min and rinsed with double distilled water using ultrasonic equipment(Shinde et al., 2017).

For synthesis of Mn(OH)_2 thin film, the cathodic constant potential value of 1.1 V(vs. SCE) was applied for the time period of 2400 s and to synthesize Co(OH)_2 thin films 1.0 V(vs. SCE) was applied for the time period of 600 s. After deposition films were dried and used for the further characterization. The deposited thin films were characterized for their structural, morphological and electrochemical properties. For the phase confirmation, X-ray diffraction analysis (Bruker D2 phaser table top model) was performed with copper ($\text{Cu-K}\alpha$ radiation ($\lambda=1.54 \text{ \AA}$) target within a diffraction angle 2θ from 10 to 80 degree. The surface morphology of films were studied by FESEM (Mira-3, Tescan Pvt. Brno-Czech Republic.). Elemental analysis was performed by Energy-dispersive X-ray spectroscopy (EDS) analysis (Oxford Instrument analyzer attached with FESEM). The electrochemical testing was carried out using the cyclic voltammetry, charge-discharge techniques using CH instrument (Model CHI-660-D).

1.3 Electrode preparation and electrochemical measurement

The deposited Mn(OH)_2 and Co(OH)_2 on SS were directly used for electrochemical test without any preparation. The electrochemical measurements were carried out using three electrode cell configurations with Mn(OH)_2 and Co(OH)_2 electrodes as the working electrode, platinum as the counter electrode and SCE as the reference electrode. The electrochemical performance of Mn(OH)_2 was tested in 2 M Na_2SO_4 and the electrochemical performance Co(OH)_2 was tested in 1 M KOH. The cyclic voltammetry (CV) and galva-



-nostatic charge discharge (GCD) measurements of the $Mn(OH)_2$ electrode were performed in a potential window of 0 to 0.8 V. The CV and GCD measurements of the $Co(OH)_2$ electrode were performed in a potential window of -0.4 to 0.4 V.

1.4 Electrochemical parameters

From the cyclic voltammetry (CV) measurements, the specific capacitance was calculated by the following formula (Ratha et al., 2015; Sahoo, Ratha, & Rout, 2015);

$$C_{sp}^{CV} = \frac{\oint I(V)dV}{2 \times m \times r \times (V_f - V_i)} \quad F g^{-1} \quad (1)$$

Similarly, from the constant current charge-discharge (CD) measurements, the specific capacitance of the material was evaluated using the following formula;

$$C_{sp}^{CD} = \frac{I_{dis} \times \Delta t}{m \times (V_f - V_i)} \quad F g^{-1} \quad (2)$$

Where, C_{sp}^{CV} and C_{sp}^{CD} is the specific capacitance calculated using CV and charge-discharge measurements respectively. m is the mass on electrode, r is the scan rate, $V_f - V_i$ is the potential window and $\oint I(V)dV$ is the area under the cyclic voltammetry. I_{dis} is the discharge current density where the measurement was performed. Δt is discharge time

2. Result and discussion

2.1 Potentiostatic deposition curve

The potentiostatic deposition curve of the $Mn(OH)_2$ and $Co(OH)_2$ are shown in figure 1(a-b). The rapid increase in the cathodic current was observed initially and it suddenly decreases with time.

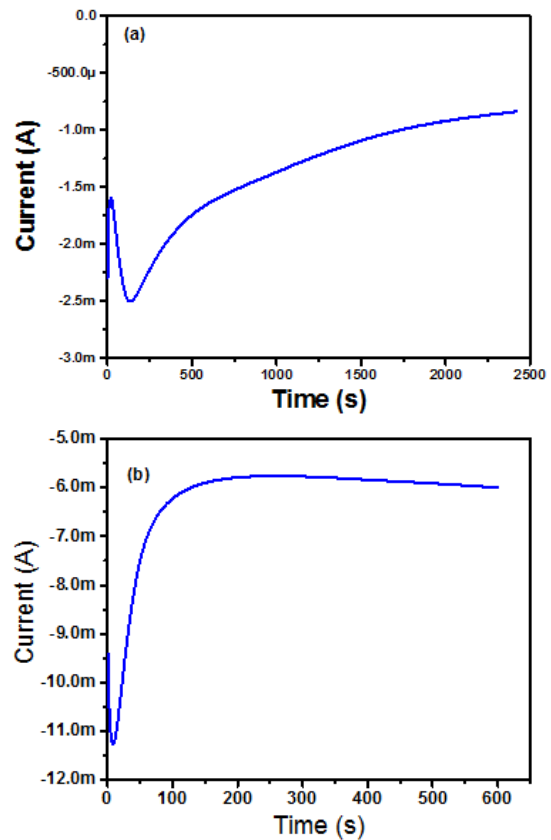
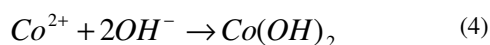
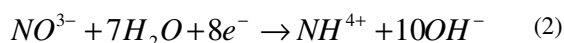
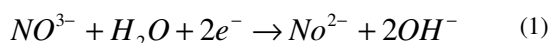


Fig-1 The potentiostatic deposition curve of the (a) $Mn(OH)_2$ and (b) $Co(OH)_2$

The initial increase in current is due to the growth of a new phase or to an increase of the number nuclei center. During this stage the deposit grows, the nuclei develop diffusion zones around themselves leads to hemispherical mass transfer then linear mass transfer resulting in the effecti-

vely planar surface. Subsequently, the current falls down corresponding to linear diffusion. This nature of curves is a typical example of a three-dimensional (3D) multiple nucleations with diffusion controlled growth (Bento & Mascaro, 2002; Moharam, Elsayed, Nino, Abou-Shahba, & Rashad, 2016).

For the applied potential more than -1.0 V at the SS substrate both Hydrogen evolution reaction and the reduction of NO_3^- is possible. Both reactions lead to increase of OH^- ion concentration at SS surface. The OH^- ions react with Mn^{2+} and Co^{2+} ions from the electrolyte leads to the formation of brownish colored $\text{Mn}(\text{OH})_2$ and bluishgreen colored $\text{Co}(\text{OH})_2$ coating on the SS surface. The deposition of $\text{Mn}(\text{OH})_2$ and $\text{Co}(\text{OH})_2$ on the SS surface can be expressed by the following possible reactions



The mass of deposited films were measured by gravimetric weight difference method. The measured mass was found to be 1.2 and 3.7 mg respectively of effective surface area of 3 cm^2 .

2.2 X-ray diffraction study

The crystallinity and chemical composition of the as-prepared $\text{Mn}(\text{OH})_2$ and $\text{Co}(\text{OH})_2$ thin films characterized by XRD. Figure 2 shows the XRD pattern of (a) $\text{Mn}(\text{OH})_2$ and (b) $\text{Co}(\text{OH})_2$ samples

Typical XRD pattern as shown in figure 2(a) can be attributed to hexagonal pyrochroite structure of $\text{Mn}(\text{OH})_2$ (JCPDS card no-073-1604) (Liu et al., 2013; Yu et al., 2009). The peaks located at 18.3° , 30.7° , 36.2° , 49.4° , 55.1° , 58.7° , 67.7° and 77.4° could be attributed to (001), (100), (011), (012), (110), (111), (103) and (202) planes of $\text{Mn}(\text{OH})_2$.

The diffraction planes of XRD as shown in figure 2(b) can be attributed to the hexagonal phase of $\alpha\text{-Co}(\text{OH})_2$ (JCPDS Card 46-0605) (Dai et al., 2017; Li et al., 2014; Ramesh, 2011). The peaks located at about 10.4° , 21.6° , 33.0° and 58.8° could be attributed to (003), (006), (012) and (110) plane of $\alpha\text{-Co}(\text{OH})_2$. In addition, some broad peaks are there having low intensity suggesting the formation of nanocrystalline material (Bae et al., 2015; Pillai et al., 2015). A small number of reflection peaks are an indication of poorly ordered samples. The strong low angle- reflection peak at $2\theta = 10.4^\circ$ for $\text{Co}(\text{OH})_2$ can be found with d-spacing of 8.6 \AA . This can be associated with nitrate groups intercalated into hydrotalcite-like α - of $\text{Co}(\text{OH})_2$ (Kelpšaitis, Baltrušaitis, & Valatka, 2011).

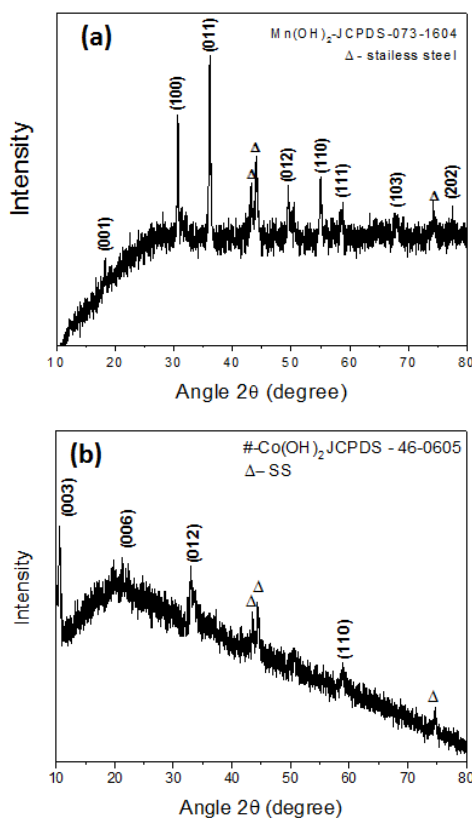


Fig-2 The XRD patterns of as prepared (a) $\text{Mn}(\text{OH})_2$ and (b) $\text{Co}(\text{OH})_2$ thin films

The EDS analysis is shown in figure 3. for (a) $\text{Mn}(\text{OH})_2$ and (b) $\text{Co}(\text{OH})_2$. The figure 3(a) shows, the



elements Mn and O were present in sample with ~1:2 confirms the $Mn(OH)_2$ phase. Similarly, figure 3(b) shows, the elements Co and O were present in sample with ~1:2 confirms the phase $Co(OH)_2$. Excess amount of oxygen percentage was due to adsorbed water at surface.

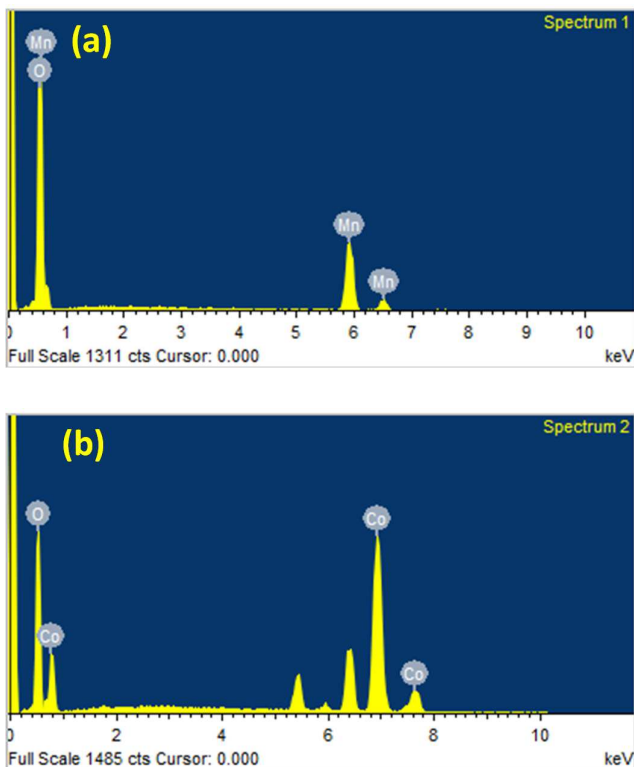


Fig-3 The EDS spectrum (a) $Mn(OH)_2$ and (b) $Co(OH)_2$ as prepared samples.

2.3 Structural and morphological study

Most of the electrochemical properties depends upon the surface morphology of thin films. In supercapacitor, the charge storage mechanism is different for electrostatic double layer capacitor (EDLC) and pseudocapacitor. In EDLC, the most of the charges gets accumulated at the surface of electrode material. So, large surface area it requirement for EDLC material. In the case of pseudocapacitor, the charge gets stored by means of faradic reaction at the interface between electrolyte and electrode, where the phase of the material gets changed during charging and discharging

process For pseudocapacitor, the electrode surface must be highly porous so the ions of electrolyte must diffuse and interact with the material (Chen, 2016).

Figure 4 shows the FESEM images of (a-b) $Mn(OH)_2$ and (c-d) $Co(OH)_2$ at two different magnification. Both images shows formation of interconnected nanoflakes structure. The interconnected nanostructure could help for electrolyte ions in intercalation process during charging discharging

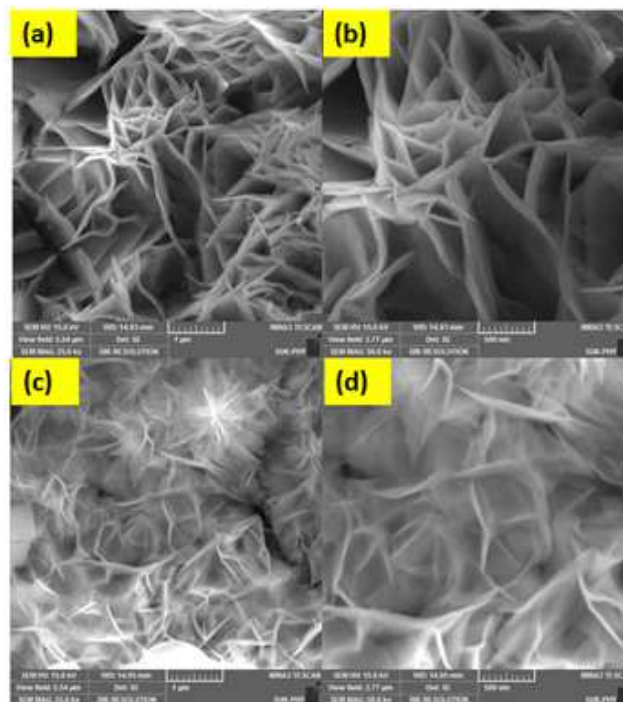


Fig-4 The FESEM images of (a-b) $Mn(OH)_2$ and (c-d) $Co(OH)_2$

2.4 Electrochemical study

The electrochemically deposited thin films of $Mn(OH)_2$ and $Co(OH)_2$ on stainless steel were directly used for electrochemical study without any further process. The $Mn(OH)_2$ thin film was tested in 2 M Na_2SO_4 electrolyte and the $Co(OH)_2$ thin film was tested in 1 M KOH electrolyte. The cyclic voltammetry (CV) and galvanostatic charge-discharge performance (GCD) were performed in three electrode configuration. The electrodeposited thin films were used as

working electrode, the platinum used as counter electrode and SCE used as reference electrode.

The CV for $\text{Mn}(\text{OH})_2$ was performed (Figure 5a) in the potential window from 0 to 0.8 V (vs SCE) at different scan rate as 5 - 100 mV s^{-1} . It was seen that, area under the curve increases with increase in scan rate. The current under curve increasing with scan rate indicates voltammetric current is directly proportional to scan rates. So, electrochemical Figure 5. The cyclic voltammetry(CV), galvanostatic charge discharge (GCD), specific capacitance vs scan rate plot and specific capacitance vs current density plot for $\text{Mn}(\text{OH})_2$. So, electrochemical reaction of $\text{Mn}(\text{OH})_2$ in electrolyte is a diffusion-controlled process which signifies ideal capacitive behavior. The observed rectangular shape of voltammogram without any redox current peaks indicates the ideal capacitive behavior of $\text{Mn}(\text{OH})_2$ nanoflakes. The similar results were reported elsewhere (Anandan et al., 2013). The specific capacitance was measured from equation 1. The specific capacitance (Figure 5 c) calculated were 127, 75, 41, 32, 26, and 23 F g^{-1} for scan rate 5, 10, 30, 50, 80 and 100 mV s^{-1} respectively.

The galvanostatic charge discharge of $\text{Mn}(\text{OH})_2$ was performed at different current densities as 0.6 – 5 mA cm^{-2} in the potential range of 0 to +0.8 V (vs. SCE). Charge-discharge curves have the linear profile (Figure 5b) indicating without deviations in each cycle there has a good electrochemical reversibility. Which exhibits good capacitive characteristics of the $\text{Mn}(\text{OH})_2$ nanoflakes (Anandan et al., 2013).

The specific capacitance values were calculated from discharge times using equation 2. $\text{Mn}(\text{OH})_2$ shows specific capacitance of 147, 132, 119, 85, 69, 59 and 52 F g^{-1} for discharge current densities values 0.6, 0.8, 1.0, 2.0, 3.0, 4.0 and 5.0 mA cm^{-2} respectively. Such specific capacitance properties may be due to the reversible transition of $\text{Mn}(\text{OH})_2$ to MnO_2 . Which is possible due to the transition from oxidation from Mn^{2+} to Mn^{3+} and then to Mn^{4+} (Kao & Weibel, 1992).

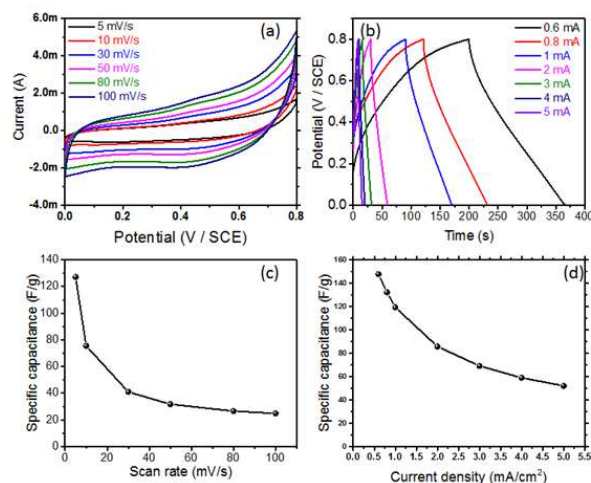


Fig-5 The (a)cyclic voltammetry (CV), (b)galvanostatic charge discharge (GCD), (c)specific capacitance vs. scan rate plot and (d)specific capacitance vs. current density plot for $\text{Mn}(\text{OH})_2$.

The CV for $\text{Co}(\text{OH})_2$ was performed (Figure 6a) in the potential window from -0.4 to 0.4 V (vs. SCE) at different scan rate as 5 - 100 mV s^{-1} . The scan rate of CV increases, it shows an increase in the oxidation and reduction potential value which is due limiting diffusion of ions into the active material. Diffusion process gets less time for electrolyte ions as scan rates increases

Peaks arising in the CV curves were corresponding to the oxidation and reduction peaks of surface faradic reaction. The anodic peak (+ ve current density) observed corresponds to an oxidation reaction $\text{Co}(\text{OH})_2$ to CoOOH , while cathodic peak (- ve current density) occurred indicates the reverse process (Jagadale, Jamadade, Pusawale, & Lokhande, 2012; Nguyen et al., 2015).The specific capacitance (Figure 6c) calculated were 456, 436, 377, 347, 317, and 308 F g^{-1} for scan rate 5, 10, 30, 50, 80 and 100 mV s^{-1} respectively.

The galvanostatic charge discharge curve (Figure. 6b) was performed for different current densities as 1.0 – 5.0 mA cm^{-2} in the potential range from -0.4 to +0.4 V (vs SCE).It is seen that the discharge time increases with decrease in current density values. Non-linear shape extant for $\text{Co}(\text{OH})_2$ indicating that the capacity results mainly from a pseudocapacitive mechanism. Wherever, the redox reaction

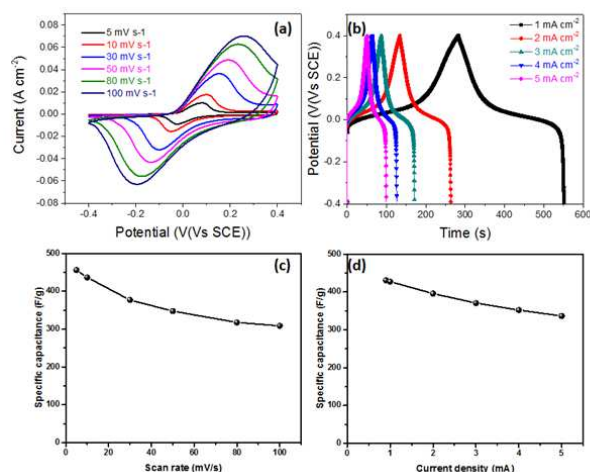


Fig-6 The (a)cyclic voltammetry (CV), (b)galvanostatic charge discharge (GCD), (c)specific capacitance vs. scan rate plot and (d)specific capacitance vs. current density plot for Co(OH)_2 .

for Co(OH)_2 is usually considered as an intercalation and de-intercalation of charges into and out of the bulk of the solid phase. From graph (Figure 5d), It was seen that, the specific capacitance decreases with increase in GCD current densities. Due to a surface confined redox process occurring at higher charging rates (Kulkarni et al., 2014). The decrease in specific capacitance is consequence of less active material access, which reduces effective utilization of material at higher charging-discharging rates. The specific capacitance values were calculated from discharge times using equation 2. Co(OH)_2 shows specific capacitance of 430, 395, 370, 352, and 336 F g^{-1} for discharge current densities values, 1.0, 2.0, 3.0, 4.0 and 5.0 mA cm^{-2} respectively.

Conclusion

Nanoflakes of Mn(OH)_2 and Co(OH)_2 were successfully synthesized by simple and low cost electrodeposition method on stainless steel substrate. XRD patterns confirmed the formation Mn(OH)_2 with hexagonal pyrochroite structure and Co(OH)_2 material with a double hydroxide layered structure. The FE-SEM microimages presented the nanoflake like nanostructure. This type of morphologies offers the higher surface area, which is favorable for ion surface intercalation. The maximum specific

capacitance measured for Mn(OH)_2 found to be 147 F g^{-1} for 0.6 mA cm^{-1} current density value and The Co(OH)_2 exhibited a maximum specific capacitance of 456 Fg^{-1} at a scan rate of 5 mVs^{-1} . All results suggesting that Mn(OH)_2 and Co(OH)_2 material is a promising material for supercapacitor.

Acknowledgment

The author acknowledges the financial assistance of UGC major research project (F.No.43-532/2014 (SR) MRP-MAJOR-PHYS-2013-35168 dated 07/10/2015) for the setting up of Project at the Department of Physics, Shivaji University, Kolhapur.

References

- Anandan S., Gnana Sundara Raj B., Lee G.-J., & Wu J. J. (2013). Sonochemical synthesis of manganese (II) hydroxide for supercapacitor applications. *Materials Research Bulletin*, 48(9), 3357–3361.
- Bae S., Cha J.-H., Lee J. H., & Jung D.-Y. (2015). Nanostructured cobalt hydroxide thin films as high performance pseudocapacitor electrodes by graphene oxide wrapping. *Dalton Transactions*, 44(36), 16119–16126.
- Bento F. R., & Mascaro L. H. (2002). Analysis of the initial stages of electrocrystallization of Fe, Co and Fe-Co alloys in chloride solutions. *Journal of the Brazilian Chemical Society*, 13(4), 502–509.
- Chen G. Z. (2016). Supercapacitor and supercapattery as emerging electrochemical energy stores. *International Materials Reviews*, 0(0), 1–30.
- Dai P., Yan T., Hu L., Pang Z., Bao Z., Wu M., Peng Z. (2017). Phase engineering of cobalt hydroxides using magnetic fields for enhanced supercapacitor performance. *Journal of Materials Chemistry A*, 5(36), 19203–19209.

- Dubal D. P., Chodankar N. R., Holze R., Kim D.-H., & Gomez-Romero P. (2017).** Ultrathin Mesoporous RuCo₂O₄ Nanoflakes: An Advanced Electrode for High-Performance Asymmetric Supercapacitors. *Chem Sus Chem*, 10(8), 1771–1782.
- Dubal D. P., Wu Y. P., & Holze R. (2016).** Supercapacitors: from the Leyden jar to electric busses. *ChemTexts*, 2(3), 13
- Fayazfar H., Dolati A., & Ghorbani M. (2011).** Electrochemical characterization of electrodeposited carbon nanotubes. *Thin Solid Films*, 519(19), 6230–6235.
- Gong X., Cheng J. P., Liu F., Zhang L., & Zhang X. (2014).** Nickel-Cobalt hydroxide microspheres electrodeposited on nickel cobaltite nanowires grown on Ni foam for high-performance pseudocapacitors. *Journal of Power Sources*, 267, 610–616.
- Jagdale A. D., Jamadade V. S., Pusawale S. N., & Lokhande C. D. (2012).** Effect of scan rate on the morphology of potentiodynamically deposited α -Co(OH)₂ and corresponding supercapacitive performance. *Electrochimica Acta*, 78, 92–97.
- Kao W.-H., & Weibel V. J. (1992).** Electrochemical oxidation of manganese (II) at a platinum electrode. *Journal of Applied Electrochemistry*, 22(1), 21–27.
- Kelpšaitė I., Baltrušaitis J., & Valatka E. (2011).** Electrochemical deposition of porous cobalt oxide films on AISI 304 type steel. *Medziagotyra*, 17(3), 236–243.
- Kong L. Bin, Liu M. C., Lang J. W., Liu M., Luo Y. C., & Kang L. (2011).** Porous cobalt hydroxide film electrodeposited on nickel foam with excellent electrochemical capacitive behavior. *Journal of Solid State Electrochemistry*, 15(3), 571–577.
- Kulkarni S. B., Patil U. M., Shackery I., Sohn J. S., Lee S., Park B., & Jun S. (2014).** High-performance supercapacitor electrode based on a polyaniline nanofibers/3D graphene framework as an efficient charge transporter. *J. Mater. Chem. A*, 2(14), 4989–4998.
- Li C., Zhang X., Wang K., Zhang H., Sun X., & Ma Y. (2014).** Dandelion-like cobalt hydroxide nanostructures: morphological evolution, soft template effect and supercapacitive application. *RSC Adv.*, 4(103), 59603–59613.
- Liu J.-S., Hu Y., Chuang T.-L., & Huang C.-L. (2013).** Mn(OH)₂/multi-walled carbon nanotube composite thin films prepared by spray coating for flexible supercapacitive devices. *Thin Solid Films*, 544, 186–190.
- Moharam M. M., Elsayed E. M., Nino J. C., Abou-Shahba R. M., & Rashad M. M. (2016).** Potentiostatic deposition of Cu₂O films as p-type transparent conductors at room temperature. *Thin Solid Films*, 616, 760–766.
- Nguyen T., Boudard M., Rapenne L., Chaix-Pluchery O., Carmezim M. J., & Montemor M. F. (2015).** Structural evolution, magnetic properties and electrochemical response of MnCo₂O₄ nanosheet films. *RSC Adv.*, 5(35), 27844–27852.
- Pillai A. S., Rajagopalan R., Amruthalakshmi A., Joseph J., Ajay A., Shakir I., ... Balakrishnan A. (2015).** Mesoscopic architectures of Co(OH)₂ spheres with an extended array of microporous threads as pseudocapacitor electrode materials. *Colloids and Surfaces A: Physicochemical and Engineering Aspects*, 470, 280–289.
- Ramesh T. N. (2011).** Synthesis and thermal stability study of cobalt hydroxynitrate in different polytypic modifications. *Inorganic Chemistry Communications*, 14(2), 419–422.



- Ratha S., Marri S. R., Lanzillo N. A., Moshkalev S., Nayak S. K., Behera J. N., & Rout C. S. (2015).** Supercapacitors based on patronite–reduced graphene oxide hybrids: experimental and theoretical insights. *J. Mater. Chem. A*, 3(37), 18874–18881.
- Sahoo S., Ratha S., & Rout C. S. (2015).** Spinel NiCo₂O₄ Nanorods for Supercapacitor Applications. *American Journal of Engineering and Applied Sciences*, 8(3), 371–379.
- Shinde S. K., Dubal D. P., Ghodake G. S., Kim D. Y., & Fulari V. J. (2014).** Nanoflower-like CuO/Cu(OH)₂ hybrid thin films: Synthesis and electrochemical supercapacitive properties. *Journal of Electroanalytical Chemistry*, 732, 80–85.
- Shinde S. K., Ghodake G. S., Dubal D. P., Patel R. V., Saratale R. G., Kim D.-Y., Fulari V. J. (2017).** Electrochemical synthesis: Monoclinic Cu₂Se nano-dendrites with high performance for supercapacitors. *Journal of the Taiwan Institute of Chemical Engineers*, 75, 271–279.
- Thombare J. V., Fulari V. J., Rath M. C., & Han S. H. (2012).** Optical absorption study of electrochemically synthesized polypyrrole (Ppy) thin films. In *2012 International Conference on Optical Engineering (ICOE)* (Vol. 1, pp. 1–4). IEEE.
- Yu T., Moon J., Park J., Park Y. Il, Na H. Bin Kim B. H., ... Hyeon, T. (2009).** Various-Shaped Uniform Mn₃O₄ Nanocrystals Synthesized at Low Temperature in Air Atmosphere. *Chemistry of Materials*, 21(11), 2272–2279.
- Zhang S., & Pan N. (2015).** Supercapacitors Performance Evaluation. *Advanced Energy Materials*, 5(6), 1401401.





Sol-Gel Deposition of Nanocrystalline TiO₂ Films and Natural dye for Dye Sensitized Solar Cell Application

M. T. Sarode

^aDepartment of Physics, Mahatma Phule A.S.C. College, Panvel, 410206, India.

KEYWORDS

TiO₂ film; Sol-gel;
Anatase; Nanocrystalline,
Strawberry.

Corresponding Author
Email
sarodemadhav@gmail.com

ABSTRACT

The dye sensitized solar cell (DSSC) that was proposed by O'Regan and Grätzel has attracted considerable interest since 1991. In the present work TiO₂ thin films were deposited on indium tin oxide (ITO) coated glass substrates by Sol-Gel dip coating method. As deposited films were annealed at temperature between 300, 400 and 500°C for 1hr in air. The XRD studies revealed that the films are nanocrystalline anatase phase. The crystallite sizes of TiO₂ films obtained from XRD are between 12 and 18 nm. The effects of annealing temperature between 300, 400 and 500°C were studied on the structural, optical and photovoltaic properties of TiO₂ thin films. The optical band gap is between 3.29 and 3.21 eV. The absorption coefficients are in the order of 10⁴ cm⁻¹. SEM of films on ITO substrate showed spherical morphology and distribution of TiO₂ particles with sizes between 10 and 100 nm. The dye sensitized solar cell device was prepared of the films annealed between 300, 400 and 500°C. Better photovoltaic properties are noteworthy that open circuit voltage (V_{oc}) = 0.550 V and Current density (J_{sc}) = 0.46 mA/cm² · efficiency = 0.178 % with fill factor (FF) 52.2 % using natural dye (Strawberry) and redox polyiodide electrolyte in acetonitrile of the film annealed at temperature 500°C.

Introduction

TiO₂ is an important inorganic functional material with good physical properties, which make it suitable for thin film applications. TiO₂ is one of the potential semiconductor materials in DSSC due to its fine physical, chemical and optical properties (M.C.Kao et al 2009). The TiO₂ thin films have been prepared by many growth techniques, such as electrochemical process (H.H. Park et al 2010, X. Chen et al 2007), anodization techniques (T. Stergiopoulos et al 2003) and sol-gel process (M. Grätzel 2001).

Among these methods, the sol-gel method has drawn a considerable amount of attention in scientific and technological fields because of its considerable advantages of generally low temperature processing conditions, easy composition control and homogeneity, easy fabrication of thin films with large area and low cost. The sol-gel dip coating method can also allow more precise control of film thickness, particle size and porosity by allowing the adjustment of different parameters such as: sol concentration, annealing conditions, numerous literature reports on the fabrication of TiO₂ thin films by sol-gel dip coating technique using many types of titanium tetra

In this work we have synthesized the Nanocrystalline TiO₂ thin films due to the post deposition annealing and correlated the annealing conditions with structure and optical properties. The results of this study will update the data on sol-gel prepared TiO₂ films and its applications in dye sensitized solar cell. Also annealed films between temperature 300, 400 and 500 °C was prepared for dye sensitized solar cells. The optical constants such as band gap (E_g) and absorption coefficient of the films have been estimated by using Tauc plot^[9]. The deposited TiO₂ thin films were characterized using X-ray diffractometer (XRD), Raman spectroscopy, Transmission electron microscopy (TEM), Scanning electron microscopy (SEM) and UV-vis spectroscopy. Photovoltaic properties were studied by solar simulator.

2. Experimental

2.1. Preparation of thin films of TiO₂

In the preparation of Ti-precursor sol, One mole of titanium tetraisopropoxide (TTIP) was added into four mole of isopropanol and stirred 30 min. Further the sol was kept 11 hr for aging. For the deposition of film, indium tin oxide (ITO) coated glass substrates were first degreased, cleaned thoroughly and dried before deposition. Then the substrate was dipped in the Ti-precursor sol and pulled out with a uniform pulling rate of ~ 1mm s⁻¹, and then dried at room temperature. Further film was heated at 100 °C for 10 min. Each dipping process repeated 10 times. As deposited films were further annealed at temperature 300, 400 and 500 °C for 1hr in muffle furnace. The deposited TiO₂ thin films were characterized using XRD, Raman spectroscopy, TEM, SEM and UV-vis spectroscopy. Further the films deposited on ITO glass substrates were studied their structural, optical and photovoltaic properties.

2.2. Fabrication of Dye Sensitized Solar Cell (DSSC)

In fabrication of DSSC, the resultant film of as-heated 300, 400 and 500 °C was initially kept in 1mM solution of Natural dye (Strawberry) for 48 hr at room temperature.

The color of film was found to be changed due to absorption of dye and formation of complex with Ti (IV). Then film was rinsed with DDW & ethanol and then dried in tissue paper gently. The carbon coated ITO was used as counter electrode. The carbon along the perimeter of three sides of the carbon-coated ITO was removed by using a cotton swab. The counter electrode was placed (carbon-coated side touching to film) on the top of film. This sandwich was used as DSSC. The few drops of electrolyte solution of polyiodide in acetonitrile were poured from exposed side of DSSC. The solution gets absorbed into DSSC by capillary action. The devices are ready for photovoltaic characteristics

Result and Discussion

3.1 Structural Properties

Fig. 1 shows the XRD pattern recorded for TiO₂ films annealed between 300, 400 and 500 °C for 1hr in air deposited on the ITO coated glass substrate. The films showed several diffraction peaks at 2θ = 25.1°, 47.9° and 53.8° ranging 2θ from 20° to 60° angle with the inter-planar spacing of 3.53 Å, 1.89 Å and 1.69 Å, respectively. The relative peak intensity of these diffraction peaks also increases as the annealing temperature increases and resulted in nanocrystallinity. The evolution of phase is started at 300 °C. Also, the films annealed at 400 and 500 °C clearly indicate the anatase (tetragonal) phase of TiO₂ which marks by 'A' and ITO marks by 'I' as shown in fig.1. Since all the reflections are perfectly matching with the peaks given in the JCPDS data file for anatase TiO₂ [PDF-21-1272]. The peaks of the (101) plane for samples became sharper and the full width at half-maximum (FWHM) decreased indicating better crystallinity and an increase in grain size with increasing annealing rate. The average grain size of the samples is estimated by the Scherer's formula (W. Que et al 2006)

$$D = \frac{0.9\lambda}{\beta \cos\theta} \quad (1)$$

Where D, λ, θ and β are the mean grain size, the X-ray wavelength (0.154056 nm), the Bragg diffraction angle and the FWHM of (101) peak, respectively.

From equation (1) the average grain size from the XRD peak (1 0 1) with $\theta = 25.1^\circ$ at an annealing temperature between 300, 400 and 500°C was found to be 12, 15 and 17 nm respectively. In the present study, after heat treatment at 300 °C, TiO₂ thin films exhibit anatase phase with moderate grain growth. Hence, the film nanocrystallinity depends on deposition parameters especially with annealing temperature. The structural properties are tabulated in table 1.

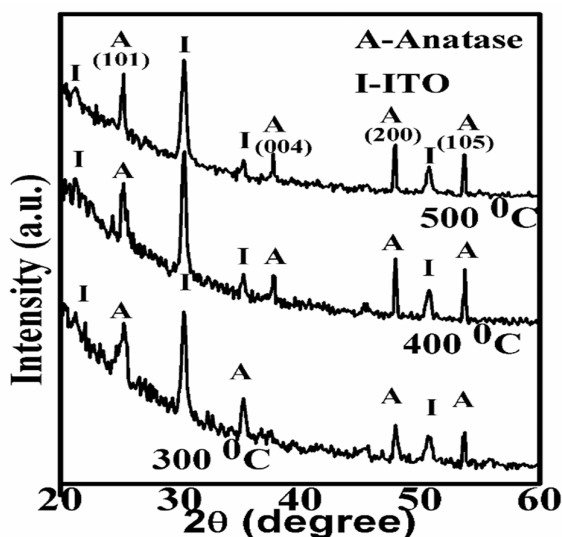


Figure 1. XRD patterns of TiO₂ films annealed at 300, 400 and 500 °C

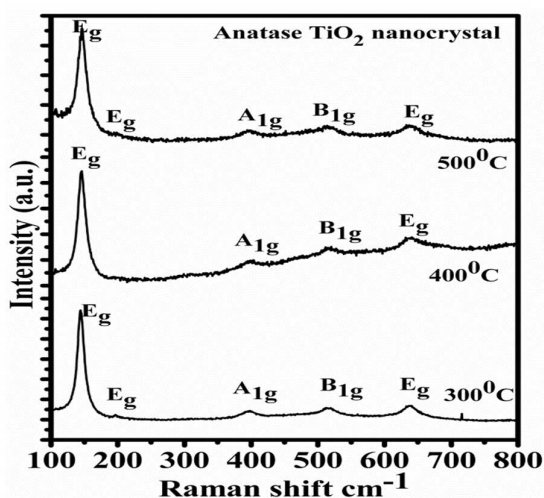


Figure 2. Raman spectrum of the titanium dioxide film annealed at 300, 400, 500 °C

Fig. 2 shows the Raman spectrum of the TiO₂ nanocrystalline film annealed between 300, 400 and 500 °C. The results of X-ray diffraction analysis are supported by the Raman spectra of TiO₂ thin film. The Raman spectra shows well defined peaks and the absence of overlapping peaks confirm that the films are well crystallized with low number of imperfect sites. Anatase TiO₂ has six Raman active modes: A_{1g} + 2B_{1g} + 3E_g. For TiO₂ single crystal have reported the following allowed bands (T. Ohsaka et al 1978): 142±2cm⁻¹ (E_g), 194±3cm⁻¹ (E_g), 393±2cm⁻¹ (B_{1g}), 512±1cm⁻¹ (A_{1g}), 519cm⁻¹ (B_{1g}) and 634±2cm⁻¹ (E_g). Five distinct peaks (Fig. 2) are observed in the Raman spectra of the dip coated TiO₂ films which can be assigned according to the above given allowed modes of anatase. The observed peaks have bands centered at 144.2 cm⁻¹ (E_g), 195.9 cm⁻¹ (E_g), 394.7cm⁻¹ (B_{1g}), 517.3cm⁻¹ (A_{1g}) and 637.4cm⁻¹ (E_g). The lowest-frequency E_g mode at 144.2 cm⁻¹ is the strongest of all the observed modes in anatase TiO₂ nanocrystals. Its frequency is quite close to 142±2 cm⁻¹ in anatase phase of single-crystal. The measured Raman spectrum shows that the as-prepared TiO₂ nanocrystals are well crystallized in the anatase structure. Also the results of the Raman studies confirm that the TiO₂ thin films prepared by the sol-gel dip coating method are suitable for the fabrication of TiO₂ based quantum dot solar cells (Y. Djaoved et al 2002). Fig.3. shows SEM micrographs of the pure TiO₂ film on ITO coated glass substrate. The surface morphologies of the as-deposited TiO₂ thin films annealed between 300, 400 and 500 °C are shown in Fig. 3. From Fig. 3 can be observed that the film is composed of an open porous structure with the average grain size of about 10 to 100 nm. With the increase of annealing temperature, the grain size becomes bigger, which results in the increase of the density of TiO₂ thin films.

This is also reflected by the enlargement of the refractivity. The SEM image shows the following observations: (i) particles are spherical, (ii) particle size distribution is nearly uniform, (iii) particles are soft agglomerates in nature, (iv) each spherical agglomerate contains many particles in the nanometric range and (v) the agglomerate size is in between 20 and 100 nm.

Table 1: STRUCTURAL PROPERTIES OF RESULTANT FILMS

Temperature (°C)	Crystalline Size (nm)	'd' spacing (nm), Phase		Phase symmetry	Plane	Lattice parameter			Unit cell volume (nm) ³
		Obs.	Std.			a (nm)	b (nm)	c (nm)	
300	12.09	0.3519	0.352	Anatase	101	0.3771	0.3771	0.9497	0.1354
400	15.75	0.3518	0.352			0.3764	0.3764	0.9495	0.1349
500	17.59	0.3517	0.352			0.3759	0.3759	0.9486	0.1339

The image also reveals the porous/less densification nature of the film at the surface. The voids are clearly seen at the surface of the film.

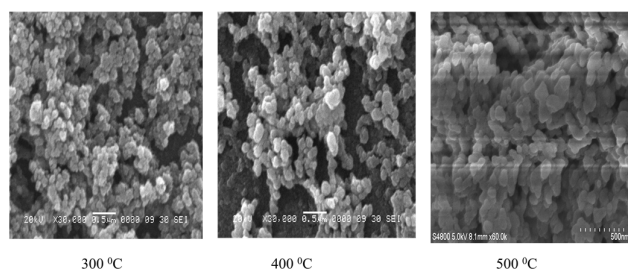


Figure 3. SEM images of titanium dioxide films annealed between 300, 400 and 500 °C

3.2 TEM studies

To confirm the crystalline structure and particle size, the dip coated TiO₂ film was peeled out from the substrate and subjected to transmission electron microscopy analysis (TEM). The transmission electron microscope image of the dip coated TiO₂ film annealed at 500 °C is shown in Fig.4.

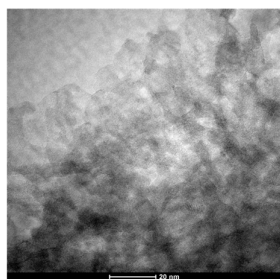


Figure 4. TEM images of 500 °C annealed TiO₂ film

Using the particle number (frequency %) and the average

particle diameter of the particles in the transmission electron microscope image the particle size has been calculated and is found to be 18.2 nm. This is in agreement with the X-ray diffraction results

3.3 Optical Properties

Thickness of films were determined by surface profiler (KLA Tencor P-16+), also confirmed by (i)UV-visible spectroscopy using the method proposed by Swanepoel (R.Swanepoel 1983) and (ii) the gravimetric weight difference method (C. Xu et al 1991).

The optical transmittance spectra of TiO₂ thin films annealed at different temperatures are shown in Fig.5. The percentage transmittances are 79, 87 and 82% at 675nm annealed films between temperature 300, 400 and 500°C respectively. TiO₂ films exhibit high transmittance annealed at 400 °C is 87% at 675 nm. All films showed good transmittance in the visible wavelength regions.

3.3.1. Optical band gap determination

The optical band gap of the TiO₂ thin films was determined by using Tauc's plot (P. Chrysicopoulou et al 1998).

$$(\alpha h\nu)^{1/2} = A(h\nu - E_g) \quad (2)$$

Where, α = absorption coefficient, A = constant independent of photon energy and $h\nu$ (eV) = energy of excitation. The



value of E_g is obtained by extrapolation of the straight-line portion of the plot to zero absorption edge in a graph of $(\alpha h\nu)^{1/2}$ versus $h\nu$ as shown in Fig. 6. The optical band gap of the as-deposited TiO₂ thin films annealed at 300, 400 and 500 °C are found to be 3.29, 3.24 and 3.21 eV respectively. The band gap of the TiO₂ films was decreased with the increase in the annealing temperature. The absorption coefficient is order of 10⁴ per sec.

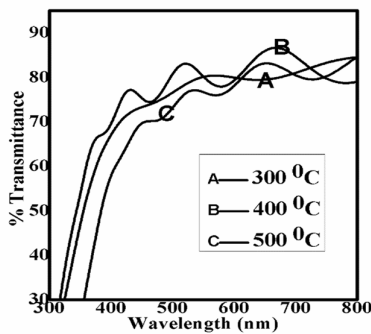


Figure 5. Transmittance spectra of the nanocrystalline TiO₂ thin films for different temperature

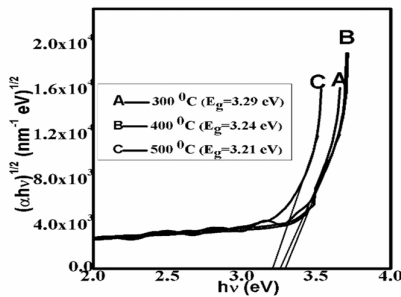


Figure 6 Variation of $(\alpha h\nu)^{1/2}$ vs. $h\nu$ of nanocrystalline TiO₂ thin films for different temperature

3.4 Photovoltaic properties of Dye Sensitized Solar Cells

The as deposited film heated at 300, 400 and 500°C was used for dye sensitized solar cell characteristics study. The cell under test was illuminated under standard AM 1.5 simulated sunlight (power density of 100mW/cm²). The solar cell J - V curves was recorded for this cell immediately after its fabrication. Fig. 7 shows the current density vs voltage curve for different temperature. The solar cell parameters obtained under condition are summarized into table 2

All the data as compared to reported data which might be good for prepared strawberry dye. The better performance of this solar cell under condition might be due to the lower stability of strawberry dye under the ambient surroundings.

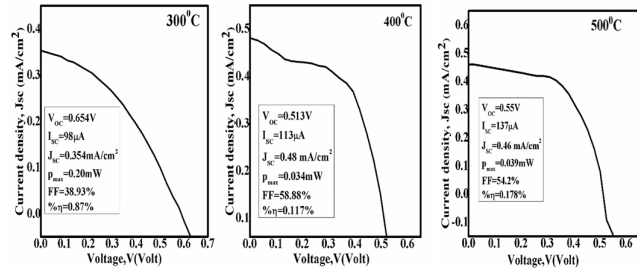


Figure 7. Current density vs Voltage curve for different temperatures.

Table 2 PHOTOVOLTAIC PROPERTIES FOR DSSCs

Parameter	Film annealed at		
	300°C	400°C	500°C
Thickness, d (nm)	778	748	702
Open circuit voltage, V _{OC} (volt)	0.654	0.513	0.550
Short circuit current, I _{SC} (μA)	98	113	137
Maximum voltage, V _{MAX} (volt)	0.347	0.361	0.374
Maximum current, I _{MAX} (μA)	58	95	97
Maximum power, P _{MAX} (mW)	0.20	0.034	0.036
Current density, J _{SC} (mA/cm ²)	0.354	0.48	0.46
Fill Factor, FF (%)	38.93	58.88	54.2
Efficiency, η (%)	0.87	0.117	0.178
Series resistance, R _S (Ω)	2352.1	2132.2	1843.1
Shunt resistance, R _{SH} (kΩ)	28.71	27.76	23.29

4. Conclusions

The sol-gel processing is simple, cheap and versatile route for the preparation of thin films. The TiO₂ films prepared by sol-gel dip coating method in the present work showed the phase pure anatase nanocrystalline nature of film material. The measured Raman spectrum shows that the as-prepared TiO₂ nanocrystals are well crystallized in the anatase structure. The optical properties showed the indirect band gap between 3.29 and 3.21 eV with corresponding crystallite sizes between 12 and 18 nm.. The SEM studies showed spherical morphology and uniform size distribution of TiO₂ particles with sizes between 10 and 100 nm.

It is also observed that refractive index of the film increases with increasing the annealing temperature and hence the crystallite size. Hence, the nanocrystalline TiO₂ thin films prepared in the present work might be having tremendous potential for the applications dye sensitized solar cells. Better photovoltaic properties is noteworthy that open circuit voltage (Voc) = 0.550 V and Current density (Jsc) = 0.46 mA/cm² · efficiency = 0.178 % with fill factor (FF) 52.2 % using natural dye (Strawberry) and redox polyiodide electrolyte in acetonitrile of the film annealed at temperature 500°C.

Acknowledgments

The author is thankful to Prin. G. A. Thakur M.P.A.S.C. College, Panvel, India and Director, SES, UoP, India for kind support.

References

Xu CJ, Tamaki J, Miura N, Yamazoe N, (1991)

Sensor. Actuat. B, 3: 147.

Park HH, Park S., Kim KS, Jeon WY., Park BK., Kim HS, Bae TS, Lee MH, (2010)

J. Electrochim. Acta 55: 6109.

Kao MC, Chen HZ, Young SL, (2009)

J. Appl. Phys. A 97: 469.

Grätzel MJ, (2001)

J. Sol Gel Sci. Technol. 22 7.

Kao MC, Chen HZ, Young SL, Kung CY, Lin CC, (2009)

Thin Solid Films 517: 5096.

Chrysicopoulou P, Davazoglou D, Trapalis C, (1998)

Thin Solid Films 323: 188.

Swanepoel R, (1983)

J. phys E,sci. instrum 16: 1214-1222.

Stergiopoulos T, Ghicov A, Likodimos V, (2006)

Nanotechnology 19: 235602.

Que W, Uddin A, Hu X, (2003)

J. Power Sources 159: 353.

Chen X, Schriver M, Suen T, Mao SS, (2007)

Thin Solid Films 515: 8511

Djaoved Y, Badilescu S, Vashirt P, Robichaud J, (2002)

Int. J. Vib. Spectrosc. 5: 4



Phytochemical constitute and antioxidant potential of *Lantana camera*

¹S.B.Patil and S.K.Mengane*

*Department of Botany, M.H.Shinde Mahavidyalaya, Tisangi, Kolhapur, India.

¹Anandibai Raorane Arts,Commerce and Science College,Vaibhavwadi, India

KEYWORDS

Phytochemical,
antioxidants, *Lantana
camera*

ABSTRACT

Traditional knowledge of medicine has long been used since ages for curing various human diseases. Most of world populations still rely on plant based medicines. the traditional Indian system of medicine has a long history of use, but they lack adequate scientific documentation. The medicinal value of plant lies in the bioactive phytochemical constituents of the plant and which shows various physiological effects on human body. So through phytochemical screening one could detect the various important compounds which could be used as the base of modern drugs for curing various diseases. The present study was aimed to analyze the chemical composition, antioxidant potential in the leaf extract of *Lantana camera*. Methanol extract, alcohol and water extracts of *Lantana camera* were assessed to determine phytochemical analysis like tannin, flavonoides, saponin, steroid, carbohydrate, glycoside, protein, emodins, anthocyanin, coumarins, phlobatanins, anthraquinones. The antioxidant activity was determined by Free-Radical Scavenging Ability (DPPH-assay). The methanolic extracts of *Lantana camera* leaves show the maximum free-radical scavenging activity (69.97%) at 500 ppm, while the synthetic antioxidant Gallic acid showed 90.93% inhibition at the same concentration in DPPH assay.

Corresponding Author
Email

skmengane@rediffmail.com

Introduction

Medicinal plants besides therapeutic agents are also a big source of information for a wide variety of chemical constituents which could be developed as drugs with precise selectivity. These are the reservoirs of potentially useful chemical compounds which could serve as newer leads and clues for modern drug design (Vijyalakshmi and Ravindran,2012)The most important of these bioactive constituents of plants are alkaloids, tannins, flavonoides and phenolic compounds (Doss,2009) Correlation between the

phytoconstituents and the bioactivity of plant is desirable to know for the synthesis of compounds with specific activities to treat various health ailments and chronic diseases as well Pandey et al.(2013). Owing to the significance in the above context, such preliminary phytochemical screening of plants is the need of the hour in order to discover and develop novel therapeutic agents with improved efficacy. Numerous research groups have also reported such studies throughout the world (Raphael 2012;Kumari ,2013; Kavitha,2013;Dasgupta,2013; Kharat,2013). Thus, the present study deals with the screening based on

Lantana camera (Family: Verbinaceae) is perennial flowering plant. *Lantana* leaves can display antimicrobial, fungicidal and insecticidal properties. *L. camera* has also been used in traditional herbal medicines for treating a variety of ailments, including cancer, skinitches, leprosy, rabies, chickenpox, measles, asthma and ulcers.

Materials and Methods

2.1 Collection of Plant Material

The leaves of *Lantana camera* were collected from the college campus. Air dried and pulverized to obtained fine powder. It was kept in air tight container and used further for phytochemical and antioxidant potential analysis.

2.2 Preparation of plant extract

10 gm of air dried powder were taken in 100 ml of methanol, ethanol and water. Plugged with cotton wool and then kept on a rotary shaker at 199-220 rpm for 24 hours. The supernatant were collected and the solvent were evaporated to the final volume one-fourth of the original volume and stored at 4 °C in air tight containers.

2.3 Preliminary Phytochemical Screening

The condensed extracts were used for preliminary screening of phytochemicals such as tannin, flavonoides, saponin, steroid, carbohydrate, glycoside, protein, emodins, anthocyanin, coumarins, phlobatanins, anthraquinones.

Tannins (**Braymer's Test**) :2ml extract + 2ml H₂O + 2-3 drops FeCl₃ (5%) Green precipitate

Flavonoids :1ml extract + 1ml Pb(OAc)₄ (10%) Yellow coloration

Saponins: (**Foam Test**) :5ml extract + 5ml H₂O + heat Froth appears

Steroids :(**Salkowski Test**) 2ml extract + 2ml CHCl₃ + 2ml H₂SO₄ (conc.) Reddish brown ring at the junction

Glycosides (**Liebermann's Test**) 2ml extract + 2ml CHCl₃ + 2ml CH₃COOH Violet to Blue to Green coloration

Coumarins : 2ml extract + 3ml NaOH (10%) Yellow coloration

Proteins: (**Xanthoproteic Test**) 1ml extract + 1ml H₂SO₄(conc.) White precipitate

Emodins: 2ml extract + 2ml NH₄OH + 3ml Benzene Red coloration

Anthraquinones: (**Borntrager's Test**) 3ml extract + 3ml Benzene + 5ml NH₃(10%)
Pink, Violet or Red coloration in ammonical layer

Anthocyanins :2ml extract + 2ml HCl (2N) + NH₃
Pinkish red to bluish violet coloration

2.4 Free-Radical Scavenging Ability (DPPH-assay) :

Radical scavenging activity of *S. lanceolatum* leaf essential oil was determined spectrophotometrically. 27,28 2 ml of different concentrations of essential oil and standard gallic acid (50-500 ppm) were prepared in methanol and add 1mM methanolic DPPH [1,1-diphenyl-2-picrylhydrazyl] solution to all the samples. Then the samples were shaken vigorously and kept at dark in room temperature for 30 minutes before measuring the absorbance at 517 nm against a reagent blank. The DPPH radical scavenging ability was calculated according to the following equation:

$$\% \text{ DPPH radical scavenging activity} = (A_0 - A_1) / A_0 \times 100\%$$

where A₀ is the absorbance of the control reaction and A₁ is the absorbance in the presence of the standard or sample of the tested extracts. Percentage radical scavenging activity was plotted against the corresponding antioxidant substance concentration to obtain the IC₅₀ value, which is defined as the amount of antioxidant substance required to scavenge 50% of free-radicals present in the assay system. IC₅₀ values are inversely proportional to the antioxidant potential.

Result and Discussion

Tannins have amazing stringent properties. They are known to hasten the healing of wounds and inflamed mucous membranes. The biological functions of **flavonoids** apart from its antioxidant properties include protection against



Result:

Sr. No	Phytochemicals	Methanol Extract	Alcohol Extract	Aqueous Extract
1	Tannins	+	+	+
2	Flavonoides	-	+	+
3	Saponin	+	+	+
4	Steroid	+	+	+
5	Carbohydrate	+	+	+
6	Glycoside	+	+	-
7	Protein	-	-	-
8	Emodins	-	-	-
9	Anthocynins	-	-	-
10	Coumarins	-	-	+
11	Phlobatannins	-	-	-
12	Anthraquinones	-	-	-

membranes. The biological functions of **flavanoids** apart from its antioxidant properties include protection against allergies, inflammation, free radicals, platelet aggregation, microbes, ulcers, hepatoxins, viruses and tumors. Flavonoids are also present in leaf extract as a potent water-soluble antioxidant and free radical scavenger, which prevent oxidative cell damage and also have strong anticancer activity [9-10]. It also helps in managing diabetes induced oxidative stress. Numerous studies have confirmed that saponins possess the unique property of precipitating and coagulating red blood cells [11-12], **Saponins** has natural tendency to ward off microbes makes them good candidates for treating fungal and yeast infections. These compounds served as natural antibiotics, which help the body to fight infections and microbial invasion. **Steroids** are responsible for cholesterol-reducing properties. Steroids also help in regulating the immune response [13] Plants containing **carbohydrates, glycosides** are known to exert a beneficial action on immune system by increasing body strength and hence are valuable as dietary supplements. **Free-radical scavenging activities**

The free-radical scavenging ability of *Lantana camera* was determined DPPH. Maximum free-radical scavenging activity (69.97%) was observed at 500 ppm, while the synthetic antioxidant Gallic acid showed 90.93% inhibition at the same concentration in DPPH assay.

Conclusion

The presence of various phytochemicals such as tannin, flavonoides, saponin, steroid, carbohydrate, glycoside in the leaf extract (methanolic, alcoholic and aqueous) confirms that this genus is a potent source for modern drugs. The present study not only paves way for preliminary contribution to the medico-botany investigation but also shows a way for pharmacological research in future for the discovery of new sources of drugs from these phytochemicals. Antioxidant capacity is widely used as a parameter to characterize nutritional health food or plants and their bioactive components. Recently, interest has considerably increased in finding naturally occurring antioxidant to replace synthetic antioxidants, which were restricted due to their side effects such as carcinogenesis. The leaf extract of *L. camera* contain high capacity of antioxidant.

References

- Vijyalakshmi R, Ravindran R (2012).** Preliminary comparative phytochemical screening of root extracts of *Diospyrus ferrea*(Wild.) Bakh and *Arva lanata* (L.) Juss. Ex Schultes. Asian J Plant Sci Res; 2:581-587.
- Doss A (2009)** Preliminary phytochemical screening of some Indian medicinal plants. Anc Sci Life; 29:12-16.

Pandey P, Mehta R, Upadhyay R. (2013) Phytochemical screening of aqueous extract collected from fertilizers affected two medicinal plants. *J Chem Bio Phy Sci* 2012; 2:1326-1332.

Kharat SS, Kumkar PB, Siddhesh RR, Sonawane KS. (2013) Qualitative phytochemical screening of *Gnidia glauca* (Fresen) Gilg. Plant extract. *Int J Pharm Bio Sci*; 4:144-148.

Kavitha R, Premalakshmi V. (2013) Phytochemical analysis of ethanolic extract of leaves of *Clitoria ternatea* L. *Int J Pharm Bio Sci* 2013; 4:236-242.

Dasgupta S, Parmar A, Patel H. (2013) Preliminary phytochemical studies of *Kalanchoe Gastonis-bonniieri*. *Int J Pharm Bio Sci*; 4:550-557.

Rio DA, Obdulio BG, Casfillo J, Marin FG and Ortuno A. (1997) Uses and properties of citrus flavonoids. *J Agric Food Chem*; 45:4505-4515.

Salah N, Miler NJ, Pagange G, Tijburg L, Bolwell GP, Rice E, et al. (1995) Polyphenolic flavonoids as scavenger of aqueous phase radicals as chain breaking antioxidant. *Arch Biochem Broph*; 2:339-46.

Okwu DE. (2004) Phytochemicals and vitamin content of indigenous spices of southeastern Nigeria. *J Sustain Agric Environ* ; 6:30-37.

Sodipo OA, Akiniyi JA, Ogunbamosu JU. (2000) Studies on certain characteristics of extracts of bark of *Pansinystalia macruceras* (K schemp) *Pierre Exbeille*. *Global J Pure Appl Sci* ; 6:83-87.

Shah BA, Qazi GN, Taneja SC. (2009) Boswellic acids: a group of medicinally important compounds. *Nat Prod Rep* ; 26:72-89.



Green synthesis of silver nanoparticles from *Lantana camera*

*S.K.Mengane and ¹S.S.Patil

*Department of Botany, M.H.Shinde Mahavidyalaya, Tisangi, Kolhapur

¹Shivraj College of Arts,Commerce and Science and D.S.Kadam Science College,Gadhinglaj.

KEYWORDS

Green synthesis,silvernano particles,plant extract,*Lantana camera*.

Corresponding Author Email

skmengane@rediffmail.com

ABSTRACT

The field of nanotechnology is one of the most active researches nowadays in modern material science and technology. Eco friendly methods of green mediated synthesis of nanoparticles are the present research in the limb of nanotechnology. The silver nanoparticles synthesized biologically have been widely used in medicinal field. In this research article we present a simple and eco-friendly bio synthesis of silver nanoparticles using *Lantana camera* leaf extract as reducing agent. The aqueous silver ions when exposed to leaf extract were reduced and resulted in silver nanoparticles whose average size was 35 nm. The silver nanoparticles were characterized by UV-Visible and transmission electron microscopy (TEM) techniques.

Introduction

The synthesis of noble metal nanoparticles attracts an increasing interest due to their new and different characteristics as compared with those of macroscopic phase, that allow attractive applications in various fields such as antimicrobials, medicine, biotechnology, optics, microelectronics, catalysis, information storage and energy conversion. Silver nanoparticles (AgNPs) have the properties of high surface area, very small size (<20 nm) and high dispersion. Silver is a safe and effective bactericidal metal because it is non-toxic to animal cells and highly toxic to bacteria. Silver nanoparticles (AgNPs) are one of the most commonly used nanomaterials. AgNPs are known to have antioxidant and antimicrobial properties (Patil et.al.2017) AgNPs are used in coating or embedding for medical purposes. In addition to their medical uses, AgNPs are also used in clothing, food industry, paints, electronics and other fields. Several techniques have demonstrated that AgNPs can be synthesized

chemical and physical methods, but due to the fact of usage of a huge amount of toxic chemicals and high temperature conditions, it becomes a mandate to find an alternative method (Ayman et. al.) Green chemistry approach emphasizes that the usage of natural organisms has offered a reliable, simple, nontoxic and eco-friendly. Therefore, researchers in the last years have turned to biological systems for nanoparticle synthesis. Synthesis of nanoparticles by biological methods, using microorganisms, enzyme and plant or plant extract, has been suggested as possible eco-friendly alternatives to chemical and physical methods. Biosynthesis of nanoparticles by plant surpasses other biological methods by reducing the complicated process of maintaining cell culture. *Lantana camera* which belongs to the family Verbenaceae is being used since ancient period to alleviate various ailments (Doss,2009).In the present investigation, we report the easy, one step, ecofriendly synthesis of silver

silver nanoparticles by an environmental friendly procedure involving the in situ reduction of Ag by *Lantana camera* leaf extract .

2. Material and methods:

2.1. Plant material and preparation of the extract

Fresh and healthy *Lantana camera* leaves were collected, washed thoroughly with distilled water, incised into small pieces and air-dried. About 25 g of thus finely cut *Lantana camera* leaves were weighed and transferred into 500-ml beaker containing 100 ml distilled water, mixed well and boiled for 25 min. The extract obtained was filtered through Whatman No.1 filter paper and the filtrate was collected in a 250-ml Erlenmeyer flask and stored in refrigerator for further use.

2.2. Synthesis of silver nanoparticles

Aqueous solution (1 mM) of silver nitrate (AgNO_3) was prepared and used for the synthesis of silver nanoparticles. 5 ml of *Lantana camera* leaf extract was added into 95 ml of aqueous solution of 1 mM silver nitrate for reduction into Ag ions. Reduction of silver nitrate to silver ions was confirmed by the color change from colorless to brown. The formation of silver nanoparticles was also confirmed by spectrophotometric determination. The fully reduced solution was centrifuged at 5000 rpm for 30 min. The supernatant liquid was discarded and the pellet obtained was redispersed in deionized water. The centrifugation process was repeated two to three times to wash off any absorbed substances on the surface of the silver nanoparticles.

2.3. Characterization of silver nanoparticles

2.3.1. UV-Visible

To determine the time point of maximum production of silver nanoparticles, the absorption spectra of the samples were taken 300–540 nm using a UV-vis spectrophotometer (HITACHI, Model U-2800 spectrophotometer). The deionized water was used as the blank. The reduction of pure Ag

the reaction medium after diluting a small aliquot of the sample into deionized water. One milliliter of the sample was pipetted into a test tube and diluted with 4 ml of deionized water and subsequently analyzed at room temperature. The nanoparticle solution showed maximum absorbance at 438 nm.

2.3.2. Transmission electron microscopy (TEM)

TEM technique was employed to visualize the size and shape of Ag nanoparticles. The 200 kV Ultra High Resolution Transmission Electron Microscope (JEOL-2010) was used. TEM grids were prepared by placing a drop of the particle solution on a carbon-coated copper grid and drying under lamp.

Result and Discussion

It is well known that silver nanoparticles exhibit yellowish brown color in aqueous solution due to excitation of surface plasmon vibrations in silver nanoparticles. Fig.1 shows as the *Lantana camera* leaf extract was mixed with aqueous solution of the silver nitrate, it started to change the color from light green to brown due to reduction of silver ion; which indicated the formation of silver nanoparticles (S Ahmed,2015) It is generally recognized that UV-Vis spectroscopy could be used to examine size and shape-controlled nanoparticles in aqueous suspensions. Fig. 2 shows the UV-Vis spectra recorded from the reaction medium after heating the solution at 75^o C for 60 min. Absorption spectra of silver nanoparticles formed in the reaction media has absorbance peak at 438 nm similar to those reported in literature (Krishraj et.al.2010) and broadening of peak indicated that the particles are polydispersed.

Fig. 3 shows the TEM micrograph of the synthesized Ag nanoparticles. Transmission electron microscopy (TEM) has been used to identify the size, shape and morphology of nanoparticles. It reveals that the silver nanoparticles are well dispersed and predominantly spherical in shape. It is observed that most of the Ag nanoparticles were spherical in shape with average diameter of around 35 nm. A few agglomerated

CONCLUSION

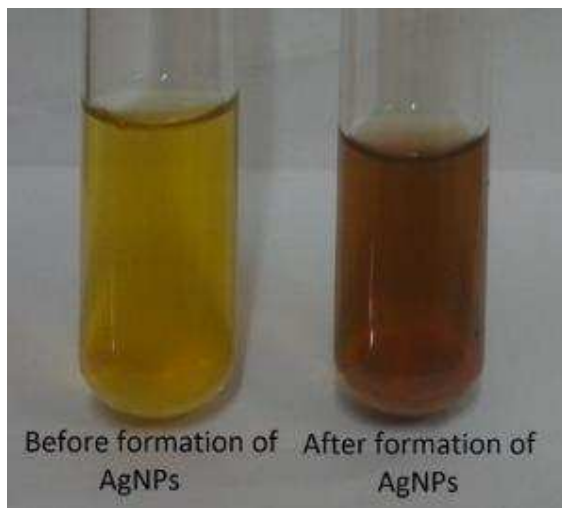


Fig 1: Color of *Lantana camera* leaf extract changing from light green to brown

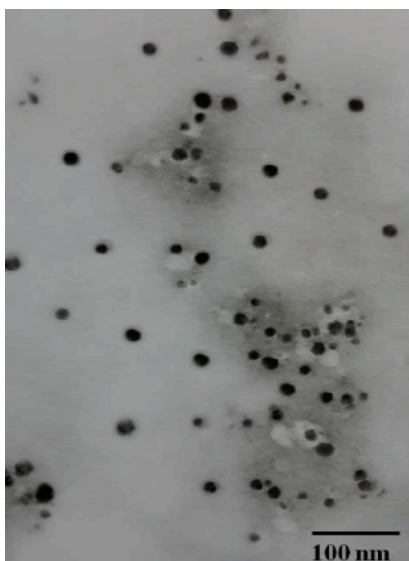


Fig 3: the TEM micrograph of the synthesized Ag nanoparticles.

Ag nanoparticles were also observed in some places, thereby indicating possible sedimentation at a later time.

Patil and Mengane (2016) also observed a simple and ecofriendly bio synthesis of silver nanoparticles using *Clerodendrum serratum* leaf extract as reducing agent. The aqueous silver

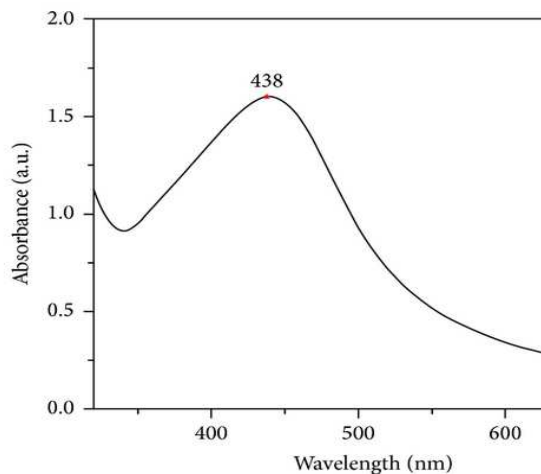


Fig 2: UV-Vis spectra of AgNPs of *Lantana camera*

ions when exposed to leaf extract were reduced and resulted in silver nanoparticles whose average size was 35 nm. According to Patil et. al. the prepared spherical shape nanoparticles using a medicinal plant *Tridax procumbens* are in the size range of 20–50 nm. The synthesized AgNPs was found higher antioxidant activity than plant extract thus signification of the present study is the production of biomedical products.

Conclusion

A simple green synthesis of stable silver nanoparticles using *Lantana camera* leaf extract at room temperature was reported in this study. Synthesis was found to be efficient in terms of reaction time as well as stability of the synthesized nanoparticles which exclude external stabilizers or reducing agents. It proves to be an eco-friendly, rapid green approach for the synthesis providing a cost effective and an efficient way for the synthesis of silver nanoparticles. Therefore, this reaction pathway satisfies all the conditions of a 100% green chemical process. The silver nanoparticles have been produced by *Lantana camera* extracts, which is an economical, efficient and eco-friendly process. UV-vis spectrophotometer and TEM techniques have confirmed the reduction of silver nitrate to silver nanoparticles.

Reference

- A. Ayman, A. G. Medhat, F. Manal, B. M. Mona, and A. M. Mohamed, (2013).** Phytosynthesis of Au, Ag, and Au–Ag Bimetallic Nanoparticles Using Aqueous Extract of Sago Pondweed (*Potamogeton pectinatus* L.) ACS Sustainable chem. Eng. 1, 1520.
- Doss A. (2009)** Preliminary phytochemical screening of some Indian medicinal plants. Anc Sci Life; 29:12-16.
- Krishnaraj, E. G. Jagan, S. Rajasekar, P. Selvakumar, P. T. Kalaichelvan, and N. Mohan. ((2010).** Synthesis of silver nanoparticles using *Acalypha indica* leaf extracts and its antibacterial activity against water borne pathogens. Colloids and Surfaces B: Biointerfaces 76, 50.
- Patil AB, Mengane SK. (2016)** Biosynthesis of Silver Nano Particles from *Tridax procumbens* and Its Antioxidant Potential: A Novel Biological Approach. Journal of Bionanoscience. 10(6) 491-494.
- Patil AB, Panse CS, Mengane SK. (2017)** Biosynthesis of Silver Nano Particles from *Tridax procumbens* and Its Antioxidant Potential: A Novel Biological Approach. Journal of Bionanoscience. 11(5) 442-445.
- S. Ahmed, M. Ahmad, Swami. B.L. S. Ikram (2015)** Plants extract mediated synthesis of silver nanoparticles for antimicrobial applications: a green expertise. Journal of Advance Research , 10.1016/j.jare.2015.02.007.



STUDIES ON LPG SENSING BEHAVIOUR OF Cs DOPED PHOSPHOMOLYBDIC ACID BY HYDROTHERMAL ROUTE

S. N. NADAF¹, V. A. KALANTRE³, B. M. SARGAR⁴, K. S. PAKHARE⁵ AND S. R. MANE²

¹Nanasaheb Mahadik polytechnic Institute .Peth, 415407, (MS) India.

²Department of Chemistry, Smt. K. R. Patil Kanya Mahavidyalaya, Islampur, 415409, (MS) India.

³P.G Department of Chemistry, Balasaheb Desai College Patan, 415206, (MS) India.

⁴Materials Science Research Laboratory, P.G Dept. of Chemistry, Jaysingpur College, Jaysingpur, (MS) India.

⁵Anandibai Raorane Arts, Commerce and Science College, Vaibhavwadi, Sindhudurg. (MS) India.

KEYWORDS

Hydrothermal, heteropolyoxometalate, thin films, gas sensing.

Corresponding Author
Email: samnadaf2010@rediffmail.com

ABSTRACT

In this study, we successfully synthesized Cs₃ (PMO₁₂O₄₀) by hydrothermal route. The electrical and gas sensing properties of Cs₃ (PMO₁₂O₄₀) synthesized material have been investigated. Scanning electron microscopy (SEM) and X-ray diffraction (XRD) techniques were used to study the structural properties of the materials. Morphological study shows after doping Cs⁺ there is formation of spherical shaped grains of Cs₃ (PMO₁₂O₄₀) heteropolyoxometalate. X-ray diffraction study revealed that, the material is polycrystalline in nature having simple cubic spinel structure. After doping Cs⁺ intensity of prominent peak (311) increases and other peaks are suppressed indicating intercalations of Cs⁺ in the octahedral lattice of phosphomolybdate anion without change in crystal structure. The optical absorption study revealed that, there is decrease in band gap (E_g) of material after doping Cs⁺. During gas sensing analysis it is found that, Cs⁺ doped material showing highest gas response 39.52 % at 325^oc with gas concentration 30 ppm for LPG gas.

1. Introduction

The heteropolyoxometalate (HPOM) materials of Vanadium, Molybdenum and Tungsten are an exciting class of materials whose properties are intermediate between atoms or molecules and bulk materials [1]. Metal ion doped HPOM materials are technologically important due to its high electrical and thermal conductivities [2], redox ion exchange behaviors [3-5]. The heteropolyanions of V, Mo, and W find applications in biochemical industrial catalysis, proton conductor [6], ion exchange materials, thin layer chromatography, materials for separation of amino acids [7]. Heteropolyoxometalates (HPOM), in addition to their considerable applications in catalysis and medicine,

are attracting attention for advanced materials. So, in the present investigation, we are reporting influence of Cs+ doping on gas sensing of hydrothermally grown molybdenum heteropolyoxometalate thin films.

2. Materials and Methods

2.1 Thin film deposition of CsPMA

The cesium doped molybdenum HPOM (CsPMA) thin films were deposited on FTO substrates. The aqueous solution of 0.05M Phosphomolybdic acid (H₃PMO₁₂O₄₀) and disodium salt of ethylene diamine tetra acetic acid (EDTA) was used as a complexing agent. A complexing agent of about 20 ml is obtained by mixing PMA (0.05M) and EDTA (0.1M) this mixing solution was adjusted to P^H of about 9.5 by adding

drop wise ammonia .Resulting solution of complexing agent along with 20 ml CsCl (0.2M) was poured in the Teflon of autoclave arrangement set up. Precleaned fluorine doped tin oxide (FTO) substrates were immersed vertically in autoclave containing reaction mixture and temperature was kept at 150°C for three hours. After cooling deposited thin films were washed with distilled water and dried. The dried films were annealed at 200°C by keeping in a furnace. Thickness of the deposited films was measured by surface profilometer.

3. Result and Discussions:

3.1 Optical characterization:

Fig.1 shows the plot of $(\alpha h\nu)^2$ verses $h\nu$ for CsPMA thin films. The presence of single slope in the curves suggests that films are single phase in nature and type of transition is direct and allowed. From Fig. 1 it was found that for Cs⁺ doped material optical band gap is 2.06eV [8-9].

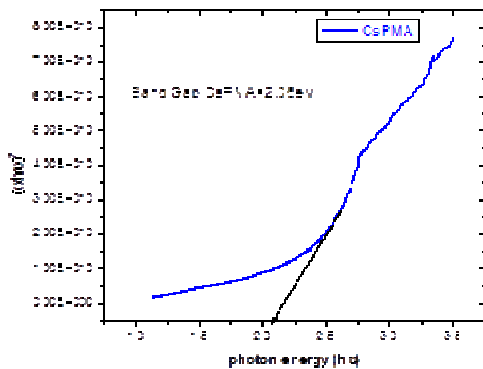


Fig.1: Plot of $(\alpha h\nu)^2$ verses $h\nu$ for CsPMA thin film.

3.2 Morphological Analysis:

The morphological investigations of CsPMA HPOM materials were analyzed by SEM technique. The scanning electron microphotographs of Cs⁺ doped PMA thin films annealed at 200°C for 2 hours are shown in Fig.2. From this figure it is found that, there is uniform distribution of grains for Cs⁺doped PMA.The grains of Cs⁺doped material becomes spherical this indicates that Cs⁺ plays an important role to improve optostructural and electrical properties. Spherical grains achieve good electrical properties.

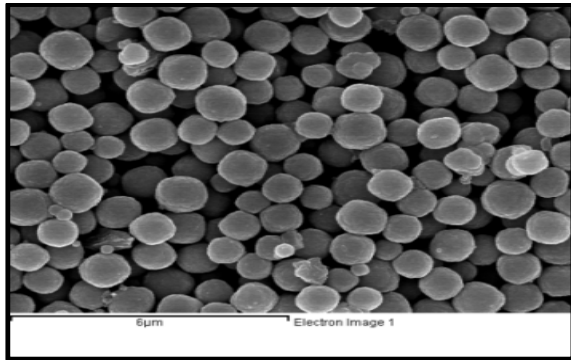


Fig. 2: SEM of CsPMA

3.3 Compositional analysis by EDS:

Required atomic percentage of Phosphorus, Oxygen, Molybdenum and Cesium composition under investigation was confirmed by analyzing annealed thin film on Energy Dispersive X-ray Analyzer. Fig.3 shows the EDS spectra of CsPMA.

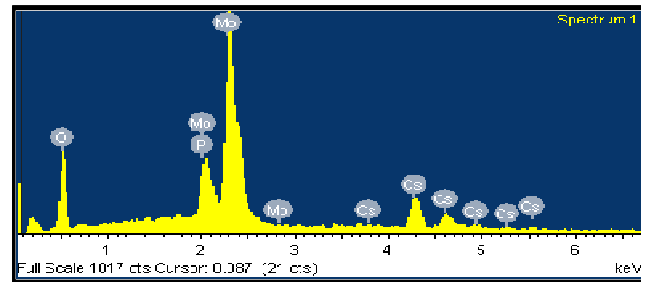


Fig.3: EDS of CsPMA

The EDS pattern shows the presence of O, P, Mo and Cs in the films without any major impurity. Table 1 shows theoretical and practical atomic percentage of O, P, Mo and Cs.

Elements	Theoretical atomic %	Practical Atomic %
O	25.50	67.82
P	2.01	2.76
Mo	50.36	22.34
Cs	22.13	7.09

Table 1: Theoretical and practical atomic percentage of O, P, Mo and Cs.



3.4 Structural analysis of CsPMA by XRD:

The X-ray diffractograms of CsPMA is presented in Fig. 4. The presence of prominent peak having 311 planes in the XRD pattern shows that the material possesses simple cubic spinel structure. The crystallite size, lattice constant and average grain size of CsPMA is shown in Table 2 which indicate that, Cs⁺ doping crystallite size (D), lattice constant (a) and average grain size (Ga) values decreases [10-11].

Table 2: Effect of Cs⁺ doping on crystallite size, lattice constant and average grain size.

Sample	Crystallite size 'D' (nm)	Lattice constant 'a' (Å)	Average grain size 'Ga' (nm)
CsPMA [Cs ₃ (PMo ₁₂ O ₄₀)]	31.34	10.89	1031

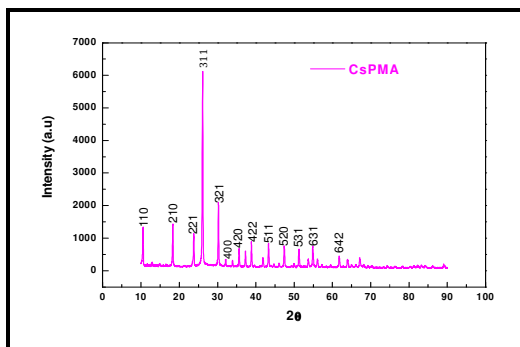


Fig.4: XRD of Cs⁺ doped phosphomolybdic acid (CsPMA)

3.5. Gas sensing properties of Cs⁺ doped Phosphomolybdic acid (CsPMA):

Fig.5 shows that, the gas response for Cs⁺ doped thin films shows 39.52 % at 325°C temperature with gas concentration 30 ppm for LPG gas. The temperature of the sensor surface is one of the major parameter. The temperature affects the physical properties of the semiconductor such as charge carrier concentration. The optimum operating temperature for an effective sensor performance corresponds to that value at which material able to catalytically reduce or oxidize the target gas.

Response of sensor depends on speed of chemical reaction on the surface and the diffusion of gas molecule to that surface. At low temperature the sensor response restricted by the speed of chemical reaction while at higher temperature it is restricted by the speed of the diffusion of gas molecule to the surface on the surface. At some intermediate temperature, the speeds of two processes become equal and at that point the sensor response reaches to its maximum. [12].

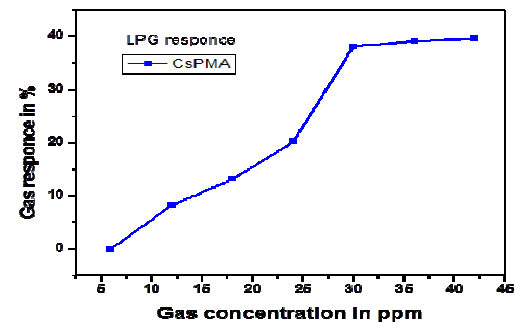
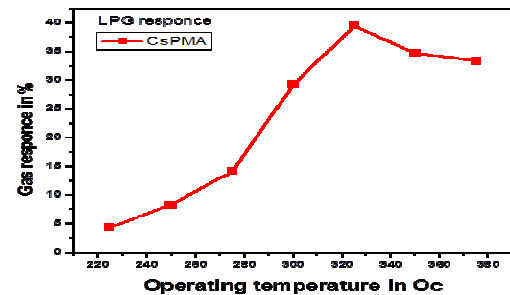


Fig.5: Gas sensing of CsPMA material.

4. Conclusion:

Thin films of the CsPMA were prepared by hydrothermal process. X-ray diffraction study confirms well formation of simple cubic spinel spherical nanocrystals. Band gap, crystallite size, lattice constant decreases with Cs⁺ doping. Gas sensing analysis shows that after, Cs⁺ doping material showing highest gas response 39.52 % at 325°C with gas concentration 30 ppm for LPG gas. Thus Cs₃(PMo₁₂O₄₀) HPOM material is applicable for gas sensor.

Acknowledgment:

One of the authors Dr.V.A.Kalantre P.G Department of Chemistry, Balasaheb Desai College Patan is very much thankful to DST New Delhi for DST-FIST grants.

References:

1. Sun, Y.H.; Xu, J.Q. ; Ling, Y.; Cui, X.B. ; Yong, L. *J. Mol. Str.* 2005, 740, 193-201.
2. Lisnard, L.; Dolbecq, A.; Mialane, P.; Marrot, J.; and Secheresse F. *Inorganica Chimica Acta* 2004,357, 845-852. Feng, W.; Zhang, T.; Liu, Y.; Lu, R.; Guan, C.; Zhao, Y. and Yao *J. Mater. Chem. Phy.*2003, 77, 294-298.
3. Keita, B.; Nadjo, L. *J. Mat. Chem. Phy.* 1989, 22, 77. DOI: 10.1016/0013-4686(94)00294-B.
4. Feng, W.; Zang, T.; Liu, Y.; Lu, R.; Zhao, Y.; Li, T. and Yao, J. *J. Solid State Chem.* 2002, 169, 1.
5. Mioc, U.; Todorovic, M.; Davidovic, M.; Colombari, P. and Holclajtner, I. *J. Solid State Ionics*2005, 176, 3005.
6. Fujibayashi, S.; Nakayama, K.; Hamamoto, M.; Sakaguchi, S.; Nishiyama, Y. and Ishii, Y. *J. Mol. Cat. - A: - Chemical*1996, 110,105.
7. Fu, X.K.; Chen, J.R.; Li, L.Q.; Wang, Q.; sui, Y. *Chin. Chem. Lett.*, 14,515(2003).
8. S. Shanmugam, B. Vishwanathan, T.K. Varadarajan, *Mat. Chem. phy.*, 112,863 (2008)
9. B.K. Hodnett and J.B. Moffat *J. Catl.*, 253 (1984).
10. Gomez-Romero, P. *J. Adv. Mater.*, 13,163 (2001).
11. M.M. Abd El-Raheem, *J. world Applied Science*, 2,204 (2007)
12. T. Nenov and S. Yordanov, "Ceramic Sensors-Technology and Applications", Technomic publishing: Lancaster PA USA, 1996.



The effect of Copper doping on the structural and Optical properties of ZnFe₂O₄

Deepa M Audi

Dhempe College of Arts and Science Miramar Goa.

KEYWORDS

Copper doped, Zinc Ferrite, Citrate gel, calcination, particle size, photocatalyst.

Corresponding Author
Email:
audim@rediffmail.com

ABSTRACT

This study reports the simple synthesis of ZnCuFe₂O₄ nanoparticles by Citrate gel method, followed by calcination at 300°C which has resulted in a homogeneous crystalline sample. The characterization studies were conducted by X-ray diffraction and SEM. The average particle size obtained by Debye Scherrer formula was in nanometer range. FT-IR confirmed the presence of Fe-O and Zn-O bands. Copper doped Zinc Ferrite was found to be an efficient photocatalyst in the degradation of dyes.

Introduction

Nanocrystalline spinel ferrites are the important class of materials having a variety of electronic, magnetic and catalytic properties. The Ferrite nanoparticles are having large number of applications in different areas such as biomedical, ferrofluid, magnetic media, microwave, magnetocaloric refrigeration and gas sensors. Zinc Ferrite (ZnFe₂O₄) is a normal spinel structure with a face centered cubic structure, where Zn⁺² cations occupy tetrahedral sites and Fe⁺³ cations occupy the octahedral sites. They have high thermal and chemical stability which make them to be used as semiconductors, photocatalysts and also for drug delivery, magnetic resonance imaging (MRI), high electromagnetic performance, low coercivity and moderate saturation magnetization, which makes it a good contender for the application as soft magnets and low loss materials at high frequencies. Nanomaterial Ferrites have attracted much attention because of their surface effect (large surface to volume ratio) and size dependent properties. These factors affect their physical and chemical properties which differ from the properties of their molecular and counterparts.

Spinel nanocrystals are important materials because of their electronic, optical, electrical, magnetic and catalytic properties---- (Mahmoud G et al 2012). Nanoscale ZnFe₂O₄ has been studied extensively due to their unique size dependent counterparts. Semiconductor photocatalysts show promising photocatalytic activity for the degradation of various dye organic pollutants in water----(Shirzadi A et al 2016, Jia Z et al 2015). TiO₂ is a widely used photocatalyst for dye degradation due to its high photo efficiency but it has limitations because of its high band gap--- (Krasae N et al 2015, Taoda H 2008). It is difficult to regenerate the powder photocatalysts from aqueous solutions. These difficulties are overcome by using magnetic nanoparticles. ZnFe₂O₄ has low band gap than TiO₂ and can be removed from aqueous solution by applying magnetic field--(Patil R et al , Haifeng D et al). ZnFe₂O₄ when doped with Copper it produces ZnCuFe₂O₄ I have tried to monitor the effect of doping on structure and photocatalytic properties.

In this paper Citrate Gel method was employed for synthesis of Copper doped ZnFe₂O₄.

2. Experimental methods

2.1 Synthesis

All the Chemicals used were A.R grade reagents. $\text{CuSO}_4 \cdot 5\text{H}_2\text{O}$, $\text{ZnSO}_4 \cdot 7\text{H}_2\text{O}$, Ferric ammm Sulphate and Citric acid was used as the precursior. Weights corresponding to 100ml solutions of 0.05M $\text{CuSO}_4 \cdot 5\text{H}_2\text{O}$, 0.05M $\text{ZnSO}_4 \cdot \text{H}_2\text{O}$, 0.1M FAS and 0.2M Citric acid were taken. First 6.242g of $\text{CuSO}_4 \cdot 5\text{H}_2\text{O}$ and 7.187g of $\text{ZnSO}_4 \cdot \text{H}_2\text{O}$ were taken in a mortar and pestle and finely ground to a mixture , this was taken in a large evaporating dish and to it 19.730g of FAS was added and the mixture was heated , to this 19.71g of Citric acid was added. And the mixture was heated till it formed a sticky gel like residue. This was cooled, dried and heated in an incinerator at 300°C for about 2 hrs. The yield was reported as 5.25g. The Copper doped Ferrite so prepared had equimolar proportion of Copper and Zinc.

2.2 Characterisations

The structural Characterisation of Copper doped ZnFe_2O_4 nanoparticles were performed by X-ray diffractometer using $\text{Cu K}\alpha$ radiation ($\lambda = 1.542 \text{ \AA}$) t generate diffraction patterns from powder crystalline samples at ambient temperature in a 2θ range of 10° to 70° . Morphological studies were done using high resolution scanning electron microscope. FT-IR spectra were recorded using FT-IR Shimadzu spectrometer. Before recording the spectra the samples were placed on a Universal ATR sampling Accessory (diamond coated with CsI) and pressed, and then the spectra were recorded.

3.0 Results and Discussion

3.1 X-ray diffraction

The single phase and purity of Copper doped Ferrite were confirmed by analyzing with X-ray diffraction patterns. It showed the reflection planes (220), (311),(400),(422),(511),(440) and (533) which are characteristic of single cubic phase.(JCPDS Card No 22-2012).

There are additional peaks which correspond to $\alpha\text{-Fe}_2\text{O}_3$. The XRD pattern of Copper doped Zinc Ferrite when compared that with Zinc Ferrite showed additional peaks which clearly indicates that the dopant Copper has incorpotated in the Ferrite structure by replacing some of the Zn^{+2} ions from the tetrahedral sites.

The average crystallite size of Copper doped Zinc Ferrite is calculated from the diffraction peak of (311) plane in accordance with Debye Scherrer formula--- (Jia Z et al 2015, Nguyen.A.T et al 2016).

$$D = 0.9\lambda/\beta \cos\theta$$

Where D is the average particle size, λ is the wavelength (0.1542nm), β is the full width at half maxima (FWHM) and θ the Bragg's angle of the (311) plane.

$$= \frac{0.9 \times 1.542}{0.22 \times \cos(17.61)}$$

Convert $\cos(17.61)$ to radians

$$\begin{aligned} \theta &= \frac{22 \times (\text{angle})}{180 \times 7} \\ &= \frac{22 \times (17.61)}{180 \times 7} \\ &= 0.307 \\ &= \frac{0.9 \times 1.542}{0.22 \times \cos(0.307)} \\ &= 6.31 \text{ nm.} \end{aligned}$$

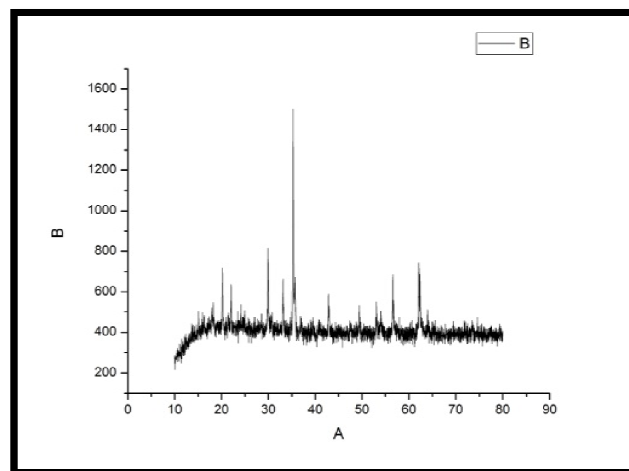


Fig 1 XRD of Copper doped Zinc Ferrite

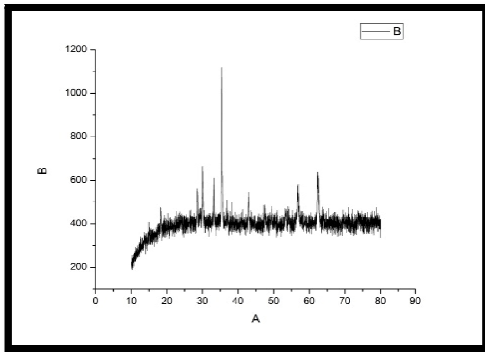


Fig 2 XRD of Zinc Ferrite

3.2 Scanning Electron Microscopy

The morphological characteristics of $ZnCuFe_2O_4$ were studied by high resolution scanning electron microscopy (HR-SEM) and are shown in fig 3 it exhibits a compact arrangement of homogeneous nanoparticles with spherical shape. This has been compared with SEM image of $ZnFe_2O_4$ in fig 4 which shows cluster of tetragonal particles. Both the images reveal agglomeration of nanoparticles due to magnetic interactions among the particles---(Prithviraj Swami.P.M et al 2011).

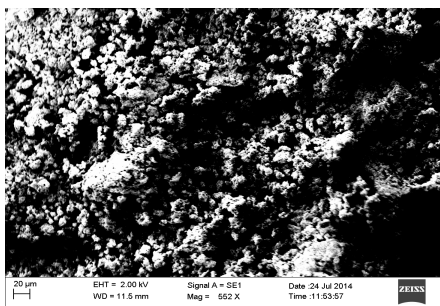


Fig 3.SEM image of $ZnFe_2O_4$

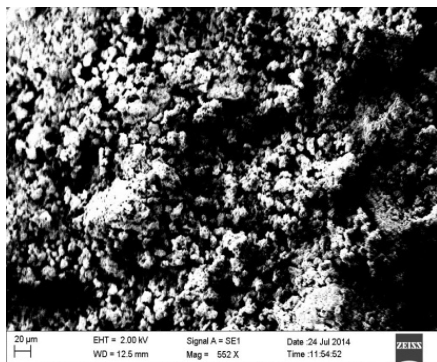


Fig 4. SEM image of $ZnCuFe_2O_4$

3.3 FT-IR Spectroscopy

The spectra of $ZnCuFe_2O_4$ nanoparticles show two principle absorption bands in the range of $300 - 600\text{cm}^{-1}$, these can be assigned to intrinsic lattice vibrations of Zn-O,Cu-O in the tetrahedral sites and Fe- O in the octahedral sites of the spinel structure.The band with peak around $1200-1250\text{cm}^{-1}$ is assigned to C-N stretching vibration, the bands in the range of $1400-1450\text{cm}^{-1}$ was attributed to C-H bending vibration from the methylene groups. Finally the bands in the region $3200 - 3400\text{cm}^{-1}$ is associated to N-H and O-H stretching vibration respectively. This has been compared with the FT-IR spectra of $ZnFe_2O_4$ which has less bands. The prominent principle bands were in the range of $300 - 600\text{cm}^{-1}$ due to vibrations of Zn-O and Fe-O in the tetrahedral and octahedral sites of spinel structure--- (Thankachan R M et al 2015). There were other bands in the region 1350cm^{-1} , 2400cm^{-1} and a broad band around $3200-3400\text{cm}^{-1}$ which are due to C-N stretching, and O-H stretching vibrations respectively.

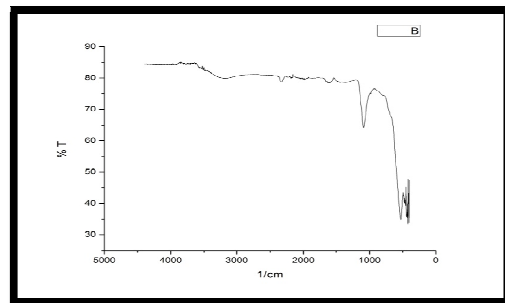


Fig 5 FT-IR of $ZnFe_2O_4$

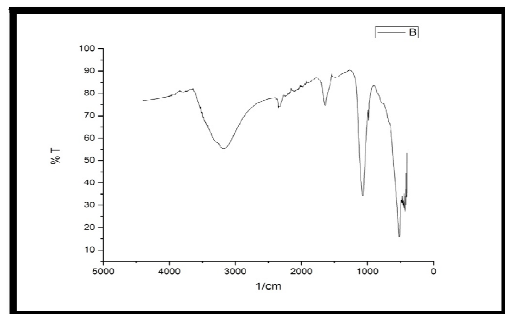


Fig 6 FT-IR of $ZnCuFe_2O_4$

3.3 Photocatalytic properties

The photocatalytic properties of $ZnCuFe_2O_4$ was studied using methylene blue. For this purpose 16 ppm of methylene blue was prepared. 25 ml of this was taken in round bottom flask and to it 0.01g of $ZnCuFe_2O_4$ was added and then kept in sunlight and the absorbance was recorded on a uv-visible spectrophotometer after every 30 mins for a period of 3 hrs. The absorbance values of dye solution steadily decrease with time, and this was found to be more pronounced for the methylene blue solution containing Copper doped Ferrite than $ZnFe_2O_4$ as seen from the optical density measurements. The O.D graph of $ZnFe_2O_4$ is shown along with doped Ferrite for the sake of comparison. This indicates that Copper doped Ferrite is degrading the methylene blue to a greater extent, which lowers their absorption in the visible region. This can be therefore used for treatment of waste waters likely to be contaminated with organic dyes. Therefore when Copper doped Ferrite when served as a photo catalyst for degradation of Methylene blue in an aqueous solution it exhibited a relatively high performance than $ZnFe_2O_4$ ---(Yan Xu et al 2017). This is attributed to higher crystallite size and high uv absorption thus enhancing the dye degradation--- (karnaji et al – 2017).

Time in mins	O.D of M.B with $ZnFe_2O_4$	O.D of M.B with $ZnCuFe_2O_4$
0	0.16	0.12
30	0.2	0.16
60	0.17	0.13
90	0.14	0.10
120	0.1	0.08
150	0.09	0.06
180	0.05	0.02

Table 1 O.D values of Methylene Blue using $ZnCuFe_2O_4$ and $ZnFe_2O_4$

4. Conclusion:

The Citrate Gel method is well suited for the synthesis of Copper doped Zinc Ferrite nanoparticles. The XRD graph clearly shows that dopant Copper is well incorporated into

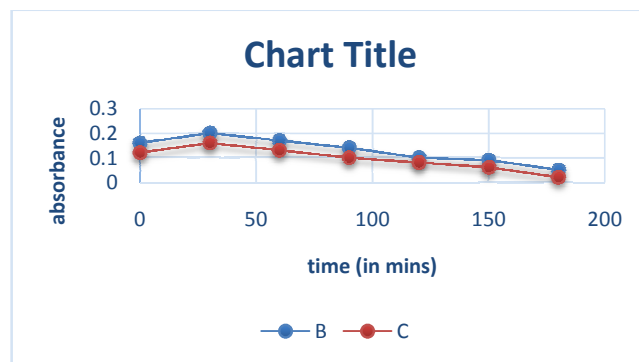


Fig 7 Dye degradation of Methylene Blue using $ZnCuFe_2O_4$ (C) and $ZnFe_2O_4$ (B)

spinel structure, which can be confirmed from the additional peaks obtained which are missing in the diffractogram of $ZnFe_2O_4$. $ZnCuFe_2O_4$ is found to degrade Methylene blue to a greater extent than $ZnFe_2O_4$ and is found to be an efficient photocatalyst for the treatment of waste waters.

5. Acknowledgements:

I thank University Grants Commission (UGC), for providing financial assistance in the minor research project. I also thank National Institute of Oceanography Donapaula Goa for carrying out XRD analysis, Instrumentation Centre Goa University for SEM analysis, Research Cell of Dhempe College of Arts and Science Miramar Goa for FT-IR analysis, and also my students Rajat Vaskar, Shanti Naik, Deepshika Naik, Namrata Naik for providing assistance.

6 .References:

- 1.Manikandan A, Judith Vijaya J, Sundaranjan M, Meghanathan C, John Kennedy L, Boudoudina M.(2013) Optical and Magnetic properties of Mg-doped $ZnFe_2O_4$ nanoparticles by rapid microwave combustion method Superlattices and Microstructures Elsevier 64: 118-131
2. Mahmoud G, Elias B, Ahmad K (2012) An overview on nanocrystalline $ZnFe_2O_4$, $MnFe_2O_4$ and $CoFe_2O_4$ ISRN Nanotechnology604241:1-11.



3. Shirzadi A, Alizera N (2016) *J. Mol. Catalyst A: Chem* 411 222-229.
4. Jia Z et al (2015) *Suplatt Micro* 82 174-187.
5. Krasae N, Wantala K (2015) *App Surf Sc* 380 309-317.
6. Taoda H (2008) *Res. Chem. Intermed.* 34 417- 426.
7. Nguyen. A. T, Phan. Ph. H. Nh et al (2016) The Characterisation of nanosized ZnFe₂O₄ material prepared by co-precipitation *Nanosystems: Physics, Chem, Mathematics*, 7,3: 459-463.
8. Prithviraj Swami .PM, Basavaraja. S et al (2011) *Bull Mater Sc* 34,7: 1325-1330.
9. Thankachan R M et al (2015) *J. Powr Sourc.* 282 462-470.
10. Yan Xu, Shumin Wu et al (2017) Synthesis, characterization, and photocatalytic degradation properties of ZnO/ZnFe₂O₄ magnetic heterostructures *New Journal of Chemistry* 24 ,41 :15433-15438.
11. Karnaji, Nurhasanah I, (2017) Photodegradation of Rhodamine B by using ZnFe₂O₄ Nanoparticles Synthesised through Precipitation method 4th International Conference on Advanced Materials Science and Technology doi: 10.1088/1757-899X/2021/012044.